MARTIN MARIETTA ENERGY SYSTEMS LIBRARIES
3 4456 0050308 8

ORNL-4791

cy. 2

Chemistry Division

ANNUAL PROGRESS REPORT

Period Ending May 20, 1972

OAK RIDGE NATIONAL LABORATORY
CENTRAL RESEARCH LIBRARY
DOCUMENT COLLECTION
LIBRARY LOAN COPY
DO NOT TRANSFER TO ANOTHER PERSON
If you wish someone else to see this document, send in name with document and the library will arrange a loan.

OAK RIDGE NATIONAL LABORATORY
OPERATED BY UNION CARBIDE CORPORATION • FOR THE U.S. ATOMIC ENERGY COMMISSION

Printed in the United States of America. Available from
National Technical Information Service
U.S. Department of Commerce
5285 Port Royal Road, Springfield, Virginia 22151
Price: Printed Copy $3.00; Microfiche $0.95

This report was prepared as an account of work sponsored by the United States Government. Neither the United States nor the United States Atomic Energy Commission, nor any of their employees, nor any of their contractors, subcontractors, or their employees, makes any warranty, express or implied, or assumes any legal liability or responsibility for the accuracy, completeness or usefulness of any information, apparatus, product or process disclosed, or represents that its use would not infringe privately owned rights.

ORNL-4791
UC-4 – Chemistry

Contract No. W-7405-eng-26

CHEMISTRY DIVISION ANNUAL PROGRESS REPORT

for Period Ending May 20, 1972

E. H. Taylor, Director
Sheldon Datz, Associate Director
Ralph Livingston, Associate Director
B. H. Ketelle, Assistant Director

G. E. Moore, Editor of Annual Report

AUGUST 1972

OAK RIDGE NATIONAL LABORATORY
Oak Ridge, Tennessee 37830
operated by
UNION CARBIDE CORPORATION
for the
U.S. ATOMIC ENERGY COMMISSION

MARTIN MARIETTA ENERGY SYSTEMS LIBRARIES
3 4456 0050308 8

Reports previously issued in this series are as follows:

ORNL-2386	Period Ending June 20, 1957
ORNL-2584	Period Ending June 20, 1958
ORNL-2782	Period Ending June 20, 1959
ORNL-2983	Period Ending June 20, 1960
ORNL-3176	Period Ending June 20, 1961
ORNL-3320	Period Ending June 20, 1962
ORNL-3488	Period Ending June 20, 1963
ORNL-3679	Period Ending June 20, 1964
ORNL-3832	Period Ending May 20, 1965
ORNL-3994	Period Ending May 20, 1966
ORNL-4164	Period Ending May 20, 1967
ORNL-4306	Period Ending May 20, 1968
ORNL-4437	Period Ending May 20, 1969
ORNL-4581	Period Ending May 20, 1970
ORNL-4706	Period Ending May 20, 1971

Contents

INTRODUCTION ix

1. NUCLEAR CHEMISTRY

Thermal-Neutron Capture Cross Section and Resonance Integral for 10.7-Year ^{85}Kr 1
Search for Beta Decay of ^{96}Zr 1
Gamma-Ray Studies on the Decay of 2.42-min ^{108}Ag 2
^{136}Nd Decay 2
Discovery of New Isotopes Far from Stability 4
Branching Ratios of ^{150}Dy, ^{151}Dy, and ^{149m}Tb 5
Coulomb Excitation of 10^+ States in ^{162}Dy and ^{164}Dy 6
Band Mixing in ^{156}Gd and ^{158}Gd 8
$M1$ Admixtures of Transitions in ^{156}Gd 11
Level Structure of ^{178}Hf 12
Transitions of Low Intensity in the Decay of ^{206}Tl 14
Single-Particle Transfer Reactions in ^{208}Pb Induced by High-Energy ^{12}C Ions 15
Coulomb Excitation with Heavy-Ion Beams at ORIC 15
The Effect of Hexadecapole Moments on the Coulomb Excitation of the Actinides 16
Search for Conversion Electrons from the ^{236}U Fission Isomer 16
Abundances of Primordial and Cosmogenic Radionuclides in Apollo 14 Rocks and Fines 17
Studies of Primordial Radioelements and Cosmogenic Radionuclides in Apollo 15 Samples by Nondestructive Gamma-Ray Spectrometry 19

2. CHEMISTRY AND PHYSICS OF TRANSURANIUM ELEMENTS

Calculations of Spallation-Fission Competition in the Reactions of Protons with Heavy Elements at Energies $\leqslant$3 GeV 21
Compound-Nuclear and Transfer Reactions in ^{12}C Reactions with ^{238}U and ^{239}Pu 22
Nuclear Charge Distribution of Heavy Fission Fragments in the Reaction ^{239}Pu(n_{th},f) 23
States in ^{236}U via the (d,d') Reaction and in the Alpha Decay of ^{240}Pu 24
Intrinsic Quadrupole and Hexadecapole Moments for Even-Even Transuranium Nuclei and the Equilibrium Deformations 25
Neutron Multiplicity Distribution Measurements in the Spontaneous Fission of ^{246}Cm, ^{248}Cm, and ^{252}Cf 26
Absolute Specific Activity of ^{249}Cf and Half-Lives for ^{249}Cf, ^{250}Cf, ^{251}Cf and ^{252}Cf 27
Neutron-Induced Fission Cross Sections for ^{249}Cf in the Energy Range 0.32 eV $\leqslant E_n \leqslant$ 1.5 MeV 27

Further Experiments on the New Isotope, Nobelium-259 29
Attempted Z Identification of ^{255,256}Lr and ^{257,261}Rf 31
Radioactivity Associated with Radiohalos 33
Search for Superheavy Elements in Nature 33
Neutron Emission Measurements of Natural Samples 34
Samples Counted in LBL Neutron Multiplicity Counter in a Search for Superheavy Elements in Nature 36
Search for Superheavy Elements in Tantalum Targets from SLAC 37
Search for Superheavy Elements in Tungsten and Uranium Targets from BNL 38
Search for Superheavy Elements in U-Zr Targets from Rutherford High-Energy Laboratory 39
Relative Energies of the Lowest Levels of the $f^q ps^2$, $f^q ds^2$, and the $f^{q+1}s^2$ Electron Configurations of the Lanthanide and Actinide Neutral Atoms 39
Electron-Transfer and $f \rightarrow d$ Absorption Bands of Some Lanthanide and Actinide Complexes and the Standard (II-III) Oxidation Potentials for Each Member of the Lanthanide and Actinide Series 40
Systematics Correlating Some Thermodynamic Properties of the Lanthanide and Actinide Metals 40
Electron Binding Energies in Americium 40
Evaluation of Atomic Energy Levels and X-Ray Energies for the Actinide Elements 41
Spectrophotometric Study of the Formation of Americium Thiocyanate Complexes 44
Stability Constants of the Monochloro Complexes of Bk(III) and Es(III) 45
Stabilization of Divalent Californium in the Solid State: Californium Dibromide 45
Preparation of Anhydrous Lanthanide Halides by Ligand Exchange 46
Organolanthanides 46
Studies with Heptavalent Neptunium: Identification and Crystal-Structure Analysis of $LiCo(NH_3)_6Np_2O_8(OH)_2 \cdot 2H_2O$ 47
Crystal Structure and Lattice Parameters of Curium-248 Oxychloride, ^{248}CmOCl 48
Crystal Structures of Californium Trichloride 49
Crystal Structure of Californium Tribromide 50
Microchemical Preparations of Heavy-Element Metals 51

3. ISOTOPE CHEMISTRY

Fractionation of Carbon Isotopes: The CYANEX System 52
Separation of Cobalt Isotopes by Ion Exchange 53
Solvent Extraction of Cesium and Rubidium Triphenylcyanoboron 53
Identity of the COCO System Complex 54
Search for a New Sulfur Isotope Separation System 55
Molecular Spectroscopy and Photochemistry 56
Isotopic Mass Spectrometry 61

4. RADIATION CHEMISTRY

Effects of H_2O, NH_3, H_2, and SF_6 on Ozone Yields and Kinetics in the Pulse Radiolysis and Flash Photolysis of Oxygen 62
Absorption Spectrum and Reaction Kinetics of the HO_2 Radical in the Gas Phase 63

Elementary Processes in the Radiolysis of Aqueous Sulfuric Acid Solutions: Determinations of Both G_{OH} and $G_{SO_4^-}$ 63
Role of Water Activity in Sulfuric Acid Solutions 63
Radiolytic Decarboxylation of α,ω-Dicarboxylic Acids in the Liquid State 65

5. ORGANIC CHEMISTRY

Transformation Graphs for Norbornyl Carbonium Ion Rearrangements 67
Mechanism of Hydride Shifts in Norbornyl Cations 70
Reaction of 5-*exo*-Hydroxy-5-Phenyl-2-*endo*-Norbornylamine with Nitrous Acid 71
β-Deuterium Isotope Effect in the Reaction of α-Phenylethylamine-α-*d* with Nitrous Acid 72
Vinyl Cations 73
Pyrolysis of Acetophenone-2-^{14}C in the Presence of Iron 73
Preparation and Purification of *p*-Sexiphenyl 73

6. PHYSICAL CHEMISTRY

AQUEOUS SYSTEMS

Thermodynamic Properties of Aqueous HCl-$LaCl_3$ Solutions to Ionic Strength 5.0 75
Thermodynamic Properties of Aqueous HCl-NaCl-$LaCl_3$ Mixtures 76
Thermodynamic Properties of Aqueous HCl-KCl-$CaCl_2$ Mixtures 77
Extension of the Two-Structure Concept for Electrolyte Solutions to Osmotic Coefficients 79
Recalculation of the Standard Potential of the Ag, AgCl Electrode 79
The Tetrad Effect in Lanthanide(III) Ion Exchange Reactions 80
Application of Laser Raman Spectroscopy to the Identification of Complex Ions in Ion Exchangers 82
Extension of the Radiometric Porous-Frit Method to the Measurement of Diffusion Coefficients of Nonradioactive Counterions in Ion Exchange Membranes 86
Self-Diffusion Coefficients of Na^+ in Poly(Acrylic Acid)–Water Mixtures 86
Thermodynamics of Water-Organic Solvent-Salt Solutions. Polyelectrolyte Organics 87
Filtration and Adsorption 88
Adsorption of Cr(VI) and Cr(III) by Organic and Inorganic Exchangers 90
Filtration Techniques for Treatment of Aqueous Solutions 94
Stability of the Extended Nernst-Planck Equations in the Description of Hyperfiltration through Ion Exchange Membranes 98
Preliminary Analysis of Donnan Softening 98
Sorption of Cations by Polyaminoresins 99
Temperature Effects on Equilibria in the System: Poly(hydroxypropyl acrylate–co–tetraethylene glycol dimethacrylate), Water, and Electrolyte 99
Cross-Flow Filtration of Municipal Sewage 100

MOLTEN SALTS AND RELATED NONAQUEOUS SYSTEMS

Nonideality of Mixing in Alkali Metal Tetrafluoroberyllate–Iodide Systems 101
The Lithium Fluoride–Tetrafluoroborate Phase Diagram 102

Enthalpy of Lithium Tetrafluoroborate 103
Evaluation of Fusion Entropies of Uranium and Zirconium Tetrafluorides 103
The Free Energies of Formation of Lanthanide Halides by an EMF Technique 103

CALORIMETRY

Preparation of Certain Oxides of Technetium 104
High-Temperature Enthalpy of Potassium Perrhenate 105

ELECTROCHEMISTRY

The Electrochemical Behavior of Technetium and of Iron Containing Technetium 106
Electrochemical Behavior of Titanium 106
Potentiostatic Method for the Determination of Specific Conductance: Application to Molten Salt Electrolytes 108
An Electrochemical Method for Monitoring the Oxygen Content of Aqueous Streams at the Part-per-Billion Level 110
Analysis with Packed-Bed Electrodes 111
Direct Electrochemical Pretreatment of Waters for Hardness and pH Control 112
Electrochemical Cell for Generation of Base 113
Electrochemical Demonstration Unit for Copper Removal from Distillation Plant Blowdown 113

7. CHEMICAL PHYSICS

NEUTRON AND X-RAY DIFFRACTION

Hydrogen Isotope Partitioning in a Crystal Containing Both Short and Long Hydrogen Bonds 115
The Tri-Aquated Hydrogen Ion $H_7O_3^+$. A Neutron Diffraction Study of Sulfosalicylic Acid Trihydrate 118
Neutron Diffraction Study of Lithium Hydroxide Monohydrate 118
Nonplanarity of Hydroxamic Acids. A Neutron Diffraction Study of Hydroxyurea 120
Sucrose: Further Refinement of the Crystal-Structure Parameters from Neutron Data 122
Solution of the Crystal Structure of Fluocinolone Acetonide, a Steroidal Anti-Inflammatory Agent, and Comparison of Its Molecular Geometry with Active and Inactive Steroids 125
Structure of a Crystalline Acid-Catalyzed Cyclization Product of the 14-Membered Ring Diterpene Hydrocarbon, Cembrene 126
A Method for Predicting the Conformation of an Isolated Molecule from Its Crystal Structure 128
A New Form for the Torsional Potential in Molecules 129
Analytical Approximation for the Crystallographic Least-Squares Matrix 130
Liquid Water: Atom-Pair Correlation Functions from Neutron and X-Ray Diffraction 131
Toward a Molecular Theory for the Structure of Liquid Water 132

INFRARED AND RAMAN SPECTROSCOPY

Raman Spectra of Molten Alkali-Metal Carbonates 133
Raman Spectra of $Be_2F_7^{3-}$ and Higher Polymers of Beryllium Fluorides in the Crystalline and Molten States 135

Raman Spectra of Neutron-Irradiated SiO_2 137
Raman Spectra of O_2^- and O_3^- Ions in Alkali-Metal Superoxides and Ozonides 139
Vibrational Spectra of Molten and Aqueous $NaClO_3$ and $KClO_3$ 140
Raman Spectra of Crystalline Cyclopropane, Cyclopropane-d_6, and C_3H_6-C_3D_6 Solid Solutions 142

MICROWAVE AND RADIO-FREQUENCY SPECTROSCOPY

Paramagnetic Resonance Studies of Liquids During Photolysis 145
Electron Spin Resonance Study of Fremy's Radical in Single Crystals of Potassium Hydroxylamine Trisulfonate 148
ESR Study of Radical Interconversions in Single Crystals of Strontium Nitrate at 77°K 148

ELECTRON SPECTROSCOPY

Study of the Angular Distribution for the Photoelectron Spectra of Halogen-Substituted Methane Molecules 149
Use of X-Ray Photoelectron Spectroscopy to Study Bonding in Cr, Mn, Fe, and Co Compounds 150
Study of the X-Ray Photoelectron Spectrum of Tungsten–Tungsten Oxide as a Function of Thickness of the Surface Oxide Layer 150
Study of Core Binding Energies of Simple and Complex Salts Using X-Ray Photoelectron Spectroscopy 150
X-Ray Analysis by Photoelectron Spectrometry 151

ATOMIC AND MOLECULAR COLLISONS

Velocity Dependence of Electronic to Vibronic Energy Conversion for $Hg(6^3P_2)$ in Molecular Collisions 152
Ionizing Collisions of Fast Alkali Atoms with Cl_2, Br_2, and O_2 152
Spectator Stripping in Fast Alkali Atom and Ion Collisions with Diatomic Molecules 153
"Hot-Atom" Beam Sources from Electron Sputtering of Alakli Halides 153
Inner-Shell Ionization in Fast Heavy-Ion Collisions 153
Inner-Shell Ionization by Proton and Alpha-Particle Bombardment 154
The Z^2 Dependence of the X-Ray Production Cross Section by 5-MeV/amu Heavy Ions 154

PUBLICATIONS 157
PAPERS PRESENTED AT SCIENTIFIC AND TECHNICAL MEETINGS 166
LECTURES 172
SUPPLEMENTARY ACTIVITIES 174

Introduction

With support for research still declining, chemists at ORNL are being converted to other occupations, some drawing partly on chemical training and others only on the general problem-solving abilities of persons educated and experienced in science. The Chemistry Division is, of necessity, participating in this conversion; it has supplied members of its staff to the task of evaluating the impact of reactors on their environments, to the Environmental Information Center, and to the Mathematics Division. A few other instances of conversion will probably occur by the time this appears. These ventures seem to be stimulating to the persons concerned and may bring new and rewarding careers to some. In a less obvious way, other members of the Division are turning to problems that require broader considerations than do, for example, the discovery and characterization of a new radioisotope or a new steroid. Members of the Water Research Program, largely drawn from the Chemistry Division, have been balancing chemistry, engineering, economics, and practical sociology for years, and more and more of the staff are being brought into committees, study groups, and other part-time exercises that deal with multidisciplinary problems and the Laboratory's role in attacking them. Again, this broadening of outlook is welcomed by the participants and, one hopes, will be valuable to the Laboratory and to society.

However, not all of the problems of the world will go away with thinking about them, no matter how broadly, and not all of the information necessary for solving technical aspects of them will be available or quickly acquired by obvious measurements. We need a continuing, relatively free search for understanding of natural phenomena if we are going to continue to live in reasonable comfort and safety in a world of great natural complexity.

This has been an article of faith among scientists for many years, but one that does not now hold so much respect elsewhere as it once did. This report is too parochial to be a useful forum for converting nonbelievers, but perhaps the congregation itself would be heartened by a few examples that tend to support the faith.

If one wishes to be generous, he can admit to three kinds of discovery that demonstrate the role of undirected science in the support of practical matters. The first and most convincing is the discovery of a new phenomenon or substance that can then be put to practical use — like the transistor. The second (in a way a nondiscovery) is the realization in the course of practical work that a necessary understanding of the underlying science is deficient. And the third is a discovery in pure science that demonstrates an error or deficiency in some part of science. As long as unexpected results keep turning up, one can hardly say we understand the natural world well enough to stop poking around in it.

So, where do we stand in this? What have we done for us today?

With transistors, this year's score (like most years' for most people) is zero. We do keep busy taking advantage of earlier such discoveries like dynamically formed membranes for hyperfiltration. Or like last year's realization that a voltage pulse technique for studying electrode kinetics could provide a new, practical method for measuring electrolytic conductivity. Neither, of course, ranks with the transistor, but you've got to do the best you can with what you've got, either in burlesque or in chemistry.

As we enter further into more directly practical studies, we learn more about deficiencies in our fundamental knowledge — the nondiscoveries that need to be made so that we can reach an already recognized practical objective. An almost continuous example of this is those areas of work combining hydrodynamics and chemistry. It is not possible to proceed entirely rationally with even so long used an art as filtration (hyper or otherwise) because of deficient understanding, and this year it came once more to our attention in proposing a study of bacterial production of methane. What, in fact, are the kinetic limits to such a process if it is carried out with some control of the mass transfer? Almost anything useful we try to do with packed beds, slurries, porous electrodes, and so on demonstrates that we don't know enough about the fundamentals to do practical things easily and surely.

The final kind of discovery, the one which shows our fundamental edifice is not yet perfect, is probably the easiest to document, since most of our interest is in just those experiments that probe the adequacy of theory. Regrettably, we have not shattered any conservation laws this year, but a couple of results are so unexpected that they put considerable pressure on current theories of the phenomena involved.

Fission, our favorite phenomenon, is still understood largely on the liquid-drop model, somewhat embellished since the days of Bohr and Wheeler. However, during this year, Coulomb excitation experiments on heavy nuclei have revealed that even-even nuclides in the actinide region have measurable hexadecapole moments, the largest at ^{234}U. The shape indicated, a football that has swallowed a discus the hard way, would certainly not have been predicted by the liquid-drop model. We had better have better models if nuclear reactions continue to be of great practical interest.

Another surprise turned up outside the nucleus. For several years, free radicals have been studied here by ESR after they were produced photolytically in solution. It proved to be a good way to study the structure and chemical reactivity of numerous interesting species, but no particular surprises emerged from this closer (or sometimes first) look at a number of radicals. However, with tartaric acid a surprise has indeed appeared. Radicals are normally born in approximate equilibrium with their environment (except for the big step that makes them radicals) and are more than half in the lower spin state and hence are detected in absorption. The radical from tartaric acid is different – it is born mostly in the upper spin state and appears in emission – a little microwave firefly winking through the solution. Theory can explain a rather small polarization, but nothing like that observed.

So, we have two more hints that we've not yet gotten back to that unhappy state (first reached just before Röntgen discovered x rays) in which all natural phenomena were thought to be predictable by existing theories. And if they aren't, we'd better press on, not only because it's fun but because among the remaining mysteries may be some unexpected benefits. We can be happy that there are new challenges outside of our original bounds, but we should not forget that future opportunities will be poorer if we cannot continue to study Nature for her own sake.

Finally, a note of regret. On June 22, Quentin Larson, a member of the Laboratory for nearly 29 years, most of them in the Chemistry Division, died suddenly at work. His formal training was as a printer, but he became a chemist through self-education and practice and was a talented experimentalist. The Laboratory will miss his abilities, and his associates will miss his friendship.

1. Nuclear Chemistry

THERMAL-NEUTRON CAPTURE CROSS SECTION AND RESONANCE INTEGRAL FOR 10.7-YEAR ^{85}Kr[1]

C. E. Bemis, Jr. J. Halperin
R. E. Druschel J. R. Walton[2]

The long-term storage and/or disposal of the radioactive noble gas fission products recovered in the processing of spent power-reactor fuels poses especially difficult technological problems. Perhaps the most important rare gas fission product presenting such problems is the 10.7-year ^{85}Kr (1.3% cumulative ^{235}U fission yield). We have measured the thermal-neutron capture cross section and resonance integral of ^{85}Kr in order to evaluate the burnup that might be experienced in reactor spectra. By irradiating 99.992% ^{85}Kr in carefully monitored experiments and measuring the increase in the ^{86}Kr produced, we have found $\sigma_{th}(^{85}Kr) = 1.66 \pm 0.20$ b and $I(^{85}Kr) = 1.8 \pm 1.0$ b respectively. We conclude from our results that the burnup of radioactive ^{85}Kr in power reactors as a possible means of disposal is not feasible.

1. Published as a technical note, *Nucl. Sci. Eng.* **47**, 371–72 (1972).
2. Analytical Chemistry Division.

SEARCH FOR BETA DECAY OF ^{96}Zr

E. Eichler J. S. Eldridge[1]
G. D. O'Kelley J. B. Ball[2]

Of the nuclei with masses below $A = 150$, nine are energetically unstable with respect to beta decay but possess half-lives long enough to permit them to exist in nature in measurable amounts. We note that the heaviest isotope of zirconium should be considered a member of this group, and we report below a preliminary attempt to detect the radioactive decay of ^{96}Zr.

The *1971 Atomic Mass Adjustment* by Wapstra and Gove[3] lists the Q value for beta decay of ^{96}Zr to ^{96}Nb as 183 ± 6 keV. The low-lying levels of ^{96}Nb shown in Fig. 1.1 are taken from the study of the reaction ^{96}Zr(^{3}He,t)^{96}Nb by Comfort et al.[4] Figure 1.1 shows schematically that the only energy levels of ^{96}Nb which lie within the energy available for beta decay are the ground state (6^+) and the excited states at 45 keV (5^+) and 152 keV (4^+). All of the possible beta transitions are highly forbidden, namely, $\Delta J \geqslant 4$ and no parity change. The low decay energy available and the highly forbidden nature of the possible transitions are consistent with the long half-life of ^{96}Zr. The beta transition most amenable to detection is expected to be the fourth-forbidden, nonunique transition to the 152-keV excited state of ^{96}Nb. The energy of this transition is expected to be only about 31 keV.

We attempted to detect the beta decay of ^{96}Zr by the presence of its daughter nuclide, 23.4-hr ^{96}Nb, whose characteristic gamma-ray spectrum is well known.[5] In the ORNL low-background gamma spectrometer, the pattern of coincident gamma transitions from ^{96}Nb yields both a high detection sensitivity and an identification of the radionuclide. The sample consisted of

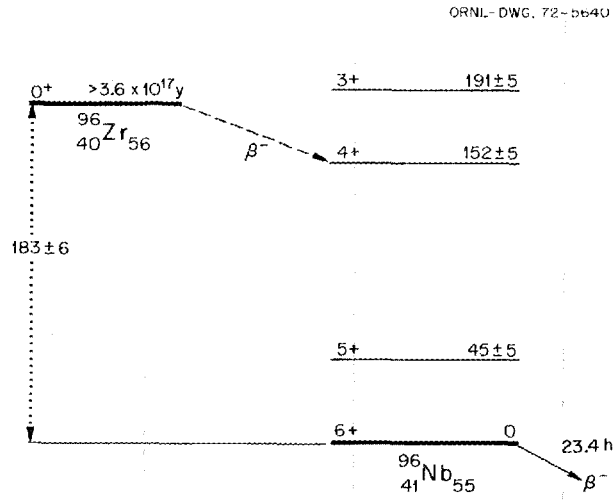

Fig. 1.1. Low-lying energy levels in ^{96}Nb shown with respect to the ground state of ^{96}Zr. The Q value for beta decay of ^{96}Zr is taken from ref. 3. Energies are in keV.

9.64 g of zirconium enriched to 57.4% ^{96}Zr. The zirconium as the chemical compound ZrO_2 was compressed into a cylinder and loaded into a plastic holder.

The sample was measured in the low-background gamma spectrometer for 9573 min and the background for 6637 min. A preliminary analysis of the data showed that the ZrO_2 sample contained detectable amounts of thorium and uranium. Spectrum libraries for calibration of the instrument were prepared from ZrO_2 samples of natural isotopic composition, each containing a known amount of either ^{96}Nb, Th, or U.

The data analysis followed the general approach used for lunar sample studies.[6] The experimental singles and coincidence spectra were fitted by use of a least-squares computer program developed by Schonfeld.[7] The computer analysis showed that our ability to detect ^{96}Nb in the enriched zirconium sample was seriously impaired by the presence of 3.8 ppm Th and 0.8 ppm U. No ^{96}Nb was detected in this experiment. An upper limit of $\leq$0.13 dis/min of ^{96}Nb was established by least-squares analysis, from which we infer a half-life of at least 3.6×10^{17} years, possibly the longest half-life known for a beta-unstable nucleus.

The energy of 31 keV for the $0^+ \rightarrow 4^+$ beta transition and the lower limit for the half-life lead to a value of log *ft* $\geq$21.6. This result is consistent with values[8] of log *ft* for two fourth-forbidden, nonunique beta transitions computed from experimental data, 22.6 for the transition ^{115}In($9/2^+$) $\rightarrow$ ^{115}Sn($1/2^+$) and 23.2 for the transition ^{113}Cd($1/2^+$) $\rightarrow$ ^{113}In($9/2^+$). The near agreement between the measured values of log *ft* for similar cases and the lower limit on log *ft* for the decay of ^{96}Zr, together with the uncertainty in the beta transition energy, suggest that the half-life of ^{96}Zr may be measurable by the method described here, provided that a large source of zirconium of sufficient purity can be found.

1. Analytical Chemistry Division.
2. Physics Division.
3. A. H. Wapstra and N. B. Gove, *Nucl. Data Tables* 9, 265 (1971).
4. J. R. Comfort, J. V. Maher, G. C. Morrison, and J. P. Schiffer, *Phys. Rev. Lett.* 25, 383 (1970).
5. H. W. Taylor, B. Singh, R. J. Cox, and A. H. Kukoc, *Z. Phys.* 239, 42 (1970).
6. G. D. O'Kelley, J. S. Eldridge, E. Schonfeld, and P. R. Bell, pp. 1407–23 in *Proceedings of the Apollo 11 Lunar Science Conference, Geochim. Cosmochim. Acta,* suppl. 1, vol. 2, Pergamon, 1970.
7. E. Schonfeld, *Nucl. Instrum. Methods* 52, 177 (1967).
8. S. Raman and N. B. Gove, to be published in the *Physical Review.*

GAMMA-RAY STUDIES ON THE DECAY OF 2.42-MIN ^{108}Ag[1]

N. C. Singhal[2] E. Eichler
N. R. Johnson J. H. Hamilton[3]

Gamma-ray singles and coincidence measurements following the decay of 2.42-min ^{108}Ag have been performed with 40-cm^3 Ge(Li) and 3 × 3 in. NaI(Tl) detectors. A total of 13 gamma rays have been assigned to ^{108}Ag decay, and their energies and intensities have been measured accurately. From the coincidence measurements and energy sum relationships, 12 gamma rays have been fitted into the level scheme of ^{108}Pd as shown in Fig. 1.2. The levels populated have the following energies (and spins): 433.96 (2^+), 931.06 (2^+), 1052.82 (0^+), 1314.22 (0^+), 1441.18 (2^+), and 1539.97 (1,2) keV. The first excited state of ^{108}Cd at 632.98 keV (2^+) is also populated by the beta decay of ^{108}Ag.

The spins of the 1052.82- and 1314.22-keV levels were determined uniquely as 0 from the Ge(Li)-NaI(Tl) directional-correlation measurements. The 1441.18-keV level has been assigned a spin of 2, and the multipolarity of the 1007.22-keV transition is established as $E2$ + <2% $M1$. A discussion of the ^{108}Pd levels within the vibrational framework is included in the account to be published[1] soon.

1. Modified abstract of a paper submitted for publication in the *Physical Review.* A preliminary account of the measurements appeared previously: N. C. Singhal, N. R. Johnson, E. Eichler, and J. H. Hamilton, *Chem. Div. Annu. Progr. Rep. May 20, 1971,* ORNL-4706, p. 12.
2. Graduate student from Vanderbilt University, Nashville, Tenn.
3. Physics Department, Vanderbilt University, Nashville, Tenn.

^{136}Nd DECAY

A. R. Brosi B. H. Ketelle

Neodymium-136 decays with a 50-min half-life, largely by electron capture through a 109-keV transition to 13.1-min ^{136}Pr. One of the puzzling aspects of ^{136}Nd decay has been that it appeared to decay to a 2^+ ground state, whereas the nuclear spin systematics suggested that the ground-state spin would be 3^+. Another puzzling aspect of ^{136}Nd decay has been that the total intensity of the ^{136}Nd radiations appeared to be about 20% lower than would be expected from the intensities of the ^{136}Pr daughter radiations.

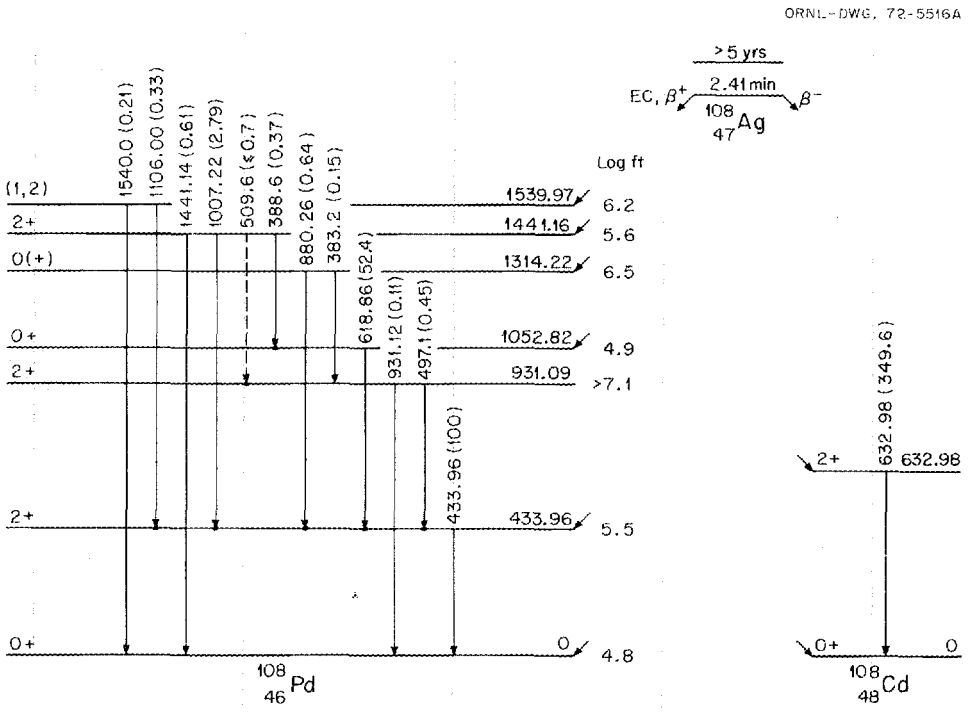

Fig. 1.2. Energy levels in ^{108}Pd and ^{108}Cd populated in the decay of 2.41-min ^{108}Ag. The excitation energies are given in keV. A dot on the tail of the arrow indicates that the transition was observed in coincidence with the 433.96-keV gamma ray.

The first puzzle appears to have been solved when we found a new 40-keV gamma ray which follows the 109-keV transition. Conversion coefficients indicate that the new 40-keV transition has $M1$ multipolarity and that a 149-keV transition is an essentially pure $E2$ transition. Since beta decay from the 0^+ level of ^{136}Nd to the 149-keV level in ^{136}Pr is allowed, the 149-keV level must have a 1^+ spin assignment, and the most probable spin for the ^{136}Pr ground state is 3^+.

In earlier attempts to measure gamma-gamma coincidences the rates were extremely low, and any net counts were obscured by coincidences which resulted from scattering between detectors and by random coincidence counts. New coincidence measurements made with a high-efficiency coaxial germanium detector with excellent energy and time resolution on one side and a small planar germanium detector with good energy and time resolution on the other side have given statistically valid net coincidence counts. When the planar detector was a 1-cm^3 high-resolution x-ray counter, gamma spectra coincident with praseodymium x rays and with the 40-keV gamma transition were obtained. When a planar detector with a volume of 5 cm^3 was used, net gamma spectra coincident with some of the low-energy gamma transitions were obtained. It now appears that the discrepancy between the total intensity of the ^{136}Nd radiations and the number of ^{136}Pr daughter disintegrations can be accounted for by the presence of many low-intensity gamma transitions following ^{136}Nd decay, which were not seen in earlier work. Some of the level energies deduced from coincidence measurements are given in Table 1.1, along with level spin assignments which are based on conversion coefficients.

Table 1.1. Energy levels populated by ^{136}Nd decay

Approximate level energy (keV)	Probable spin assignment
Ground state	3^+
40	2^+
149	1^+
183	
475	
575	
794	
942	

DISCOVERY OF NEW ISOTOPES FAR FROM STABILITY[1]

K. S. Toth[2] M. A. Ijaz[3]
R. L. Hahn C. R. Bingham[4]
R. F. Walker, Jr.[5]

We have continued our search at ORIC for new isotopes far from stability by combining the helium gas-jet technique and alpha-particle spectroscopy. Over the past few years the effort[6–10] has been directed toward the production of previously unknown rare-earth isotopes with neutron numbers of 86 and 87. In that time a total of ten such alpha-emitting nuclear species have been discovered ranging in atomic number from 67 (holmium)[6,9] to 70 (ytterbium).[8] Last year we began the search for the lutetium (Z = 71) and hafnium (Z = 72) nuclides. In a series of bombardments of ^{144}Sm with 160-MeV ^{20}Ne ions, the alpha decay of ^{159}Hf was indeed observed, with E_α = 5.09 ± 0.01 MeV and $T_{1/2}$ = 5.6 ± 0.5 sec. More work is being done to confirm this assignment. The data indicated that at least one of the lutetium isotopes was also seen; a more definitive experiment is now being planned to make ^{157}Lu and ^{158}Lu by bombarding ^{144}Sm with ^{19}F ions.

We have also extended our studies to a new region of the periodic table by bombarding ^{156}Dy with the ^{20}Ne beam to produce ^{171}Os and ^{170}Os, located 19 and 20 mass units away from the line of beta stability. In the experiments, alpha spectra were measured at various ^{20}Ne bombarding energies, covering the range from 152 to 101 MeV. In addition to the 19-sec 5.105-MeV alpha group that had previously been assigned[11] to ^{172}Os, two new alpha emitters were observed. Their half-lives and alpha-decay energies were as follows: (1) $T_{1/2}$ = 7.1 sec, E_α = 5.40 ± 0.01 MeV and (2) $T_{1/2}$ = 8.2 sec, E_α = 5.24 ± 0.01 MeV. The three alpha groups can be seen in Fig. 1.3, which shows spectra measured at 141.5, 130.6, and 119.2 MeV. The intensities of the alpha peaks relative to one another vary with bombarding energy in a manner that indicates that the mass numbers of the new alpha emitters are less than 172.

Figure 1.4 shows yields measured as a function of bombarding energy for the three alpha groups. The yields were corrected for differences in beam intensity and half-lives; the ordinate scale in Fig. 1.4, however, is in relative units because the alpha/total branching ratios for the alpha emitters are not known. Curves shown in the figure represent excitation functions for various

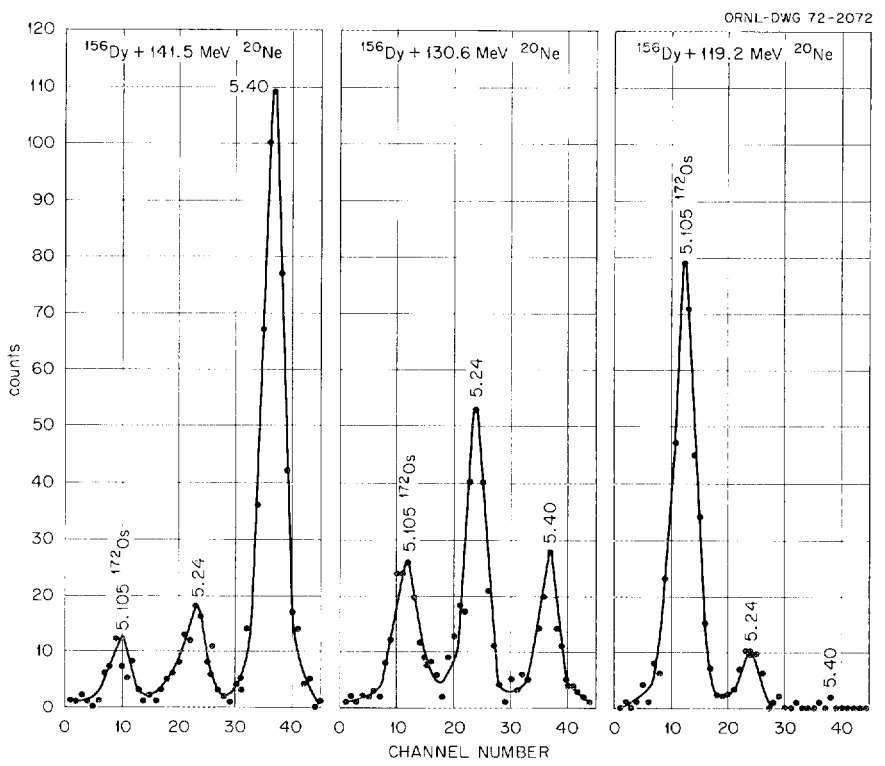

Fig. 1.3. Alpha spectra measured at ^{20}Ne bombarding energies of 141.5, 130.6, and 119.2 MeV.

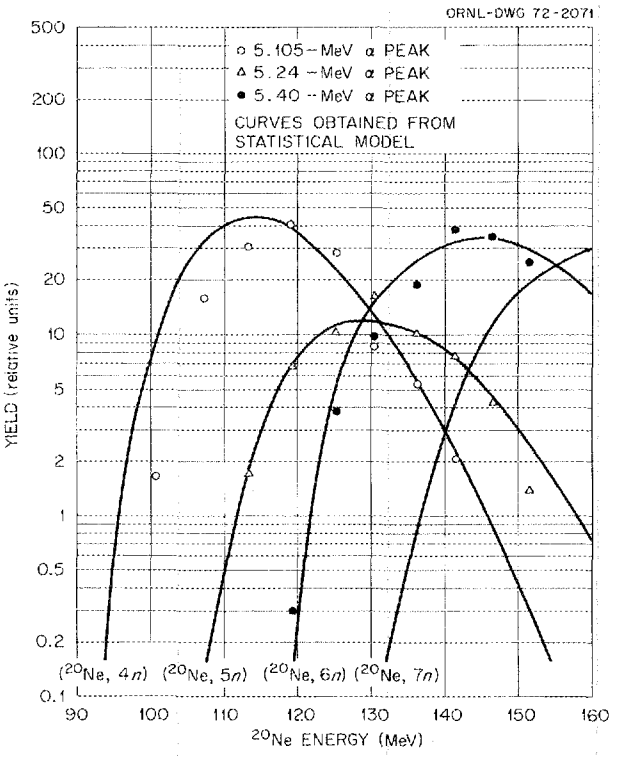

Fig. 1.4. Yields measured as a function of bombarding energy for ^{172}Os and the two new alpha groups observed in this study. Curves represent excitation functions calculated from the statistical model for various ^{156}Dy(^{20}Ne,xn) reactions.

(^{20}Ne,xn) reactions obtained by statistical-model calculations. The magnitudes of the theoretical excitation functions were normalized separately to each set of data points by assuming that the three alpha emitters were produced by the emission of four, five, and six neutrons from the compound nucleus ^{176}Os. It is seen that not only do our results support the assignment[11] of the 5.105-MeV alpha group to ^{172}Os but the (^{20}Ne,5n) and (^{20}Ne,6n) curves reproduce the data points for the new alpha activities reasonably well. The indication, then, is that the 5.23- and 5.40-MeV alpha groups are due to the decay of ^{171}Os and ^{170}Os respectively. Confirmatory evidence for these assignments comes from the agreement of the observed alpha-particle energies with those expected from alpha-decay systematics.

1. Portions of this work appeared in *Phys. Div. Annu. Progr. Rep. Dec. 31, 1971*, ORNL-4743, p. 77.
2. Physics Division.
3. Virginia Polytechnic Institute and State University, Blacksburg.
4. University of Tennessee, Knoxville.
5. Centenary College, Shreveport, La.

6. R. L. Hahn, K. S. Toth, and T. H. Handley, *Phys. Rev.* **163**, 1291 (1967).
7. K. S. Toth, R. L. Hahn, M. F. Roche, and D. S. Brenner, *Phys. Rev.* **183**, 1004 (1969).
8. K. S. Toth, R. L. Hahn, M. A. Ijaz, and W. M. Sample, *Phys. Rev. C* **2**, 1480 (1970).
9. K. S. Toth and R. L. Hahn, *Phys. Rev. C* **3**, 854 (1971).
10. K. S. Toth, R. L. Hahn, and M. A. Ijaz, *Phys. Rev. C* **4**, 2223 (1971).
11. J. Borggreen and E. K. Hyde, *Nucl. Phys. A* **162**, 407 (1971).

BRANCHING RATIOS OF ^{150}Dy, ^{151}Dy, AND ^{149m}Tb[1]

D. U. O'Kain[2] K. S. Toth[4]
C. R. Bingham[3] R. L. Hahn

Many of the neutron-deficient rare-earth nuclides have been characterized only by their alpha-decay branches. In an initial attempt to study the electron-capture (EC) decay of such nuclei, we have determined alpha/x-ray ratios for ^{150}Dy, ^{151}Dy, and ^{149m}Tb.

The radioactivities were produced at ORIC by bombarding ^{141}Pr with ^{14}N and ^{12}C ions. Recoil nuclei were collected in a gas-jet system and deposited upon aluminum foils for assay. To obtain the alpha/x-ray ratios, the alpha particles were detected with an Si(Au) detector and the x rays with a Ge(Li) detector. Corrections to the data were made for detector efficiencies, radioactive decay, and fluorescence yields.

If we assume, as has been done previously for these nuclides,[5] that the observed x rays arise primarily from orbital electron capture, then we can obtain good estimates of the alpha/EC ratios. This assumption will be valid if the β^+-decay mode that competes with electron capture is energetically unfavored and if few low-energy, highly internally converted gamma-ray transitions occur in the decay scheme. The resulting alpha/EC ratios are given in Table 1.2. Agreement between the present work and previously published results[5] for ^{151}Dy and ^{149m}Tb is good, although our results are slightly higher than those of ref. 5. For ^{150}Dy our value is not only higher than previous results but significantly outside the estimated limit of error.

Table 1.2. Alpha/EC ratios

Nuclide	Alpha/EC	
	This work	From ref. 5
^{150}Dy	0.32 ± 0.06	0.18 ± 0.02
^{151}Dy	0.068 ± 0.015	0.06 ± 0.006
^{149m}Tb	0.00041 ± 0.00008	0.00025 ± 0.00005

This discrepancy may indicate a systematic error in one of the values and suggests some of the difficulties inherent in measurements of alpha/EC.

1. A discussion of this work has appeared in the M.S. thesis of D. U. O'Kain, University of Tennessee, Knoxville.
2. University of Tennessee, Knoxville, and ORGDP.
3. University of Tennessee, Knoxville.
4. Physics Division.
5. R. D. Macfarlane and D. W. Seegmiller, *Nucl. Phys.* **53**, 449 (1964).

COULOMB EXCITATION OF 10^+ STATES IN ^{162}Dy AND ^{164}Dy

R. O. Sayer[1] Noah R. Johnson
E. Eichler D. C. Hensley[2]
L. L. Riedinger[3]

We have measured the multiple Coulomb excitation of ^{162}Dy and ^{164}Dy as a sensitive test of the rotational predictions for $B(E2)$ ratios in the ground-state bands of rare-earth nuclei. Since deviations from the rotational energies increase rapidly with increasing spin, one might expect $B(E2)$ ratios between high-spin states to be significantly different from simple ratios of Clebsch-Gordan coefficients. It is important to measure $B(E2)$ values accurately because they should be quite sensitive to details of the nuclear structure not reflected by the level energies.

Multiple Coulomb excitation with heavy ions is a natural tool for getting $B(E2)$ values for high-spin states. The dysprosium nuclei were chosen because they are midway between proton shell closures; they are good rotors, and their levels lie low in energy and thus are relatively easy to excite.

A Ge(Li) detector was used to observe the deexcitation gamma rays in singles and in coincidence with projectiles backscattered into a ring counter. Coincidence data were taken in a three-parameter (gamma-ray, heavy-ion, and time) mode using a Tennelec analog-to-digital converter interfaced to an SEL 940A computer. Data were stored on magnetic tape in list mode.

States in the ground band up to $J = 10$ were populated in these measurements. Figure 1.5 shows a singles (ungated) spectrum for 126.5-MeV ^{35}Cl ions on ^{162}Dy, while Fig. 1.6 shows the backscattered-heavy-ion–gamma-ray coincidence spectrum. The $10 \rightarrow 8$ transition appears strongly in the coincidence spectrum of Fig. 1.6. Since the germanium detector was at 0°, the transitions from higher-lying, shorter-lived states exhibit appreciable Doppler shifts. This makes it hard to see weak transitions. Thus we also took coincident data at 90° to minimize Doppler effects.

Peak areas were corrected for detector efficiency, internal conversion, gamma-ray absorption by target and mount, angular distribution of gamma rays, cascades from higher-lying states, and number of backscattered ions to obtain experimental excitation probabilities, $(P_j)_{\text{exp}}$. These are compared with theoretical values $(P_J)_{\text{theory}}$ calculated with the Winther–de Boer computer code for $E1$, 2, 3, and 4 excitation of a thick target. However, ratios of excitation probabilities yield a more sensitive comparison with theory, because only the relative germanium efficiency enters and because the $E2$ matrix elements for lower states cancel. For

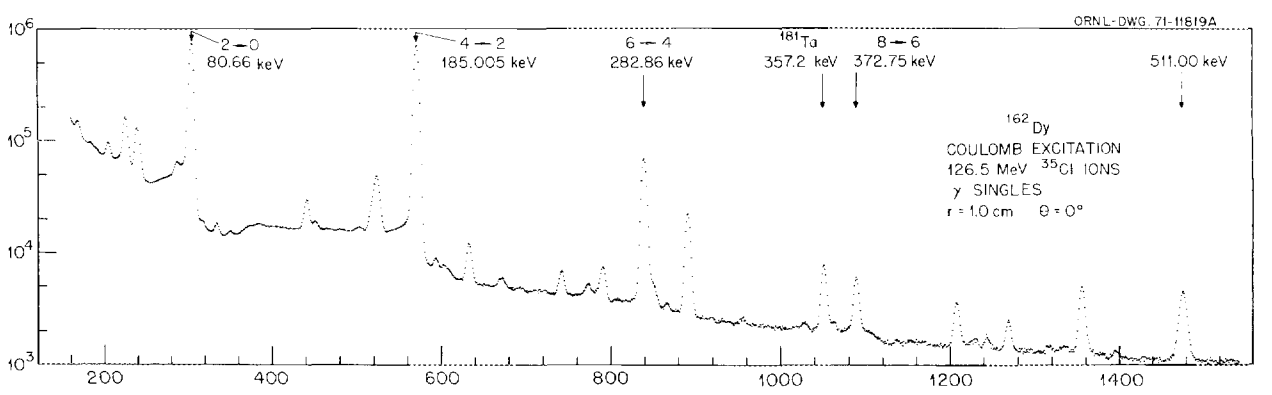

Fig. 1.5. Gamma-ray spectrum (ungated) of ^{162}Dy following Coulomb excitation by 126.5-MeV ^{35}Cl^{7+} ions.

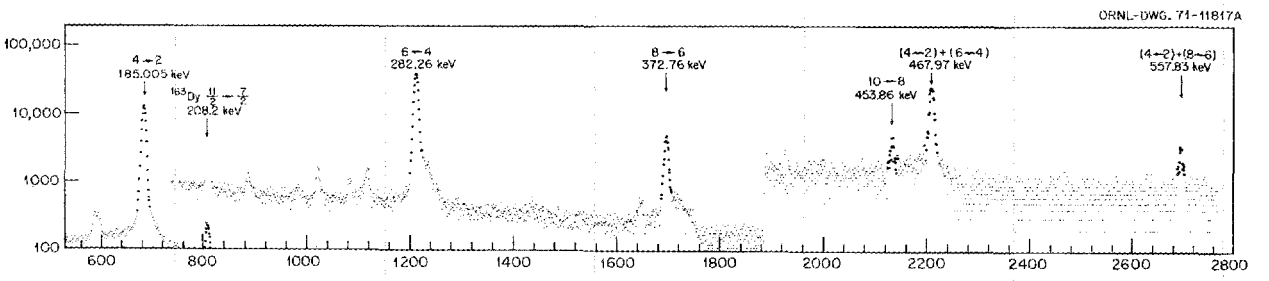

Fig. 1.6. Gamma-ray spectrum of ^{162}Dy in coincidence with backscattered 126.5-MeV $^{35}Cl^{7+}$ ions.

Table 1.3. Summary of best values for probability ratios and α parameters

Nucleus	β_4	Experiment/theory			$\alpha \times 10^4$				
		$R(^6/_4)$	$R(^8/_6)$	$R(^{10}/_8)$	$\alpha(^6/_4)$	$\alpha(^8/_6)$	$\alpha(^{10}/_8)$	$\langle\alpha\rangle^a$	B/A^b
^{162}Dy	0	0.892 ± 0.046	0.916 ± 0.042	1.176 ± 0.148	−20 ± 9	−8 ± 4	10 ± 8	−11 ± 4	8.5
	+0.05	0.844 ± 0.044	0.857 ± 0.043	1.086 ± 0.139	−29 ± 9	−14 ± 4	5 ± 8	−20 ± 4	
^{164}Dy	0	0.907 ± 0.053	0.878 ± 0.038	1.107 ± 0.132	−17 ± 10	−12 ± 4	6 ± 7	−12 ± 4	7.0
	+0.05	0.865 ± 0.053	0.822 ± 0.038	1.029 ± 0.132	−25 ± 10	−17 ± 4	2 ± 8	−19 ± 4	

[a]Weighted average of α values extracted from $R(J/I)$ values according to

$$Q_{exp}(I, J) = Q_{rot}(I, J)\ \{1 + \frac{\alpha}{2}\ [I(I+1) + J(J+1) - 6]\},$$

where $Q(I, J)$ is a transitional matrix element.

[b]Extracted from energy levels according to $\alpha = B/A$, where $E(I) = AI(I+1) - BI^2(I+1)^2$.

example, the ratio $R(^6/_4) = P_6/P_4$ is, to first order, proportional to $B(E2; 4 \rightarrow 6)$ because $B(E2; 0 \rightarrow 2)$ and $B(E2; 2 \rightarrow 4)$ cancel.

A comparison of the experimental probability ratios to Winther–de Boer calculations using rotational $E2$ matrix elements is shown in Table 1.3. The data taken at 0 and 90° in coincidence with beams of neon and chlorine ions are in good agreement for $R(^8/_6)$ and $R(^{10}/_8)$ but not for $R(^6/_4)$. However, the corresponding singles values for $R(^6/_4)$ are in good agreement. We used the singles data for $R(^6/_4)$ and the coincidence data for other ratios to derive the weighted-average values shown in Table 1.3.

Theoretical values used to obtain the ratios in Table 1.3 were calculated with the Winther–de Boer computer code using: (1) rotational $E2$ reduced matrix elements only, that is, $\beta_4 = 0$, and (2) rotational $E2$ and $E4$ matrix elements which correspond to $\beta_{40} = +0.05$ where the usual Y_{40} deformation is assumed.

For the case of no $E4$ matrix elements, the $R(^6/_4)$ and $R(^8/_6)$ experimental values are 9 and 12% smaller than rotor predictions respectively. Riedinger and co-workers[4] at Notre Dame have used ^{16}O ions to obtain preliminary results which indicate possible agreement with our values for the 6^+ and 8^+ levels. Our $R(^{10}/_8)$ values are somewhat larger than, though still consistent with, theory. The three values do seem to indicate a jump upward at the 10^+ state. The main error in $R(^6/_4)$ and $R(^8/_6)$ is the relative germanium detector efficiency, while statistical errors are more important for $R(^{10}/_8)$.

It is important to point out that the $R(J/I)_{theory}$ values used for Table 1.3 were obtained from a semiclassical calculation sufficient for many experimental situations involving heavy ions. However, quantum corrections could be very important for high-spin states. Recently, Roesel, Alder, and Morf[5] estimated corrections of 30 to 50% for multiple excitation of a 6^+ state with alpha particles. If one assumes that quantal corrections go as $1/\eta$, this means a 4 to 7% correction for excitation of a 6^+ state with ^{35}Cl ions. Inclusion of quantum corrections would increase the $B(E2)$ values extracted from our data. This would bring our experimental values of $R(^6/_4)$ and $R(^8/_6)$ closer to theory but would increase the variance between experiment and theory for the $R(^{10}/_8)$ value. It can be seen that when $\beta_4 = 0.05$ is used in the theoretical calculation, the overall agreement between the experimental and theoretical ratios is not helped appreciably.

In Table 1.3 we also show our results in terms of the α parameter. This parameter is spin-independent and describes the effect of centrifugal stretching. The three α values are not consistent. The values from $R(^6/_4)$ and $R(^8/_6)$ are negative, whereas those from the energy levels are positive, so our results contradict the simple centrifugal stretching picture.

It is well known that a reduction in the pair correlations by the Coriolis force contributes significantly to the level depression. From the present dysprosium data and from earlier work at Berkeley and Oak Ridge on erbium and ytterbium nuclei, it is clear that effects other than stretching produce changes in the $B(E2)$ values. Unfortunately, it is not known whether the Coriolis antipairing would tend to increase or decrease $B(E2)$. There may be other spin-dependent contributions as well.

1. Oak Ridge Associated Universities Research Participant from Furman University, Greenville, S.C., summer 1971.
2. Physics Division.
3. Physics Department, University of Tennessee, Knoxville.
4. L. L. Riedinger et al., private communication.
5. F. Roesel, K. Alder, and R. Morf, to be published.

BAND MIXING IN ^{156}Gd AND ^{158}Gd

A. F. Kluk[1] Noah R. Johnson J. H. Hamilton[2]

In even-even deformed nuclei, the ground-state rotational and β- and γ-vibrational levels are well known to couple with each other through the rotation-vibration interaction. For interband transitions this coupling alters the ratios of reduced transition probabilities from the simple adiabatic predictions based on the collective model of Bohr and Mottelson.[3,4] The extent of the coupling between the β- and γ-vibrational bands and the ground-state rotational band has been analyzed in terms of Z_β and Z_γ, respectively, the spin-independent band mixing parameters.

In the first approximation, a single value of Z_β is expected to explain all of the observed branching ratios for transitions between members of the β-vibrational and ground-state bands, and likewise a single value of Z_γ should account for transition intensities between the γ-vibrational levels and the ground-state band. However, it has been necessary to make further developments of the theory in which the effects of interactions between the β- and γ-vibrational bands are considered.[5] Investigations[6] have shown that in ^{152}Sm and ^{154}Gd a consistent Z_γ parameter is obtained only after the effects of mixing between the β- and γ-vibrational bands are included. Unfortunately, this new consideration of β-γ mixing still did not yield an internally consistent Z_β mixing parameter for ^{152}Sm and ^{154}Gd (see ref. 5).

These studies of β and γ vibrations have been extended to the more highly deformed systems ^{156}Gd and ^{158}Gd, and in a previous report[6] we described some of our preliminary results on the properties of excited $K = 0$ and $K = 2$ bands in these nuclei. Since that time we have made numerous additional measurements in an effort to achieve minimal error limits on the ratios of reduced electric quadrupole ($E2$) transition probabilities from these $K = 0$ and $K = 2$ bands.

Sources of radioactive ^{156}Eu and ^{158}Eu were used in the present experiments. Ge(Li) detectors were employed in both singles and coincidence modes. In both the ^{156}Eu and ^{158}Eu singles spectra, several complex gamma-ray peaks exist that make it difficult to extract accurate intensities for the transitions from the $K^\pi = 2^+$ and $K^\pi = 0^+$ states of interest. However, by carefully selecting the coincidence gating energies, we were able to obtain these transition intensities. The coincidence data were analyzed quantitatively by using several well-known cascades in each experiment to normalize the data for other cascades. Wherever possible we used our singles intensities, since they were determined with greater accuracy, but in all cases the coincidence measurements are in good agreement with them.

Summarized in Table 1.4 are the data on the $K^\pi = 0^+$ and 2^+ bands observed in ^{156}Gd. The error limits assigned to the experimental branching ratios (as well as those in Table 1.5) are conservative estimates that include both the contributions from detector-efficiency calibrations and peak area determinations as well as a contribution to account for any indeterminable behavior of the entire experimental system. It is felt that the improved resolution of our detection system, the careful cross checks provided by the large number of coincidence measurements, and the definitive information gained by gating on transitions that directly feed some of the vibrational states considered lend to these branching-ratio values a degree of reliability not previously realized.

Applying the first-order perturbational corrections (i.e., corrections only due to mixing between the vibrational and ground-state bands) in the same manner as described in our previous work[6] on ^{152}Sm and ^{154}Gd leads to the spin-independent band mixing parameters Z_β and Z_γ shown in column 5 (Table 1.4). In column 6 these mixing parameters are compared with those obtained by McMillan et al.[7] from a study of the ^{156}Gd levels populated in the decay of ^{156}Tb; in column 7 a comparison is made with the values from

Table 1.4. $B(E2)$ ratios and band mixing parameters for transitions between the $K^\pi = 0^+$ and $K^\pi = 2^+$ bands and the ground-state band of ^{156}Gd

$\frac{I^\pi{}_i \to I^\pi{}_f}{I^\pi{}_i \to I'^\pi{}_f}$	$\frac{E(I_i \to I_f)}{E(I_i \to I'_f)}$	$\frac{B(E2, K_i I_i \to K_f I_f)}{B(E2, K_i I_i \to K_f I'_f)}$ Experimental value	Adiabatic theory[a]	Z_β or $Z_\gamma \times 10^3$ Present work	McMillan et al.[b]	Greenwood and Reich[c]	With β-γ mixing
			β-vibrational band				
$\frac{2^+ \to 0^+}{2^+ \to 2^+}$	$\frac{1129.47}{1040.44}$	0.185 ± 0.019	0.70	83 ± 4	87 ± 6	74 ± 4	64 ± 13
$\frac{2^+ \to 4^+}{2^+ \to 2^+}$	$\frac{841.16}{1040.44}$	1.36 ± 0.10	1.80	-9 ± 2	-17 ± 4	-15 ± 2	-5 ± 4
$\frac{2^+ \to 0^+}{2^+ \to 4^+}$	$\frac{1129.47}{841.16}$	0.137 ± 0.016	0.39	28 ± 3	25 ± 5	18 ± 2	24 ± 5
			$K^\pi = 0^+$ band				
$\frac{2^+ \to 0^+}{2^+ \to 2^+}$	$\frac{1258.03}{1169.12}$	0.223 ± 0.025	0.70	72 ± 5	68 ± 30	77 ± 5	54 ± 13
$\frac{2^+ \to 4^+}{2^+ \to 2^+}$	$\frac{969.83}{1169.12}$	3.35 ± 0.27	1.80	26 ± 4	24 ± 12	18 ± 4	31 ± 7
$\frac{2^+ \to 0^+}{2^+ \to 4^+}$	$\frac{1258.03}{969.83}$	0.070 ± 0.007	0.39	48 ± 3	$44 {}^{+10}_{-8}$	47 ± 4	39 ± 4
			γ-vibrational band				
$\frac{2^+ \to 0^+}{2^+ \to 2^+}$	$\frac{1154.09}{1065.14}$	0.67 ± 0.03	0.70	7 ± 6	13 ± 10		9 ± 8
$\frac{2^+ \to 4^+}{2^+ \to 2^+}$	$\frac{865.98}{1065.14}$	0.086 ± 0.017	0.05	48 ± 22	47 ± 13		39 ± 23
$\frac{2^+ \to 0^+}{2^+ \to 4^+}$	$\frac{1154.09}{865.98}$	7.9 ± 1.6	13.9	32 ± 12	34 ± 8		28 ± 13
$\frac{3^+ \to 2^+}{3^+ \to 4^+}$	$\frac{1159.14}{959.89}$	1.52 ± 0.08[b]	2.50		39 ± 4		

[a]This is simply the ratio of squares of Clebsch-Gordan coefficients.
[b]From ref. 7.
[c]From ref. 8.

the recent neutron capture work of Greenwood and Reich.[8] The Z_β mixing parameters obtained by these various techniques are in rather good agreement but show no indication of a consistent value. A first-order perturbational treatment leaves a similar inconsistency in the Z_γ mixing parameters, as was found in the work[5] on ^{152}Sm and ^{154}Gd.

We have proceeded to include in the Hamiltonian those matrix elements that account for mixing of the wave functions of the β- and γ-vibrational bands. The Z_β and Z_γ parameters that result from including these second-order effects are shown in column 8. It is evident that the β-vibrational band mixing parameters still are not brought into alignment but that within just

Table 1.5. Ratios of reduced transition probabilities and values of Z_γ and $Z_{\beta\gamma}$ for transitions from the γ-vibrational band of ^{158}Gd to the ground-state rotational band

$\frac{I^\pi_i \to I^\pi_f}{I^\pi_i \to I'^\pi_f}$	$\frac{E(I_i \to I_f)}{E(I_i \to I'_f)}$	$\frac{B(E2, K_iI_i \to K_fI_f)}{B(E2, K_iI_i \to K_fI'_f)}$ Experimental value	Adiabatic theory[a]	$Z_\gamma \times 10^3$ Present work	Paperiello et al.[b]	$Z_{\beta\gamma} \times 10^3$
$\frac{2^+ \to 0^+}{2^+ \to 2^+}$	$\frac{1187.1}{1107.63}$	0.608 ± 0.030	0.70	24 ± 8	41 ± 15	−23 ± 8
$\frac{2^+ \to 4^+}{2^+ \to 2^+}$	$\frac{925.6}{1107.63}$	0.057 ± 0.012	0.05	9 ± 17	9 ± 16	8 ± 9
$\frac{2^+ \to 0^+}{2^+ \to 4^+}$	$\frac{1187.1}{925.6}$	10.6 ± 2.5	13.9	14 ± 13	17 ± 12	22 ± 16
$\frac{3^+ \to 2^+}{3^+ \to 4^+}$	$\frac{1004.2}{1186.0}$	0.37 ± 0.04	0.40	−7 ± 7		

[a]From the predictions of the adiabatic symmetric rotor model.
[b]Values calculated from the data of Paperiello et al., ref. 9.

over one standard deviation in the error limits, these mixing parameters for the other $K^\pi = 0^+$ band are consistent. The values for Z_γ shown in column 8 appear to be consistent as a result of including β-γ mixing.

A perturbational treatment similar to that used above was applied to the 2^+ and 3^+ members of the γ-vibrational band of ^{158}Gd. In column 5 of Table 1.5 are listed our Z_γ values for ^{158}Gd and in column 6 are shown the Z_γ values calculated from the ^{158}Tb decay data of Paperiello et al.[9] Although conservative error limits have been set on our gamma-ray intensities, it is evident that just as was the case for ^{156}Gd, there is very poor agreement among the values of the Z_γ parameter. Contrary to the case of ^{156}Gd, including β-γ mixing effects does not improve the agreement with theory. This can be seen from the values of $Z_{\beta\gamma}$ shown in column 7.

Perhaps an appropriate approach to the solution of this problem for these two nuclei is a perturbational calculation involving in each case mixing between both $K = 0$ bands, the γ-vibrational band and the ground-state band. The recently suggested procedure of Stokstad et al.[10] also deserves consideration. In the latter approach, which involves three bands and matrix diagonalization, energy-level information is introduced into the rotation-vibration interaction by means of the variable moment of inertia model.[11]

A detailed account[12] of this research will appear shortly in the open literature.

1. Oak Ridge Graduate Fellow from Vanderbilt University, Nashville, Tenn., under appointment with Oak Ridge Associated Universities.
2. Vanderbilt University, Nashville, Tenn.

3. A. Bohr and B. R. Mottelson, *Kgl. Dan. Vidensk. Selsk. Mat.-Fys. Medd.* 27(16) (1953).
4. A. Bohr and B. R. Mottelson, "Lectures on Nuclear Structure and Energy Spectra," Copenhagen, 1962 (unpublished)
5. See, for example, L. L. Riedinger, N. R. Johnson, and J. H. Hamilton, *Phys. Rev.* 179, 1214 (1969).
6. A. F. Kluk, N. R. Johnson, and J. H. Hamilton, *Chem. Div. Annu. Progr. Rep. May 20, 1970,* ORNL-4581, p. 15.
7. D. J. McMillan, J. H. Hamilton, and J. J. Pinajian, *Phys. Rev. C* 4, 542 (1971).
8. R. C. Greenwood and C. W. Reich, Progress Report IN-1317, p. 78, Idaho Nuclear Corporation (1970).
9. C. J. Paperiello, E. G. Funk, and J. W. Mihelich, *Nucl. Phys. A* 140, 261 (1970).
10. R. G. Stokstad, J. S. Greenberg, I. A. Fraser, S. H. Sie, and D. A. Bromley, *Phys. Rev. Lett.* 27, 748 (1971).
11. M. A. J. Mariscotti, G. Scharff-Goldhaber, and B. Buck, *Phys. Rev.* 178, 1864 (1969).
12. A. F. Kluk, N. R. Johnson, and J. H. Hamilton, *Z. Phys.* (in press).

$M1$ ADMIXTURES OF TRANSITIONS IN ^{156}Gd

J. H. Hamilton[1] Noah R. Johnson
E. Collins[1] A. V. Ramayya[1]
P. E. Little[1] J. J. Pinajian[2]
A. F. Kluk[3]

We have pointed out the difficulties encountered in our work[4] on the β- and γ-vibrational bands of ^{156}Gd and ^{158}Gd. The behavior of these states disagrees significantly with the collective-model predictions. It has been suggested[5] that the difficulties may be due to the presence of significant magnetic dipole ($M1$) contributions in the $2^{+\prime} \rightarrow 2_g^+$ transitions. Although this idea has not been borne out in other recently tested cases, we felt it necessary to make a careful check for any such possibilities in ^{156}Gd. Due to the short half-life of ^{158}Eu, it was not deemed feasible to attempt such determinations in ^{158}Gd.

These ^{156}Gd experiments involved a measurement of the gamma-gamma directional correlations of the 88.95-keV $2_g^+ \rightarrow 0_g^+$ transition with the $2_\beta^+ \rightarrow 2_g^+$ and $2_\gamma^+ \rightarrow 2_g^+$ transitions and with as many other transitions that feed the 88.95-keV state as possible. The equipment included a movable NaI(Tl)-Ge(Li) fixed-detector arrangement with a 4096-channel analyzer for data storage.

The directional-correlation data were fitted to the function

$$W(\theta) = 1 + A_2 G_2 Q_2 \, P_2(\cos\theta) + A_4 G_4 Q_4 \, P_4(\cos\theta) ,$$

where θ represents the angle of emission between the two successive radiations and A_2 and A_4 are coefficients of the Legendre polynomials. The factors G_2Q_2 and G_4Q_4 are correction coefficients which include solid-angle corrections for both detectors and attenuation corrections which arise because of the relatively long life of the 88.95-keV state. Since $0 \rightarrow 2 \rightarrow 0$ cascades have unique values of A_2 (0.357) and A_4 (1.14) it was possible to take our data on two such cascades in ^{156}Gd and deduce these solid-angle and attenuation corrections.

A summary of the results on all of the consecutive gamma-ray cascades measured is given in Table 1.6. The 1040.44-keV transition originating from the 2^+ level at 1129.41 keV in the $K^\pi = 0^+ \beta$-vibrational band is one of the primary transitions under consideration here. In Table 1.6 it can be seen that this transition has only

Table 1.6. The results of a directional correlation study of the consecutive cascades in ^{156}Gd

The gating transition was the 88.95-keV, $2^+ \rightarrow 0^+$ ground-state transition.

Energy (keV) (transition)	Spin sequence ($x \rightarrow 2_g^+ \rightarrow 0_g^+$)	$A_2{}^{a,b}$	$A_4{}^{a,b}$	δ^c	Admixture (%)
961.0	0^+	0.357^d	1.14^d		$E2$ (100)
1040.44	2_β^+	0.054 (43)	0.25 (9)	$-5.9^{+1.4}_{-2.8}$	$E2\left(97.2^{+1.5}_{-2.1}\right)$
1065.14	2_γ^+	−0.035 (6)	0.337 (12)	−18 ± 3	$E2$ (99.7 ± 0.1)
1079.16	0^+	0.357^d	1.14^d		$E2$ (100)
1153.47	1^-	−0.254 (10)	0.004 (9)	$\lvert\delta\rvert < 0.023$	$E1$ (>99.95)
1230.71	2^-	0.260 (10)	0.002 (9)	$0.018^{+0.018}_{-0.010}$	$E1\left(99.97^{+0.03}_{-0.05}\right)$
1277.43	1^-	−0.237 (12)	−0.016 (15)	−0.01 ± 0.01	$E1\left(99.99^{+0.01}_{-0.03}\right)$
1857.42	1	−0.22 (9)	−0.12 (16)	$-0.03^{+0.03}_{-0.07}$	$\left.\begin{matrix}E1\\ \text{or}\\ M1\end{matrix}\right\}\left(99.91^{+0.09}_{-0.90}\right)$
1877.03	1^+	−0.580 (28)	−0.126 (34)	0.40 ± 0.05	$E2\left(13.8^{+3.0}_{-2.9}\right)$
1937.71	1^+	0.321 (21)	−0.198 (27)	−0.57 ± 0.03	$E2\left(24.5^{+2.0}_{-1.9}\right)$
2097.70	1^+	0.581(22)	−0.410 (20)	−1.2 ± 0.2	$E2\left(59.0^{+25.2}_{-9.0}\right)$

[a]The last digit of the error, in parentheses, occurs in the third decimal place.

[b]$G_2Q_2 = 0.624 \pm 0.021$, $G_4Q_4 = 0.385 \pm 0.008$.

[c]The mixing ratio of the two multipole contributions in the transition.

[d]Theoretical values which were compared with the experimental values to obtain G_2Q_2 and G_4Q_4 of footnote *b*.

Table 1.7. Results of a directional correlation study of several one-three correlations in ^{156}Gd

The gating transition was the 88.95-keV, $2^+ \to 0^+$ ground-state transition.

Energy (keV) (transition)	Spin sequence ($x \to y \to 2_g^+ \to 0_g^+$)	$A_2{}^{a,b}$	$A_4{}^{a,b}$	δ	Admixture (%)
599.47	$1^+ \to 1^-$	0.149 (36)	−0.005 (67)	$-0.036^{+0.036}_{-0.044}$	$E1\left(99.87^{+0.13}_{-0.51}\right)$
646.29	$1^+ \to 2^-$	−0.136 (07)	0.003 (12)	−0.025 ± 0.014	$E1\left(99.94^{+0.04}_{-0.02}\right)$
723.47	$1^+ \to 1^-$	0.152 (11)	−0.011 (18)	$-0.038^{+0.011}_{-0.014}$	$E1\left(99.86^{+0.07}_{-0.09}\right)$
811.77	$1^+ \to 2_\gamma^+$	0.045 (07)	−0.012 (13)	−0.035 ± 0.035	$E2\left(0.1^{+0.4}_{-0.1}\right)$

[a]The last digit of the error, in parentheses, occurs in the third decimal place.

[b]$G_2Q_2 = 0.624 \pm 0.021$, $G_4Q_4 = 0.385 \pm 0.008$.

2.8% $M1$ admixture. This is far less than the 64.3% $M1$ component needed to fit the observed branching ratios[4] for a one-parameter (Z_β) band mixing of the ground state and the β band. Hence, there remains a clear discrepancy between experiment and theory. Since the 1258.0-keV level ($K^\pi I = 0^+ 2$) is very weakly populated in the ^{156}Eu decay, our γ-$\gamma(\theta)$ measurements involving the 1169.11-keV transition from this state are of poor statistical quality, and we are unable to obtain a meaningful value for its $M1$ component. In line with most of the measured cases, we find that the transition from the 2^+ member of the γ band going to the 2^+ member of the ground band is essentially pure $E2$. In addition to these consecutive cascades we were able to measure four one-three (intermediate transition unobserved) cascades, all of which depopulate the 1^+ level at 1965.89 keV. These data are summarized in Table 1.7.

A further interesting result of this work is that we have now shown that the transitions from three 1^+ states at 1965.89, 2026.60, and 2186.71 keV in ^{156}Gd to the ground band are predominately $M1$. These data are the first such information on the properties of $K^\pi I = 1^+ 1$ quasi-particle excitations. Note that the δ values in the $1^+ \to 2g^+$ transitions have different signs as well as magnitudes. Thus these results provide sensitive tests of any microscopic theory of such excitations.

For a detailed account of this work, see ref. 6.

1. Vanderbilt University, Nashville, Tenn.
2. Isotopes Division.
3. Oak Ridge Graduate Fellow from Vanderbilt University, Nashville, Tenn., under appointment with Oak Ridge Associated Universities.
4. A. F. Kluk, N. R. Johnson, and J. H. Hamilton, "Band Mixing in ^{156}Gd and ^{158}Gd," the previous contribution, this report.
5. B. R. Mottelson, *J. Phys. Soc. Jap., Suppl.* 24, 87 (1968).
6. J. H. Hamilton, P. E. Little, A. V. Ramayya, E. Collins, N. R. Johnson, J. J. Pinajian, and A. F. Kluk, *Phys. Rev. C* 3, 899 (1972).

LEVEL STRUCTURE OF ^{178}Hf

P. E. Little[1] J. H. Hamilton[1]
A. V. Ramayya[1] Noah R. Johnson

During this past year we have completed an extensive study of the level structure of ^{178}Hf populated in the decay of 9.4-min ^{178}Ta, and a detailed account of this work has been published.[2] Our main interest in the ^{178}Hf nucleus was to obtain information to provide a better understanding of rotation-vibration interactions in deformed nuclei.

Earlier work by our group[3,4] has shown that in samarium and gadolinium nuclei, which are just at the onset of permanent shape deformation, there are significant disagreements between the observed behavior of the β- and γ-vibrational states and that predicted by the Bohr-Mottelson collective model. The nucleus ^{178}Hf lies near the middle of the deformed rare-earth nuclei and should show whether the problems with the quadrupole vibrational states of ^{152}Sm and ^{154}Gd are peculiar to the transition from spherical to deformed shapes or whether they are a generalization of the entire deformed region. In previous reports on this problem[5,6] we have pointed out that in fact this anomalous behavior is also evident in ^{178}Hf and that it cannot be accounted for by the rather large amount of magnetic dipole ($M1$) radiation present in the transitions from the $K = 0$ states. Therefore, it seemed most important to carefully check the properties of all near-lying states which may present any perturbations on the β vibration whose strength appears to be spread

over several $K = 0$ states in ^{178}Hf in the excitation range of 1 Mev.

The half-life of ^{178}Ta is only 9.4 min. However, for these measurements we have used the parent activity ^{178}W, which has a 21.5-day half-life and decays by electron capture to the ground state of ^{178}Ta. Sources were prepared by proton bombardment of 10-mil tantalum foils in the Oak Ridge Isochronous Cyclotron. The ^{178}W resulted from the ^{181}Ta$(p,4n)^{178}$W reaction. After chemical purification the activity was precipitated as H_2WO_4 and then dissolved in a minimum of NaOH. Aliquots of this solution were used for the sources.

The experiments involved gamma-ray singles measurements with a large-volume, high-resolution Ge(Li) detector and two-parameter gamma-gamma coincidence and angular-correlation studies with Ge(Li) detectors. A total of 32 gamma rays were assigned to 15 states in ^{178}Hf. Additionally, the correlation measurements provided spin assignments for most of these states. All

ORNL-DWG. 70-14627A

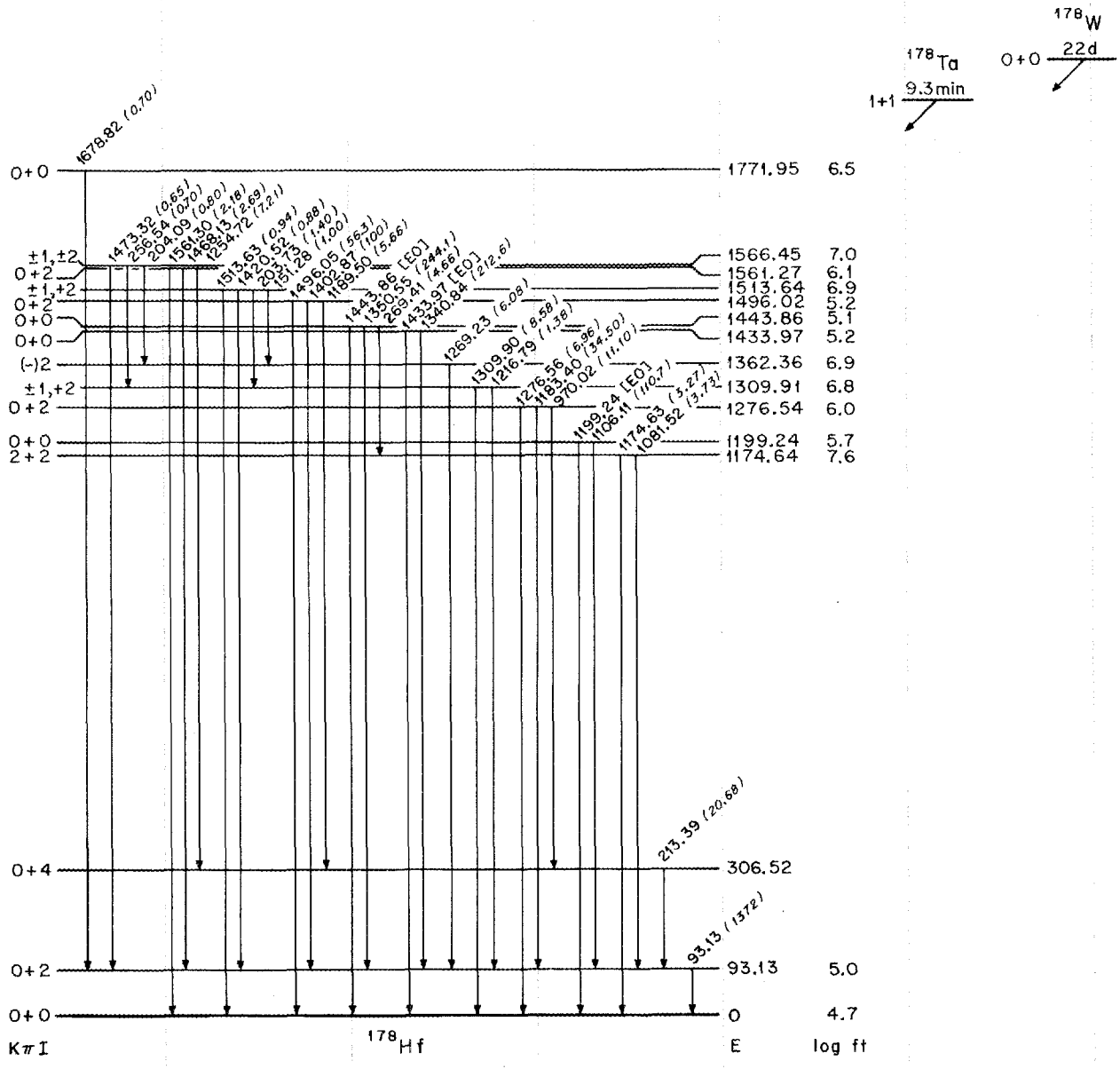

Fig. 1.7. Level scheme of ^{178}Hf populated in the decay of ^{178}Ta.

of these data are summarized in the level scheme shown in Fig. 1.7. Note that this scheme contains 13 gamma-ray transitions and five excited states which were previously unassigned.

Despite having arrived at a rather detailed knowledge of the excited states of ^{178}Hf, we are still unable to determine the cause of the variance between experiment and theory for two of the observed $K = 0$ bands. We have accurately established the amount of $M1$ radiation in the $2^+ \rightarrow 2^+_{ground}$ transitions from these $K = 0$ bands but still find a discrepancy with the perturbational treatment of the associated reduced electric quadrupole ($E2$) transition probabilities.

It is interesting that if we assume the 1496-keV level is the 2^+ member of a $K = 0$ band, we are able to use our measured $M1$ admixture and get agreement with theory for its $E2$ branching ratios. Yet our study reveals no 0^+ state which, on the basis of the moment of inertia, could be considered the band head.

The results of our measurements, coupled with the fact that recent Coulomb excitation experiments[7] indicated very little collective nature for the $K\pi I = 0+2$ states at 1276, 1496, and 1561 keV, lead us to conclude that they are not β vibrational in character. Rather, they are most likely quasi-particle excitations.

1. Vanderbilt University, Nashville, Tenn.
2. P. E. Little, J. H. Hamilton, A. V. Ramayya, and N. R. Johnson, *Phys. Rev. C* **5**, 252 (1972).
3. L. L. Riedinger, N. R. Johnson, and J. H. Hamilton, *Phys. Rev.* **179**, 1214 (1969).
4. L. L. Riedinger, N. R. Johnson, and J. H. Hamilton, *Phys. Rev. C* **2**, 2358 (1970).
5. J. H. Hamilton, P. E. Little, A. V. Ramayya, and N. R. Johnson, *Chem. Div. Annu. Progr. Rep. May 20, 1971*, ORNL-4706, p. 21.
6. J. H. Hamilton, P. E. Little, A. V. Ramayya, and N. R. Johnson, *Phys. Rev. Lett.* **25**, 946 (1970).
7. L. Varnell, J. H. Hamilton, and R. L. Robinson, *Phys. Rev. C* **3**, 1265 (1971).

TRANSITIONS OF LOW INTENSITY IN THE DECAY OF ^{206}Tl

L. L. Collins, Jr.[1] G. D. O'Kelley
E. Eichler

We have investigated the decay of two excited states in ^{206}Pb populated by beta transitions of low intensity from the 0^- ground state of ^{206}Tl. Sources of ^{206}Tl were prepared by irradiating $TlNO_3$ of natural isotopic composition in the Oak Ridge Research Reactor (ORR). A chemical procedure to reduce contamination from a trace of indium was required for some of the

ORNL-DWG. 72-5645

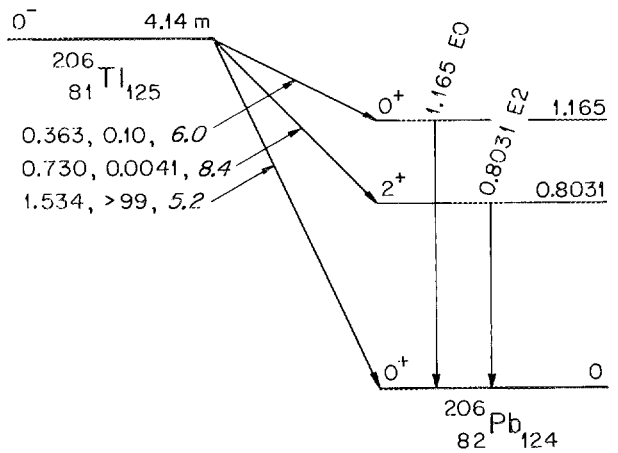

Fig. 1.8. Decay scheme proposed for ^{206}Tl. Energies are given in MeV. For each beta transition is given the energy in MeV, the branching in percent, and the value of log *ft*.

measurements. The half-life of ^{206}Tl as determined from anthracene detector data and analyzed by a least-squares computer program yielded a half-life of 4.14 ± 0.05 min.

The $E2$ gamma transition from the well-known first excited state in ^{206}Pb at 803.1 keV was readily detected with a Ge(Li) spectrometer. Absolute beta counting, combined with absolute gamma spectrometry, yielded an intensity for the 803.1-keV gamma ray of $(4.1 \pm 0.6) \times 10^{-5}$ per disintegration. This measurement compares favorably with recently published determinations of $(5.5 \pm 0.6) \times 10^{-5}$ by Zoller and Walters[2] and $(4 \pm 1) \times 10^{-5}$ by Griffin and Donne.[3] Because the 0^+ ground state of ^{206}Pb is populated so readily in the decay of ^{206}Tl (log *ft* = 5.2), it seemed possible that the excited state of 0^+ at 1165 keV might also be populated to a detectable extent. We searched unsuccessfully for the 362-keV transition between the second 0^+ state and the first 2^+ state (see Fig. 1.8). The upper limit (2σ) for the intensity of the 362-keV gamma ray is $\leqslant 2.6 \times 10^{-6}$ per disintegration of ^{206}Tl, somewhat lower than limits set by other groups.[2,3]

A study with a high-resolution Ge(Li) x-ray detector disclosed a prominent spectrum of x rays which could be assigned unambiguously to the K x-ray spectrum of lead. Absolute determination of the x-ray intensity led to an x-ray abundance of 12×10^{-4} per disintegration of ^{206}Tl, of which 2×10^{-4} were attributed to electron shakeoff.[4] The remainder of the x-ray intensity, $(10 \pm 2) \times 10^{-4}$, is in good agreement with the

recent measurement of Griffin and Donne,[3] who obtained an intensity of $(8 \pm 2) \times 10^{-4}$. As shown by Griffin and Donne, these lead x rays most likely arise from the $E0$ transition in ^{206}Pb from the 1165-keV excited state of 0^+.

The results are summarized in the decay scheme of Fig. 1.8. If all of the x-ray intensity reported here is due to the $E0$ transition, then our upper limit on the intensity of the $E2$ transition from the 0^+ excited state leads to an intensity ratio $E0/E2 \geqslant 435$, which is surprisingly high compared with other cases in this same mass region.[5]

1. Graduate student from the University of Tennessee, Knoxville.
2. W. H. Zoller and W. B. Walters, *J. Inorg. Nucl. Chem.* **32**, 3465 (1970).
3. H. C. Griffin and A. C. Donne, *Phys. Rev. Lett.* **28**, 107 (1972).
4. T. C. Carlson, C. W. Nestor, Jr., T. C. Tucker, and F. B. Malik, *Phys. Rev.* **169**, 27 (1968).
5. L. H. Goldman, B. L. Cohen, R. A. Moyer, and R. C. Diehl, *Phys. Rev. C* **1**, 1781 (1970).

SINGLE-PARTICLE TRANSFER REACTIONS IN ^{208}Pb INDUCED BY HIGH-ENERGY ^{12}C IONS

J. B. Ball[1] R. L. Hahn
J. L. C. Ford, Jr.[1] J. S. Larsen[2]
K. S. Toth[1]

Neutron pickup and proton stripping from light ions on ^{208}Pb to low-lying excited states of neighboring nuclei have been extensively studied and reported in the literature. The character of these states is well established, thus making ^{208}Pb a convenient target to use for a study of single-nucleon transfer reactions induced by heavy ions. In the present experiment the reactions ^{208}Pb(^{12}C,^{13}C)^{207}Pb and ^{208}Pb(^{12}C,^{11}B)^{209}Bi were initially studied with 98- and 92-MeV ^{12}C beams from ORIC. The ^{13}C and ^{11}B ions were detected with a position-sensitive proportional counter in the broad-range spectrograph facility. Particle groups corresponding to the ground states and the four lowest single-particle states in both ^{207}Pb and ^{209}Bi were identified. Angular distributions were measured in the region 20 to 70° (laboratory angle) at 98 MeV and for three angles near the maxima of the distributions at 92 MeV. Data at other angles and bombarding energies will be obtained in future experiments.

The shapes of the angular distributions appear to be dominated by kinematic effects. The positions of the maxima seem to be closely related to the grazing angle, yielding grazing radii r_g = 1.70 F and 1.66 F for neutron pickup and proton stripping respectively. Cross sections at the maxima were in the range from 1 to 10 mb/sr and, in contrast to (^{3}He,α) and (α,t) reactions, were larger for low l-transfer values.

1. Physics Divison.
2. Visiting scientist from the Niels Bohr Institute, Copenhagen.

COULOMB EXCITATION WITH HEAVY-ION BEAMS AT ORIC

E. Eichler R. O. Sayer[1]
N. R. Johnson D. C. Hensley[2]
L. L. Riedinger[3]

This past year the Coulomb excitation program grew in several directions. First, our list of collaborators has lengthened. We now make routine use of the Tennelec ADC—on-line-computer system at ORIC. Also, a new beam room devoted exclusively to in-beam spectroscopy was brought into use this year. Next year will see its completion and the addition of a large lead shield to permit singles measurements. We have constructed a Ge(Li) detector goniometer for the measurement of gamma-ray angular distributions.

We made headway toward a solution of the heavy-ion detector saturation effect which has limited the heavy-ion counting rates. After reduction of the feedback resistance in the charge-sensitive preamplifier, the system tolerated 10 to 15 nA of beam, as compared with 1 to 2 nA previously.

A major effort next year will be the design and construction of a Doppler-shift plunger device to measure the lifetimes of the Coulomb-excited states directly. The experimental results of Coulomb excitation studies of ^{232}Th, ^{238}U, and two dysprosium isotopes are described in other reports.[4]

1. Oak Ridge Associated Universities Research Participant from Furman University, Greenville, S.C., summer 1971.
2. Physics Division.
3. Physics Department, University of Tennessee, Knoxville.
4. R. O. Sayer, E. Eichler, N. R. Johnson, D. C. Hensley, and L. L. Riedinger, "Coulomb Excitation of 10^+ States in ^{162}Dy and ^{164}Dy," a previous contribution, this report; E. Eichler, N. R. Johnson, R. O. Sayer, D. C. Hensley, and L. L. Riedinger, "The Effect of Hexadecapole Moments on the Coulomb Excitation of the Actinides," the following contribution, this report.

THE EFFECT OF HEXADECAPOLE MOMENTS ON THE COULOMB EXCITATION OF THE ACTINIDES

E. Eichler R. O. Sayer[1]
N. R. Johnson D. C. Hensley[2]
L. L. Riedinger[3]

We have Coulomb-excited ^{238}U and ^{232}Th with about 144-MeV ^{40}Ar beams. To check for possible attenuation of the theoretical gamma-ray angular distributions, we measured gamma-ray yields at 0, 45, and 90° to the beam direction. Within statistics the distributions agreed with theory.

An ORNL group[4] working at the Tandem Van de Graaff accelerator has measured alpha-particle-induced Coulomb excitation of ^{238}U and ^{232}Th. Their observations require that these two nuclei possess large hexadecapole moments corresponding either to $ME4$ = +1.123 or −1.860 for ^{238}U and either $ME4$ = +1.640 or −2.220 for ^{232}Th. Although nuclear liquid-drop calculations suggest positive values, the ambiguity cannot be resolved from their data.

Our multiple excitation of these nuclei up to the 12^+ state makes it possible to choose a single $E4$ matrix element. By a modified version of the de Boer–Winther[5] coupled-equations Coulomb-excitation computer program, we computed excitation probabilities for three cases. In the first of these, only $E2$ matrix elements were used. In the second and third cases we included, respectively, the positive and the negative $ME4$ values of McGowan et al.[4] All of these calculations assumed pure rotational behavior. Various experimental probability ratios are compared in Tables 1.8 and 1.9 with corresponding theoretical ratios for the three cases cited above. The P 10/8 ratio comparison gives unequivocal support for the positive $E4$ matrix element, which indicates a positive hexadecapole deformation.

Table 1.8. Coulomb excitation of ^{238}U with 143.5-MeV ^{40}Ar

Probability ratio	Experimental	Theoretical		
		$E2$ only	$+ME4^a$	$-ME4^b$
P 4/6	1.75	1.79	1.73	1.88
P 6/8	4.01	3.88	3.64	4.10
P 10/8	5.78	6.84	6.29	7.01
P 10/6	23.2	26.6	22.9	28.5

[a] $ME4$ = +1.123.
[b] $ME4$ = −1.860.

Table 1.9. Coulomb excitation of ^{232}Th with 144.2-MeV ^{40}Ar

Probability ratio	Experimental	Theoretical		
		$E2$ only	$+ME4^a$	$-ME4^b$
P 6/8	4.46	4.78	4.18	4.91
P 8/10	6.68	8.24	6.8	7.85
P 6/10	28.0	39.5	28.3	38.6
P 6/12	218	500	277	419

[a] $ME4$ = +1.640.
[b] $ME4$ = −2.220.

Our results also require that all the permissible $E4$ matrix elements be included. Inclusion of the 0^+ to 4^+ entry and the static $E4$ moment of the 2^+ and 4^+ states gives essentially the $E2$ only predictions.

1. Oak Ridge Associated Universities Research Participant from Furman University, Greenville, S.C., summer 1971.
2. Physics Division.
3. Physics Department, University of Tennessee, Knoxville.
4. F. K. McGowan, C. E. Bemis, Jr., J. L. C. Ford, Jr., W. T. Milner, R. L. Robinson, and P. H. Stelson, *Phys. Rev. Lett.* **27**, 1741 (1971). See also C. E. Bemis, Jr., F. K. McGowan, J. L. C. Ford, Jr., W. T. Milner, R. L. Robinson, and P. H. Stelson, "Intrinsic Quadrupole and Hexadecapole Moments for Even-Even Transuranium Nuclei and the Equilibrium Deformations," chap. 2, this report.
5. A. Winther and J. de Boer, p. 303 in *Coulomb Excitation*, K. Alder and A. Winther, eds., Academic Press, New York, 1966.

SEARCH FOR CONVERSION ELECTRONS FROM THE ^{236}U FISSION ISOMER[1]

E. Konecny[2] P. Ostermann[5]
R. L. Ferguson H. Weigmann[4]
H. J. Specht[3] G. Siegert[6]
J. Weber[3]

In the past few years, spontaneously fissioning isomers have been a subject of extensive study. Their systematics has given support to the interpretation that fission occurs from shape isomeric states associated with a secondary minimum in the nuclear potential energy surface at large deformations. However, there is so far no direct experimental evidence demonstrating that isomeric fission is, in fact, connected with a deformation larger than the equilibrium ground-state deformation.

If we consider the usual "double-humped" fission barrier with two potential wells corresponding to the ground state and shape isomeric state, respectively, we can interpret the behavior of the ^{236}U compound

nucleus formed with an excitation energy of 6.45 MeV by thermal-neutron capture as follows. The compound nucleus may decay either by prompt fission or by electromagnetic transitions within the first or – with very low probability – the second potential well. If an isomeric level is the lowest state in the second well, the final decay in this well should proceed via $E2$ transitions within the rotational band built on the isomeric level. These transitions should be highly converted with lifetimes less than 0.1 nsec. The nucleus would then undergo spontaneous fission with a half-life characteristic of the shape isomer. Thus, a measurement of delayed coincidences between conversion electrons and fission fragments not only would allow one to identify thermal-neutron-induced isomeric fission with half-lives in the nanosecond to microsecond region, but it might also yield direct information about deformation, namely, the moment of inertia of the shape isomer.

We have searched for conversion electrons from the isomeric fission of ^{236}U formed by the thermal-neutron capture in ^{235}U. The existence of an isomeric state with a half-life of ~110 nsec has been reported previously[7] in other reactions leading to the formation of ^{236}U. The experiment was carried out at the research reactor of the Technische Universität München. Conversion electrons were detected with a superconducting electron spectrometer[8] and fission fragments with a silicon surface-barrier detector. Correlations between the electron energy and the time interval between electron and fragment detection were recorded in a two-parameter analyzer.

After a two-week run, the electron spectrum *not* in coincidence with fission fragments exhibited L_{II}, L_{III}, M_{II} plus M_{III}, and N conversion lines from the $2^+ \rightarrow 0^+$ and $4^+ \rightarrow 2^+$ transitions within the ^{236}U ground-state rotational band, in agreement with previous observations.[9] However, the background-corrected spectrum of delayed coincidences corresponding to a time interval between 50 and 220 nsec before fission did *not* show any statistically significant structure of a similar type, for example, one or several quadruplets of lines arising from $E2$ transitions within the second potential well. In addition, no recognizable tail resulting from delayed fission is visible, within the statistical uncertainties, in the measured time spectrum.

Two alternative explanations can be given for the negative result of this experiment: (1) Either the ratio r of isomeric to prompt fission in the ^{235}U thermal-neutron capture reaction is so low that any delayed coincidences are below our experimental sensitivity or (2) the 110-nsec isomeric level in ^{236}U does not correspond to the 0^+ ground state within the second potential well. For case 1 we can use the observed delayed coincidence spectrum to estimate a limit of $\leqslant 5 \times 10^{-5}$ for r. In case 2, any transitions within a rotational band built on the necessary spin-isomeric state of the ^{236}U shape isomer would be undetectable either because the energies would be too low or because the relative population of high-spin states would be too weak in the thermal-neutron capture reaction.

---

1. Abstracted from a paper to be published in *Nuclear Physics*.
2. Technische Universität München, Germany.
3. Universität München, Germany.
4. EURATOM, Geel, Belgium.
5. Universität Frankfurt, Germany.
6. Universität Giessen, Germany.
7. J. Pedersen and B. Rasmussen, *Nucl. Phys. A* **178**, 449 (1972), and references therein.
8. M. Waldschmidt and P. Ostermann, *Nucl. Instrum. Methods* **89**, 65 (1970).
9. M. R. Schmorak, *Nucl. Data Sect. B* **4**, 623 (1970).

ABUNDANCES OF PRIMORDIAL AND COSMOGENIC RADIONUCLIDES IN APOLLO 14 ROCKS AND FINES[1]

G. D. O'Kelley J. S. Eldridge[2]
K. J. Northcutt[2]

Nondestructive gamma-ray spectrometry methods developed for Apollo 11 and 12 samples[3-5] were used for the determination of K, Th, U, ^{26}Al, and ^{22}Na in eight rock samples and three soils returned by the Apollo 14 mission. All of the rock samples were fragmental, and the soils were from the top, middle, and bottom of the Soil Mechanics Experiment trench.

Our suite of samples is distinguished by its uniformity in primordial radioelement content. Potassium concentrations ranged from 4000 to 5800 ppm, thorium ranged from 10.9 to 15.6 ppm, and uranium ranged from 3.1 to 4.5 ppm. The only samples from previous Apollo missions yielding this high level of primordial radioelements (average rock values) were 12013 and 12034 from the Ocean of Storms. Soils measured from the Apollo 15 collection show K, Th, and U contents 3 to 8 times lower than the Apollo 14 soils and breccias.[6]

From extensions of our simple two-component mixing model for Apollo 12 soils[4] we deduced that our Apollo 14 samples contain 60 to 80% of a foreign component believed to be the lunar material KREEP.[7] This lends support to the predictions of many investigators that the Fra Mauro formation would be rich in KREEP.

All of our Apollo 14 samples fit into a tight grouping of the K/U systematics presented in Fig. 1.9. This

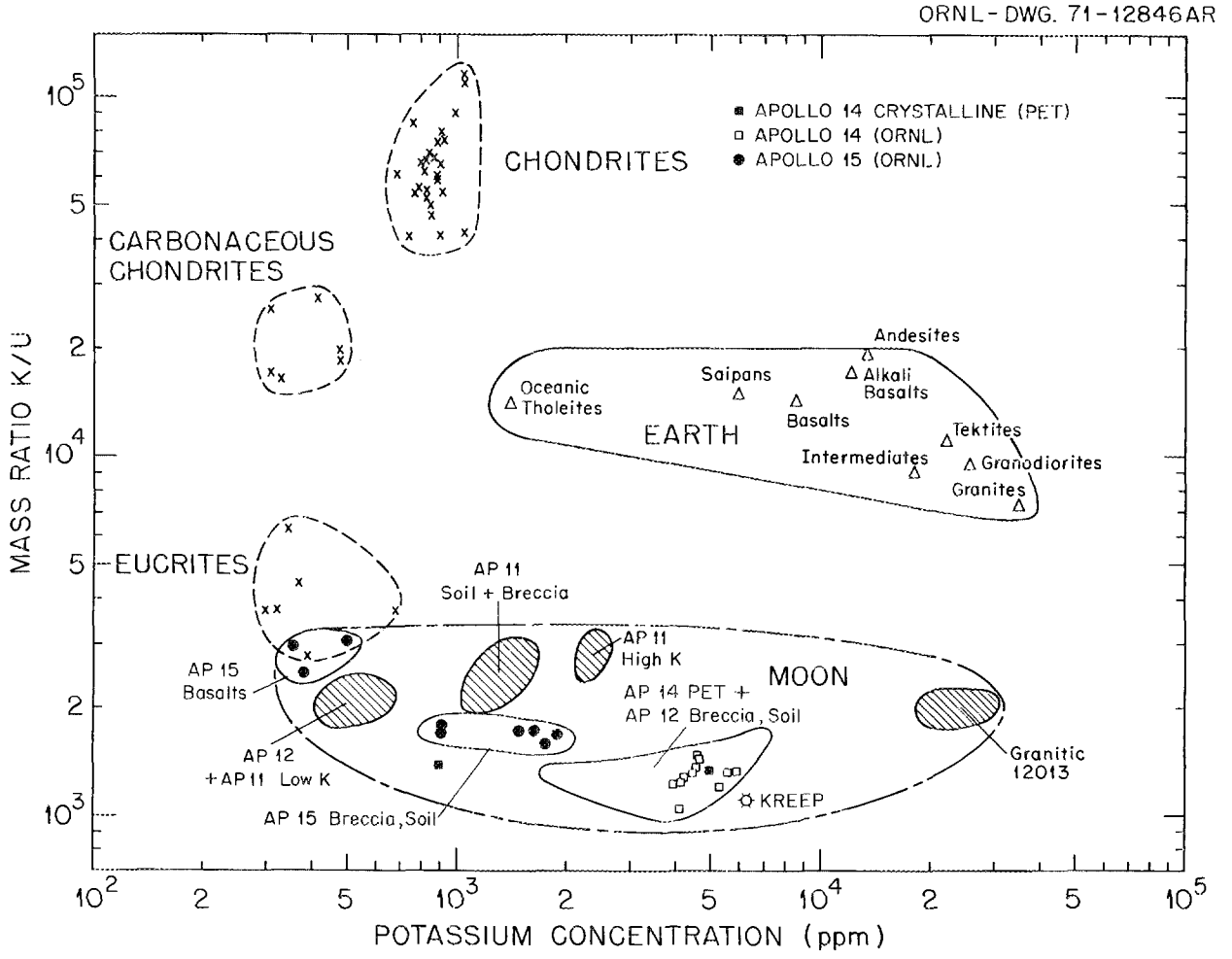

Fig. 1.9. Plot of concentration ratios K/U as a function of K concentration for terrestrial, meteoritic, and lunar materials. Data obtained at ORNL are shown as open squares (Apollo 14) and as solid circles (Apollo 15).

grouping shows that the Fra Mauro samples are very similar to the dark portion of sample 12013[4] and to KREEP.

Breccia 14321, the largest rock returned, originally weighed 9 kg. Our sample (14321, 38) is an 1100-g piece cut from one end of the rock. Sample 14321, 256 is sawdust from cutting of 14321. We obtained good agreement for radioactive concentrations in the two samples of 14321, which shows that the distribution of primordial nuclides within the whole rock is uniform despite its small-scale inhomogeneity.

Cosmogenic radionuclide determinations show few differences from those found in previous missions with the exception of the three soil samples, which deserve special discussion. The Apollo 14 Soil Mechanics Experiment trench was planned to be 60 cm deep at station G, with one vertical sidewall to provide a means for sampling at depth. The trenching did not yield a vertical sidewall; sloping occurred with walls of 60 to 80°, and a maximum depth of only 36 cm was achieved. Samples 14148, 14149, and 14156 were taken from the top, bottom, and middle, respectively, of the trench, and all were <1 mm sieved fractions. From the concentrations of K, Th, and U, it would appear that the soil at the trench site is uniform throughout its sampled depth of 0 to 36 cm. We expected to find pronounced decreases in the concentrations of the cosmogenic species ^{26}Al and ^{22}Na with depth. Instead, all three samples show a surprising uniformity in concentrations of these nuclides. We would predict values of ~40 and ~35 dis min^{-1} kg^{-1} for ^{26}Al and ^{22}Na at the depth of 36 cm for sample 14149.[8] Because of the uniform distribution of ^{26}Al and ^{22}Na and their high concentrations at depth, we

must conclude that extensive mixing occurred and our trench-bottom sample (14149, 62) is not representative of the soil at a 36-cm sampling depth. This also gives reason to question the uniformity of K, Th, and U concentrations in the different soil layers. In addition, the separation of the <1 mm fraction from the trench-bottom samples has further emphasized the sampling defect, since the bottom sample has a median grain size of 0.41 mm, compared with 0.09 and 0.007 mm for the surface and middle-trench samples.[9]

Our studies with similar trench samples from Hadley Base[6] yielded the expected decrease in ^{26}Al and ^{22}Na content with increasing depth.

---

1. Sponsored by the National Aeronautics and Space Administration through interagency agreements with the U.S. Atomic Energy Commission. Summary of a paper accepted for publication in the *Proceedings of the Third Lunar Science Conference,* vol. 2, to be published in *Geochimica et Cosmochimica Acta.*

2. Analytical Chemistry Division.

3. G. D. O'Kelley, J. S. Eldridge, E. Schonfeld, and P. R. Bell, pp. 1407–23 in *Proceedings of the Apollo 11 Lunar Science Conference, Geochim. Cosmochim. Acta,* suppl. 1, vol. 2, Pergamon, 1970.

4. G. D. O'Kelley, J. S. Eldridge, E. Schonfeld, and P. R. Bell, pp. 1159–68 in *Proceedings of the Second Lunar Science Conference, Geochim. Cosmochim. Acta,* suppl. 2, vol. 2, MIT Press, 1971.

5. G. D. O'Kelley, J. S. Eldridge, E. Schonfeld, and P. R. Bell, pp. 1747–55 in *Proceedings of the Second Lunar Science Conference, Geochim. Cosmochim. Acta,* suppl. 2, vol. 2, MIT Press, 1971.

6. G. D. O'Kelley, J. S. Eldridge, E. Schonfeld, and K. J. Northcutt, *Science* **175,** 440 (1972), and the following contribution.

7. C. Meyer, Jr., R. Brett, N. J. Hubbard, D. A. Morrison, D. S. McKay, F. K. Aitken, H. Takeda, and E. Schonfeld, pp. 393–441 in *Proceedings of the Second Lunar Science Conference,* suppl. 2, vol. 1, MIT Press, 1971. KREEP is an acronym which designates a class of material of distinctive high potassium, rare-earth elements, and phosphorus content.

8. T. W. Armstrong and R. G. Alsmiller, Jr., pp. 1729–45 in *Proceedings of the Second Lunar Science Conference, Geochim. Cosmochim. Acta,* Suppl. 2, vol. 2, MIT Press, 1971.

9. Lunar Sample Preliminary Examination Team, "Preliminary Examination of Lunar Samples," pp. 117–18 in NASA-MSC Apollo 14 Preliminary Science Report SP-272 (1971).

STUDIES OF PRIMORDIAL RADIOELEMENTS AND COSMOGENIC RADIONUCLIDES IN APOLLO 15 SAMPLES BY NONDESTRUCTIVE GAMMA-RAY SPECTROMETRY[1]

G. D. O'Kelley E. Schonfeld[3]
J. S. Eldridge[2] K. J. Northcutt[2]

Nine samples from Apollo 15 were analyzed at ORNL by nondestructive gamma-ray spectrometry. The first samples were received from the Lunar Receiving Laboratory (LRL) about nine days after liftoff from the moon. Other samples were received at intervals beginning about two weeks later.

The equipment and techniques of nondestructive gamma-ray spectrometry are essentially those we developed for use at the LRL[4,5] during the Apollo 11 and Apollo 12 missions. Spectrum libraries for all samples except one were obtained from replicas which accurately reproduced the electronic and bulk densities of the lunar samples. Bulk densities were obtained for six of the samples from known sample weights and measured volumes of the replicas.

As we have shown previously,[4,5] mass ratios K/U for the earth and moon fall into separate groups whose average values appear characteristic of each planet. The constancy of the ratio of K (a volatile element, depleted on the moon) to U (a refractory element) appears to be the result of early chemical fractionation which is not affected by later igneous processes.

Basalts 15015, 15475, and 15495 have potassium concentrations which are similar to those of the Apollo 11 low-potassium basalts and the Apollo 12 basalts. As shown in Fig. 1.9, the Apollo 15 basalts have average K/U ratios of about 2900, somewhat higher than the K/U ratio of about 2000 for Apollo 11 and 12 basalts of the same potassium concentration. The range of K/U values for eucrites slightly overlaps the data region for the Apollo 15 crystalline rocks, which suggests that both materials underwent similar genetic processes in the early history of the solar system.

As was the situation for the Apollo 12 samples,[5] the soils and breccia from Apollo 15 are much higher in K, Th, and U than the Apollo 15 basalts. Therefore, the soils and breccia are very likely mixtures of Apollo 15 basalt and a foreign component high in K, Th, and U. Our K/U systematics suggest that the most likely candidate for the foreign component is the lunar material KREEP.[6] A two-component mixture requires only about 10 to 20% KREEP for the Apollo 15 breccia and soil samples, lower than the range of KREEP concentrations estimated for Apollo 12 samples.[5] Sample 15601 and the dark portion of 15455 are similar in their primordial radioelement concentrations and are lowest in KREEP (about 10%) of the Apollo 15 samples we have examined.

The general concentration patterns for ^{22}Na and ^{26}Al resemble those observed on previous Apollo missions. Because chemical analyses are lacking for most of the samples, it is not possible to make detailed interpretations of the concentrations of ^{22}Na and ^{26}Al. However, the low ratio ^{26}Al/^{22}Na for two rocks

(15475 and 15495) from the rim of Dune Crater suggests that the ^{26}Al content did not attain saturation; the data imply that these samples were ejected onto the lunar surface within the last 2,000,000 years. The cosmogenic radionuclide yields, especially of ^{56}Co, show that the rocks were all collected from the surface, in agreement with preliminary documentation.

The radioactivity of the soil samples can be related to depth effects. The high concentrations of ^{22}Na, ^{26}Al, and ^{56}Co are consistent with a sampling depth of about 3 cm for 15101 and a somewhat shallower depth of 1.5 to 3.0 cm for 15601, assuming a chemical composition similar to that of Apollo 12 soils. Similarly, soil 15031, taken from a 35-cm depth at the ALSEP site, shows the low levels of cosmogenic radioactivity characteristic of deep samples. The radioactivity of 15041, taken from the top of the trench at station 8, is consistent with sampling within the top 3 cm of the surface.

During the preliminary examination of the Apollo 11 and Apollo 12 samples in the LRL, we were able to detect in six rocks the ^{48}V produced by solar-flare protons. From the ^{48}V content of rock 12062, which appeared to have been buried, we inferred a yield from galactic proton bombardment of about 40 ± 20 dis/min per kilogram of iron.

We determined ^{48}V quantitatively in the first two Apollo 15 samples received; however, the results on 15061 were superior, because weak components of the gamma-ray spectra of lunar basalts suffer less interference from the Th and U decay series than spectra of lunar soils and breccia. The concentration of ^{48}V in 15016 leads to a galactic production rate for ^{48}V of 57 ± 11 dis/min per kilogram of iron, in good agreement with our earlier estimate.

Although no measurements of the intensity of the solar flare of January 25, 1971, have been published, the ^{56}Co concentrations in Apollo 15 rocks suggest that this flare was about twice the intensity of the well-characterized event of November 3, 1969.

---

1. Sponsored by the National Aeronautics and Space Administration through interagency agreements with the U.S. Atomic Energy Commission. Summary of paper accepted for publication in the *Proceedings of the Third Lunar Science Conference*, vol. 2, to be published in *Geochimica et Cosmochimica Acta*. A preliminary account of some of this work was published by G. D. O'Kelley, J. S. Eldridge, E. Schonfeld, and K. J. Northcutt, *Science* **175**, 440–43 (1972).
2. Analytical Chemistry Division.
3. NASA Manned Spacecraft Center, Houston, Tex.
4. G. D. O'Kelley, J. S. Eldridge, E. Schonfeld, and P. R. Bell, pp. 1407–23 in *Proceedings of the Apollo 11 Lunar Science Conference, Geochim. Cosmochim. Acta*, suppl. 1, vol. 2, Pergamon, 1970.
5. G. D. O'Kelley, J. S. Eldridge, E. Schonfeld, and P. R. Bell, pp. 1159–68 in *Proceedings of the Second Lunar Science Conference, Geochim. Cosmochim. Acta*, suppl. 2, vol. 2, MIT Press, 1971; ibid., pp. 1747–55.
6. C. Meyer, Jr., R. Brett, N. J. Hubbard, D. A. Morrison, D. S. McKay, F. K. Aitken, H. Takeda, and E. Schonfeld, pp. 393–411 in *Proceedings of the Second Lunar Science Conference*, suppl. 2, vol. 1, MIT Press, 1971. KREEP is an acronym which designates a class of material of distinctive high potassium, rare-earth elements, and phosphorus content.

2. Chemistry and Physics of Transuranium Elements

CALCULATIONS OF SPALLATION-FISSION COMPETITION IN THE REACTIONS OF PROTONS WITH HEAVY ELEMENTS AT ENERGIES ≤3 GeV

R. L. Hahn H. W. Bertini[1]

Modification of the intranuclear cascade codes to include the competition between spallation and fission (as expressed by the ratio Γ_n/Γ_f) has been discussed previously.[2] It was found that calculations with these codes could reasonably account for cross-section data obtained from irradiations of ^{231}Pa and ^{232}Th targets with <85-MeV protons.[3]

To test the codes further, additional calculations have been performed at several proton energies up to 3 GeV for comparison with much of the extensive data published for ^{238}U, ^{235}U, and ^{232}Th.

Figure 2.1 shows radiochemical ^{238}U(p,pxn) yields at 1.8 GeV and three calculated curves taken from the work of Pate and Poskanzer.[4] The solid curves were obtained (1) by ignoring fission effects and (2) by including fission with energy-independent Γ_n/Γ_f values, while the dot-dash curve comes from calculations done by Dostrovsky et al. with energy-dependent Γ_n/Γ_f values.[4,5] The dashed curves are calculations from the present work done at 2.0 GeV, with and without fission effects. Error bars on the dashed curves represent the statistical uncertainties of the Monte Carlo computations. It is apparent from this figure that the calculations that include fission with energy-independent Γ_n/Γ_f values follow the rapid decrease in cross section with decreasing mass number A more closely than do those calculations that either ignore fission or treat fission with energy-dependent Γ_n/Γ_f formulas.

It should be pointed out that the calculation (ca. 1960) taken from ref. 4, with Γ_n/Γ_f independent of energy, and illustrated in Fig. 2.1 is similar in broad concept to the present calculations; that is, the intranuclear cascade, followed by particle evaporation in competition with fission, was used with empirical estimates of Γ_n/Γ_f. Despite these similarities that characterize the calculations shown in Fig. 2.1, there are many differences in detail[6] between the calculations of ref. 4 and the present work. The most striking difference between the solid and dashed curves in Fig. 2.1 is most likely due to the inclusion of a diffuse

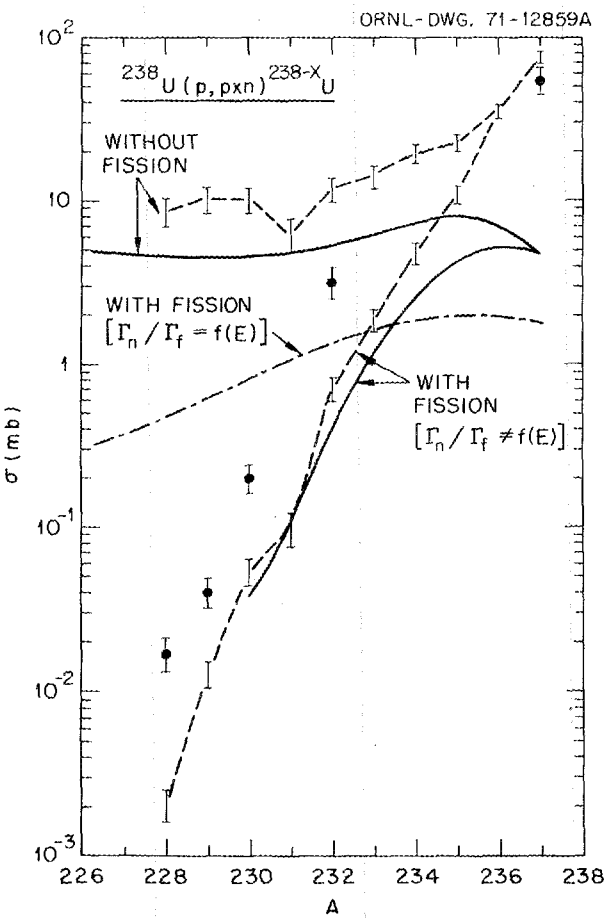

Fig. 2.1. Comparison of the present calculations at 2.0 GeV (dashes) with experimental spallation yields (points). Solid curves are calculations for the reaction ^{238}U(p,pxn)$^{238-x}$U studied by Pate and Poskanzer[4] at 1.8 GeV. Calculations with and without the effects of fission competition are shown. Errors on the dashed curves are statistical uncertainties of the Monte Carlo computations.

nuclear surface in recent cascade calculations.[7,8] That is, the low yields from the early cascade calculations for (p,pxn) products close to the target nucleus do not occur in the more recent calculations; thus the dashed curves in Fig. 2.1 reproduce the value of the (p,pn) cross section leading to ^{237}U, while the solid curves are low by a factor of ~10.

Especially significant about the comparison shown in Fig. 2.1 is the fact that although our calculated curves tend to be lower than the data points by a factor of ~3 to 5, they do reproduce the observed rapid decrease in cross section with decreasing A over an interval that spans ten mass numbers and more than three orders of magnitude in cross section.

Besides predicting spallation yields, the modified codes also compute total fission cross sections. Figure 2.2 illustrates the comparison with experiment for the energy range 0.15 to 3.0 GeV; the data points were obtained by many different workers[6] with track-detection, instead of radiochemical, techniques.

The different fission curves in Fig. 2.2 were calculated for various values of the parameter Z_f, which is the atomic number above which fission effects are considered to be significant in the calculations. We see that allowing Z_f to be as low as 88 overestimates the fission cross section over much of the energy range investigated. Although the often large discrepancies between different experimental results make a detailed comparison difficult, we conclude that the calculation with Z_f = 91 (and possibly 90) reproduces the general trend of the data.

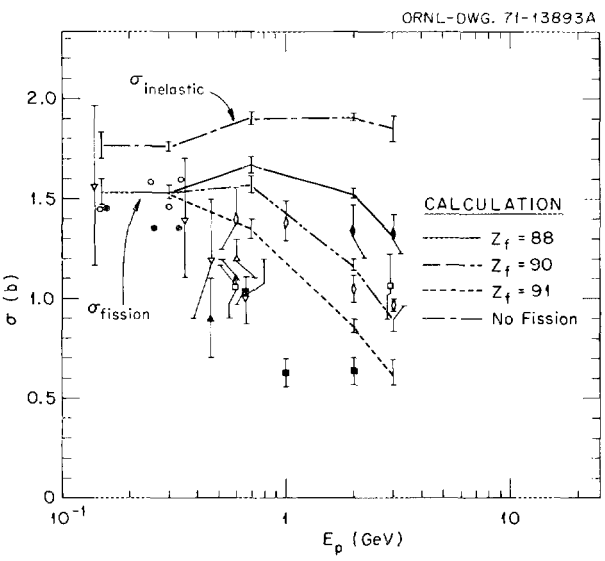

Fig. 2.2. Calculated inelastic and total fission cross sections at 0.15, 0.30, 0.70, 2.0, and 3.0 GeV compared with experimental fission cross sections at different energies. For references to the original experimental work, see ref. 6. Errors on the calculations are statistical uncertainties in the Monte Carlo computations.

In summary, we see that the modified cascade codes, originally intended to treat proton interactions with heavy elements at low energies, ≲100 MeV, also can be used to analyze data at much higher energies, up to 3 GeV.

---

1. Neutron Physics Division.

2. R. L. Hahn and O. W. Herman, *Chem. Div. Annu. Progr. Rep. May 20, 1971*, ORNL-4706, p. 32.
3. R. L. Hahn, K. S. Toth and M. F. Roche, *Chem. Div. Annu. Progr. Rep. May 20, 1971*, ORNL-4706, p. 34.
4. B. D. Pate and A. M. Poskanzer, *Phys. Rev.* **123**, 647 (1961)
5. I. Dostrovsky, Z. Fraenkel, and P. Rabinowitz, Paper P/1615, *Proc. U.N. Int. Conf. Peaceful Uses At. Energy, 2nd, 1958*, vol 15.
6. For details, see R. L. Hahn and H. W. Bertini, *Phys. Rev.*, in press.
7. H. W. Bertini, *Phys. Rev.* **131**, 1801 (1963); *Phys. Rev.* **188**, 1711 (1969).
8. K. Chen, Z. Fraenkel, G. Friedlander, J. R. Grover, J. M. Miller, and Y. Shimamoto, *Phys. Rev.* **166**, 949 (1968).

COMPOUND-NUCLEAR AND TRANSFER REACTIONS IN ^{12}C REACTIONS WITH ^{238}U AND ^{239}Pu

R. L. Hahn K. S. Toth[1]
P. F. Dittner O. L. Keller

Studies of the interactions of heavy ions (H.I.) with heavy elements, besides adding to our knowledge of the different mechanisms operative[2] in reactions such as (H.I.,xn) and (H.I.,αyn), and of the ensuing competition between particle emission and fission,[3] also have application in attempts to produce and identify new nuclides. For example, knowledge of the details of the angular distributions of recoil nuclei has been used as support for the identification of transactinide elements.[4]

At the Oak Ridge Isochronous Cyclotron, we have investigated the reactions $^{238}U(^{12}C,5n$ and $6n)$ and $^{239}Pu(^{12}C,\alpha 2n$ and $\alpha 3n)$, which lead to the same products, ^{245}Cf and ^{244}Cf. Relative excitation functions were determined by collection of recoil nuclei with a gas-jet system followed by alpha-particle spectrometry.[5] Separate experiments involving radiochemical techniques gave absolute cross-section values. The results for the ^{238}U target were consistent with published data[2] that indicated that the $(^{12}C,xn)$

reaction proceeds via the compound-nucleus mechanism with cross sections of ~50–100 μb. For the ^{239}Pu + ^{12}C reactions, maximum cross sections of 7.1 μb at 69 MeV, and 4.8 μb at 74 MeV, were found respectively for ^{245}Cf and ^{244}Cf. Furthermore, no activity ascribable to Fm nuclides from ^{239}Pu(^{12}C,xn) reactions was detected in these experiments; a limit of (^{12}C,xn)/(^{12}C,αyn) $\lesssim$0.01 was set. These results clearly indicate that ^{244}Cf and ^{245}Cf are not produced from ^{239}Pu + ^{12}C in compound-nuclear interactions, because evaporation of charged particles from such heavy nuclei is much less probable than that of neutrons.

To learn more about the reaction mechanisms involved, we measured, at different ^{12}C energies, the range and angular distributions for ^{245,244}Cf that recoiled out of thin ^{238}U and ^{239}Pu targets. Figure 2.3 shows range distributions obtained with stacks of thin carbon foils that collected recoils from 0–10° with respect to the beam (corrections for energy loss in the targets are not included in the figure). The distributions for ^{238}U + ^{12}C are approximately Gaussian, with centroids (average ranges) that increase with increasing ^{12}C energy in a manner consistent with full-momentum transfer. For ^{239}Pu the results are quite different. The distributions are asymmetric with tails that extend to large range values, yet the centroids decrease rapidly with increasing ^{12}C energy.

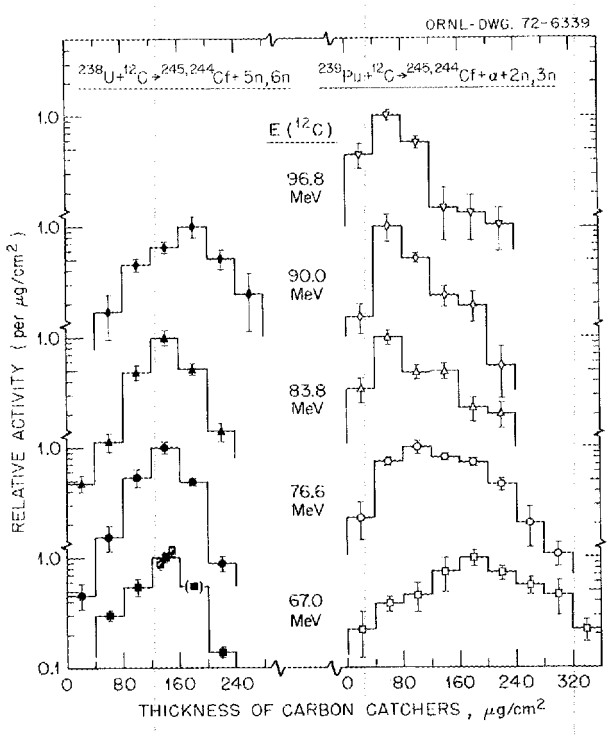

Fig. 2.3. Range-distribution measurements for ^{245}Cf and ^{244}Cf from the reactions of ^{12}C with ^{238}U and ^{239}Pu.

The angular distributions, determined by collecting recoils in ~9-mg/cm^2 aluminum foils placed at various angles with respect to the beam, are also different for the two targets. For ^{238}U + ^{12}C, the angular distributions monotonically decrease with increasing lab angle, while for ^{239}Pu + ^{12}C, they display a peak at ≈15–20°.

All of the data support the conclusion that the ^{238}U(^{12}C,xn) reactions occur via compound-nucleus formation and decay. The results for the ^{239}Pu (^{12}C,αyn) reactions are clearly not ascribable to compound-nuclear processes, and qualitatively agree with work[6] that concludes that direct transfer to the target nucleus of part of the projectile, possibly ^{8}Be, occurs in such reactions, followed by neutron emission from the excited residual nucleus.

---

1. Physics Division.
2. A. Zucker and K. S. Toth, "Heavy-Ion Induced Nuclear Reactions," in *Nuclear Chemistry*, Vol. 1, L. Yaffe, ed., Academic Press, New York, 1968.
3. T. Sikkeland et al., *Phys. Rev.* **169**, 1000 (1968); **172**, 1232 (1968).
4. G. N. Flerov et al., JINR (Dubna) Preprint P7-5164, 1970.
5. R. L. Hahn, P. F. Dittner, K. S. Toth, O. L. Keller, and P. J. Hammons, *Chem. Div. Annu. Progr. Rep. May 20, 1971*, ORNL-4706, p. 44.
6. R. Bimbot, D. Gardes, and M. F. Rivet, *Nucl. Phys.*, to be published.

NUCLEAR CHARGE DISTRIBUTION OF HEAVY FISSION FRAGMENTS IN THE REACTION ^{239}Pu(n_{th},f)

R. L. Ferguson E. Konecny[2]
H. Gunther[1] G. Siegert[1]

The division of nuclear charge is probably more directly related to the mechanism of fission than is the division of mass, since the distribution of protons most likely occurs at an earlier stage of the fission process than does that of the neutrons. In spite of this, much more reliable data exist on the mass distribution in fission than on the charge distribution. We have attempted to improve this situation by determining the charge distribution of heavy fragments in the thermal-neutron-induced fission of ^{239}Pu.

We have used the fission-product mass spectrograph[3] at the research reactor of the Technische Universität München to irradiate nuclear emulsion plates with mass-separated fission products in the range 131 $\leqslant A \leqslant$ 140. After these plates were processed, tracks of

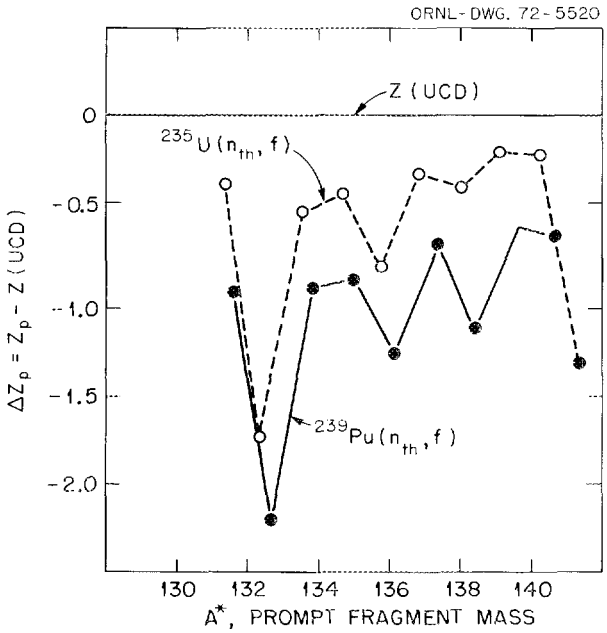

Fig. 2.4. Most probable charge Z_p as a function of fragment mass for the reactions ^{239}Pu(n_{th},f) and ^{235}U(n_{th},f). The charge values are plotted as differences from Z(UCD), which corresponds to the charge ratio of the fissioning nucleus.

individual fission fragments, and of the beta particles radiating from their termini, were examined with an optical microscope. The number of beta-particle tracks per fragment track, with minor corrections,[3] gives the beta-decay chain length as a function of fragment mass. The average chain lengths thus obtained were converted to values of the most probable charge Z_p by subtracting them from the charge of the stable end product of each mass chain.

These Z_p values are shown, in the representation of Wahl et al.,[4] in Fig. 2.4, along with Z_p values obtained from a similar measurement of the ^{235}U(n_{th},f) reaction. In the figure, Z(UCD) refers to unchanged charge distribution, namely, that charge which would give the fragments the same ratio of protons to neutrons as the fissioning nucleus, and A^* refers to the fragment mass corrected for prompt neutron emission. It is obvious that the structure in the two charge distribution curves is quite similar, but the curve for the ^{239}Pu(n_{th},f) reaction is displaced ~0.4 charge unit further from the Z(UCD) line. Considering the relative positions of the valley of beta stability, however, corresponding Z_p's for the fragment masses investigated here are approximately equidistant from it for both fission reactions.

1. Universität Giessen, Germany.
2. Technische Universität München, Germany.
3. E. Konecny, H. Gunther, H. Rösler, G. Siegert, and H. Ewald, *Z. Phys.* **231**, 59 (1970).
4. A. C. Wahl, R. L. Ferguson, D. R. Nethaway, D. E. Troutner, and K. Wolfsberg, *Phys. Rev.* **126**, 1112 (1962).

STATES IN ^{236}U VIA THE (d,d') REACTION AND IN THE ALPHA DECAY OF ^{240}Pu

C. E. Bemis, Jr. J. S. Boyno[1]
P. F. Dittner Th. W. Elze[2]
J. R. Huizenga[1] M. J. Zender[3]

The collective states in ^{236}U have recently been investigated in the (d,d') reaction at 16 MeV on the University of Rochester MP tandem Van de Graaff in a collaborative experiment.[4] Inelastically scattered deuterons were observed at 90 and 125° using an Enge split-pole spectrograph and nuclear emulsions. Spin assignments were made by comparing the differential cross-section ratios for the excitation of a particular state, $d\sigma_{90°}/d\sigma_{125°}$, to calculated ratios in the distorted-wave Born approximation. The states observed in the ^{236}U(d,d') reaction together with differential cross sections and spin assignments are listed in Table 2.1.

States in ^{236}U have also been investigated following the alpha decay of ^{240}Pu, using high-resolution x-ray and gamma-ray semiconductor detectors. A portion of

Table 2.1. States observed in the ^{236}U(d,d') reaction together with differential cross sections at 90 and 125°

Energy (keV)	$d\sigma/dr_{90°}$ (μb/sr)	$d\sigma/dr_{125°}$ (μb/sr)	I^π
0 ± 2	44489 ± 911	9322 ± 201	0^+
44 ± 2	6434 ± 361	2718 ± 120	2^+
149 ± 2	588 ± 38	270 ± 14	4^+
310 ± 3	42 ± 4	51 ± 3	6^+
524 ± 2		3.3 ± 0.6	8^+
686 ± 2	13 ± 2	30 ± 2	1^-
746 ± 2	216 ± 15	89 ± 5	3^-
848 ± 2	18 ± 2	23 ± 2	5^-
919 ± 2		3.0 ± 0.5	(0^+)
959 ± 2	104 ± 8	42 ± 3	(2^+)
1002 ± 2		4.3 ± 0.4	
1037 ± 2	95 ± 8	53 ± 3	
1060 ± 2	25 ± 2	15 ± 1	
1150 ± 2	66 ± 6	44 ± 3	
1240 ± 2		4.7 ± 0.9	
1262 ± 2		13 ± 1	
1333 ± 2		5.6 ± 0.9	

the gamma-ray work covering only the ground-state rotational band has already been published.[5] The higher lying states in ^{236}U populated in the (d,d') reaction and in the alpha decay of ^{240}Pu will be the subject of a future publication.

1. Nuclear Structure Laboratory, University of Rochester, Rochester, N.Y.
2. Present address: Institut für Kernphysik der Universität, 6 Frankfurt 90, West Germany.
3. Present address: Department of Physics, Fresno State College, Fresno, Calif.
4. J. S. Boyno, Th. W. Elze, J. R. Huizenga, and C. E. Bemis, Jr., *Bull. Amer. Phys. Soc.* 17, 463 (1972).
5. M. Schmorak, C. E. Bemis, Jr., M. J. Zender, N. B. Gove, and P. F. Dittner, *Nucl. Phys.* A178, 410 (1972).

INTRINSIC QUADRUPOLE AND HEXADECAPOLE MOMENTS FOR EVEN-EVEN TRANSURANIUM NUCLEI AND THE EQUILIBRIUM DEFORMATIONS[1]

C. E. Bemis, Jr. W. T. Milner[2]
F. K. McGowan[2] R. L. Robinson[2]
J. L. C. Ford, Jr.[2] P. H. Stelson[2]

The ground-state rotational bands for ^{230,232}Th, ^{234,236,238}U, ^{238,240,242,244}Pu, ^{244,246,248}Cm, and ^{252}Cf have been studied in precision Coulomb excitation experiments with alpha particles, using the Oak Ridge EN tandem Van de Graaff. Scattered alpha particles, elastic and inelastic, were analyzed using a split-pole magnetic spectrograph equipped with a position-sensitive proportional counter in the magnet focal plane. Early accounts of this work have recently been published.[3,4]

In these experiments with alpha particles, single and multiple $E2$ transitions populate the 2^+ and 4^+ states of the ground-state rotational bands and higher 2^+ states. The $E3$ transitions have also been observed to directly populate the 3^- states of the $K = 0$ octupole bands. However, strong electric hexadecapole ($E4$) transitions (100–250 single particle units) have been observed in the ground-state bands, and multiple $E4$ excitations account for 10 to 40% of the population of the 4^+ states. The remainder of the 4^+ excitation is via multiple $E2$ excitation.

Detailed analyses of the Coulomb excitation probabilities in the rigid-rotor limit, which include the quantum mechanical corrections for $E2$ excitations, have yielded $B(E2, 0^+ \rightarrow 2^+)$ and most $B(E4, 0^+ \rightarrow 4^+)$ values for these targets. The transition probabilities are related to the intrinsic quadrupole and hexadecapole moments, which in turn may be related to model-dependent deformation parameters. For a uniform charge distribution with axial symmetry $[R(\theta) = 1 + \beta_{20}Y_{20} + \beta_{40}Y_{40}]$, the relations are as follows:

$$B(E2, 0^+ \rightarrow 2^+) = 5e^2Q_{20}^2/16\pi\, e^2bn^2 \,, \quad (1)$$

$$B(E4, 0^+ \rightarrow 4^+) = 9e^2Q_{40}^2/16\pi\, e^2bn^4 \,, \quad (2)$$

$$Q_{20} = 3ZR_0^2\beta_{20}(1 + 0.36\beta_{20} + 0.967\beta_{40} + 0.328\beta_{40}^2/\beta_{20})/\sqrt{5\pi} \,, \quad (3)$$

$$Q_{40} = ZR_0^4\beta_{40}(1 + 0.983\beta_{20} + 0.725\beta_{20}^2/\beta_{40} + 0.411\beta_{40})/\sqrt{\pi} \,. \quad (4)$$

A summary of our results to date is given in Table 2.2. Figure 2.5 shows the dependence of our measured intrinsic hexadecapole moments on neutron number. The correlation is strong and the trends are similar to that observed in the rare-earth deformed region. The hexadecapole moments are zero at the beginning of the deformed region, rapidly rise to large positive values, cross zero at the middle (^{248}Cm), and are negative for the remainder of the deformed region.

The nucleus ^{234}U has the largest intrinsic hexadecapole moment of all cases studied. If a model of the ^{234}U nucleus is constructed based on the deformation parameters, β_{20} and β_{40}, listed in Table 2.2, the nucleus develops a pronounced bulge in the middle, as shown in Fig. 2.6. This Coulomb excitation work is continuing and will result in a firmer understanding of

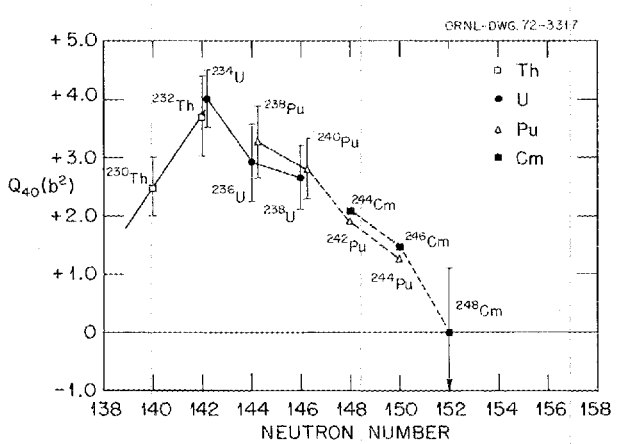

Fig. 2.5. Intrinsic hexadecapole moments for even-even transuranium nuclei as a function of neutron number. The points for ^{242,244}Pu and ^{244,246}Cm are interpolated but will be measured in future experiments.

Table 2.2. Summary of electric quadrupole and hexadecapole Coulomb excitation experiments with 17.00-MeV alpha particles

Nucleus	$B(E2, 0^+ \rightarrow 2^+)$ (e^2b^2)	$Q_{20}(b)$	$B(E4, 0^+ \rightarrow 4^+)$ (e^2b^4)	$Q_{40}(b^2)$	$\beta_{20}{}^a$	$\beta_{40}{}^a$
^{230}Th	8.01 ± 0.11	+8.975 ± 0.053	1.10 ± 0.44	2.48 ± 0.50	0.204 ± 0.006	0.110 ± 0.030
^{232}Th	9.18 ± 0.15	+9.607 ± 0.078	2.56 ± 0.86	3.78 ± 0.64	0.201 ± 0.009	0.177 ± 0.030
^{234}U	10.51 ± 0.20	10.28 ± 0.10	2.89 ± 0.34	4.02 ± 0.24	0.206 ± 0.007	0.188 ± 0.030
^{236}U	11.56 ± 0.15	10.78 ± 0.07	1.51 ± 0.69	2.90 ± 0.66	0.230 ± 0.009	0.124 ± 0.038
^{238}U	11.70 ± 0.15	+10.84 ± 0.07	1.26 ± 0.52	2.65 ± 0.55	0.235 ± 0.006	0.100 ± 0.028
^{238}Pu	12.64 ± 0.11	11.27 ± 0.05	1.90 ± 0.72	3.26 ± 0.62	0.231 ± 0.006	0.135 ± 0.026
^{240}Pu	13.26 ± 0.15	+11.55 ± 0.07	1.39 ± 0.53	2.79 ± 0.53	0.244 ± 0.007	0.099 ± 0.027
^{242}Pu	13.26 ± 0.35	+11.55 ± 0.15				
^{244}Pu	13.83 ± 0.37	+11.79 ± 0.16				
^{244}Cm	14.86 ± 0.35	+12.22 ± 0.15				
^{246}Cm	15.03 ± 0.45	+12.29 ± 0.18				
^{248}Cm	14.99 ± 0.14	12.276 ± 0.057	$0^{+0.23}_{+2.69}$	$0^{+1.1}_{-3.88}$	0.271 ± 0.006	0
^{250}Cf						
^{252}Cf	16.7 ± 1.1	12.9 ± 0.4				

[a]Deformation parameters are based on uniform charge distribution; $R(\theta) = R_0(1 + \beta_{20}Y_{20} + \beta_{40}Y_{40})$.

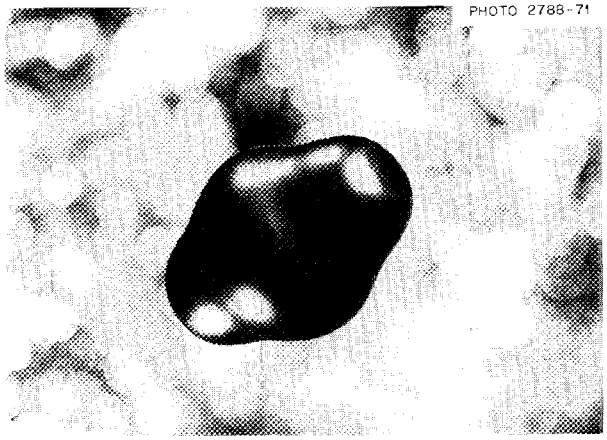

Fig. 2.6. Model of the ^{234}U nucleus based on a uniform charge distribution and the measured intrinsic quadrupole and hexadecapole moments of this work.

the nuclear systematics and deformation in the heavy-element region and should provide a more accurate basis for calculations relating to the stability of proposed superheavy nuclei.

1. A portion of these results appear in the *Phys. Div. Annu. Progr. Rep. Dec. 31, 1971*, ORNL-4743, p. 86.
2. Physics Division.
3. J. L. C. Ford, Jr., P. H. Stelson, C. E. Bemis, Jr., F. K. McGowan, R. L. Robinson, and W. T. Milner, *Phys. Rev. Lett.* **27**, 1232 (1971).
4. F. K. McGowan, C. E. Bemis, Jr., J. L. C. Ford, Jr., W. T. Milner, R. L. Robinson, and P. H. Stelson, *Phys. Rev. Lett.* **27**, 1741 (1971).

NEUTRON MULTIPLICITY DISTRIBUTION MEASUREMENTS IN THE SPONTANEOUS FISSION OF ^{246}Cm, ^{248}Cm, and ^{252}Cf

J. Halperin R. W. Stoughton
C. E. Bemis, Jr. F. M. Glass[1]
H. W. Schmitt[2] R. T. Roseberry[1]
J. H. Oliver

Our neutron multiplicity counter[3] has been adapted to count neutrons in coincidence with fission fragments in a gated mode for small samples by using a surface-barrier fission-fragment detector. When only the detector plus sample (with a small stand to locate the sample centrally in the sample chamber) were present, the single neutron efficiency was about 0.26, based on a $\bar{\nu}$ for ^{252}Cf of 3.73.[4] This contrasts with a calculated efficiency[3] of 0.30 on the assumption that the sample cavity was filled with $MgCO_3$. We filled the chamber with graphite (cylinders) except for a 2-in.-diam by 4-in.-long cavity for detector and sample and obtained an efficiency of 0.360. With graphite cylinders on both ends but with the central 8 in. of cavity containing a tank of D_2O with a 1¼-in. hole down the center (for sample and detector), we observed an efficiency of 0.450.

Our previous electronic equipment[3] was modified to allow scalar measurements of the various multiplicities from zero through twelve, as well as the number of fissions detected.

We measured multiplicities n of zero through six for ^{252}Cf with both D_2O plus graphite and with graphite only. Then on the assumption of a Gaussian[5] distribution $p(\nu)$ for the emitted neutrons, we fitted our observed distribution of multiplicities $P(n)$ to values predicted by the model by the method of least squares, using the above measured efficiencies ϵ. The Gaussian σ_ν and $\bar{\nu}$ were the parameters of fit; when we tried to pick up the value of ϵ in addition to σ_ν and $\bar{\nu}$, we did not get convergence because of the strong correlation between the values of ϵ and $\bar{\nu}$. Our values with graphite were $\sigma_\nu = 1.21 \pm 0.06$ and $\bar{\nu} = 3.72 \pm 0.06$, which compare favorably with Terrell's value[5] of 1.21 for σ_ν and with the 3.73 value of $\bar{\nu}$ mentioned above. By using the customary reciprocal mathematical equations, values of $p(\nu)$ were calculated from the computed (by the least-squares fit) values of $P(n)$. These values of $p(\nu)$ were in good agreement with literature values.[6] The distribution calculated from the experimental multiplicities agreed reasonably well for multiplicities of 1, 2, 3, and 4 but were considerably different for 0, 5, and 6 (due to especial sensitivity of the reciprocal equations to experimental scatter). The experimental distribution $P(n)$ showed higher values for the higher multiplicities than predicted from a Gaussian function.

Samples of ^{246}Cm and ^{248}Cm were counted in our multiplicity counter in the gated mode. Values of $\bar{\nu}$ and σ_ν obtained were 2.86 ± 0.06 and 1.13 ± 0.06 for ^{246}Cm and 3.14 ± 0.06 and 1.10 ± 0.06 for ^{248}Cm. In contrast to Thompson's value[7] of 3.19 for $\bar{\nu}$ of ^{246}Cm, our values for both nuclides fall on a straight line connecting the nuclides ^{242}Cm, ^{244}Cm, ^{248}Cm, and ^{250}Cm in a plot of $\bar{\nu}$ vs mass number.[8] The experimental distribution for both ^{246}Cm and ^{248}Cm showed even higher values at higher multiplicities than did ^{252}Cf when compared with the values from a Gaussian prediction.[9]

1. Instrumentation and Controls Division.
2. Physics Division.
3. R. L. Macklin, F. M. Glass, J. Halperin, R. T. Roseberry, R. W. Stoughton, and M. Tobias, *Chem. Div. Annu. Progr. Rep. May 20, 1971*, ORNL-4706, p. 87; *Nucl. Instrum. Methods*, in press.
4. Our weighted average of literature values: A. De Volpi and K. G. Porges, *Phys. Rev. C* **1**, 683 (1970); J. C. Hopkins, and B. C. Diven, *Nucl. Phys.* **48**, 433 (1963).
5. James Terrell, *Phys. Rev.* **108**, 783 (1957).
6. D. A. Hicks, J. Ise, and R. V. Pyle, *Phys. Rev.* **101**, 1016 (1956); B. C. Diven, H. C. Martin, R. F. Taschek, and J. Terrell, *Phys. Rev.* **101**, 1012 (1956).
7. M. C. Thompson, *Phys. Rev. C* **2**, 763 (1970).
8. C. J. Orth, *Nucl. Sci. Eng.* **43**, 54 (1971).
9. We wish to thank R. D. Baybarz for making the ^{248}Cm available to us.

ABSOLUTE SPECIFIC ACTIVITY OF ^{249}Cf AND HALF-LIVES FOR ^{249}Cf, ^{250}Cf, ^{251}Cf, AND ^{252}Cf

J. R. Stokely[1] R. D. Baybarz[2]
C. E. Bemis, Jr. R. E. Eby[1]

Experiments are in progress to determine the absolute specific activity of ^{249}Cf in a manner similar to that recently used[3] for ^{248}Cm. This determination relies on the absolute microchemical analysis of californium, using a complexometric titration of californium with ethylenediaminetetraacetic acid (EDTA). An excess of a standard EDTA solution is added to complex completely the californium in solution, and the excess EDTA is determined by a complexometric titration with mercury(II).

Instrumentation to provide a direct digital record of the differential complexometric titration (potential vs differential charge) has been developed and tested which will allow determination of californium at the 0.5 micromole level to an absolute accuracy of 1–2%. Purification of approximately 2 mg of ^{249}Cf is being performed, and replicate chemical determinations coupled with absolute activity measurements should provide a half-life for ^{249}Cf accurate to 2–3%. The half-lives for ^{250}Cf, ^{251}Cf, and ^{252}Cf will be determined relative to ^{249}Cf, using a combination of mass spectrometric, chemical, and absolute-activity determinations.

1. Analytical Chemistry Division.
2. Chemical Technology Division.
3. J. E. McCracken, J. R. Stokely, R. D. Baybarz, C. E. Bemis, Jr., and R. Eby, *J. Inorg. Nucl. Chem.* **33**, 3251 (1971).

NEUTRON-INDUCED FISSION CROSS SECTIONS FOR ^{249}Cf IN THE ENERGY RANGE $0.32\ \text{eV} \leqslant E_n \leqslant 1.5\ \text{MeV}$[1]

C. E. Bemis, Jr. M. S. Moore[3]
J. W. T. Dabbs[2] A. N. Ellis[3]
N. W. Hill[4]

On the basis of preliminary experiments with ^{235}U performed at the Oak Ridge Electron Linear Accelerator (ORELA),[1] a new technique for the measurement of fission cross sections has been developed which is applicable to extremely small samples (25 to 500 μg). The preliminary experiments with ^{235}U were performed at an ~8.5-m flight path and used an Si diffuse junction detector[5] located directly in the neutron flight path and nearly in contact with the sample. The type of

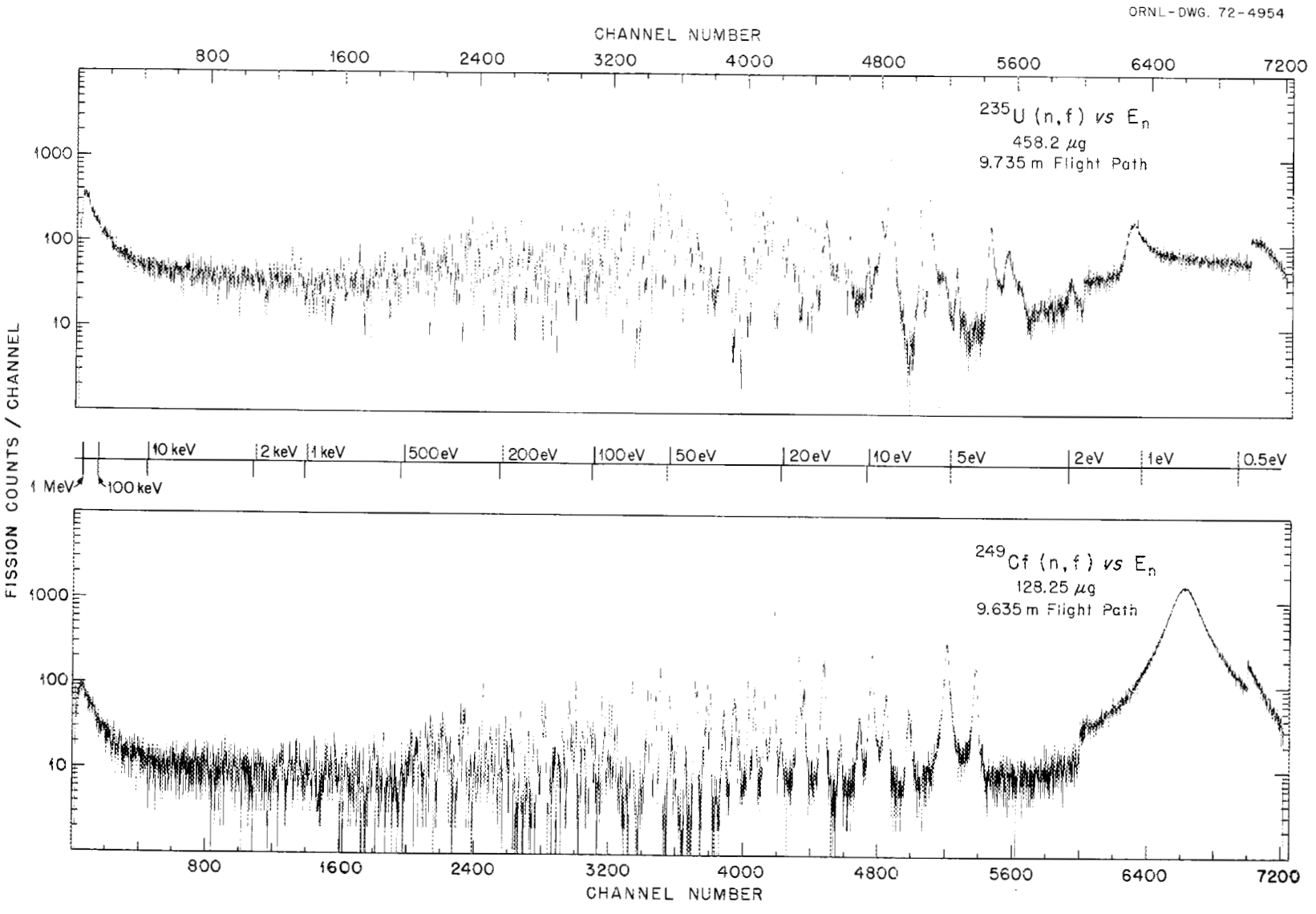

Fig. 2.7. A portion of the raw experimental fission cross-section results for ^{249}Cf (lower curve) together with the results for ^{235}U (upper curve), which was measured simultaneously to provide an absolute cross-section reference.

fission-fragment semiconductor detector used is especially resistant to neutron damage and to the intense gamma-ray flash which accompanies each accelerator beam burst. It was found that the gamma-ray flash pulse in the detector was approximately equivalent to a 100-MeV fission-fragment pulse and could easily be handled by the system electronics. A rapid recovery from the gamma flash pulse is essential at the relatively short flight paths used here (~10 m) so that fission events induced by the high-energy neutrons might be recorded.

The time-of-flight information was processed and stored using a digital clock in conjunction with the ORELA data acquisition computer.

Based on the success of our feasibility experiments[6] with ^{235}U, an experiment to measure the fission cross section for ^{249}Cf in the energy range 0.3 eV $\leqslant E_n \leqslant$ 1.5 MeV was performed. A target consisting of 128.3 μg of isotopically pure ^{249}Cf (>99.999%) was prepared by electrodeposition on a thin stainless steel target mount. Because of the high alpha disintegration rate from this target (>10^7 αdps), a high-speed current pulse amplifier was developed and integrally mounted with the ^{249}Cf fission detector-target assembly. The pulse rise and fall times of this amplifier were 10 and 30 nsec respectively. A 408-μg/cm^2 ^{235}U target was run simultaneously with the ^{249}Cf target in the same neutron beam to provide an absolute fission cross-section reference for the ^{249}Cf experiment. The experiment was performed on flight path 2 at the ORELA at a flight path distance of 9.74 m. The ORELA was operated at ~25 kW with a 25- to 30-nsec pulse width. The fission-fragment detector for the ^{249}Cf target required replacement after 15 to 20 hr exposure, due to radiation damage from the intense alpha activity of the target (10^{11} to 10^{12} alphas/cm^2 integrated dose).

Figure 2.7 shows a portion of the uncorrected data for both the ^{235}U target (upper curve) and the ^{249}Cf target (lower curve) resulting from an ~20-hr experiment.

One prominent feature in the ^{249}Cf spectrum is the large resonance at ~0.71 eV, which accounted for approximately 60% of all ^{249}Cf fissions observed in the experiment. A preliminary estimate of the peak cross section is ~5500 b, with a width, full width at half maximum (FWHM), of ~150 mV. Our data for ^{249}Cf overlap with, and extend to much lower energies, the unpublished results of Silbert[7] measured on the Physics-8 underground test explosion. We are in the process of normalizing our ^{249}Cf results to the ^{235}U reference results to yield absolute cross sections and appropriate resonance parameters for ^{249}Cf. We believe these results for ^{249}Cf demonstrate that fission cross sections for odd A and odd-odd transuranium nuclei may conveniently and reliably (±5 to 10% accuracy) be measured at the ORELA, using samples of the order 25 to 500 μg. Extension of this technique to the measurement of other transuranics, ^{245}Cm, ^{247}Cm, ^{249}Bk, ^{251}Cf, is being contemplated. The possibility of measurements on even-even nuclei will depend on a detailed examination of the spontaneous-fission background level.

---

1. Another, somewhat different, account of this work appears in the *Phys. Div. Annu. Progr. Rep. Dec. 31, 1971*, ORNL-4743, p. 88.
2. Physics Division.
3. Los Alamos Scientific Laboratory.
4. Instrumentation and Controls Division.
5. Solid State Radiation, Inc., Los Angeles, Calif. (type 600-PIN-125).
6. J. W. T. Dabbs, C. E. Bemis, Jr., M. S. Moore, A. N. Ellis, and N. W. Hill, "Small Sample Fission Cross Section Measurements at ORELA," *Phys. Div. Annu. Progr. Rep. Dec. 31, 1971*, ORNL-4743, p. 88.
7. M. G. Silbert, Los Alamos Scientific Laboratory, private communication, March 1972.

FURTHER EXPERIMENTS ON THE NEW ISOTOPE, NOBELIUM-259

R. J. Silva M. L. Mallory
P. F. Dittner O. L. Keller, Jr.

We previously reported[1] the discovery of a long-lived alpha-emitting isotope of element 102 produced in the bombardment of ^{248}Cm with ^{18}O ions from the Oak Ridge Isochronous Cyclotron. The new nuclide was assigned mass 259 from nuclear reaction data and alpha-particle decay energy systematics. Our data indicated that ^{259}No decays primarily by the emission of 7.52-MeV alpha particles, with a half-life of 1.5 ± 0.5 hr. Preliminary results showed the elution position of the 7.52-MeV alpha activity from a cation exchange column, using 3 M ammonium α-hydroxyisobutyrate, was as expected for nobelium. We have since carried out further irradiations, using about four times as much target material (~1.5 mg of ^{248}Cm), and have studied chemically separated samples more fully in order to (1) chemically identify any other alpha groups belonging to ^{259}No decay, (2) establish the genetic linkage of ^{259}No to the known daughter ^{255}Fm for further mass identification, and (3) search for the spontaneous fission decay branch expected for ^{259}No.

Figure 2.8 shows an alpha-particle energy spectrum accumulated from 14 two-hour bombardments of a

350-μg/cm^2 ^{248}Cm target with 97-MeV ^{18}O ions, using the recoil technique.[1] The rather broad alpha peak observed at 7.52 MeV in our previous report appears to be due to at least two alpha groups, one at 7.500 MeV and another at 7.533 MeV. Additional alpha groups were observed at 7.455, 7.605, and 7.685 MeV.

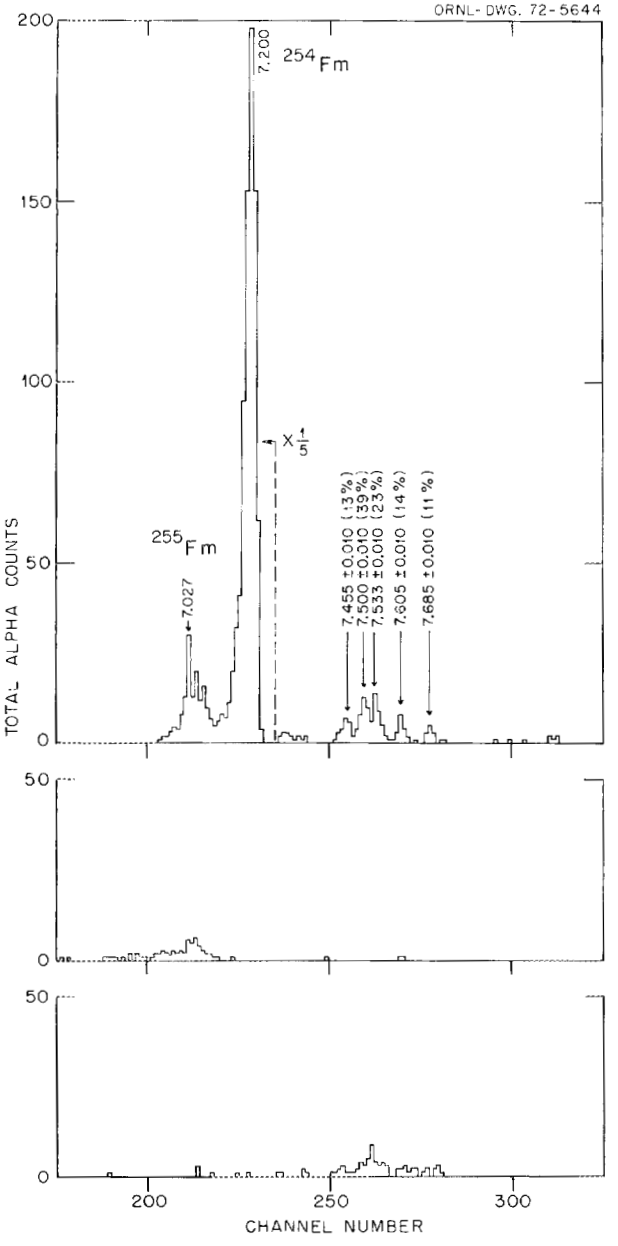

Fig. 2.8. Alpha-particle energy spectra accumulated from bombardments of ^{248}Cm with 97-MeV ^{18}O ions. (*a*) Without chemical separations; (*b*) nobelium fraction from chemical separations; (*c*) nobelium fractions accumulated for three days after (*b*).

Assuming that all of these alpha groups belong to ^{259}No decay, the percent abundance of each group was determined and is given in Fig. 2.8*a*.

Figure 2.8*b* shows an alpha-particle energy spectrum accumulated from nobelium samples obtained from three 2-hr bombardments of 1.5-mg/cm^2 ^{248}Cm targets. After these irradiations the targets were dissolved, and the nobelium was separated from most of the target and Be backing material by elution from cation exchange resin with hydrochloric acid. The final nobelium purification was accomplished by elution from cation exchange resin with ammonium α-hydroxyisobutyrate; Fig. 2.9 shows the results. The decontamination of the nobelium from the target material and other trivalent actinides was greater than 10^7. The energy resolution of the peaks in Fig. 2.8*b* was somewhat broader than in Fig. 2.8*a*, due to finite sample thickness. However, the alpha groups between 7.4 and

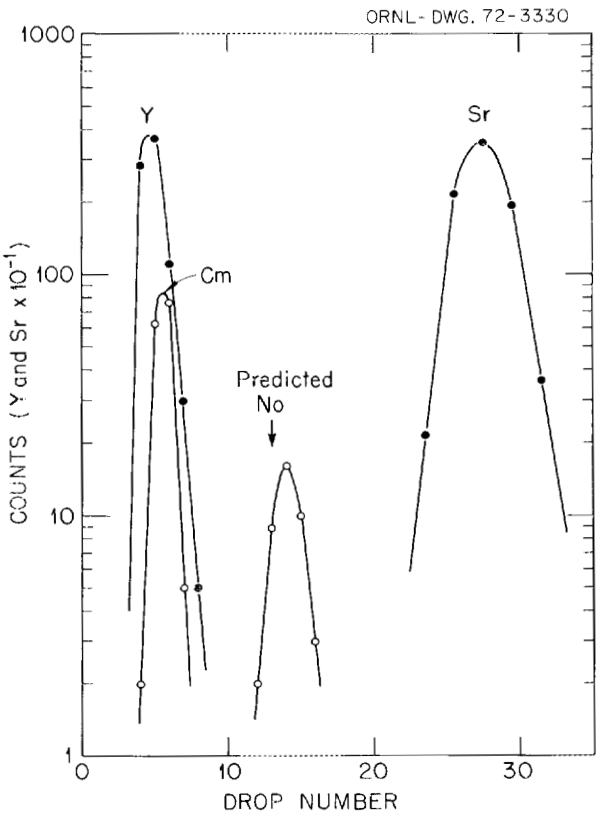

Fig. 2.9. Elution position of the nobelium alpha activity relative to ^{90}Y, ^{90}Sr, and ^{248}Cm, using 3 *M* ammonium α-hydroxyisobutyrate (pH 5.0) as eluant. The arrow indicates the expected elution position for nobelium relative to the tracers from a 2-mm-diam by 2-cm-long Dowex 50-X12 resin bed at 75°C. See ref. 2.

7.7 MeV in Fig. 2.8*a* also can be seen in Fig. 2.8*b* and thus are indeed associated with the nobelium decay.

Figure 2.8*c* shows the alpha-particle energy spectrum accumulated from the chemically separated nobelium fractions over a period of three days after spectrum 2.8*b* was obtained. The energy of the alpha group near channel 200 is about 7.03 MeV, and this activity decays with a half-life of approximately one day. These properties correspond closely to those of ^{255}Fm (E_α = 7.027 MeV, $T_{1/2}$ = 20 hr). We can estimate from our chemical separation data that the counts in this peak cannot be due to contamination by ^{255}Fm made directly in the bombardment; it must all have come from nobelium decay. The observed number of ^{255}Fm alpha decay events (atoms) in Fig. 2.8*c* is approximately equal to the number of ^{259}No alpha decay events (atoms) in Fig. 2.8*b*. For our experimental setup, the mother-daughter decay relationships would predict equal numbers of alpha events. The total half-life of ^{259}No derived from an accumulation of all of our present data is 54 ± 5 min.

Spontaneous-fission counting was also carried out on two of the chemically separated nobelium samples. A spontaneous-fission activity decaying with a half-life of about 1 hr was observed and is very likely associated with the ^{259}No decay; we estimate this mode of decay to be ~20% of the total. This branching corresponds to a spontaneous-fission half-life of ~4.5 hr and leads to an estimate of 10^{10} for the spontaneous-fission hindrance factor over the trends given by nuclei with even numbers of protons and neutrons.

1. *Chem. Div. Annu. Progr. Rep. May 20, 1971*, ORNL-4706, p. 65.
2. J. Malý, T. Sikkeland, R. Silva, and A. Ghiorso, *Science* **160**, 1114 (1968).

ATTEMPTED *Z* IDENTIFICATION OF ^{255,256}Lr AND ^{257,261}Rf

P. F. Dittner
C. E. Bemis, Jr.
D. C. Hensley[1]
C. D. Goodman[1]
R. J. Silva
R. L. Hahn

We have attempted to apply our $K\alpha$ x-ray coincidence technique[2] for identifying the atomic number of new elements to isotopes of lawrencium (Z = 103) and rutherfordium (Z = 104). Our primary goal was the Z identification of the 4.5-sec ^{257}Rf. In order to work with isotopes having half-lives of the order of seconds, an automated rapid activity transfer system (ARATS) was developed. The salient features of ARATS are:

1. A helium gas jet (issuing from the helium-filled recoil chamber) deposits the activity on the centers of thin aluminum disks ("rabbits").
2. The rabbits are transferred penumatically from the activity collection point to the counting station, where they are positioned between an alpha detector and a photon detector.
3. The elapsed time from the end of the collection time to the start of the counting time is $\leqslant$1 sec.

The reaction ^{249}Cf(^{12}C,4n)^{257}Rf did indeed produce alpha activities of the same energy and half-life as observed at Berkeley[3] for ^{257}Rf (see Fig. 2.10), but the number of coincident K x rays after two days' accumulation was extremely small. Extrapolating our yield to a five-day accumulation convinced us that an unequivocal Z identification would not be possible under existing conditions, and the experiment was halted.

We then turned to our secondary goal, the Z identification of ^{256}Lr ($T_{1/2}$ = 31 sec) produced by bombarding ^{249}Cf with ^{11}B. Previous measurements indicated that the cross section for the production of ^{256}Lr would be larger than the production cross section for ^{257}Rf, and indeed this was the case (Fig. 2.11). However, theoretical estimates of the K x-ray yield per alpha decay are smaller for ^{256}Lr compared with ^{257}Rf, and unfortunately this fact was confirmed by our experiment. Preliminary experiments, which produced the 22-sec ^{255}Lr and the 70-sec ^{261}Rf via the reactions ^{249}Cf(^{10}B,4n)^{255}Lr and ^{249}Cf(^{18}O; α,2n)^{261}Rf, respectively, convinced us that the latter two isotopes were even poorer candidates for a successful Z identification experiment.

At this time it appears that with improvements we have made in our x-ray detection efficiency and a planned improvement of ARATS, a further attempt at the Z identification of ^{257}Rf is warranted.

1. Physics Division.
2. P. F. Dittner, C. E. Bemis, Jr., D. C. Hensley, R. J. Silva, and C. D. Goodman, *Phys. Rev. Lett.* **26**, 1037 (1971).
3. A. Ghiorso, M. Nurmia, J. Harris, K. Eskola, and P. Eskola, *Phys. Rev. Lett.* **22**, 1317 (1969).

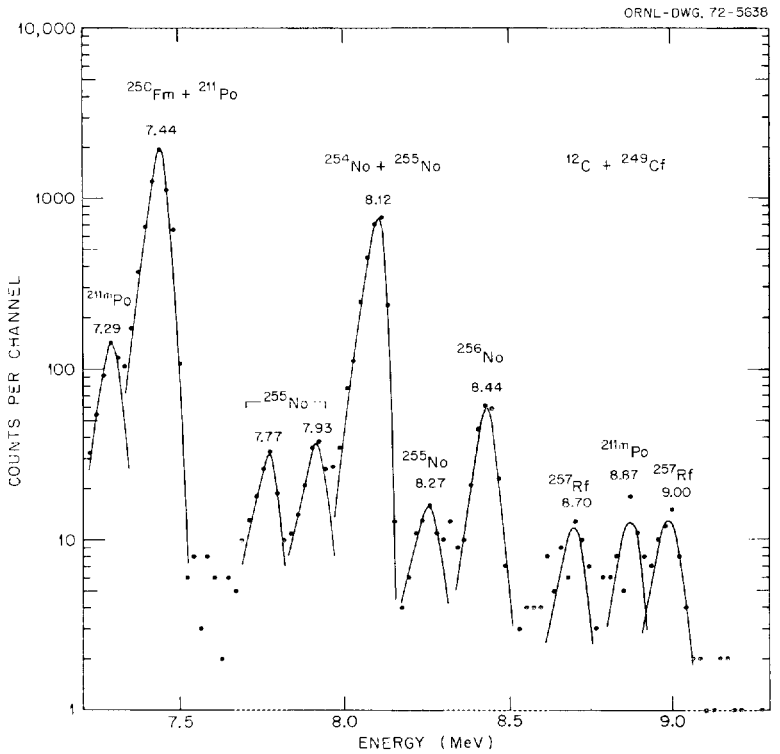

Fig. 2.10. Alpha-particle energy spectrum for activities produced in the bombardment of ^{249}Cf with 76-MeV $^{12}C^{4+}$ ions.

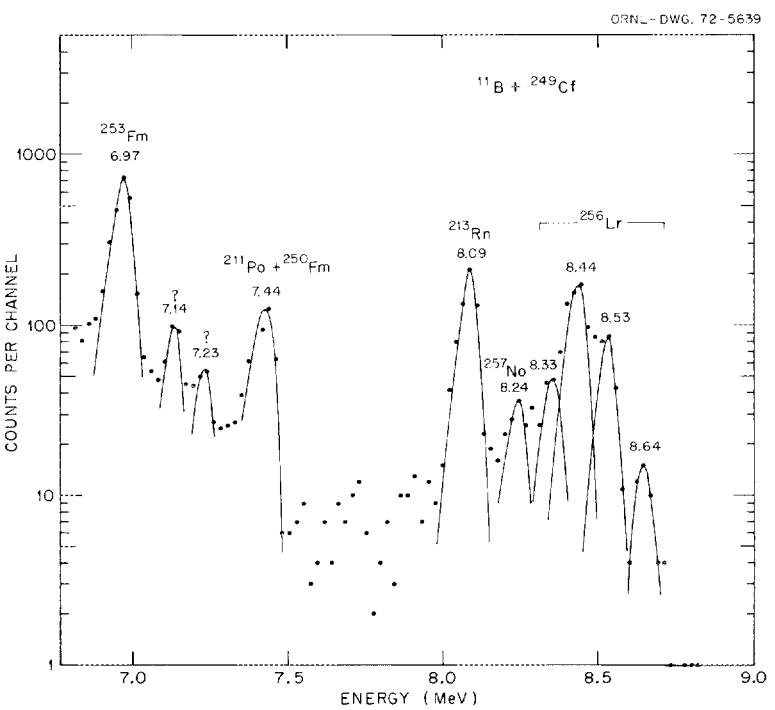

Fig. 2.11. Alpha-particle energy spectrum for activities produced in the bombardment of ^{249}Cf with 62-MeV $^{11}B^{3+}$ ions.

RADIOACTIVITY ASSOCIATED WITH RADIOHALOS

R. V. Gentry[1] J. W. Boyle

While the nature of the radioactivity associated with dwarf halos and giant halos is as yet unresolved, some interesting developments have taken place. Prior reports[2,3] of the existence of very low-energy alpha activity, which could possibly be related to the origin of the dwarf halos, were investigated by visiting some of the original investigators, F. Hernegger in Vienna and R. Coppens in Nancy, France. Follow-up contacts in France by F. Perey[4] resulted in the acquisition of certain hematite samples which purportedly contain low-energy alpha activity. Samples of this hematite have been prepared for nuclear-emulsion experiments in an attempt to duplicate the results of Coppens, who reported finding several unknown low-energy alpha emitters, using this technique.

In our experiments some short tracks similar in length to those described by Coppens have been found, but more experiments are necessary before any definite statement can be made as to the origin of these tracks. Additional alpha spectrometric studies on these and other samples extracted from dwarf-halo-bearing minerals are being carried out using a conventional solid-state detector.

Ion microprobe analyses of the various halo inclusions have been somewhat delayed by problems associated with installation and calibration of the ion probe at the Y-12 Plant. Ion probe results on NBS standard Pb show good agreement with NBS-determined Pb isotope ratios. Those results give confidence that the Pb isotope ratios (and other heavy nuclides) existing in small halo inclusions can be determined in situ by this technique.[5]

Another phase of the research on radiohalos has been with respect to the question of relating halo radii to alpha ranges in mica. It was reported several years ago[6] that alpha ranges determined by Van de Graaff irradiation seemed to agree with halo radii. However, since a recent report[7] has raised this question again, new experiments were performed on the ORNL Van de Graaff and on the University of Maryland Van de Graaff. In addition to mica, fluorite and cordierite were also irradiated to determine an experimental range-energy curve in these minerals. These induced ranges, together with a comparison of halo radii, will be published soon.

1. Visiting scientist from Columbia Union College, Takoma Park, Md.
2. A. Brukl, F. Hernegger, and H. Hilbert, *Akad. Wiss. Math. Naturwiss. Kl. Sitzungber. Abt. IIA* **160**, 129 (1951).
3. R. Coppens, *C.R. Acad. Sci.* **243**, 582 (1956).
4. Neutron Physics Division.
5. R. V. Gentry, *Science* **173**, 727 (1971).
6. R. V. Gentry, *Science* **169**, 670 (1970).
7. R. M. Spector, *Phys. Rev. A* **3**, 1323 (1972).

SEARCH FOR SUPERHEAVY ELEMENTS IN NATURE

J. S. Drury

During this report period several different techniques were employed at ORNL to detect superheavy elements in nature. This contribution summarizes only the work involving the use of the fire-assay technique, followed by spontaneous-fission counting.[1]

Our search was extended to a wide variety of ores and minerals. Following is a tabulation of the samples by type and location:

Sample	Source
Barite	Flathead Mine, Montana, and Northumberland, England
Enargite	Montana
Enstatite (bronzite)	Webster, N.C.
Forsterite	Bigelow Twp., Quebec, Canada
Galena	Park City, Utah
Gersdorffite	Rankin Inlet, Northwest Territories, Canada
Glauconite	Hazlet, N.J.
Glauconitic sandstone	Afton, Minn.
Goethite	Story Point, Virginia, and Biwabik, Minn.
Gold (auriferous conglomerate)	Central Rand, Transvaal, Africa
Gold (in quartz)	Lead, S.D.
Hausmannite	Iwate-Ken, Hanshu, Japan
Hematite	Clinton, N.Y., and Ironton, Minn.
Hematite (micaceous)	Ishpeming, Mich.
Ilmenite Sand	Melbourne, Fla.
Jamesonite	Bolivia, South America
Löllingite	South Lorraine, Ontario, Canada
Magnetite (lodestone)	Iron County, Utah
Magnetite sand	Los Angeles County, Calif.
Magnetite in chlorite schist	Chester County, Pa.
Olivine	Jackson County, N.C.
Pyrargyrite	Beaverdell, British Columbia
Pyrochroite	Iwate-Ken, Honshu, Japan
Pyroxene (diopside)	Hull, Quebec, Canada
Pyroxene (hedenbergite)	Silverstar, Mont.
Pyroxene (pigeonite)	Loudoun County, Va.
Pyroxenite (fassaite)	Helena, Mont.
Pyroxenite (harzburgite)	Nye, Mont.
Rhodonite	Butte, Mont.
Rhodonite (fowlerite)	Franklin, N.J.
Riebeckite	El Paso County, Colo.
Serpentine	Snarum, Norway, and Cornwall, England
Tennantite	Sells Mine, Alta, Utah

No evidence for the presence of superheavy elements was found in any of the samples.

1. J. S. Drury, *Chem. Div. Annu. Progr. Rep. May 20, 1970*, ORNL-4581, p. 46.

NEUTRON EMISSION MEASUREMENTS OF NATURAL SAMPLES

R. W. Stoughton R. V. Gentry[1]
J. Halperin R. M. Milton[2]
J. S. Drury J. H. McCarthy[3]
R. L. Macklin[4]

In a continuing effort to measure neutron emission in natural samples for evidence of superheavy elements, a number of ores, minerals, concentrates, and special samples have been examined in the neutron multiplicity counter.[5] This counter, containing 20 ^{3}He detectors in a paraffin matrix, enables the examination of large samples (20-liter volume) with little or no chemical processing to evaluate the emitted neutron multiplicity spectrum. This is an effective tool in the search for superheavy elements, since either their decay or the decay of daughter nuclides is expected to proceed by spontaneous fission. Furthermore, the parameter $\bar{\nu}$ (average number of prompt neutrons emitted in the fission act) has been estimated[6] to be very high for superheavy nuclides; for example, $\bar{\nu}(114^{298}) \simeq 10$ in contrast to $\nu \lesssim 4$ for all known spontaneously fissioning nuclides. Thus, in addition to providing a unique indicator, this predicted high value of $\bar{\nu}$ enhances the absolute counting sensitivity. A neutron multiplicity counter with a single neutron counting efficiency $\epsilon^0 = 0.30$ would exhibit an efficiency of $\epsilon(\geqslant 3) = 0.62$ for observing multiplicities of three or greater and $\epsilon(\geqslant 4) = 0.35$ for observing multiplicities of four or greater in a fission event in which ten neutrons were emitted. On the basis of a capability for detecting 1.0 fission event per day for a nuclide with a 10^8-year half-life (approximately the shortest half-life for a nuclide to have survived geologic times), the maximum sensitivity of the counter for such a measurement can be estimated to be $\sim 5 \times 10^{10}$ atoms or $\sim 10^{-15}$ g/g.

The results of this study are summarized in Table 2.3. The first four columns include the description of the sample, weight, and length of time measured. The fifth and sixth columns list the observed rate (counts/day) of triplets, and quadruplets and greater respectively. The last column gives the neutron multiplicity rate for ($\geqslant$4's) following corrections for variable factors in the background. Although the counter is some 50 ft below grade and the nucleonic component of the cosmic-ray spectrum has been largely filtered out, the muon component contributes appreciably to the background of samples of high Z. An empty counter gives rise to a background Bgd(3) $\simeq$ 1.2 counts/day and Bgd($\geqslant$4) $\simeq$ 0.2 count/day. If iron is introduced into the counter, it contributes a rate of $R(3) \simeq 0.35$ count day^{-1} kg^{-1} and $R(\geqslant 4) \simeq 0.12$ count day^{-1} kg^{-1}; lead contributes a rate of $R(3) \simeq 0.4$ count day^{-1} kg^{-1} and $R(\geqslant 4) \simeq 0.8$ count day^{-1} kg^{-1}. The nuclide ^{238}U is the only significant neutron emitter in nature [$T_{1/2}$(S.F.) = 8.2 $\times 10^{15}$ years, $\bar{\nu} = 2.0$] and gives rise to a rate of $R(3)$ = 7 counts day^{-1} g^{-1} and $R(\geqslant 4) = 0.7$ count day^{-1} g^{-1} in the counter.

In general, the corrections applied were small except for large samples of high Z such as lead and for samples containing appreciable quantities of uranium. The measurements of multiplicities ($\geqslant$4) were used to evaluate evidence for high-multiplicity spontaneous fission (i.e., possible superheavy elements). However, none of the samples we have examined gave evidence of spontaneous fission rates in excess of the detection limit [~0.5 count/day for multiplicities ($\geqslant$4)]. The corrected rates were in every case less than 0.5 count/day, with many observed rates less than the estimated backgrounds. However, the uncertainties due to low counting statistics and background corrections suggest that an upper limit of 0.5 count/day be placed on the samples listed in the table with the following exceptions. The uncertainties in the measurement of the 46.2-kg galena due to its high lead content and the 22-kg monazite due to its high uranium content indicate that these samples be considered as exhibiting less than 2 counts/day.

Theoretical estimates[6,7] identify Z = 110–124 as the anticipated region of enhanced nuclear stability associated with the double-shell closure at Z = 114 and N = 184. We have examined a massive galena sample with respect to our interest in element 114, ekalead. Further, the sample listed as galena-barite came from the top of a galena vein incorporating some elemental gold. We have examined several other chalcophilic samples, iron and zinc sulfides, as well as the mineral cerussite, $PbCO_3$. The two flue dust samples were collected at different stages in Cottrell precipitators from the roasting of pentlandite, iron nickel sulfide. Calculations by Keller et al.[8] indicate that element 114 can be expected to be even more volatile than mercury, and intermediate between lead and gold in nobility. In this connection, we attempted a technique successfully developed to locate mercury ore bodies.[9] Air in the vicinity of such ore bodies is passed over gold or silver foils; these are subsequently heated to release mercury, which can be

Table 2.3. Neutron multiplicity measurements of natural samples

Sample	Principal components	Wt (kg)	Time (days)	Observed neutron multiplicity (counts/day)		Corrected neutron multiplicity (counts/day)
				(3's)	(≥4's)	(≥4's)
Galena Colorado	Pb, S	46.3	4.22	14	15	(−5)
Galena, barite, some Au Colorado	Pb, S, Ba, $(SO_4)^{2-}$	14.5	1.50	1.5	0.7_3	−0.8
Pyrrhotite, mill conc. Ontario, Canada	Fe, S	30	2.84	3.7	0.0	−0.5
Pyrite Mexico	Fe, S	0.25	6.63	1.9	0.0	−0.2
Sphalerite, mill conc. Colorado	Zn, S	29.5	4.07	4.3	0.8_7	+0.2
Cerussite S. W. Africa	Pb, CO_3^{2-}	3	4.89	1.8	1.0	−0.2
Flue dust, Cottrell recov. — Fe Ontario, Canada	Fe, Ni, Cu, O	13.6	4.26	2.5	0.8_1	+0.2
Flue dust, Cottrell recov. — Ni Ontario, Canada	Fe, Ni, Cu, O	16.3	3.06	2.6	0.7_6	+0.2
Au, Ag foils — Hg mine Nevada, Arizona	Ag, Au	0.5	3.90	0.3	0.3	+0.1
Silica gel, crude Xe Linde Plant, New York	Xe	0.5	3.97	2.2	0.5	+0.3
Felsic norite Ontario, Canada	Mg, Fe, Ca, $(Si_2O_6)^{4-}$	30	3.26	1.4	0.7_1	+0.2
Dark norite Ontario, Canada	Mg, Fe, Ca, $(Si_2O_6)^{4-}$	30	3.12	1.3	0.4_2	−0.1
Kimberlite Tennessee	Mg, Fe, Al, $(Si_2O_6)^{4-}$	10.4	2.94	1.6	0.0	−0.3
Potash ore New Mexico	K, CO_3^{2-}	24.5	4.94	0.94	0.0	−0.3
Potash ore Ontario, Canada	K, CO_3^{2-}	24.5	3.89	1.19	0.0	−0.3
Salt fraction — bittern Great Salt Lake, Utah	Cs, Rb, Li, Mg, Cl	8	3.12	1.5	0.0	−0.2
Salt fraction — potash Great Salt Lake, Utah	K, Cl	20.2	2.03	0.6	0.0	−0.2
Salt fraction — sodium Great Salt Lake, Utah	Na, Ca, Cl	19.5	4.01	0.3	0.0	−0.2
Native bismuth Saxony, Germany	Bi	1.0	5.73	3.85	0.8_1	0.0
Refined bismuth unknown	Bi, O	1.5	4.69	2.8	1.2	+0.1
Meteorites — Canyon Diablo Arizona	Fe, Ni	31.3	4.05	5.8	2.0	−0.2
Meteorites — Odessa, Texas Brenham, Kansas	Fe, Ni	12.2	5.84	4.3	0.5_1	−0.3
Mica and monazite Sweden and Madagascar	K, Mo, Fe, $(AlSi_3O_{10})$, $^{5-}$ R. E., Th, U, $(PO_4)^{3-}$	0.5	5.03	2.5	0.4_1	+0.1

Table 2.3 (continued)

Sample	Principal components	Wt (kg)	Time (days)	Observed neutron multiplicity (counts/day)		Corrected neutron multiplicity (counts/day)
				(3's)	(≥4's)	(≥4's)
Monazite Australia	R. E., Th, U, $(PO_4)^{3-}$	22	1.05	220	16	(−4)
Hematite and magnetite Elba	Fe, O	5	4.85	3.6	0.2_4	−0.2
Hematite California	Fe, O	31.8	4.26	1.1	0.2_7	−0.2

detected spectroscopically. We exposed two gold foils and one silver foil in the adit of the Pershing Mine, Nevada (adit air flow: 9 fps; 0.6 μg Hg/m^3), for 15 days. The mine is an ex-mercury producer and has ore containing pyrite and stibnite. We similarly exposed two gold foils and one silver foil for eight days in the adit of the Ord Mine, Arizona (adit air flow: 3 fps; 20 μg Hg/m^3), which is another ex-mercury producer. Presumably, some of the elements between 112 (ekamercury) and 116 (ekapolonium), if they exist, might be collected in this manner.

In connection with element 118 (ekaradon), we have examined a sample of silica gel previously used over a period of months in the Linde plant at Tarrytown, New York, for sorbing and desorbing gases for the production of noble gases, together with a 1-liter sample of a gas mixture of crude xenon. With respect to our interest in element 110 (ekaplatinum), several ultrabasic rocks were examined (the norites and kimberlite); in some cases such rocks have been found to support platinum values. In connection with element 119 (ekafrancium), we have examined several potash ores as well as fractions from the Great Salt Lake, Utah. The bittern (rich in Cs, Rb, Li, and Mg) is a concentrate of the brine following removal of the sodium chloride and the potash fractions.

A sample of native bismuth as well as some reagent bismuth has been examined (element 115 is ekabismuth). Malý had previously reported[10] unexplained fission tracks in Lexan which had been placed in contact with bismuth for a period of months. Several iron-rich meteorites (Canyon Diablo, Odessa, and Brenham) have been examined which presumably sample the siderophilic phase. We have examined samples of biotite from Sweden in which rare dwarf halos have been found together with some monazite from Madagascar associated with giant halos.[11] We have also examined a larger sample of Australian monazite. We have examined some hematite and magnetite samples from the Island of Elba reported[12] to contain some unexplained low-energy alphas. We have also looked at a more massive hematite sample from California.

1. Visiting scientist from the Institute of Planetary Science, Columbia Union College, Takoma Park, Md.
2. Union Carbide Corp., Linde Laboratories, Tarrytown, N.Y.
3. U.S. Dept. of the Interior, Geological Survey, Denver, Colo.
4. Physics Division.
5. R. L. Macklin, F. M. Glass, J. Halperin, R. T. Roseberry, R. W. Stoughton, and M. Tobias, *Chem. Div. Annu. Progr. Rep. May 20, 1971*, ORNL-4706, p. 87; *Nucl. Instrum. Methods*, in press.
6. J. R. Nix, *Phys. Lett. B* **30**, 1 (1969).
7. M. Bolsteri, E. O. Fiset, J. R. Nix, and J. L. Norton, *Phys. Rev. C* **5**, 1050 (1972).
8. O. L. Keller, J. L. Burnett, T. A. Carlson, and C. W. Nestor, *J. Phys. Chem.* **74**, 1127 (1970).
9. J. H. McCarthy et al., "Mercury in Soil Gas and Air – A Potential Tool in Mineral Exploration," Geological Survey Circular 609 (1969); W. W. Vaughn, "A Simple Mercury Detector for Geochemical Prospecting," Geological Survey Circular 540 (1967).
10. J. Malý, private communication (1971).
11. R. V. Gentry, *Science*, **169**, 670 (1970); **173**, 727 (1971).
12. R. V. Gentry and F. G. Perey, private communication (1971).

SAMPLES COUNTED IN LBL NEUTRON MULTIPLICITY COUNTER IN A SEARCH FOR SUPERHEAVY ELEMENTS IN NATURE

R. C. Jared[1] J. S. Drury
E. Cheifetz[1] R. L. Silva
E. R. Giusti[1] R. W. Stoughton
S. G. Thompson[1] J. Halperin

In collaboration with the Lawrence Berkeley Laboratory, a number of natural samples were counted in the LBL scintillation neutron multiplicity counter, which is located in a tunnel under about 800 ft of dirt, giving it a low background even for large amounts of high-Z

material. None of these samples has shown evidence of the presence of superheavy elements, as far as we can tell. Such results are consistent with a half-life for spontaneous fission of about 10^{23} years (3 kg) to 10^{24} years (20 kg) for the principal component(s). (Alternatively, if the half-life of the superheavy element is 10^9 years, an upper limit of about 10^{-14} g of superheavy element per gram of sample is indicated.)

Many of these samples came from mines, smelters, etc., of the Sudbury region of Canada;

Wt (kg)	Description
3	Composite sample, precious metals
4	Ni conc
3	Blast furnace dust
3	Flue dust, Intern. Nickel
4	CuS, mill conc, Intern. Nickel
3	Blast furnace dust
3	Smelter flue dust

several others came from mines, smelters, etc., of Colorado:

Wt. (kg)	Description
4	Ag, Cu, Pb conc from Creede
10	PbS conc, Silverton
4	Pb, Ag, Zn sulfide, Creede
4	Cu, Ag, Pb, Au, Zn conc, Telluride
4	Pb, Ag, Au, Zn sulfide conc, Telluride
10	Pb, Zn sulfide ore, Creede
3	Zn, Pb, Cu, Ag, Au sulfide ore, Silverton
4	Cu, Pb, Zn sulfide ore, Silverton
4	Pb, Ag, Fe, Zn sulfide ore, Creede
4	Pb, Ag, Zn sulfide ore, Creede
4	PbS ore containing Ag, Au, Zn, Telluride
4	PbS ore, Telluride

In addition we sent 20 kg of PbS concentrate (from Ivigtut, Greenland) which shows a high ^{204}Pb content, indicating more primordial lead than any lead ore except that from the Rosetta Mine in Africa, as far as we know, and three separate 10-kg samples of an ultrabasic magma, similar in composition to kimberlite, from the Norris Lake Region in Tennessee.

In addition, other miscellaneous ores investigated were as follows:

Wt (kg)	Description
3	Pt, Pd bearing rock, Transvaal
3	Composite chromite, S. Rhodesia
3	Composite strontium ore, Hamm, Westphalia
3	Quartz containing Au, S. Dakota
4	Cinnabar, Arizona
3	Chromite + Zn conc, S. Rhodesia
3	Unburned bag house fume dust, Tooele, Utah
3	Serpentinite from mid-Atlantic ridge at equator
3	KCl ore, Hobbs, N.M.
20	Bastnasite ($CeFCO_3$), Mt. Pass, Calif.
20	Canyon Diablo iron meteorites
12	Cerussite ($PbCO_3$), New Mexico
7	Barite, Sweetwater, Tenn.
10	Galena, Cour D'Alene Region, Idaho

1. Lawrence Berkeley Laboratory (formerly the Lawrence Radiation Laboratory, University of California, Berkeley).

SEARCH FOR SUPERHEAVY ELEMENTS IN TANTALUM TARGETS FROM SLAC[1]

J. Halperin — R. E. Druschel
Donald Busick[1] — R. L. Macklin[2]
Dieter Walz[1] — R. W. Stoughton

Marinov et al.[3] have given some evidence for the production of ^{262}Cf and possibly a superheavy element in tungsten targets which had been irradiated with about 10^{18} protons of 24 GeV at CERN. Malý[4] has presented evidence for the production of high-energy fission fragments when U, Pb, and W foils were irradiated with 550- and 1300-MeV electrons. Since sufficiently high-energy fragments could penetrate a target nucleus, we thought it would be interesting to look at heavy-metal targets or beam stops from SLAC with our neutron multiplicity counter. We obtained two sets of Ta targets: Ta-I consisting of 12 sheets ($4 \times 4 \times 0.040$ in.) which had been irradiated with 1.46×10^{19} electrons of about 20 GeV, and Ta-II consisting of two such sheets which had been exposed to $(6.8 \pm 0.7) \times 10^{19}$ electrons of similar energy. Unfortunately, when the Ta-I sheets were irradiated, water in the vicinity produced many secondary neutrons of relatively low energy. These in turn produced 115-day ^{182}Ta and 42-day ^{181}Hf in large quantities which caused a serious radiation hazard in handling the sheets. We were able to count Ta-I by using some Pb and Al shielding inside the counter and by raising the lower limit of our energy window. We counted separately: (1) all twelve sheets, and (2) the three considered most likely to contain superheavy elements. The background was obtained with the Pb-Al shielding in place. Ta-II was much less radioactive, having been associated with a minimal amount of cooling water during the irradiation. Aluminum shielding was sufficient, together with a slight raising of the lower limit of the energy window, to enable measurement of this sample. None of the samples counted showed multiplicities of 3 or greater to

be above background. The results of Ta-II are:

Sample	Time counted (days)	Multiplicity count rate (day^{-1})	
		(3's)	(≥4's)
Ta-II	4.90	2.2_5	1.4_3
Bkgd	4.06	3.6_9	1.4_7

One square inch was cut out of the sheet (Ta-I) considered most likely to contain superheavy elements for chemical studies and was dissolved in an HNO_3-HF mixture. In addition to the ^{182}Ta and ^{181}Hf, the 107-day ^{88}Y and the 70-day ^{175}Hf spallation products were readily identified. An LaF_3 precipitation removed lanthanides and actinides from this solution; after metatheses to $La(OH)_3$ with NaOH, it was dissolved in HCl. The solution was put successively through a Dowex 1 and Dowex 50 column to decrease activities other than lanthanides and actinides, and was then put through two successive α-hydroxyisobutyric acid columns to fractionate the lanthanides and actinides. No actinides were seen. A number of beta-gamma-emitting spallation products were seen, as was the 3.18-MeV alpha of 93-year ^{148}Gd. The one square inch of Ta appeared to have received about one-half of the beam by visual inspection. The observed alpha rate of the ^{148}Gd was 3.6×10^7 dis/day, which is equivalent to a formation cross section of about 50 μb for 20-GeV electrons on Ta.

1. Stanford Linear Accelerator Center, Stanford, Calif.
2. Physics Division.
3. A Marinov et al., *Nature (London)* **229**, 464 (1971); **234**, 212 (1971).
4. J. Malý, *Phys. Lett. B* **35**, 148 (1971).

SEARCH FOR SUPERHEAVY ELEMENTS IN TUNGSTEN AND URANIUM TARGETS FROM BNL

J. Halperin J. H. Oliver
R. W. Stoughton R. L. Macklin[1]
J. Hudis[2]

As mentioned last year,[3] in view of the possible production of ekamercury in a tungsten target irradiated with 24-GeV protons at CERN,[4] we obtained two tungsten targets and one of natural uranium from colleagues at BNL. One was a 5-g piece of Heavimet (90% W, 7% Ni, 3% Cu) of shape 0.25 × 0.5 × 2.0 cm, another was a 43-g piece of W of shape 0.25 × 1.3 × 7.6 cm, and the uranium was a 290-g piece of larger dimensions. All had been irradiated with $\sim 1.3 \times 10^{17}$ protons of about 25 GeV over periods of many months. The Heavimet, the tungsten, and the uranium had cooled 2 years, 3 months, and several months, respectively, before our receiving them.

The Heavimet, inside the can in which it came, was counted in our neutron multiplicity counter.[5] The tungsten was more radioactive, so it was counted inside a 346-g lead pig to decrease counts due to gamma-ray "pileup." Subsequently, the Heavimet and the tungsten pieces were counted together in the lead pig. The uranium piece was dissolved in concentrated nitric acid, and the uranium was removed from a 12% aliquot of the aqueous phase (1.5 *M* HNO_3) by repeated extractions with 30% TBP in dodecane. The aqueous phase should have contained nearly everything except the uranium, and was counted in the neutron multiplicity counter. None of these samples showed neutron multiplicities ≥4 above background. Some of the results obtained are:

Sample	Time counted (days)	Multiplicity count rate (day^{-1})	
		(3's)	(≥4's)
W + Heavimet	4.09	0.4_9	0.2_4
Bkgd (346 g Pb)	8.56	1.0_4	0.8_2
Aq phase from U ext'n	2.59	1.9_3	0
Bkgd	2.09	0	0

The apparent high number of (3's) in the second sample may have been due to incomplete removal of uranium.

The aqueous solution from the uranium extraction was chemically treated by 100% TBP extractions and ion exchange to yield a solution which should have contained the actinides and lanthanides. These were then electrodeposited onto a Pt plate and counted for alphas. Many beta-gamma-emitting or alpha-emitting spallation products were found, including members of the natural radioactive series; the alpha emitters diminished the sensitivity for detecting actinides. We did observe the 3.18-MeV alpha of the 93-year ^{148}Gd, which was produced in good yield (450,000 dis/day). This would be equivalent to a cross section for production of ^{148}Gd from proton interaction with uranium of about 7 μb.

The activities on this plate were dissolved off with an HNO_3-HCl mixture. Then the lanthanides and actinides were further purified with two successive Dowex 50, Dowex 1 cycles. Polonium-210 and ^{208}Po were removed by chemically depositing them onto a silver disk. An oxidation-reduction cycle with CeF_3 precipitations was used to separate plutonium from lanthanides (and

difficultly oxidizable actinides, if present). After electrodeposition, the lanthanide fraction contained about two-thirds as much ^{148}Gd as mentioned above. The plutonium fraction contained ^{236}Pu, ^{238}Pu, and ^{239}Pu in alpha ratios relative to ^{148}Gd of 2.6_6: 0.3_3:0.3_0:1.00. These results are equivalent to cross sections of about 0.5_7 μb, 2.2 μb, and 0.54 mb for producing the respective Pu isotopes, on the assumption that they were formed in a reaction of U with the primary protons. No other actinides were found; this means that their alpha activities were less than about 10^{-3} times that of ^{148}Gd.

1. Physics Division.
2. Brookhaven National Laboratory, Upton, Long Island, N.Y.
3. J. Halperin et al., *Chem. Div. Annu. Progr. Rep. May 20, 1971*, ORNL-4706, p. 71.
4. A Marinov et al., *Nature (London)* **229**, 464 (1971); **234**, 212 (1971).
5. R. L. Macklin et al., *Chem. Div. Annu. Progr. Rep. May 20, 1971*, ORNL-4706, p. 87; *Nucl. Instrum. Methods*, in press.

SEARCH FOR SUPERHEAVY ELEMENTS IN U-Zr TARGETS FROM RUTHERFORD HIGH-ENERGY LABORATORY

G. G. J. Boswell[1] R. E. Druschel
J. Halperin H. W. Schmitt[2]
G. W. A. Newton[3] R. W. Stoughton

Two rods of 1:1 (atomic ratio) alloy of uranium and zirconium (37 g each) were irradiated for three weeks with 7-GeV protons at the Rutherford High-Energy Laboratory in March and April of 1970. One of the rods (UZr-1) had been irradiated with 3.0×10^{16} protons, the other (UZr-2) with 1.6×10^{17} protons. They were dissolved in HNO_3-HF mixtures to avoid the explosive hazard,[4] and boric acid was added to complex the fluoride. UZr-1 was extracted with dioctyl phosphate to remove most of the uranium, zirconium, and thorium, while leaving most other elements in the aqueous phase. UZr-2 was further treated with TBP extractions and by ion exchange to remove thorium to a greater extent. The aqueous phases containing most elements in the targets other than U, Zr, and Th were sent to ORNL and counted about a year after the irradiations in our neutron multiplicity counter.[5]

The measurements were carried out both with and without an anticoincidence mantle above the counter to decrease neutron bursts resulting from reactions of cosmic-ray muons with nuclei. The results are as follows:

Sample	Anticoincidence mantle	Counting time (days)	Rate (per day)		
			(2's)	(3's)	(≥4's)
Bkgd	Yes	1.94	26.7	1.22	0
Bkgd	No	5.31	29.6	1.31	0.19
UZr-1	Yes	1.70	22.1	2.12	0
UZr-1	No	4.12	30.6	1.46	0
UZr-2	Yes	6.79	16.3	2.41	0
UZr-2	Yes	2.68	19.3	0.88	0

These rates have been corrected for an ~15% "dead time" when the anticoincidence mantle was in operation. For $\bar{\nu}$ = 10 neutrons per fission, our efficiencies for multiples of (≥3) and (≥4) are 62 and 35% respectively. We conclude that there was less than about one fission per day with a large $\bar{\nu}$ (say greater than ~7).

We looked for actinides, which might have been formed in secondary reactions, in 200-μl aliquots of the initial UZr-1 solution. The procedure involved removing a CeF_3 precipitate, metathesizing with NaOH, and dissolving in HCl. Then followed three precipitations of $Ce(OH)_3$ with NH_4OH, each one being dissolved in HCl. The material containing the Ce(III) was then passed through a Dowex 50 and a Dowex 1 column to remove much of the Ce(III) and extraneous activities. Finally, any actinides and lanthanides present were electroplated onto a Pt plate and counted for alphas. No actinides were seen. Gadolinium-148 (3.18 MeV) and ^{210}Po (5.30 MeV) were definitely identified.

1. University of Salford, England.
2. Physics Division.
3. University of Manchester, England.
4. R. P. Larsen et al., *A Study of the Explosive Properties of Uranium-Zirconium Alloys*, ANL-5135 (July 1954).
5. R. L. Macklin et al., *Chem. Div. Annu. Progr. Rep. May 20, 1971*, ORNL-4706, p. 87; *Nucl. Instrum. Methods*, in press.

RELATIVE ENERGIES OF THE LOWEST LEVELS OF THE $f^q ps^2$, $f^q ds^2$, AND THE $f^{q+1}s^2$ ELECTRON CONFIGURATIONS OF THE LANTHANIDE AND ACTINIDE NEUTRAL ATOMS[1]

K. L. Vander Sluis[2] L. J. Nugent

Linearity of the differences between the lowest levels of the $f^q ps^2$, $f^q ds^2$, and the $f^{q+1}s^2$ electron configurations as a function of q was demonstrated for the lanthanide and actinide series. A linear extrapolation of these differences estimates the energy of the lowest level of the $4f^{14}6p6s^2$ electron configuration of

Lu to be 3.5 kK (1 kilokayser = 10^3 cm^{-1}) higher than the measured value. This deviation from linearity is attributed to expected discontinuities at the $q = 0$ and $q = 14$ end of the $f^q ds^2$ series. In the actinide series the corresponding linear extrapolation predicts the lowest level of the $5f^{14}7p7s^2$ electron configuration of Lr to be 2.3 ± 3 kK above the expected $5f^{14}6d7s^2$ ground state, after correction for a corresponding 3.3-kK deviation expected at the end of the actinide series.

1. Accepted for publication in the *Physical Review.*
2. Physics Division.

ELECTRON-TRANSFER AND $f \rightarrow d$ ABSORPTION BANDS OF SOME LANTHANIDE AND ACTINIDE COMPLEXES AND THE STANDARD (II-III) OXIDATION POTENTIALS FOR EACH MEMBER OF THE LANTHANIDE AND ACTINIDE SERIES[1]

L. J. Nugent R. D. Baybarz
J. L. Burnett[2] J. L. Ryan[3]

A powerful new correlation technique, based on theoretical and experimental results of atomic spectroscopy, is shown[1] to be generally applicable for intraseries correlations of various physical and chemical properties, such as oxidation potentials, first electron-transfer-absorption-band energies, and first $f \rightarrow d$ absorption-band energies of the compounds and complexes of the lanthanide and actinide series. For many of the members of these series, representative values of some of these properties were available from the literature; for others new measurements were made. Thus sufficient data were available to provide a convincing test of the general validity of the theory, and hence to map out many of these properties for all the members of both series. The most important new results of this work are the determination or verification of the following standard oxidation potentials (E°), all relative to the standard oxidation potential of the normal hydrogen electrode:

Sm(II-III)	+1.55 V
Eu(II-III)	+0.35 V
Tm(II-III)	+2.3 ± 0.2 V
Yb(II-III)	+1.15 V
Am(II-III)	+2.3 ± 0.2 V
Cm(II-III)	+4.2 ± 0.2 V
Bk(II-III)	+2.8 ± 0.2 V
Cf(II-III)	+1.6 ± 0.2 V
Md(II-III)	+0.15 V
No(II-III)	−1.45 V

1. To be submitted for publication in the *Journal of Physical Chemistry.*
2. Division of Research, United States Atomic Energy Commission, Washington, D.C.
3. Pacific Northwest Laboratories, Richland, Washington.

SYSTEMATICS CORRELATING SOME THERMODYNAMIC PROPERTIES OF THE LANTHANIDE AND ACTINIDE METALS[1]

L. J. Nugent J. L. Burnett[2]
L. R. Morss[3]

Systematics correlating some of the thermodynamic and spectroscopic properties of the metals, M, of the lanthanide and actinide series have been used to treat the enthalpy of sublimation at 298°K, $\Delta H_S{}^0(M)$, the standard aqueous enthalpy of formation of the metal aquo ion at 298°K, $\Delta H_f{}^0(\mathrm{III})$, and the difference in energy, $\Delta(M)$, between the lowest lying energy level of the trivalent $f^n s^2 d^1$ electronic configuration and the lowest lying energy level of the divalent $f^{n+1}s^2$ electronic configuration of the neutral gaseous atoms. Previously reported data most likely in error can be pointed out, and best values of $\Delta H_S{}^0(M)$ and $\Delta H_f{}^0(\mathrm{III})$ for each member of the lanthanide and actinide series have been determined. The trends observed in $\Delta H_S{}^0(M)$ and $\Delta H_f{}^0(\mathrm{III})$ across each series are related to the number of valence electrons per atom in the metal crystal and in the gaseous metal atoms.

1. Accepted for publication in the *Journal of Chemical Thermodynamics.*
2. Division of Research, United States Atomic Energy Commission, Washington, D.C.
3. School of Chemistry, Rutgers University, New Brunswick, N.J.

ELECTRON BINDING ENERGIES IN AMERICIUM[1]

M. O. Krause F. Wuilleumier[2]

Employing the technique of photoelectron spectrometry we determined the binding energies of the electrons in the $4d$ to $6p$ levels of americium. Both the Mg $K\alpha$ and Al $K\alpha$ lines were used for excitation, and the resulting photoelectrons were dispersed in a 15-cm electrostatic double-focusing energy analyzer. The energy resolution $\Delta E/E$ was set to 0.16% (FWHM), and the deflection voltages were measured to an accuracy of better than 50 ppm. The Cu $2p_{3/2}$ level, $E_B = 932.9(4)$ eV, was taken as primary standard and the C 1s level,

Table 2.4. Experimental electron binding energies (in eV) of americium in $Am(OH)_3$ compared with theoretical and critically evaluated values for free Am atoms

Level	Expt., this work	Theory, ref. 3	Evaluations	
			Ref. 4	Ref. 5
$4d_{3/2}$	882.6(7)	877.4	888	878.7(1.0)
$4d_{5/2}$	832.1(5)	825.7	837	827.6(1.0)
$4f_{5/2}$	463.6(4)	470.1	471	
$4f_{7/2}$	449.3(4)	456.0	458	
$5s$	351.4(4)[a]	362.2	380	
$5p_{1/2}$		294.8	301	
$5p_{3/2}$	215.7(5)	224.8	227	
$5d_{3/2}$	121.0(5) 118.9(5)[b]	124.9	128	115.8(1.3)
$5d_{5/2}$	111.0(4) 109.4(4)[b]	114.3	116	103.3(1.1)
$6s$	50.4(6)[a]	54.9	87	
$6p_{1/2}$	40.2(6)[a]	35	69	
$6p_{3/2}$	31.7(5)	23.8	57	
$5f_{5/2}$	11.9(4)	7.9 6.6	6	
$5f_{7/2}$	11.9(4)		6	
$\Delta 4d$	50.5(6)	51.7	51	51.1
$\Delta 4f$	14.3(1)	14.1	13	
$\Delta 5d$	9.7(2)	10.6	12	
$\Delta 6p$	8.5[a]	11.2	12	

[a]Tentative assignment.
[b]Indicates the more intense peak.

E_B = 285.0(4) eV, as secondary standard. Americium was electrodeposited onto a 50-μm Pt foil from a near-neutral nitrate solution. The deposit was between 10 and 20 μg and, according to the preparation and handling procedure, very probably consisted of the trivalent americium hydroxide. Table 2.4 lists the measured values and compares them with theoretical predictions[3] and semiempirical evaluations.[4,5] Although the theoretical entries represent eigenvalues only, a surprisingly good accord exists with the experimental data. This recommends the calculation of Lu et al.[3] for use as a guide in cases where no dependable experimental data or evaluations or precise theoretical calculations exist.

1. Synopsis of paper published in *Electron Spectroscopy*, p. 759, D. A. Shirley, ed., North-Holland, Amsterdam, 1972.
2. Visiting scientist from Laboratoire de Chimie Physique de l'Université Paris VI, France.

3. C. C. Lu, T. A. Carlson, F. B. Malik, T. C. Tucker, and C. W. Nestor, Jr., *Atomic Data* 3, 1 (1971).
4. W. Lotz, *J. Opt. Soc. Amer.* 60, 206 (1970).
5. J. A. Bearden and A. F. Burr, *Rev. Mod. Phys.* 39, 125 (1967).

EVALUATION OF ATOMIC ENERGY LEVELS AND X-RAY ENERGIES FOR THE ACTINIDE ELEMENTS

M. O. Krause F. Wuilleumier[1]

Now that more than a sprinkling of measured values of level and x-ray energies of the actinides exists in literature, we considered it timely to check the mutual consistency of the reported values, to improve and, where necessary, adjust these values by injecting Moseley's modified prescription, and, most important, to determine values not yet measured. We are still in the process of completing the task, but would like to point out briefly here the procedure we have adopted and to present a few results for K, L, and M shells. We have at our disposal a number of accurate (order 1 eV) photoelectron determinations of levels of the light actinides, and a number of fairly accurate measurements (order 10 ev) from internal-conversion spectrometry for the elements Cm, Bk, Cf, and Fm. Also available are a number of x-ray energy measurements of the K and L series. In all, about one-half of the levels of K, L, and M shells have been measured in the actinide series. From our point of view, these are the raw data which need to be smoothed and from which we can also derive values for the remaining unknown levels. Previously, Bearden[2] and Bearden and Burr[3] recommended a set of values for x-ray energies and level energies on the basis of the few data and calculations available prior to 1966; and Lotz[4] offered a set of new values by reevaluating Bearden and Burr's set.

Our approach is the following: We "align" the measured electron spectrometric values of the levels that have been measured most frequently, that is, L_3 and M_5, by means of a modified Moseley diagram[5] corresponding to the function $f(E_B,Z) = [(E_B)^{1/2} - (AZ + B)]^{1/2} - (CZ + D)$. This version of the Moseley diagram has proven useful before in other regions of the Periodic Table, including the region of the lanthanides. A line according to $f(E_B,Z)$ without breaks (viz., no changes in the parameters A, B, C, and D) could be drawn through the measured level energies of the K and L electrons of the lanthanides.[5] We assume the modified Moseley diagram to be equally valid for the inner levels (K to N) of the actinides. Figures 2.12 and 2.13 show the measured basis points for the L_3 and M_5

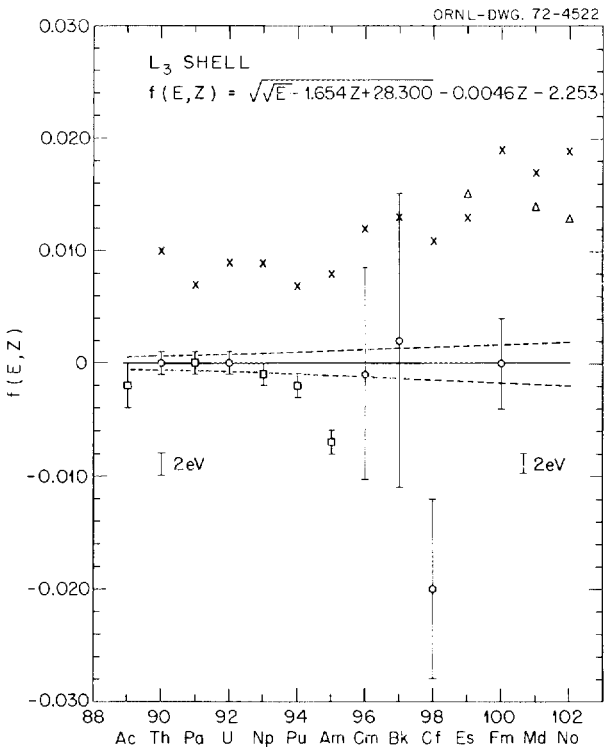

Fig. 2.12. Modified Moseley diagram fit to the measured L_3-level energies of the actinides. Dashed lines indicate our estimated error limits. Open circles are electron spectroscopic measurements (ESCA or internal conversion). They are the basis for the Moseley line fit. Squares are values recommended by ref. 3, and triangles are extrapolated values from the same source. Crosses are eigenvalues from ref. 6.

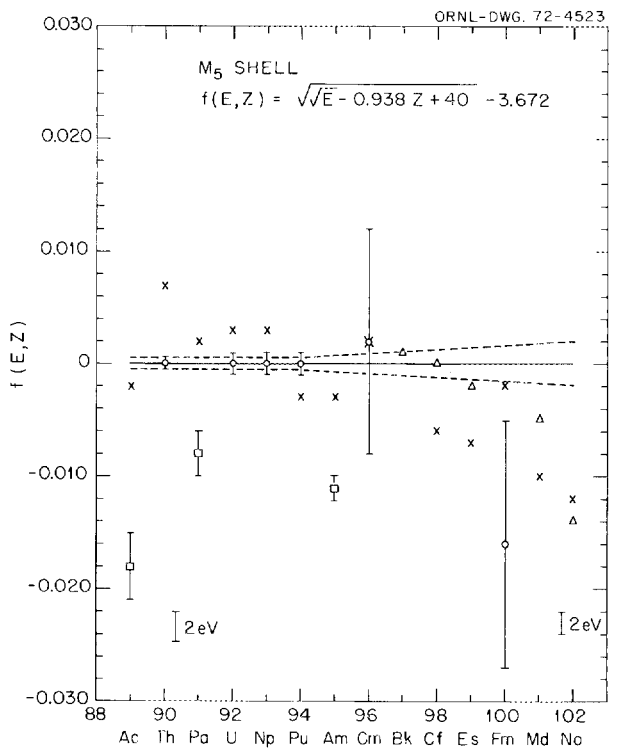

Fig. 2.13. Modified Moseley diagram fit to the reported M_5-level energies of the actinides. Key of symbols is the same as for Fig. 2.12. Dashed lines give estimated uncertainties.

shells respectively and the corresponding best-fit Moseley lines $f(E_B,Z)$. To evaluate the K-level energies, we preferred, however, to draw a best-fit Moseley line through the points of the measured energies of the $K\alpha_1$ x rays, and then derived the K levels from $L_3 + K\alpha_1$. This we felt gave the more accurate evaluation, since the $K\alpha_1$ energies are much better known than the K-level energies, few of which have been measured directly. Figure 2.14 gives the Moseley diagram for the $K\alpha_1$ x rays. As a second step we derived the "best" values from the Moseley lines of Figs. 2.12 to 2.14 for every element for L_3 and M_5 levels and $K\alpha_1$ x rays. Tables 2.5 to 2.8 list our "best" values for the actinide series of the K_1, L_3, and M_5 levels and of $K\alpha_1$ and $L\alpha_1$ lines. In the same tables, we also list the energy differences between the values obtained from earlier evaluations,[2–4] calculations,[6,7] and experiments,[8–17] and the values given by our present evaluation. Note that $L\alpha_1$ $(L_3 - M_5)$ is obtained as the difference between our values for L_3 and M_5 shells, and that the K levels are obtained from $L_3 + K\alpha_1$. The accuracy of the

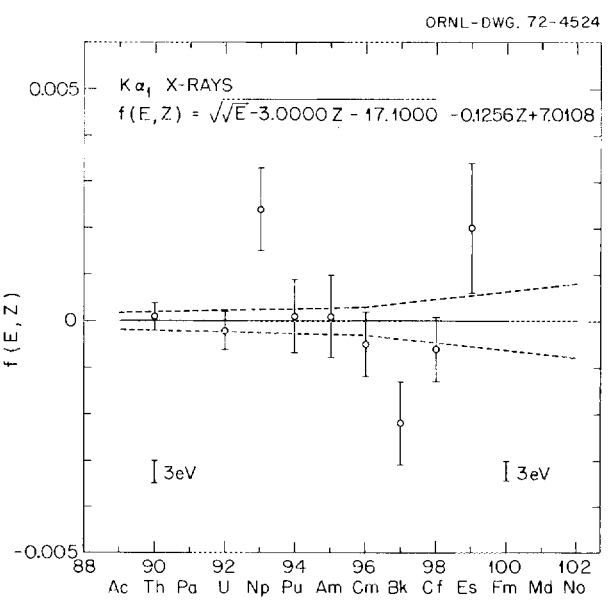

Fig. 2.14. Modified Moseley diagram fit to the measured (open circles) $K\alpha_1$ x-ray energies of the actinides. Triangles are interpolated values from ref. 3. Dashed lines indicate estimated error range.

Table 2.5. Binding energies (eV) of L_3 electrons for Z = 89 to 102

Accuracy of our values is estimated to be better than ±2 eV. Values from this work are compared with values from other evaluations and calculations.

Z	This work	ΔE(eV) = E(others) − E(ours)				
		Expt.[a]	Lotz[4]	Bearden[3]	Lu et al.[6]	Carlson et al.[7]
89	15,874		−3	−3	+8	
90	16,300	0	0	0	+14	
91	16,733		−1	0	+9	
92	17,169	0	−1	−3	+12	
93	17,612		−3	−2	+13	
94	18,059		−3	−2	+11	
95	18,514		−5	−10	+11	
96	18,974	−1	−6	−44	+18	0
97	19,439	+13	−7	+13	+21	+1
98	19,910	−29	−8	+20	+18	−3
99	20,386		−0	+24	+21	−3
100	20,869	−1	−12	+31	+30	+3
101	21,358		−16	+32	+26	−4
102	21,850		−18	+30	+31	−1

[a] Z = 90, ref. 8; Z = 92, ref. 9; Z = 96, ref. 10; Z = 97, ref. 11; Z = 98, ref. 12; Z = 100, ref. 13.

Table 2.6. Binding energies (eV) of M_5 electrons for Z = 89 to 102

Accuracy of our values is estimated to be better than ±2 eV. Values from this work are compared with values from other evaluations and calculations.

Z	This work	ΔE(eV) = E(others) − E(ours)				
		Expt.[a]	Lotz[4]	Bearden[3]	Lu et al.[6]	Carlson et al.[7]
89	3225		−5	−6	−2	
90	3332	0	0	0	+6	
91	3441		+2	+1	+2	
92	3552	0	+2	0	+2	
93	3664	0	+3	+2	+3	
94	3778	0	+2	0	−3	
95	3894		+2	−7	−3	
96	4012	+2	+1	−41	+2	+2
97	4131		+3	+1	+2	+2
98	4253		+3	0	−6	−6
99	4376		+4	−2	−7	−7
100	4500	−16	+5	−2	−2	−2
101	4627		+6	−5	−11	−11
102	4755		+8	−14	−12	−12

[a] Z = 90, ref. 8; Z = 92, ref. 9; Z = 93, ref. (14); Z = 94, ref. 15; Z = 96, ref. 10; Z = 100, ref. 13.

Table 2.7. Binding energies (eV) of K electrons for Z = 89 to 102

Accuracy of our values is estimated to be better than ±4 eV for $Z < 96$ and ±6 eV for $Z \geqslant 96$. Values from this work are compared with values from other evaluations and calculations.

Z	This work	ΔE(eV) = E(others) − E(ours)				
		Expt.[a]	Lotz[4]	Bearden[3]	Lu et al.[6]	Carlson et al.[7]
89	106,757		+2	−2	+429	
90	109,650		+4	+1	455	
91	112,601		+3	0	473	
92	115,609		+4	−3	491	
93	118,678		−2	0	519	
94	121,806		−6	12	534	
95	124,997		−13	+30	562	
96	128,251		−22	−31	596	+10
97	131,566	+24	−30	+24	632	+20
98	134,946	−146	+960	+1014	665	+21
99	138,389		+951	+1091	711	+51
100	141,899	+64	+1040	+1191	768	+63
101	145,476		+1048	+1304	825	+95
102	149,117		+919	+1423	901	+156

[a] Z = 97, ref. 11, Z = 98, ref. 12; Z = 100, ref. 13.

values which we now recommend for the actinides is better than ±6 eV for the K shell, better than ±2 eV for L_3 and M_5 shells, better than ±4 eV for $K\alpha_1$ x rays, and better than ±3 eV for $L\alpha$ x rays.

A consistency test yet to be executed will involve Moseley diagram fits of the K-level energies and of the $L\alpha_1$ x-ray energies, which will allow us to make a final adjustment to the values reported. We do not, however, expect any changes that would exceed the estimated error limits. We intend to extend this evaluation to other inner levels, whereas an evaluation of the levels beyond the N shell must await further experimentation.

Note that the values of the atomic energy levels are referred to the Fermi level in our case and in Bearden and Burr's tables, whereas the calculations of Lu et al. and Carlson et al. give free-atom values. We referred Lotz's values to the Fermi level by adding for the work function a value of −3 eV.

1. Visiting scientist from Laboratoire de Chimie Physique de l'Université Paris VI, France.

2. J. A. Bearden, *Rev. Mod. Phys.* **39**, 78 (1967).
3. J. A. Bearden and A. F. Burr, *Rev. Mod. Phys.* **39**, 125 (1967).
4. W. Lotz, *J. Opt. Soc. Amer.* **69**, 206 (1970).
5. S. Hagström, *Z. Phys.* **178**, 82 (1964).
6. Lu et al., *Atomic Data* **3**, 1 (1971). Eigenvalues are reported.

Table 2.8. Energies (eV) of $K\alpha_1$ and $L\alpha_1$ x rays for $Z = 89$ to 102

Accuracy of our values is estimated as follows: ±2 eV for $K\alpha_1$ and $L\alpha_1$ energies for $Z < 96$; ±4 eV for $K\alpha_1$ and ±3 eV for $L\alpha_1$ energies for $Z \geqslant 96$.

Z	This work	$K\alpha_1$ x rays, $\Delta E = E$(others) − E(ours)			This work	$L\alpha_1$ x rays, $\Delta E = E$(others) − E(ours)		
		Expt.[a]	Lu et al.[6]	Carlson et al.[7]		Expt.[b]	Lu et al.[6]	Carlson et al.[7]
89	90,883		+421		12,649	+3	+10	
90	93,350	0	441		12,968	+1	8	
91	95,868		464		13,292	−1	7	
92	98,440	−1	479		13,617	−2	10	
93	101,066	+14	506		13,948	−4	10	
94	103,747	+1	523		14,281	−2	14	
95	106,483	+1	551		14,620	−3	14	
96	109,277	−4	578	+10	14,962	−3	16	−2
97	112,127	−15	611	19	15,308		19	−1
98	115,036	−5	647	24	15,657		24	+3
99	118,003	+15	690	54	16,010		28	4
100	121,030		738	60	16,369		32	5
101	124,118		799	99	16,731		37	7
102	127,267		870	157	17,095		43	11

[a] $Z = 90$ and 92, ref. 2; $Z = 93$ to 95, ref. 16; $Z = 96$ to 99, ref. 17.
[b] $Z = 89$ to 95, ref. 2; $Z = 96$, ref. 10.

7. Carlson et al., *Nucl. Phys. A* **135**, 57 (1969). This is a calculation with a semiempirical correction.
8. C. Nordling and S. Hagström, *Z. Phys.* **178**, 418 (1964).
9. C. Nordling and S. Hagström, *Ark. Fys.* **15**, 431 (1959).
10. Y. Y. Chu, M. L. Perlman, P. F. Dittner, and C. E. Bemis, *Phys. Rev. A* **5**, 67 (1972).
11. J. M. Hollander, M. D. Holtz, T. Novakov, and R. L. Graham, *Ark. Fys.* **28**, 375 (1965).
12. I. Ahmad, et al., *Phys. Rev. C* **3**, 390 (1971).
13. F. T. Porter and M. S. Freedman, *Phys. Rev. Lett.* **27**, 293 (1971).
14. S. Hagström, *Bull. Amer. Phys. Soc.* **11**, 389 (1966).
15. A Fahlman, et al., *Phys. Lett.* **19**, 643 (1966).
16. G. C. Nelson, B. G. Saunders, and S. I. Salem, *Z. Phys.* **235**, 308 (1970).
17. P. F. Dittner and C. E. Bemis, Jr., *Phys. Rev. A* **5**, 481 (1972).

SPECTROPHOTOMETRIC STUDY OF THE FORMATION OF AMERICIUM THIOCYANATE COMPLEXES[1]

H. D. Harmon[2] J. T. Bell[4]
J. R. Peterson[3] W. J. McDowell[4]

The results of a spectrophotometric study of the formation of Am(III) complexes with thiocyanate at an ionic strength of 1.0 *M* have enabled calculation of the overall stability constants of $Am(SCN)^{2+}$ and $Am(SCN)_2^+$. The values of these constants were found to be 5.79 ± 0.33 (β_1) and 6.77 ± 1.05 (β_2), where the error limits represent one standard deviation. The small spectral changes observed in the formation of $Am(SCN)^{2+}$ are in agreement with the conclusions of Choppin and Ketels[5] and Choppin[6] that this complex is of the outer-sphere type. The more marked spectral changes observed above 0.1 *M* SCN^- indicated that $Am(SCN)_2^+$ and any additional complexes are possibly of the inner-sphere type.

The observed Am(III) spectral changes in concentrated KSCN solutions suggested that the Am(III) ion is strongly complexed. The existence of Am(III) thiocyanate complexes with coordination numbers considerably greater than 4 in ~5 to 10 *M* KSCN solutions is implied tentatively by the magnitude of the shift in wavelength of maximum absorbance. The "effective stability constant (β_1*)" approach of Marcus and co-workers[7,8] was employed to calculate the value for $Am(SCN)^{2+}$ (7.6 ± 2.5) from the data obtained at variable ionic strength in the KSCN concentration range 0 to 0.45 *M*.

1. Summary of paper, *J. Inorg. Nucl. Chem.* **34**, 1711 (1972); a more detailed account of this work is available in ORNL-TM-3486 (July 1971).
2. Graduate student from the University of Tennessee, Knoxville, and supported by a National Defense Education Act Title IV Fellowship. Present address: Chemistry Department, Walters State Community College, Morristown, Tenn.
3. Consultant, Department of Chemistry, University of Tennessee, Knoxville.
4. Chemical Technology Division.
5. G. R. Choppin and J. Ketels, *J. Inorg. Nucl. Chem.* **27**, 1335 (1965).

6. G. R. Choppin, U.S. Atomic Energy Commission Document No. TID-25671 (1970).
7. Y. Marcus and M. Shiloh, *Isr. J. Chem.* 7, 31 (1969).
8. M. Shiloh, M. Givon, and Y. Marcus, *J. Inorg. Nucl. Chem.* 31, 1807 (1969).

STABILITY CONSTANTS OF THE MONOCHLORO COMPLEXES OF Bk(III) AND Es(III)[1]

H. D. Harmon[2] J. R. Peterson[3]
W. J. McDowell[4]

The stability constants of the chloro complexes of Pu(III), Am(III), and Cm(III) have been determined in a variety of ionic strengths. The present study was carried out to extend these investigations to some of the heavier members of the trivalent actinide series, which were unavailable to earlier workers. In this work, a solvent extraction technique was employed to study the complex formation of Bk(III) and Es(III) in NaCl-$NaClO_4$ solutions at constant ionic strength (I = 1.0) and pH = 2.0. The stability constants we determined are the first values that have been reported for the monochloro complexes of Bk(III) and Es(III).

The values of the stability constant (β_1) for $BkCl^{2+}$ and $EsCl^{2+}$, along with previously reported values for $AmCl^{2+}$ and $AmCl_2^+$ (β_2) at I = 1.0, are listed in Table 2.9. The error limits for the β_1 values from our work and those of Khopkar and Narayanankutty[5] are equal to one standard deviation, as calculated by the curve-fitting analyses. The exact meaning of the error limits given by the other authors[6,7] is not known.

It is evident that the β_1 values for the monochloro complexes of Bk(III) and Es(III) are very close to the average of those reported for the similar Am(III) complex. Therefore, these results indicate that no significant change occurs in the stability or structure of the monochloro complexes of the trivalent actinides as the atomic number increases. Hence, it may be concluded that the monochloro complexes of the actinide(III) ions, at least through Es(III), are weak and of the outer-sphere type.[8]

1. Summary of paper, *Inorg. Nucl. Chem. Lett.* 8, 57 (1972); a more detailed account of this work is available in ORNL-TM-3486 (July 1971).
2. Graduate student from the University of Tennessee, Knoxville, and supported by a National Defense Education Act Title IV Fellowship. Present address: Chemistry Department, Walters State Community College, Morristown, Tenn.
3. Consultant, Department of Chemistry, University of Tennessee, Knoxville.
4. Chemical Technology Division.
5. P. K. Khopkar and P. Narayanankutty, *J. Inorg. Nucl. Chem.* 33, 495 (1971).
6. D. F. Peppard, G. W. Mason, and I. Hucher, *J. Inorg. Nucl. Chem.* 24, 881 (1962).
7. B. M. L. Bansal, S. K. Patil, and H. D. Sharma, *J. Inorg. Nucl. Chem.* 26, 993 (1964).
8. A. D. Jones and G. R. Choppin, *Actinides Rev.* 1, 311 (1969).

STABILIZATION OF DIVALENT CALIFORNIUM IN THE SOLID STATE: CALIFORNIUM DIBROMIDE[1]

J. R. Peterson[2] R. D. Baybarz[3]

In recent years a number of papers have appeared offering experimental evidence for the stability of divalent californium. A lesser number of papers has been published refuting the evidence or the interpretation of the experimental results as indicative of divalent californium. We report here the preparation of $CfBr_2$, the first known compound of Cf(II).

Individual cation exchange resin beads, saturated with 1 to 5 μg of ^{249}Cf, were calcined in air at ~1200°C and treated with anhydrous HBr gas at temperatures between 500 and 625°C to produce $CfBr_3$.

Table 2.9. Chloro complex stability constants of some trivalent actinides at I = 1.0

Actinide ion	β_1	β_2	Medium	Reference
Am(III)	0.9 ± 0.2		HCl-$HClO_4$	6
	0.9 ± 0.1		HCl-$HClO_4$	7
	1.4 ± 0.1		NaCl-$NaClO_4$	7
	0.56 ± 0.02		LiCl-$LiClO_4$	5
	0.72 ± 0.04	0.30 ± 0.03	HCl-$HClO_4$	5
	1.04 ± 0.05	0.43 ± 0.05	NaCl-$NaClO_4$	5
	1.31 ± 0.05	1.08 ± 0.05	NH_4Cl-NH_4ClO_4	5
Bk(III)	0.96 ± 0.01		NaCl-$NaClO_4$	Present work
Es(III)	0.96 ± 0.01		NaCl-$NaClO_4$	Present work

The $CfBr_2$ samples were prepared from $CfBr_3$ by hydrogen gas reduction at ~650°C. At this temperature the reaction proceeds rapidly in a 1-atm H_2 gas flow to produce the amber-colored $CfBr_2$. It was noted that, at the lower temperature of ~500°C, the reaction failed to proceed at a noticeable rate. At temperatures in moderate excess of 700°C the $CfBr_2$ formed underwent decomposition.

During the course of our experimentation it was noted that when samples of $CfBr_3$, sealed at room temperature in an x-ray capillary containing ¾ atm of HBr, were heated at or above 675°C, they would darken considerably. This color change was reversed upon cooling the sample. It is proposed that the following equilibrium system is established in the capillary system: $2CfBr_3 \rightleftharpoons 2CfBr_2 + Br_2$.

The samples of $CfBr_2$ exhibited the tetragonal structure characteristic of $SrBr_2$ and $EuBr_2$. The x-ray diffraction patterns obtained did not have good high-angle detail, a common problem with powder patterns of such compounds.

The room-temperature lattice parameters derived from the best $CfBr_2$ diffraction pattern are $a_0 = 11.500 \pm 0.007$ Å and $c_0 = 7.109 \pm 0.006$ Å, where the error limits given represent one standard deviation, reflecting only the internal consistency of this particular data set. Lattice parameters derived from the diffraction patterns of other $CfBr_2$ samples were in agreement with these values, usually differing by not more than 0.01 Å. These values indicate that the Cf(II) ionic radius is smaller than that of Eu(II) by just about 0.01 Å, a result in agreement with the relative magnitudes of the Cf(III) and Eu(III) ionic radii. The calculated density (x-ray) of $CfBr_2$ for ten formula units per unit cell is 7.22 g/cc, and the molecular volume is 94.0 $Å^3$.

The preparation of divalent californium is slightly more difficult than that for divalent samarium under similar conditions. Samarium tribromide could be reduced with hydrogen gas at a significantly lower temperature than was needed for the reduction of $CfBr_3$. Samarium trichloride (pale yellow) could be reduced with hydrogen gas to the (dark reddish-brown) dichloride, whereas californium trichloride (green) could not be reduced to the dichloride in a similar manner; in every case the californium product was either the unreacted trichloride or the oxychloride. Even at temperatures well above the californium trichloride melting point, there was no darkening of the sample as would be expected if Cf(II) were being formed. Thus, the reducibility of Cf(III) relative to Sm(III) indicates that its reduction potential should be similar to, though slightly more negative[4] than, that of samarium.

1. Summary of paper, *Inorg. Nucl. Chem. Lett.* 8, 423 (1972).
2. Consultant, Department of Chemistry, University of Tennessee, Knoxville.
3. Chemical Technology Division.
4. The sign convention here is as in W. M. Latimer, *Oxidation Potentials*, Prentice-Hall, New York, 1952.

PREPARATION OF ANHYDROUS LANTHANIDE HALIDES BY LIGAND EXCHANGE

C. E. Higgins W. H. Baldwin

Solvated anhydrous rare-earth halides have been prepared and reported earlier.[1] Anhydrous lanthanide halide dialcoholates resulted from reaction of the water in hydrated lanthanide chlorides with triethyl orthoformate or dimethoxypropane. Water was also quantitatively removed in the analysis of the hydrate, using a high-boiling ligand exchanger such as tributyl phosphate or hexamethylphosphoramide. After exchange, the water was pumped to a trap, while the anhydrous salt remained in solution in the ligand exchanger.

The latter method has now been modified with the use of lower-boiling ligand exchangers, such as methylcellosolve and dimethylformamide (DMF), to produce anhydrous salts both in solution and as residues from evaporation. Water and solvent were removed from solutions of cerium trichloride hexahydrate in DMF; removal was accomplished at 1 torr and 25–30°C. All the water was pumped off during the first half of the DMF distillation. The average composition of the residue after being treated in vacuo at 1 torr for 7 hr at 25–30°C was $CeCl_3 \cdot 3.5DMF$, and after further treatment for 1 hr at 97–99°C the entire residue analyzed $CeCl_3 \cdot 2.4DMF$.

1. C. E. Higgins and W. H. Baldwin, *Chem. Div. Annu. Progr. Rep. May 20, 1971*, ORNL-4706, p. 80.

ORGANOLANTHANIDES

F. H. Fink[1] J. H. Burns
W. H. Baldwin

Cyclopentadienides of Cm, Bk, and Cf have been prepared[2,3] and were studied by several techniques, but an attempt to deduce the nature of the bonding by determination of the crystal structure failed because of inherent tendencies in the structure toward disorder

and/or twinning. Two compounds have now been synthesized which are related to the cyclopentadienides closely enough to show the same metal-to-cyclopentadiene bonds but sufficiently dissimilar to have a different crystal structure. These are tris(methylcyclopentadienyl)neodymium, $Nd(C_6H_7)_3$, and tricyclopentadienyl samarium-cyclohexylisonitrile, $Sm(C_5H_5)_3 \cdot C_7H_{11}N$.

For purposes of developing techniques and obtaining preliminary crystal information, the lanthanide compounds have been made using published methods,[4,5] but the techniques will soon be extended to transuranium elements. The melting point of $Nd(C_6H_7)_3$ was observed to be 160°C (value in ref. 4: 165°C). Large blue-violet tabular crystals obtained by sublimation showed monoclinic symmetry. Unit-cell dimensions are $a = 14.24$, $b = 26.68$, $c = 9.28$ Å, and $\beta = 120°\ 18'$. The space group is $P2_1/c$. The density was measured to be 1.68 g/cm^3; the calculated value for $Z = 8$ is 1.67 g/cm^3. The compound $Sm(C_5H_5)_3 \cdot C_7H_{11}N$ (mp 148°C) was found by x-ray powder diffraction to be isomorphous with the Pr analog (mp 138–139°C) reported previously.[6]

1. Visiting scientist from the Chemistry Department, Birmingham Southern College, Birmingham, Ala.
2. P. G. Laubereau and J. H. Burns, *Inorg. Chem.* 9, 1091 (1970).
3. P. G. Laubereau and J. H. Burns, *Inorg. Nucl. Chem. Lett.* 6, 59 (1970).
4. L. T. Reynolds and G. Wilkinson, *J. Inorg. Nucl. Chem.* 9, 86, (1959).
5. E. O. Fischer and H. Fischer, *J. Organometal. Chem.* 6, 141 (1966).
6. P. G. Laubereau, J. H. Burns, and L. Ganguly, *Chem. Div. Annu. Progr. Rep. May 20, 1970,* ORNL-4581, p. 52.

STUDIES WITH HEPTAVALENT NEPTUNIUM: IDENTIFICATION AND CRYSTAL-STRUCTURE ANALYSIS OF $LiCo(NH_3)_6Np_2O_8(OH)_2 \cdot 2H_2O$

J. H. Burns W. H. Baldwin
J. R. Stokely[1]

In a previous report[2] we noted that when a solution of $Co(NH_3)_6Cl_3$ was added rapidly to an alkaline solution of Np(VII), minute green crystals of $Co(NH_3)_6NpO_5 \cdot 3H_2O$ were obtained, while slow diffusion together of the same components produced large black crystals of unknown composition. The latter product has since been identified by combining methods of analytical chemistry and single-crystal x-ray diffraction. For the large crystals grown from LiOH solution, the formula is $LiCo(NH_3)_6Np_2O_8(OH)_2 \cdot 2H_2O$. From NaOH solution the same compound with Li replaced by Na was obtained, but from KOH solution no crystals were produced.

The results of the crystal-structure determination on the Li compound are shown in Fig. 2.15, which portrays the basic components of the structure in their positions in the unit cell. The two kinds of Np atoms are each octahedrally coordinated by O atoms, and these octahedra share corners to form chains along the c axis. Lithium ions are attached to the chains periodically, and the chains are cross-linked by octahedral $Co(NH_3)_6^{3+}$ ions between them. Details of the significant bond lengths are given in Fig. 2.16. Note that Np(2) has four short bonds to O atoms in a square array and has two oxygen bonds perpendicular to this which are considerably longer. Next along the chain is Np(1), which has a square (slightly distorted because of corner sharing) of O atoms and two long bonds to O atoms perpendicular to it. Each Li^+ ion shares four of the O atoms bonded to Np atoms and has two of its own.

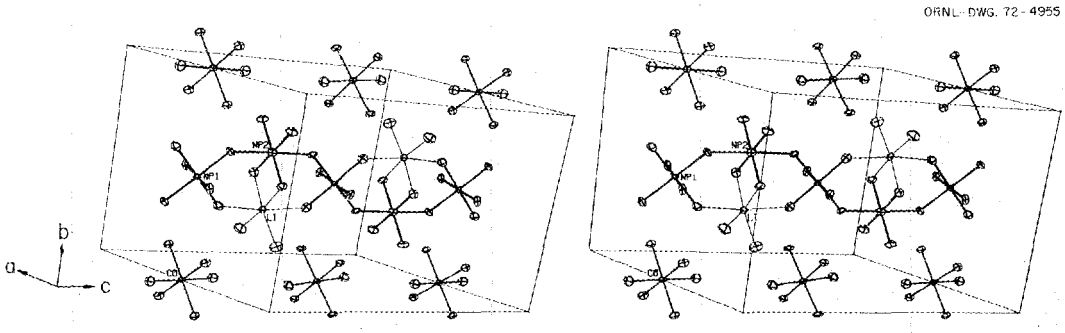

Fig. 2.15. Stereoscopic view of one monoclinic unit cell of the structure of $LiCo(NH_3)_6Np_2O_8(OH)_2 \cdot 2H_2O$. Portions are omitted for clarity. Unlabeled atoms are oxygens.

ORNL-DWG. 72-3322A

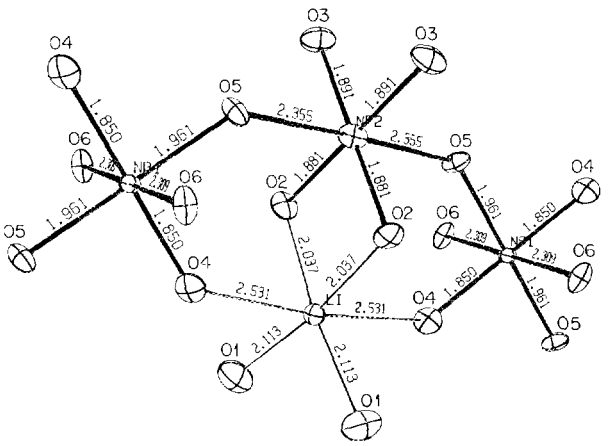

Fig. 2.16. Bond lengths in the chain portion of $LiCo(NH_3)_6Np_2O_8(OH)_2 \cdot 2H_2O$. Orientation of the chain is nearly the same as in Fig. 2.15.

The distribution of H atoms, while not determined directly, may be assigned on physical-chemical grounds. The two atoms designated O(2) in Fig 2.16 must belong to H_2O molecules because of their relatively isolated positions. The two labeled O(8) are believed to be OH^- ions because of their bond lengths to Np(1) and the requirements of electroneutrality. All the other O atoms appear to be doubly bonded to Np atoms because of their short distances from them, comparable to the U = O distances in the uranyl ion.

From the nature of the structure, two conclusions may be drawn: (1) Heptavalent Np exists in this crystal as a quadruply double-bonded, square-planar species, NpO_4^-, and is probably stabilized thereby, as are the 5- and 6-valent states by existence of the linear NpO_2^+ and NpO_2^{2+} ions. (2) In alkaline solution the anion is likely $[NpO_4(OH)_2]^{3-}$ instead of the previously postulated[3] NpO_5^{3-}. If the second conclusion is correct, a plausible explanation for the precipitation of two different compounds can be offered. On rapid addition of $Co(NH_3)_6^{3+}$, it reacts with $[NpO_4(OH)_2]^{3-}$ to yield $Co(NH_3)_6NpO_4(OH)_2 \cdot 2H_2O$ (which is a regrouping of the empirical formula given above for the green compound), while slow diffusion splits out OH^- and adds Li^+ to produce the polymeric form:

$$LiCo(NH_3)_6Np_2O_8(OH)_2 \cdot 2H_2O.$$

1. Analytical Chemistry Division.
2. W. H. Baldwin, J. H. Burns, J. R. Stokely, and G. K. Werner, *Chem. Div. Annu. Progr. Rep. May 20, 1971*, ORNL-4706, p. 83.
3. V. I. Spitsyn et al., *J. Inorg. Nucl. Chem.* **31**, 2733 (1969).

CRYSTAL STRUCTURE AND LATTICE PARAMETERS OF CURIUM-248 OXYCHLORIDE, $^{248}CmOCl$[1]

J. R. Peterson[2]

In a continuing effort to study the properties of curium in the absence of intense self-irradiation by using the long-lived isotope of mass number 248 ($t_{1/2}$ = 3.5 × 10^5 years), the oxychloride has been prepared and found to exhibit the PbClF-type tetragonal structure. Prior to this work there were no x-ray data or lattice parameters available in the literature for this compound.

The source of ^{248}Cm was the same as reported elsewhere.[3] Single ion exchange resin bead techniques were employed to prepare ~1-μg samples of CmOCl by treatment at 500 to 600°C of either $CmCl_3$ or Cm_2O_3 with the vapor in equilibrium with a 10 *M* HCl solution. Unlike $CmCl_3$, CmOCl is not hygroscopic. All samples were examined by standard x-ray powder diffraction techniques.[3]

It is apparent that curium oxychloride is thermodynamically quite stable with respect to the sesquioxide whenever there is chloride ion available. However, in the absence of a source of chloride ion, the oxychloride will decompose at 600°C to form the cubic form of the sesquioxide.

Room-temperature, average lattice parameters were determined to be a_0 = 3.985 ± 0.003 Å and c_0 = 6.752 ± 0.008 Å, where the error limits represent the 95% confidence level calculated using the standard statistical method for the average of seven independent determinations.

Oxychlorides of the type MOCl have been characterized for all the trivalent lanthanides and for Ac, U, Pu, Am, Cm, Bk, Cf, and Es. All of the known actinide oxychlorides, as well as the oxychlorides of La through Er, exhibit the same type of tetragonal structure. The heaviest three lanthanides and one form of ErOCl exhibit an as yet uncharacterized structure type.

It has been pointed out previously[4] that these oxychlorides are a good illustration of the limitation of the ionic radius concept, in that different values for the trivalent metal ionic radius are obtained from the various metal-chlorine and metal-oxygen distances. The structure is characterized by layers of coplanar oxygen atoms and of coplanar chlorine atoms arranged in repeating units of O-Cl-Cl. The metal atoms are located in holes between the oxygen and chlorine atom layers. Each metal atom is surrounded by four oxygen atoms, four chlorine atoms in the adjacent layer, and one chlorine atom in the second halogen layer. However, due to

anion-anion interactions (chlorine-oxygen and chlorine-chlorine), the trivalent metal ion does not reach its closest approach to all of the anions around it. Thus, a meaningful trivalent metal ionic radius cannot be calculated taking into account all nine metal-anion distances. As would be expected on the basis of electrostatic attraction forces, the metal ion favors contact with the divalent oxygen atoms over the monovalent chlorine atoms. In fact, the metal-oxygen distances in the lanthanide and actinide oxychlorides are in good accord with the metal-oxygen distances in the corresponding sesquioxides.

1. Summary of paper, *J. Inorg. Nucl. Chem.* **34**, 1603 (1972).
2. Consultant, Department of Chemistry, University of Tennessee, Knoxville. Work carried out in part at the ORNL Transuranium Research Laboratory and in part at the University of Liège (Belgium) while in residence as a North Atlantic Treaty Organization Postdoctoral Fellow in Science.
3. J. R. Peterson and J. Fuger, *J. Inorg. Nucl. Chem.* **33**, 4111 (1971).
4. J. R. Peterson and B. B. Cunningham, *Inorg. Nucl. Chem. Lett.* **3**, 579 (1967).

CRYSTAL STRUCTURES OF CALIFORNIUM TRICHLORIDE

J. H. Burns J. R. Peterson[1]
R. D. Baybarz[2]

Single-crystal specimens of two modifications of $CfCl_3$ have been grown from melts, and their structures were determined by x-ray diffraction. The least-squares refined parameters for the high-temperature, hexagonal UCl_3 form (h-$CfCl_3$) were given previously;[3] and the results for the low-temperature, orthorhombic $PuBr_3$ form (o-$CfCl_3$) are as follows: a = 3.869(2), b = 11.748(7), c = 8.561(4) Å, space group: *Cmcm*, Z = 4.

	x	10^4y	10^4z	$10^3\beta_{11}$	$10^4\beta_{22}$	$10^4\beta_{33}$	$10^4\beta_{23}$
Cf	0	2434(1)	2500	13.7(7)	28(1)	32(1)	0
Cl(1)	0	5845(8)	2500	24(4)	26(4)	60(9)	0
Cl(2)	0	1467(5)	5667(6)	22(3)	28(3)	28(5)	−3(3)

In comparing the two forms of $CfCl_3$, the main point of structural interest is that in h-$CfCl_3$ the Cf ion has nine Cl-ion neighbors, while in o-$CfCl_3$ this is reduced to eight. Thus the Cf ion is of a size such that it represents the point in the contracting actinide series at which 8- and 9-coordination are about equally stable; the corresponding element in the lanthanide series is Gd.[4]

In Fig. 2.17 are shown the two coordination polyhedra in a similar orientation for comparison. In each case there is a trigonal prism of six Cl ions, but the h-$CfCl_3$ has three equatorial Cl ions and the o-$CfCl_3$ has only two. How these prisms are shared with others to make up the structures is shown in Fig. 2.18. In both cases the trigonal prisms share bases to form continuous columns along the vertical direction; it is in the cross-linking that the structures differ. In h-$CfCl_3$ each column is cross-linked in three horizontal directions, while in o-$CfCl_3$ the linking occurs in only two, which results in sheets of cross-linked columns. The hexagonal to orthorhombic phase transition probably occurs through the breaking of one-third of the equatorial linkages, with the remainder of the structure remaining largely intact and undergoing small shifts in positions.

ORNL-DWG. 72-2919

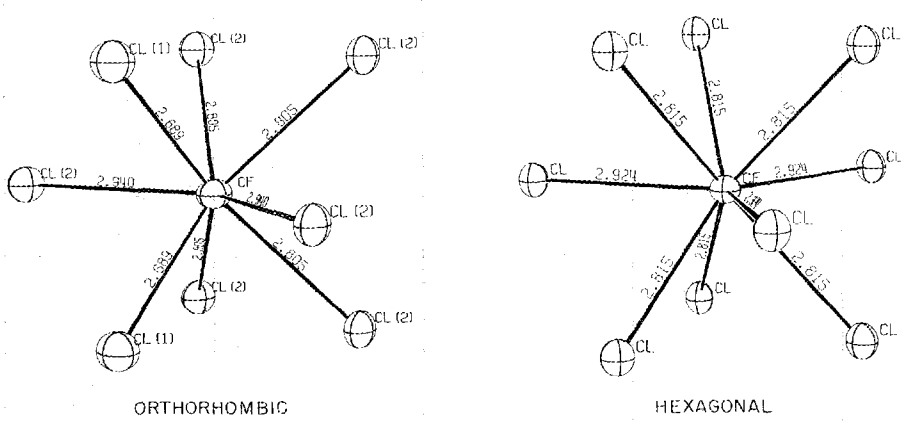

Fig. 2.17. Coordination polyhedra in the two forms of $CfCl_3$.

ORNL-DWG. 72-2920

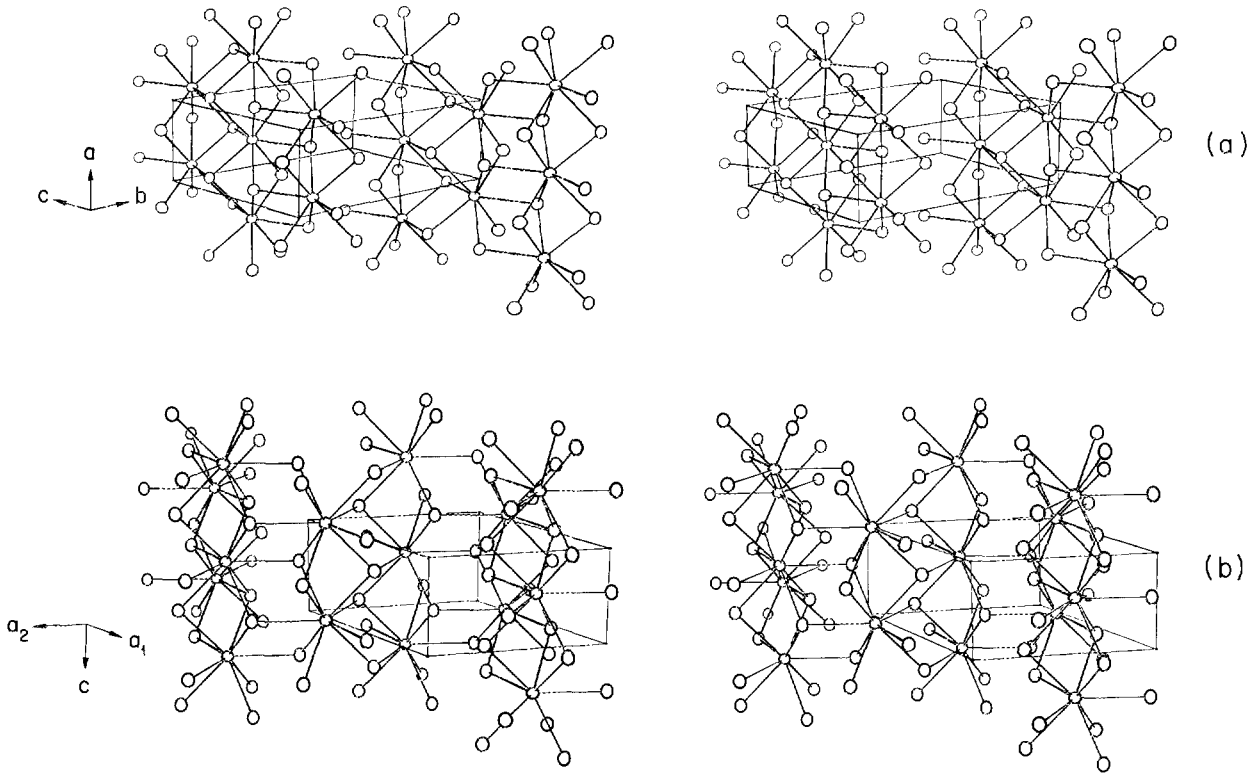

Fig. 2.18. (*a*) Orthorhombic $CfCl_3$; (*b*) hexagonal $CfCl_3$.

1. Consultant, Department of Chemistry, University of Tennessee, Knoxville.
2. Chemical Technology Division.
3. J. H. Burns, J. R. Peterson, and R. D. Baybarz, *Chem. Div. Annu. Progr. Rep. May 20, 1971*, ORNL-4706, p. 86.
4. A. L. Harris and C. R. Veale, *J. Inorg. Nucl. Chem.* 27, 1437 (1965).

CRYSTAL STRUCTURE OF CALIFORNIUM TRIBROMIDE

J. H. Burns J. R. Peterson[1]

With decreasing cationic size the lanthanide trichlorides and tribromides exhibit a series of structural types which range from UCl_3 to $PuBr_3$ to $AlCl_3$ (trichlorides) or $FeCl_3$ (tribromides). Previous studies on the actinide analogs have shown them to follow the same pattern through the UCl_3 and $PuBr_3$ structure types; but when $CfBr_3$ and one form of $BkBr_3$ were prepared,[2,3] the expected $FeCl_3$ structure did not explain the x-ray powder patterns obtained.

Consequently, we applied our single-crystal growth methods used on transplutonium trichlorides to grow a crystal of $CfBr_3$ and then analyzed it by x-ray diffraction. A sample of Cf_2O_3 in a quartz capillary was treated with anhydrous HBr(g), the temperature raised above the melting point, and a single crystal produced by slow cooling of the melt. At or near the melting point, the green $CfBr_3$ darkened as a result of some decomposition to $CfBr_2$ and Br_2.

The structure obtained was of the $AlCl_3$ (or YCl_3) type,[4] and from it the previously obtained powder patterns could be explained. In this structure the Cf^{3+} ions are octahedrally coordinated by Br^- ions. These octahedra share edges to form pseudo-hexagonal sheets parallel to (001). A view of one unit cell of the structure is shown in Fig. 2.19. All Cf-Br distances within each octahedron are 2.82 Å, but the three shared octahedral edges are slightly compressed compared with the unshared edges. We have preliminary evidence that the $FeCl_3$-type structure is also formed by $CfBr_3$, so the compound may be dimorphic.

ORNL-DWG. 72-4956

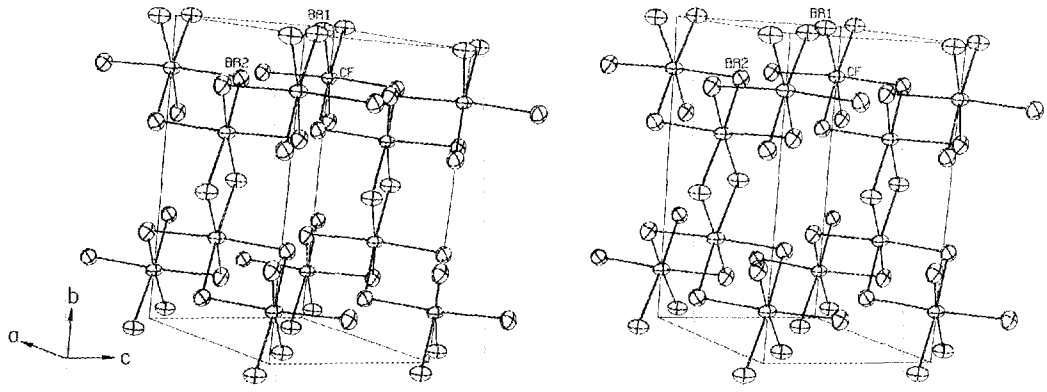

Fig. 2.19. Stereoscopic view of one unit cell of $CfBr_3$.

1. Consultant, Department of Chemistry, University of Tennessee, Knoxville.
2. D. K. Fujita, Ph.D. thesis, Lawrence Berkeley Laboratory, University of California, UCRL-19507, November 1969.
3. D. Cohen, S. Fried, S. Siegel, and B. Tani, *Inorg. Nucl. Chem. Lett.* **4**, 257 (1968).
4. D. H. Templeton and G. Carter, *J. Amer. Chem. Soc.* **58**, 940 (1954).

MICROCHEMICAL PREPARATIONS OF HEAVY-ELEMENT METALS

J. N. Stevenson[1] J. R. Peterson[2]

Various attempts were made to prepare 4- to 6-μg samples of lanthanide metals by reduction of the corresponding trifluorides. These trifluoride samples were derived from single ion exchange resin beads which were saturated with the tripositive lanthanide, calcined in air to produce the oxide, and converted to the trifluoride by treatment at about 600°C with HF gas. The lanthanide elements used (Ce, Pr, Eu, and Yb) were chosen because of their low melting points and/or high volatilities, in order to serve as stand-ins during the development of techniques for the production of Cf metal in bulk (5- to 10-μg) quantities. The techniques used in the production of Am, Cm, and Bk metals cannot be applied to Cf because of the high volatility of Cf metal[3] and the limited quantities of ^{249}Cf available for such "possible-loss" experimentation. Rapid heating of the reactants (lanthanide trifluoride and Li metal) and cooling of the product (lanthanide metal) is accomplished by the use of a minimal-volume matrix of LiF supported by a loop or spiral of 5-mil Pt wire. Analyses of the metal products from experiments in which visual observation indicated significant reduction of the trifluoride show that some oxide formation occurred. The source of the oxygen contamination is thought to be the LiF matrix material (powder melted in air) and/or the inert gas (Ar) in which the reductions took place. Therefore the experimental apparatus will be transferred into an inert-atmosphere glove box, and high-purity LiF crystals will be used as the matrix material.

Samples of CfF_3, before reduction to the metal, will be used to study the high-temperature form predicted to exist at temperatures greater than or equal to about 700°C.[4] This LaF_3-type trigonal structure exists for EuF_3 at temperatures above 700°C.[5] One sample of EuF_3 (prepared for use in the metal production experiments) exhibited this structure when examined by x-ray powder diffraction at room temperature immediately after preparation. Other attempted preparations resulted in samples exhibiting either the low-temperature form (orthorhombic) of the trifluoride or a structure characteristic of the oxyfluoride. Further attempts to stabilize the high-temperature trifluoride structure at room temperature will be made with the apparatus in the inert-atmosphere glove box.

1. Oak Ridge Graduate Fellow from the University of Tennessee, Knoxville, under appointment from the Oak Ridge Associated Universities.
2. Consultant, Department of Chemistry, University of Tennessee, Knoxville.
3. J. A. Fahey, J. R. Peterson, and R. D. Baybarz, *Inorg. Nucl. Chem. Lett.* **8**, 101 (1972).
4. J. R. Peterson and B. B. Cunningham, *J. Inorg. Nucl. Chem.* **30**, 1775 (1968).
5. R. E. Thoma and G. D. Brunton, *Inorg. Chem.* **5**, 1937 (1966).

3. Isotope Chemistry

FRACTIONATION OF CARBON ISOTOPES: THE CYANEX SYSTEM

L. L. Brown

Continuing studies of the use of cyanohydrins to separate the isotopes of carbon have resulted in several process improvements:

$$R_2C(OH)^{12}CN(org) + {}^{13}CN^-(aq) = R_2C(OH)^{13}CN(org) + {}^{12}CN^-(aq) . \quad (1)$$

In previously reported studies, the cyanohydrin of methyl isobutyl ketone was dissolved in xylene and equilibrated with an aqueous KCN solution containing $KHCO_3$. This implementation of reaction (1) was characterized by an attractive single-stage separation factor (1.034 at 25°C), thermally refluxable product-end and waste-end reactions, and chemical and mechanical stability over extended periods of operation. Unfortunately, however, the rate of isotopic exchange was slow, resulting in excessively long theoretical plate lengths in the exchange column. This development threatened the economic competitiveness of the CYANEX process, and a new cyanohydrin having a faster exchange rate was therefore sought. The results of these studies are summarized in Table 3.1, which shows very favorable exchange rates for the diethyl ketone cyanohydrin, even in the presence of sufficient HCO_3^- to effect readily the waste-end reflux reaction. The greater aqueous-phase solubility of diethyl ketone, compared with methyl isobutyl ketone, caused a lowering of the effective isotopic separation factor from 1.034 to 1.033, but this slight decrease was a small price to pay for the economic advantages of the faster exchange rate.

The use of diethyl ketone, rather than methyl isobutyl ketone, gave other benefits in addition to the faster exchange rate. Both reflux reactions occur more readily and require less length of contacting column for completion. Further, the difficult waste-end reflux reaction can now be effected with smaller amounts of excess bicarbonate than formerly.

Studies are in progress to confirm the long-term stability of the process materials.

Table 3.1. Rates of exchange of cyanide in selected two-phase aqueous-organic systems

Organic phase		Aqueous phase mole ratio, HCO_3^-/CN^-	Half-time of exchange (sec)
Cyanohydrin	Diluent		
Acetone	Methyl isobutyl ketone	0	<8
Methyl isobutyl ketone	Methyl isobutyl ketone	0	13
		1.25	38
		1.50	125
	Xylene	1.20	60
	Hexane	1.20	72
Dipropyl ketone	Xylene	0	40
		1.29	300
Diethyl ketone	Xylene	0	<1.5
		1.10	<6

SEPARATION OF COBALT ISOTOPES BY ION EXCHANGE

D. A. Lee

There is a great need in isotope separation work to measure single-stage separation factors accurately. A program has recently been initiated to determine single-stage separation factors for isotopes of various elements. Since these factors are usually small, ion exchange and extraction chromatography will be used to multiply the separation effect. The methods of Glueckauf[1] and Spedding[2] will be used in the same manner as we previously used them in the determination of the separation factors for lithium isotopes.[3] To reduce the cost of isotopic assay, radioisotopes will be employed. Ideally, a pair of radioisotopes which can be resolved by radioactive counting would be preferred. In some cases it may be possible to use a stable isotope and a radioisotope if the analytical precision is adequate.

Some preliminary experiments have been conducted with cobalt isotopes. Mixtures of ^{60}Co and natural cobalt (^{59}Co) have been eluted from ion exchange columns under various conditions. The ratios of ^{60}Co to total cobalt have been determined for all samples eluted. The total cobalt in each sample was determined by the accurate potentiometric method of Lingane.[4] Our preliminary results indicate that the accuracy of the separation factor will be limited by the precision of the counting technique. Therefore, a large number of samples must be counted for long periods of time, and the columns must have large numbers of theoretical plates so that the total isotopic separation will be maximized.

A band of $CoCl_2$ was eluted from a column of cationic exchanger (Dowex 50-X12, 400 mesh) with 2 *N* HCl. From the elution curve the number of theoretical plates was calculated to be 2000. The single-stage separation factor for $^{59}Co/^{60}Co$ was determined to be approximately 1.00009. Cobalt-59 concentrated in the resin phase. We believe that the value of this separation factor can be established more precisely as we become more familiar with the analytical techniques.

In strongly acidic chloride solutions, cobalt forms anionic complexes which are readily sorbed on anionic exchange resins.[5] A band of $CoCl_2$ in 4 *N* HCl was eluted from an anion exchange column (Dowex 1-X10, 400 mesh) with 4 *N* HCl. The anionic species was probably $CoCl_3^-$. The retention of cobalt in 4 *N* HCl on Dowex 1 was not very good; there were only 500 theoretical plates in the column. For these conditions the single-stage separation factor was estimated to be 1.0004. This is significantly larger than the factor for cobalt isotopes on a cationic exchanger, and it may be that anionic complexes of cobalt have a larger separation potential than the cationic species.

However, this work is only in the preliminary stages. Many more data must be gathered before accurate values can be determined and the effect of the nature of the solution on the separation factors can be established. Yet the method appears to be workable, and isotopic separation factors for a variety of chemical species may be forthcoming.

---

1. E. Glueckauf, "Isotope Separation by Chromatographic Methods," AERE-R2896, Atomic Energy Res. Estab., Harwell, Berkshire, 1959.
2. F. H. Spedding, J. E. Powell, and H. J. Svec, *J. Amer. Chem. Soc.* 77, 6125 (1955).
3. D. A. Lee and G. M. Begun, *J. Amer. Chem. Soc.* 81, 2332 (1959); D. A. Lee, *Advan. Chem. Ser.* 89, 57 (1969).
4. J. J. Lingane, *Anal. Chim. Acta* 30, 319 (1964).
5. K. A. Kraus and F. Nelson, "Anion Exchange Studies of the Fission Products," *Proc. Int. Conf. Peaceful Uses Atomic Energy*, Vol. 7, p. 113, Session 9B.1, P/837, United Nations, New York, 1956.

SOLVENT EXTRACTION OF CESIUM AND RUBIDIUM TRIPHENYLCYANOBORON

D. A. Lee

A comparison has been made between the extraction of cesium(I) and rubidium(I) from aqueous sodium nitrate solutions with sodium triphenylcyanoboron ($Na\phi_3CNB$) and sodium tetraphenylboron ($Na\phi_4B$) in *o*-nitrotoluene. Although the magnitude of the distribution coefficients for alkali-metal ions was not as large with ϕ_3CNB^- as with ϕ_4B^-, the increased stability and improved phase separation make ϕ_3CNB^- an attractive reagent for Cs^+ and Rb^+ extraction. Differences in Rb^+ and Cs^+ distribution coefficients indicate that the two elements can be readily separated from one another in a multistage extraction facility.

The effect of alkali-metal ion concentration on the extraction of cesium and rubidium triphenylcyanoboron was determined over a concentration range of two orders of magnitude. The log-log plots of the loading isotherms were linear with composition with a slope of 1 for $Cs\phi_3CNB$, $Rb\phi_3CNB$, $Cs\phi_4B$, and $Rb\phi_4B$ extracted into *o*-nitrotoluene from aqueous $NaNO_3$ solutions. The loading isotherms for $Cs\phi_4B$ and $Rb\phi_4B$ extracted into 2,6-dimethyl-4-heptanone also had a slope of 1. This is expected since the ions involved are very large, and the dielectric constants of the organic solvents are relatively high.

The dependence of distribution coefficients on pH for $Cs\phi_3CNB$, $Rb\phi_3CNB$, $Cs\phi_4B$, and $Rb\phi_4B$ extracted into *o*-nitrotoluene from aqueous solutions at constant ionic strength, reagent concentration, and metal ion concentration was studied. For ϕ_4B^- systems, the expected slope of 1, indicating first-power hydrogen ion dependence, occurred between pH 8 and 9; therefore, $Cs\phi_4B$ and $Rb\phi_4B$ extractions should be made from basic aqueous solutions. For ϕ_3CNB^- systems it was necessary to go to strongly acidic solutions before first-power hydrogen ion dependence was noted. Thus, $Cs\phi_3CNB$ and $Rb\phi_3CNB$ can be extracted from acidic solutions as well as from basic solutions. The first-power slopes support the supposition that the extracted species are simply ion pairs M^+A^- or dissociated ion pairs $M^+ + A^-$.

Experiments were made to determine the dependence of the distribution coefficients on reagent concentration for cesium and rubidium triphenylcyanoboron. For $Cs\phi_3CNB$ the slope of a log-log plot of the reagent dependence curve was 1; however, that for $Rb\phi_3CNB$ was less than 1. A slope of less than 1 may be due to partial dissociation of the ion pair in the organic phase.[1] Dissociation is probable because of the high dielectric constant of the organic solvent, *o*-nitrotoluene ($E = 27.4$).

In ϕ_4B^- systems the reagent dependence slope for $Cs\phi_4B$ was 1.77; for $Rb\phi_4B$ it was 1.39. This difference from the behavior of the $Cs\phi_3CNB$ case suggested that there was some larger ion aggregation in the extracted species. An experiment was undertaken to confirm the association of $Cs\phi_4B$ with $Na\phi_4B$ in the organic phase. $Na\phi_4B$ tagged with ^{22}Na was extracted from 2 *N* $LiNO_3$ in the presence of 0.001 *N* Cs^+ and from 2 *N* $LiNO_3$ without Cs^+. The Na^+ extracted 25% more in the presence of Cs^+ than in the absence of Cs^+. The same experiment was done in the presence of Rb^+, but there was no significant difference in the Na^+ extraction in the presence of Rb^+. These results suggest association of $Cs\phi_4B$, though not $Rb\phi_4B$, with $Na\phi_4B$ in the organic phase. Presumably, the anomolous reagent dependence for $Rb\phi_4B$ is due to self-association. The distribution coefficient for Cs^+ was 1000 times the Na^+ coefficient.

Mixtures of *o*-nitrotoluene and 2,6-dimethyl-4-heptanone were used to extract $Cs\phi_3CNB$ from $NaNO_3$ solutions. As the concentration of *o*-nitrotoluene in the solvent mixture increased, the distribution coefficient increased. More than a fiftyfold increase in the distribution coefficient was noted for *o*-nitrotoluene as compared with 2,6-dimethyl-4-heptanone.

Cs^+ and Rb^+ were stripped from the organic phase with NH_4NO_3 solutions. The distribution of M^+ between the organic and aqueous phases decreased as the NH_4NO_3 concentration increased. A log-log plot of the dependence of the distribution coefficient on NH_4NO_3 activity had a slope of -2 for Cs^+ and Rb^+. Concentrated HCl also stripped Cs^+ from the organic phase; however, the reagent $H\phi_3CNB$ was partially decomposed.

p-Toluenesulfonic acid added to the aqueous phase increased the extraction of $Cs\phi_3CNB$ into *o*-nitrotoluene by 50%. This may be similar to the effect found by Flynn[2] in which the extraction of Cs^+ by phenol-nitrobenzene was enhanced by the addition of sodium dodecylbenzene sulfonate. No detailed analysis of *p*-toluenesulfonic acid dependence on $Cs\phi_3CNB$ extraction has been made.

It can be concluded that triphenylcyanoboron anion is an effective reagent for the solvent extraction of cesium and rubidium ions, and that the extracted species is probably the simple ion pair M^+A^-. The reagent is much more stable than tetraphenylboron and may be used in acidic as well as basic solutions.

This work has been accepted for publication in the *Journal of Inorganic and Nuclear Chemistry*.

1. R. M. Diamond and D. G. Tuck, "Extraction of Inorganic Compounds into Organic Solvents," pp. 139–43 in *Progress in Inorganic Chemistry*, F. A. Cotton, ed., Vol. II, Interscience, New York, 1960.
2. W. W. Flynn, *Anal. Chim. Acta* **50**, 365 (1970).

IDENTITY OF THE COCO SYSTEM COMPLEX

L. Landau D. Ahlgren[1]
W. H. Fletcher[2]

The COCO System[3] is a recently developed chemical exchange process for separating carbon isotopes. In this system, isotopic fractionation is based upon the reaction

$$^{13}CO(g) + Cu_2Cl_2 \cdot 8NH_4Cl \cdot {}^{12}CO(aq) = {}^{12}CO(g) + Cu_2Cl_2 \cdot 8NH_4Cl \cdot {}^{13}CO(aq)\,, \quad (1)$$

where the formula $Cu_2Cl_2 \cdot 8NH_4Cl \cdot CO$ represents the stoichiometric composition of the aqueous phase solute which yields the greatest isotopic fractionation. Determining the structure of this complex was considered pertinent to the problem of optimizing the performance of the COCO process. In pursuit of this objective, we

Table 3.2. Raman frequencies (cm^{-1})

H_2O	NH_4Cl(aq)	Cu_2Cl_2 in NH_4Cl	$Cu_2Cl_2 \cdot NH_4Cl \cdot {}^{12}CO$	$Cu_2Cl_2 \cdot NH_4Cl \cdot {}^{13}CO$	Polarization	Assignment
			301.2	296.1	1.0 D	Cu-C-O bend
			386.2	380.2	0.47 P	Cu-C stretch
	1431.2	1430.0	1433.0	1433.2	0.77 D	ν_4 NH_4^+
1637			1640.0			ν_2 H_2O
	1663.0	1659.0	1665.0	1669.0	0.82	Composite of ν_2 H_2O and ν_2 NH_4^+
			1691.0		0.98 D	ν_2 NH_4^+
			2051.5	2053.5	0.52 P	^{13}C-O stretch
			2101.1	2101.4	0.48 P	^{12}C-O stretch
	2879.0	2875.0	2867.0	2858.0	0.50 P	$2\nu_4$ NH_4^+
	3090.0	3101.0	3091.0	3103.0	0.32 P	ν_1 NH_4^+
3262	3242.0	3227.0	3225.0	3203.0	0.34 P	$2\nu_2$ H_2O
3430	3439.0	3450.0	3444.0	3438.0	0.41 P	ν_1 H_2O

examined the Raman spectra of H_2O, NH_4Cl(aq), $Cu_2Cl_2 \cdot NH_4Cl$(aq), $Cu_2Cl_2 \cdot NH_4Cl \cdot {}^{12}CO$(aq), and $Cu_2Cl_2 \cdot NH_4Cl \cdot {}^{13}CO$ in the region 250 to 4000 cm^{-1}. The observed Raman frequencies, as well as their polarizations and assignments, are shown in Table 3.2.

The infrared spectrum of the ${}^{12}CO$ complex was examined in the region 4000 to 400 cm^{-1}. The C-O stretch was observed and measured at 2098 cm^{-1}, in good agreement with the Raman measurement (2101.1 cm^{-1}).

In order to obtain further indications of the structure of the complex, CO was added at 20°C to a solution containing Cu_2Cl_2, NH_4Cl, and H_2O in concentrations usually employed in the COCO system. The pressure on the system was progressively increased to 3000 torr. The composition of the liquid phase was then computed as a function of CO pressure. The data indicated that more than one molecule of CO can be absorbed by each Cu_2Cl_2 molecule. A plot of the data suggests that a CO/Cu ratio of 1 would probably be attained at sufficiently high CO pressure.

The Cu^+ has a $3d^{10}$ configuration. Most commonly it has a coordination number of 4 and a tetrahedral geometry corresponding to $4sp^3$ hybrid bonding. In strong concentrations of Cl^- the $CuCl_4^{3-}$ species is the most abundant.[4] Our spectral and vapor pressure data support the thesis that, upon addition of CO to such solutions, the ion $CuCl_3CO^{2-}$ is formed. This species would have tetrahedral geometry and C_{3v} symmetry.

1. Student participant in the Great Lakes Colleges Association Science Semester, fall 1971, from DePauw University, Greencastle, Ind.

2. Consultant, Department of Chemistry, University of Tennessee, Knoxville.

3. A. A. Palko, L. Landau, and J. S. Drury, *Ind. Eng. Chem., Process Des. Develop.* **10**, 79 (1971).

4. T. G. Sukhova, O. N. Temkin, R. M. Flid, and T. K. Kaliya *Russ. J. Inorg. Chem.* **13**, 1072 (1968).

SEARCH FOR A NEW SULFUR ISOTOPE SEPARATION SYSTEM

J. S. Drury L. Landau

In response to anticipated interest in the availability of low-cost, high-purity, stable sulfur isotopes, we have undertaken the development of a suitable chemical separation process. Despite considerable research by subsequent investigators,[1,2] the best existing method[3] for separating stable sulfur isotopes is still the process based on the chemical exchange of sulfur between gaseous SO_2 and an aqueous solution of HSO_3^-, which was suggested by Thode in 1938. This process, though superior to other existing systems, suffers from two characteristics which prevent its successful application to the production of low-cost sulfur isotopes. First, the rate of exchange of sulfur between SO_2(g) and aqueous HSO_3^- is slow in the solution phase, and poor stage heights are obtained even in exchange columns of well-designed cascades. Second, Thode's process requires chemical refluxing. Both of these factors limit the economic potential of the process and preclude its use in the production of low-cost, high-purity isotopes.

The objectives of the present research are to identify a two-phase chemical exchange reaction, preferably gas-liquid, which can be thermally refluxed, and which has a single-stage separation factor of about 1.02 for ${}^{32}S/{}^{34}S$ separations.

The stipulation of a thermally refluxable process is crucial; it eliminates the necessity and expense of

chemical refluxing. It also virtually dictates the consideration of molecular addition compounds of the simple sulfur-containing molecules. We therefore planned to examine the 1:1 molecular addition compounds of H_2S, R_2S, CS_2, SO_2, COS, $SOCl_2$, SCl_2, and S_2Cl_2. From prior experience we believe molecular addition compounds having enthalpies of formation in the range 10–20 kcal/mole may be best suited to our purpose. Because of the basicity of the sulfur atom, obvious choices of moieties to form molecular addition compounds with the above sulfur molecules are compounds of elements of group IIIA of the Periodic Chart. These elements exhibit a wide range of Lewis acidity in their trivalent state: thus, for the trimethyl derivatives, the order of electron acceptor properties is B < Al > Ga > In > Tl. Among this group of Lewis acids we expect to find a suitable candidate of the proposed isotope separation system.

From the standpoint of isotope separation theory, the electron donor of choice, among the various sulfur species previously listed, is H_2S. We soon discovered, however, that Lewis acids sufficiently strong to form stable molecular addition compounds with this molecule readily abstracted protons from it to form not molecular addition compounds, but more advanced reaction products. Thus we soon were obliged to replace H_2S with its homologue, $(CH_3)_2S$. This compound forms a 1:1 molecular addition compound with diborane which is stable at room temperature, but its use was not considered practical because of the hazards involved in handling large quantities of the uncomplexed acceptor compound. Boron trifluoride forms stable 1:1 complexes with alkyl sulfides which we previously examined during the development of the ANCO System for separating boron isotopes. These molecular addition compounds are unsuitable for use in our proposed sulfur isotope separation system, however, because the mechanics of the separation process require the Lewis acid to be liquid, rather than gaseous, under operating conditions. No triaryl or trialkyl boron compounds were found which formed stable 1:1 coordination compounds with $(CH_3)_2S$ at or near ambient temperatures; we therefore turned our attention to a class of stronger Lewis acids, the trialkyl aluminum compounds.

No difficulty was experienced in obtaining 1:1 complexes with $(CH_3)_2S$ and $(CH_3)_3Al$ or $(C_2H_5)_3Al$. The enthalpy of formation of the first adduct is 19 kcal/mole, and that of the second adduct about 9 kcal/mole. The latter complex proved stable toward chemical decomposition in an inert environment, and was sufficiently promising otherwise that it was chosen for further investigation.

To determine if the complex could be used to fractionate sulfur isotopes, we equilibrated it with $(CH_3)_2S$ for 1 hr at 47°C, sampling the gas phase before and after contact. Mass analysis of these samples will indicate the single-stage separation factor for the exchange reaction,

$$(CH_3)_2{}^{34}S(g) + (CH_3)_2{}^{32}S\cdot Al(C_2H_5)_3(liq)$$
$$= (CH_3)_2{}^{32}S(g) + (CH_3)_2{}^{34}S\cdot Al(C_2H_5)_3(liq)\ .$$

Analysis of the samples awaits the development of a satisfactory procedure for quantitatively converting $(CH_3)_2S$ to a molecular species suitable for mass analysis. Initially we planned to convert $(CH_3)_2S$ to SF_6 by treatment with F_2 and heat, but this procedure introduced a by-product which interfered with the mass analysis. Recent studies indicate that $(CH_3)_2S$ may be converted quantitatively to CS_2 by pyrolysis, in vacuo, at 900°C. When this technique has been adequately tested, we plan to apply it in the mass analysis of our isotopic samples.

1. K. E. Holmberg, British Pat. 736,459, Sept. 7, 1955.
2. A. C. Rutenberg and J. S. Drury, *J. Chem. Eng. Data* **9**, 43 (1964).
3. H. G. Thode, J. E. Gorham, and H. C. Urey, *J. Chem. Phys.* **6**, 296 (1938).

MOLECULAR SPECTROSCOPY AND PHOTOCHEMISTRY

G. M. Begun

Observations of infrared and Raman vibrational frequencies of isotopic molecules have been employed since the early days of isotope separation to furnish data from which isotopic exchange equilibrium constants can be calculated. For this reason, and because molecular spectroscopy is one of the fastest developing and most powerful fields of science, we have built up and maintained a capability for research in this area. The advent of the laser has hastened developments in these disciplines and greatly expanded the uses of optical methods. It is our belief that these fields will continue to grow at a rapid rate, and that many more applications will be found. Our Raman spectrometer (originally a Cary model 81 employing a mercury arc source) has been modified to use two laser sources: a helium-neon red laser and an argon-ion blue-green laser. Our infrared capabilities consist of a Perkin-Elmer 521 spectrophotometer with accessories.

The possible photochemical separation of isotopes has, since the early days of the Manhattan Project, inspired the imagination of those interested in their separation. The experimentalists, however, have been able to obtain significant separation in only one case, that of mercury isotopes. In this example, mercury resonance radiation causes reaction of a selected isotope to occur with a substrate in low-pressure gaseous mercury. Small quantities (milligram amounts) of mercury isotopes have been photochemically enriched in this way. Recent proposals suggest the use of laser radiation to initiate preferential isotopic reactions. We have previously[1] reported our results with reactions of chlorine excited by the 514.5-nm green line from the argon-ion laser. In all cases which we examined, a chain reaction was initiated by the laser light which made isotope enrichment impossible. The pressures used were, however, relatively high, and we have assembled a quadrupole mass spectrometer with the hope of examining such reactions at low pressures. The assembly of the instrument is nearly complete, and testing of the mass spectrometer will be started shortly. We plan to examine chlorine reactions initially, since the argon-ion laser is the only suitable light source available to us at present. Several tunable lasers are now marketed, and it is hoped that eventually we may be able to use one of these in our experiments.

The Molten-Salt Reactor Project at Oak Ridge National Laboratory has resulted in considerable fundamental research on the properties of molten salt systems. Laser Raman spectroscopy has proven to be an especially powerful tool for the investigation of the actual species present in such fused salt systems. We have continued our collaborative work in this field.

In our previous molten-salt studies,[2,3] sealed sample tubes were wrapped with lengths of Nichrome or platinum heating wire spaced widely enough to allow passage of light between the turns. The sample was melted by passing current through the wire, and the Raman spectrum was observed.

This simple method of operation gave good results with fused salt samples up to 500°C. In attempting to observe the Raman spectrum of fused Cs_2ZnCl_4 at 610°C, however, we found that thermal losses from the sample tube became excessive, and temperature fluctuations resulted. It was apparent that a furnace was necessary to ensure even heating of the sample, and the simple furnace pictured in Fig. 3.1 was fabricated from grade A Lava[4] in a few hours. Good Raman spectra of molten Cs_2ZnCl_4 at 620° (see below) were obtained in this manner.

ORNL-DWG. 71-9123

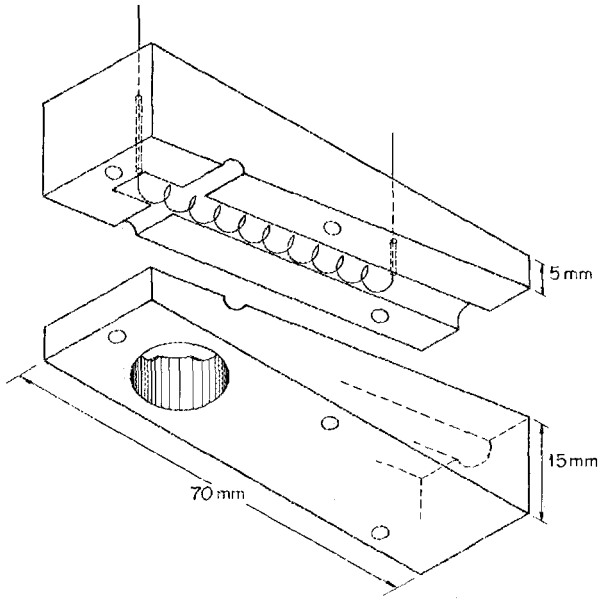

Fig. 3.1. Furnace for fused-salt Raman studies.

The Raman spectra of molten and glass $ZnCl_2$ have been studied by several investigators, and Raman spectra of molten mixtures of $ZnCl_2$ with alkali chlorides have been examined. These studies showed that $ZnCl_2$ is a strong chloride acceptor. In nonaqueous media the order of acceptor strength of the two compounds $AlCl_3$ and $ZnCl_2$ is different in different solvents. The question arises, Which of the two compounds is a better chloride acceptor in the molten state? Since both salts are very hygroscopic and molten $AlCl_3$ is highly volatile, direct investigation of the phase diagram of this system is very difficult. Palkin and Belousov[5] deduced the phase diagram of the $AlCl_3$-$ZnCl_2$ system from a study of the Al-$ZnCl_2$ system. A solid compound of the formula $4AlCl_3 \cdot 3ZnCl_2$ was suggested. The x-ray examination of the system, however, failed to give results because of glass formation in the frozen mixture. We have examined the Raman spectra of molten mixtures and glasses containing various mole ratios of $ZnCl_2$-$AlCl_3$. In addition, we have examined the Raman spectra of polycrystalline and molten Cs_2ZnCl_4 for comparison with the $AlCl_3$-$ZnCl_2$ system. Samples prepared in a nitrogen-filled dry box were sealed in quartz tubes. The tubes were wrapped with heating wire, and the Raman spectra were recorded using laser excitation.

Representative Raman spectra of various molten $AlCl_3$-$ZnCl_2$ mixtures, as well as the spectra of molten $ZnCl_2$ and $AlCl_3$, are reproduced in Fig. 3.2. The

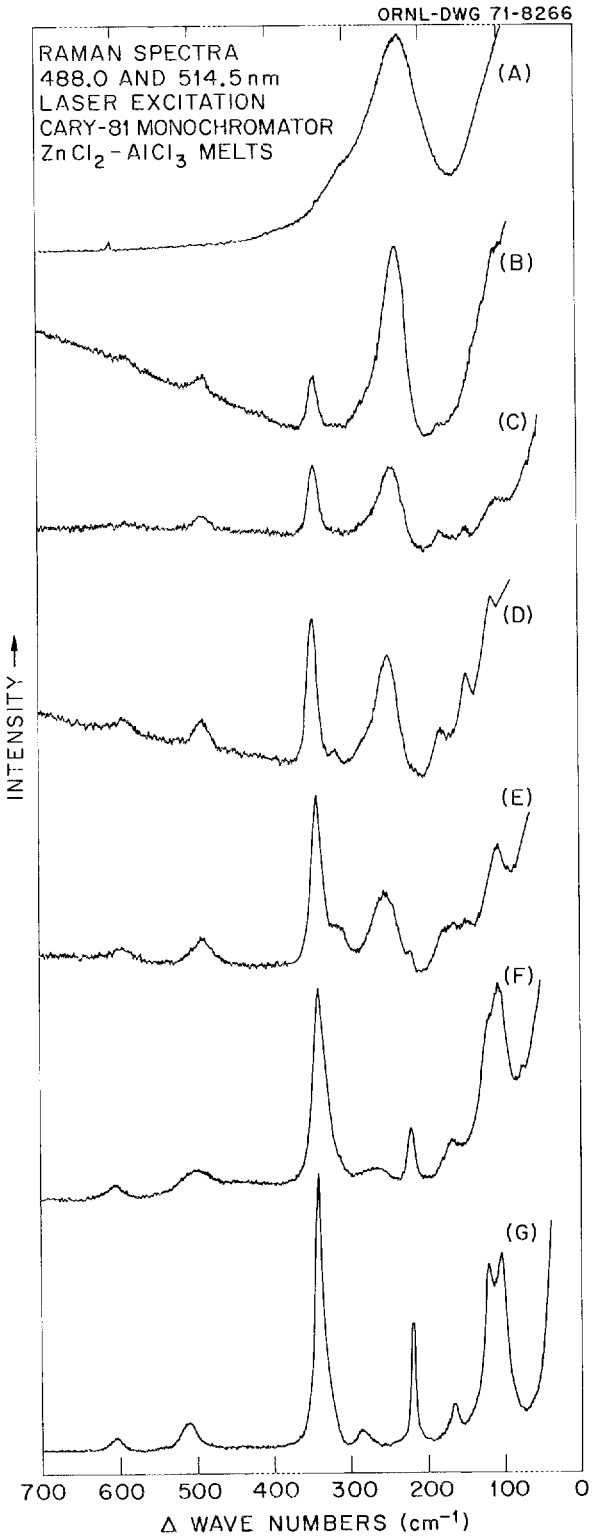

Fig. 3.2. Raman spectra of molten or glass $AlCl_3$-$ZnCl_2$ samples, mole % $AlCl_3$; A, 0; B, 20; C, 40; D, 50; E, 70; F, 90; G, 100.

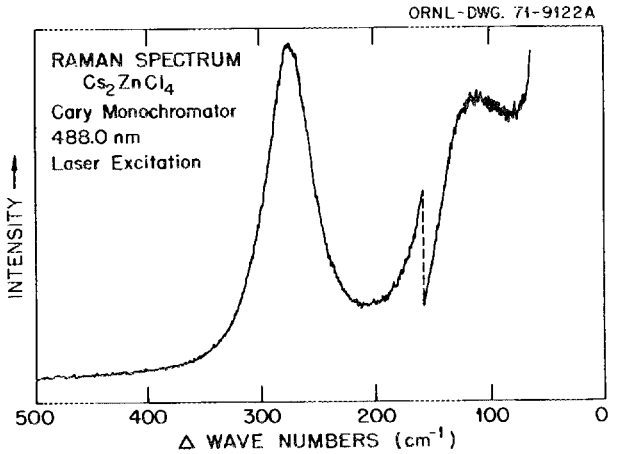

Fig. 3.3. Raman spectra of Cs_2ZnCl_4; A, molten; B, polycrystalline.

frequencies of the peaks observed for samples of various mole ratios are recorded in Table 3.3. The Raman spectra of polycrystalline and of molten Cs_2ZnCl_4 are shown in Fig. 3.3. The frequencies of the peaks observed for polycrystalline Cs_2ZnCl_4 are 115, 140, 288, and 298 cm^{-1}, while the two broad peaks for the molten salt center at 110 and 277 cm^{-1}. Our Raman spectrum of molten Cs_2ZnCl_4 shows a remarkable resemblance to that published[6] for 2.88 *M* $ZnCl_2$ + 9.35 *M* HCl in aqueous solution. It appears that with both aqueous and molten $ZnCl_4^{2-}$ ion the four tetrahedral vibrational modes merge into two broad bands with ν_1 coalescing with ν_3, and ν_2 with ν_4. That this effect is due to more than just a broadening of bands in the liquid is shown by the lack of resolution of ν_1 and ν_3 when the polarization rotator was turned 90°. These frequencies must be quite close in the molten spectra. Transition from the solid to the liquid state thus produces a greater lowering of the antisymmetrical (F_2) vibration than of the symmetrical (A_1) stretching frequency. These data also support the contention of Quicksall and Spiro[6] that aqueous $ZnCl_4^{2-}$ maintains its tetrahedral structure rather than forming $ZnCl_4(H_2O)_2^{2-}$ with D_{4h} symmetry as postulated by Irish, McCarroll, and Young.[7]

The most obvious conclusion from the $AlCl_3$-$ZnCl_2$ data is that no appreciable quantities of the discrete complex species $AlCl_4^-$, $Al_2Cl_7^-$, or $ZnCl_4^{2-}$ were formed in any of the samples. The strong peaks[2] for $AlCl_4^-$ at 351 cm^{-1}, $Al_2Cl_7^-$ at 313 cm^{-1}, and $ZnCl_4^{2-}$ at 277 cm^{-1} do not appear in any of the spectra. The strongest Al_2Cl_6 peak, the polarized ν_2 vibration at 341 cm^{-1}, remains virtually unchanged in the various

Table 3.3. Raman frequencies of the molten $AlCl_3$-$ZnCl_2$ system

$AlCl_3$ (mole %)	Peak positions (Δcm^{-1})[b]									
0	80 w					233 s,P	268 sh 306 sh	335 sh		
10						234 s,P	275 sh	342 w,P		
20[a]	102 w			178 w		235 s,P	274 sh	342 m,P	486 w,P	
40[a]	100 w		146 w	176 w		240 s,P	265 sh	343 s,P	486 w,P	
45[a]	103 w		144 w	174 w		242 s,P	264 sh	342 s,P	483 w,P	
50	110 w		143 w,P	174 w,P		244 s,P	274 sh 310 w,P	345 s,P	484 m,P	586 w
55	106 w			173 w		242 s,P		342 s,P	488 m,P	
70	104 m,P		142 w	165 w	218 w	250 s,P	312 w	340 s,P	490 m,P	592 w,P
80	104 m,P	118 w			219 w			340 s,P		
90	105 s,P	119 m		165 w	218 m,P	261 w		339 s,P	500 w,P	605 w,P
100	104 s,P	119 s		166 w	218 s,P	290 w,P		341 s,P	512 m,P	608 m,P

[a]Data from glass samples, verified by melt spectra.
[b]w, weak; m, medium, s, strong; sh, shoulder; P, polarized.

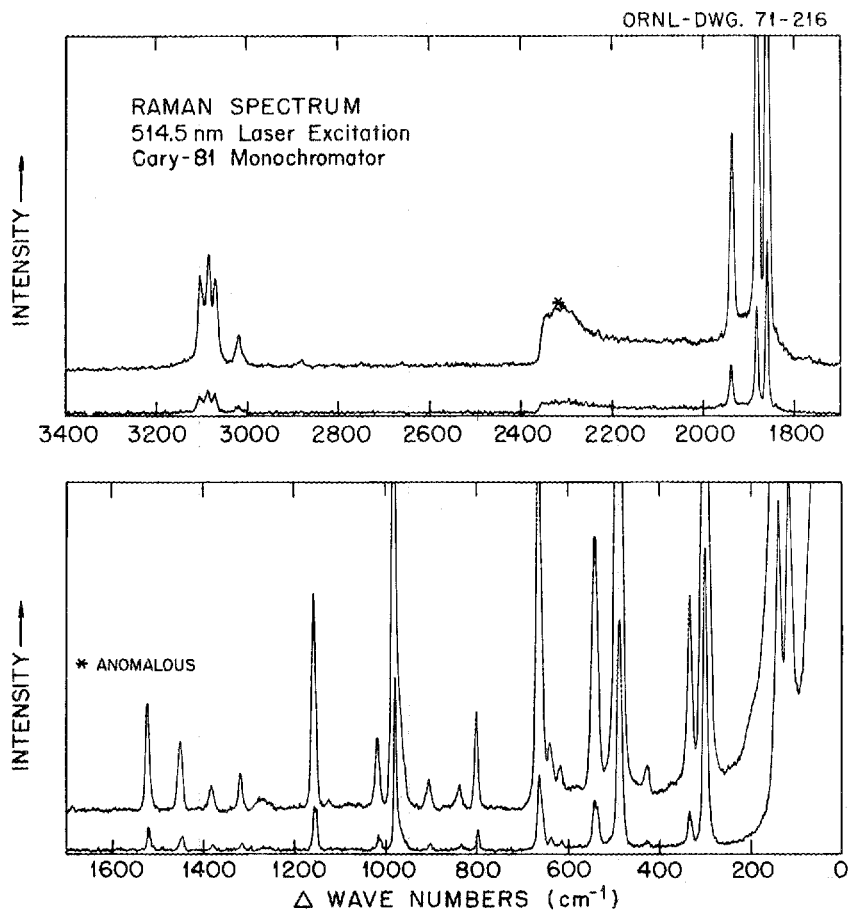

Fig. 3.4. Raman spectrum of polycrystalline benzene chromium tricarbonyl.

mixtures, and we conclude that dimeric Al_2Cl_6 does not appreciably dissociate or react in the molten mixture. The Raman spectrum of pure molten $ZnCl_2$ shows a broad peak centered at 233 cm^{-1} with several shoulders on the high-frequency side. The band at 233 cm^{-1} has previously been assigned to the bridged Zn-Cl stretching frequency of a polynuclear $(ZnCl_2)_n$ aggregate. Higher-frequency bands have been assigned to smaller fragments of the tetrahedral $ZnCl_4$ (260–270 cm^{-1}) and $ZnCl_2$ (305 cm^{-1}) monomers. As pure $ZnCl_2$ is diluted with Al_2Cl_6, we find a gradual change in the major $ZnCl_2$ peak frequency from 233 to 261 cm^{-1}. A reasonable interpretation of this effect is an interaction between $ZnCl_2$ and Al_2Cl_6 whereby the polynuclear aggregate of $ZnCl_2$ is being broken up by Al_2Cl_6 molecules, resulting in smaller Zn-Cl-Zn aggregates.

With the development of laser light sources, it is possible to obtain Raman spectra of colored compounds that previously could not be examined. Benzene chromium tricarbonyl is such a compound. We have recorded the Raman spectra of solid polycrystalline samples and of solutions in benzene. The Raman spectrum of the polycrystalline solid is shown in Fig. 3.4. The numerical values of the frequencies are given in Table 3.4 together with the relative intensities and the half-widths of the observed absorptions. Based on x-ray diffraction results,[8] which indicate a molecular model

Table 3.4. Vibrational frequencies of benzene chromium tricarbonyl

Freq. No.	Species	Vibration type	Raman[a] (solid)	Infrared[b] (solid)	Solution[c] in CS_2	Solution[c] in C_6H_6
28	E	OC-Cr-CO asym. def.	110 (96; 30)			
24	E	ϕH-Cr-CO rock	132 (90; 30)			
21	A_1	ϕH-Cr sym. st.	298 (100; 30)	298 (5)	301 P	301 P
27	E	Cr-CO asym. st.		306 (0)		
23	E	Cr-ϕH wag	332 (10; 14)	330 (5)	331 D?	332 D
16	E	C-C-C bend	426 (1; 11)	422 (5)		
26	A_1	Cr-CO sym. def.	486 (78; 30)	483 (6)	477 P	480 P
25	A_1	Cr-CO sym st.	535 (12; 15)	535 (10)		532 P?
34	E	Cr-C-O band	543 (16; 15)			
6	E	C-C-C bend	614 (1; 14)	612 (3)		
33	E	Cr-C-O bend	644 (3; 17)	633 (10)		
31	A_1	Cr-C-O sym. bend	664 (23; 11)	664 (10)		657 P
11	A_1	C_2C-H bend	800 (5; 11)	784 (9)		793 P
10	E	C_2C-H bend	842 (2; 11)	965 (3)		
17	E	C_2C-H bend	902 (1; 17)	902 (6)		
1	A_1	C-C sym. st.	980 (46; 9)	978 (4)	977 P	
18	E	C-C-H bend	1017 (5; 11)	1016 (5)		1122 D?
15	A_1	H-C_2-H bend	1152 (13; 10)	1147 (5)		1150 P?
9	E	CC-H bend	1158 (14; 10)	1157 (4)		
			1272 (1; 34)			
14	A_1	H-C_2-H bend	1317 (2; 9)	1314 (1)		
			1348 (0.6; 23)		1356 P	
			1381 (2; 11)		1374 P	
19	E	H-C_2-H bend	1451 (5; 11)	1445 (10)		1443 D?
			1521 (7; 11)		1516 D?	1517 D?
8	E	C-C asym. st.		1631		
30	E	C-O asym. st.	1865 (51; 9)	1862 vs	1903 D	1898 D
			1887 (33; 9)	1882 sh		
29	A_1	C-O sym. st.	1943 (16; 11)	1967 vs		1971 P
20	E	C-H deg. st.	3023 (3; 14)	*3040 w		
7	E	C-H deg. st.	3076 (7;	*3073 sh		
2	A_1	C-H sym. st.	3090 (9; 40)	*3089 s		
			3108 (7;	*3100 s		

[a]The solid Raman data are from 514.5 nm excitation. The numbers in parentheses refer to the relative peak height (first number) and the half-width in cm^{-1} (second number).

[b]Data from H. P. Fritz and J. Manchot, *Spectrochim. Acta* **18**, 171 (1962).

[c]Solution data using 632.8 and 514.4 nm laser excitation. P = polarized, D = highly depolarized.

with a staggered C_{3v} symmetry, we have assigned the vibrational frequencies of the molecule (Table 3.4). The assignment of threefold symmetry to the molecular structure of $C_6H_6Cr(CO)_3$ should not be taken to mean a distortion of the benzene ring from sixfold to threefold symmetry. On the contrary, no significant distortion of the π-bonded benzene ring from sixfold symmetry (D_{6h}) is found by the x-ray study. The threefold symmetry suggested for $C_6H_6Cr(CO)_3$ by the vibrational spectra describes the overall molecular symmetry, not a local symmetry. Using the assignment of the vibrations given in Table 3.4, force field and mean amplitude of vibration calculations will be made for benzene chromium tricarbonyl.

1. W. H. Fletcher, *Chem. Div. Annu. Progr. Rep. May 20, 1971*, ORNL-4706, p. 91.
2. G. M. Begun, *Chem. Div. Annu. Progr. Rep. May 20, 1970*, ORNL-4581, p. 65.
3. G. M. Begun, *Chem. Div. Annu. Progr. Rep. May 20, 1971*, ORNL-4706, p. 92.
4. American Lava Company, Chattanooga, Tenn.
5. A. P. Palkin and O. K. Belousov, *Zh. Neorg. Khim.* **2**, 1620 (1957).
6. C. O. Quicksall and T. G. Spiro, *Inorg. Chem.* **5**, 2232 (1966).
7. D. E. Irish, B. McCarroll, and T. F. Young, *J. Chem. Phys.* **39**, 3436 (1963).
8. M. F. Bailey and L. F. Dahl, *Inorg. Chem.* **4**, 1314 (1965).

ISOTOPIC MASS SPECTROMETRY

L. Landau D. Ahlgren[1]

Samples of CO_2 and O_2 were derived from all of the columns and reservoirs of the ^{17}O facility, and were analyzed for ^{17}O and ^{18}O abundances, as part of the shutdown procedure for the plant, prior to transferring the enriched material to the Isotopes Division.

Samples of CO_2 were examined for isotopic separation factors arising from various modifications of the CYANEX system. Rates of isotopic exchange in the CYANEX system were also monitored under several different conditions.

A study was undertaken to find a suitable molecular species for analysis of samples containing isotopically fractionated sulfur. Gaseous SF_6 was found to behave well in the mass spectrometer. The use of a fluoride for this application is advantageous, for, not having other isotopes, it cannot be fractionated during any experimental procedure. In preliminary work, samples of SF_6 readily pumped out of the mass spectrometer and errors attributable to memory of previous samples were negligible.

Table 3.5. Isotopic abundance measurements on SF_6

Number of measurements	Species	Ratio $^{34}S/^{32}S$	95% C.L.
2	SF_4^+	0.04490	±0.00127
2	SF_3^+	0.04495	±0.00064
2	SF_2^+	0.04545	±0.00064
4	SF^+	0.04619	±0.00015
5	S^+	0.0588	±0.00442

The isotopic abundance ratios for $^{34}S/^{32}S$ were examined at m/e 34 and 32 (S^+), 53 and 51 (SF^+), 72 and 70 (SF_2^+), 91 and 89 (SF_3^+), 110 and 108 (SF_4^+), and 129 and 127 (SF_5^+). Essentially no SF_6^+ was observed; SF_5^+ was the major component of the cracking pattern, followed in order by SF_3^+, SF^+, SF_4^+, SF_2^+, and S^+.

Our ratio mass spectrometer uses extremely wide slits and would not resolve the peaks at 127 and 129 well enough to run the ratios. The data from the other peaks are listed in Table 3.5. The data obtained from mass positions 34 and 32 were not reproducible and were at variance with the other data points. Measurements at all of the other mass positions appeared to be acceptable, and SF^+ was chosen as the species of preference, because we had better resolution in that mass range, and 53/51 ratios could be run without modifications to the mass spectrometer.

Methods for the preparation of SF_6 were investigated: apparatus was set up to fluorinate elemental sulfur directly by passing F_2 slowly over S in a stainless steel tube. The reaction went readily and a good yield was obtained, although some of the other sulfur fluorides were observed in the infrared spectra. Spiked samples are being prepared, and isotopic constancy will be checked.

1. Student participant in the Great Lakes Colleges Association Science Semester, fall 1971, from DePauw University, Greencastle, Ind.

4. Radiation Chemistry

EFFECTS OF H_2O, NH_3, H_2, AND SF_6 ON OZONE YIELDS AND KINETICS IN THE PULSE RADIOLYSIS AND FLASH PHOTOLYSIS OF OXYGEN

J. A. Ghormley J. W. Boyle
C. J. Hochanadel P. J. Ogren[1]

We had previously shown that small concentrations of H_2O, NH_3, H_2, and SF_6 greatly inhibit O_3 formation in the pulse radiolysis of O_2.[2] We have carried out additional studies employing both pulse radiolysis and flash photolysis in order to determine mechanisms of inhibition.

The O_3 yield was measured over the entire composition range for O_2-SF_6 mixtures in order to delineate accurately the scavenging and direct-action effects. While it is still not clear how to calculate accurately the energy partition in the radiolysis of a gas mixture, a simple plot of $G(O_3)$ vs electron fraction (which is nearly equal to the stopping power fraction in this system) gave a value $G(O_3) = 6.2$ on extrapolation to zero SF_6 concentration, compared with 13.8 in pure O_2. The effect of SF_6 has been interpreted[3] in terms of electron scavenging by SF_6, which prevents dissociative neutralization of O_2^+ by O_2^- or e^-. The decrease in yield of 7.6 is greater than $2G(e^-) = 6.6$ (obtained from measurements of W), indicating an additional effect of the SF_6. Similar measurements were made for O_2-NH_3 and O_2-H_2 mixtures for the concentration ranges outside the explosion limits (~25 and 75% for NH_3, and ~15 and 90% for H_2). Ammonia has a very marked effect, giving an extrapolated yield of ~3.3 molecules of O_3 per 100 eV. Yields were also measured for O_2-H_2O (up to saturation at ~3%) and for O_2-NH_3, O_2-H_2, and O_2-H_2O with added SF_6. It is clear that, in addition to interfering with O_3 formation from ionic precursors, these additives also inhibit O_3 formation from neutral precursors, which may be excited O atoms [O (^1D), O (^1S), or hot O (^3P)] or excited O_2 molecules.

Measurements of the O_3 yield in the flash photolysis (>1600 Å) of O_2 in mixtures with He, Ar, N_2, or SF_6 over the entire composition range showed that these molecules act only as diluents, affecting only the rate of O_3 formation as third body M in the reaction $O + O_2 + M \rightarrow O_3 + M$. The molecules H_2, H_2O, and NH_3 lower the O_3 yield. Reaction of these molecules with ground-state, thermal oxygen atoms, O (^3P), is known to be very slow. The molecules H_2 and H_2O are known to react rapidly with O (^1D), but the rate with NH_3 has not been measured. We are studying the reaction of these and other molecules with O (^1D). The O (^1D) are produced by photolysis of O_3 at wavelengths greater than 2300 Å (oxygen-free 2 M NaBr filter). The filter prevents photolysis of O_2 and the other additives and allows adequate absorption by O_3 (peak at 2560 Å). Dissociation of O_3 at $\lambda > 2300$ Å produces O (^1D) and O_2 ($^1\Delta$). In a system containing mostly O_2 (0.04 M) with a small amount of O_3 (~10^{-5} M), there is no net loss of O_3, since the O (^1D) and O_2 ($^1\Delta$) are deactivated by O_2, and the O (^3P) are then reconverted to O_3. We observe dissociation of the O_3 by the flash, followed by re-formation of the O_3. The addition of He, Ar, N_2, or SF_6 causes no net loss of O_3, whereas the addition of NH_3, H_2, or H_2O, which react with O (^1D). does produce a net loss. Most of the decrease in O_3 concentration occurs during the flash, but with NH_3 or H_2 added, there is an additional small loss on a millisecond time scale. The percentage loss of O_3 increases with (1) the ratio of concentration of additive to oxygen, since these molecules compete for O (^1D), and (2) the ratio of concentrations $[O_3]/[O_2]$, indicating competition of these two molecules for products of the reaction of the additive with O (^1D).

In addition to the absorption by ground-state O_3 centered at 2560 Å, we also observe transient absorption at slightly longer wavelengths in the range ~2500 to ~3500 Å, with a peak at ~2800 Å. We had previously observed[4] this absorption in the pulse radiolysis of O_2 and attributed it to vibrationally

excited O_3. Riley and Cahill[5] disagree with this assignment. The photolysis system offers simplifications for studying this transient, since the only primary species are O (^1D) and O_2 ($^1\Delta$). We are now studying the kinetics of formation and decay of the transient and the effects of various additives on the transient. Most of the transient forms during the flash, and at 1 atm of O_2 it undergoes first-order decay with $t_{1/2} \cong 6$ μsec, about the same as for re-formation of ozone. All of the additives, including He, Ar, N_2, SF_6, H_2, NH_3, and H_2O, affect the kinetics of formation and decay, and at least the last three affect the amount of transient produced.

1. Department of Chemistry, Maryville College, Maryville, Tenn.
2. C. J. Hochanadel, J. A. Ghormley, and P. J. Ogren, *Chem Div. Annu. Progr. Rep. May 20, 1971*, ORNL-4706, p. 102.
3. C. Willis et al., *Can. J. Chem.* **48**, 1505, 1515 (1970).
4. C. J. Hochanadel, J. A. Ghormley, and J. W. Boyle, *J. Chem. Phys.* **48**, 2416 (1968).
5. J. F. Riley and R. W. Cahill, *J. Chem. Phys.* **52**, 3297 (1970).

ABSORPTION SPECTRUM AND REACTION KINETICS OF THE HO_2 RADICAL IN THE GAS PHASE[1]

C. J. Hochanadel J. A. Ghormley P. J. Ogren[2]

Perhydroxyl radicals were produced in the gas phase by flash photolysis of water vapor (3%) in an atmosphere of hydrogen, helium, or argon containing ~2% oxygen. Water is dissociated in the first continuum to H and OH, and O_2 converts the H atoms to HO_2. Hydrogen nearly doubled the amount of HO_2 produced by converting OH to H. The absorption spectrum of HO_2 is a broad band with a peak at 2050 Å. The molar extinction coefficient, ϵ_{max}, based on measurement of the H_2O_2 formed in the hydrogen system, is 1770 ± 150 M^{-1} cm^{-1}. The rate constant for the bimolecular combination reaction, $HO_2 + HO_2 \rightarrow H_2O_2 + O_2$, was evaluated as $5.7 \pm 0.5 \times 10^9$ M^{-1} sec^{-1} at 298°K, and for the reaction $HO_2 + OH \rightarrow H_2O + O_2$, $k = 1.2 \pm 0.2 \times 10^{11}$ M^{-1} sec^{-1}.

From auxiliary measurements of the rate of O_3 formation it was also found that, in the flash photolysis of O_2 (2%) in H_2, hot O atoms react with H_2 to form OH and H which are then converted to HO_2.

1. Abstract of published paper: *J. Chem. Phys.* **56**, 4426 (1972).
2. Department of Chemistry, Maryville College, Maryville, Tenn.

ELEMENTARY PROCESSES IN THE RADIOLYSIS OF AQUEOUS SULFURIC ACID SOLUTIONS: DETERMINATIONS OF BOTH G_{OH} AND $G_{SO_4^-}$[1]

R. W. Matthews[2] H. A. Mahlman T. J. Sworski

We have obtained evidence for the proposal of Boyle[3] that two oxidizing radicals are produced concurrently in the radiolysis of aqueous sulfuric acid solutions: OH and SO_4^- radicals that are presumed to result from the direct action of ionizing radiation on water and sulfuric acid anions respectively. The evidence is the dependence of $G(Ce^{III})$ on both cerium(III) and either formic acid or 2-propanol concentrations in the radiolysis of cerium(IV)–cerium(III)–formic acid mixtures and cerium(IV)–cerium(III)–2-propanol mixtures. G_{OH} and $G_{SO_4^-}$ were determined by using the generalized least-squares program of Lietzke[4] to fit experimental data to complex kinetic equations that contain up to 22 dependent variables.

Validity of the kinetic equations was originally indicated[5] by the excellent agreement for two determinations in 4.0 M sulfuric acid: $G_{OH} = 1.76 \pm 0.19$ and $G_{SO_4^-} = 0.95 \pm 0.18$ with 2-propanol solutions; $G_{OH} = 1.78 \pm 0.03$ and $G_{SO_4^-} = 0.94 \pm 0.03$ with formic acid solutions. Further validity is indicated by the successful evaluation of radical yields in 0.4 M sulfuric acid: $G_{OH} = 2.60 \pm 0.04$ and $G_{SO_4^-} = 0.20 \pm 0.04$. Despite this low yield of SO_4^- radicals, there is gratifying agreement between the values obtained in 0.4 and 4.0 M sulfuric acid solutions for the relative reactivities of SO_4^- radical with cerium(III), formic acid, 2-propanol, and water.

The significance of this research is the conclusion that G_{OH} is proportional to energy absorption by water. There is no evidence for oxidation of sulfuric acid anions by H_2O^+, a commonly assumed precursor of the OH radical.

1. Abstract of published paper: *J. Phys. Chem.* **76**, 1265 (1972).
2. Visiting scientist from the Australian Atomic Energy Commission Research Establishment, Lucas Heights, New South Wales.
3. J. W. Boyle, *Radiat. Res.* **17**, 427 (1962).
4. M. H. Lietzke, *A Generalized Least Squares Program for the IBM-7090 Computer*, ORNL-3259 (March 1962).
5. R. W. Matthews, H. A. Mahlman, and T. J. Sworski, *Chem. Div. Annu. Progr. Rep. May 20, 1969*, ORNL-4437, p. 52.

ROLE OF WATER ACTIVITY IN SULFURIC ACID SOLUTIONS

T. J. Sworski

The rate of cerium(IV) reduction by hydrogen peroxide in sulfuric acid solutions from 2.0 to 13.0 M

adheres well to Eq. (I):

$$d[Ce^{IV}]/dt = -2k_{obs}[Ce^{IV}]^2[H_2O_2]/[Ce^{III}] \ . \qquad (I)$$

A marked decrease in k_{obs} with increase in sulfuric acid concentration from 2.0 to 8.0 M is quantitatively explicable[1] by postulation of virtual equilibrium between HO_2 and $H_2O_2^+$ according to the following reaction mechanism:

$$Ce^{IV} + H_2O_2 \rightleftharpoons Ce^{III} + H_2O_2^+ \ , \qquad (1)$$

$$H_2O_2^+ \rightleftharpoons H^+ + HO_2 \ , \qquad (2)$$

$$Ce^{IV} + HO_2 \rightarrow Ce^{III} + HO_2^+ \ , \qquad (3)$$

$$HO_2^+ \rightarrow H^+ + O_2 \ , \qquad (4)$$

$$Ce^{IV} + H_2O_2^+ \rightarrow Ce^{III} + H_2O_2^{2+} \ , \qquad (5)$$

$$H_2O_2^{2+} \rightarrow H^+ + H_2O_2^+ \ , \qquad (6)$$

with

$$k_{obs} = \frac{k_1 k_5}{k_{-1}}\left(1 + \frac{k_3 K_{H_2O_2^+}}{k_5 h_0}\right) . \qquad (II)$$

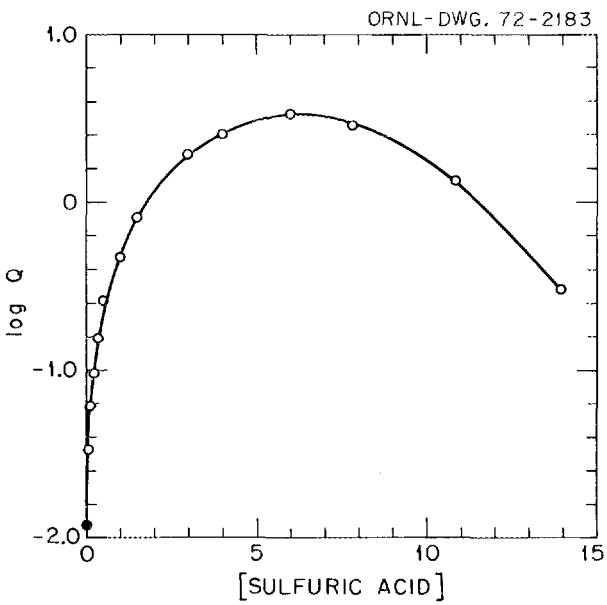

Fig. 4.1. Dependence of the second dissociation quotient of sulfuric acid on the sulfuric acid concentration. ○ Calculated values from the data of Young, Maranville, and Smith. Solid curve illustrates the least-squares fit of the data to Eq. (III).

A marked increase in k_{obs} with further increase in sulfuric acid concentration from 8.0 to 13.0 M is quantitatively explicable[1] by postulation of virtual equilibrium between H_2O_2 and $H_3O_2^+$. However, as previously noted,[2] the minimum in k_{obs} occurs at about the same sulfuric acid concentration at which $[SO_4^{2-}]$ is a maximum.[3,4] This qualitative correlation suggests a common cause for the minimum in k_{obs} and the maximum in $[SO_4^{2-}]$. A search for this common cause indicates that both k_{obs} and $[SO_4^{2-}]$ may be dependent on water activity (a_w).

The second dissociation quotient of sulfuric acid, $Q = [H^+][SO_4^{2-}]/[HSO_4^-]$, is shown in Fig. 4.1 as a function of sulfuric acid concentration. The curve in Fig. 4.1 illustrates an excellent least-squares fit of the data to Eq. (III):

$$\log Q = \log K^0 + 4AI^{1/2}/(1 + BI^{1/2}) + q \log a_w \ , \qquad (III)$$

where A is the Debye-Hückel limiting slope of 0.509 at 25°C for a singly charged ion, K^0 is the complete equilibrium constant

$$K^0 = \frac{(a_{H^+})(a_{SO_4^{2-}})}{(a_w^q)(a_{HSO_4^+})}$$

that contains water as a reactant,[5,6] I is the ionic strength, and B is an adjustable parameter in an extended Debye-Hückel equation. Values for $\log K^0$, B, and q are listed in Table 4.1 for the data of Young, Maranville, and Smith[3] and of Chen and Irish.[4] The significance of Eq. (III) is the constancy of K^0, even at extremely high ionic strengths, with an extended Debye-Hückel equation for activity coefficients.

Figure 4.2 shows the dependence of k_{obs} on sulfuric acid concentration. The dashed curve in Fig. 4.2 illustrates the least-squares fit of the data obtained by postulation of protonation equilibria between HO_2 and $H_2O_2^+$ and between H_2O_2 and $H_3O_2^+$.[1] The solid curve illustrates the least-squares fit of the data to Eq. (IV):

Table 4.1. Dependent variables in Eq. (III) obtained by method of least squares with experimental data of Young, Maranville, and Smith (YMS) and Chen and Irish (CI)

	YMS	CI
$\log K^0$	-1.92 ± 0.02	-2.116 ± 0.007
B	0.445 ± 0.008	0.428 ± 0.003
q	0.66 ± 0.02	0.419 ± 0.006

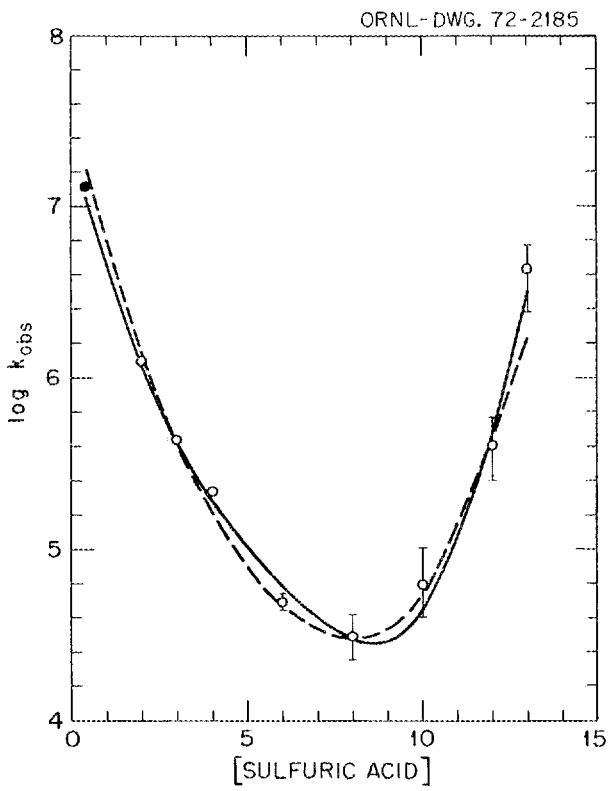

Fig. 4.2. Dependence of k_{obs} on sulfuric acid concentration. ○ Data of Mahlman, Matthews, and Sworski; ● data of Czapski, Bielski, and Sutin.[8] Dashed curve illustrates the least-squares fit of the data obtained by postulating protonation of both HO_2 and H_2O_2. Solid curve illustrates the least-squares fit of the data to Eq. (IV).

$$k_{obs} = \frac{k_1 k_5}{k_{-1}} \left(1 + \frac{k_3 K_{H_2O_2^+}}{k_5 h_0}\right) a_w^q , \qquad \text{(IV)}$$

with $k_1k_5/k_{-1} = (1.7 \pm 0.6) \times 10^2\ M^{-1}\ \text{sec}^{-1}$, $k_3K_{H_2O_2^+}/k_5 = (4.8 \pm 1.5) \times 10^4\ M$ and $q = -2.32 \pm 0.09$. Least-squares analysis indicates that the better fit of the data is obtained with Eq. (IV). The applicability of Eq. (IV) is only further confirmation of the discovery of Bunnett[7] that the rates of most acid-catalyzed reactions are dependent on water activity in moderately concentrated aqueous acids.

1. H. A. Mahlman, R. W. Matthews, and T. J. Sworski, *J. Phys. Chem.* 75, 250 (1971).
2. H. A. Mahlman, R. W. Matthews, and T. J. Sworski, *Chem. Div. Annu. Progr. Rep. May 20, 1968,* ORNL-4306, p. 61.
3. T. F. Young, L. F. Maranville, and H. M. Smith in *The Structure of Electrolytic Solutions,* W. J. Hamer, ed., p. 35, Wiley, New York, 1959.
4. H. Chen and D. E. Irish, *J. Phys. Chem.* 75, 2672 (1971).
5. E. U. Franck, *Z. phys. Chem.* (*Frankfurt am Main*) 8, 107 (1956).
6. W. L. Marshall and A. S. Quist, *Proc. Nat. Acad. Sci. U.S.* 58, 901 (1967).
7. J. F. Bunnett, *J. Amer. Chem. Soc.* 83, 4956 (1961).
8. G. Czapski, B. H. J. Bielski, and N. Sutin, *J. Phys. Chem.* 67, 201 (1963).

RADIOLYTIC DECARBOXYLATION OF α,ω-DICARBOXYLIC ACIDS IN THE LIQUID STATE

A. R. Jones P. S. Rudolph

The radiolytic decarboxylation of the linear aliphatic carboxylic acids has been extended to include α,ω-dicarboxylic acids irradiated in the liquid state by ^{60}Co gamma rays at 145°C. The dibasic acids studied (C_5 through C_{13}, C_{16}, and C_{18}) showed that $G(CO_2)$ decreased with increasing chain length, as was observed with monobasic acids in the liquid state.[1] These results and the comparison are shown in Fig. 4.3.

If the simple model previously proposed[1,2] is applicable to the dibasic acids, $G(CO_2)$ for the dibasic acids of N carbon atoms should be equal to $G(CO_2)$ for the monobasic acids of one-half that number of carbon atoms. For example, $G(CO_2)$ for the C_{12} dibasic acid should be equal to $G(CO_2)$ for the C_6 monobasic acid. The applicability of the model, on this basis, to the dibasic acids can be seen in Fig. 4.3, where $G(CO_2)$ is

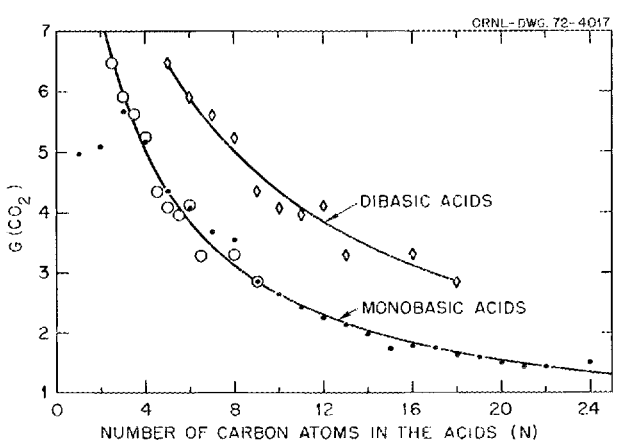

Fig. 4.3. The ^{60}Co gamma-ray-induced radiolytic yields of CO_2 from the liquid linear monocarboxylic and dicarboxylic acids as a function of the total number of carbon atoms in the acids. The dots represent the monobasic acids irradiated at 38°C (N = 1 to 10), 57°C (N = 11 to 15), and 92°C (N = 16 to 22). The diamonds represent the dibasic acids, all irradiated at 145°C. The circles represent $G(CO_2)$ of the dibasic acids at $N/2$ carbon atoms.

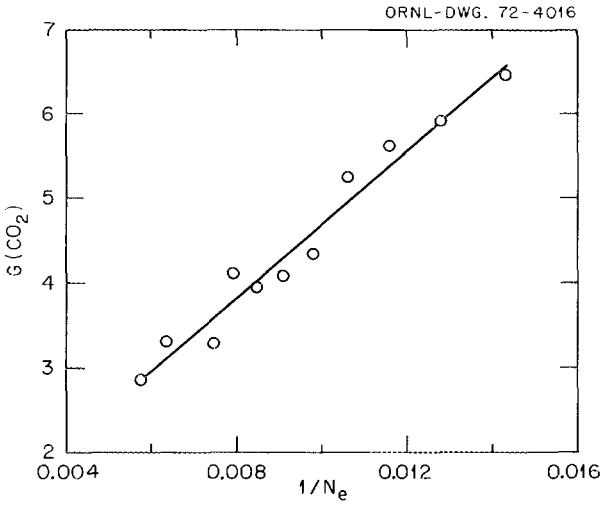

Fig. 4.4. Radiolytic yields of CO_2 from liquid dicarboxylic acids as a function of the reciprocal of the total number of electrons in the acids.

plotted as a function of $N/2$ for the dibasic acids; these points fall on the monobasic acid line within experimental error.

The chain length and the energy absorbed by the molecule are related to the total number of electrons in the molecule (N_e). A plot of $G(CO_2)$ vs $1/N_e$ for the α,ω-dicarboxylic acids is shown in Fig. 4.4. The slope of the line is practically a factor of 2 greater than that for the liquid monobasic acids. This is in agreement with the previously proposed model[1,2] applied to α,ω-dicarboxylic acids.

1. A. R. Jones, *Radiat. Res.* 48, 447 (1971).
2. A. R. Jones, *Chem. Div. Annu. Progr. Rep. May 20, 1971*, ORNL-4706, p. 107.

5. Organic Chemistry

TRANSFORMATION GRAPHS FOR NORBORNYL CARBONIUM ION REARRANGEMENTS

C. K. Johnson B. M. Benjamin
C. J. Collins

The three most important transformations which norbornyl cations undergo are Wagner-Meerwein rearrangement, 6,2-hydride shift, and 3,2-hydride shift. When several substituents are present on the norbornyl cation, a large number of products are possible from different combinations of the three reactions. An exhaustive enumeration of the products and reaction paths is a formidable task, using the traditional manual methods for manipulating chemical formulas, and there is an obvious need for computer automation of this process.

We have devised a mathematical model for the norbornyl rearrangements based on permutations of the 11 letters A–K, which designate specific positions in the right-handed or left-handed carbonium ions shown in Fig. 5.1*a*. An abbreviated notation containing $n + 1$ characters is used to represent any configuration of n nonhydrogen substituents on the right-handed (+) or left-handed (–) framework as shown by example in Fig. 1*b*. The algorithm we devised to do the symbolic manipulation was coded in the PL-1 language by P. R. Coleman (Mathematics Division). The output from the program[1] is a complete and nonduplicative list of all products and all nonblocked reactions (see caption of Fig. 5.2) starting from any given precursor. The output list can be rearranged to form "symmetric transformation graphs" such as those shown in Figs. 5.2 and 5.3. At present the symmetrization step is performed by hand, but we are examining the possibility of using group-theoretic methods to automate this step, so that the computer output might be a Calcomp plot of a symmetrized transformation graph.

Figure 5.3 may be employed to demonstrate the use of the graph by applying it to an older problem. We reported several years ago[2,3] that the diol **1**, in cold, concentrated sulfuric acid, yields ketone **2** quantitatively. The initial carbonium ion is 2-phenyl-3-*endo*-hydroxy[2,2,1]bicycloheptan-2-yl-cation, which may

ORNL-DWG. 72-4959

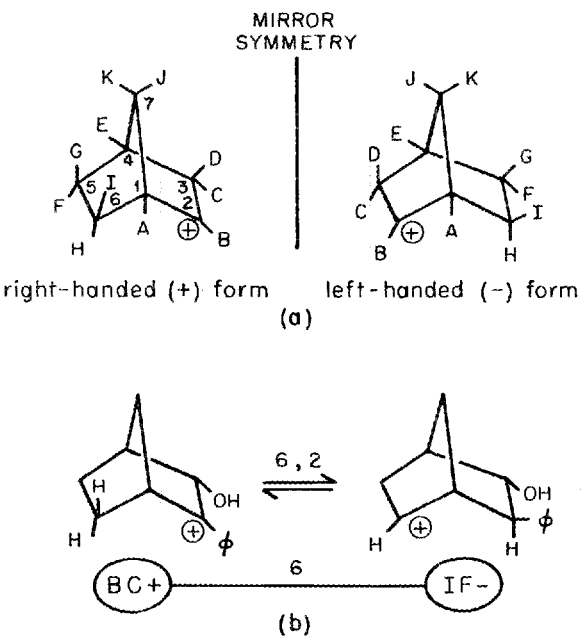

Fig. 5.1. (*a*) Notational convention adopted to represent positions on the right- and left-handed norbornyl cations; (*b*) a comparison of the conventional diagramatic representation for a particular 6,2-hydride shift transformation and the abbreviated symbolism used herein. In this example the first character denotes the phenyl position, the second character denotes the hydroxyl position, and the third character (+ or –) designates the handedness of the framework.

ORNL-DWG. 72-4961

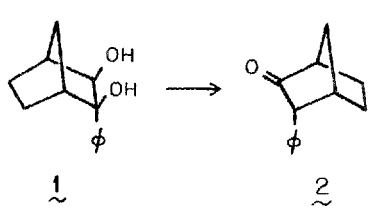

ORNL-DWG. 72-4958

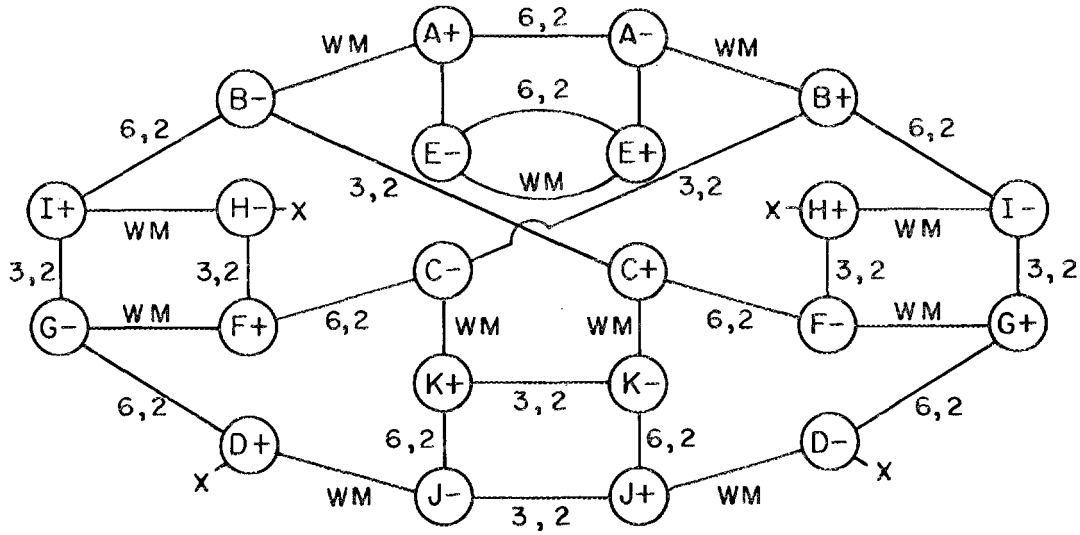

Fig. 5.2. Complete transformation graph for the monosubstitution case. The broken paths from positions D and H designate blocked reactions, since the substituted group cannot undergo 3,2- and 6,2-shift reactions. The graph contains 22 vertices (products) and 31 edges (reactions).

be abbreviated as BD+ (i.e., phenyl on position B and hydroxyl on position D of a right-handed cation). The rearrangement reactions will terminate with formation of a ketone whenever the hydroxyl group and the positive charge occur on the same carbon atom; consequently, any symbol with a B in the second position represents a possible product (e.g., AB±, CB±, DB±, HB±, and IB± in Fig. 5.3). Furthermore, it is generally assumed that the 3,2-hydride shift reaction is at least 100 times slower than the other two reactions; thus the most probable reaction paths are those with the minimum number of 3,2-hydride shifts (i.e., one). On this basis, the important reaction sequences are found easily from Fig. 5.2 and may be rewritten as

BD+ —[WM/6,2/WM/3,2]→ CB+ , I*a*

BD+ —[WM/6,2/WM/6,2/3,2/WM/6,2]→ CB− , I*b*

BD+ —[WM/6,2/WM/6,2/WM/3,2/6,2]→ CB− , I*c*

BD+ —[6,2/3,2/6,2]→ DB− , II*a*

BD+ —[6,2/WM/3,2/WM/6,2]→ DB− . II*b*

The products from an isomer of BD± containing deuterium in the *exo*-5 and *exo*-6 positions have been studied.[2,3] If the symbol for this deuterated isomer is written as BDGI+, then the products corresponding to the above reaction sequences become CBGK+, CBGJ−, CBEG−, DBFG−, and DBEG− respectively. The major product was established by NMR[2,3] as CBGK± (i.e., deuterium in the *exo*-5 and *anti*-7 positions). A neutron-diffraction crystal-structure analysis[4] confirmed this result and also showed that CBGJ± from reaction sequence I*b* is present, since the deuterium percentages observed were 85% in *exo*-5, 80% in *anti*-7, and 3% in *syn*-7. The fact that the product CBEG− corresponding to reaction sequence I*c* was not detected in the neutron diffraction experiment may reflect a kinetic isotope effect, since the rate-determining step in I*b* is the 3,2-hydride shift, while I*c* contains a slower 3,2-deuteride shift. The products derived from II*a* and II*b* were not detected as major components of the reaction.

1. Henceforth this program will be referred to as ORNOCARE (*O*ak *R*idge *NO*rbornyl *CA*tion *RE*arrangement Program).

2. C. J. Collins, Z. K. Cheema, R. G. Werth, and B. M. Benjamin, *J. Amer. Chem. Soc.* **86**, 4913 (1964).

3. B. M. Benjamin and C. J. Collins, *J. Amer. Chem. Soc.* **88**, 1556 (1966).

4. C. K. Johnson, *Chem. Div. Annu. Progr. Rep. May 20, 1967*, ORNL-4164, p. 115.

ORNL-DWG. 72-4530

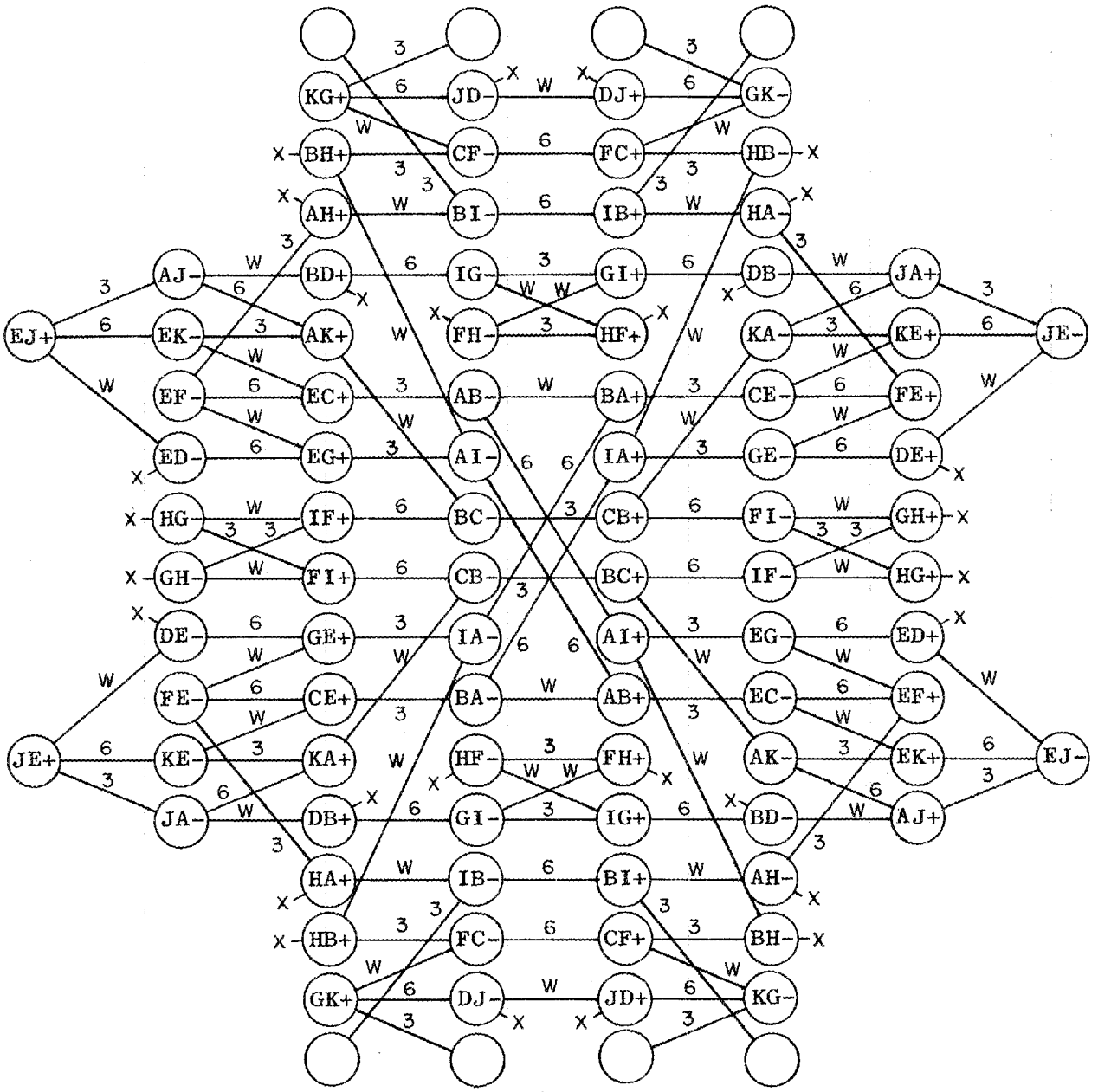

Fig. 5.3. Partial transformation graph for the disubstitution case using the conventions shown in Figs. 5.1 and 5.2. The complete transformation graph contains 204 vertices. Connections to the remaining portions of the graph are indicated by open circles. The 16 products with both substituents on the same carbon atom (i.e., $CD^{\pm}$, $FG^{\pm}$, $HI^{\pm}$, and $JK^{\pm}$ with permutations) form a separate graph. The total of 220 products reflects the fact that there are $11!/9! = 110$ linear sequences of 11 objects, 9 of which are identical. Introducing chirality brings the total to 220.

MECHANISM OF HYDRIDE SHIFTS IN NORBORNYL CATIONS

V. F. Raaen B. M. Benjamin
C. J. Collins

Last year[1] we reported on the fates of the deuterium label in the products (**2** and **3**, Charts I and II) obtained when 1-methyl-7,2-carbolactone-2-d (**1**) is treated with concentrated sulfuric acid. We formulated the transformations **1** → **2** and **1** → **3** as proceeding through the pathways shown in Charts I and II. It was apparent at once that the three processes by which these cations can interconvert — namely, 6,2-, and 3,2-hydride (or deuteride) shift and Wagner-Meerwein rearrangement — could conceivably produce many more intermediates than the ten cations shown. It is therefore conceivable that the pathways shown in Charts I and II are not unique, and that other routes exist which are also compatible with the experimental results. In collaboration with C. K. Johnson (Chemistry Division) and P. R. Coleman (Mathematics Division), a computer program[2] was therefore adapted for determining the total number of possible intermediates and the pathways interrelating them. From the program we learned that 204 cations are possible, starting from **1** containing no deuterium, and that 1836 species are possible if a single deuterium label is included. The route from **1** to **2** shown in Chart I [62; WM; 62; 32] is the only simple pathway connecting the two compounds.

The situation for **1** → **3** is much different. In addition to the route [32; WM; 62; WM; 32] shown in Chart II, another route [32; 62; WM; 62; 32] gives the same end result. Further, there is an easy alternate pathway, namely, [62; 32; WM; 62; 32], which places the deuterium in the *exo*-2 position of lactone **3**, but which clearly is not used.

The pathways involved may be summarized as follows:

Path 1	~~32~~	~~WM~~	~~62~~	WM	~~32~~
Path 2	~~32~~	~~62~~	~~WM~~	62	~~32~~
Path 3	~~62~~	~~32~~	~~WM~~	62	~~32~~

Those processes which are common to all three routes have been crossed out, from which it is clear that path 1 differs from paths 2 and 3 only by Wagner-Meerwein rearrangement vs 6,2-hydride shift. Paths 1 and 2 both are consistent with the experimental result, whereas path 3 is not; we believe path 1 to be the route followed, since the Wagner-Meerwein rearrangement should proceed with much lower activation energy than the 62 shift.[3–5]

ORNL-DWG. 72-4010

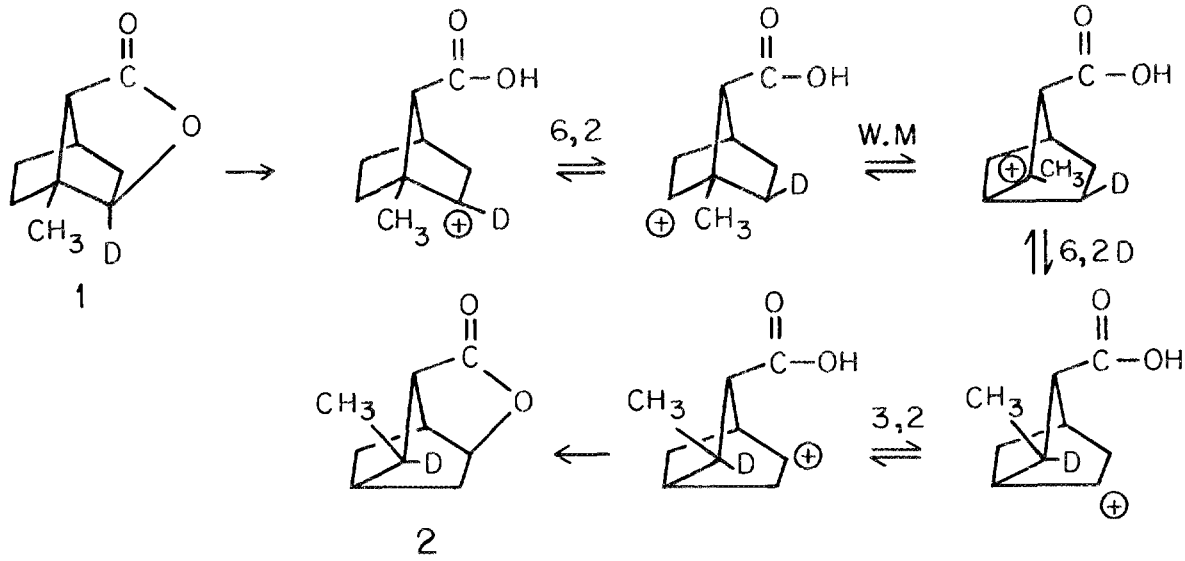

Chart I

ORNL-DWG. 72-4011

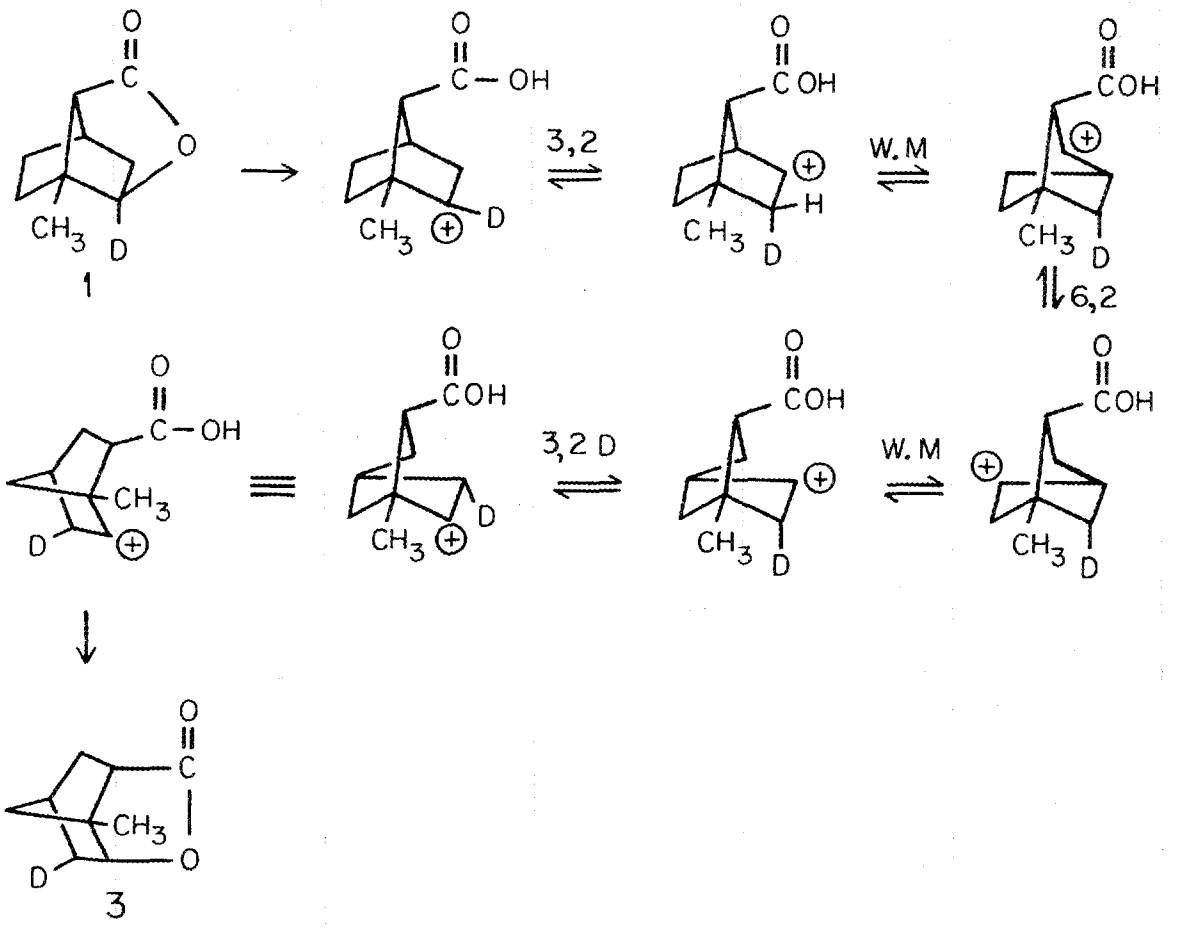

Chart II

1. V. F. Raaen, C. J. Collins, B. M. Benjamin, and D. Houser, *Chem. Div. Annu. Progr. Rep. May 20, 1971*, ORNL-4706, p. 116.

2. ORNOCARE: Oak Ridge Norbornyl Cation Rearrangement Program; C. K. Johnson, B. M. Benjamin, and C. J. Collins, "Transformation Graphs for Norbornyl Carbonium Ion Rearrangements," the preceding contribution, this report.

3. M. Saunders, P. von R. Schleyer, and G. A. Olah, *J. Amer. Chem. Soc.* **86**, 5680 (1964).

4. G. A. Olah and A. M. White, *J. Amer. Chem. Soc.* **91**, 3957 (1969).

5. G. A. Olah, A. M. White, J. R. DeMember, A. Commeyras, and C. Y. Lui, *J. Amer. Chem. Soc.* **92**, 4627 (1970).

REACTION OF 5-*exo*-HYDROXY-5-PHENYL-2-*endo*-NORBORNYLAMINE WITH NITROUS ACID

B. M. Benjamin C. J. Collins

In 1970 we reported[1] that the title compound (1) on nitrous acid deamination in acetic acid yields, among other products, 1.8% of the monoacetate of 2-*exo*-phenylnorbornane-2,5-*cis*-*endo*-diol (2). This was an unprecedented observation, quite in contradiction to what would be predicted on the basis of Winstein's original formulation[2] of "hot" carbonium ions as the

intermediates in such deaminations. Seemingly, the originally produced cation had undergone Wagner-Meerwein rearrangement and then had been attacked from the *endo* direction to give the monoacetate of 2. The mechanism just described is shown in Eq. (1) together with the expected result of deuterium labeling in the *exo*-2 position of the starting amine 1:

ORNL-DWG. 72-4529

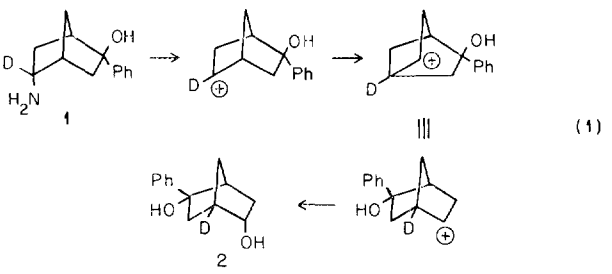

(1)

The observation[3] of Hückel and Kern that *endo*-fenchylamine, on treatment with nitrous acid, yields 3.5% of borneol provides evidence for the possibility of an alternate pathway from 1 → 2, and this alternate pathway is shown in Eq. (2) together with the expected result of deuterium labeling:

ORNL-DWG. 72-4528

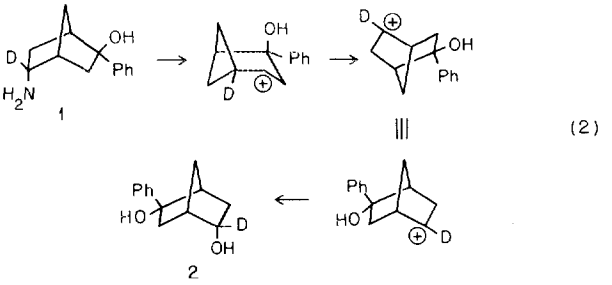

(2)

We prepared compound 1 labeled with deuterium as shown, and determined with NMR that within experimental error of about 2%, the product 2 contained deuterium only in the No. 4 bridgehead position, corresponding to the mechanism shown in Eq. (1).

1. C. J. Collins and B.M. Benjamin, *J. Amer. Chem. Soc.* **92**, 3182 (1970).

2. D. Semenow, C. H. Shih, and W. G. Young, *J. Amer. Chem. Soc.* **80**, 5472 (1958), give Prof. Winstein credit for proposing to them the "hot" carbonium ion.

3. W. Hückel and H.-J. Kern, *Justus Liebigs Ann. Chem.* **728**, 49 (1969).

β-DEUTERIUM ISOTOPE EFFECT IN THE REACTION OF α-PHENYLETHYLAMINE-α-*d* WITH NITROUS ACID

F. A. Shirley[1] V. F. Raaen
C. J. Collins

The amine–nitrous acid reaction is unique among those organic reactions which proceed through carbocations, for the rate-determining step precedes cation formation:[2]

$$RHNO_2 \rightarrow N_2O_3 + H_2O\,, \tag{1}$$

$$RNH_2 + N_2O_3 \rightarrow RNH_3^+NO + NO_2^-\,, \tag{2}$$

$$RNH_3^+NO \rightarrow RNH_2NO + H^+\,, \tag{3}$$

$$RNH_2NO \rightarrow RN{=}NOH\,, \tag{4}$$

$$RN{=}NOH \rightarrow RN_2^+ + OH^-\,, \tag{5}$$

$$RN_2^+ + OH^- \rightarrow R^+ + OH^- + N_2\,, \tag{6}$$

$$R^+ + OH^- \rightarrow ROH + \text{other products}\,. \tag{7}$$

Thus of the equations [(1)–(7)] which describe the appropriate processes, it is either reaction (1) or reaction (2) which is presumed[2] to be rate determining, depending upon the initial concentrations of the reactant and the acidity of the solution. This poses a problem in studying the mechanism of the reaction, for usual kinetic techniques cannot be employed. Thus the reaction has been studied, historically, by product analyses,[3] and the older work[2,3] upon which the mechanism [Eqs. (1)–(7)] rests has seldom been challenged. We therefore decided to study the isotope effect during reaction of $PhCD(NH_2)CH_3$ with nitrous acid, using techniques previously[4] invented by us. In the experiment, $PhCD(NH_2)CH_3$, also labeled with ^{14}C in the phenyl group, was mixed with an excess of $PhCH(NH_2)CH_3$, and the mixture was treated with sufficient nitrous acid to react with less than 10% of the amine; solvents used were acetic acid–sodium acetate solution and an aqueous solution containing 1.1 mole of HCl per mole of amine. Carbon-14 assay of the α-phenylethanol or α-phenylethyl acetate so produced and comparison with the molar radioactivity of the starting amine allowed calculation of the isotope effect. We found a normal β-deuterium isotope effect of 2.4 ± 0.1% when acetic acid–sodium acetate was the solvent, and no isotope effect at all in dilute aqueous hydro-

chloric acid. A subsidiary experiment for the formation of the acetate of α-phenylethylamine in acetic acid—acetic anhydride showed an isotope effect of 2.5%. The implications of these experiments are not fully understood, and the studies will be continued.

1. Student participant in the Great Lakes Colleges Association Science Semester, fall 1971, from DePauw University, Greencastle, Ind.
2. J. H. Ridd, *Quart. Rev. Chem. Soc.* **15**, 418 (1961).
3. For reviews, see H. Söll, in Houben-Weyl, *Methoden der organische Chemie*, E. Müller, ed., Georg Thieme, Stuttgart XI/2, 1958, pp. 133–81; C. J. Collins, *Accounts Chem. Res.* **4**, 315 (1971).
4. V. F. Raaen, T. K. Dunham, D. D. Thompson, and C. J. Collins, *J. Amer. Chem. Soc.* **85**, 3497 (1963).

VINYL CATIONS

B. M. Benjamin C. J. Collins

In continuation of our study of the properties of vinyl cations,[1] we prepared the trifluoromethylsulfonate (triflate) ester of two vinyl intermediates, ^{14}C-labeled triphenylvinyl and 1,1-diphenylpropene. We were interested in producing vinyl cations by solvolysis of these triflate esters and in determining the amount of rearrangement in the products produced by reactions of the resulting vinyl cations with solvent. The degree of rearrangement was expected to give us some insight into the structure of the cationic intermediates and to help us design future experiments to study the stereochemistry of the intermediates. The stereochemistry of intermediates is essential to the understanding of their structures and is a field which has been neglected in the study of vinyl cations.[2]

During preparation of the triflate ester from benzhydryl-^{14}C phenyl ketone the ^{14}C label became scrambled to the extent of 1%. Hydrolysis of triphenylvinyl triflate in 60% acetone-water containing potassium carbonate produced benzhydryl phenyl ketone with no further scrambling of the ^{14}C. Solvolysis of triphenylvinyl triflate in the less nucleophilic solvent, acetic acid saturated with sodium acetate, produced triphenylvinyl acetate with 3% scrambling of the ^{14}C. It appears that the positive charge in the triphenylvinyl cation is highly localized.

The hydrolysis, in water-acetone mixture, of 1,1-diphenylpropene-2-trifluoromethyl sulfonate (2,2-diphenyl-1-methylvinyl triflate, a viscous oil) produced a 50-50 mixture of benzhydryl methyl ketone (rearranged product) and 2-phenylpropiophenone (unrearranged product). Solvolysis of 2,2-diphenyl-1-methylvinyl triflate in acetic acid—sodium acetate mixture resulted in more than 99% rearrangement to produce almost exclusively 2-phenylpropiophenone. Therefore rearrangement is favored in the less nucleophilic solvent.

1. B. M. Benjamin and C. J. Collins, *Chem. Div. Annu. Progr. Rep. May 20, 1971*, ORNL-4706, p. 113.
2. M. Hanack, *Accounts Chem. Res.* **7**, 209 (1970).

PYROLYSIS OF ACETOPHENONE-2-^{14}C IN THE PRESENCE OF IRON

V. F. Raaen

In an earlier report[1] I described the ketonic decarboxylation of the iron(II) salts of aromatic carboxylic acids; in no instance was the expected symmetrical ketone isolated. Thus only 1,2′-dinaphthyl ketone was obtained when iron(II) naphthoate was pyrolyzed.

It therefore seemed important to determine whether the unsymmetrical ketones were formed by thermal rearrangement of symmetrical ketones of the type expected. Compounds such as 4,4′-dimethylbenzophenone were unaffected by 24-hr heating with iron powder (in excess) at temperatures as high as 335°. Prolonged (one month) heating of acetophenone results in 80% conversion to condensation products, water, and char. Two major products of the acetophenone pyrolysis are 3-phenylbutyrophenone (**1**) and 1,3,5-triphenylbenzene (**2**). The aromatization reaction that leads to **2** may be responsible for the reduction that occurs in the formation of **1**; it is accompanied by scrambling of the ^{14}C. Oxidation of **2** produces radioactive benzoic acid.

1. W. F. Raaen, *Chem. Div. Annu. Progr. Rep. May 20, 1967*, ORNL-4164, p. 46.

PREPARATION AND PURIFICATION OF *p*-SEXIPHENYL

W. H. Baldwin P. T. Perdue[1]
J. H. Burns

The linear molecule *p*-sexiphenyl is being studied because of its superior properties as a scintillator for particle counting.[2] The importance of isolation of the product from the reaction mixture has already been emphasized.[3] In a quest of further purification of sexiphenyl, the product of highest purity was sublimed in a helium atmosphere at elevated temperature to grow

crystals. Two different crystal forms were obtained, thin plates and dendrites. Samples were separated mechanically and examined.

The plates melted at 490°C, while the dendrites melted over a range 450 to 480°C. Mass spectra of the two samples were nearly identical; the largest yield of ions corresponded to the sexiphenyl parent, with small yields of ions corresponding to heptaphenyl, pentaphenyl, quaterphenyl, and an even smaller yield corresponding to monochlorosexiphenyl.

In the preparation step, two terphenyl molecules are condensed in the presence of aluminum chloride and cupric chloride. The compounds containing 4, 5, and 7 phenyl groups in the chain result from chain scission. Chlorination also occurs to a small extent in the condensation step. A measure of the quantity of Cu (64 ppm) and Cl (4 ppm) in the material before crystal growth was obtained by neutron activation analysis, emphasizing the small yield of chlorinated products.

Infrared spectra of the plates are identical with those reported by Cade and Pilbeam[3] for sexiphenyl. The spectra of the dendrites show additional absorption peaks at 6.8, 7.0, 11.3, and 13.2 μ. These spectra, in conjunction with the other data (above) and the method of preparation of the compound, show that the dendrites are composed chiefly of molecules with six rings per chain and with partial hydrogenation of one or more rings.

The formation of plates by crystallization is typical of long molecules.[4] Brief x-ray crystallographic examination of a single plate confirms the presence of a long repeat distance perpendicular to the largest face of the plate and a short repeat distance within the plate. These data are consistent with the expected properties of *p*-sexiphenyl. The dendritic crystals are unsuitable for single-crystal x-ray studies.

---

1. Health Physics Division.
2. W. H. Baldwin and P. T. Perdue, *Chem. Div. Annu. Progr. Rep. May 20, 1971,* ORNL-4706, p. 117.
3. J. A. Cade and A. Pilbeam, *J. Chem. Soc. London* **1964**, 114.
4. C. W. Bunn, *Chemical Crystallography,* p. 279, Oxford University Press, London, 1958.

6. Physical Chemistry

AQUEOUS SYSTEMS

THERMODYNAMIC PROPERTIES OF AQUEOUS HCl-$LaCl_3$ SOLUTIONS TO IONIC STRENGTH 5.0[1]

M. H. Lietzke M. D. Danford

In a previous paper[2] we reported the results of a study of the thermodynamic properties of aqueous HCl-$LaCl_3$ mixtures in the temperature range 25–175°C in solutions of total ionic strength (I) 0.5 and 1.0. Recently we have made a study[3] of the HCl-NaCl-$LaCl_3$ system to I = 5 over the temperature range 25–75°C. In connection with this latter study, we found it desirable to extend the measurements in the HCl-$LaCl_3$ system to I = 5 but only in the temperature range 25–70°. Using the new data, we have recalculated the activity coefficient of both the HCl and the $LaCl_3$ in the mixtures. Although at I = 1 the values of log γ_{HCl} were affected but little, inclusion of the data at the higher ionic strengths resulted in considerable change in the values of log γ_{LaCl_3} at the higher fractions of acid. Hence, it seems desirable to report separately our recent results on the HCl-$LaCl_3$ system to I = 5. As before, emf measurements of the cell

$$\text{Pt-H}_2(p = 1)|\text{HCl}(m_2), \text{LaCl}_3(m_3)|\text{AgCl, Ag}$$

have been combined with values of the activity coefficient of $LaCl_3$ obtained isopiestically[4] to compute the thermodynamic properties of both HCl and $LaCl_3$ in the HCl-$LaCl_3$ mixtures.[1]

The treatment of the data followed that used previously.[2] The activity coefficient corresponding to each experimental emf value E was calculated by using the Nernst equation and previous values[5] of the standard potential E° of the Ag, AgCl electrode.

$$E = E^\circ - \frac{RT}{F} \ln [m_2(m_2 + 3m_3)] - \frac{2RT}{F} \ln \gamma_\pm \quad (1)$$

In this equation m_2 and m_3 are the molalities of HCl and $LaCl_3$, respectively, while the remaining quantities have their usual significance. The total log γ values are obtained by adding a Debye-Hückel term to the appropriate expression used for the excess activity coefficient (γ^e); these excess expressions are identical to Eqs. (5) and (6) of ref. 2. Even at the higher ionic strengths, Harned's rule appears to hold for the HCl in the mixtures.

The activity coefficients of HCl in the HCl-$LaCl_3$ mixtures (including both the present and former data) were fitted by the method of least squares using an equation identical to Eq. (5) of ref. 2, simplified by the introduction of Harned's rule. Over the wide range of total ionic strengths covered, the temperature dependence of the coefficients in the activity coefficient equations could be expressed by an algebraic series [similar to Eqs. (7) and (8) of ref. 2]. The form of these equations gives rise to excess enthalpies varying linearly with temperature and excess entropies varying linearly with log T. The values of the parameters of these equations were obtained directly by the least-squares fit.[1] The additional parameters needed for calculating log $\gamma_3{}^e$ were obtained either by the application of Harned's rule or by evaluation by the method of least squares using activity coefficient data on pure $LaCl_3$ solutions.[4] Since the activity coefficient of $LaCl_3$ has been measured only at 25°C, it was possible to compute the activity coefficient of $LaCl_3$ in the HCl-$LaCl_3$ mixtures only at 25°.

Plots of log γ_{HCl} vs fraction of $LaCl_3$ in the mixtures at constant total ionic strength are all very similar to those previously reported[2] at I = 0.5 and 1.0. At all total ionic-strength values and temperatures in the range investigated the log γ_{HCl} values become more negative as the fraction of $LaCl_3$ in the mixture increases.

As mentioned above, inclusion of data on the HCl-$LaCl_3$ mixtures to a total ionic strength of 5 results in a considerable change in the values of log γ_{LaCl_3} previously reported[2] when data only at I = 0.5 and 1.0 were available. The values of log γ_{LaCl_3} calculated from the derived parameters[1] are shown plotted in Fig.

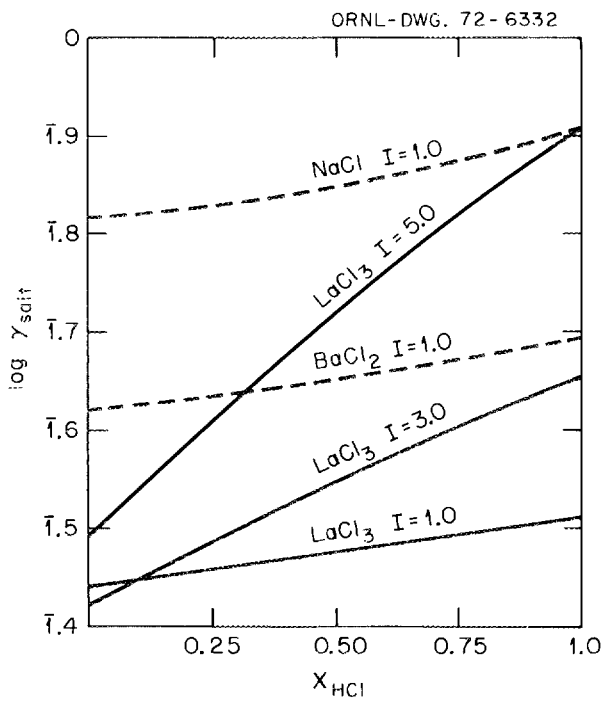

Fig. 6.1. Plots of log γ_{LaCl_3} vs X_{HCl} in HCl-$LaCl_3$ mixtures.

6.1 vs the fraction of acid in the mixtures. As the fraction of HCl increases in the mixtures at constant total ionic strength, the log γ_{LaCl_3} values increase (become less negative), the effect being greater the higher the total ionic strength. Hence the plots now resemble the corresponding plots of log γ_{salt} in HCl-NaCl[6] and HCl-$BaCl_2$[7] mixtures, also shown plotted in Fig. 6.1.

1. This is an abbreviated version of part of a paper being prepared for publication. A more complete text, including values of derived constants, is available at once from M. H. Lietzke.

2. M. H. Lietzke and R. W. Stoughton, *J. Phys. Chem.* **71**, 662 (1967).

3. M. H. Lietzke and M. D. Danford, "Thermodynamic Properties of Aqueous HCl-NaCl-$LaCl_3$ Mixtures," the following contribution, this report.

4. R. A. Robinson and R. H. Stokes, *Electrolyte Solutions*, 2d ed. (revised), p. 489, Butterworths, London, 1965.

5. M. H. Lietzke and R. W. Stoughton, *J. Phys. Chem.* **68**, 3043 (1964).

6. M. H. Lietzke, H. B. Hupf, and R. W. Stoughton, *J. Phys. Chem.* **69**, 2395 (1965).

7. M. H. Lietzke and R. W. Stoughton, *J. Phys. Chem.* **70**, 756 (1966).

THERMODYNAMIC PROPERTIES OF AQUEOUS HCl-NaCl-$LaCl_3$ MIXTURES[1]

M. H. Lietzke M. D. Danford

Very little is known about the thermodynamic properties of aqueous electrolyte mixtures containing trivalent ions. One such mixture which has been studied isopiestically is the NaCl-$LaCl_3$ system.[2] As far as we know, no aqueous three-electrolyte system containing a trivalent ion has been reported. Hence it seemed a logical extension of our program of investigating the properties of three-electrolyte systems to combine the results of the isopiestic study of the NaCl-$LaCl_3$ system with emf measurements of the cell

$$\text{Pt-H}_2(p = 1)|\text{HCl}(m_2), \text{NaCl}(m_3), \text{LaCl}_3(m_4)|\text{AgCl, Ag}$$

to calculate the activity coefficient of each component in HCl-NaCl-$LaCl_3$ solutions. With these results a direct comparison can be made with the activity coefficient behavior of each component in the previously studied HCl-NaCl-$MgCl_2$ system,[3] differing only in the polyvalent electrolyte.

The treatment of the emf data was the same as that used with the HCl-NaCl-$MgCl_2$ system. The derivation of the equations used for expressing log γ_{HCl}, log γ_{NaCl}, and log γ_{LaCl_3} in the mixtures also parallels that used previously and will not be given.

The activity coefficients of HCl in the HCl-NaCl-$LaCl_3$ mixtures (along with the values for pure HCl,[4] for HCl in HCl-NaCl mixtures,[5] and for HCl in HCl-$LaCl_3$ mixtures[6]) were fitted by the method of least squares. Over the wide range of total ionic strength covered, it was found possible to express the temperature dependence of both the B and C coefficients by an algebraic series [similar to Eqs. (8) and (8′) of ref. 3]. The form of these equations gives rise to excess enthalpies varying linearly with temperature and excess entropies varying linearly with log T. The additional parameters needed for calculating log γ_{NaCl} and log γ_{LaCl_3} in the HCl-NaCl-$LaCl_3$ mixtures were obtained by fitting isopiestic data on NaCl-$LaCl_3$ solutions.[2]

Plots of log γ_{HCl} vs total salt fraction in the mixtures at $I = 1.0$ and 5.0 and at temperatures of 25 and 70° are shown in Fig. 6.2. As can be seen, the plots are essentially linear at 25° at both total ionic strengths (i.e., Harned's rule is obeyed by the acid in the mixtures at 25°). At higher temperatures, however (e.g., 70°), the plots are slightly concave downward, the amount of curvature increasing as the total ionic strength increases.

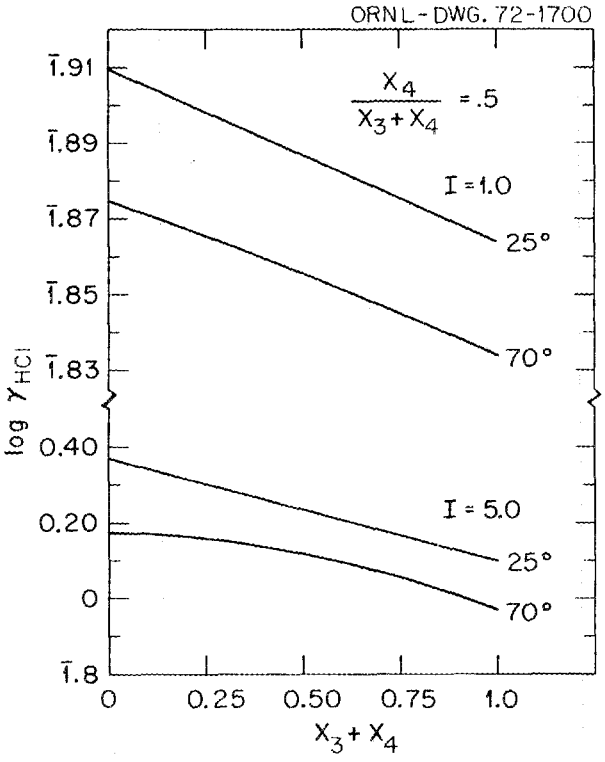

Fig. 6.2. Plots of log γ_{HCl} vs $X_3 + X_4$ (total salt fraction) in HCl-NaCl-$LaCl_3$ mixtures.

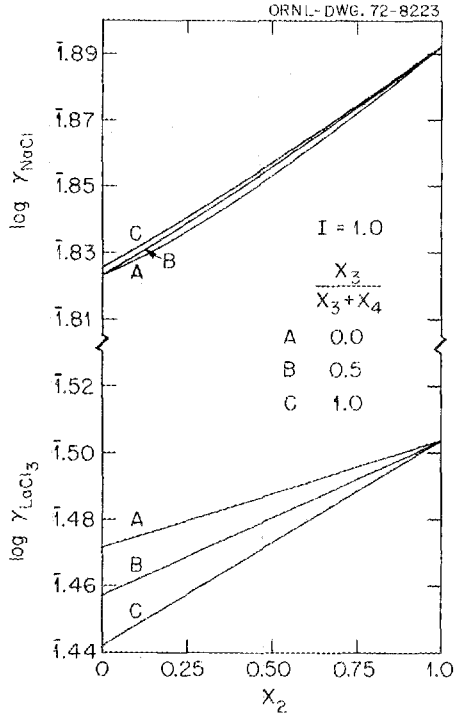

Fig. 6.3. Plots of the logarithms of the activity coefficients of NaCl and $LaCl_3$ in HCl-NaCl-$LaCl_3$ mixtures vs X_2 at I = 1.0 and 25°C.

This downward curvature is similar to that displayed by the HCl in the HCl-NaCl-$MgCl_2$ system[3] at all temperatures and ionic strengths.

The calculated variation of the logarithms of the activity coefficients of NaCl and $LaCl_3$ in the HCl-NaCl-$LaCl_3$ mixtures with X_2, the fraction of HCl in the mixtures, at I = 1.0 and 25° is shown in Fig. 6.3. As the fraction of $LaCl_3$ in any of the mixtures increases at the same total fraction of acid, the activity coefficient of the NaCl increases. The same is true with the $LaCl_3$ activity coefficient: as the fraction of NaCl increases at constant fraction of acid, the activity coefficient of the $LaCl_3$ also increases. These trends are exactly in the same direction as those observed for the corresponding salts in the HCl-NaCl-$MgCl_2$ system.[3] At higher ionic strengths the same relative orders are preserved.

1. This is an abbreviated version of part of a paper being prepared for publication. A more complete text, including values of derived constants, is available at once from M. H. Lietzke.

2. A. N. Kirgintsev and A. V. Luk'yanov, *Zh. Fiz. Khim.* **39**, 744 (1965).

3. M. H. Lietzke and R. J. Herdklotz, *J. Inorg. Nucl. Chem.* **33**, 1649 (1971).

4. M. H. Lietzke and R. W. Stoughton, *J. Phys. Chem.* **68**, 3043 (1964).

5. M. H. Lietzke, H. B. Hupf, and R. W. Stoughton, *J. Phys. Chem.* **69**, 2395 (1965); also ref. 4.

6. M. H. Lietzke and R. W. Stoughton, *J. Phys. Chem.* **70**, 756 (1966); also M. H. Lietzke and M. D. Danford, to be submitted.

THERMODYNAMIC PROPERTIES OF AQUEOUS HCl-KCl-$CaCl_2$ MIXTURES[1]

M. H. Lietzke Cynthia Daugherty[2]

Emf measurements of the cell

$$Pt\text{-}H_2(p = 1)|HCl(m_2), KCl(m_3), CaCl_2(m_4)|AgCl, Ag$$

have been combined with isopiestic measurements of the system KCl-$CaCl_2$ to compute the activity coefficient of each component in aqueous HCl-KCl-$CaCl_2$ mixtures. The emf measurements were carried out in the range 25–75°C, using a water bath controlled to better than ±0.1°C, on solutions of total ionic strength 1.0, 3.0, and 5.0. At each total ionic strength, solutions were prepared containing 0.75, 0.50, and 0.25 ionic

strength fraction of HCl. The salt fraction of each solution consisted of approximately equal ionic strength fractions of KCl and $CaCl_2$. Isopiestic data on the KCl-$CaCl_2$ system were taken from the literature.[3] The reported osmotic coefficient values were fitted by the method of least squares to an equation suggested by Scatchard.[4] The parameters estimated by this fit were then converted to the additional coefficients needed to calculate the activity coefficient of each salt in the mixtures, as described by Hupf.[5]

As before, the neutral-electrolyte treatment[4] has been used in fitting the data. The activity coefficient $\gamma_{\pm}$ of HCl corresponding to each emf value E was calculated by using the Nernst equation and previous values[6] of the standard potential E° of the Ag, AgCl electrode.

Plots of log γ_{HCl} vs the total salt fraction in the mixtures at constant total ionic strength and temperature were linear, indicating that Harned's rule was obeyed by the acid in the mixtures. Hence the equation used for fitting the log γ_{HCl} values, as derived from the neutral-electrolyte treatment, will not contain any cross terms or quadratic terms in the ionic strength fraction of either salt in the mixtures. The equation used in fitting the log γ_{HCl} values was

$$\log \gamma_{HCl} = \frac{-S_T \rho^{1/2}\sqrt{I}}{1 + 1.5\sqrt{I}} + 2I\left[B_{22} + (B_{23} - B_{22})X_3 + \left(\frac{B_{24}}{3} - B_{22}\right)X_4\right] + 3I^2\left[C_{222} + 2(C_{223} - C_{222})X_3 + 2\left(\frac{C_{224}}{3} - C_{222}\right)X_4\right], \quad (1)$$

where the B_{ij} and C_{ijk} are interaction coefficients, X_3 and X_4 are the ionic strength fractions of KCl and $CaCl_2$ respectively, I is the total ionic strength of the solution, S_T represents the Debye-Hückel limiting slope at temperature T for a univalent electrolyte, and ρ is the density of water, which corrects I to a volume basis as required by the Debye-Hückel theory. The equations for representing the log γ_{salt} values in the HCl-KCl-$CaCl_2$ mixtures were the same as those used in the HCl-CsCl-$BaCl_2$ system.[4] The additional coefficients needed for calculating values of log γ_{KCl} and log γ_{CaCl_2} in the mixtures were obtained by fitting isopiestic data on KCl-$CaCl_2$ mixtures.[3]

Since the isopiestic measurements on the KCl-$CaCl_2$ solutions were made at 25° only, the activity coefficients of the KCl and the $CaCl_2$ in the HCl-KCl-$CaCl_2$ mixtures could be computed at this temperature only. However, the emf measurements were performed in the temperature range 25–75°, and hence the variation with temperature of the activity coefficient of the HCl in the mixtures could be computed. In order that all the emf data could be used simultaneously in estimating the values of the B and C coefficients in Eq. (1), it was necessary to make these coefficients temperature dependent. Over the wide range of total ionic strengths covered, the temperature dependence of the coefficients in Eq. (1) could be expressed by an algebraic series [similar to Eqs. (8) and (8′) of ref. 7]. The form of these coefficients is consistent with excess enthalpies varying linearly with temperature and with excess entropies varying linearly with log T.

Values of the logarithms of the activity coefficient of HCl in HCl-KCl-$CaCl_2$ mixtures at various temperatures, total ionic strengths, and fractions of acid and salts in the mixtures may be calculated using Eq. (1) and values of the B and C coefficients obtained by least squares. When these values are plotted at constant total ionic strength vs the fraction of salt in the mixture at a fixed ratio of salt fractions, the plots are linear. [This is a consequence of the omission of terms in X_3^2, X_4^2, and X_3X_4 from Eq. (1) for the reason previously stated.] Hence the behavior of the HCl in this system, where Harned's rule is obeyed, is in contrast to the behavior in HCl-NaCl-$MgCl_2$ mixtures,[7] where the corresponding plots are concave downward, and to the behavior in HCl-CsCl-$BaCl_2$ mixtures,[4] where the corresponding plots are concave upward.

The variation of the logarithms of the activity coefficients of KCl and $CaCl_2$ in the HCl-KCl-$CaCl_2$ mixtures with X_2, the fraction of HCl in the mixtures, at I = 1.0 and 25° is shown in Fig. 6.4. As the fraction of $CaCl_2$ in any of the mixtures increases at the same total fraction of acid, the activity coefficient of the KCl increases. This trend is the same as that observed for the activity coefficient of NaCl in HCl-NaCl-$MgCl_2$ mixtures at all fractions of acid and for the activity coefficient of CsCl in HCl-CsCl-$BaCl_2$ mixtures at fractions of acid below about 0.06. Whereas in both of the latter systems the log γ_{NaCl} and γ_{CsCl} vs X_2 plots show pronounced curvature at both high and low fractions of the bivalent salt, the plots of log γ_{KCl} vs X_2 are all nearly linear at I = 1.0. Even at ionic strengths of 3.0 and 5.0 the curves show very little curvature.

When the fraction of KCl at any one ionic strength increases at the same total fraction of acid, the activity coefficient of the $CaCl_2$ decreases. This is just the reverse of the corresponding trend in log γ_{MgCl_2} in HCl-NaCl-$MgCl_2$ mixtures and the same as the trend displayed by the log γ_{BaCl_2} in HCl-CsCl-$BaCl_2$ mixtures.

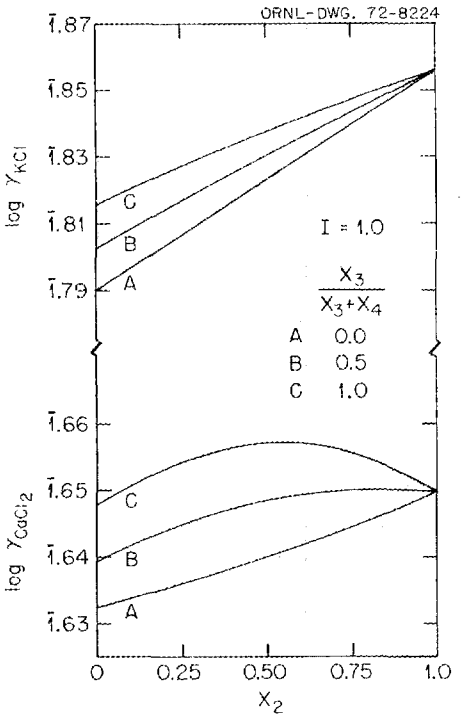

Fig. 6.4. Plots of the logarithms of the activity coefficients of KCl and $CaCl_2$ in HCl-KCl-$CaCl_2$ mixtures vs X_2 at I = 1.0 and 25°C.

1. This is an abbreviated version of part of a paper being prepared for publication. A more complete text, including values of derived constants, is available at once from M. H. Lietzke.
2. Graduate student, University of Tennessee, Knoxville.
3. R. A. Robinson and A. K. Covington, *J. Res. Nat. Bur. Stand., Sect. A* **72**, 239 (1968).
4. M. H. Lietzke, H. B. Hupf, and R. W. Stoughton, *J. Inorg. Nucl. Chem.* **31**, 3481 (1969).
5. H. B. Hupf, "The Thermodynamic Properties of Aqueous Hydrochloric Acid–Cesium Chloride–Barium Chloride Mixtures," Ph.D. thesis, The University of Tennessee, Knoxville, June 1969.
6. M. H. Lietzke and R. W. Stoughton, *J. Phys. Chem.* **68**, 3043 (1964).
7. M. H. Lietzke and R. J. Herdklotz, *J. Inorg. Nucl. Chem.* **33**, 1649 (1971).

EXTENSION OF THE TWO-STRUCTURE CONCEPT FOR ELECTROLYTE SOLUTIONS TO OSMOTIC COEFFICIENTS

M. H. Lietzke D. W. Gosbin[1]
R. W. Stoughton

Previous work[2] in the development of a two-structure model for electrolytic solutions showed that at concentrations of the order of a few tenths molar the Debye-Hückel term contributed only very slightly to the activity coefficient of an electrolyte in solution. The same holds true for the osmotic coefficient of a solution. We have demonstrated, using isopiestic data on a variety of electrolytic solutions, that the ionic strength (I) dependence of the osmotic coefficient (ϕ) may be expressed by an equation of the type

$$\phi = 1.0 + A_1 I^{1/3} + A_2 I + A_3 I^2 + A_4 I^3 \qquad (1)$$

about as well as by the usual expression containing a Debye-Hückel term. The quadratic and cubic terms contribute significantly to the value of ϕ only at higher ionic strengths.

In integrating the activity coefficient expression for an electrolyte to obtain the corresponding expression for the osmotic coefficient, a definite numerical relationship is seen to exist between the coefficients of terms involving the same power of the ionic strength. If, in the two-structure model, the coefficient of the $I^{1/3}$ term in the activity coefficient expression is B_1, then the A_1 coefficient in the osmotic coefficient expression [Eq. (1)] is given by $B_1/4$; that is, $B_1 = 4A_1$.

When osmotic coefficients were fitted using Eq. (1), it was found that the coefficient A_1 had an average value of ca. −0.1676 for 1-1 electrolytes and a value of ca. −0.2608 for 2-1 and 1-2 electrolytes. The corresponding B_1 coefficients are then −0.67 for 1-1 electrolytes and −1.04 for 2-1 and 1-2 electrolytes. These values are in excellent agreement with the values −0.66 and −1.07 obtained previously in fitting activity coefficients directly with a two-structure equation. This agreement is gratifying, since the activity coefficient expression did not contain terms in I^2 and I^3. The consistency demonstrates the importance of the $I^{1/3}$ term and adds support to the two-structure concept of electrolyte solutions.

Future work in this area will include an extension of the two-structure concept to electrolyte mixtures.

1. Graduate student, Chemistry Department, University of Tennessee, Knoxville.
2. M. H. Lietzke, R. W. Stoughton, and R. M. Fuoss, *Proc. Nat. Acad. Sci. U.S.* **59**, 39 (1968).

RECALCULATION OF THE STANDARD POTENTIAL OF THE Ag, AgCl ELECTRODE

M. H. Lietzke

The standard potential $E°$ of the Ag, AgCl electrode has been determined as a function of temperature both in protonated[1–4] and in deuterated[5,6] media. In all cases except ref. 6, the $E°$ values were determined by

extrapolation or calculation at each of a number of temperatures separately. In ref. 6 all emf data at each temperature and concentration of acid were used simultaneously in one least-squares fit to calculate the E° of the Ag, AgCl electrode both in HCl and DCl media. Although the data of Greeley et al.[3] were used, slightly different values of E° (at variance with the other values) were obtained.

In using the emf data at all temperatures and concentrations simultaneously, the thermodynamic assumption was made that ΔC_p for the cell reaction was independent of temperature. An attempt to fit the data with the further assumption that ΔC_p showed a linear dependence on temperature was not successful at that time. Recently, however, the calculations were repeated in double-precision arithmetic on the IBM-360 computer and were completely successful. The equation describing the temperature dependence of the E° value in protonated media is given by

$$E^\circ = 0.477241 - 0.00866664T + 0.00162255T \ln T - 4.8048 \times 10^{-6} T^2 , \quad (1)$$

Table 6.1. E° values for the Ag, AgCl electrode in protonated media

Temperature (°C)	E°(V)				
	Eq. (1)	Ref. 1	Ref. 2	Ref. 3	Ref. 4
25	0.2225	0.2224	0.2223	0.2224	0.2225
50	0.2045	0.2044		0.2047	0.2044
60	0.1965	0.1962	0.1965	0.1965	0.1964
90	0.1697		0.1696	0.1697	0.1694
125	0.1326			0.1330	0.1325
150	0.1019			0.1033	0.1025
175	0.0676			0.0706	0.0697
200	0.0296			0.0349	0.0338

Table 6.2. E° values for the Ag, AgCl electrode in deuterated media

Temperature (°C)	E°(V)	
	Eq. (2)	Ref. 5
25	0.2099	0.2127
50	0.1918	0.1931
60	0.1833	
90	0.1533	
125	0.1110	
150	0.0767	
175	0.0393	
200	−0.0009	

while that for deuterated media is

$$E^\circ = -0.528448 + 0.022694T - 0.00364466T \ln T + 1.83884 \times 10^{-6} T^2 . \quad (2)$$

Values of the standard potential E° in volts of the Ag, AgCl electrode both in protonated and in deuterated media as reported by different investigators are given in Tables 6.1 and 6.2. Both sets of values are on a molal basis. The reason for the discrepancy between the two sets of values in Table 6.2 is unknown.

1. H. S. Harned and R. W. Ehlers, *J. Amer. Chem. Soc.* **54**, 1350 (1932); ibid. **55**, 2179 (1933).
2. R. G. Bates and V. E. Bower, *J. Res. Nat. Bur. Stand.* **53**, 283 (1954).
3. R. S. Greeley, W. T. Smith, R. W. Stoughton, and M. H. Lietzke, *J. Phys. Chem.* **64**, 652 (1960).
4. T. Izaki and K. Arai, *Suiyokawai* **16**(7), 367 (1968).
5. R. Gary, R. G. Bates, and R. A. Robinson, *J. Phys. Chem.* **68**, 1186 (1964).
6. M. H. Lietzke and R. W. Stoughton, *J. Phys. Chem.* **68**, 3043 (1964).

THE TETRAD EFFECT IN LANTHANIDE(III) ION EXCHANGE REACTIONS

G. E. Boyd[1] Q. V. Larson[1,2]

The effect of a half-filled shell in the electronic structure of the lanthanide(III) ions on their relative ion exchange affinities has been known for some time.[3] Recently, however, Peppard and coworkers[4,5] have found a more complex atomic number, Z, dependence of the partition of Ln(III) and An(III) between various immiscible solvents. In addition to a break at the half-filled shell, discontinuities in the logarithm of the liquid-liquid separation factors also appear to be present when the $4f$ shell is one-quarter and three-quarters filled respectively. This novel behavior contrasts with the Z dependence of many of the physical chemical properties of the rare earths in aqueous solutions observed by Spedding[6] and others. It has been explained by Nugent[7] on the basis of a stabilization by interelectron repulsion and by Jørgensen[8] as a consequence of a variation of the nephelauxetic ratio in the third decimal place.

In 1957 Surls and Choppin[9] conducted a systematic investigation of ion exchange equilibria involving the lanthanide(III) cations in dilute perchloric acid solutions and reported that the relative affinities decreased from La to Dy but that from Dy to Lu almost no change in the log K_d with crystallographic radius was

observed. Not only were no ¼ or ¾ point discontinuities evident in their data, but neither was a half-filled-shell effect seen. We have repeated the work of Surls and Choppin, and, additionally, we have measured the integral heat of ion exchange with a sensitive solution calorimeter. Our results are presented in Figs. 6.5 and 6.6. Although data are yet to be obtained with Pm, it would appear that a tetrad effect exists in the equilibrium constant as approximated by the mass law concentration product quotient. The integral heat of exchange, $Q_{Ln}{}^{Ce}$, showed an unexpected dependence on Z with maximum exothermicity at Tb. Neither a tetrad nor a dyad effect can be discerned in the variation of $Q_{Ln}{}^{Ce}$ with Z. Values of ΔG°, ΔH°, and ΔS° will be derived from the data given in Figs. 6.5 and 6.6 when the measurements of solute activity coefficients in, and apparent molal heat contents of, aqueous rare-earth perchlorate solutions are completed.

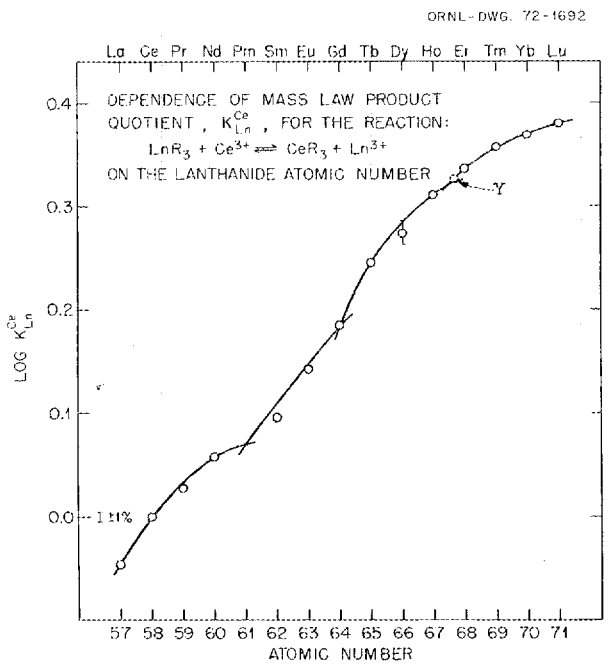

Fig. 6.5. Dependence of the mass law concentration product quotient, $K_{Ln}{}^{Ce}$, on the lanthanide(III) atomic number. Symbol diameter indicates maximum error except as shown.

1. Director's Division.
2. Deceased.
3. B. H. Ketelle and G. E. Boyd, *J. Amer. Chem. Soc.* **69**, 2800 (1947).
4. D. F. Peppard, G. W. Mason, and S. Lewey, *J. Inorg. Nucl. Chem.* **27**, 2065 (1965); ibid. **31**, 2271 (1969).
5. D. F. Peppard C. A. A. Bloomquist, E. P. Horwitz, S. Lewey, and G. W. Mason, ibid. **32**, 339 (1970).
6. F. H. Spedding, M. J. Pikal, and B. O. Ayers, *J. Phys. Chem.* **70**, 2440 (1966).
7. L. J. Nugent, *J. Inorg. Nucl. Chem.* **32**, 3485 (1970).
8. C. K. Jørgensen, ibid. **32**, 3127 (1970).
9. J. P. Surls, Jr., and G. R. Choppin, *J. Amer. Chem. Soc.* **79**, 855 (1957).

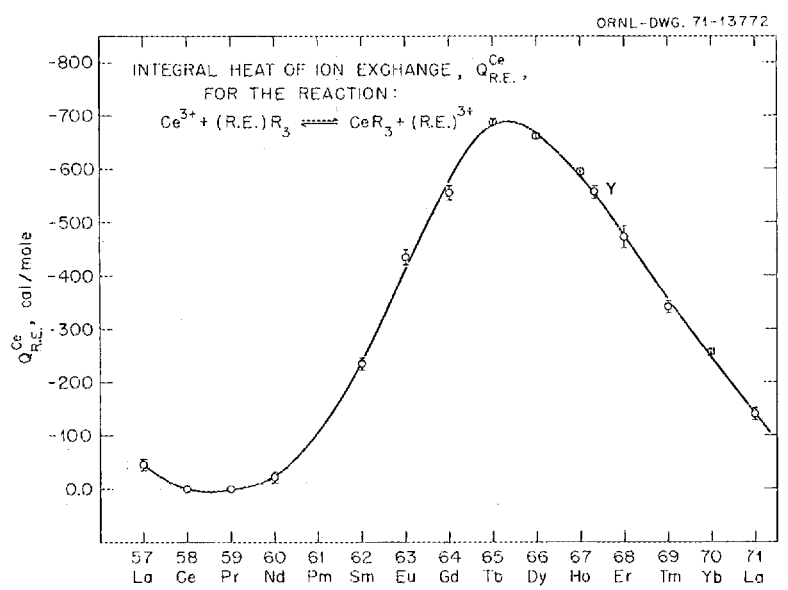

Fig. 6.6. Dependence of the integral heat of ion exchange between Ce(III) and Ln(III) cations on atomic number.

APPLICATION OF LASER RAMAN SPECTROSCOPY TO THE IDENTIFICATION OF COMPLEX IONS IN ION EXCHANGERS[1]

G. E. Boyd[2]

A knowledge of the identity of ions in ion exchangers is an essential prerequisite to the formulation of the chemical equation for an ion exchange reaction, and hence to the quantitative formulation of mass law expressions to describe ion exchange equilibria. Measurements of visible and ultraviolet absorption spectra[3,4] and infrared transmission spectra[5] have been employed to identify ions in ion exchangers. However, the use of Raman spectra should have substantial advantages over either of the foregoing techniques, as measurements can be performed easily at the small frequencies which characterize the binding of heavy atoms together to form complex ions. Further, scattering by water is negligible, and the use of high-intensity gas laser light sources for excitation makes feasible the examination of quite small samples because of the small diameter and nondivergent character of the laser beam. In the work described below, Kimax glass capillaries were employed to contain microcrystalline powders, microliter volumes of aqueous solutions, or single ion exchanger spheres which were illuminated with 4880-Å laser light to excite the Raman spectra. Tyndall (i.e., refractive index) scattering and sample fluorescence gave difficulty when strong-acid cation exchangers were examined. However, satisfactory results were obtained with strong-base anion exchangers.

The first complex ion system examined was that formed by Au(III) with concentrated solutions of chloride ion. Trivalent gold has been known since the work of Kraus and Nelson[6] to be strongly absorbed by anion exchangers from aqueous HCl and LiCl solutions.

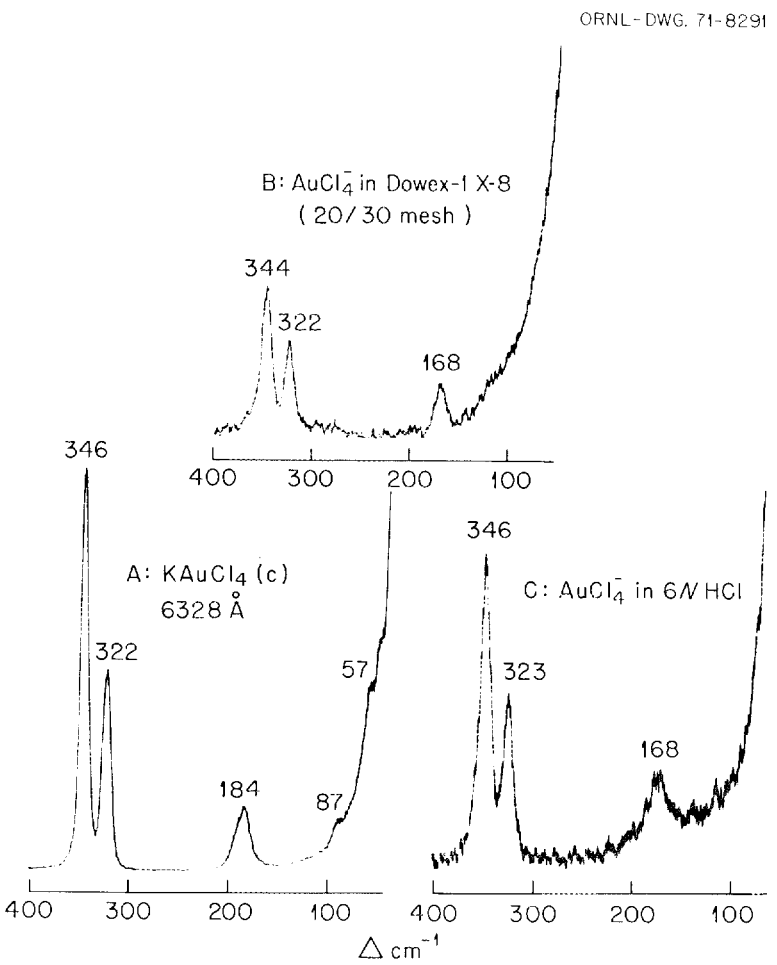

Fig. 6.7. Raman spectra of (*A*) $KAuCl_4$(c); (*B*) $AuCl_4^-$ in Dowex 1-X8; (*C*) $AuCl_4^-$ in 6 *N* HCl.

Presumably, Au(III) is extracted as $AuCl_4^-$, as this complex ion is exceptionally stable. On the other hand, Au(III) is a strong oxidizing agent, and reduction to Au metal may occur. Other gold halocomplex ions, such as $AuBr_6^{3-}$, are known to be formed by the reaction of $AuBr_4^-$ with bromide ions in nonaqueous solvents; conceivably $AuCl_6^{3-}$ also may be formed and taken up by the anion exchanger in preference to $AuCl_4^-$. Evidence for the nature of the Au(III) complex ion in aqueous solutions and in anion exchanger gels is given in Fig. 6.7, where typical recordings of the Raman spectra of crystalline $KAuCl_4$, of Au(III) in 6 *N* HCl, and of Dowex 1 in equilibrium with the foregoing aqueous solution are given.

X-ray diffraction results with $KAuCl_4$(c) have established that square planar $AuCl_4^-$ ions occur in the solid. The point group symmetry of a square planar ion is D_{4h}, and from group theory there should be three Raman-active vibrational frequencies, one of which, the symmetric stretch frequency, ν_1, should be polarized. The polarized line was shown to be that at 346 cm^{-1}, which is the strongest line. The other two lines at about 170 and 322 cm^{-1} can be assigned to ν_3 and ν_5 respectively. If $AuCl_4^-$ were tetrahedral (T_d point group symmetry), there should be four Raman lines. There is no evidence for $AuCl_6^{3-}$, which, if it were a distorted octahedron, would possess five Raman-active lines, two of which would be polarized. Note the similarity between spectra *B* and *C* (Fig. 6.7): The spectrum for the ion exchanger is virtually identical with that for the aqueous solution except for the absolute intensities of the lines. The spectrum, *A*, for the solid differs in that the frequency of the ν_3 planar deformation vibration is shifted to 184 cm^{-1}. This ca. 16 cm^{-1} shift reflects the effect of the crystal environment.

Raman spectra for another very similar ion, $AuBr_4^-$, are given in Fig. 6.8. The $AuBr_4^-$ ion is even more stable than $AuCl_4^-$, and it possesses the same symmetry, D_{4h}.

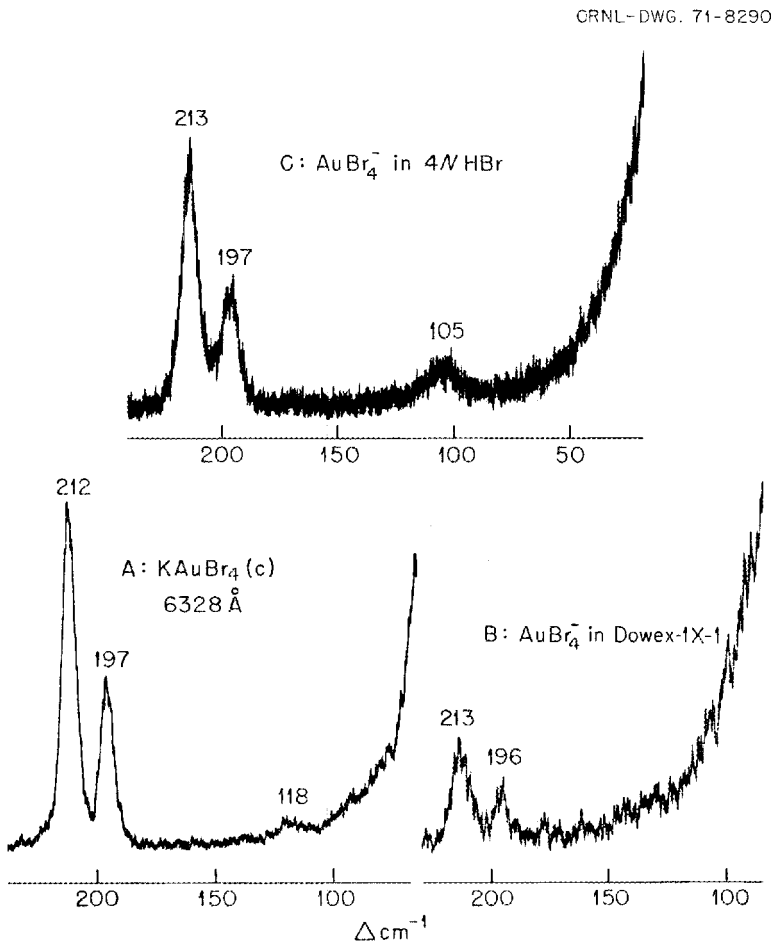

Fig. 6.8. Raman spectra of (*A*) $KAuBr_4$(c); (*B*) $AuBr_4^-$ in Dowex 1-X1; (*C*) Au(III) in 4 *N* HBr.

The ion $AuBr_6^{3-}$ has been reported to be formed in nitrobenzene solution in the presence of excess bromide, and frequently, the same ions are taken up by ion exchange resins and organic extractants, so that a search for $AuBr_6^{3-}$ in Dowex 1 seemed justified. A three-line Raman spectrum characteristic of square planar Au(III) complex ions was observed, with one frequency strongly polarized and the other two depolarized. There was no evidence for a higher complex bromoanion. The line pattern resembles that for $AuCl_4^-$, except that, as expected, all frequencies come at lower values. Again, the spectra for the aqueous solution and the ion exchange gel are very similar.

A complex anion known to possess tetrahedral symmetry (T_d) in the solid state was chosen as the next example (Fig. 6.9). Indium(III) has been reported[7] to be strongly absorbed ($K_d \sim 2 \times 10^4$) by Dowex 1 from 4 *M* HI solution, where presumably the InI_4^- ion is formed. Four Raman-active lines, one of which should be strongly polarized, are expected for a species with T_d point group symmetry; such a spectrum was observed with the aqueous solution, where scattering at low frequencies is minimal. Interestingly, in the solid the degenerate ν_3 (F_2) band at 187 cm^{-1} is split because of crystal field effects. The suggestion that this same band may be split by interactions in Dowex 1 is tempting. Further work on this point is required. In its general character, however, the Raman spectrum for the anion exchanger closely resembles that for the aqueous HI solution.

A complex ion with octahedral symmetry in its crystals was chosen (Fig. 6.10) as a final example. The

ORNL-DWG. 71-8292

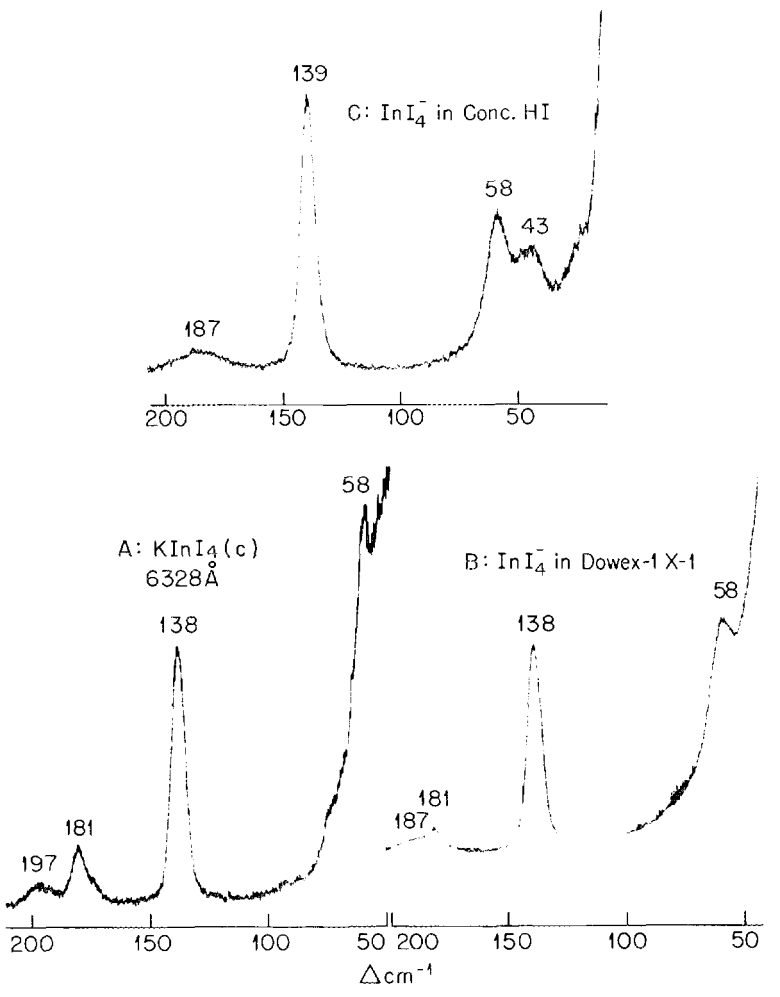

Fig. 6.9. Raman spectra of (*A*) $KInI_4$(c); (*B*)InI_4^- in Dowex 1-X1; (*C*) In(III) in 4 *M* HI.

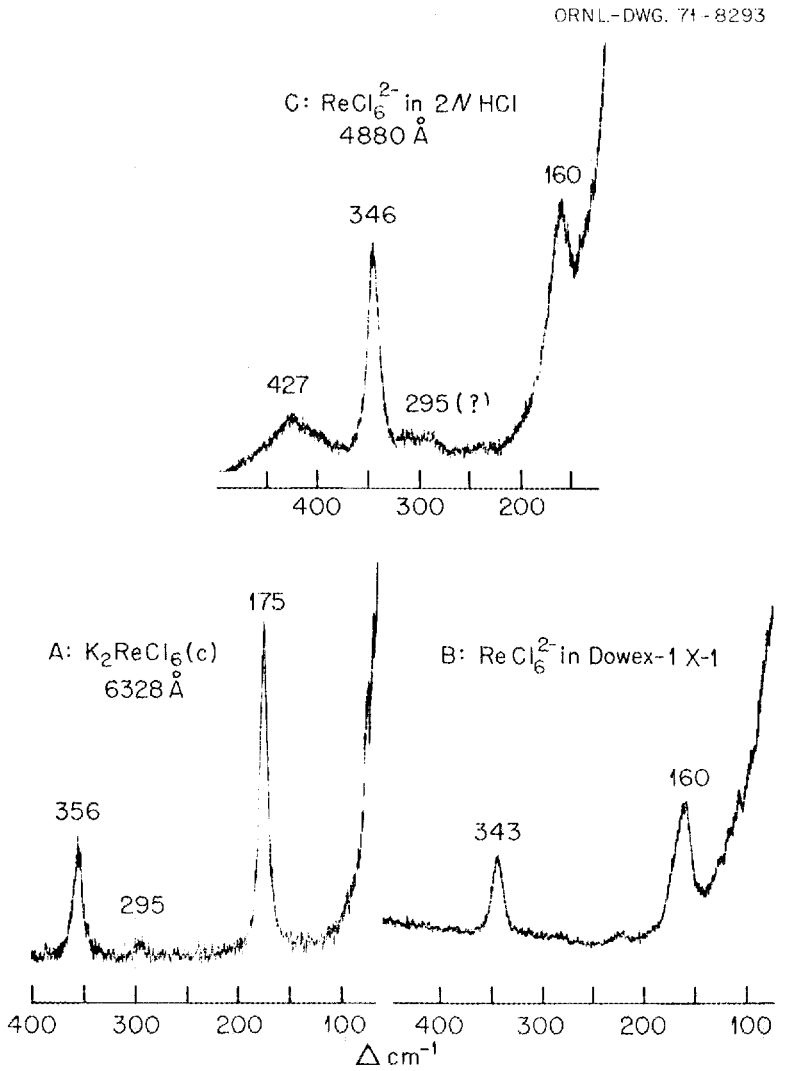

Fig. 6.10. Raman spectra of (*A*) K_2ReCl_6(c); (*B*)$ReCl_6^{2-}$ in Dowex 1-X1; (*C*) Re(IV) in 2 *N* HCl.

point group symmetry of an undistorted octahedron is O_h, and the Raman spectrum is predicted to consist of three lines — one of which, the symmetric stretch, or ν_1, vibration, should be polarized. The spectrum of aqueous 2 *N* HCl solution of K_2ReCl_6 conforms to this expectation, and the lines at 346, 295, and 160 cm^{-1} can be assigned to the fundamental vibrational modes. The band at 427 cm^{-1} cannot be assigned; it did not appear in the spectrum for crystalline K_2ReCl_6. This frequency may be caused by a hydrolysis product of $ReCl_6^{2-}$, and further study seems to be necessary. Again, except for the unassigned 427-cm^{-1} band, there is a near identity of the spectra for the aqueous HCl solution and for the exchanger gel phase.

The principal conclusion from the limited observations reported is that measurements of Raman spectra constitute a direct method for the identification of molecular ions in strong-base anion exchangers. The Raman method surpasses the infrared method and is distinctly superior to chemical methods, which depend on the chemical analysis of changes in solution composition, for inferring complex ion stoichiometry. However, there are limitations in the employment of Raman spectroscopy. In some cases, spectra cannot be observed because of the strong absorption of the exciting laser radiation. Solutions of U(IV) are an example. Further, deductions of the symmetry of the ion in solution or in ion exchanger gels from the number and polarization of

the Raman lines observed are not invariably unambiguous.

1. Excerpted from an invited lecture to the Gordon Research Conference on Ion Exchangers, Meriden, N.H., Aug. 9–14, 1971.
2. Director's Division.
3. J. L. Ryan, *J. Phys. Chem.* **65**, 1099, 1856 (1961); **64**, 1375 (1960).
4. G. E. Boyd and S. Lindenbaum, *J. Phys. Chem.* **66**, 1383 (1962).
5. L. H. Jones and R. A. Penneman, *J. Chem. Phys.* **22**, 965 (1954).
6. K. A. Kraus, D. C. Michelson, and F. Nelson, *J. Amer. Chem. Soc.* **81**, 3204 (1959).
7. P. Dobud, H. M. Lee, and D. G. Tuck, *Inorg. Chem.* **9**, 1990 (1970).

EXTENSION OF THE RADIOMETRIC POROUS-FRIT METHOD TO THE MEASUREMENT OF DIFFUSION COEFFICIENTS OF NONRADIOACTIVE COUNTERIONS IN ION EXCHANGE MEMBRANES[1]

Lawrence Dresner

A way is suggested by which the porous-frit[2–6] method may be used to measure the diffusion coefficients of nonradioactive counterions in ion exchange membranes. The (nonradioactive) counterion, whose diffusion coefficient in the membrane is to be determined, is used to elute from the membrane another (radioactive) counterion of known diffusion coefficient. The transient, rather than the asymptotic, time behavior of the membrane activity is recorded. For very short times, the fractional decrease in the activity of the membrane is proportional to the square root of the elapsed time of elution. The dependence of the coefficient of proportionality on the ratio of the diffusion coefficient of the nonradioactive ion (1) to that of the radioactive ion (2) has been calculated and is shown in Fig. 6.11.

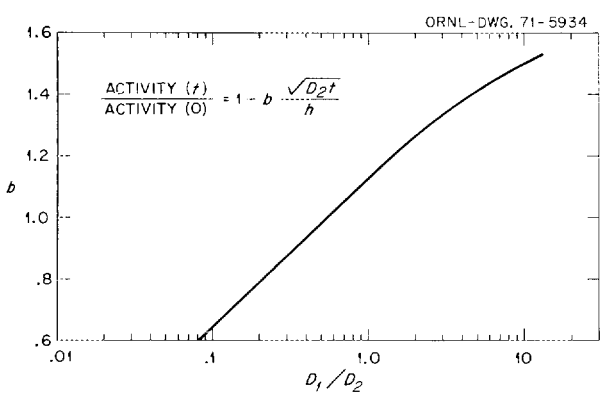

Fig. 6.11. Time dependence of the tracer activity of the membrane for early times. h is the thickness of the membrane.

1. Research sponsored by the National Science Foundation under Union Carbide Corporation's contract with the U.S. Atomic Energy Commission. Published as ORNL-4708, July 1971.
2. F. Nelson, *J. Polym. Sci.* **40**, 137, 563 (1959).
3. F. Nelson and K. A. Kraus, in *Production and Use of Short-Lived Isotopes from Reactors*, vol. I, pp. 191–213, IAEA, Vienna, 1962.
4. A. E. Marcinkowsky, F. Nelson, and K. A. Kraus, *J. Phys. Chem.* **69**, 303 (1965).
5. F. T. Wall, P. F. Grieger, and C. W. Childers, *J. Amer. Chem. Soc.* **74**, 3562 (1952).
6. A discussion of the case of the radioactive counterion may be found in: L. Dresner, *Theory of the Porous-Frit Method of Measuring Self-Diffusion Constants*, ORNL-4667 (March 1971).

SELF-DIFFUSION COEFFICIENTS OF Na^+ IN POLY(ACRYLIC ACID)–WATER MIXTURES[1]

A. J. Shor[2] D. C. Michelson
H. O. Phillips R. E. Meyer

As part of our study of transport properties in water-organic mixtures, we have been studying self-diffusion coefficients of sodium ion in poly(acrylic acid)–water mixtures. Two techniques have been used for these studies, the radiometric porous frit method[3–5] and the open-end capillary method. In the former method, a rectangular porous frit saturated with a solution containing a tracer of interest is placed into the center of a tube through which an identical solution not containing the tracer is pumped. The rate of removal of the tracer is monitored, and diffusion coefficients are calculated after appropriate calibration with a tracer of known diffusion coefficient. A flow regime has to be selected under which diffusional resistance in the boundary layer at the surface of the frit is small and reproducible, and appropriate allowances for this diffusional resistance must be made. Because there were some questions as to the applicability of the radiometric porous frit method to highly viscous solutions, such as poly(acrylic acid)–water mixtures, a second and independent method of determining diffusion coefficients seemed desirable. The open-end capillary method was selected for its simplicity and for its suitability to highly viscous solutions. In this method a small-bore capillary, open on one end and closed on the other, is filled with the solution containing the radioactive tracer. This capillary is immersed in a bath

Table 6.3. Self-diffusion coefficients of sodium ion in poly(acrylic acid)–water mixtures (0.1 *m* NaCl)

Temperature (°C)	$\mathbb{D} \times 10^5$ (cm²/sec)				
	0% PAA	25% PAA, frit	25% PAA, capillary	40% PAA, capillary	56% PAA, capillary
25	1.28	0.617	0.673	0.51	0.37
40	1.78	0.928	1.04		
60	2.58	1.43	1.43		
85	3.82	2.02			

containing an identical but nonlabeled solution. After a time interval, the capillary is removed, and the reduction in total activity, C_t/C_0, is determined. The diffusion coefficient $\mathbb{D}$ is calculated from the relation $\ln(\pi^2 C_t/8C_0) = -\pi^2 \mathbb{D}t/4L^2$, where L is the length of the capillary and t is the time interval of immersion.

Table 6.3 shows some of the results we have obtained so far. At 25° and 40°C the open-end capillary method yielded slightly higher results than the frit method, but at 60°C the results were identical. The lower temperature solutions are more viscous than the higher temperature solutions, and the differences in the diffusion coefficients might be due to an incomplete allowance for the diffusional resistance in the boundary layer for the porous frit method. More determinations are planned to confirm these results and to extend them to higher temperatures.

1. Research sponsored by the Office of Saline Water, U.S. Department of the Interior, under Union Carbide Corporation's contract with the U.S. Atomic Energy Commission.
2. On loan from the Reactor Chemistry Division.
3. F. Nelson, *J. Polym. Sci.* **40**, 563 (1959).
4. F. Nelson and K. A. Kraus, pp. 191–213 in *Production and Use of Short-Lived Isotopes from Reactors*, vol. I, IAEA, Vienna, 1962.
5. A. E. Marcinkowski, F. Nelson, and K. A. Kraus, *J. Phys. Chem.* **69**, 303 (1965).

THERMODYNAMICS OF WATER-ORGANIC SOLVENT-SALT SOLUTIONS. POLYELECTROLYTE ORGANICS[1]

R. E. Meyer J. Csurny

The solubility of sodium chloride in water mixtures of a number of organic materials was determined by a packed-column technique in which the organic-water mixture slowly flows over pure NaCl. The organic materials include a sodium polymethacrylate (pH 9.6, M.W. 5000), a poly(acrylic acid) (PAA, M.W. 150,000), sodium acrylate, and acrylic acid ($CH_2{:}CHCOOH$). Because the polyelectrolyte solutions were highly viscous, the solubilities were determined at 50°C to increase the flow of solutions through the column. The solubilities of NaCl in water mixtures of acetic and propionic acids were also determined, but at 25°C. Solubilities were determined by analysis of the chloride ion in the solution that passed through the column. All of these solutions were selected as possible models for hyperfiltration membranes containing PAA.

Sodium polymethacrylate is available as a water-organic mixture of 70% water content, and PAA as a 75% water mixture. Higher organic contents could be obtained by evaporation of the water, but the resulting solution would be too viscous to pass through the column at 50°. In order to obtain some data at high organic content, solubilities were also determined in water-organic mixtures of monomeric acrylic acid. In this case, data were obtained only for organic contents greater than 75%; in the presence of sodium chloride, a miscibility gap appeared at lower organic contents.

Only one measurement was obtained for poly(acrylic acid), at 95% water. At higher organic contents, poly(acrylic acid) appeared to salt out as the solution passed through the column of sodium chloride.

The results for the different compounds can be compared in terms of an activity coefficient ratio $\Gamma^* = \gamma_\pm{}^*/\gamma_\pm$, where the activity coefficient in the mixed solvent, $\gamma_\pm{}^*$, is computed on the same basis as that in water ($\gamma_\pm$), namely, by using the same standard state as in water and expressing concentrations in moles per kilogram of water. The Γ^* thus measures the relative selectivity of the medium for salt and water; it is a useful quantity for evaluation of model solutions for hyperfiltration membranes.

The activity coefficient ratios can be calculated[2] from the relation $\Gamma^* = s_{aq} f_w / [m_{Na^+(o)} m_{Cl^-(o)}]^{1/2}$, where s_{aq} is the molality of sodium chloride in a saturated 100% aqueous solution (6.274 m at 50°C), f_w is the fractional water content of the water-organic mixture (kg of water per kg of solvent), and $m_{Na^+(o)}$ and

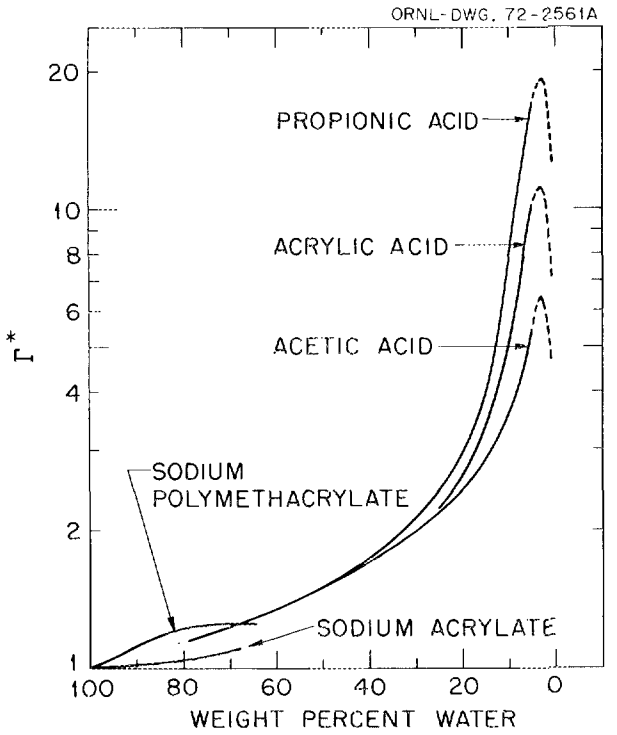

Fig. 6.12. Activity coefficient ratios in water-organic mixtures. Dotted portion of curves calculated from interpolated solubilities.

$m_{Cl^-(o)}$ are the molalities (moles per kilogram of solvent) of Na^+ and Cl^- in the water-organic mixture.

Activity coefficient ratios for all of the mixtures studied here are shown in Fig. 6.12. For the case of the sodium salts of acrylic and poly(methacrylic acid), the activity coefficient ratios are close to unity. This is not unexpected, for the solutions are composed of salts at high water contents. In addition, the ratio for the single determination with PAA is also close to unity. Again, this is not unexpected because the water content is so high. It would be desirable to determine activity coefficient ratios at higher organic contents, but the salting out of the PAA at high concentrations of NaCl precludes these measurements.

Knowledge of activity coefficients allows calculation of minimum asymptotic salt rejection R_∞ by hyperfiltration membranes. The limiting rejection R_∞ of a membrane at sufficiently high fluxes of water through it is related to a distribution coefficient D^* at the entrance interface by $R_\infty = 1 - \beta D^*$. Here β is a coupling coefficient which for neutral membranes is usually presumed to be between 0 and 1; the minimum value of R occurs for $\beta = 1$. The distribution coefficient (for neutral membranes) is related to the activity coefficient ratio by $D^* = 1/\Gamma^*$. Hence $R_\infty (\beta = 1) = 1 - 1/\Gamma^*$.

Thus, insofar as these acid solutions can serve as models for neutral membranes formed from poly(acrylic acid), asymptotic salt rejections can be computed from the solubilities. From the solubilities in water–acrylic acid mixtures, a rejection of about 90% is computed at a water content of 5%, and a rejection of about 50% at 25% water ($\beta = 1$). For propionic acid–water mixtures, the corresponding rejections are slightly higher, and for acetic acid somewhat lower.

---

1. Research sponsored by the Office of Saline Water, U.S. Department of the Interior, under Union Carbide Corporation's contract with the U.S. Atomic Energy Commission.

2. W. H. Baldwin, R. J. Raridon, and K. A. Kraus, *J. Phys. Chem.* 73, 3417 (1969).

FILTRATION AND ADSORPTION

F. Nelson H. O. Phillips K. A. Kraus[1]

In the development of cross-flow filtration[2] in this laboratory, two principal objectives were hoped to be achieved: the removal of finely divided (highly dispersed) materials from feed streams, and the removal of low-level contaminants by a combination of adsorption on such finely divided materials and removal by filtration of the "loaded" material from the feed stream. The application of cross-flow filtration to sewage treatment in the presence of a clarifying agent such as hydrous iron oxide[3] belongs to this latter class of applications. For practical applications, the filtration rate should be as large as possible; the hydrodynamic control implied in the term "cross-flow filtration" was hoped to assist in the attainment of high production rates per unit area at modest pressures by preventing buildup of a thick filter cake on the filtering surface ("porous support").

The cross-flow filtration equipment developed at this laboratory, while achieving the objectives originally set and at the same time being suitable for pilot-plant studies, seemed too cumbersome and expensive for "bench-top" research designed for the rapid evaluation of the many important variables and of the many systems to which it should be applicable. In a search for a relatively simple desk-top device, we developed a few years ago the "axial filter" by which the hydrodynamic aspects of cross-flow filtration might be approximated without the need for large pumps and loops. In the axial filter the filtration surface is located on the outside of a small (about a 1-in.-diam) rotor which spins

in a cylindrical chamber made from a section of transparent pipe. The annulus between jacket and rotor (the filter chamber) contains the feed under modest pressure. Filtrate flows radially from the annulus through the filter to the axis of the rotor, where it is collected. The device has some similarities to an experimental arrangement developed by Sherwood and co-workers[4] for the study of concentration polarization in hyperfiltration. It is similar to a device developed by Wilke and co-workers[5] primarily for the study of fermentation at high cell densities (Rotorfermentor).[6]

We have used the axial filter for a variety of studies during the year. It can be operated in three principal modes, which we shall briefly illustrate.

In the first mode the axial filter is used to filter continuously a dilute slurry containing a finely divided material. In this case the rotor is operated at high rotational speed to prevent thickening of the filter cake; the filtered solids concentrate as a slurry in the filter chamber. While we operated this device on a semicontinuous basis, it can in principle be operated on a continuous basis by controlled withdrawal of concentrated slurry from the annulus.

Most of the experiments in this mode of operation dealt with filtration characteristics of freshly precipitated hydrous oxides of metallic ions, such as those of Fe(III) and Mg(II). The filtration rates were in the range 0.5 to 2 cm/min [180 to 700 gallons per square foot per day (gfd)] at applied pressures between 10 and 30 psi. Presumably because of compaction of the thin residual layer of solids adhering to the porous support, fluxes were relatively independent of applied pressure. Fluxes depended strongly on rotational velocities; the fluxes quoted apply to rotational velocities larger than 3000 to 4000 rpm (13 to 17 fps linear velocity).

In an attempt to "model" lime-soda softening of brackish waters, an extensive series of experiments was carried out on axial filtration of freshly precipitated mixtures of magnesium hydroxide and calcium carbonate. As expected, at a given rotational velocity, calcium carbonate filters very much faster than magnesium hydroxide. In the mixtures, calcium carbonate seems to act as a "filter aid," and fluxes are in general higher than for pure magnesium hydroxide.

In a second mode of operation, finely divided adsorbents are first introduced into the filter chamber, and then a clear solution containing a contaminant is introduced. The rotor is operated at sufficiently high speed to minimize deposition of the adsorbent particles and to stir the mixture in the filter chamber. This operation simulates a single-plate chromatographic process.

This technique was tested on a variety of solutions selected because of their connection to pollution control problems. The experimental program included removal of Cu(II) from dilute solutions, using Dowex 50 and the chelating resin Chelex-100 as adsorbents; removal of Hg(II) from 0.1 to 5 *M* NaCl solutions by adsorption on Dowex 1; adsorption of Cd(II) on Dowex 50 from dilute chloride solutions; and adsorption of Cr(VI) by Dowex 1 from dilute ammonium sulfate solutions in the pH range 3.5 to 8.

Two of these systems were studied in considerable detail by MIT School of Chemical Engineering Practice teams.[7,8] As one might expect, in this mode of operation, mass transfer from the solution to the adsorbent is strongly dependent on rotational velocity (mixing), on the volume fraction of adsorbent, and on its particle size. Under favorable conditions [adsorption of trace Cu(II) by Dowex 50], decontamination factors in excess of 100 could be achieved at production rates of the order of 40 cm/min (14,000 gfd).

In a third mode of operation, finely divided material is introduced into the chamber of the axial filter; the rotor is stationary or (preferably) rotates at sufficiently low velocity to allow buildup of a uniform filter cake of significant thickness. The solution to be decontaminated is then caused to pass by the application of slight pressure from the filter chamber through this cake, which operates as a thin multiple-plate chromatographic "column." With micron-sized particles, a layer of a few millimeters thickness constitutes a bed with a very large number of theoretical plates. In addition, with such

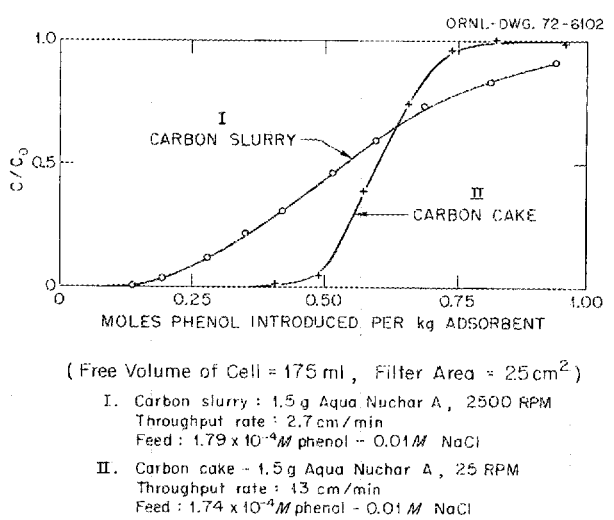

Fig. 6.13. Adsorption of phenol by activated carbon in an axial filter.

layers very high flow rates can still be achieved at modest pressures.

With this mode of operation, some experiments were carried out with "beds" of finely divided ion exchange resins, but most of the experiments were with powdered adsorbent carbon with average particle size of the order of 3–5 μ. The adsorption characteristics were tested with dilute solutions of phenol and chlorophenols. Excellent removal can be achieved in this system at very high flow rates. A typical breakthrough curve is shown in Fig. 6.13, where phenol was adsorbed by a 2-mm-thick layer of Aqua Nuchar-A at a flow rate of 13 cm/min (4600 gfd) at 20 psi. For comparison, Fig. 6.13 also shows the "breakthrough curve" when this system is operated at high rotational velocity, where the carbon is present as a dilute slurry.

1. Director's Division.
2. J. A. Dahlheimer, D. G. Thomas, and K. A. Kraus, *Ind. Eng. Chem., Process Des. Develop* **9**, 565 (1970).
3. H. A. Mahlman, W. G. Sisson, J. S. Johnson, K. A. Kraus, and N. Harrison, "Cross-Flow Filtration of Municipal Sewage," another contribution in this chapter, this report.
4. T. K. Sherwood, P. L. T. Brian, and R. E. Fischer, *Ind. Eng. Chem., Fundam.* **6**, 2 (1967).
5. A. K. Bhagat and C. R. Wilke, *Filtration Studies with Ultrafine Particles,* UCRL-16574, University of California Lawrence Berkeley Laboratory (September 1966).
6. A. Margaritis and C. R. Wilke, *Engineering Analysis of the Rotorfermentor,* LBL-222, University of California Lawrence Berkeley Laboratory (August 1971).
7. M. M. Irizarry and D. B. Anthony, *Adsorption and Filtration of Trace Contaminants in Aqueous Effluents,* ORNL-MIT-129 (1971).
8. J. A. J. Sobota and U. M. R. Lima, *Adsorption and Filtration of Chromium from Aqueous Effluents,* ORNL-MIT-133 (1971).

ADSORPTION OF Cr(VI) AND Cr(III) BY ORGANIC AND INORGANIC EXCHANGERS

F. Nelson D. C. Michelson
H. O. Phillips K. A. Kraus[1]

Because of current interest in the removal of chromium and particularly of Cr(VI) from waste streams, several series of adsorption studies were carried out with organic anion exchangers and with a variety of hydrous oxides, which can be operated as anion exchangers. While a few experiments were carried out with supporting electrolytes containing monovalent anions, principal interest was on sulfate-containing solutions, since these simulate cooling-tower wastes which have been treated with sulfuric acid to control pH.

Adsorption of Cr(VI) by Dowex 1 from Sulfate Solutions

In this system, two types of experiments were carried out: measurement of adsorbabilities at trace chromate concentrations as a function of ammonium sulfate concentration, and measurement of adsorbability of chromate at constant ionic strength as a function of conversion of the resin from the sulfate to the chromate form (range of chromate loading from 0 to 80%). The measurements were carried out near pH 8 with Dowex 1-X10 in the sulfate form. Characteristics of this resin have been described earlier.[2]

Distribution coefficients D (amount per kg dry resin/amount per liter solution) decrease from about 1100 to 20 as the concentration of ammonium sulfate increases from 0.018 to 5.4 m.

From these distribution coefficients and the known water contents, the activity coefficient ratio

$$\Gamma = \frac{\gamma^3_{\pm(NH_4)_2SO_4}\gamma^3_{\pm(NH_4)_2CrO_4(r)}}{\gamma^3_{\pm(NH_4)_2SO_4(r)}\gamma^3_{\pm(NH_4)_2CrO_4}} \qquad (1)$$

may be determined[2] for the chromate-sulfate ion exchange equilibrium

$$CrO_4^{2-} + (SO_4^{2-})(r) \rightleftharpoons (CrO_4^{2-})(r) + SO_4^{2-} . \qquad (2)$$

With our usual assumption that the standard states of all components are the same in the aqueous and resin phases, the relationship between the various measured quantities is given by

$$1 = \frac{m_{SO_4} m_{CrO_4(r)}}{m_{CrO_4} m_{SO_4(r)}} \Gamma = K^{(m)} \Gamma$$

$$= D^* \frac{m_{SO_4}}{m_{SO_4(r)}} \approx D^* \frac{m_{SO_4}}{C^*} . \qquad (3)$$

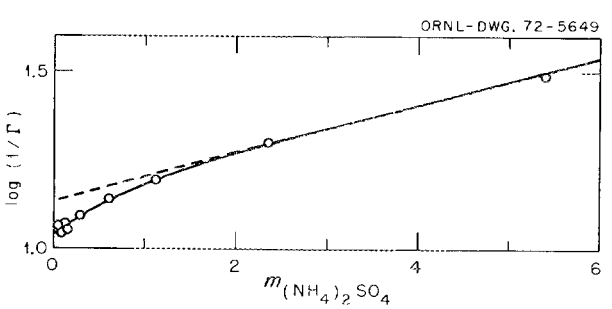

Fig. 6.14. Activity coefficient function for trace CrO_4^{2-}.

In these equations, subscript r designates the resin phase, m is moles per kg of water, and C^* is capacity (equivalents/kg water).

A plot of log $1/\Gamma$ vs m_{SO_4} is shown in Fig. 6.14; log $1/\Gamma$ increases almost linearly with m_{SO_4}. While separation of the activity coefficient terms is not possible, we suspect that the change in $1/\Gamma$ with m_{SO_4} is largely due to variations of the activity coefficient ratio in the resin phase.

The Chromate–Sulfate–Dowex 1 System at High Loading

Adsorbabilities of Cr(VI) were measured from ammonium sulfate–ammonium chromate mixtures at constant molality $m = 0.1$. The distribution coefficients D_v (moles per liter of bed/moles per liter solution) decrease only moderately with Cr(VI) loading; D_v is 85, 56, and 23 at 0, 50, and 90% Cr(VI) loading. Thus, effective removal of Cr(VI) may be accomplished with nearly complete utilization of resin capacity.

Effect of Acidity on Cr(VI) Adsorption by Dowex 1

A number of years ago we showed that anion exchangers in polyvalent anion form are capable of adsorbing acids.[2,3] A typical reaction studied in the past was the adsorption of sulfuric acid by the sulfate-form exchanger according to the equation

$$H_2SO_4 + SO_4^{2-}(r) \rightleftharpoons 2HSO_4^-(r) . \qquad (4)$$

In this reaction the sulfate form of the exchanger changes to the bisulfate form. A similar conversion of the exchanger from the chromate form to the dichromate form was to be expected according to the equation

$$H_2CrO_4 + CrO_4^{2-}(r) \rightleftharpoons 2HCrO_4^-(r) . \qquad (5)$$

To demonstrate the occurrence of this or similar reactions, adsorption of chromic acid by the chromate form of Dowex 1 was studied. The results are summarized in Fig. 6.15, which also includes the earlier results on sulfuric acid adsorption on the sulfate form of the exchanger. Distribution coefficients of chromic acid are much higher than those of sulfuric acid, implying that (except for slow oxidative degradation of the resin) this technique of chromium removal should be more successful than the equivalent sulfuric acid adsorption reaction (which has since been named by others the Sul-Bisul process).

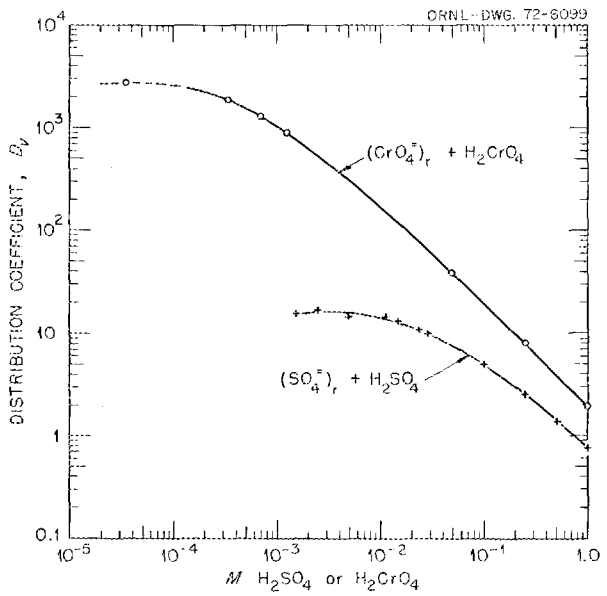

Fig. 6.15. Adsorption of H_2CrO_4 and H_2SO_4 by a strong-base anion exchange resin.

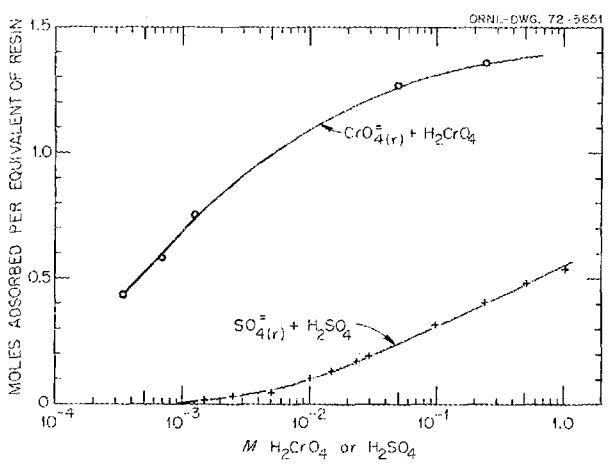

Fig. 6.16. Adsorption of H_2CrO_4 and H_2SO_4 by a strong-base anion exchange resin.

Figure 6.16 summarizes the results of Fig. 6.15 in terms of moles of H_2CrO_4 (or H_2SO_4) adsorbed per equivalent of exchanger. One expects that on complete conversion to the $HCrO_4^-(Cr_2O_7^{2-})$ form, 0.5 mole of H_2CrO_4 should be adsorbed per equivalent of exchanger. Actually, at high chromic acid concentrations this ratio is significantly larger, implying that chromic acid adsorption occurs beyond the dichromate form of the resin. If the resin would contain the species $HCr_2O_7^-$, the ratio would become 1.5.

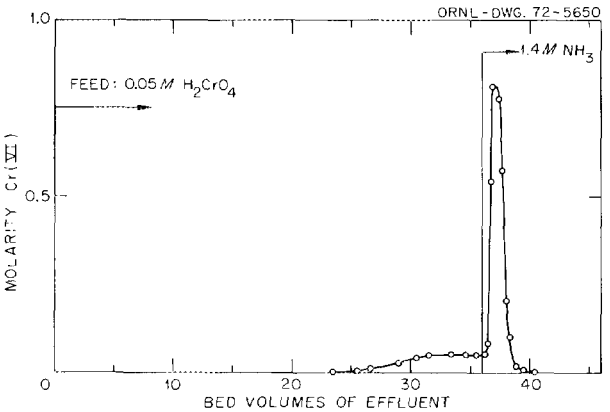

Fig. 6.17. Recovery of H_2CrO_4 with a strong-base resin.

Adsorption of chromic acid by the chromate-form exchanger can, of course, be reversed by a suitable increase in pH of the medium. These properties allow development of a unique separations and recovery procedure for chromium wherein Cr(VI) is adsorbed at low pH and eluted at high pH while retaining the exchanger at all times in the Cr(VI) form. A column experiment demonstrating this technique is shown in Fig. 6.17; Cr(VI) was adsorbed to breakthrough from 0.05 M H_2CrO_4 and eluted with 1.5 M NH_3. Elution was extremely rapid and essentially complete in two column volumes. In a similar experiment with 0.005 M H_2CrO_4 feed, the recovered $(NH_4)_2CrO_4$ solution was concentrated by more than a factor of 100 compared with the feed solution.

Adsorption of Cr(VI) by Weak-Base Anion Exchange Resins

It has been suggested that weak-base anion exchangers have advantages over strong-base exchangers in the recovery of chromates, since in principle they are easier to regenerate with base. Three experimental weak-base exchangers were supplied to us by the Dow Chemical Company. They were compared on the basis of relative capacities. The results are given in Table 6.4. The capacities were determined by passing 0.05 m $(NH_4)_2Cr_2O_7$ solutions (pH 4.0) into small beds of the exchangers and determining breakthrough curves. With all three exchangers the adsorbed Cr(VI) could be removed essentially quantitatively by elution with 1 to 2 M NH_3.

Table 6.4. Adsorption of Cr(VI) on some experimental weak-base resins

Dowex resin	Type	Capacity[a]
FPS-4004 L	Tertiary amine	1.45
FPS-4015 L	Modified tertiary amine	1.56
FPS-4024 L	Tertiary amine	1.48

[a]Moles of Cr(VI) per liter of bed.

During the adsorption cycle, a small amount of chromium (0.1%) "leaked" through the columns. This presumably represents slow reduction of Cr(VI) to Cr(III) by the exchanger; Cr(III) is expected not to adsorb under these conditions on organic anion exchangers.

Adsorption of Cr(VI) by Hydrous Oxides

Hydrous oxides in their anion exchange mode have long been known[4] to be excellent adsorbents for chromates, at least when the supporting electrolyte contains principally monovalent anions. Hydrous oxides might offer some advantages over organic anion exchangers for the recovery of Cr(VI), since they would not be oxidized by chromate as are the organic exchangers and since, in principle at least, they are cheaper than organic exchangers. Use of the hydrous oxides in the past for such applications has been retarded because of unavailability of commercial hydrous oxide particles of sufficient size and strength to permit column operation. It was hoped that the materials could also be used in colloidal form or as flocs, provided that adsorption could be combined with reasonably rapid filtration. We are attempting to do the latter under another part of the program.[5] We have evaluated the "capacity" for chromate of a large number of simple and mixed hydrous oxides (Table 6.5).

Table 6.5. Adsorption of Cr(VI) on freshly precipitated hydrous oxides

(0.005 M Na_2SO_4)

Hydrous oxide	D_M	D	pH
Al(III)	400	8×10^3	6
Bi(III)	10^4	4×10^4	6
Cr(III)	200	2.5×10^3	6
Fe(III)	250	3×10^3	6
La(III)	500	3×10^3	(7.5–8)
Sn(IV)	25	2×10^2	3.4
Th(IV)	2000	8×10^3	5–6
Zr(IV)	1000	8×10^3	6
1 Bi(III)–1 Zr(IV)	6000	3×10^4	6
1 Cr(III)–1 Zr(IV)	300	3×10^3	6.5
2 Mg(II)–1 Zr(IV)	200	3×10^3	6

To determine chromate uptake by the hydrous oxides and the effect of pH on it, dilute slurries of freshly precipitated hydrous oxides were mixed in beakers in a ratio of 1 mole of Cr(VI) to 10 moles of metal and the systems titrated with acids and bases. At convenient intervals, samples were withdrawn, centrifuged, and the supernatants analyzed for chromium by atomic absorption spectroscopy. Typical titration curves for hydrous zirconium oxide are shown in Fig. 6.18. This system as well as most, though not all, of the others seems reversible; that is, distribution coefficients observed during the titrations with acid were, within experimental error, equal to those observed during titration with base. Figure 6.18 shows three curves. Very high distribution coefficients were observed with 0.05 *M* NaCl as supporting electrolyte. Substantially lower distribution coefficients occur in 0.005 *M* Na_2SO_4 and still lower values in 0.05 *M* Na_2SO_4. The sulfate system was expected to show substantially lower distribution coefficients than the chloride system.

The distribution coefficient–pH functions show pronounced maxima, which in the sulfate system are located near pH 6. Presumably in the lower pH range, adsorption is decreased because of conversion of chromate to dichromate in the aqueous phase and because presumably $HCrO_4^-$ is less strongly adsorbed by these hydrous oxides than the divalent ion CrO_4^{2-}. Adsorbability decreases at pH values above the maxima presumably because of the competition from the hydroxide-chromate exchange reaction.

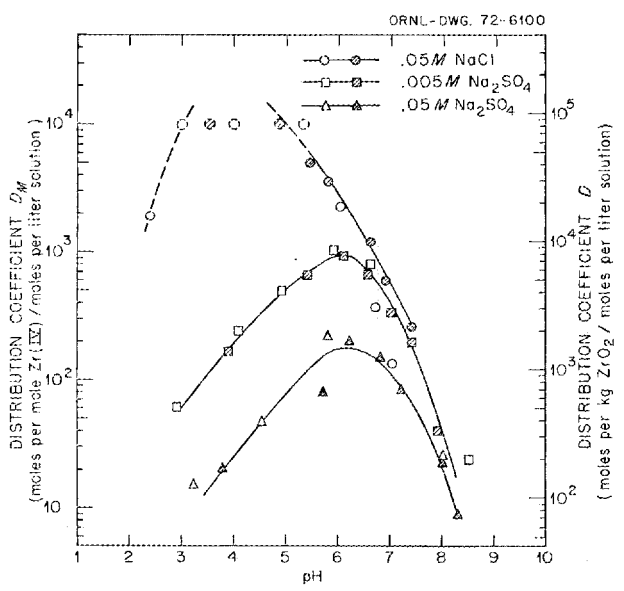

Fig. 6.18. Adsorption of Cr(VI) by freshly precipitated hydrous Zr(IV) oxide.

Table 6.5 lists for various hydrous oxides the pH values and distribution coefficients at the absorption maxima. Two sets of distribution coefficients are listed: D_M, which is [amount of Cr(VI) adsorbed per mole of metal]/[amount per liter of solution]; and D, which is [amount per kg of (anhydrous) oxide]/[amount per liter of solution].

The relatively acidic and common hydrous oxides Al(III), Cr(III), and Fe(III) seem to have values D_M of the order of several hundred. The hydrous oxide of Sn(IV) has a value of D_M about an order of magnitude smaller, while the hydrous oxide of Zr(IV) has D_M about a factor of 5 larger. Adsorbabilities by the very basic oxides, Th(IV), Bi(III), and La(III), are substantially higher. While with the basic oxides Cr(VI) is difficult to elute by treatment with excess base, such removal seems satisfactory for the more acidic oxides.

A few experiments were also carried out with lead oxide. Adsorption of Cr(VI) from these solutions [5×10^{-4} *M* Cr(VI) originally] was extremely good. In this case, however, we presume that we are dealing with conversion of lead oxide to lead chromate rather than with an anion exchange–adsorption reaction.

For the mixed oxide Bi(III)-Zr(IV) (mole ratio 1:1), adsorption seemed to be similar to that with Bi_2O_3; the mixed material, however, is easier to handle than Bi_2O_3. The 1:1 mixture Cr(III)-Zr(IV) seemed to

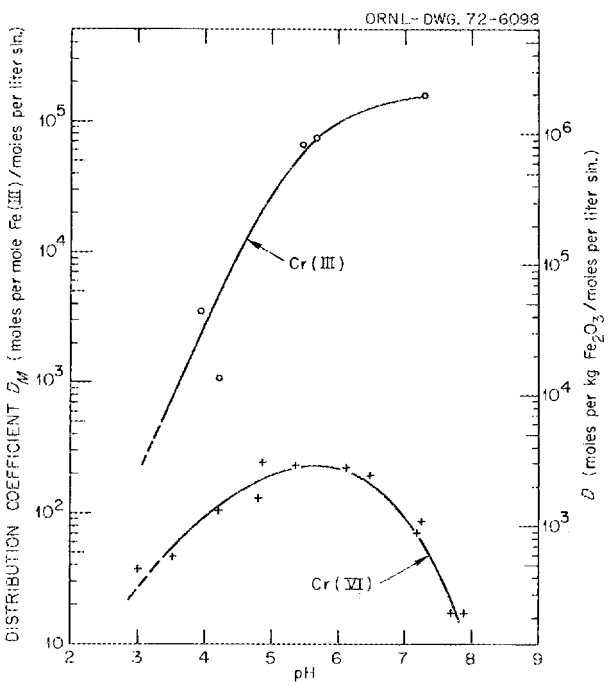

Fig. 6.19. Adsorption of Cr(VI) and Cr(III) on hydrous Fe(III) oxide.

behave more like Cr(III) oxide than Zr(IV) oxide. The Mg(II)-Zr(IV) mixture with 2:1 mole ratio was investigated because it was hoped that in this mixture advantage might be taken of the very basic characteristics of Mg(II) hydrous oxide. This did not seem to be the case.

Adsorption of Cr(III) by Hydrous Oxides

One of the advantages of hydrous oxides for the removal of chromium is the possibility of finding a single adsorbent which would remove both Cr(III) and Cr(VI) in a practical pH range. It was anticipated that Cr(III) would adsorb strongly on acidic hydrous oxides such as Fe(III) or Zr(IV) oxides if the pH was high enough.[4] This expectation was confirmed, and distribution coefficients D of the order of 10^5 and 10^6 were found when the pH of the solutions exceeded about 6. A comparison of adsorption of Cr(III) and Cr(VI) by hydrous Fe(III) oxide is given in Fig. 6.19.

1. Director's Division.
2. F. Nelson and K. A. Kraus, *J. Amer. Chem. Soc.* **80**, 4154 (1958).
3. F. Nelson and K. A. Kraus, *J. Amer. Chem. Soc.* **77**, 329 (1955).
4. K. A. Kraus, H. O. Phillips, T. A. Carlson, and J. S. Johnson, *Ion Exchange Properties of Hydrous Oxides,* Proceedings of the Second United Nations International Conference on the Peaceful Uses of Atomic Energy, vol. 28, pp. 3–16, United Nations, Geneva (1958).
5. F. Nelson, H. O. Phillips, and K. A. Kraus, "Filtration and Adsorption," the previous contribution, this report.

FILTRATION TECHNIQUES FOR TREATMENT OF AQUEOUS SOLUTIONS

R. E. Minturn	P. M. Lantz
C. G. Westmoreland	K. A. Kraus[2]
J. Csurny	J. T. Day[3]
Neva Harrison	W. H. Baldwin
J. S. Johnson	C. E. Higgins
G. E. Moore	S. Amin[3]
A. J. Shor[1]	S. D. Harms[3]
L. L. Fairchild[1]	W. D. Franklin[3]

Development of filtration methods for desalination and for pollution control applications continued to occupy much of the attention of the Water Research Program. Support for non-AEC applications came from the Office of Saline Water (OSW)/Research and from the ORNL Environmental Program, funded by the National Science Foundation-RANN.

Desalination

The focus has been on development of dynamically formed hydrous Zr(IV) oxide–polyacrylate membranes[4-6] [Zr(IV)-PAA] for use with typical brackish waters. A concurrent program, sponsored by the OSW/Membrane Division, on engineering development of dynamic membranes, has added impetus in this direction; this program, carried out by D. G. Thomas' group in the Reactor Division, culminates in a 1000-gpd pilot plant, to be field tested at the OSW station in Roswell, N.M.

One area of emphasis has been on location of porous supports suitable for practical application. Much attention has also been given to detailed delineation of the deleterious effects of polyvalent counterions [mainly Ca(II) and Mg(II)] on performance of Zr(IV)-PAA membranes and the alleviation of these effects by pretreatment to remove various fractions of these ions.

A 55-day run exemplifies efforts toward these objectives. The membrane was formed on a ceramic tube, under development by Selas Flotronics for practical modules. Outer dimensions of the tube are $^3/_8$ in., and in it are seven $^1/_{12}$-in. channels, on the surface of which membranes are dynamically formed. This configuration allows feed pressurized to about 1000 psi to be circulated on the inside, an unusual capability for ceramic tubes. As we outlined in last year's report,[4] initially a hydrous Zr(IV) oxide membrane is formed by circulation of a solution containing the colloidal oxide, and an organic polyanionic layer is then attached by exposure to poly(acrylic acid) solution at acidic pH. The pH is then gradually raised to neutrality by additions of base.

The first membrane formed on the tube was tested for 121 hr with a simulated pretreated Colorado River water, and performance was satisfactory until Ca(II) and Mg(II) concentrations were increased to the amounts normally found in the water. The first membrane was stripped from the support by chemical washes, and a new membrane formed. This membrane was tested for 584 hr with a variety of solutions simulating treated and untreated natural waters. Again, fluxes and rejections were good except for those cases when appreciable concentrations of divalent cations were present. Water recoveries of from 60 to 73% were carried out at various times throughout the run.

A third membrane was formed, and a chronological record of a 524-hr run is given in Fig. 6.20. The feed brines, indicated by name at the top of the figure, are simulated natural waters in which the divalent cation concentrations had either been reduced by chemical

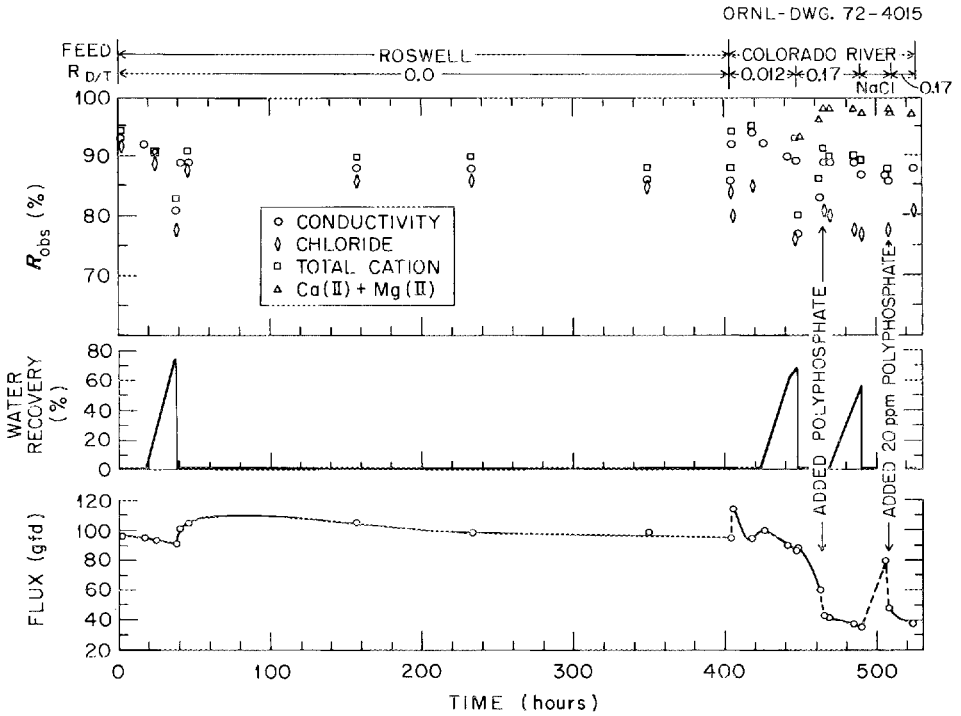

Fig. 6.20. Hyperfiltration of simulated pretreated brackish waters by Zr(IV)-PAA membrane on Selas ceramic tube. $R_{D/T}$ is the ratio of divalent cation concentration to total ion equivalents in feed (950 psig, 15 fps, 25°C, pH 8).

treatment to precipitate $CaCO_3$ and $Mg(OH)_2$, which were then removed by cross-flow filtration, or omitted entirely when the feed was prepared. The value of $R_{D/T}$ is the ratio of the equivalents of divalent cation to total ion equivalents; for Roswell water the normal value of $R_{D/T}$ is about 0.38, total salinity being 2010 ppm, while for Colorado River water it is about 0.47, with total salinity of 1060 ppm.

At certain times during the 524-hr test, we discarded product and thereby increased brine concentration. These periods are indicated in the central portion of the figure by increases in water recovery. For example, at 18 hr we began to concentrate the feed, a simulated Roswell water with no divalent cations, and had removed about 73% of the water by 38 hr. During this period, all rejections being monitored dropped from about 90% to about 80%, and the flux decreased from about 95 gfd to about 91 gfd. Both rejections and fluxes recovered, however, when the concentrated brine was replaced with fresh solution of the original composition.

After more than 400 hr of operation, the rejections had fallen somewhat, with chloride rejection the lowest at 84%, while the fluxes remained greater than 90 gfd. At that point we rinsed the simulated pretreated Roswell water from the loop and replaced it with a simulated Colorado River water that had been cross-flow filtered[7] after chemical treatment. At this point, $R_{D/T}$ was 0.012. The flux increased abruptly, probably because of the water rinse, but soon fell to values near those for the Roswell water. The rejection of total cations increased, although the rejection of chloride ion fell to about 80%. Again, fluxes and rejections decreased as feed concentration increased. When a pretreated Colorado River water which still contained most of the Mg(II), but little of the Ca(II), was added at 447 hr, rejections decreased, but fluxes were not appreciably affected. In subsequent experiments, attempts to complex the Mg(II) in the feed by adding an equivalent amount of polyphosphate did not give promising results.

After 55 days of operation, the ceramic tube was removed and placed in a small loop for lifetime tests of the support.

For brackish waters whose Ca(II) and Mg(II) content is not too high for economical removal, these results indicate that adequate rejections can be attained by Zr(IV)-PAA membranes which generally give fluxes

much higher than those with usual commercial hyperfiltration membranes. Prospects for availability of cheap porous supports also appear good; besides the Selas ceramics discussed here, Union Carbide is investigating carbon tubes, while Ferro ceramics have given excellent results in modules developed by Thomas' group for the Roswell pilot plant.

Membrane formation procedures were optimized for Acropor and Millipore filter sheets, and performance is favorable with these at higher divalent cation concentrations than with membranes on potentially practical supports. It may be that delineation of the best procedures for ceramic and carbon supports will decrease the level of pretreatment needed.

Pollution Control Applications

Major participation by us in the evaluation of dynamic membranes for textile dyeing wastes[8,9] has been completed during the year, and the results have been reported. Our Clemson University collaborators are continuing the work, hopefully with support from the Environmental Protection Agency.

Our heaviest effort at present, carried out in collaboration with the International Paper Co., is on treatment of waste streams generated in the kraft pulping process. One example is hyperfiltration by Zr(IV)-PAA membranes of the waste effluents from the bleaching of kraft pulp, specifically the caustic extraction stage effluent neutralized with the acidic bleaching waste.

ORNL-DWG. 71-9677A

	REJECTION R_{obs} (%)	CONCENTRATE	PRODUCT
COLOR (Pt-Co Units)	99.9	9000 - 45,000	5 - 35
TOTAL CARBON (ppm)	94 - 97	775 - 3200	25 - 100
CHLORIDE (ppm)	BELOW	1000 - 5000	150 - 1000

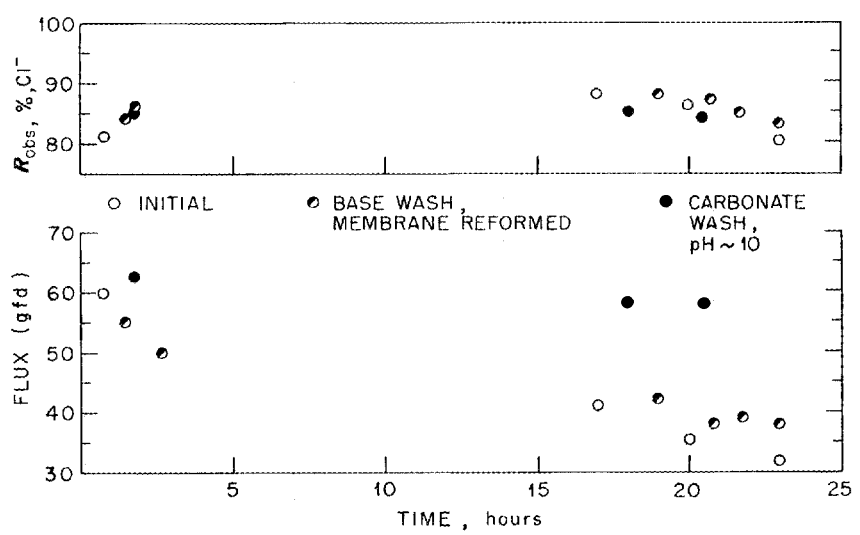

FEED: CAUSTIC EXTRACT, ACID BLEACH ADDED TO pH 7-7.5
SUPPORT: 6C CARBON TUBES, UNION CARBIDE
PRESSURE: 950 psig
CIRC. VEL.: 12.4 fps
TEMPERATURE: 58-67°C

Fig. 6.21. Hyperfiltration of bleach plant wastes from kraft pulping process by Zr(IV)-PAA membranes on carbon tubes in small protomodule (950 psig, 12.4 fps, 58–67°C, pH 7–7.5).

Figure 6.21 summarizes some results obtained with membranes formed on porous carbon tubes in a small protomodule made by Union Carbide Corporation. Hyperfiltration was carried out at typical process temperatures, 58–67°C. Water recovery was carried to about 80%, and the rejection of color remained above 99.9% throughout, while that for total carbon varied from 97% with the dilute feed to about 94% with the concentrated feed. Chloride rejection was 80 to 90% throughout the run. Membranes were regenerated twice, once by washing with base and acid and reforming the membrane in situ, and once by simply rinsing the membrane with bicarbonate at pH 10. In the latter case, no membrane re-formation was necessary, and the subsequent flux decline, when once again the membrane was subjected to the kraft waste, was slower than before regeneration.

The process described above, hyperfiltration of kraft wastes at high pressure, was designed to yield a product pure enough to be returned to the environment or to be recycled in the process. Another possibility is to operate under conditions where color and other organics in the waste are removed and the permeate retains the process salts. The salts could thus be reused, while the organics, in more concentrated form, would be more amenable to disposal. An example of this approach is summarized in Fig. 6.22, which shows a pH scan (the pH of the caustic extract was adjusted with acid bleach waste) during a low-pressure hyperfiltration by a single-layer hydrous Zr(IV) oxide membrane on a porous carbon tube. There is good separation between the organics (color and carbon) and the salts (conductivity and Cl^-) with high fluxes, ranging from 80 to 100 gfd. Hydrous Zr(IV) oxide membranes are expected to reject salt poorly in this pH range and at this pressure.

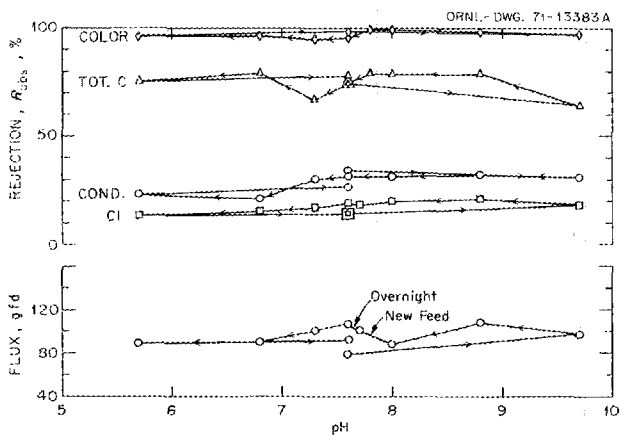

Fig. 6.22. Low-pressure hyperfiltration of kraft bleaching waste as a function of pH. Caustic extract with added acid bleach; Zr(IV) membrane on porous carbon tube (200 psig, 9 fps, 65°C).

Applications of Nuclear Energy Interest

Cooling tower blowdown. Blowdown from cooling towers contains chromate at concentrations from 10 to ≥70 ppm, and in the past has been discharged into streams and rivers. Chromate is now recognized as a dangerous contaminant and will, in the future, have to be removed from any effluent released to the environment. We tried with some success to remove chromate from aqueous wastes either by cross-flow filtration or by hyperfiltration. However, the most promising approach appears to be that of removing other contaminants, for example, calcium, magnesium, and zinc, from the blowdown and recirculating the chromate and softened water to the tower. Cross-flow filtration after addition of appropriate amounts of carbonate and base to precipitate $CaCO_3$ and $Mg(OH)_2$ and of H_2O_2 to convert reduced chromium to Cr(VI) appears to be an effective way of attaining almost complete conservation of the chromium in the cooling tower water.

Waste streams with low-level radioactivity. We have also addressed the problem of processing low-level wastes, exemplified by ORNL process water. By a two-stage process, a softening step involving cross-flow filtration followed by hyperfiltration, we were able to remove about 99.96% of the ^{90}Sr (final value 0.062 dpm/ml) and more than 99.8% of the gross beta activity, while the gamma activity was removed to below background levels. Very little alpha activity was found in the feed solution. The hyperfiltration was carried to 90% water recovery at fluxes from 40 to 75 gfd. A process involving softening as in the first stage above, with addition of Fe(III) as a specific adsorbent for ^{90}Sr, also appears to be promising. This should be cheaper, since only cross-flow filtration is required. Here 99% of the ^{90}Sr was removed. Fluxes were from 350 to 500 gfd at 10 psig.

---

1. Reactor Chemistry Division.
2. Director's Division.
3. MIT School of Chemical Engineering Practice, Oak Ridge Station, J. T. Day, Director; S. Amin, Assistant Director.
4. *Chem. Div. Annu. Progr. Rep. May 20, 1971*, ORNL-4706, p. 140.
5. J. S. Johnson, R. E. Minturn, and P. Wadia, *J. Electroanal. Chem. Inter-facial Electrochem.*, in press.

6. J. S. Johnson, "Polyelectrolytes in Aqueous Solutions. Filtration, Hyperfiltration and Dynamic Membranes," to appear in *Reverse Osmosis Membrane Research*, H. K. Lonsdale and H. E. Podall, eds., Plenum, New York.

7. J. A. Dahlheimer, D. G. Thomas, and K. A. Kraus, *Ind. Eng. Chem., Process Des. Develop.* 9, 565 (1970).

8. C. Aurich, C. A. Brandon, J. S. Johnson, R. E. Minturn, K. C. Turner, and P. Wadia, *J. Water Pollut. Contr. Fed.*, in press.

9. C. A. Brandon, J. S. Johnson, R. E. Minturn, and J. J. Porter, American Society of Mechanical Engineering, Publication 72-PID-3, Joint ASME/EPA, *Reuse and Treatment of Waste Water General Industry and Food Processing Symposium*, New Orleans, La., March 28–30, 1972.

STABILITY OF THE EXTENDED NERNST-PLANCK EQUATIONS IN THE DESCRIPTION OF HYPERFILTRATION THROUGH ION EXCHANGE MEMBRANES[1]

Lawrence Dresner

One of the most interesting features of nonlinear differential equations is that their solutions may depend discontinuously on the initial conditions. Such behavior, which is related to the stability of the differential equations, is found when the extended Nernst-Planck equations (ENPE) are used to describe the hyperfiltration of multicomponent solutions through ion exchange membranes. The case most thoroughly analyzed is that of two counterions and one coion. In this case, there are two different kinds of solutions of the ENPE, distinguishable by their behavior in the limit of infinite membrane thickness: the limiting behavior of the first kind may be easily calculated from certain algebraic equations related to the ENPE, but the limiting behavior of the second kind cannot. In the limit of infinite membrane thickness, there is complete rejection of a particular one of the counterions from any feed which leads to a solution of the second kind. Under certain circumstances solutions of the first kind exhibit negative rejection of the other counterion. (Negative rejection means that the effluent solution is more concentrated in the particular ion than the feed.) An experiment is quoted in the paper on which this summary is based exhibiting both of these phenomena.

In an earlier paper,[2] also discussed in last year's annual report,[3] I found an approximate solution of the ENPE, which turns out to be an approximate form of the solution of the second kind. From this approximate solution, I recognized the possibility of complete rejection that is associated with solutions of the second kind in the present paper. The earlier paper was based on the restrictive assumption of good coion exclusion from the membrane, an assumption that is dropped in the present paper.

1. Research jointly sponsored by the ORNL-NSF Environmental Program and by the Office of Saline Water, U.S. Department of the Interior, under Union Carbide Corporation's contract with the U.S. Atomic Energy Commission. Accepted for publication in the *Journal of Physical Chemistry*.

2. L. Dresner, *Desalination* **10**, 27 (1972).

3. L. Dresner, *Chem. Div. Annu. Progr. Rep. May 20, 1971*, ORNL-4706, p. 146.

PRELIMINARY ANALYSIS OF DONNAN SOFTENING[1]

Lawrence Dresner

Donnan softening[2] is a name given to a dialytic method of removing divalent cations from the feed water of desalination plants. The feed to the plant and the brine from it flow countercurrent to each other in adjacent channels, the common wall of which is a cation exchange membrane.[3] Divalent cations migrate from feed to brine, while univalent cations migrate in the opposite direction. In a variation of the process, the brine is enriched in a salt of the univalent cation from an external source. Donnan softening of the feed water would be extremely valuable in suppressing scale formation in desalination plants.

The paper on which this summary is based presents a simplified economic analysis of Donnan softening. Only the costs of the membrane and added salt are considered. Four specific examples are discussed, based on using electrodialysis membranes to soften the feed waters at Yuma, Ariz., Webster, S.D., Roswell, N.M., and a synthetic seawater. Table 6.6 summarizes the costs estimated in the examples, together with the cost

Table 6.6. Summary of cost estimates (¢/kgal)

Feed		50% softening	90% softening	Cost of chemicals for soda-lime softening	
				50%	100%
Yuma	No salt	7.87	14.7	1.67	7.65
	Salt	6.34			
Webster	No salt	23.8	32.0	6.80	13.6
	Salt	5.14	9.87		
Syn. seawater	No salt	49.4	156	6.80	13.6
	Salt		144		
Roswell	No salt	25.4	66.5	5.20	18.8
	Salt				

of chemicals for 50 and 100% softening by the soda-lime process. It appears that Donnan softening with present-day electrodialysis membranes is too costly for use with feed waters of high salinity, for example, seawater or the water at Roswell. Even with less saline waters like those at Yuma or Webster, Donnan softening does not always compete favorably with the soda-lime process. It seems fair to say that with present-day electrodialysis membranes, Donnan softening is not very interesting economically. However, a drastic reduction in membrane cost, for example, by a factor of 10, would make Donnan softening an attractive candidate for intensive development.

The most hopeful avenue for drastically reducing membrane costs is to make the membranes thinner. The typical thickness of a present-day electrodialysis membrane is 200 μ. A tenfold reduction in thickness to 20 μ, for example, would permit a tenfold reduction in membrane area required. This would be reflected in a tenfold reduction in cost when (1) no salt is added to the brine, and (2) the cost per unit area is the same for the thinner as for the thicker membrane. The savings could conceivably be even greater, since the thinner membrane would have only a tenth as much material per unit surface area as the thicker membrane. With a very cheap membrane surface, salt addition to the brine would probably not produce any savings. This is good, since adding salt may complicate the brine disposal problem of inland desalting plants. Finally, it may be noted that ordinary dialysis membranes are often manufactured in the form of tubes, and such a configuration appears an excellent choice for Donnan softening.

---

1. Research sponsored by the Office of Saline Water, U.S. Department of the Interior, under Union Carbide Corporation's contract with the U.S. Atomic Energy Commission. Submitted to *Industrial and Engineering Chemistry Process Design and Development.*

2. J. L. Eisenmann and J. Douglas Smith, *Donnan Softening as a Pretreatment to Desalination Processes,* OSW R&D Progress Report No. 406, U.S. Government Printing Office (February 1970); J. D. Smith, *Exchange Diffusion (Donnan Softening) as a Pretreatment to Desalination Processes,* OSW R&D Progress Report No. 655, U.S. Government Printing Office (May 1971).

3. The use of ion exchange membranes as dialysis membranes in separations processes was pioneered by R. M. Wallace, *J. Phys. Chem.* **68,** 2418 (1964); **70,** 3922 (1966); *Ind. Eng. Chem., Process Des. Develop.* **6,** 423 (1967).

SORPTION OF CATIONS BY POLYAMINORESINS

Neva Harrison W. H. Baldwin C. E. Higgins

Interest in polyaminoresins for chelation or for use as polyelectrolytes was expressed previously.[1] Some of these resins were equilibrated with aqueous solutions to define the limitations of sorption.

Insolubilized PEI Polymers

Poly(ethylene imine) was insolubilized by reaction with methyl acrylate as described.[1] The solid was equilibrated with aqueous electrolyte solutions to measure their distribution between solid and liquid. Equilibrium was attained in times significantly less than 1 hr when the mixture was tumbled end over end at the rate of 20 rpm.

Mercury(II) was sorbed from 1 *M* HNO_3 solutions with distribution coefficients in the range 2 to 10, depending on the Hg(II) concentration. The distribution coefficient is defined here as the ratio of the concentration of Hg(II) in the dry resin to the concentration per ml of solution. The concentration of Hg(II) in the aqueous feed solutions ranged from 0.005 to 0.07 *M.*

Copper (II) was sorbed on the same kind of resin with larger distribution coefficients in favor of the resin. It appears from these preliminary tests that the sorption of Cu(II) is more sensitive than that of Hg(II) to the acidity of the solution.

Cadmium(II) was not sorbed on the resin from solutions ranging in HNO_3 concentration from 0.3 to 2 *M.*

Poly(vinylpyridine-co-divinylbenzene)

Vinylpyridine (4 g) was copolymerized with divinylbenzene (1 g) and ground to a powder suitable for equilibration tests. Distribution coefficients of the order of 5 were observed when this resin was equilibrated with 0.05 *M* Hg(II) in 0.1 *M* HNO_3. This result identifies another polymer that has properties favorable for the sorption of cations.

---

1. W. H. Baldwin, Neva Harrison, and C. E. Higgins, *Chem. Div. Annu. Progr. Rep. May 20, 1971,* ORNL-4706, p. 145.

TEMPERATURE EFFECTS ON EQUILIBRIA IN THE SYSTEM: POLY(HYDROXYPROPYL ACRYLATE--CO--TETRAETHYLENE GLYCOL DIMETHACRYLATE), WATER, AND ELECTROLYTE

C. E. Higgins W. H. Baldwin

During our investigation of unfamiliar properties of polymers that may be related to desalting of aqueous electrolytes, the effect of temperature on the absorp-

tion of aqueous sodium chloride by poly(hydroxypropyl acrylate–co–tetraethylene glycol dimethacrylate) was tested. Rods of the polymer were prepared as described[1,2] from the monomers hydroxypropyl acrylate and tetraethylene glycol dimethacrylate in the weight ratio of 19 to 1.

The polymer was equilibrated with water at 24°C and then transferred to a large excess of 0.5 *M* NaCl at 1°C. The weight of the polymer increased by 43%, but this was accompanied by 34% rejection of sodium chloride. The blotted cylinder of polymer was then warmed to 24°C. The exudate that separated was 0.45 *M* in NaCl, representing another 70% rejection during this step.

Although this polymer does not appear useful for desalination by thermal cycling, it should be an interesting candidate for a dynamically formed membrane.

1. N. Harrison, J. Csurny, C. E. Higgins, and W. H. Baldwin, *Chem. Div. Annu. Progr. Rep. May 20, 1970,* ORNL-4581, p. 112.
2. C. E. Higgins and W. H. Baldwin, *J. Appl. Polym. Sci.* **12**, 1471 (1968).

CROSS-FLOW FILTRATION OF MUNICIPAL SEWAGE

H. A. Mahlman J. S. Johnson
W. G. Sisson[1] K. A. Kraus[2]
Neva Harrison

Results last year[3] indicated that cross-flow filtration, combined with physical-chemical clarification, had great promise in treatment of municipal sewage. Hydrolyzable salts, for example of Al(III) and Fe(III), are added to the effluent from primary settling, and the effluent is then circulated past filtering surfaces. The cross flow hinders the thickening of filter cake and, consequently, slows flux decline. One attempts to recover most of the water in the filtrate and to retain impurities in a concentrated stream. Filtrate quality usually exceeds that given by biological secondary processes and is comparable with effluents from several tertiary treatments: turbidity near that of tap water (JTU < 1); phosphate, a fraction of a ppm; and organic carbon, typically 5 to 15 ppm.

During the past year, we have made considerable progress toward delineating conditions for efficient cleanup and good flux. Besides the cross-flow variables (primarily pressure, circulation velocity, filtration medium, and backwash intervals), such conditions as additive level and manipulation of pH appear important.

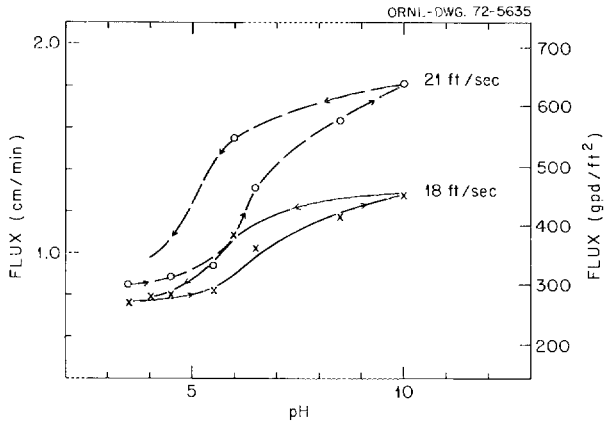

Fig. 6.23. Effect of pH on cross-flow filtration of primary sewage effluent. Fire-hose jackets, 40 psi, 100 ppm Fe(III).

In earlier work, acidic conditions (pH 3 to 4) seemed necessary for best removal of contaminants at high flux. We have since found that, although a cycle to acidic pH indeed improves performance, flux is greater, with product quality at least as high, if pH is again increased before filtration. The effect of increasing and then decreasing pH is illustrated in Fig. 6.23 for sewage effluent that had been digested overnight at pH 3 after addition of Fe(III). There is hysteresis, but the trend to higher flux at higher pH is clear.

Figure 6.24 summarizes a run carried out by procedures so far found to be favorable, though they are by no means established as optimum. Primary effluent was introduced into the feed tank at pH 6, after addition of 100 ppm of Fe(III) and digestion for about 1 hr. As filtrate was removed, the tank was replenished with similarly treated sewage effluent. About 93% of the water introduced into the system was recovered as filtrate. Organic carbon buildup does not completely reflect this recovery, probably owing to bacterial action. After 20 hr operation with no backwash, flux was still 500 gal day^{-1} ft^{-2}. From a preliminary analysis carried out during the year,[4] such a production rate should make cross-flow filtration quite feasible economically. Product quality, as the table below the figure indicates, was excellent.

The filter surfaces were fire-hose jackets, supported inside by porous metal tubes, with pressurized feed circulated in an annulus outside. Filter-aid pretreatment of these fabric supports has been found greatly to increase the efficiency of backwashing in restoring flux, and woven materials are at present favored for this application.

Further reduction of organic carbon can be effected by a second-stage treatment with powdered adsorbent

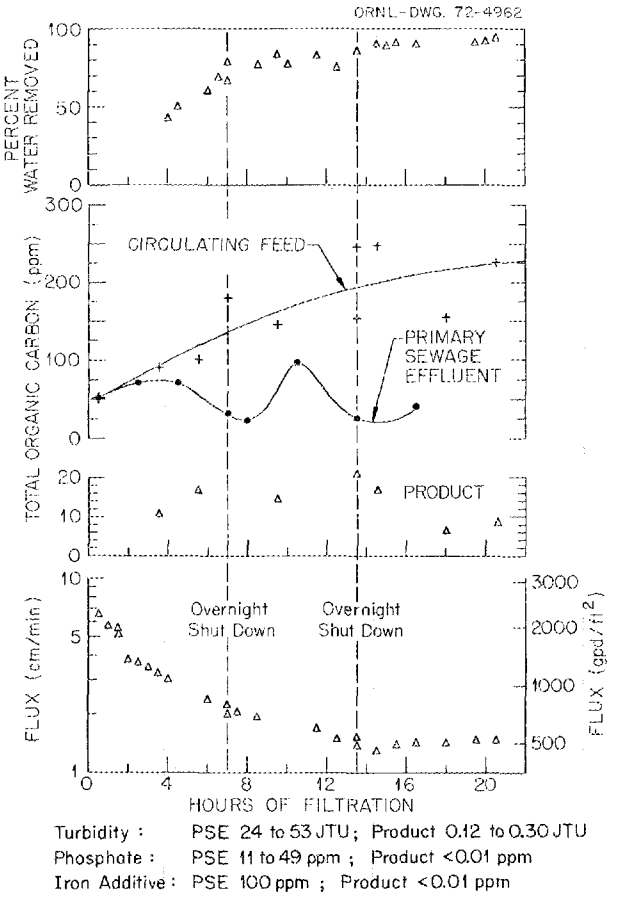

Fig. 6.24. Cross-flow filtration of primary sewage effluent. Fire-hose jacket, 40 psi, 15 fps.

carbon, followed by cross-flow filtration. It is not clear, however, that in most cases such further processing will be needed.

---

1. Chemical Technology Division.
2. Director's Division.
3. H. A. Mahlman, K. A. Kraus, and W. G. Sisson, *Chem. Div. Annu. Progr. Rep. May 20, 1971*, ORNL-4706, p. 148.
4. P. H. Wadia, K. A. Kraus, A. J. Shor, and L. Dresner, *Preliminary Economic Analysis of Cross-Flow Filtration*, Oak Ridge National Laboratory report ORNL-4729 (1971).

MOLTEN SALTS AND RELATED NONAQUEOUS SYSTEMS

NONIDEALITY OF MIXING IN ALKALI METAL TETRAFLUOROBERYLLATE–IODIDE SYSTEMS[1]

A. S. Dworkin M. A. Bredig

Effects of ion size, charge, and polarizability in systems with a complex anion, BeF_4^{2-}, were studied by determining the phase diagrams of the systems M_2BeF_4-MI (M = Li, Na, Cs). These are shown in Fig 6.25, together with ideal diagrams where the MI and M_2BeF_4 liquiduses are calculated for one particle per solute molecule (undissociated BeF_4^{2-} or I^- respectively, n = 1). The calculated effect of complete dissociation of BeF_4^{2-} to one Be^{2+} and four F^- ions (n = 5) is also shown.

The experimental iodide liquidus is similar in the three systems. The BeF_4^{2-} seems to show a high degree of dissociation only in very dilute solution. At the lowest concentration measured, about 3 mole % M_2BeF_4, only about 10 to 15% dissociation is indicated. The rate at which the degree of dissociation decreases with increasing M_2BeF_4 concentration is difficult to estimate because of the nonideal mixing of I^- and BeF_4^{2-} ions evident at and near the eutectic composition. The CsI liquidus appears slightly less curved than the NaI or the LiI liquidus. The positive deviation from ideality for the iodide liquidus, that is, excess partial free energy of mixing $\mu^E_{MI} > 0$, at concentrations greater than about 20 mole % M_2BeF_4 (and probably at even lower concentrations) may be compared with that for the LiF liquidus in the LiF-Li_2BeF_4 system, which is ideal up to approximately 45 mole % of Li_2BeF_4.[2] In mixtures with a common anion the overall increase in the polarization of the anion on mixing usually makes the overwhelming (negative) contribution to the interaction potential, that is, stabilizes the mixture. On the other hand, the much smaller interaction potentials for mixtures with a common cation result from a delicate balance between the positive contribution of the change in the van der Waals (e.g., I^-) or multipole (e.g., BF_4^-) interactions between anions, the negative contribution of the increase in anion polarization, and the positive or negative contribution of the change in the anion-anion Coulomb repulsion. It is tempting to offer an explanation for the more positive deviation from ideality when Li_2BeF_4 is added to LiI than to LiF by juggling the changes in magnitude of the effects above with a change from I^- to F^-. However, we must also remember that the differences reflected in the phase diagrams are due to partial excess *free energy* of mixing and not necessarily to the enthalpy of mixing, which determines the interaction potential. The explanation for differences in degree of nonideality must, then, include differences in the entropy of mixing, for which few data exist for these systems.

The M_2BeF_4 liquidus lines all show positive deviation from ideality, although to a much lesser extent than the MF liquidus in MF-MI mixtures,[2] especially in the

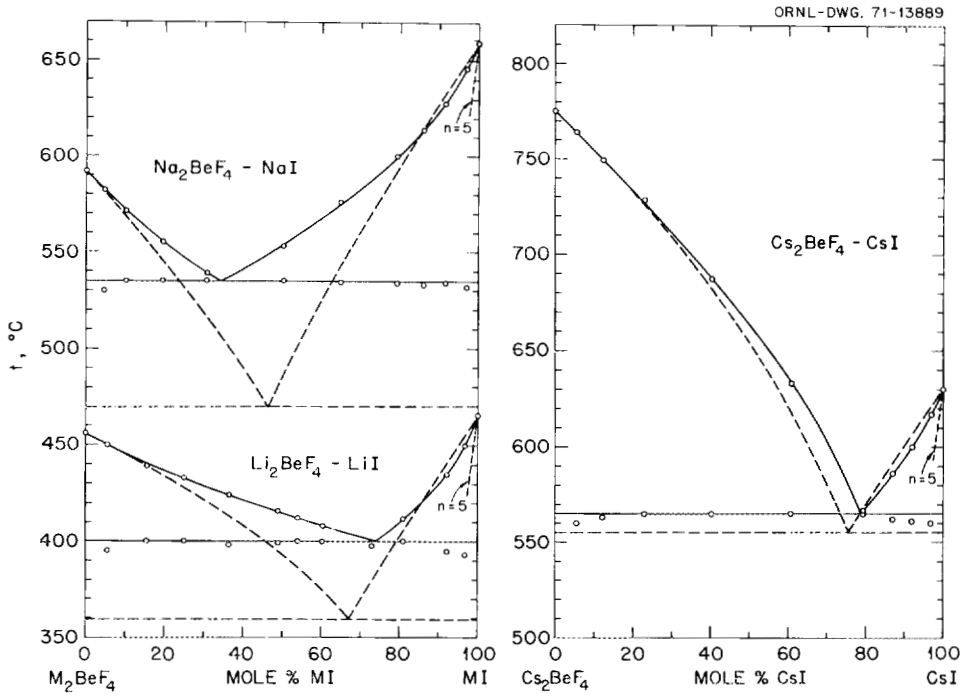

Fig. 6.25. Experimental and ideal phase diagrams of the systems Li_2BeF_4-LiI, Na_2BeF_4-NaI, and Cs_2BeF_4-CsI.

dilute MI region. An interaction parameter

$$(\Delta\bar{\mu}_{M_2BeF_4}/X^2_{MI})_{X_{MI}=0}$$

is 900, 1950, and 150 cal for the lithium, sodium, and cesium systems respectively. Again, an explanation for the differences in nonideality will depend on a knowledge of the entropies of mixing.

Fusion enthalpies of Na_2BeF_4 and Cs_2BeF_4 were calculated from the initial liquidus slopes to be 6.5 and 11.0 kcal, with a probable error of ±5%. Fusion entropies, 7.5 and 10.5 cal deg^{-1} $mole^{-1}$, are considerably less than the ΔS_m = 14.5 cal deg^{-1} $mole^{-1}$ for Li_2BeF_4. This is as expected, considering that crystalline Na_2BeF_4 and Cs_2BeF_4 are isostructural with the corresponding alkali metal sulfates while the Li_2BeF_4, with a structure similar to Be_2SiO_4 and very low tetrahedral coordination of the cations, must suffer much less profusion disordering than the former crystals.

1. This work has also been reported in *MSR Program Semiannu. Progr. Rep. Feb. 28, 1972*, ORNL-4782.

2. M. A. Bredig, *Chem. Div. Annu. Progr. Rep. May 20, 1971*, ORNL-4706, pp. 155–56.

THE LITHIUM FLUORIDE–TETRAFLUOROBORATE PHASE DIAGRAM

A. S. Dworkin M. A. Bredig

Determination of this phase diagram rounded out the studies of the alkali metal fluoride–tetrafluoroborate binary systems at ORNL. The diagram shown in Fig. 6.26 must be considered tentative because capsule failure precluded measurements between 10 and 50 mole % $LiBF_4$ as well as confirmation of the reported high-temperature point. However, we believe the diagram to be correct in its essential character and will perform experiments with capsules of improved design to confirm this.

A comparison of activity coefficients calculated from Fig. 6.26 with those for the sodium, potassium, and rubidium systems calculated by Moulton and Braunstein[1] shows an increasing positive deviation from ideality with decreasing cation size. At 1000°K and mole fraction $X_{BF_4^-}$ of 0.2, 0.4, and 0.6, activity coefficients γ_{LiF} = 1.16, 1.32, and 1.40 while γ_{NaF} = 1.10, 1.20, and 1.23. The potassium system shows slight positive deviation, while the rubidium system is essentially ideal. This trend most likely reflects the smaller distance and consequently greater multipole

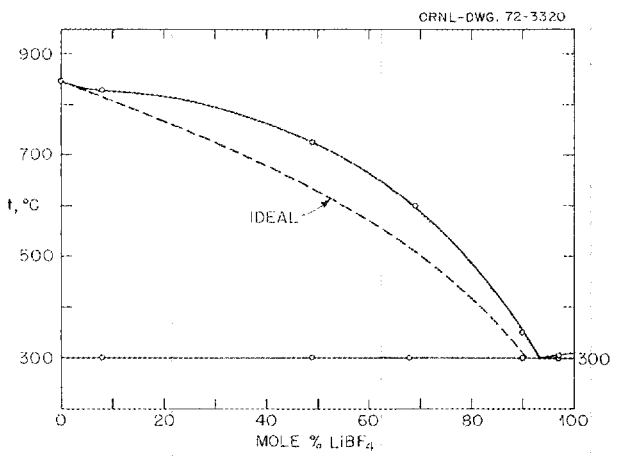

Fig. 6.26. Phase diagram of the system LiF-$LiBF_4$.

interaction between BF_4^- ions in the presence of smaller cations.

1. D. M. Moulton and J. Braunstein, *MSR Program Semiannu. Progr. Rep. Feb. 28, 1971*, ORNL-4676, p. 100.

ENTHALPY OF LITHIUM TETRAFLUOROBORATE

A. S. Dworkin

The enthalpy measurements for lithium tetrafluoroborate reported previously[1] were corrected for the presence of 3 mole % LiF. Thermal analysis showed two breaks, at 304° and 300°C, indicating a liquidus and eutectic in the $LiBF_4$-LiF system. From the liquidus temperature, the mole % LiF impurity as determined by chemical analysis, and the heat of fusion of $LiBF_4$, the true temperature of fusion of $LiBF_4$ is calculated to be 310°C rather than 304° as reported earlier.

The following equations represent our measured enthalpy data for $LiBF_4$ (corrected for LiF impurity) in calories per mole:

$$H_T - H_{298} = -11{,}440 + 31.89T + 1.0 \times 10^{-3}\, T^2 + 5.50 \times 10^5\, T^{-1} \quad (298\text{–}583°K)$$

$$\Delta H_{fusion} = 3{,}460 \text{ cal/mole};$$

$$\Delta S_{fusion} = 5.94 \text{ cal deg}^{-1} \text{ mole}^{-1} \quad (583°K)$$

$$H_T - H_{298} = -11{,}490 + 40.1T \quad (583\text{–}700°K)$$

The correction amounted to about 0.5% for enthalpies below the melting point and about 1.5% for those above.

1. A. S. Dworkin, *Chem. Div. Annu. Progr. Rep. May 20, 1971*, ORNL-4706, p. 154.

EVALUATION OF FUSION ENTROPIES OF URANIUM AND ZIRCONIUM TETRAFLUORIDES

A. S. Dworkin M. A. Bredig

We have shown[1] the entropy of fusion of UF_4 to be about 4 e.u. (32%) less than that for isostructural ZrF_4. The difference in $S°_{298}$ between UF_4 and ZrF_4 (for UF_4 about 11 e.u. greater than for ZrF_4) is due to the difference in size, mass, and magnetic entropy. From room temperature to the melting points the entropy is very similar. We conclude, therefore, that the difference in ΔS_{fusion} reflects ionic vs molecular structure of UF_4 and ZrF_4, respectively, in their molten states. The very large volume change on melting for ZrF_4 as contrasted to the small change for UF_4 (and ThF_4) lends further credence to this conclusion. The melting of ZrF_4 may be compared with that of $AlCl_3$, where the large entropy change and volume change on melting reflect the change from an ionic solid to a molecular liquid, Al_2Cl_6. We would predict that the electrical conductivity of molten ZrF_4 is small.

1. A. S. Dworkin, *J. Inorg. Nucl. Chem.* **34**, 135 (1972).

THE FREE ENERGIES OF FORMATION OF LANTHANIDE HALIDES BY AN EMF TECHNIQUE

H. R. Bronstein

The free energies of halide formation of the fission product lanthanides are of great importance to the fuel reprocessing technology of both the Molten-Salt Breeder Reactor and the Liquid-Metal Fast Breeder Reactor but, at present, are not too well established. The free energy values which now appear in the literature are for the most part derived from estimates and contradictory measured data. Commonly, the standard free energy of formation, $\Delta G°_f$, of a compound at elevated temperature is derived from third-law entropies and heat data, namely, the heat of formation at room temperature as well as the enthalpies above room temperature and heat capacities below room temperature of the compound and of the elements from which it is formed.

One direct method of obtaining this information is the use of galvanic cells of the type

R.E. metal/molten R.E. halide/halogen electrode (1)

where $E = E^\circ = -\Delta G^\circ_f/nF$, with all reactants in their standard states. However, since the rare-earth metals are somewhat soluble in their molten halides,[1] the above cell cannot give the correct information. Cells of the type

R.E. metal/0.005 mole % R.E. halide in molten

LiX-KX eutectic/halogen electrode (2)

where the solubility of the rare-earth metal is quite negligible, have been used to obtain activities, activity coefficients, and the partial molar entropies of mixing,

$$\Delta\bar{S}^M = nF\left(\frac{dE}{dT} - \frac{dE^\circ}{dT}\right),$$

with the assumption of the correctness of the standard free energy of formation (and, therefore, E°) in the literature.

If the activity of the rare-earth metal is decreased substantially by alloying with a more noble metal, for instance nickel, its solubility in the pure rare-earth halide would be so reduced as not to interfere with the emf measurement of the cell

$$\text{R.E. metal alloy} \Big/ \begin{matrix}\text{R.E. halide}\\ \text{(molten)}\end{matrix} \Big/ \text{halogen electrode} \qquad (3)$$

The needed activity of the rare-earth metal in the alloy may be obtained by substituting the alloy electrode for the halogen electrode of cell 2. Cell 3 would then give the free energy of formation of the pure rare-earth halide,

$$\Delta G^\circ_f = -nFE^\circ = -nFE + RT \ln a_{\text{R.E. metal in alloy}}$$

where E is the measured voltage and $a_{\text{R.E.}}$ is the activity of the rare-earth metal in the alloy.

A cerium-nickel compound of composition $CeNi_5$,[2] melting point 1315°C, was prepared, and the cerium activity in the compound was determined by measuring the emf of the cell

$$CeNi_5 \Big/ \begin{matrix}\text{1 mole \% } CeCl_3\\ \text{99 mole \% KCl}\\ \text{(molten)}\end{matrix} \Big/ Ce^0 \text{ at } 806^\circ\text{C} \qquad (4)$$

The activity of the cerium in this compound was calculated from the equation

$$E = -RT \ln a_{Ce}; \quad a_{Ce} = 3.7 \times 10^{-13}.$$

Further experiments are planned where the solvent for the $CeCl_3$ will be varied, such as using the eutectic melt of KCl-LiCl, in order to show that the voltage of cell 4 is independent of the solvent. The cerium activity will be determined as a function of temperature, and then cell 3 will be measured to give the standard free energy of formation of the rare-earth halide.

1. J. D. Corbett in *Fused Salts*, ed. B. R. Sundheim, pp. 341–407, McGraw-Hill, New York, 1964.

2. M. Hansen, ed., *Constitution of Binary Alloys*, 2d ed., p. 457, McGraw-Hill, New York, 1958.

CALORIMETRY

PREPARATION OF CERTAIN OXIDES OF TECHNETIUM

A. Y. Herrell[1] R. H. Busey

The need to prepare very pure technetium heptoxide, Tc_2O_7, has arisen in the course of an extensive research study to determine the enthalpies of formation at 25°C of the oxides of technetium by solution calorimetry. The thermochemical scheme to be employed in this study follows that used by King et al.[2] to determine similar data on the oxides of rhenium by solution calorimetry. According to the literature, the oxidation of technetium metal in oxygen at moderately high temperatures leads only to Tc_2O_7.[3] This behavior would be anticipated by comparison with the reaction of rhenium metal heated in oxygen, where only Re_2O_7 is obtained.[4] We have observed, however, that the combustion of technetium in oxygen is complex, leading to some side products in addition to Tc_2O_7. A preliminary account of the products of the combustion process will be briefly presented in this report.

The Pyrex combustion tube, in which the Tc was heated by an electric furnace (temperature controlled) in an atmosphere of pure, dry oxygen, was attached to a high-vacuum line so that all traces of moisture and air could be removed before oxygen introduction. The oxidation of the Tc was carried out in a manner similar to that used for production of Re_2O_7,[4] using a combustion tube closed at one end. Invariably, the initial product that sublimes out of the furnace during the oxidation is a highly volatile pink or red oxide.

Although it is most evident in the initial stages of the oxidation, this side product is produced during the entire course of the oxidation. This red oxide is a little more volatile than Tc_2O_7 and tends to collect farthest from the furnace.

Fried and coworkers[5,6] observed a pink volatile compound when they burned Tc in oxygen but did not characterize their product, since they were only interested in the combustion process as a purification procedure. Boyd and coworkers[3] obtained only pale yellow Tc_2O_7 with no mention of a darker product. We have varied conditions in an attempt to reduce or eliminate the small amount of red oxide formed during the combustion but with no success. We have used Tc metal made both from $KTcO_4$ and from NH_4TcO_4, metal formed at relatively low temperature (about 500°C), and metal heated to 1000°C in a high vacuum to remove any trace of hydrogen. The reaction zone has been increased by employing a lone furnace, thus increasing the residence time of the red product in the hot zone.

In an attempt to separate the volatile red oxide from our desired Tc_2O_7, we have employed a two-furnace arrangement, one furnace at 500°C providing the reaction zone to oxidize the Tc, and the second furnace at 150°C acting as a condenser for the Tc_2O_7 but subliming the red oxide on down the tube. This arrangement also produced a second technetium oxide by-product, which collected as a purple compound between the two furnaces, where liquid Tc_2O_7 should and did collect.

The red oxide can be produced in apparently pure form by low-temperature oxidation of Tc. A sample of Tc metal has been heated in oxygen at 150°C for approximately three months, during which time a significant amount of volatile red oxide has collected. An analysis of this product as well as the state of the technetium within the furnace will be made soon. Low-temperature oxidation of rhenium over an extended period of time yields only nonvolatile ReO_3. The volatility of the red technetium oxide tends to rule out its being TcO_3. At the present time we feel that the red oxide is probably the pentoxide, although the evidence is too involved to present in this preliminary report. Future experiments are planned to establish the identity of this oxide.

We have prepared and characterized TcO_3 for the first time anywhere. Rhenium trioxide (ReO_3) may be prepared by reduction of Re_2O_7 with CO at 175° to 280°C.[7] When this method was tried for producing TcO_3, only technetium metal resulted. Obviously a milder reducing agent is required, and reference to free energy tables indicated that the SO_2-SO_3 system might be suitable. The use of SO_2 as the reducing agent resulted in successful production of TcO_3. The oxidation state was established by ceric perchlorate titration, and the technetium content was established spectrophotometrically after oxidation to TcO_4^-. Technetium trioxide appears black but under certain conditions (e.g., thin films) has a reddish-purple color. In some of our oxidations of technetium, we obtained a small amount of trioxide along with the red oxide as side products. A considerable quantity of trioxide was apparently produced when the two-furnace arrangement described above was used in the technetium oxidation.

A procedure has been developed to make very high purity Tc_2O_7. The essential and necessary step in the procedure involves sealing off with a torch that portion of the Pyrex combustion tube which contains the products of the combustion (contaminated with lower oxides) under a pressure of 1 atm of oxygen. This tube is placed wholly within a furnace and heated to 400°C. Under these conditions the lower technetium oxides are kept in the reaction zone in the presence of oxygen and converted to the heptoxide. When this step is incorporated in the preparation procedure, only pale-yellow, high-purity Tc_2O_7 results.

---

1. National Science Foundation Science Faculty Fellow, Wayne State University, Detroit, Mich.

2. E. G. King, D. W. Richardson, and R. V. Mrazek, *U.S. Bur. Mines Rep. Invest.* 7323, 1969.

3. G. E. Boyd, J. W. Cobble, C. M. Nelson, and W. T. Smith, Jr., *J. Amer. Chem. Soc.* **74**, 556 (1952).

4. A. D. Melaven, J. N. Fowle, W. Brickell, and C. F. Hiskey, *Inorg. Syn.* **3**, 188 (1950).

5. S. Fried, A. H. Jaffey, N. F. Hall, and L. E. Glendenin, *Phys. Rev.* **81**, 741 (1951).

6. S. Fried and N. F. Hall, *Abstracts of Papers, 117th Meeting, American Chemical Society,* abstract 25, p. 13-O (April 1950).

7. A. D. Melaven, J. N. Fowle, W. Brickell, and C. F. Hiskey, *Inorg. Syn* **3**, 187 (1950).

HIGH-TEMPERATURE ENTHALPY OF POTASSIUM PERRHENATE

R. A. Gilbert

In a previous report[1] it was noted that the use of Nichrome V capsules as containers for enthalpy determinations could lead to systematic errors even though the capsules were made from adjacent sections of the same rod. For this reason, new data using platinum–10% rhodium capsules were obtained for the enthalpy of $KReO_4$ at selected temperatures over the range

0–900°C to correct for such an error possibly present in the original measurements on this compound.[2] These new data differed by (0.3 ± 0.1)% from the previous values. The enthalpy and entropy of fusion are unchanged, but the melting point is increased to 828.5°K.

1. C. W. Linsey, R. A. Gilbert, and R. H. Busey, *Chem. Div. Annu. Progr. Rep. May 20, 1970,* ORNL-4581, p. 122.
2. R. H. Busey and R. A. Gilbert, *Chem. Div. Annu. Progr. Rep. May 20, 1967,* ORNL-4164, p. 103.

ELECTROCHEMISTRY

THE ELECTROCHEMICAL BEHAVIOR OF TECHNETIUM AND OF IRON CONTAINING TECHNETIUM

G. H. Cartledge

Studies on the electrochemical behavior of pure technetium and of iron containing 0.1 wt % technetium in sulfuric acid solutions were completed. It was found that evolution of hydrogen on technetium has a Tafel slope approximating −40 mV/decade. At overvoltages noble to the hydrogen-evolution potential, oxidation of technetium or its surface oxides has a rate of ca. 10^{-6} A/cm^2 until the potential becomes high enough to form soluble pertechnic acid. The current density then rises rapidly. The presence of technetium in iron modifies the electrochemical behavior because dissolution of iron leads to enrichment of the surface in residual technetium. This causes the open-circuit potential to ennoble, with lowering of the overvoltage for evolution of hydrogen. Passivation is also rendered more difficult and much less effective in lowering the passive corrosion current density. Detailed results of the investigation have been published in the *Journal of the Electrochemical Society.*[1]

1. G. H. Cartledge, *J. Electrochem. Soc.* 118, 1752 (1971).

ELECTROCHEMICAL BEHAVIOR OF TITANIUM

E. J. Kelly

On the basis of steady-state electrochemical polarization measurements described in earlier reports,[1–5] a mechanism for the active-state dissolution and passivation of titanium in acidic sulfate solutions has been proposed.[6] Reduced to its essentials, the mechanism may be represented by Eqs. (1)–(6):

$$\mathrm{Ti} + \mathrm{H_2O} \rightleftharpoons (\mathrm{TiOH})_s + \mathrm{H}^+ + \mathrm{e}^- \qquad (1)$$

$$(\mathrm{TiOH})_s \rightleftharpoons (\mathrm{TiO})_s + \mathrm{H}^+ + \mathrm{e}^- \qquad (2)$$

$$(\mathrm{TiO})_s \rightarrow \mathrm{TiO}^+ + \mathrm{e}^- \text{ (rate-determining)} \qquad (3)$$

$$(\mathrm{TiO})_s + \mathrm{H_2O} \rightleftharpoons (\mathrm{TiO{\cdot}OH})_s + \mathrm{H}^+ + \mathrm{e}^- \qquad (4)$$

$$(\mathrm{TiO{\cdot}OH})_s + \mathrm{H}^+ \rightarrow \mathrm{TiO}^+ + \mathrm{H_2O} \qquad (5)$$

$$(\mathrm{TiO{\cdot}OH})_s \rightleftharpoons (\mathrm{TiO_2})_s + \mathrm{H}^+ + \mathrm{e}^- \qquad (6)$$

where the subscript s indicates a surface intermediate. According to this mechanism, the steady-state anodic current density corresponding to the oxidation of titanium to Ti(III) ions in solution increases, reaches a maximum (i_m) at the "critical potential," E_m, and then decreases (passivation) as the potential of the titanium electrode, initially at the open-circuit or corrosion potential, is made increasingly positive (noble). The steady-state current-potential relationship is given by

$$i = 3Fk_3\theta_{\mathrm{TiO}} \exp(FE/2RT)\,, \qquad (7)$$

where θ_{TiO} is the fractional surface coverage by TiO, E is the potential of the titanium electrode relative to an arbitrary reference electrode, and the other symbols have their conventional significance. In the vicinity of E_m, we have

$$\theta_{\mathrm{TiO}} \cong 1/[1 + Ka_{(\mathrm{H}^+)}^{-2} \exp(3FE/2RT)]\,, \qquad (8)$$

where $K = k_4k_6/k_{-6}k_5$. Moreover, $\theta_{\mathrm{TiO}} + \theta_{\mathrm{TiO_2}} \cong 1$ and $\theta_{\mathrm{TiO}}/\theta_{\mathrm{TiO_2}} \cong 2$; that is, $\theta_{\mathrm{TiO}} \cong 2/3$. Equations (7) and (8) are consistent with the experimental facts that $d \log i_m/d\,\mathrm{pH} = -2/3$ and $d \ln i_m/dE_m = F/2RT$. Passivation results from the increase in $\theta_{\mathrm{TiO_2}}$ at the expense of θ_{TiO}.

In order to obtain further evidence in support of the postulated mechanism, a study of the non-steady-state (transient) polarization behavior of titanium was initiated. A typical potentiostatic current vs time curve is shown in Fig. 6.27, together with the corresponding total charge vs time curve. The observed current (i) is given by

$$i = i_f - R_sC(di/dt)\,, \qquad (9)$$

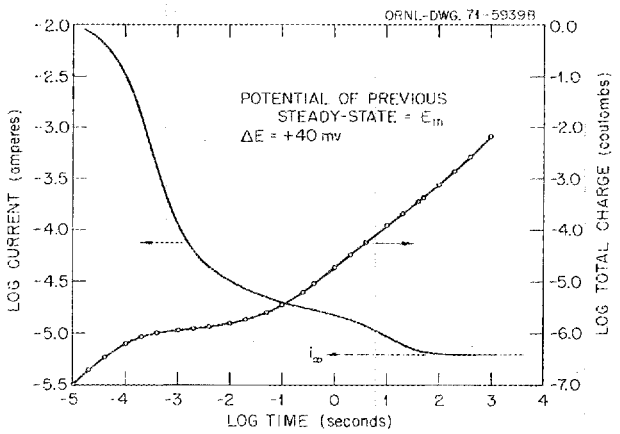

Fig. 6.27. Potentiostatic current vs time and total charge vs time transient on titanium in 1 N H_2SO_4. Area = 0.124 cm^2, T = 30°C.

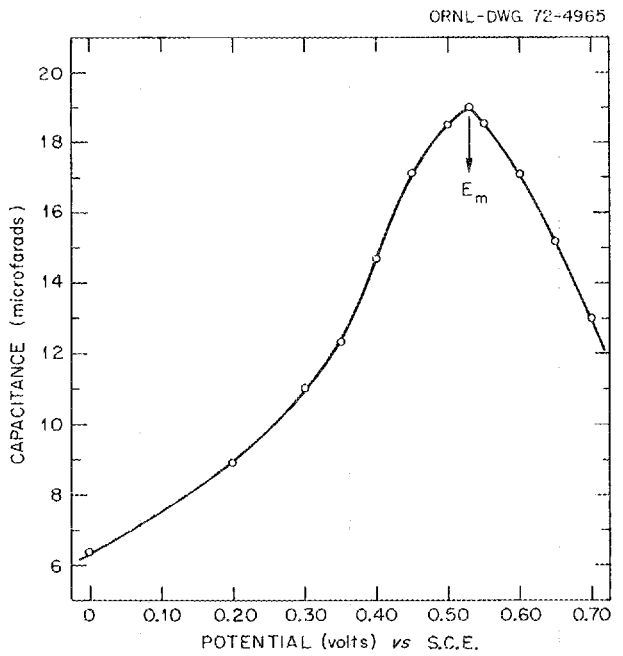

Fig. 6.28. Differential capacitance as a function of potential for titanium in 1 N H_2SO_4. Area = 0.124 cm^2, T = 30°C.

where R_s is the resistance of the electrolyte between the titanium surface and the reference electrode, C is the double-layer capacitance, and i_f is the current associated with Faradaic (charge-transfer) reactions. A study of numerous transients in the microsecond time region has established that $(d \ln i/dt)_{t\to 0}$ is a constant which, if $i_f = 0$, would be equal to $-1/R_sC$, according to Eq. (9). However, from the known values of R_s, the calculated values of C are much too great to be attributed to just the double-layer capacitance. Moreover, as shown in Fig. 6.28, the calculated capacitance values are a function of potential and exhibit a maximum at E_m, thus reflecting the reaction mechanism in addition to double-layer charging. Since the values of $|d \ln i/dt|$ are less than $1/R_sC$, it can be shown that i_f must be of the form

$$i_f = -R_sC_f(di/dt)\,, \tag{10}$$

where C_f is an adsorption pseudocapacitance. Insertion of this value of i_f into Eq. (9) leads to

$$d \ln i/dt = -1/R_s(C + C_f)\,, \tag{11}$$

which is in agreement with the experimental data. If i_f corresponds to a very fast non-rate-determining reaction [Eqs. (1) or (2)] which is in pseudoequilibrium for all values of ψ (the potential difference between the metal and a point just inside the electrolyte phase), then, at constant E, i_f is given by

$$i_f = \beta F(d\theta/d\psi)\,(d\psi/dt)$$
$$= C_f(d\psi/dt) = -R_sC_f(di/dt)\,, \tag{12}$$

where β is the surface concentration (moles/cm^2) per unit coverage of the surface intermediate formed by the fast reaction.

Equation (12) shows the origin of Eq. (10) and the meaning of C_f. Consequently, one concludes that the early stage (up to 1 msec) of the current-time curve shown in Fig. 6.27 reflects both double-layer charging and a fast charge-transfer reaction [Eq. (1)]. The charge corresponding to monolayer coverage is ca. 2×10^{-5} coulomb for the electrode area used in the experiment shown in Fig. 6.27. At the end of 1 msec, the total charge vs time curve in Fig. 6.27 shows that the electrode reaction responsible for C_f involves the formation of less than 5% of a monolayer of the intermediate. Since θ_{TiO} and θ_{TiO_2} are virtually constant during this time region and since $\theta_{TiO} + \theta_{TiO_2} \cong 1$, this result is entirely consistent with the identification of C_f with the fast reaction [Eq. (1)]. From approximately 1 sec onward, the slow decrease in current results from the slow increase in θ_{TiO_2} at the expense of θ_{TiO} [cf. Eq. (7)]. The double-layer-charging process is essentially complete by the end of 1 msec [i.e., $d\psi/dt \cong 0$ (cf. Fig. 6.29)], and, consequently, i is equal to i_f at times greater than 1 msec. The drop in current between 1 msec and 1 sec cannot be attributed to the fast reaction [Eq. (1)] nor to the slowest reaction (conversion of TiO to TiO_2) and

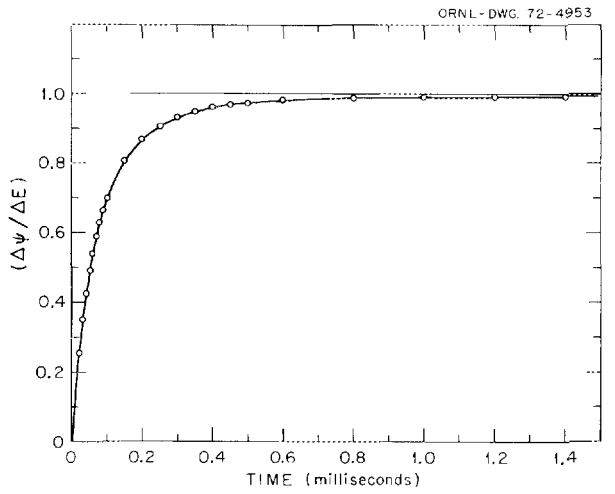

Fig. 6.29. **Double-layer charging.** Plot of $\Delta\psi/\Delta E$ vs time for the data shown in Fig. 6.27.

therefore corresponds to a second relatively fast charge-transfer reaction [i.e., to the reaction shown in Eq. (2)]. Thus the results of the transient measurements appear to support the postulated reaction mechanism.

1. E. J. Kelly, *Chem. Div. Annu. Progr. Rep. May 20, 1967*, ORNL-4164, p. 90.
2. E. J. Kelly, *Chem. Div. Annu. Progr. Rep. May 20, 1968*, ORNL-4306, p. 108.
3. E. J. Kelly, *Chem. Div. Annu. Progr. Rep. May 20, 1969*, ORNL-4437, p. 89.
4. E. J. Kelly, *Chem. Div. Annu. Progr. Rep. May 20, 1970*, ORNL-4581, p. 125.
5. E. J. Kelly, *Chem. Div. Annu. Progr. Rep. May 20, 1971*, ORNL-4706, p. 175.
6. E. J. Kelly, "Anodic Dissolution of Titanium in Acidic Sulfate Solutions," 5th International Congress on Metallic Corrosion, Tokyo, May 22, 1972.

POTENTIOSTATIC METHOD FOR THE DETERMINATION OF SPECIFIC CONDUCTANCE: APPLICATION TO MOLTEN SALT ELECTROLYTES

E. J. Kelly H. R. Bronstein

The basic principles involved in the potentiostatic method for the determination of specific conductance, together with the application of the method to aqueous electrolytes, have been described in earlier reports.[1,2] The method may be understood by reference to the schematic drawing shown in Fig. 6.30. The potential (E) of input A with respect to circuit ground is determined by a precision variable "reference voltage" source. Any voltage difference detected between the

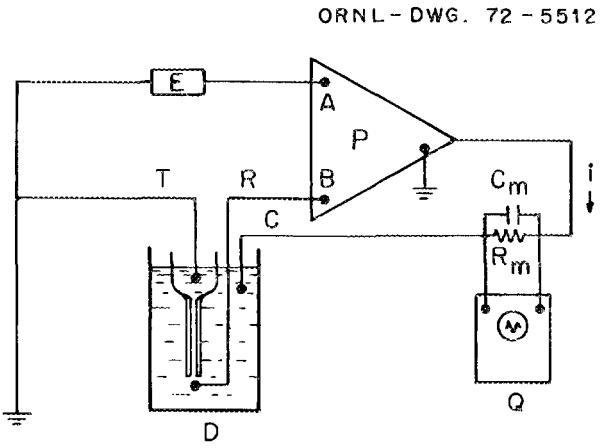

P , Fast-rise Potentiostat
Q , Fast-rise Oscilloscope
D , Cell With Capillary Conductance Tube
T, R, C , Test, Reference and Counter Electrodes
E , Reference Voltage
A, B , Inputs to Voltage Difference-Detector Stage of Potentiostat
R_m , C_m , Current (i) Measuring Precision Resistors and Capacitors

Fig. 6.30. **Schematic diagram of potentiostatic method for specific conductance measurements.** (P) Fast-rise potentiostat, (Q) fast-rise oscilloscope, (D) cell with capillary conductance tube, (T, R, C) test, reference, and counter electrodes, (E) reference voltage, (A, B) inputs to voltage-difference-detector stage of potentiostat, (R_m, C_m) current (i) measuring precision resistors and capacitors.

inputs A and B of the voltage-difference-detector input stage of the potentiostat results in a change in the output current (i) in such a direction as to reduce the voltage difference to "virtual" zero. Since essentially no current flows in the high-resistance inputs, the potential of a test electrode with respect to a reference is given by

$$E = V + iR_s + \beta , \qquad (1)$$

where V is the potential difference between the test electrode and a point just inside the electrolyte phase, R_s is the electrolyte resistance between the test and reference electrodes, and β is a constant which depends upon the particular reference electrode used. To measure specific conductance, E is abruptly changed (<1 μsec) from an initial value, E_1, to a second constant

value, E_2, and the resulting current-time transient at E_2 is displayed on an oscilloscope and recorded on film. The quantity $(i_2)_{t=0}$, the current at E_2 for $t = 0$, is determined by extrapolation of the current-time curve in the microsecond time region to $t = 0$. At $t = 0$, $(\Delta V)_{t=0} = 0$ (cf. refs. 1 and 2), and, consequently, it follows from Eq. (1) that the electrolyte resistance is given by

$$R_s = \frac{E_2 - E_1}{(i_2)_{t=0} - i_i} = \frac{\Delta E}{(\Delta i)_{t=0}} . \qquad (2)$$

The specific conductance of the electrolyte, κ, is calculated on the basis of the relationship $R_s = k/\kappa$, where k, the cell constant, depends only on the geometry of the system. The cell constant is determined by measuring R_s for a reference electrolyte, usually a standard KCl solution.

In view of certain advantages over the conventional ac bridge method,[1,2] it was thought that the potentiostatic method should be of special value in determining specific conductances of molten salts. To test its applicability to such systems, the specific conductance of molten KNO_3 was measured over a temperature range from 350 to 550°C. A typical current-time transient is shown in Fig. 6.31, where it is apparent from the upper curve that no difficulty is encountered in obtaining an accurate extrapolation to $t = 0$. The small current overshoot observed in the first few microseconds is instrumental in origin, has no effect on the accuracy of the measurement, and can be eliminated by choosing the proper value for C_m (cf. Fig. 6.30). As in the work on aqueous systems, it was shown that Eq. (2) was obeyed; that is, $(\Delta i)_{t=0}$ was a linear function of ΔE for a given cell constant and temperature.

If R_s is too small (roughly speaking, less than 1 Ω), not only do the lead resistances become significant, but the current decay becomes too rapid to permit an accurate determination of $(\Delta i)_{t=0}$. Since the specific resistance of molten KNO_3 is low, a capillary conductance cell (cf. Fig. 6.30) was employed to obtain adequately large values of R_s. The enhanced conductivity of soft glass at high temperatures introduced errors

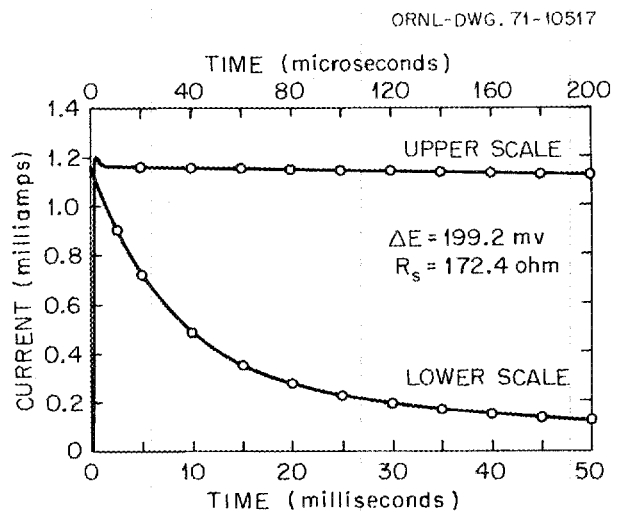

Fig. 6.31. Potentiostatic current vs time transient on Pt in molten KNO_3 at 375°C.

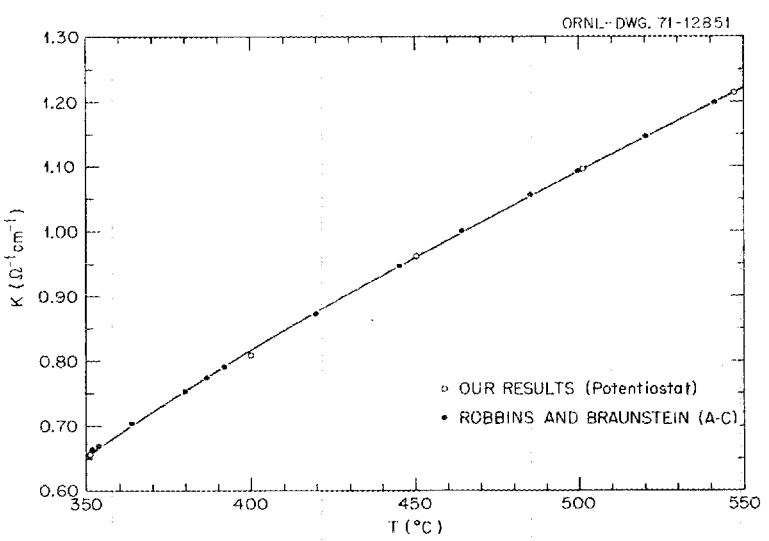

Fig. 6.32. Specific conductance vs temperature for molten KNO_3. Comparison of potentiostatic and ac methods.

in the initial experiments, and, therefore, quartz was chosen for the conductance cell. Platinum electrodes were used as a matter of convenience, not of necessity. The results are shown in Fig. 6.32. For comparative purposes, the data of Robbins and Braunstein are also shown.[3] The agreement in the two sets of data can be appreciated by comparing them with the results of others, results which show differences of as much as 5% at 350°C.[3] To prove conclusively that the measured values of R_s corresponded to the electrolyte resistances only, two capillary cells were used, the length of one capillary being roughly half that of the other. The cell constants for the two cells were accurately determined by use of a standard 1 demal solution of KCl. The ratio of the cell constants was 1.687. At 351.0°C, the ratio of the measured resistances of molten KNO_3 in the two cells was 1.685.

Two important areas of application of the potentiostatic method remain to be investigated. First, the method should be applicable to solid-state electrolytes. The second area of interest embraces those highly conducting electrolytes for which satisfactory (i.e., nonconducting and resistant to attack by the electrolyte) capillary materials cannot be found, electrolytes such as the molten fluorides and the alkali–alkali halide systems. The potentiostatic method may permit the use of metallic capillaries, thereby eliminating the problem.

1. E. J. Kelly, *Chem. Div. Annu. Progr. Rep. May 20, 1971*, ORNL-4706, p. 175.
2. E. J. Kelly and H. R. Bronstein, *Chem. Div. Annu. Progr. Rep. May 20, 1971*, ORNL-4706, p. 177.
3. G. D. Robbins and J. Braunstein, *J. Electrochem. Soc.* **116**, 1218 (1969).

AN ELECTROCHEMICAL METHOD FOR MONITORING THE OXYGEN CONTENT OF AQUEOUS STREAMS AT THE PART-PER-BILLION LEVEL

R. E. Meyer F. A. Posey
P. M. Lantz

Determination of the dissolved oxygen content of aqueous streams in the 0 to 50 part per billion (ppb) range has always been a difficult problem. Because the corrosion properties of chemical process equipment depend so strongly in many cases on the dissolved oxygen content of the aqueous streams contained by the metallic materials of construction,[1,2] it can be important to monitor the oxygen concentration with considerable precision. The principal requirements for a desirable method of determination are precision of 1 or 2 ppb and simplicity of operation so that highly skilled technicians are not required.

At present this analysis is usually carried out either by the classical Winkler method or by a modification of the polarographic sensor. The Winkler method is a difficult wet-chemistry method requiring a skilled analyst. The polarographic sensor relies for its operation on electrochemical determination of the dissolved oxygen which diffuses through a plastic membrane (usually Teflon) permeable only to gases. The response of this device therefore depends on the properties of the membrane, the temperature, and the concentration of oxygen on either side of the membrane. Current sensitivity is low, on the order of 10^{-7} to 10^{-8} A for dissolved oxygen contents in the low ppb range. These difficulties can be overcome to some extent, but only by increasing the complexity of the instrument and by periodic recalibration, usually by the Winkler method.[3]

In continuation of studies reported earlier,[4] we have developed a device for determining the dissolved oxygen content of flowing streams in the ppb range which is self-calibrating and does not possess the disadvantages of the polarographic sensor. As in the polarographic sensor, our device couples an electrochemical sensor with a permeable membrane. A schematic diagram of this device is shown in Fig. 6.33. The test stream flows through an exchanger (*B*) which contains the gas-permeable membrane. This exchanger is used to equilibrate the oxygen content of the test stream and a solution which ultimately passes through an electrochemical sensor. An exchanger is used in our device in order to separate dissolved oxygen from other reducible substances (such as iron and copper ions) which might be contained in the streams to be monitored and in order to avoid fouling of the electrochemical sensor by various substances. The sensor stream is allowed to remain in the exchanger long enough for it to attain essentially the same dissolved oxygen content as the test stream. The sensor stream is then passed through the electrolytic sensor (*C*) at a known flow rate, and the dissolved oxygen is completely reduced by a packed-bed cathode of finely divided silver. The current required to reduce the oxygen is a measure of the oxygen content, which may be calculated from the relation

$$C = I/nFU ,$$

where C is the oxygen concentration (moles per cubic centimeter), I is the current (amperes), n is the number (4) of electrons required for complete reduction of an oxygen molecule, F is Faraday's constant (coulombs

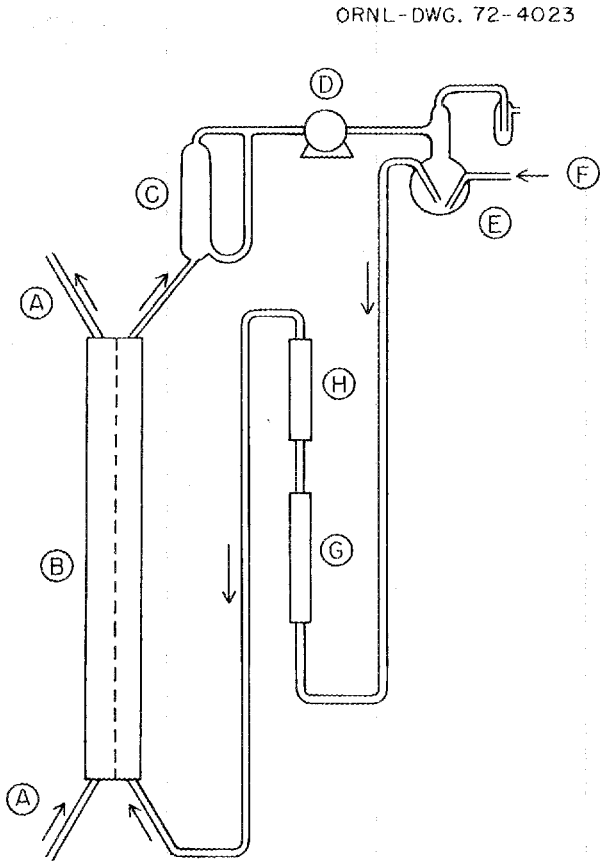

Fig. 6.33. Schematic diagram of laboratory model of ppb oxygen monitoring device. (*A*) Test solution inlet and exit, (*B*) exchanger, (*C*) oxygen sensor, (*D*) metering pump, (*E*) solution reservoir, (*F*) purging gas inlet, (*G*) flowmeter, (*H*) electrolytic oxygen stripper.

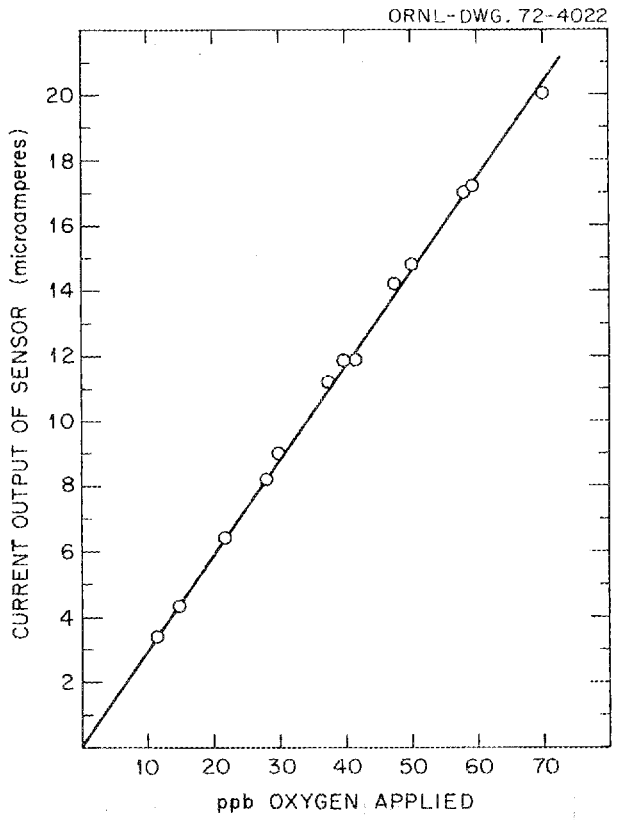

Fig. 6.34. Test of oxygen monitoring device.

per equivalent), and U is the volume flow rate (cubic centimeters per second). This sensor (cf. C in Fig. 6.33) is a simplification of a device described by Eckfeldt and Shaffer.[5]

Some results obtained with this device are shown in Fig. 6.34. In this experiment, the gas-permeable membrane was a 7-mil-thick sheet of silicone rubber which separated the two halves of an exchanger constructed from Lucite. The test stream flowed past the membrane in one half of the exchanger and the sensor stream in the other half. As shown in Fig. 6.34, the response is linear, and the current sensitivity is of the order of 10^{-5} A in the ppb range. We have examined a number of designs of sensors and exchangers and conclude on the basis of the measurements that the device described above should be especially useful for monitoring the dissolved oxygen content of desalination plant streams and other process streams where plant operation and/or corrosion behavior of metallic materials depend critically on the oxygen level.

1. E. H. Phelps, R. T. Jones, and H. D. Leckie, *J. Electrochem. Soc.* **116**, 213C (1969).

2. H. C. Behrens et al., *Sea Water Corrosion Test Program*, O.S.W. Research and Development Progress Report No. 417 (March 1969).

3. H. C. Behrens et al., *Assembly and Evaluation of an Improved PPB Oxygen Analyzer for Sea Water*, O.S.W. Research and Development Progress Report No. 572 (July 1970).

4. R. E. Meyer, P. M. Lantz, and F. A. Posey, *Chem. Div. Annu. Progr. Rep. May 20, 1971*, ORNL-4706, p. 182.

5. E. L. Eckfeldt and E. W. Shaffer, Jr., *Anal. Chem.* **36**, 2008 (1964).

ANALYSIS WITH PACKED-BED ELECTRODES

R. E. Meyer F. A. Posey

In the previous report[1] on the oxygen monitor, we described a sensor which may be used to determine the oxygen content of aqueous streams by quantitative reduction of the dissolved oxygen with a packed-bed cathode of finely divided silver. In the operation of this

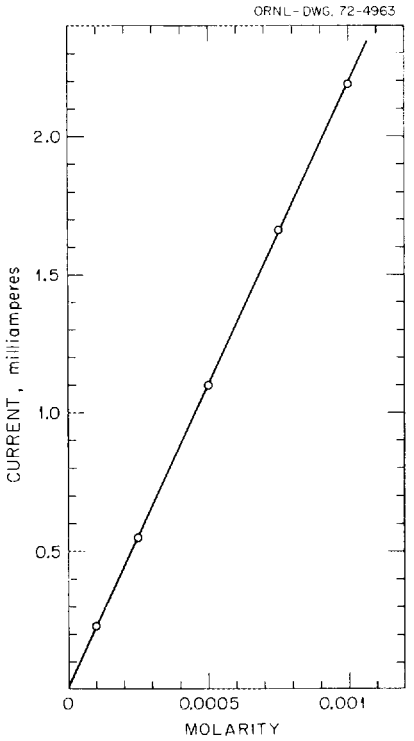

Fig. 6.35. Analysis of bromide ion with packed-bed cathode of silver. Electrode potential = +150 mV vs S.C.E.; flow = 1.3 ml/min.

sensor, a potentiostat is used to hold the electrode potential at −700 mV vs the saturated calomel reference electrode (S.C.E.). If the potentiostat is set at +300 mV vs S.C.E., any oxygen present will not be reduced; but if chloride ion is present, the following oxidation reaction will take place on the silver: $Ag + Cl^- = AgCl + e^-$. As in the oxygen monitor, the current required for this reaction will be directly proportional to the concentration of the chloride ion. This concentration may therefore be determined by passing the unknown solution through the packed bed at a known flow rate. The concentration is then calculated by use of the relation[1] $C = I/nFU$. At other potentials, it may be possible to determine other solution species. For example, Fig. 6.35 shows the determination of bromide ion with a packed bed of silver maintained at +150 mV vs S.C.E. Thus, the use of porous or packed-bed electrodes at controlled potential is a simple and general method for the quantitative monitoring of electroactive solution species.

1. R. E. Meyer, F. A. Posey, and P. M. Lantz, "An Electrochemical Method for Monitoring the Oxygen Content of Aqueous Streams at the Part-per-Billion Level," the preceding contribution, this report.

DIRECT ELECTROCHEMICAL PRETREATMENT OF WATERS FOR HARDNESS AND pH CONTROL[1]

A. A. Palko R. E. Meyer
F. A. Posey

Previously we described the operation of a prototype electrochemical cell for simultaneous removal of bicarbonate from and acidification of seawater.[2] The cell used a high-efficiency suspension electrode for the anode, in which a suspension of palladium black catalyst particles was forced to impinge upon an array of charging electrodes. The cathode consisted of an array of stainless steel rods, which were kept clean of precipitated $CaCO_3$ and $Mg(OH)_2$ from the synthetic seawater feed, thus allowing continuous, efficient operation of the cathode reaction. In addition, the cell could optionally be operated with feedback of hydrogen produced by the cathode reaction into the suspension anode assembly, thus allowing operation at greatly reduced cell voltages.

Studies during the past year have emphasized the direct electrochemical treatment of artificial seawater by investigating a number of alternative modes of operation of the cell with several electrode configurations over a reasonably wide range of power input and solution feed throughput. Such studies have demonstrated that the techniques have potential applicability to a much wider range of waters, especially brackish waters.

In one series of measurements, carried out with a solid, uncatalyzed graphite anode, decarbonated, acidified seawater (pH ~ 2) was produced with a power requirement of about 1 kWhr per 1000 gal. This product could be used for acidification pretreatment of much larger volumes of seawater, in a manner similar to conventional sulfuric acid injection pretreatment of seawater, for decarbonation prior to distillation. Use of appropriately catalyzed anode structures and/or the hydrogen cycle studied previously would allow operation at lower power consumption.

Other experiments were carried out with a catalyzed porous graphite anode assembly, with and without use of ion exchange membrane separators, to establish the feasibility and power requirements of direct electrochemical removal of substances (in addition to bicarbonate) which are contained in seawater and typical brackish water. Injection of CO_2 into the cathode loop removed essentially all the calcium ions from synthetic seawater with a power input of about 20 kWhr per 1000 gal. More extensive electrolytic pretreatment removed essentially all calcium and magnesium ions from incoming seawater at a power consumption of

about 60 kWhr per 1000 gal. Power requirements could be reduced considerably if a cell operating on a hydrogen cycle could be developed, so that the anode reaction could be oxidation of hydrogen to hydrogen ions, instead of oxidation of chloride ions to chlorine. Power requirements for direct electrolytic pretreatment of brackish waters for removal of calcium and magnesium ions are, of course, much less and may be quite competitive with more conventional pretreatment methods.

These studies have led to development of a cell to be used as part of a process for pretreatment of brackish water before desalination by hyperfiltration.[3] In future studies we plan to attempt further development of a direct electrolytic pretreatment cell based on the hydrogen cycle, in order to allow operation at the smallest possible power consumption; the cell may be used for generation of acid or base or to remove hardness from feedwaters.

1. Research carried out under the ORNL-NSF Environmental Program, sponsored by NSF-RANN, under Union Carbide Corporation's Contract with the U.S. Atomic Energy Commission.

2. A. A. Palko, R. E. Meyer, and F. A. Posey, *Chem. Div. Annu. Progr. Rep. May 20, 1971*, ORNL-4706, p. 181.

3. F. A. Posey and R. E. Meyer, "Electrochemical Cell for Generation of Base," the following contribution, this report.

ELECTROCHEMICAL CELL FOR GENERATION OF BASE

F. A. Posey R. E. Meyer

As an outgrowth of work on direct electrochemical pretreatment of waters,[1] a compact, lightweight cell for production of base was designed and constructed. An economical method for on-site production of base from the streams to be treated would be useful in a variety of applications, such as water softening and pollution abatement of contaminated streams. The cell is constructed from Lucite, with stainless steel cathodes and platinized titanium anodes (working surface area about 12 ft^2), and makes use of porous Teflon membrane separators backed by porous polyethylene sheet and nylon screen supports.

The unit is to be field-tested as part of a process for pretreatment of brackish water during hyperfiltration tests at Roswell, New Mexico.[2] In operation, the cell is to supply approximately 40 gal/day of ca. 1 *M* NaOH for pretreatment of ca. 2000 gal/day of brackish water. An anode loop is to be operated on brine made up from hyperfiltration-treated water and rock salt, while the base stream from a cathode loop will be used, together with CO_2 injection, to precipitate calcium and magnesium ions in the incoming brackish water as $CaCO_3$ and $Mg(OH)_2$. Pretreated water will subsequently be reacidified to an optimum pH for hyperfiltration.

1. A. A. Palko, R. E. Meyer, and F. A. Posey, "Direct Electrochemical Pretreatment of Waters for Hardness and pH Control," the preceding contribution, this report.

2. Engineering studies on hyperfiltration of brackish waters carried out in the Water Research Program by D. G. Thomas, Reactor Division, in collaboration with J. S. Johnson, Jr., Chemistry Division.

ELECTROCHEMICAL DEMONSTRATION UNIT FOR COPPER REMOVAL FROM DISTILLATION PLANT BLOWDOWN[1]

F. A. Posey

The copper content of typical distillation plant blowdown streams is usually in the range of several tenths of a part per million (ppm) and is a consequence of normally occurring corrosion of Cu-Ni alloy tubing used in the heat-exchanger sections of the plants. Dissolved copper at this level in brine streams is of concern because of its likely toxic effect on sea life near brine outfalls (normal copper content of seawater in open ocean is about 0.003 ppm). Up until now, there have existed no proven, economical methods for removing heavy-metal ions, especially copper, from distillation plant blowdown streams. Most proposed methods for copper removal would require the addition of various reagents and conventional chemical operations or would depend upon use of ion exchange techniques. Earlier studies[2] on the properties of porous electrodes had shown that reducible heavy-metal ions may be removed from flowing streams very efficiently by appropriately designed and operated electrodes having a sufficiently large ratio of reactive surface area to solution volume.

Accordingly, an electrochemical demonstration unit for copper removal from brine streams has been designed, constructed, and tested. The prototype unit, having a cross-sectional area of 1 ft^2, has successfully treated 7–25 gpm (10,000–36,000 gal/day) of blowdown obtained from the Office of Saline Water test site at Wrightsville Beach, North Carolina. In spite of some unavoidable nonuniformity of flow distribution within

the prototype cell, the unit removed 97% of the dissolved copper at 10,000 gal day^{-1} ft^{-2} and 85% at 36,000 gal day^{-1} ft^{-2}. Power requirements are almost negligible at the copper concentration levels expected for typical distillation plant brines; removal of 1 ppm of dissolved cupric ions at a cell voltage of 2.5 V requires only about 8×10^{-3} kWhr per 1000 gal. The unit is to be further tested for an extended period on brine blowdown at the Office of Saline Water's Freeport, Texas, test bed site.

---

1. Research carried out in collaboration with S. A. Reed, Reactor Chemistry Division. Research sponsored by the Distillation Division, Office of Saline Water, U.S. Department of the Interior, under Union Carbide Corporation's contract with the U.S. Atomic Energy Commission.

2. Research originally sponsored by the Research Division, Office of Saline Water, U.S. Department of the Interior, and later carried out under the ORNL-NSF Environmental Program, sponsored by NSF-RANN; research under both sponsors was possible under Union Carbide Corporation's contract with the U.S. Atomic Energy Commission.

7. Chemical Physics

NEUTRON AND X-RAY DIFFRACTION

HYDROGEN ISOTOPE PARTITIONING IN A CRYSTAL CONTAINING BOTH SHORT AND LONG HYDROGEN BONDS

C. K. Johnson G. D. Brunton[1]

Our initial reason for undertaking a neutron diffraction crystal-structure analysis of the $P4_2/n$ phase of the compound $YH_5O_2(C_2O_4)_2 \cdot H_2O$ was to establish the geometrical conformation of the diaquated proton $(H_2O{-}H{-}OH_2)^+$ which had been postulated for this crystal from previous x-ray diffraction studies.[2,3] Hydrogen atoms were not found by the x-ray studies because of the presence of the heavy yttrium atom which dominates the x-ray scattering. A set of 1371 neutron data was collected at 25°C from a nondeuterated crystal (a = 8.696 Å, c = 12.824 Å), and a similar set was collected from a crystal (a = 8.699 Å, c = 12.818 Å) containing 92% deuterium. Refinement of the two structures produced values of the discrepancy index $R(F^2)$ of 4.79% and 4.06% respectively. All data were included in the refinements. Figure 7.1 shows distances and angles for the deuterated ion $D_5O_2{}^+$. The short, centered hydrogen bond is 0.024 Å shorter in the nondeuterated form, but the other hydrogen bond lengths are nearly the same in both crystals.[4] In addition, we found that the deuterium fractions at the four different hydrogen atom sites of the 92% deuterated crystal were not identical and that the protium isotope seems to concentrate in the short, centered hydrogen bond.[5] To determine the partitioning more

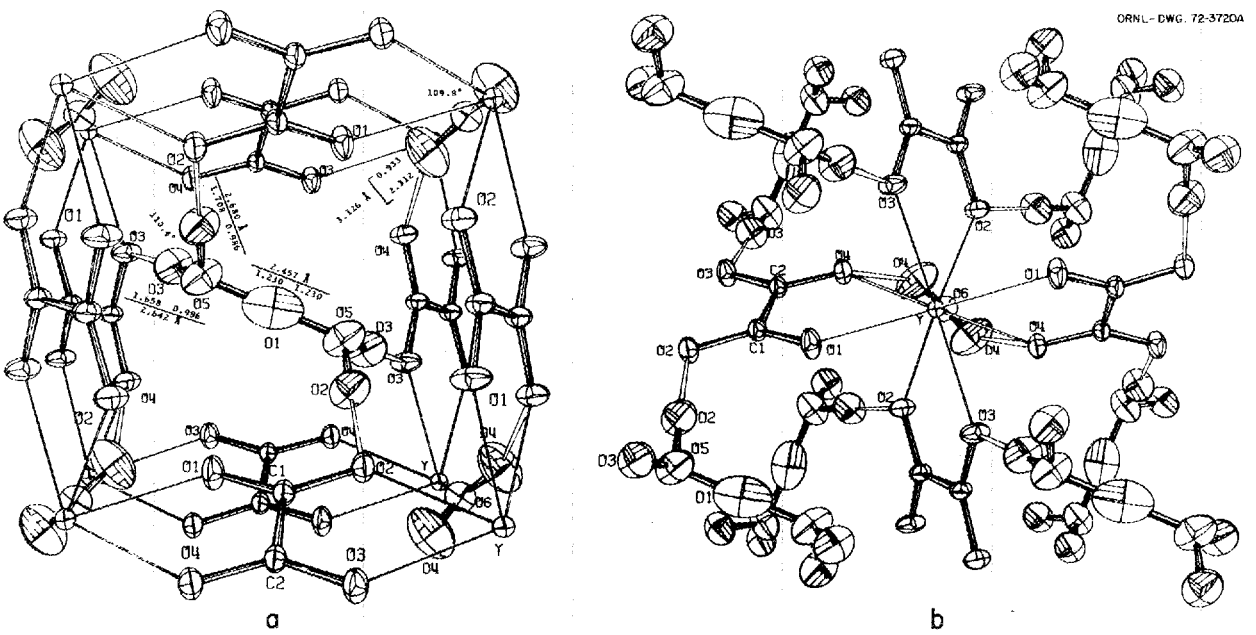

Fig. 7.1. Portions of the yttrium hydrogen oxalate trihydrate structure viewed nearly parallel to [001]. The [110] axis extends to the right. (*a*) The $D_5O_2{}^+$ ion and its environment. The atom D_1 is on a twofold rotation axis. (*b*) Coordination pattern around the yttrium atom. The ninth atom in the coordination is an oxygen atom O_6 above the yttrium atom and is not shown. The atoms Y and O_6 are on a 4_2 screw axis.

precisely, we collected still another set of neutron diffraction data at 25°C from a crystal containing 52% deuterium. The deuterium fractions found are 0.376(8) in H_1, 0.541(6) in H_2, 0.530(6) in H_3, and 0.553(6) in H_4 (see Fig. 7.1). The differences in isotope concentration between the very short hydrogen bond containing H_1 and the others are highly significant.

Hydrogen atoms bound as in this compound are readily exchangeable in aqueous solution and might also be labile in the crystal if, for example, the equilibrium $H_5O_2^+ \rightleftharpoons H_2O + H_3O^+$ occurs with an accompanying threefold rotation of the H_3O^+ ion.[6] There should then be a temperature dependence for the isotope partitioning. To test this hypothesis, we collected two additional complete neutron data sets from the 52% deuterated crystal at temperatures of −155 and 60°C. The experimental results given in Table 7.1 clearly demonstrate that equilibrium was not obtained at −155°C and suggest that 60°C was not high enough to produce a significant change from the results at 25°C. Our basic premise is that the isotope fractionation is at equilibrium at the temperature of crystallization, which was 90°C. Since the crystals were grown slowly from a large volume of solution, this premise seems reasonable.

For simple molecules in the gas and liquid states, equilibrium isotope effects often can be calculated quite accurately from theoretical considerations.[7] Such calculations can be applied to the solid-state equilibrium problem described above. The fundamental equation on which the analysis depends is the usual partition-function-ratio equation for internal-molecular harmonic vibration:

$$\frac{Q_b}{Q_o} = \prod_i \exp\left[-\frac{h(\nu_b - \nu_o)_i}{2kT}\right] \times \left[\frac{1 - \exp(-h\,\nu_{o_i}/kT)}{1 - \exp(-h\,\nu_{b_i}/kT)}\right] . \quad (1)$$

In the present case, the product with running index i is over all normal modes of vibration which contribute to the displacement of hydrogen atoms in the molecule. The normal-mode frequencies for the nondeuterated isomer and a particular deuterated isomer designated **b** are ν_o and ν_b respectively. The symbols Q_b and Q_o represent the quantum mechanical Boltzman partition function for species **b** and **o**. The remaining symbols have their normal chemical significance.

The deuterium fraction f_k at atomic site k in the crystal is obtained by summing the mole fractions $[A_b]$ of all species **b** with deuterium in the kth position. The mole fraction for any species **b** is related to the partition function ratio [i.e., Eq. (1)] by the expression

$$[A_b] = K\, r^m Q_b/Q_o , \quad (2)$$

where m is the number of deuterium atoms in species **b**. The ratio parameter r is the positive root of the following polynomial in R,

$$\sum_{j=0}^{n} \left(F - \frac{j}{n}\right) R^j \sum Q_b/Q_o = 0 , \quad (3)$$

and the constant K is given by

$$K = 1 \Big/ \sum_{j=0}^{n} r^j \sum Q_b/Q_o . \quad (4)$$

The second summations in Eqs. (3) and (4) are over all species **b** with a total of j deuterium atoms in the n possible sites, and the symbol F in Eq. (3) represents the overall deuterium fraction in the crystal. Equations (2)–(4) were derived by W. R. Busing from considerations of chemical equilibria.

The rotation and translation components of the gas-phase partition function are inappropriate for crystal-phase calculations; however, if the lattice-vibra-

Table 7.1. Observed and calculated deuterium fractions for $YH_5O_2(C_2O_4)_2 \cdot H_2O$

Observed values based on neutron scattering factors H, −0.374; D, +0.667. Calculated values based on spectroscopic normal coordinate analyses by J. B. Bates and L. M. Toth ($H_5O_2^+$: 15 internal frequencies, 32 isomers; H_2O: 3 internal frequencies, 4 isomers).

	−155°C				25°C				60°C			
	H_1	H_2	H_3	H_4	H_1	H_2	H_3	H_4	H_1	H_2	H_3	H_4
Observed	0.36	0.54	0.54	0.55	0.38	0.54	0.53	0.55	0.39	0.53	0.53	0.54
Model 1	0.15	0.58	0.61	0.56	0.37	0.55	0.56	0.52	0.39	0.55	0.56	0.52
Model 2	0.91	0.35	0.34	0.68	0.72	0.44	0.44	0.58	0.70	0.45	0.45	0.57

tion contributions can be expressed adequately as those due to small-amplitude rigid-body librations and translations, the rigid-body frequencies can simply be added to the list of internal frequencies used for Eq. (1).

A spectroscopic normal-coordinate analysis of the $H_5O_2^+$ ion in the crystal was undertaken by J. B. Bates (Director's Division) and M. R. Toth (Reactor Chemistry Division). Unfortunately, the characteristic Raman and infrared spectra for the ion appear as diffuse bands and consequently are difficult to assign. Nevertheless, two different force constant models reasonably compatible with the observed spectra were derived, and internal frequencies for each of the 32 isomers were calculated by Bates and Toth. Using these calculated frequencies and Eqs. (1)–(4), we derived the deuterium fractions shown in Table 7.1. These results illustrate that the deuterium fractionation is quite sensitive to the model used. The values are preliminary and may change considerably when the rigid-body libration frequencies are derived and included in the calculations.

Two other unusual physical phenomena besides the isotope effects were found during the studies. A rapid, reversible, order-disorder phase transition occurs at 50 to 56°C, transforming the structure from one in space group $P4_2/n$ to one in $P4/n$ with the c axis half as long. The progress of the transformation was recorded by monitoring the disappearance of the l-odd 311 reflec-

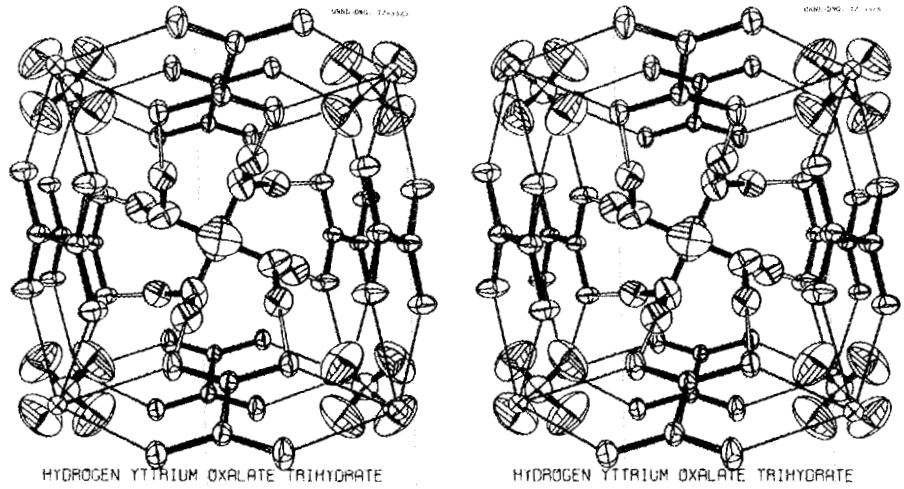

Fig. 7.2. Stereoscopic drawing showing the disordered high-temperature structure with space-group symmetry $P4/n$. The two configurations of $H_5O_2^+$ ions shown are related by a fourfold rotary inversion.

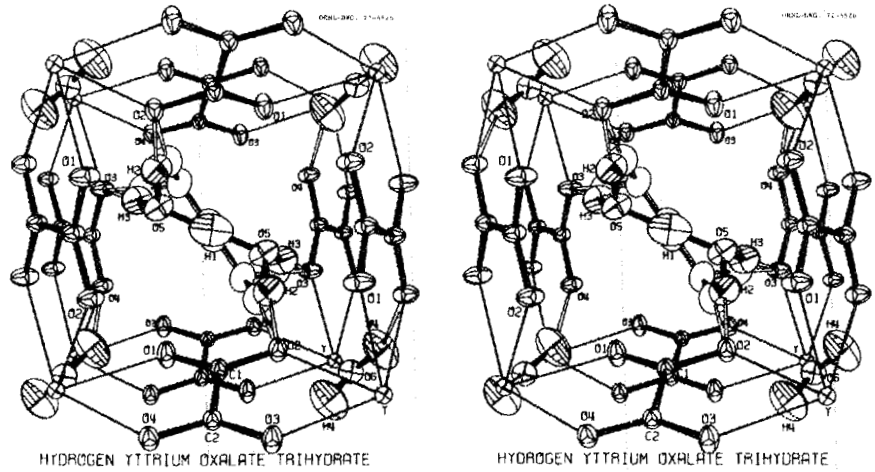

Fig. 7.3. Stereoscopic drawing showing the "inversion" disordered $H_5O_2^+$ ions. The minor configuration is related to the major configuration by a noncrystallographic approximate twofold rotation about an axis in the x-y plane.

tion with increasing temperature. Figure 7.2 shows the disordered phase at 60°C. There is also a separate temperature-dependent disordering phenomenon in which each half of the ion undergoes an "inversion" resembling that which occurs in ammonia, while maintaining the same hydrogen bonds. The resulting configuration is well represented by a twofold rotation about a noncrystallographic axis in the *x-y* plane. Figure 7.3 illustrates this disorder. We find 12% "inverted form" at 60°C, 8% at 25°C, and none at −155°C.

1. Reactor Chemistry Division.
2. H. Steinfink and G. D. Brunton, *Inorg. Chem.* **9**, 2112 (1970).
3. R. R. Ryan and R. A. Penneman, *Inorg. Chem.* **10**, 2637 (1971).
4. The paper by R. G. Delaplane and J. A. Ibers, *Acta Crystallogr., Sect. B* **25**, 2423 (1969) suggesting that all hydrogen bonds are increased significantly in length on deuteration is not supported by the present findings.
5. An unequal distribution of hydrogen isotopes was previously noted for α-oxalic acid dihydrate by P. Coppens in *Thermal Neutron Diffraction*, B. T. M. Willis, ed., p. 82, Oxford Press, 1970.
6. An NMR study on crystals of chloroauric acid tetrahydrate suggests that this process does occur. D. E. O'Reilly, E. M. Peterson, C. E. Scheie, and J. M. Williams, *J. Chem. Phys.*, in press.
7. See R. L. Schowen, *Progr. Phys. Org. Chem.* **9**, 275 (1972) and references quoted therein.

THE TRI-AQUATED HYDROGEN ION $H_7O_3^+$. A NEUTRON DIFFRACTION STUDY OF SULFOSALICYCLIC ACID TRIHYDRATE[1]

J. M. Williams[2] S. W. Peterson[2]
H. A. Levy

A recent x-ray diffraction study[3] of sulfosalicylic acid trihydrate, $C_6H_3(COOH)(OH)(SO_3H)\cdot 3H_2O$, indicated the existence in this crystal of a hydrogen ion closely associated with three water molecules. Since the x-ray study did not yield precise locations for the hydrogen atoms involved, and proper interpretation of the nature of the species depends critically on the O-H separations, the present neutron diffraction study was undertaken.

The crystal is orthorhombic, space group *Pbca*, with $a = 6.646(1)$, $b = 24.507(5)$, $c = 13.874(3)$ Å, and $Z = 8$. Complete neutron diffraction data, numbering 2696 symmetry-independent reflections, were measured at the HFIR automatic diffractometer to $\sin\theta/\lambda = 0.66 A^{-1}$. A refinement by the Fourier and least-squares methods of a scale multiplier, atomic positions parameters, anisotropic temperature factors, and isotropic

ORNL-DWG. 72-5515

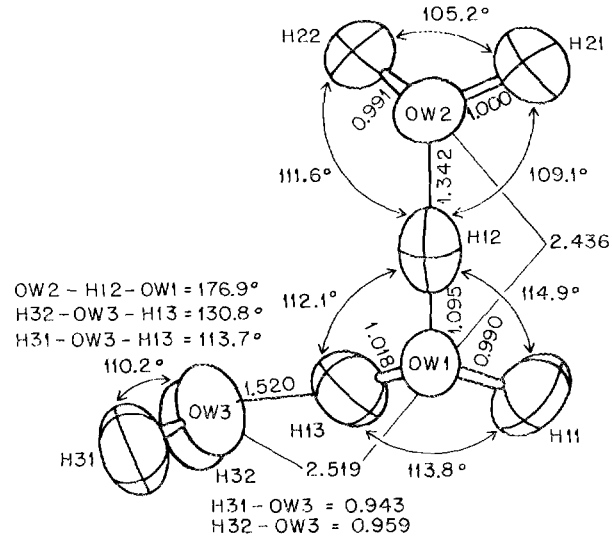

Fig. 7.4. Bond angles and bond lengths of the diaquooxonium ion. The standard deviations are in units of the last given decimal place.

extinction coefficients yielded the weighted discrepancy index value $R(wF^2) = 0.055$.

The resulting structure confirms the main conclusions of the x-ray study[3] and in addition furnishes a precise description of the tri-aquated hydrogen ion $H_7O_3^+$ shown in Fig. 7.4. This species contains a central group H_3O^+ in which hydrogen atoms surround the oxygen atom pyramidally at distances 0.990, 1.018, and 1.095 Å; to it are hydrogen-bonded the other two water molecules, one at the exceptionally short O···O distance of 2.436 Å and the other at 2.519 Å. It is of special interest that the hydrogen atom of the short hydrogen bond is not centered: the O–H distances are 1.095 and 1.342 Å. The species is thus appropriately described by the name diaquooxonium. All peripheral hydrogen atoms of the species are involved in hydrogen bonds to carboxyl, hydroxyl, or sulfonate groups.

1. Cooperative research with Argonne National Laboratory.
2. Chemistry Division, Argonne National Laboratory.
3. D. Mootz and J. Fayos, *Acta Crystallogr., Sect. B* **26**, 2046 (1970).

NEUTRON DIFFRACTION STUDY OF LITHIUM HYDROXIDE MONOHYDRATE

P. A. Agron W. R. Busing
H. A. Levy

X-ray diffraction studies of lithium hydroxide monohydrate[1-3] established the general nature of the struc-

ture as consisting of Li^+ ions coordinated into chains by OH^- ions and water molecules and further hydrogen bonded into a three-dimensional network. In the latest of these studies,[3] which was concurrent with the present work, the arrangement of hydrogen atoms was also disclosed. For an understanding of the structural chemistry of the hydroxide ion in an environment of both cations and water molecules, the hydrogen positions must be known with precision. For this purpose, the neutron diffraction study here reported was undertaken.

Our interest in $LiOH \cdot H_2O$ began in 1956, when a two-dimensional set of neutron intensity data was measured. Because the crystal specimens available were all highly perfect, the data proved to be so severely affected by extinction as to be incapable of yielding a satisfactory refined structure with analytical methods then available. Since recent theoretical advances[4] have greatly increased the tractable range of extinction-affected data, a new examination of the problem became appropriate.

Single-crystal specimens of $LiOH \cdot H_2O$ were grown by slow evaporation of a saturated aqueous solution over solid potassium hydroxide. The space group was confirmed to be $C2/m$ with $Z = 4$. The unit cell parameters were determined from Cu $K\alpha_1$ x-ray diffractometer settings ($\lambda = 1.54051$) of 13 high-angle Bragg reflections to be $a = 7.4153(2)$, $b = 8.3054(2)$, $c = 3.1950(1)$ Å, $\beta = 110.107(4)°$. Intensities of a set of 680 reflections covering two asymmetric quadrants of reciprocal space were measured with the HFIR automatic neutron diffractometer. Corrections for absorption were made in the usual way. Refinement by the method of least squares of a scale multiplier, atomic position and anisotropic thermal parameters, and anisotropic extinction coefficients[5] of type 1 yielded a final discrepancy index $R(F) = 0.045$. Fifty-two reflections having extinction corrections more severe than 0.1 were deemed to be inadequately corrected and were omitted from the refinement.

Figure 7.5 shows a drawing of the unit cell of the structure. The arrangement may be visualized as built of pairs of Li^+ ions bridged by oxygen atoms of OH^- ions into equilateral parallelograms; parallel strings of these rhombuses are bridged between Li^+ ions with oxygen atoms of water molecules, as illustrated in Fig. 7.6. These strings are further linked into a three-dimensional network by hydrogen bonding between water molecules of one string and hydroxyl ions of another. Each string contains a mirror plane of symmetry in which the OH^- ions lie and alternate two-fold rotors on which Li^+ and oxygen atoms of H_2O respectively lie. Thus all atoms are in special positions of the space group except the hydrogen atoms of the water molecules, which are in general positions.

The coordination about Li^+ ($2OH^-$ and $2H_2O$) is that of a tetrahedron with angles and distances shown in the figures. The hydroxyl ion is coordinated by two lithium

ORNL-DWG. 72-2925

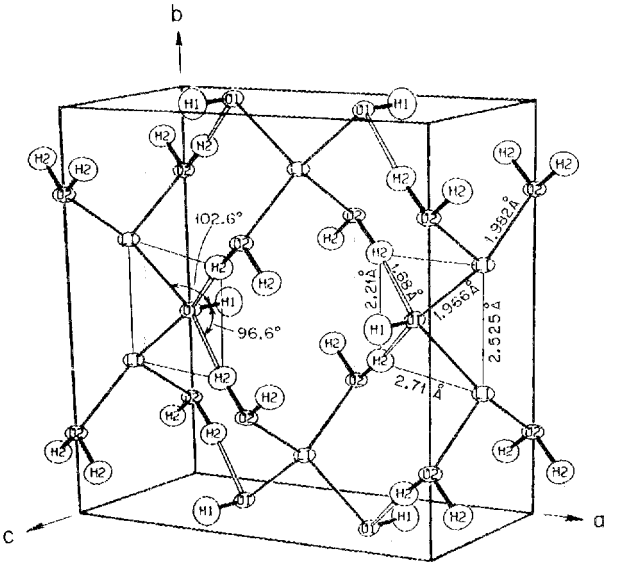

Fig. 7.5. Drawing of the unit cell of $LiOH \cdot H_2O$. The surroundings of the hydroxyl ion are indicated by light lines. Interatomic distances and bond angles are shown.

ORNL-DWG. 72-2924

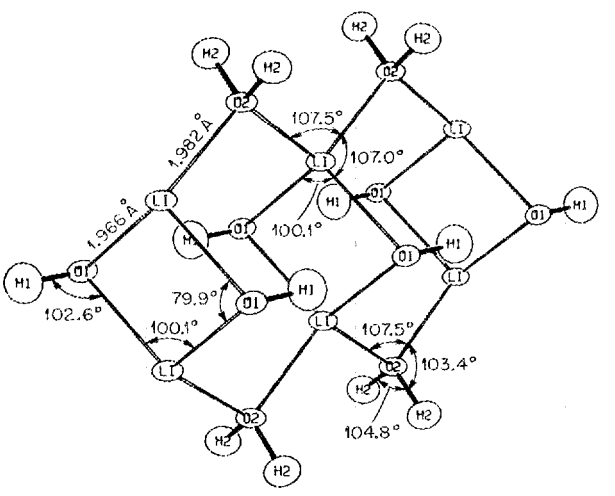

Fig. 7.6. Drawing illustrating the bridging of pairs of LiOH neutral units into strings. Distances and bond angles in the coordination shells of Li^+, OH^-, and H_2O are shown.

Table 7.2. Atomic coordinates and root-mean-square thermal displacements in $LiOH \cdot H_2O$

	Fractional coordinates			Principal rms displacements (Å)		
	x	y	z	(1)	(2)	(3)
Li	0	0.3480(5) [0.3474(11)]	0.5	0.091	0.128	0.143
O(1)	0.2858(2) [0.2857(5)	0	0.3955(5) 0.3952(12)]	0.088	0.104	0.148
O(2)	0	0.2068(2) [0.2066(4)]	0	0.095	0.107	0.146
H(1)	0.2657(4) [0.237(21)	0	0.6740(11) 0.631(61)]	0.169	0.179	0.193
H(2)	0.1121(3) [0.107(12)	0.1330(2) 0.118(10)	0.1399(7) 0.004(38)]	0.146	0.154	0.179

Note: X-ray values from ref. 3 are given in square brackets. O(1) and H(1) form the hydroxide ion; O(2) and H(2) the water molecule.

Table 7.3. Distances and bond angles in $LiOH \cdot H_2O$

Lithium coordination polyhedron	
Li–O(1)	1.966(3) Å
Li–O(2)	1.982(3)
Hydroxyl ion	
O(1)–H(1)	0.952(3)
Water molecule	
O(2)–H(2)	1.006(2)
H(2)–O(2)–H(2)	1.04.8(2)°
Hydrogen bond	
O(2)–H(2)···O(1)	174.5(2)°
O(2)–O(1)	2.683(1) Å
H(2)–O(1)	1.680(2)

ions and two hydrogen atoms from different water molecules, forming a flat trapezoidal pyramid which may be seen in Fig. 7.5. The oxygen atom of the water molecule has a nearly regular tetrahedral coordination of two Li^+ and its own two hydrogen atoms. The H–O–H angle in the water molecule is 104.8°, close to the gas-phase value.

Atomic coordinates and thermal parameters are listed in Table 7.2 and are compared with those determined in the most recent x-ray study.[3] The agreement with the x-ray study is satisfactory except for the z coordinate of H(2), for which the x-ray study yielded a value grossly in error. Some interatomic distances and bond angles are listed in Table 7.3; no corrections for thermal motion were made.

1. R. Pepinsky, *Phys. Rev.* **55**, 1115 (1939).
2. H. Rabaud and R. Gay, *Bull. Soc. Fr. Mineral. Cristallogr.* **80**, 166 (1957).
3. N. W. Alcock, *Acta Crystallogr., Sect. B* **27**, 1682 (1971).
4. W. H. Zachariasen, *Acta Crystallogr.* **16**, 1139 (1963); **23**, 558 (1967).
5. P. Coppens and W. C. Hamilton, *Acta Crystallogr., Sect. A* **26**, 71 (1970).

NONPLANARITY OF HYDROXAMIC ACIDS. A NEUTRON DIFFRACTION STUDY OF HYDROXYUREA

W. E. Thiessen H. A. Levy
B. D. Flaig[1]

Although substituted amides are generally considered to be planar, accurate knowledge of the molecular geometry of those with electronegative substituents at nitrogen is sparse. Such knowledge is needed, since the structure-dependent ionization of the N–O bond in hydroxamic acids and their esters is a crucial step in their carcinogenic action.[2] Last year[3] it was shown that the surroundings of the hydroxamic acid nitrogen atom in 3-hydroxyxanthine, a potent tumor-inducing chemical agent, were definitely pyramidal. While the explanation offered in that report was in terms of molecular bonding, it is also possible to explain the effect in terms of hydrogen bonding in the crystal of 3-hydroxyxanthine dihydrate.

Previous x-ray studies[4,5] had revealed the positions of the nonhydrogen atoms in the simpler hydroxamic acid hydroxyurea, $H_2NCONHOH$, and made it seem likely that accurate knowledge of hydrogen atom positions, potentially obtainable from a neutron diffraction study, could decide between the alternative explanations. Accordingly, a suitable 20.8-mg crystal grown from aqueous solution was selected for intensity measure-

ments on the Oak Ridge computer-controlled neutron diffractometer at the High Flux Isotope Reactor.

Intensity measurements were carried out on 1995 reflections in two quadrants below a Bragg angle of 130° at a neutron wavelength of 1.25 Å. The 1000 independent structure factor magnitudes thus obtained were phased from the nonhydrogen atom positions given by Berman and Kim[5] to yield a Fourier synthesis which indicated all hydrogen atom positions. Full-matrix least-squares refinement including an extinction correction led eventually to a conventional $R(F)$ of 0.0407 on the 1955 reflections whose extinction corrections were no greater than a factor of 2.5. Distances and angles of the refined model are given in Fig. 7.7.

In contradistinction to the 3-hydroxyxanthine case, the hydroxamic acid oxygen atom lies approximately in the plane of the rest of the nonhydrogen atoms. Table 7.4 shows the distance of all atoms from this plane. The N3–H8 bond makes an angle of 15° with the plane, while the N–O bond in 3-hydroxyxanthine is only 8° out of the plane of the aromatic rings. As can be seen from the packing diagram (Fig. 7.8), the moderate deviations of H6 and H7 from the plane can be explained by observing that they form shorter, straighter hydrogen bonds to carbonyl oxygen in other molecules than they would if moved toward the plane, keeping the same bond distance and the same bond angles projected onto the best plane.

The larger deviation of H8 from the plane cannot be explained in this way. Indeed, if H8 is allowed to move toward the plane under the constraints described above, a position is found in which its hydrogen bond becomes shorter and straighter than it was originally, showing that hydrogen bonding in the hydroxyurea crystal is tending to decrease the pyramidal character of hydroxamic nitrogen compared with that characteristic of the isolated molecule. We therefore conclude that pyramidality about hydroxamic nitrogen is a true molecular effect and is to be generally expected in hydroxamic acid derivatives.

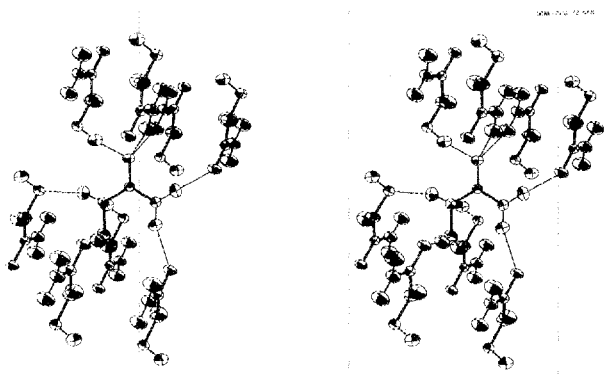

Fig. 7.8. Stereoscopic view of the molecular packing in crystalline hydroxyurea.

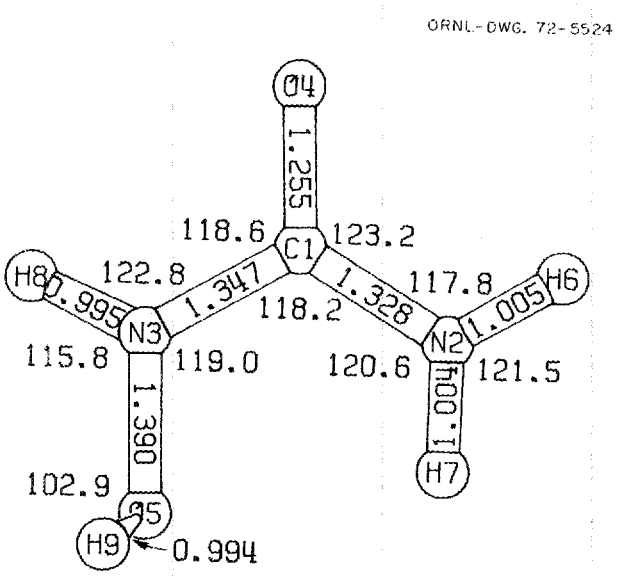

Fig. 7.7. Atom-number scheme, bond lengths (Å), and valence angles (deg) in the hydroxyurea molecule.

Table 7.4. Distances (Å) of atoms from a least-squares plane fitted to C1, N2, N3, and O4 in the hydroxyurea molecule

Atom	Distance	Atom	Distance
C1	−0.005	O5	−0.035
N2	0.002	H6	0.114
N3	0.002	H7	−0.035
O4	0.002	H8	−0.234
		H9	0.876

1. Oak Ridge Associated Universities Summer Student Trainee from Moorhead State College, Moorhead, Minn., 1971.

2. G. Stöhrer and G. B. Brown, *Science* 167, 1622 (1970).

3. W. E. Thiessen, *Chem. Div. Annu. Progr. Rep. May 20, 1971*, ORNL-4706, p. 185.

4. I. K. Larsen and B. Jerslev, *Acta Chem. Scand.* **20**, 983 (1966).

5. H. Berman and S. H. Kim, *Acta Crystallogr.* **23**, 180 (1967).

SUCROSE: FURTHER REFINEMENT OF THE CRYSTAL-STRUCTURE PARAMETERS FROM NEUTRON DATA

G. M. Brown H. A. Levy

In 1963 at the time of our original reports[1,2] on the structure of sucrose ($C_{12}H_{22}O_{11}$) as determined by neutron crystal-structure analysis, we had not reached complete convergence in least-squares refinement. The structure parameters had to be refined in blocks because of the limited core storage of the computer used, and the least-squares program had no provision for correcting the observations for the effects of extinction, as is commonly done today. We had attempted to minimize extinction effects by using data from the smaller two of three crystal specimens for the stronger intensities and data from the largest crystal only for the weaker intensities. However, although we regarded the atomic coordinates as reliable, we have been concerned recently about possible errors in the thermal parameters arising from residual effects of extinction. Knowing of the intent of a group of crystallographers[3] elsewhere to use our parameters in conjunction with their own new x-ray data to study the distribution of bonding electron density in the molecule, we have now completed the refinement of the parameters, using our original neutron data and the full-matrix least-squares method, with type I anisotropic extinction corrections.[4]

For the final refinement the data set consisted of 2813 values of $|F(hkl)|_o^2$, the observed square of the structure-factor magnitude, from a 96.3-mg crystal, 1002 values from a 10.8-mg crystal, and 145 values from a 5.1-mg crystal, with a standard error, $\sigma(|F|^2)$, for each. The standard error was computed as

$$\sigma(|F|^2) = \left\{ [\sigma_s(|F|^2)]^2 + (0.03|F|^2)^2 \right\}^{1/2} ,$$

where $[\sigma_s(|F|^2)]^2$ is the purely statistical variance, and the term $(0.03|F|^2)^2$ is an empirical variance correction. The data set for the largest crystal was essentially complete to the value 0.764 $Å^{-1}$ in $(\sin\theta)/\lambda$. The data for the three different crystals were not averaged, because the effects of extinction were different for the three.

At convergence in least-squares refinement the values of the usual measures of goodness of fit were as follows: 0.033 for $R(F)$, the usual discrepancy index; 0.037 for $R(F^2)$, the index computed on the $|F|^2$ values; 0.050 for the weighted index computed on $|F|^2$; 0.997 for the standard deviation of fit. These measures of goodness of fit indicate a significantly better fit of parameters to the data than had been attained without the inclusion of the extinction parameters. A final difference map showed a maximum positive excursion of 0.02 and a maximum negative excursion of −0.02 in units of 10^{12} cm^{-2}. For comparison, the height of the highest positive peak in the corresponding Fourier map was 6.45 units [for atom C(1)], and the depth of the deepest hole was 2.50 units [for atom H(C1)]. The final coordinates and thermal parameters are given in Table 7.5, and the extinction parameters are given in Table 7.6.

The extinction was extraordinarily anisotropic for crystal 1, slightly anisotropic for crystal 2, and essentially isotropic for crystal 3. It is interesting that for crystal 1 the principal axis of the extinction ellipsoid about which the angular mosaic spread is greatest is almost exactly along the *c* axis of the crystal. This seems consistent with the fact that the sucrose crystals show facile cleavage parallel to the (100) plane, which has already been explained in terms of the hydrogen bonding pattern established in our preliminary determination.[1,2] In contrast, however, to the situation for crystal 1, the smallest mosaic spread in crystal 2 is associated with the direction of c. The fact that crystal 2, along with 3, had been repeatedly dipped in liquid nitrogen before being used in data collection, whereas crystal 1 had not, may account for the difference.

All bond lengths and valence angles for the sucrose molecule are reported in Fig. 7.9, along with the torsion angles[5] of most interest. Included in the figure are the standard errors of all these molecular parameters as calculated from the complete least-squares covariance matrix. The calculated lengths and angles are based upon the following cell parameters determined in this laboratory at 21–24°C with the assistance of R. D. Ellison: a = 10.8633(5) Å, b = 8.7050(4) Å, c = 7.7585(4) Å, β = 102.945(6)° (space group $P2_1$). No detailed discussion of the molecular structure is necessary, since the data in Fig. 7.9 merely confirm at a higher level of precision the parameters previously reported by us or calculated by others from parameters supplied by us.

The abnormally low value of 0.9122(42) Å for the apparent O(4)–H(O4) bond length is a consequence of the unusually large amplitudes of the thermal motion of atom H(O4), which in turn are related to the fact that the O(4) hydroxyl group is not involved in hydrogen bonding (see below). For H(O4) the principal axis of greatest thermal motion (rms displacement 0.432 Å) is at 102° to the O(4)–H(O4) bond direction. The corrected bond length calculated according to the "riding" model,[6] which should be a fair approximation

Table 7.5. Coordinates and thermal parameters, with standard errors, for the crystal structure of sucrose, all times 10^5. The anisotropic temperature factor has the form $\exp(-\beta_{11}h^2 - \beta_{22}k^2 - \beta_{33}l^2 - 2\beta_{12}hk - 2\beta_{13}hl - 2\beta_{23}kl)$.

ATOM	X	Y	Z	β_{11}	β_{22}	β_{33}	β_{12}	β_{13}	β_{23}
C(1)	29961(8)	35792(0)	48487(12)	274(6)	376(9)	584(12)	6(6)	94(7)	4(9)
C(2)	31253(9)	47474(15)	63600(12)	304(6)	498(10)	641(13)	-44(7)	73(7)	-64(9)
C(3)	28545(9)	63673(15)	56447(13)	321(7)	437(10)	965(15)	-18(7)	196(8)	-72(10)
C(4)	37404(10)	67095(15)	44198(14)	400(7)	403(10)	1003(15)	-22(7)	243(9)	6(11)
C(5)	35925(9)	55107(16)	29529(13)	314(7)	525(11)	756(14)	-23(7)	133(8)	64(10)
C(6)	45754(11)	57083(17)	18455(14)	525(8)	749(14)	858(15)	-133(9)	307(9)	-2(12)
C'(1)	10301(10)	13110(15)	54380(12)	463(8)	559(11)	517(12)	-71(8)	152(8)	104(9)
C'(2)	12446(8)	19262(14)	36895(10)	307(6)	362(9)	426(11)	-6(6)	101(6)	32(8)
C'(3)	718(8)	19075(15)	21485(11)	288(6)	430(9)	521(11)	-32(6)	106(7)	19(9)
C'(4)	6478(9)	16653(15)	5476(11)	354(6)	474(10)	464(11)	-39(7)	107(7)	-2(9)
C'(5)	17635(9)	6133(15)	12864(12)	393(7)	440(10)	565(12)	27(7)	152(7)	-62(9)
C'(6)	28927(10)	8194(17)	4668(14)	482(8)	795(14)	814(15)	81(9)	303(9)	-49(12)
O(1)	17143(9)	34630(15)	39165(13)	272(7)	340(10)	611(13)	-5(7)	86(8)	18(10)
O(2)	22954(12)	43550(19)	74766(16)	488(10)	749(15)	668(16)	-67(10)	206(10)	-40(13)
O(3)	30801(13)	74770(19)	70279(21)	577(12)	656(16)	1650(27)	-213(11)	507(15)	-516(17)
O(4)	34880(18)	81412(20)	35631(24)	1042(17)	478(15)	1629(29)	151(13)	593(19)	271(18)
O(5)	37719(10)	39878(16)	36864(15)	316(8)	442(12)	837(16)	-1(8)	224(9)	-20(11)
O(6)	58144(13)	54525(21)	28621(20)	384(9)	878(19)	1425(24)	-118(11)	379(12)	-190(17)
O'(1)	3017(12)	23548(20)	62119(16)	503(9)	859(16)	690(16)	-75(11)	314(10)	-26(13)
O'(2)	21205(10)	9445(16)	31572(13)	400(8)	472(12)	540(13)	124(8)	78(8)	-17(10)
O'(3)	-7367(11)	31776(17)	20452(16)	337(8)	602(13)	856(17)	109(9)	126(10)	64(13)
O'(4)	-2123(12)	9734(19)	-8904(14)	502(10)	836(16)	541(15)	-143(10)	39(10)	-62(12)
O'(6)	32644(13)	23799(21)	4035(17)	553(11)	931(18)	852(19)	-125(12)	259(11)	36(15)
H(C1)	33468(20)	24508(27)	53880(29)	509(16)	610(22)	1155(33)	74(16)	112(18)	159(22)
H(C2)	41158(21)	46929(33)	71166(31)	440(16)	1125(32)	1123(36)	-21(19)	-65(19)	-86(28)
H(C3)	18707(20)	64476(32)	48969(34)	412(15)	947(30)	1749(44)	59(18)	146(21)	46(30)
H(C4)	47171(21)	66808(34)	52180(33)	502(17)	1118(33)	1462(39)	-183(20)	228(20)	-153(31)
H(C5)	26384(21)	56129(35)	20931(32)	492(16)	1135(34)	1347(38)	11(21)	-29(20)	149(30)
H(C6)	45305(32)	68728(40)	13445(42)	1101(31)	1212(41)	1993(58)	-11(31)	607(35)	652(42)
H'(C6)	43723(32)	49265(46)	7189(39)	1023(30)	1939(57)	1272(43)	-442(35)	454(29)	-556(40)
H(C'1)	5199(30)	2238(32)	52157(36)	1129(30)	800(30)	1425(43)	-345(25)	436(30)	80(29)
H'(C'1)	19473(24)	10908(36)	63300(31)	732(20)	1337(38)	975(32)	145(24)	102(21)	360(30)
H(C'3)	-4946(21)	8843(27)	22896(28)	556(17)	728(25)	1116(32)	-181(17)	212(19)	25(23)
H(C'4)	9840(22)	27720(27)	1551(29)	635(18)	747(25)	1101(33)	-58(18)	273(20)	231(24)
H(C'5)	14653(25)	-5988(29)	11325(32)	846(22)	610(23)	1204(35)	-74(19)	270(23)	-154(23)
H(C'6)	36724(30)	1189(42)	11947(48)	743(24)	1541(49)	2281(66)	462(29)	466(33)	491(46)
H'(C'6)	26505(31)	3991(41)	-8870(36)	1114(29)	1451(43)	1227(39)	-116(32)	580(29)	-464(36)
H(O2)	27193(26)	37235(36)	84664(31)	845(23)	1253(37)	969(34)	-77(26)	172(23)	185(31)
H(O3)	23175(29)	76597(36)	74255(44)	888(27)	1047(34)	2232(60)	-253(25)	832(34)	-598(38)
H(O4)	34066(58)	89130(40)	43250(60)	3073(88)	695(35)	2880(91)	367(47)	1812(78)	149(47)
H(O6)	60152(31)	43834(39)	28663(46)	890(28)	1052(39)	2121(62)	26(27)	340(33)	248(39)
H(O'1)	8454(27)	32466(32)	65416(35)	863(24)	905(30)	1489(42)	-138(23)	508(26)	-209(30)
H(O'3)	-3100(24)	40891(30)	17613(35)	716(21)	677(26)	1589(43)	85(19)	327(24)	159(28)
H(O'4)	-1672(25)	15381(34)	-19611(27)	849(23)	1109(33)	729(30)	-4(23)	45(21)	47(25)
H(O'6)	34766(29)	27804(37)	16026(35)	909(26)	1261(39)	1234(40)	-211(26)	287(27)	-198(32)

Table 7.6. Parameters Z'_{ij} for type I extinction[4] in the three sucrose crystals. The maximum correction factor for extinction for each crystal is also shown.

	Crystal 1	Crystal 2	Crystal 3
Weight, mg	96.3	10.8	5.1
Max. corr.	2.965	1.164	1.112
Z'_{11}	2.73(21)	0.075(18)	0.059(58)
Z'_{22}	0.22(7)	0.016	0.055(43)
Z'_{33}	2.87(10)	0.000(0)	0.005(7)
Z'_{12}	-0.14(9)	-0.009(10)	0.013(40)
Z'_{13}	0.00(14)	0.001(6)	-0.020(38)
Z'_{23}	0.00(7)	0.000(5)	-0.000(18)

in this case, is 0.9892(49) Å. The appearance of the stereoscopic molecular drawing of Fig. 7.10, in which each atom is represented by its thermal ellipsoid of 50% probability,[7] suggests that all of the apparent O—H and C—H bond lengths are significantly shorter than the actual mean interatomic separations. The average riding-model correction (probably an overcorrection) is 0.021 Å for the seven O—H groups exclusive of O(4)—H, 0.032 Å for the six C—H distances in the three CH_2OH groups, and 0.019 Å for the other eight C—H distances.

A description of the hydrogen bonds is given in Table 7.7, which includes data for the O(4)—H hydroxyl, though we do not consider this group to be hydrogen

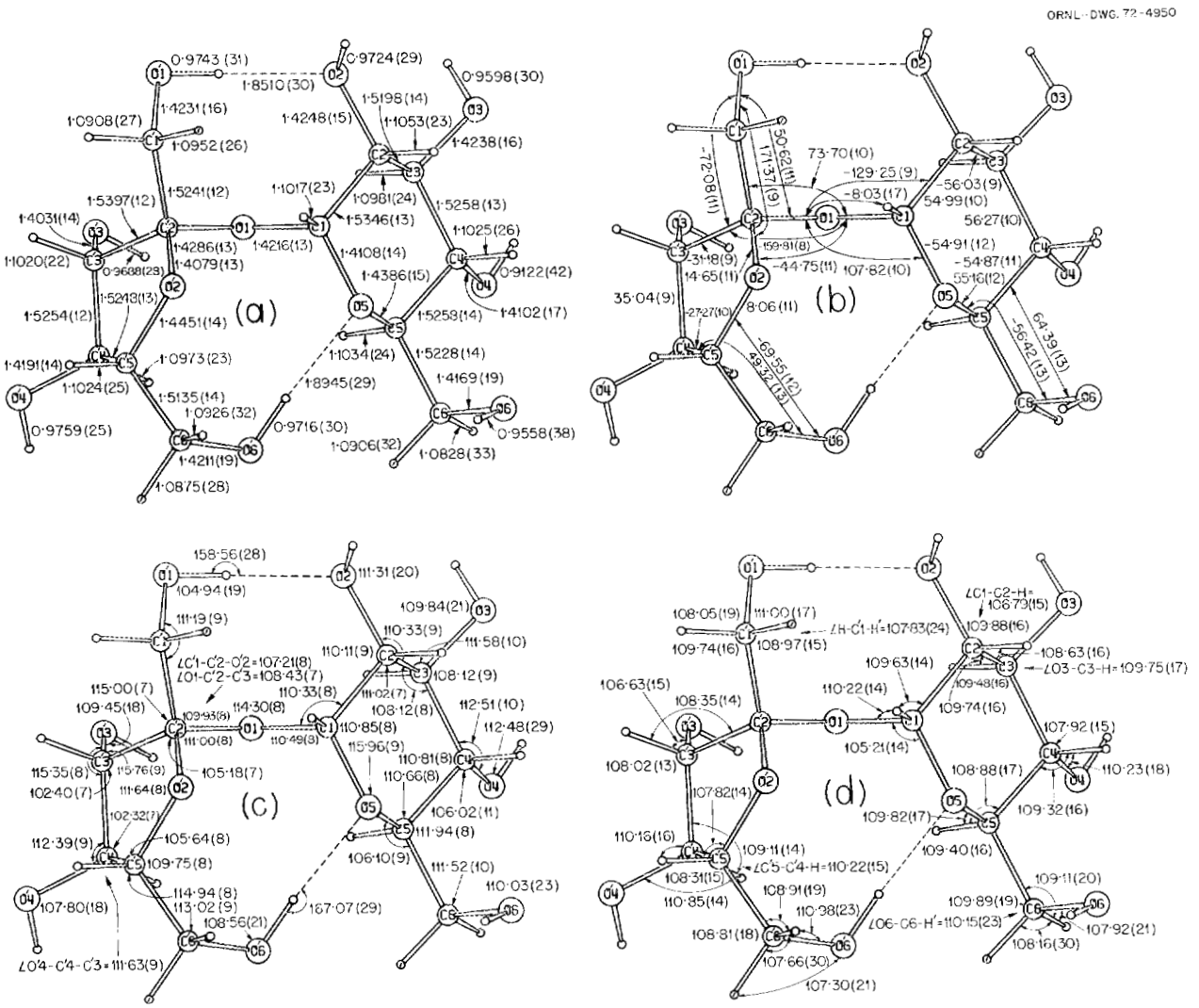

Fig. 7.9. Structure of the sucrose molecule: (*a*) bond lengths (Å); (*b*) selected torsion angles (deg); (*c*) valence angles (deg) not involving C-H bonds; (*d*) valence angles involving C-H bonds. All lengths and angles are uncorrected for effects of thermal motion. Numbers in parentheses specify the standard errors of the corresponding quantities. The two intramolecular hydrogen bonds are indicated. The atom labels correspond to those of Table 7.5, except that the parentheses have been omitted.

ORNL-DWG. 72-4952

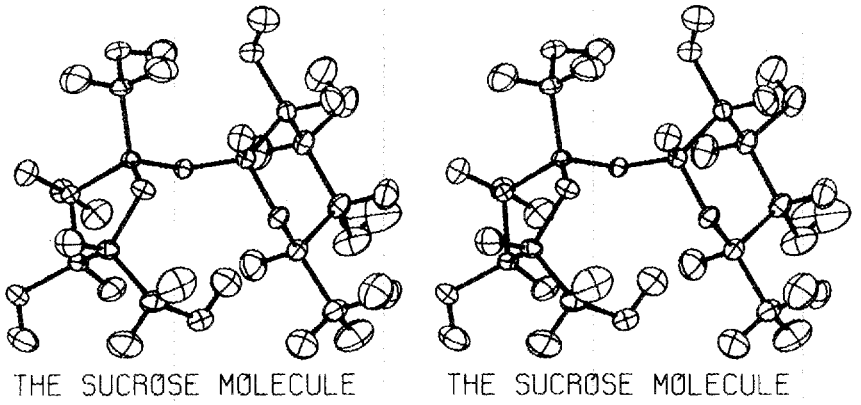

Fig. 7.10. Stereoscopic view of the sucrose molecule showing the 50% probability ellipsoids. Atoms may be identified by reference to Fig. 7.9, in which the molecular orientation is only slightly different.

Table 7.7. Description of the hydrogen bonds in sucrose

O···H···O	Sym. trans.[a]	Distances (Å)			Angle (°)
		O–H	H···O	O···O	O–H·O
Intramolecular					
O′(1)···H···O(2)	1,000	0.974	1.851	2.781	158.6
O′(6)···H···O(5)	1,000	0.972	1.895	2.850	167.1
Intermolecular					
O(2)–H···O′(6)	1,001	0.972	1.892	2.855	170.2
O(3)–H···O′(3)	2,001	0.959	1.907	2.862	172.8
O(6)–H···O(3)	2,1$\bar{1}$1	0.956	1.921	2.848	162.9
O′(3)–H···O′(4)	2,000	0.969	1.908	2.864	168.5
O′(4)–H···O′(1)	1,00$\bar{1}$	0.976	1.760	2.716	165.4
Unbonded OH					
O′(2)	1,010		2.309	2.838	116.6
O(4)–H O(3)	1,000	0.912	2.534	2.879	103.0
O(6)	2,101		2.539	3.373	152.1

[a]Symmetry transformations which generate the coordinates of the acceptor oxygen atoms. The first digit represents either (1) the position x, y, z or (2) the position $-x, y + \frac{1}{2}, -z$. The last three digits specify a lattice translation.

bonded. A drawing showing the hydrogen bonding has been published.[1,2]

1. G. M. Brown and H. A. Levy, *Chem. Div. Annu. Progr. Rep. May 20, 1963*, ORNL-3488, p. 108.
2. G. M. Brown and H. A. Levy, *Science* **141**, 921 (1963).
3. J. C. Hanson, L. C. Sieker, and L. H. Jensen, University of Washington, private communication.
4. P. Coppens and W. C. Hamilton, *Acta Crystallogr., Sect. A* **26** 71 (1970). Provision for correction for extinction by this method is incorporated in the current Oak Ridge least-squares program written by W. R. Busing, H. A. Levy, and others.
5. W. Klyne and V. Prelog, *Experientia* **16**, 521 (1960).
6. W. R. Busing and H. A. Levy, *Acta Crystalogr.* **17**, 142 (1964).
7. C. K. Johnson, *OR TEP: A Fortran Thermal Ellipsoid Plot Program for Crystal-Structure Illustrations*, ORNL-3794 (2d rev.) (1970).

SOLUTION OF THE CRYSTAL STRUCTURE OF FLUOCINOLONE ACETONIDE, A STEROIDAL ANTI-INFLAMMATORY AGENT, AND COMPARISON OF ITS MOLECULAR GEOMETRY WITH ACTIVE AND INACTIVE STEROIDS

W. E. Thiessen H. A. Levy

While engaged in a project of comparing ring conformations of medicinally active and inactive steroids, A. T. Christensen of the Syntex Research Center found that the conventional "direct-method" approach to solving crystal structures[1] did not, in his hands, elucidate the structure of fluocinolone acetonide (I), a widely used anti-inflammatory adrenocortical steroid.

Since we had previously carried out a successful "Patterson search-tangent refinement" procedure using a known molecular fragment,[2] and an accurate model of part of the known molecular structure of I was available from earlier studies,[3] Christensen kindly provided his intensity data on fluocinolone acetonide for further experimentation with Patterson search methods.

The structure was solved by a procedure closely similar to that outlined for the solution of katonic acid anomalous acetate last year,[2] assuming that the ten-atom fragment of I containing C1 through C6, C9, C10, C19, and the oxygen atom attached to C3 has the

configuration of the corresponding fragment in crystalline 2-bromo-β-santonin.[3] After refinement of atomic parameters by the method of least squares, the conventional $R(F)$ is 0.037 on 2389 reflections for which $|F|^2$ is greater than twice the value of $\sigma(|F|^2)$:

ORNL-DWG. 72-5634

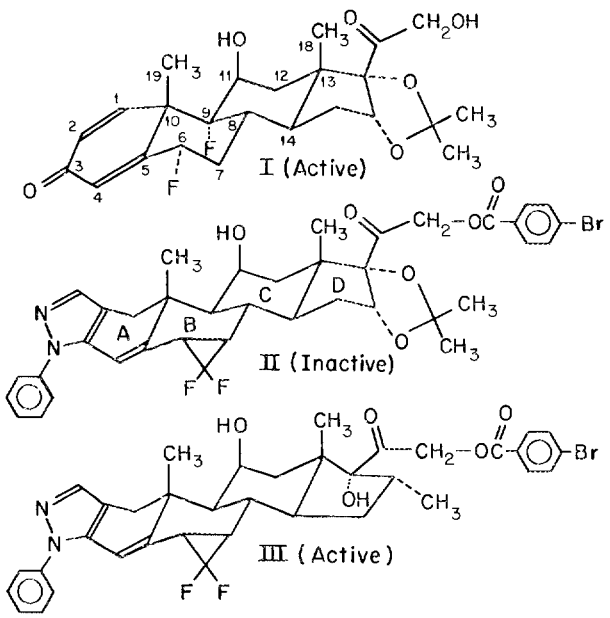

Since the presence of the 11β-hydroxyl group in ring C is known to be indispensable for corticoid activity, we have compared the conformations of ring C in fluocinolone acetonide, I, the chemically similar but inactive steroid acetonide II,[4] and the active non-acetonide III.[5] We have found an important conformational difference between the two active compounds on the one hand and the inactive compound on the other. The conformations of ring C in the three steroids are shown in Fig. 7.11. It is clear that ring C is buckled in the inactive compound II, causing the hydrogen atom on C8′ in the inactive compound (H8′ of Fig. 7.11) to be about 0.3 Å higher than is the corresponding atom H8 of the active compounds I and III. This difference in hydrogen positions is such as to suggest a blocking of access to the 11β–hydroxyl oxygen from that direction. Since access to the 11β-hydroxyl group from other directions is blocked by the methyl groups containing C18 and C19, it seems reasonable that openness of the β face of ring C could be crucial for binding of the molecule to a biochemically active site.

ORNL-DWG. 72-5633

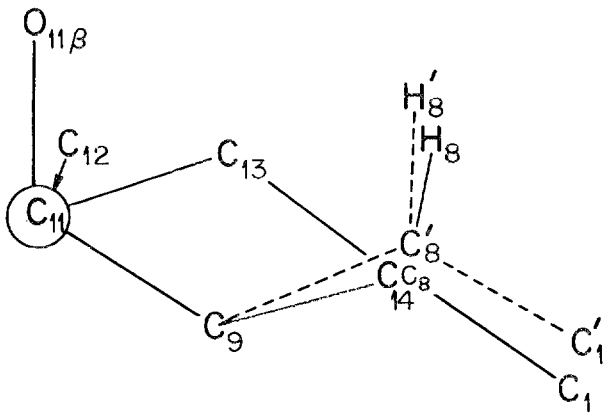

Fig. 7.11. Conformations of ring C in the steroids I, II, and III drawn so as to have C9, C11, C12, C13, C14, and O11β nearly superposed. The primed atoms and dashed lines refer to the inactive steroid II, while the unprimed atoms and solid lines refer to active steroids I and III.

1. For an example, see W. E. Thiessen, *Chem. Div. Annu. Progr. Rep. May 20, 1970,* ORNL-4581, p. 137.
2. W. E. Thiessen and H. A. Levy, *Chem. Div. Annu. Progr. Rep. May 20, 1971,* ORNL-4706, p. 183.
3. P. Coggon and G. A. Sim, *J. Chem. Soc. B* 237 (1969).
4. E. Thom and A. T. Christensen, *Acta Crystallogr., Sect. B* **27,** 573 (1971).
5. A. T. Christensen, *Acta Crystallogr., Sect. B* **26,** 1519 (1970).

STRUCTURE OF A CRYSTALLINE ACID-CATALYZED CYCLIZATION PRODUCT OF THE 14-MEMBERED RING DITERPENE HYDROCARBON, CEMBRENE

W. E. Thiessen

Certain classes of sesquiterpenoids containing two six-membered rings or one seven- and one five-membered ring are known to be formed in nature from ten-membered ring precursors.[1,2] The structures of some recently discovered di- and tricyclic diterpenes[3,4] suggest that their biogenesis proceeds through a 14-membered ring precursor. Diterpenes containing 14-membered rings have been isolated from natural sources,[3] but there has been no report of their cyclization in the laboratory to polycyclic products. Quite recently, Dauben and Oberhänsli[5] have isolated a small amount of a crystalline cyclization product from the complex reaction mixture which results when cembrene,[6] a 14-membered ring diterpene hydrocarbon

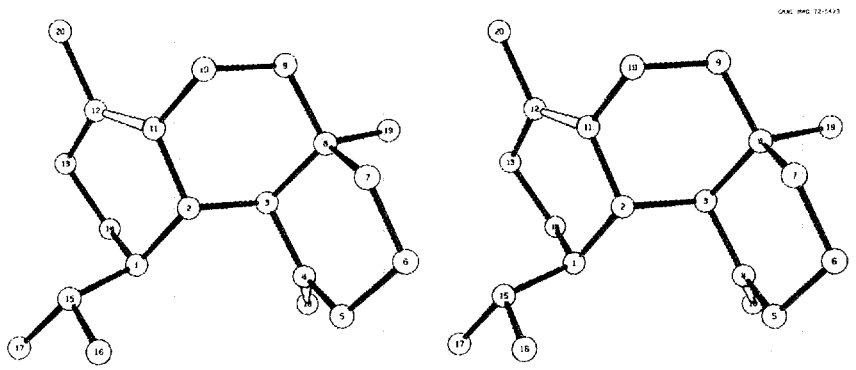

Fig. 7.12. Stereoscopic drawing of the molecule (excluding hydrogen atoms) viewed approximately along *b*. The a axis is horizontal. Atoms linked by double bonds are connected by two lines.

found in *Pinus* spp., is treated with perchloric acid in dioxane. The Raman spectrum and NMR spectrum of this product indicate the presence of only two double bonds, one tetrasubstituted and one geminally disubstituted, while its isomer cembrene has one ring and four double bonds. The cyclization product is therefore tricyclic. Because of the small yield and lack of functional groups, structural characterization of the product by chemical and spectral means would have been extremely difficult, and crystal structure analysis seemed a more fruitful approach.

Crystals of the cyclization product are monoclinic with the symmetry of space group $P2_1$; the unit cell containing two molecules has parameters $a = 9.1110(4)$ Å, $b = 11.3870(10)$ Å, $c = 8.9159(6)$ Å, and $\cos\beta = -0.32575(7)$ at 24°C. The structure was solved from 2014 independent reflections measured on the Oak Ridge computer-controlled x-ray diffractometer by the Patterson search procedure outlined in the 1971 report.[7] The six carbon atoms of the tetrasubstituted double bond were selected as a known fragment in the Patterson search; however, the procedure actually yielded another fragment, a tetrasubstituted ethane near the center of the molecule. Extension by means of the tangent formula of the phases calculated for selected reflections[8] developed the entire structure. After refinement of the atom parameters by the method of least squares, the current value of $R(F)$ is 0.04.

A stereoscopic view of the carbon skeleton of the cembrene cyclization product consistent with the known[6] absolute configuration of cembrene is shown in Fig. 7.12. A credible scheme for its formation via a dicyclic intermediate is displayed in Fig. 7.13. To yield the stereochemical arrangement observed in the final product (III), the 3,4 double bond in the dicyclic

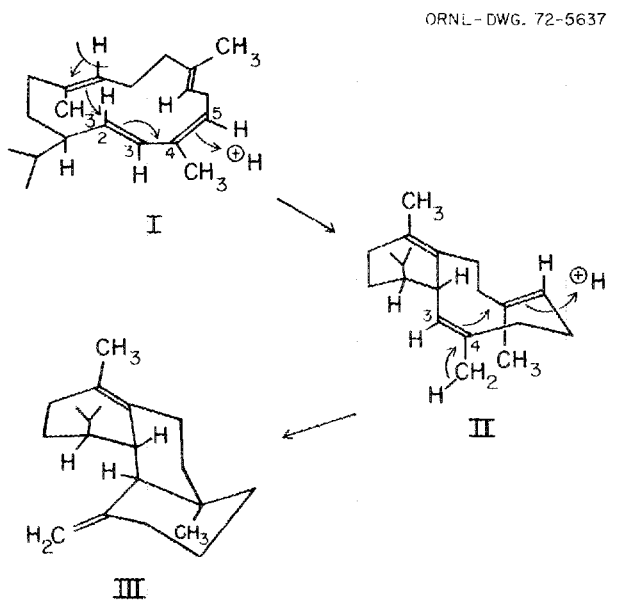

Fig. 7.13. A two-step scheme for the acid-catalyzed cyclization of cembrene.

intermediate (II) must have been *cis*, which in turn implies a *cisoid* relationship between the 2,3 and 4,5 double bonds in cembrene (I) immediately before the initial cyclization step. This conformation of cembrene is different from the *transoid* one found in crystalline cembrene[9] but can arise by a simple rotation about the 3,4 single bond. It should be noted that no compound containing the carbon skeleton of III has yet been found in nature, indicating that cembrene itself is not a biogenetic procursor of any known polycyclic diterpene.

1. J. B. Hendrickson, *The Molecules of Nature*, p. 36, Benjamin, New York, 1965.
2. J. B. Hendrickson, *Tetrahedron* **7**, 82 (1959).
3. R. McCrindle and K. H. Overton, "The Diterpenoids, Sesterpenoids and Triterpenoids," chap. 14 in *Rodds Chemistry of Carbon Compounds*, 2d ed., S. Coffey, ed., Elsevier, New York, 1969.
4. D. H. Eyre, J. W. Harrison, and B. Lythgoe, *J. Chem. Soc. C* 452 (1967).
5. W. G. Dauben and P. Oberhänsli, private communication. We are indebted to these workers for providing the crystals for this structure determination.
6. W. G. Dauben, W. E. Thiessen, and P. R. Resnick, *J. Org. Chem.* **30**, 1693 (1965).
7. W. E. Thiessen and H. A. Levy, *Chem. Div. Annu. Progr. Rep. May 20, 1971*, ORNL-4706, p. 183.
8. J. Karle, *Acta Crystallogr., Sect. B* **24**, 182 (1968).
9. M. G. B. Drew, D. H. Templeton, and A. Zalkin, *Acta Crystallogr., Sect. B* **25**, 261 (1969).

A METHOD FOR PREDICTING THE CONFORMATION OF AN ISOLATED MOLECULE FROM ITS CRYSTAL STRUCTURE

W. R. Busing W. E. Thiessen

In earlier reports[1,2] we described calculations of the minimum energy of nor-β-cubebone (N-β-C) (Fig. 7.14) both for the crystalline state and for the isolated molecule. The purpose of that work was to estimate the effect of crystal packing on the conformation of the isopropyl group. The molecule was assumed to be composed of four rigid segments, and only three intramolecular rotations were permitted.

We have now extended that work, assuming a completely flexible molecule in order to assess the effects of packing on the ring conformations and other details of the molecular geometry. The energy of either the isolated molecule or the crystal is assumed to have the form

$$\sum_{ij} - D_i D_j / r_{ij}^6$$

$$+ \sum_{ij} (B_i + B_j) \exp\left[(A_i + A_j - r_{ij})/(B_i + B_j)\right]$$

$$+ \sum_{ij} (k_{ij}/2)(r_{ij} - r_{ij}^0)^2$$

$$+ \sum_{ijk} (k_{ijk}/2)(a_{ijk} - a_{ijk}^0)^2$$

$$+ \sum_{ijkl} (V/6) \cos 3\phi_{ijkl}$$

$$+ (k_\Delta/2)(|\phi_\Delta| - \pi)^2 .$$

The first two sums are over both intermolecular and intramolecular nonbonded pairs and represent van der Waals attraction and nonbonded repulsion respectively. The next three sums are over bond distances r_{ij}, bond angles a_{ijk}, and conformation angles ϕ_{ijkl} (for $|\phi_{ijkl}| < \pi/3$) respectively. The final term involves ϕ_Δ, the conformation angle between the carbonyl group and a bisector of the cyclopropane ring, and reflects the partial double-bond character of the C(4)–C(5) bond.

Values for 19 of the 30 parameters in this expression were determined from the molecular geometries and vibrational frequencies of ethane, propane, cyclopropane, and acetone.[3] Theoretical values were used for seven more constants, and the remaining four were determined from the packing and geometry of N-β-C.

Starting with the experimental crystal structure[4] of N-β-C, the energy of the model was minimized by varying 114 structural parameters: the coordinates of the 37 atoms and the three lattice constants. The calculation was repeated for the isolated molecule, varying $3 \times 37 - 6 = 105$ coordinates.

For the comparison of molecular geometries the most sensitive quantities are the conformation angles about the carbon-carbon bonds. Some of these are listed in Table 7.8 for the observed crystal structure, the calculated crystal structure, and the calculated structure of the isolated molecule. Comparison of the first two columns provides a test of the model, and comparison of the last two yields a measure of the effect of intermolecular forces on the molecule. Root-mean-square differences of these angles are also included in the table.

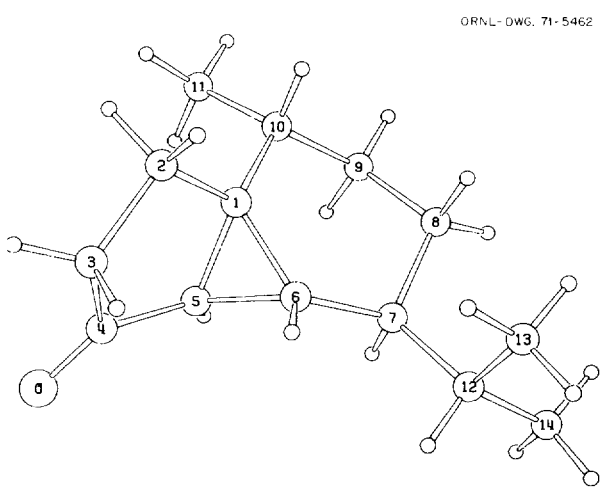

Fig. 7.14. Perspective drawing of the nor-β-cubebone molecule. The carbon atoms are numbered, the single oxygen atom is labeled O, and the hydrogen atoms are unlabeled.

Table 7.8. Some conformation angles of the nor-β-cubebone molecule (deg)

The angles are described in terms of the atom numbers in Fig. 7.14

Angle	Observed (crystal)	Calculated (crystal)	Calculated (molecule)
Six-membered ring			
10-1-6-7	−5.5	−5.4	−4.8
1-6-7-8	24.1	24.1	22.5
6-7-8-9	−53.3	−52.9	−51.8
7-8-9-10	67.3	65.4	65.3
8-9-10-1	−45.5	−43.9	−44.7
9-10-1-6	15.3	14.5	15.2
RMS differences	1.1	0.9	
Five-membered ring			
5-1-2-3	14.0	6.7	−0.5
1-2-3-4	−22.3	−15.1	−5.8
2-3-4-5	23.0	18.5	10.3
3-4-5-1	−14.4	−14.4	−10.6
4-5-1-2	0.0	4.4	6.7
RMS differences	5.4	6.7	
Isopropyl group			
6-7-12-13	−66.9	−68.8	−67.7
6-7-12-14	166.5	164.4	165.5
8-7-12-13	58.2	57.4	58.7
8-7-12-14	−68.4	−69.4	−68.1
RMS differences	1.6	1.2	

For the six-membered ring the RMS difference between the observed and calculated conformation angles in the crystal is only 1.1°, indicating that the model represents this ring quite satisfactorily. The RMS difference between the calculated angles in the crystal and in the isolated molecule is 0.9°, so that intermolecular forces have little effect on the conformation of this ring. The results lead to similar conclusions for the isopropyl group.

For the five-membered ring, however, we find the observed and calculated conformation angles for the crystal have an RMS difference of 5.4°, indicating that the model is much less satisfactory for this ring. A new torsional potential which may yield an improved fit is described below.[5]

The five-membered ring also shows an RMS difference of 6.7° between the calculated angles for the crystal and for the isolated molecule. This may mean that the geometry of this part of the molecule is appreciably affected by intermolecular forces. In fact, the crystal has a short H···H contact which tends to pucker the ring. This interpretation should be regarded as tentative, however, until calculations with an improved model are completed.

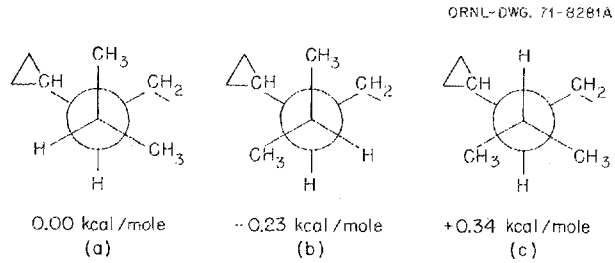

Fig. 7.15. Relative stabilities of rotational isomers calculated for the isolated molecule of nor-β-cubebone. The observed isomer is shown in (*a*) and the two alternative forms in (*b*) and (*c*).

The energy of the isolated molecule was also minimized for the two alternative rotational positions of the isopropyl group, and the calculated energy differences are shown in Fig. 7.15. These differences are small compared with RT at room temperature, so that in the gas phase there would be an appreciable fraction of each isomer with form (*b*) predominating. Form (*a*) is stable in the crystal, presumably because of packing considerations. Our earlier conclusion[1] that form (*a*) would be stable for the isolated molecule was based on the unrealistic assumption that the segments of the isopropyl group could be treated as rigid.

1. W. R. Busing and W. E. Thiessen, *Chem. Div. Annu. Progr. Rep. May 20, 1971*, ORNL-4706, p. 202.
2. W. R. Busing, ibid., p. 201.
3. W. R. Busing, ibid., p. 203.
4. W. E. Thiessen, *Chem. Div. Annu. Progr. Rep. May 20, 1970*, ORNL-4581, p. 140.
5. W. R. Busing, "A New Form for the Torsional Potential in Molecules," the following contribution, this report.

A NEW FORM FOR THE TORSIONAL POTENTIAL IN MOLECULES

W. R. Busing

A potential of the form

$$V = (V_0/2)(1 + \cos 3\phi) \qquad (1)$$

has often been used in the study of hindered rotation in ethane-like molecules.[1,2] Here ϕ is a conformation angle and V_0 is the height of the barrier to internal rotation. Spectroscopic and thermodynamic experiments yield information about the shape of the

potential near its minima, and the barrier height is derived from the assumed form of the curve.

The potential (1) is commonly used in calculations of the conformation of large molecules,[3,4] but it is not always clear how the conformation angle ϕ should be chosen when the molecule lacks threefold symmetry about the bond in question. In recent work of this kind, Busing and Thiessen[5] used a segmented cosine potential

$$V = (V_0/6) \sum_i (1 + \cos 3\phi_i) , \qquad (2)$$

where the sum is over those conformation angles ϕ_i for which $|\phi_i| \leqslant \pi/3$. For the torsional oscillation of ethane, potential (2) reduces to form (1). Unfortunately this segmented cosine potential has discontinuous second derivatives which lead to difficulties in the calculation of some other normal modes of vibration for ethane.

Another problem found by Busing and Thiessen[5] is that, although potential (2) gives a good prediction of the conformation of a six-membered ring which is relatively free of strain, it gives a poorer fit for a five-membered ring which is more strained and more nearly planar. This implies that potential (2) may be approximately correct near the energy minima but unsatisfactory near the barrier maxima.

A potential which seems to overcome all of these difficulties has the form

$$V = a \sum_i G(\phi_i, b) , \qquad (3)$$

where the summation is over all conformation angles ϕ_i. The function

$$G(\phi_i, b) \equiv \sum_{n=-\infty}^{\infty} \exp\left[-(\phi_i - 2\pi n)^2/2b^2\right]$$

is known as a "wrapped-up" Gaussian function, because the summation over n causes the tails of the exponential at $\phi_i \pm 2\pi n$ to be added to the function, thus eliminating discontinuities. For ethane, potential (3) reduces identically to the form (1) (except for an added constant) as b becomes large.[6] The two parameters a and b allow both the curvature at a potential minimum and the barrier height to be adjusted independently. This potential will be used in further efforts to explain the conformations of molecules involving five-membered rings.

1. K. S. Pitzer, *Discuss. Faraday Soc.* **10**, 66 (1951).
2. W. G. Dauben and K. S. Pitzer, p. 54 in *Steric Effects in Organic Chemistry*, M. S. Newman, ed., Wiley, New York, 1956.
3. D. A. Buckingham and A. M. Sargeson, p. 219 in *Topics in Stereochemistry*, vol 6, N. L. Allinger and E. L. Eliel, eds., Wiley-Interscience, New York, 1971.
4. N. C. Cohen, *Tetrahedron* **27**, 789 (1971).
5. W. R. Busing and W. E. Thiessen, "A Method for Predicting the Conformation of an Isolated Molecule from Its Crystal Structure," the previous contribution, this report.
6. M. A. Stephens, *Biometrika* **50**, 385 (1963).

ANALYTICAL APPROXIMATION FOR THE CRYSTALLOGRAPHIC LEAST-SQUARES MATRIX

C. K. Johnson

The results of a recent survey[1] of crystallographic computing needs and resources in the U.S. show that the structure-refinement step in crystal-structure analysis accounts for 80 to 90% of the computing time used by crystallographers. Further analysis reveals that the method of least squares is the principal refinement technique and that most of the computing time is spent building the matrix of normal equations which often fills the available computer memory. The question "How can this calculation be shortened?" is of considerable economic importance. The frequently tried procedure of omitting large segments of off-diagonal terms usually does not reduce the overall computing time, because additional cycles of refinement are required to reach convergence. We decided to try a completely different approach to the problem by utilizing some special mathematical properties of the crystallographic matrix to replace the time-consuming numerical summation by an equivalent analytical integration. The following assumptions are needed to derive the expressions for the analytical matrix:

1. The least-squares weighting scheme is chosen so that the variance of each observation F^2 is proportional to its magnitude. This is a correct weighting scheme for the idealized case where intensity background corrections are negligible.

2. The scattering factor product for any pair of atoms is approximated by a short sum of isotropic Gaussian functions. Analytical expressions of this type for individual atom scattering factors often are used for crystallographic computing.

3. The origin of the unit cell is on a crystallographic center of symmetry. This condition restricts the treatment to centrosymmetric space groups.

By incorporating these restrictions, we can write a simplified equation for any element in the crystallographic matrix L. For example, in space group $P\bar{1}$, the equation for the interaction term relating the ith component of the position vector $\mathbf{x}_m$ for atom m and

the jth component (i,j = 1,2,3) of the corresponding vector for atom n is

$$L(x_m^i, x_n^j) = K \sum_{\mathbf{y}} \sum_p \alpha_p \left[\sum_{\mathbf{q}} q_i q_j \exp(-\mathbf{q}'M\mathbf{q}/2) \cos(\mathbf{q}'\mathbf{y}) \right], \quad (1)$$

with the matrix M defined as

$$M \equiv \beta_p G + (B_m + B_n)/2\pi^2 . \quad (2)$$

In these equations, K is a constant, $\mathbf{y}$ is an interatomic vector between atoms on crystallographic sites m and n, $\mathbf{q}$ is a reciprocal-lattice vector, B_m and B_n are anisotropic temperature-factor matrices for atoms m and n, G is the metric matrix, and the scalar quantities α_p and β_p are coefficients in the Gaussian expansion of the scattering factor product for the atom pair m,n. If the summation in brackets is replaced by an integration over all of reciprocal space, we obtain

$$L(x_m^i, x_n^j) = K \sum_{\mathbf{y}} \sum_p \alpha_p [-|M|^{-1/2} H_{ij}(\mathbf{y}, M^{-1}) \exp(-\mathbf{y}'M^{-1}\mathbf{y})] , \quad (3)$$

with

$$H_{ij}(\mathbf{y}, M^{-1}) \equiv z_i z_j - M_{ij}^{-1} \quad \text{and} \quad \mathbf{z} \equiv M^{-1}\mathbf{y} .$$

The tensor component H_{ij} is a second-order three-dimensional Hermite polynomial.[2] Corresponding formulations for the position-thermal and the thermal-thermal interaction equations have the same form as the position-position equation shown in (3), except that the second-order H_{ij} is replaced by the third- and fourth-order polynomials H_{ijk} and H_{ijkl} respectively.

Equation (3) represents the asymptotically limiting situation which is realized only when the entire data set has been included. A more common experimental practice is spherical truncation of the data set at some fixed value of $|\mathbf{q}|$. When the temperature factors for the atoms are isotropic and the truncation is spherical, the finite summation over $\mathbf{q}$ in Eq. (1) can be replaced by an integration which has an analytical solution involving Legendre polynomials and error functions. An exact solution for the general case with anisotropic temperature factors has been elusive, but some success has been achieved with empirical correction terms for the spherical truncation.

Evaluation of the technique is under way. With favorable conditions (i.e., low crystallographic symmetry and extensive diffraction data), the computing time can be reduced by an order of magnitude. A novel application of the technique is the generation of the complete variance-covariance matrix for a published structure when the structural parameters are given but the diffraction data are not. The variance-covariance matrix can then be used in calculating the standard errors of various mathematical functions involving the structural parameters.

The equations given here can also be used to establish rigorously the formulism for reporting the precision of crystal-structure parameters described last year.[3]

---

1. W. C. Hamilton, introductory remarks at symposium on *Computational Needs and Resources in Crystallography*, Albuquerque, New Mexico, April 8, 1972.

2. S. Berkowitz and F. J. Garner, *Math. of Computation* **24**, 537 (1970).

3. C. K. Johnson, *Chem. Div. Annu. Progr. Rep. May 20, 1971*, ORNL-4706, p. 205.

LIQUID WATER: ATOM-PAIR CORRELATION FUNCTIONS FROM NEUTRON AND X-RAY DIFFRACTION[1]

A. H. Narten H. A. Levy

Coherent neutron scattering from deuterium oxide is largely determined by interactions involving deuterium nuclei, in contrast to x-ray scattering, for which oxygen atom pairs are of overriding importance. Consequently, x-ray and neutron data from heavy water are ideally complementary, the former disclosing the positional correlation among molecular centers, and the latter additionally disclosing orientational correlation between molecule pairs. Earlier results[2] derived from the x-ray diffraction pattern of water at 25°C have shown that positional correlation between oxygen atoms extends out to 8 Å separation.

Neutron diffraction data have been obtained with a computer-controlled diffractometer at the ORR. The results clearly indicate that orientational correlation between molecules extends only to separations of about 5 Å (see Fig. 7.16). A model has been devised which ascribes the orientational correlation to nearest-neighbor molecular pairs only, random mutual orientation being assumed for second and higher neighbors. This model adequately explains the neutron diffraction pattern; as shown in Fig. 7.17, it consists of tetrahedrally coordinated water molecules, each near-

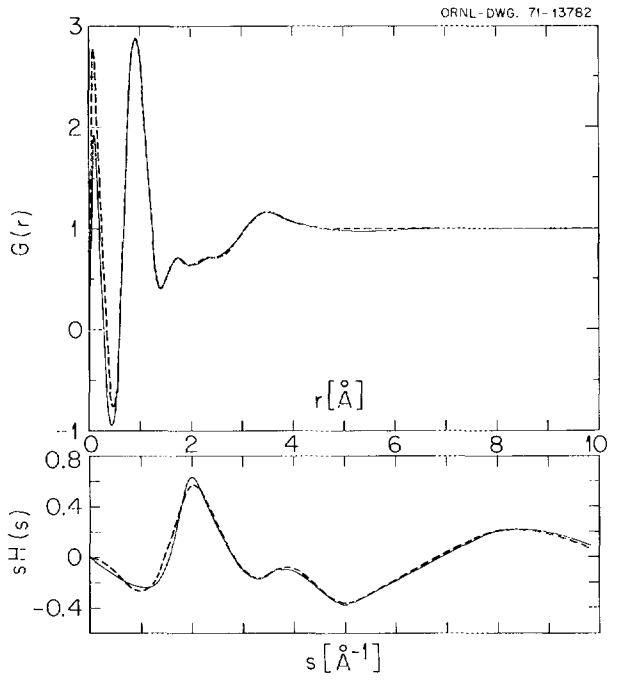

Fig. 7.16. Weighted structure functions (bottom) and correlation functions (top) for D_2O at 25°C. Solid curves are derived from neutron data. Dashed curves were calculated for the near-neighbor model shown in Fig. 7.17.

ORNL-DWG. 71-13781

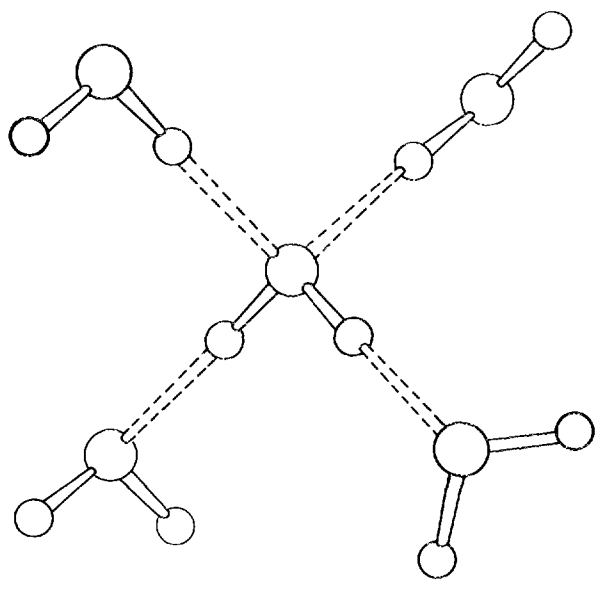

Fig. 7.17. Model for the average orientation of pairs of near-neighbor molecules in water. Large local and instantaneous deviations from this average configuration occur in the liquid.

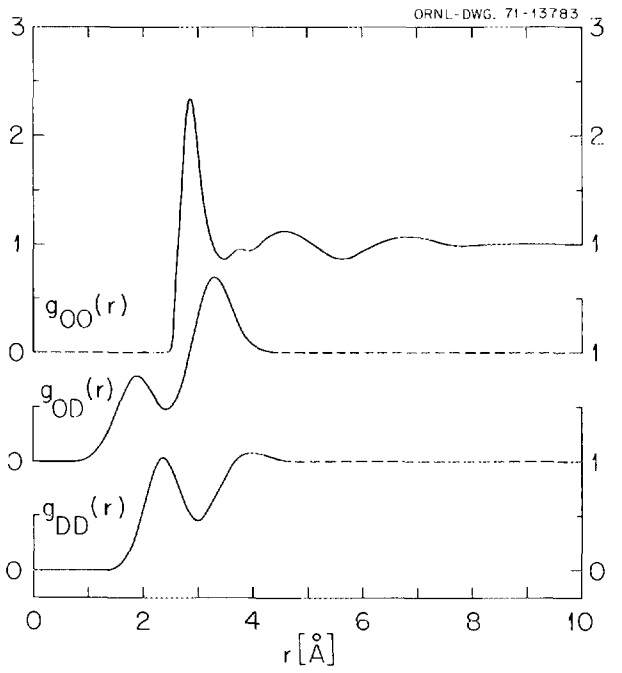

Fig. 7.18. Atom-pair correlation functions for liquid water at 25°C derived from combined x-ray and neutron scattering data.

neighbor pair being connected by a hydrogen bond which is straight on the average.

The neutron diffraction pattern indicates that the geometric structure of water molecules in the liquid is not significantly different from that in the dilute gas. However, the distribution of displacements from the average is much broader than in the gas, probably reflecting a distribution of local environments.

Atom-pair correlation functions have been extracted from the combined x-ray and neutron data (Fig. 7.18) and prove to be in qualitative agreement with correlation functions obtained by molecular dynamics calculations.[3] These results are sufficiently accurate to provide a sensitive test for molecular theories of liquid water.

1. Expanded abstract of published paper: A. H. Narten, *J. Chem. Phys.* **56**, 5681 (1972).
2. A. H. Narten and H. A. Levy, *J. Chem. Phys.* **55**, 2263 (1971).
3. A. Rahman and F. H. Stillinger, *J. Chem. Phys.* **55**, 3336 (1971).

TOWARD A MOLECULAR THEORY FOR THE STRUCTURE OF LIQUID WATER

L. Blum[1] A. H. Narten

For many purposes, the structure of liquid water can be described by a molecular pair correlation function

$g(\mathbf{r},\Omega)$, the vector $\mathbf{r}$ and three Euler angles $\Omega = (\alpha,\beta,\gamma)$ specifying the mutual configuration of pairs of molecules. The function $g(\mathbf{r},\Omega)$, not in general accessible from one-dimensional diffraction data, can be expressed as a series expansion.[2] From the coefficients of such an expansion the atom pair correlation functions can be calculated and can be compared with those derived from scattering experiments.[3]

By means of group theoretical arguments, a new expansion for the correlation functions descriptive of fluids with nonspherical molecules has been formulated.[4,5] The main feature of this expansion is a closed-form definition, not previously achieved, of the so-called direct correlation function.[6] Most of the successful theories of fluids with spherical molecules regard the direct correlation function as a central quantity and provide closure relations for the Ornstein-Zernike (O.Z.) equation.[6] In the nonspherical case, the defining matrix equation[5] is closely similar to the O.Z. equation for fluids with spherical molecules. The dimensions of the matrices are small; for example, a fluid with polarizable molecules subject to dipole and quadrupole forces will give a set of maximum dimension 6.

The problem of the structure of liquid water is of enormous complexity. To make progress, a simplified approach has been adopted as a first step toward its solution.

The first simplification concerns the potential describing the interaction between pairs of water molecules. Ben-Naim and Stillinger[7] have shown that a modified Bjerrum potential exhibits the known tendency toward tetrahedral coordination, and fits the measured second virial coefficient of water vapor reasonably well. Rahman and Stillinger[8] have used this potential in molecular dynamics calculations, and their results are in good qualitative agreement with many properties of liquid water. The Stillinger–Ben-Naim (S.B.) potential has therefore been adopted as a reasonably realistic and tractable description for the interaction between pairs of water molecules.

The second simplification concerns the relationship between the model potential and the direct correlation function. The first attempt, in progress now, is to use the mean spherical model (MSM) of Lebowitz and Percus.[9] The MSM is a linearized model in which the potential is the sum of two parts: a short-range, spherically symmetric, central hard core, plus a long-range, nonspherical part. The MSM then assumes that the direct correlation function is linearly related to the interaction potential outside the hard core. This model has been solved in closed form[5] for systems of spheres with electrostatic multipolar interactions. It has also been shown[10,11] that the MSM is a useful theory of liquids involving molecules with long-range interactions.

The S.B. potential is expandable in multipoles, and a direct check of the simplified theory against the molecular dynamics results is thus possible. Numerical work has shown that only a few of the low-order coefficients of such a multipole expansion are needed to represent the S.B. potential for liquid water. This result, together with the fact that the form of the potential admits an exact solution of the MSM integral equation, makes a numerical test of the model relatively simple.

Should the test of the MSM against the molecular dynamics calculations be successful, a search will be made for the potential which fits the largest amount of experimental information. If the model is unsatisfactory, improved theories will be tried.

---

1. Oak Ridge Associated Universities Research Participant from the University of Puerto Rico, Rio Piedras, summer 1969.
2. W. A. Steele, *J. Chem. Phys.* **39**, 3197 (1963).
3. A. H. Narten and H. A. Levy, "Liquid Water: Atom-Pair Correlation Functions from Neutron and X-Ray Diffraction," the preceding contribution, this report.
4. L. Blum and A. J. Toruella, *J. Chem. Phys.* **56**, 303 (1972).
5. L. Blum, *J. Chem. Phys.*, in press.
6. H. L. Frisch and J. L. Lebowitz, *The Equilibrium Theory of Classical Fluids*, Benjamin, New York, 1964.
7. A. Ben-Naim and F. H. Stillinger, *Water and Aqueous Solutions*, R. A. Horne, ed., p. 295, Wiley, New York, 1972.
8. A. Rahman and F. H. Stillinger, *J. Chem. Phys.* **55**, 3336 (1971).
9. J. L. Lebowitz and K. K. Percus, *Phys. Rev.* **144**, 251 (1966).
10. E. Waisman and J. L. Lebowitz, *J. Chem. Phys.* **52**, 4307 (1970).
11. L. Blum and A. H. Narten, *J. Chem. Phys.*, in press.

INFRARED AND RAMAN SPECTROSCOPY

RAMAN SPECTRA OF MOLTEN ALKALI-METAL CARBONATES[1]

J. B. Bates[2] A. S. Quist[2]
M. H. Brooker[2,3] G. E. Boyd[2]

Raman spectra of molten Li_2CO_3 (mp = 726°C) and of Li_2CO_3–60 mole % LiCl, Li_2CO_3–33 mole % $CaCO_3$, Na_2CO_3–57 mole % NaCl, and K_2CO_3–65 mole % KCl eutectic mixtures were measured from 150 to 2000 cm^{-1} because of a practical interest in carbonate melts and because of a basic problem

concerning the structure of molten alkali-metal nitrates. Molten alkali-metal carbonates recently have found application in the North American–Rockwell process for the removal of sulfur oxide from fossil fuel stack gases, and in the gasification of coal by the Lurgi-Kellogg process; hence, their physical and chemical properties are of interest. Vibrational spectra of the carbonate ion in ionic melts also are of fundamental interest from the standpoint of determining the magnitudes and causes of the spectral perturbations in this and other small polyatomic anions in the molten state. Numerous investigations of the Raman and infrared spectra of alkali-metal nitrates from dilute solutions to molten salts have shown that there is an apparent breakdown in the "free ion," D_{3h}, selection rules: the $\nu_1(A_1')$ mode of NO_3^- becomes infrared active, the $\nu_3(E')$ mode is split, and two bands are observed in the $\nu_4(E')$ region for $LiNO_3$ and $NaNO_3$ melts. Similar effects were anticipated for CO_3^{2-} ion in aqueous solution and molten salts.

Raman spectra of molten Li_2CO_3 and Li_2CO_3-LiCl eutectic are shown in Fig. 7.19 as an example of a part of our work. Band frequencies and assignments observed in the molten salt and aqueous solution spectra of these and other carbonates are presented in Table 7.9. Not unexpectedly, there appears to be a breakdown in the D_{3h} selection rules for CO_3^{2-} ion in these media. Contrary to strict selection rules, the $\nu_1(A_1')$ symmetric stretching mode appeared in the infrared spectra of saturated aqueous Na_2CO_3 and K_2CO_3 solutions, the $\nu_2(A_2'')$ bending mode was observed in the 870–880 cm^{-1} region of the Raman spectrum of the Li_2CO_3 and Na_2CO_3 melts, and the $\nu_3(E')$ antisymmetric stretching mode was split in spectra of the aqueous solutions as well as in the melt. The ν_3 splitting decreased from a maximum value of about 92 cm^{-1} in the Li_2CO_3-$CaCO_3$ eutectic to a minimum of about 27 cm^{-1} in the K_2CO_3-KCl eutectic. Further, the frequencies of two ν_3 components observed in the infrared

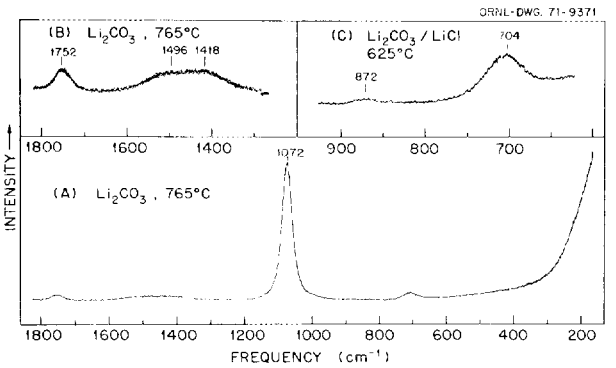

Fig. 7.19. Raman spectra of molten Li_2CO_3 at 765°C and molten Li_2CO_3-LiCl eutectic mixture (60 mole % LiCl) at 625°C.

Table 7.9. Bands observed in the Raman spectra of molten and aqueous carbonates

Assignment	Frequency (cm^{-1})[a,b]						
	Li_2CO_3			Na_2CO_3		K_2CO_3	
	Pure (765°C)	LiCl[c] (625°C)	$CaCO_3$[c] (775°C)	NaCl[c] (745°C)	Aq. soln. (25°C)	KCl[c] (670°C)	Aq. soln. (25°C)
$\nu_1(A_1')$	1072 s,p	1074 s,p	1072 s,p	1050 s,p	1067 s,p [1063][d]	1040 s,p	1064 s,p [1065]
$\nu_2(A_2'')$	878 vw	872 vw	874 vw	880 vw	[880]	n.o.	[882]
$\nu_3(E')$	1496 m	1496 m	1510 m	1440 m	1412 m [1405]	1407 m	1432 [1410]
	1418 m	1422 m	1418 m	1400 m	1380 m [1360]	1380 m	1389 [1355]
$\nu_4(E')$	702 w	704 w	712 w	695 w	681 w	687 w	686 w
$2\nu_2$	1752 w	1748 w	1742 w	1758 w	n.o.	1764 w	n.o.

[a]Frequency accuracy: ν_1 (±2), ν_2 (±5), ν_3 (±10), ν_4 (±5), $2\nu_2$ (±5).

[b]s = strong; m = medium; w = weak; v = very; p = polarized; n.o. = band not observed.

[c]Eutectic compositions: Li_2CO_3-LiCl (60 mole % LiCl, mp = 506°C); Li_2CO_3-$CaCO_3$ (33 mole % $CaCO_3$, mp = 662°C); Na_2CO_3-NaCl (57 mole % NaCl, mp = 640°C); K_2CO_3-KCl (65 mole % KCl, mp = 630°C).

[d][ ] indicates an infrared value.

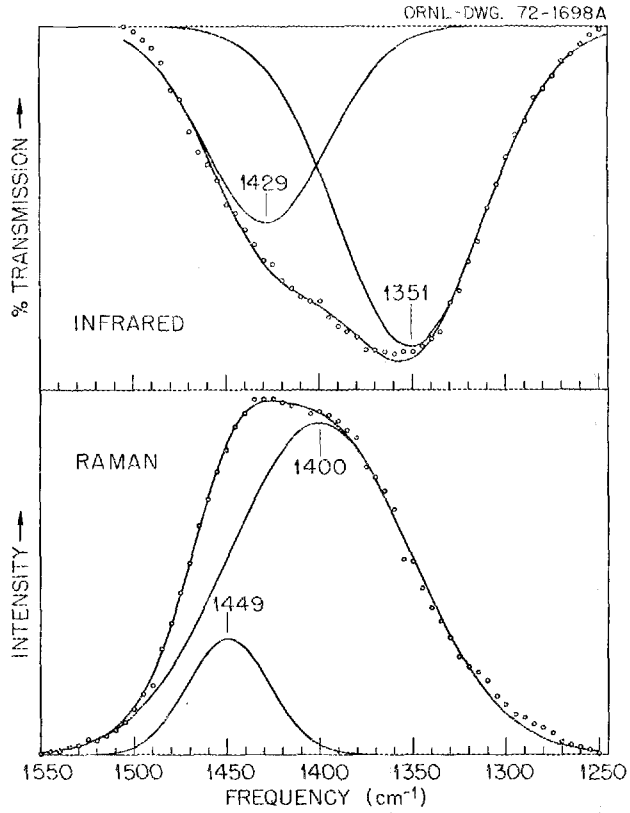

Fig. 7.20. Resolution of ν_3 band envelope observed from Raman and infrared spectra of aqueous K_2CO_3 using nonlinear least-squares computer techniques. Points represent experimental values, and curves are least-squares calculations.

spectra of Na_2CO_3 and K_2CO_3 (see Fig. 7.20) in aqueous solution were not coincident with those of the two components in the Raman spectra of the same solutions.

The splitting of ν_3 in melts with molecular ions of D_{3h} symmetry has been ascribed to (1) a lowering of the free ion symmetry by forming cation-anion contact pairs, (2) dynamic coupling of correlated motions of the ions in a unit cell possessing a quasi-crystalline structure, (3) longitudinal optical–transverse optical mode effects which also require a lattice model for molten salts, (4) local field anisotropy, and (5) vibrational-rotational coupling interactions. None of these hypotheses appears to be adequate to explain the data for nitrate and for carbonate ions in melts and aqueous solutions, because they do not account for the lack of coincidence in the frequencies of the infrared and Raman active components of ν_3.

1. Expanded abstract of published paper: *J. Phys. Chem.* 96, 1565 (1972).

2. Director's Division.

3. Present address: Chemistry Department, Mount Allison University, Sackville, N.B., Canada.

RAMAN SPECTRA OF $Be_2F_7^{3-}$ AND HIGHER POLYMERS OF BERYLLIUM FLUORIDES IN THE CRYSTALLINE AND MOLTEN STATES

L. M. Toth[1] J. B. Bates[1]
G. E. Boyd[1]

The tendency of BeF_2 to form extensive three-dimensional networks of -Be-F-Be-F- chains in its crystalline and glassy states has been shown by x-ray diffraction measurements.[2] Presumably, molten BeF_2 also is highly associated, as may be inferred from its Raman spectrum[3] and from its very large viscosity. According to Baes' polymer model,[4] the addition of basic fluoride such as LiF to molten BeF_2 is believed to cause breakage of the network links by supplying extra F^-:

$$-\overset{|}{\underset{|}{Be}}\cdots F\cdots\overset{|}{\underset{|}{Be}}\cdots + F^- \rightleftharpoons [-\overset{|}{\underset{|}{Be}}-F]^{1/2-} + [F-\overset{|}{\underset{|}{Be}}\cdots]^{1/2-} . \quad (1)$$

If an excess of fluoride ion is added, a complete disruption of the network results and free BeF_4^{2-} ions are formed.

Although Raman spectra for the two extremes in the BeF_2 system have been reported,[3,5] that is, that of pure molten BeF_2 and that of BeF_4^{2-}, no evidence has been given to support the polymer model mechanism of Eq. (1) which occurs for intermediate compositions. This region of the phase diagram is the subject of the following discussion, which includes Raman spectra in support of the polymer formation mechanism.

The approach taken was to identify simple species occurring during initial polymerization stages by comparing the Raman spectra of melts with those of known species found in solid crystalline compounds. The ion, $Be_2F_7^{3-}$, representing the first step in the polymerization process, was sought in a number of alkali-metal-fluoride, BeF_2 mixed-salt compounds.[6] Single crystals of the congruently melting compound, $Na_2LiBe_2F_7$, were grown, and, from an x-ray structure determination,[7] the presence of $Be_2F_7^{3-}$, consisting of two Be-F tetrahedra sharing a corner and having approximate C_{2v} symmetry, was verified.

The Raman spectrum of polycrystalline $Na_2LiBe_2F_7$ at 77°K is shown in Fig. 7.21. The strong band at 522

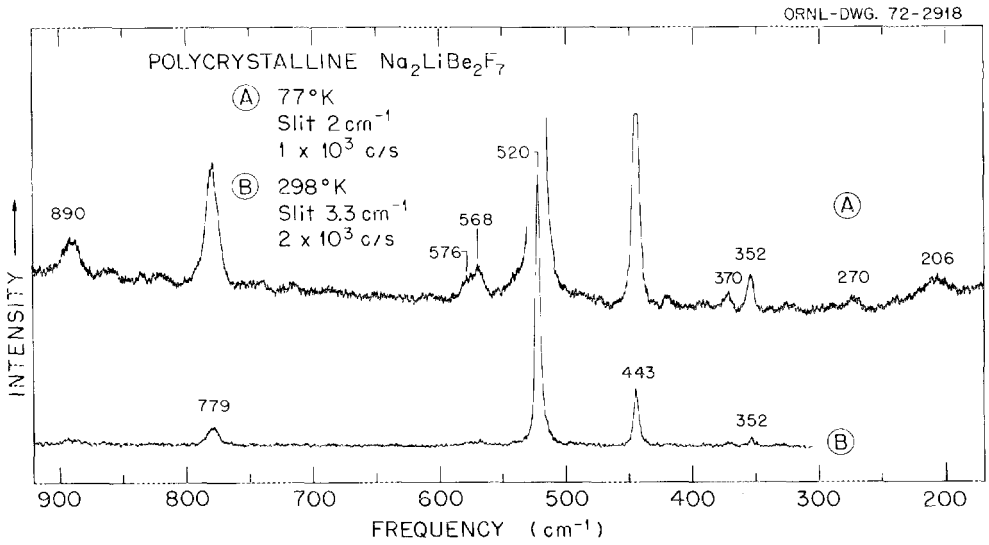

Fig. 7.21. Raman spectrum of polycrystalline $Na_2LiBe_2F_7$ at 77°K. Curve *A*, full scan at normal scale; curve *B*, expanded scale to show weaker modes.

cm^{-1} is assigned to the symmetric stretching mode involving both the bridging Be-F and the terminal Be-F bonds. This mode is related to the symmetric stretch of BeF_4^{2-} at 550–560 cm^{-1} but, it should be noted, is displaced to lower frequencies. Extensive usage of this frequency shift was made in characterizing the beryllium fluoride species as the melt compositions changed, based on the interpretation that an increase in the extent of the beryllium fluoride network formation is represented by progressively lower frequency values for the symmetric vibrational mode.

When $Na_2LiBe_2F_7$ is melted, an additional Raman band at 550 cm^{-1} appears as a shoulder on the side of the 522 cm^{-1} band in Fig. 7.22A. This band is identified as arising from the symmetric stretching mode of BeF_4^{2-} which is produced by dissociation that occurs on melting the compound:

$$xBe_2F_7^{3-} \rightleftharpoons BeF_4^{2-} + Be_{2x-1}F_{7x-4}^{(3x-2)-} \quad ; (2)$$

a similar band due to the larger component, $Be_{2x-1}F_{7x-4}^{(3x-2)-}$, is expected to lie under the 522 cm^{-1} band and is not resolved. Molten $Na_2LiBe_2F_7$ thus represents a system of various Be-F species which combine during crystal growth to form essentially pure $Be_2F_7^{3-}$ ions. The BeF_4^{2-} and $Be_2F_7^{3-}$ can be explicitly identified in the melt, because the polarized bands at 550 and 522 cm^{-1} for each, respectively, are resolved.

A more complex situation exists in melt mixtures of LiF and BeF_2, because bands of individual species other than BeF_4^{2-} and $Be_2F_7^{3-}$ cannot be resolved. In Fig. 7.23, only a shift in the strong polarized band envelope to lower frequencies is evident as the F^- concentration is decreased. The shift extends to 480 cm^{-1} for the 48-52 mole % LiF-BeF_2 composition and in the limit of pure BeF_2 should reach 282 cm^{-1} as observed previously.[3] At present, it is believed that the shift to lower frequency results from a change in form of the symmetric mode from a stretching (BeF_4^{2-}) to a bending (BeF_2) mode as the extent of polymerization increases. Furthermore, examination of this mode for the Li_2BeF_4 composition, Fig. 7.23, curve *B*, indicates that it is not entirely due to BeF_4^{2-} but already contains contributions from modes of higher polymers. The symmetric mode of BeF_4^{2-} is then more exactly represented by curve *A* with a peak still at 550 cm^{-1} but with a smaller band half-width.

The technique of identifying a complex species in solution primarily by the position and intensity of the symmetric stretching mode is frequently used in molten salt systems where temperature broadening obscures the detailed characteristics of the Raman spectrum. There are uncertainties in this method of analysis because several competing processes, such as changes in the coordination number and network formation due to cross-linking, may be occurring simultaneously and cannot be separately identified by this method alone. In

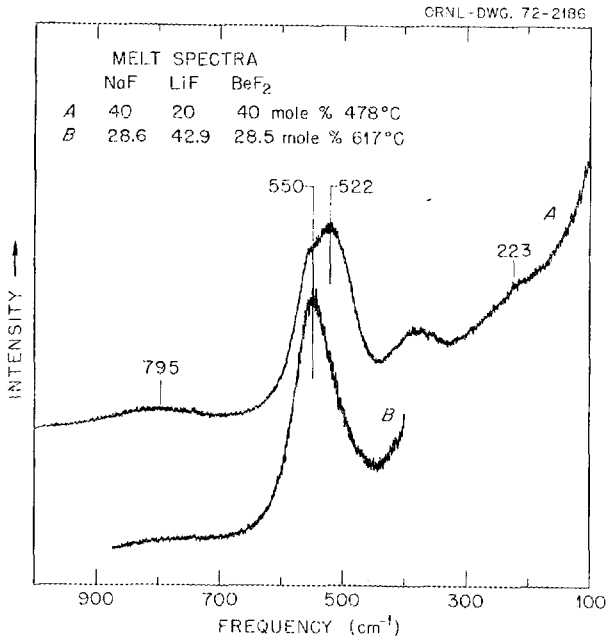

Fig. 7.22. Raman spectrum of (*a*) molten $Na_2LiBe_2F_7$ (*b*) NaF-LiF-BeF_2 (28.6-42.9-28.5 mole %). The effect of adding excess fluoride ion, curve *B*, causes the 522 cm^{-1} band to disappear and the 550 cm^{-1} band, attributed to BeF_4^{2-}, to remain.

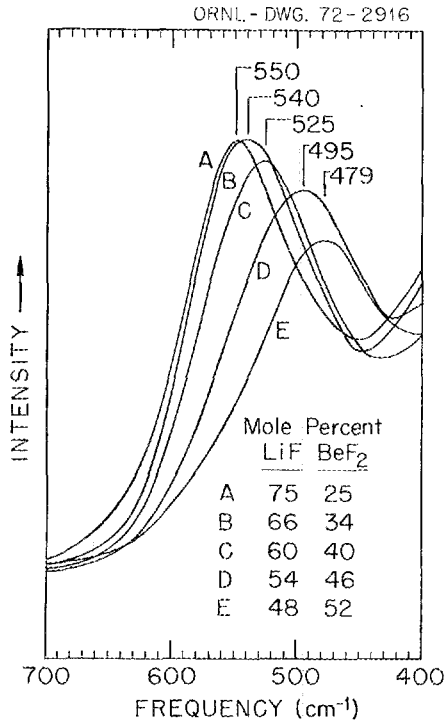

Fig. 7.23. Effect of varying LiF/BeF_2 melt composition on the strong polarized band in the Raman spectrum of the LiF-BeF_2 system at approximately 600°C.

the BeF_2 system where only tetrahedral coordination around the beryllium ion is known to occur, this procedure is valid because there appear to be no other probable processes competing with the network formation mechanism.

---

1. Director's Division.
2. A. H. Narten, *J. Chem. Phys.* **56**, 1905 (1972).
3. A. S. Quist, J. B. Bates, and G. E. Boyd, *Spectrochim. Acta, Part A* **28**, 1103 (1972).
4. C. F. Baes, Jr., *J. Solid State Chem.* **1**, 159 (1970).
5. A. S. Quist, J. B. Bates, and G. E. Boyd, *J. Phys. Chem.* **76**, 78 (1972).
6. The authors acknowledge valuable suggestions from M. A. Bredig, Chemistry Division, in this matter.
7. G. Brunton, "The Crystal Structure of $Na_2LiBe_2F_7$," to be published (1972).

RAMAN SPECTRA OF NEUTRON-IRRADIATED SiO_2[1]

J. B. Bates[2]

The structure and dynamics of vitreous silica have been discussed in recent publications from this Laboratory.[3,4] It was found that x-ray scattering data and infrared and Raman spectra of noncrystalline SiO_2 could be interpreted using a β-quartz lattice model with 12% defects in the form of SiO_2 vacancies. Two relatively sharp and polarized bands at about 604 and 490 cm^{-1} observed in Raman spectra were assigned[4] as due to modes localized about the defects in silica. To test this assignment and to explore further the nature of the defects in noncrystalline SiO_2, samples of the GE-101 material studied previously were subjected to neutron irradiation. It was anticipated that energetic neutrons would produce structural defects generally the same in type as the naturally occurring defects in silica.

Rectangular specimens of GE-101 measuring 15 × 5 × 2 mm were contained in aluminum rabbits for irradiation in the HFIR. Three samples were irradiated at doses of 1×10^{19}, 5×10^{19}, and 2×10^{20} *nvt* respectively. These levels were reported to correspond to low, maximum, and limiting (intermediate) density changes in silica as a function of dose.[5] Densities of the SiO_2 samples studied were 2.204, 2.234, 2.260, and 2.252 g/cm^3 for the unirradiated and for the 1×10^{19}, 5×10^{19}, and 2×10^{20} *nvt* irradiated specimens respectively. Because of intense laser-stimulated fluorescence from color centers in irradiated SiO_2, it was necessary to anneal the samples at 300°C for several hours. Density measurements were repeated after the annealing process and indicated only a very slight change in the density (e.g., 2.234 before vs 2.231 after

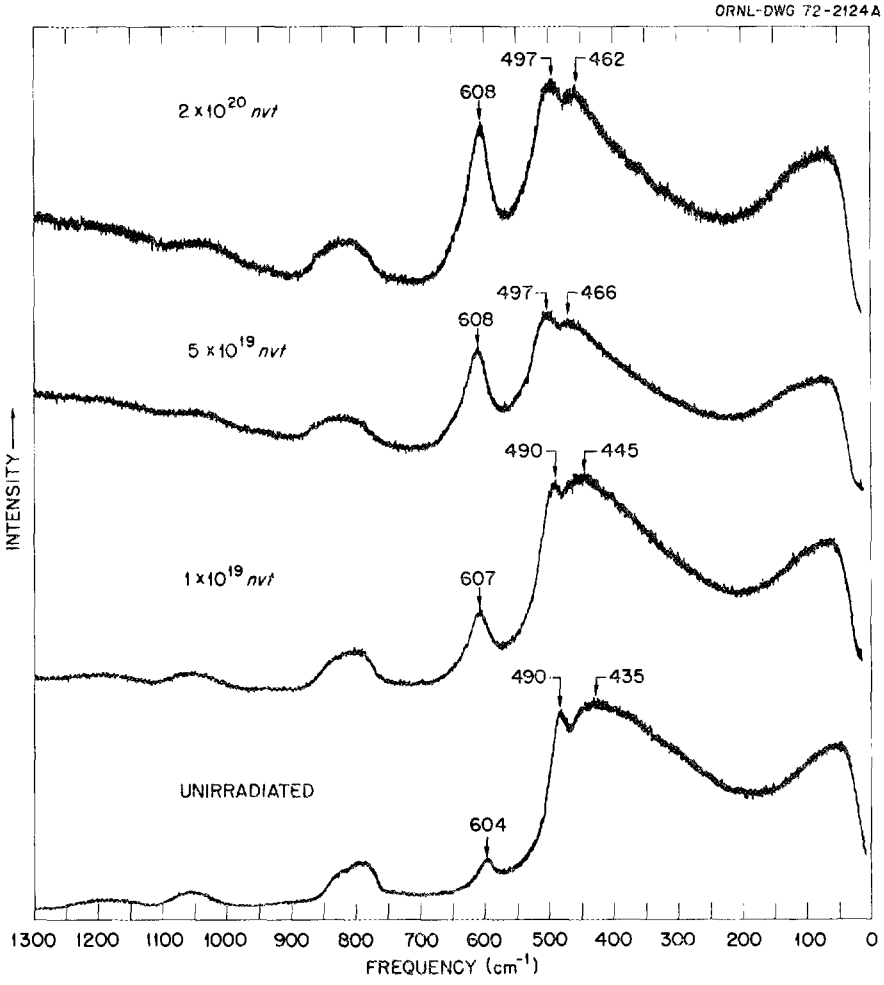

Fig. 7.24. Raman spectra of irradiated and unirradiated vitreous silica measured at 25°C. Spectra recorded in the $z(x_x{}^z)y$ orientation.

annealing). Raman spectra of the unirradiated and irradiated GE-101 samples of vitreous SiO_2 are presented in Fig. 7.24. This figure shows the marked increase in intensity of the 600 and 490 cm^{-1} bands with increasing dose.

The results obtained from Raman scattering experiments with irradiated SiO_2 support the previous assignment of the 600 and 490 cm^{-1} bands to "defect modes," that is, vibrational modes, localized about vacancies in silica. The effect of neutron irradiation was to increase the concentration of defects and, therefore, to increase the scattering intensity of the defect modes as observed (Fig. 7.24). At present, it is believed that the defect structure includes nonbridged oxygen, trivalent silicon, and centers containing hydrogen atoms such as OH or SiH, for example. The electronic structure of these types of defects has been recently considered.[6] Additional work on the defect structures in noncrystalline SiO_2 will include calculations of local mode vibrational frequencies as well as x-ray scattering experiments being conducted by R. W. Hendricks of the Metals and Ceramics Division. Hopefully, additional techniques will be employed to investigate this problem as other researchers become interested.

---

1. Abstracted from a paper submitted to the *Journal of Chemical Physics.*
2. Director's Division.
3. A. H. Narten, *J. Chem. Phys.* **56,** 1905 (1972).
4. J. B. Bates, *ibid.* **56,** 1910 (1972).
5. E. Lell, N. J. Kreidl, and J. R. Hensler, *Progress in Ceramic Science,* Vol. 4, J. E. Burke, ed., Fig. 1, p. 6, Pergamon, New York, 1966.
6. A. J. Bennett and L. M. Roth, *J. Phys. Chem. Solids* **32,** 1251 (1971).

RAMAN SPECTRA OF O_2^- AND O_3^- IONS IN ALKALI-METAL SUPEROXIDES AND OZONIDES[1]

J. B. Bates[2] M. H. Brooker[2,3]
G. E. Boyd[2]

The $\nu_4(\Sigma_g^+)$ stretching mode of the O_2^- ion has been observed from spectra of polycrystalline alkali-metal superoxides,[4] but the optically active lattice phonons of these materials have not been previously measured. The vibrational spectrum of ozonide ion, O_3^-, has not been determined, although this species, which is produced in the radiolysis of alkali-metal halates, has been extensively studied by ESR[5] and by ultraviolet diffuse reflectance spectroscopy.[6] It was desirable to obtain more nearly complete spectroscopic data on pure samples of alkali-metal superoxides and ozonides in view of the interest of O_2^- ions as impurity centers in alkali halides as well as the study of O_3^- produced on radiolysis of oxyanions such as ClO_3^-.[7]

Raman spectra of polycrystalline NaO_2, KO_2, and RbO_2 at 80°K are presented in Fig. 7.25. The frequencies of the bands observed from spectra of the superoxides and ozonides from 75 to 300°K are collected in Table 7.10. As shown, the Na, K, and Rb superoxide spectra exhibited marked changes as the temperature was lowered from 300°K. Each of these salts is known to exhibit phase transitions within the temperature range employed in the present investigation.[8–10] Three phases have been identified for NaO_2 (ref. 8) which are stable in the range $T > -50°C$, $-50°C > T > 77°K$, and $T < 77°K$, and are denoted by NaO_2(I), NaO_2(II), and NaO_2(III) respectively.

The external modes of NaO_2 were observed at 80 and 75°K but not at 200°K or above (Table 7.10). In phase II, $E_g + 2F_g$ Raman active lattice phonons are predicted, and the two bands at 226 and 142 cm^{-1} in the 80°K spectra were assigned to two of these three modes. (The sharp peak at about 65 cm^{-1} is due to a grating ghost.) The noticeable shift of the external mode frequencies on cooling to 75°K probably is a consequence of the II → III phase transition, because a shift to a lower wave number would be expected in the absence of a phase change.

Three crystal phases of KO_2 are reported to exist in the temperature range studied in this work. The room-temperature, or α-KO_2, phase has tetragonal symmetry[9] and is presumably stable from 209 to 400°K.[10,11] Except for a small increase in frequency of the Σ_g^+ mode, no change was observed in spectra recorded at 200°K, although a phase change was reported to occur below about 209°K.[11] At 80°K, the Σ_g^+ mode shifted upward by about 4 cm^{-1} from the

Table 7.10. Bands observed from Raman spectra of alkali-metal superoxides and ozonides. Frequencies in cm^{-1}

	NaO_2[a]				KO_2			RbO_2				CsO_2	
	300°K	200°K	80°K	75°K	300°K	200°K	80°K	300°K	200°K	80°K	75°K	300°K	77°C
Σ_g^+	1156 s	1155 s	1164 s	1164 s	1141 s	1144 s	1145 s	1140 s	1138 s	1141 s	1140 s 1138 w	1137	1137
ν_L[b]	----[b]	----	226 w	218 w	----	----	211 w 205 w	----	----	200 w	RNS[b]	----	----
ν_L	----	----	142 w	130 w	----	----	140 w 122 w 89 m	----	----	146 w 80 m	RNS 81 m	----	----
ν_L	----	----	----	----	----	----	81 m 65 w	----	75 w	63 m	75 m 65 m 62 m	----	----

KO_3, 300°K	CsO_3, 300°K
1017	1010

[a] s = strong, m = medium, w = weak.

[b] ν_L lattice mode, ---- = band not observed, RNS = region not scanned.

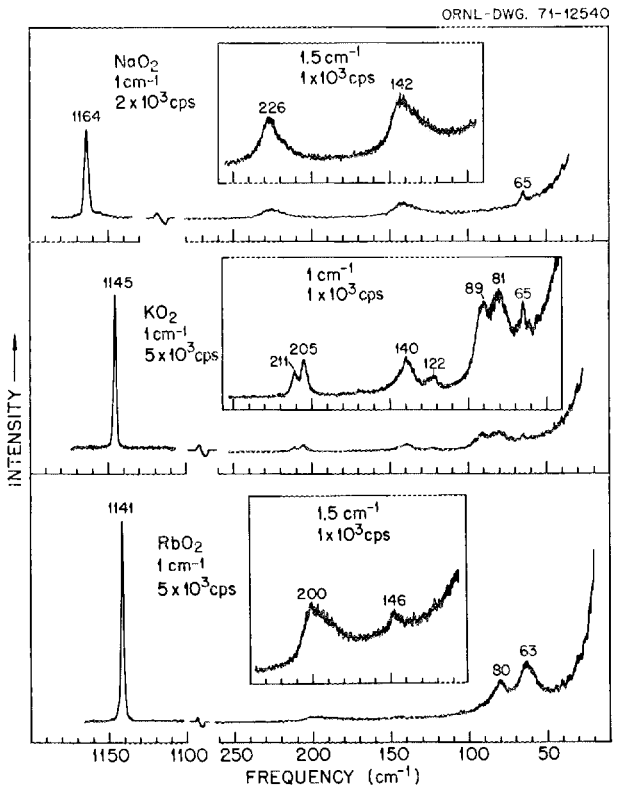

Fig. 7.25. Raman spectra of sodium, potassium, and rubdium superoxides measured at 80°K. Spectral slit width in wave numbers and sensitivity in counts per second.

room-temperature frequency, and three groups of external mode frequencies appeared (Fig. 7.25 and Table 7.10). The appearance of the external modes at 80°K may be a result of a transition to another crystal phase which occurs below 150°K.[11]

Two crystalline phases of RbO_2 have been reported between 75 and 300°K, with the transition point at 77°K.[11] As shown in Table 7.10, on cooling from 80 to 75°K, a splitting of Σ_g^+ was observed, and additional bands appeared in the 60–80 cm^{-1} region. It should be noted that the low-frequency bands (<200 cm^{-1}) measured at 80°K (Fig. 7.25 and Table 7.10) were not observed at 200°K, except for a very weak broad band at about 75 cm^{-1}.

The structure of crystalline CsO_2 apparently has been determined at room temperature only.[12] As with KO_2 and RbO_2, CsO_2 exhibits a CaC_2 structure at 300°K. The Raman spectrum of CsO_2 revealed a single component of the Σ_g^+ O_2^- mode at 1137 cm^{-1}. Because of the lack of any additional features in the 80°K spectrum, no additional measurements at a lower or intermediate temperature were made.

The large relative intensities at low frequencies (60–90 cm^{-1}) in 80°K spectra of KO_2 and RbO_2 (Fig. 7.25) suggest that these bands are caused by librational motion of the O_2^- ion. Considering the structure of NaO_2(III) (see above and ref. 8), the 226 and 142 cm^{-1} bands observed in 80°K spectra of this material (Fig. 7.25) also originate in anion libration, since the O_2^- ions occupy centers of inversion in a centric unit cell. Thus, all three groups of low-frequency bands observed in the superoxides may be attributed to O_2^- librational modes. The fact that no external mode frequencies were observed at 200°K or at higher temperatures may be a consequence of the rapid onset of anion disorder with increasing temperature.

The Raman spectra of KO_3 and CsO_3 reported in Table 7.10 exhibited single bands at 1017 and 1010 cm^{-1} respectively. Based on considerations of Walsh diagrams and CNDO/II calculations, the O_3^- ion was predicted to have a bent C_{2v} structure with an apex angle of 114–126°. Therefore, we expected to observe ν_2 and ν_3 of O_3^- in Raman spectra of KO_3 and CsO_3. The single band observed is probably due to $\nu_1(a_1)$, the symmetric stretching mode.

1. Abstracted from a paper submitted to *Chem. Phys. Lett.*
2. Director's Division.
3. National Research Council of Canada Postdoctoral Fellow 1969–71. Present address: Department of Chemistry, Mount Allison University, Sackville, N.B., Canada.
4. F. J. Blunt, P. J. Hendra, and J. R. Mackenzie, *Chem. Commun.* **1969**, 278.
5. (*a*) S. Schlick, *J. Chem. Phys.* **56**, 654, (1972); (*b*) A. Begum, S. Subramanian, and M. C. R. Symons, *J. Chem. Soc. A* **1970**, 918; (*c*) M. M. Cosgrove and M. A. Collins, *J. Chem. Phys.* **52**, 989 (1970).
6. G. E. Boyd and L. C. Brown, *J. Phys. Chem.* 74, 3490 (1970).
7. J. B. Bates and G. E. Boyd, work in progress.
8. G. F. Carter and D. H. Templeton, *J. Amer. Chem. Soc.* **75**, 5247 (1953).
9. S. C. Abrahams and J. Kalnajs, *Acta Crystallogr.* **8**, 503 (1955).
10. G. F. Carter, J. L. Margrave, and D. H. Templeton, *ibid.* **5**, 851 (1952).
11. H. G. Smith, R. M. Nicklow, L. J. Raubenheimu, and M. K. Wilkinson, *J. Appl Phys.* **37**, 1047 (1966).
12. R. W. G. Wyckoff, *Crystal Structures* Vol. I, p. 351, Wiley, New York, 1963.

VIBRATIONAL SPECTRA OF MOLTEN AND AQUEOUS $NaClO_3$ AND $KClO_3$[1]

J. B. Bates[2] A. S. Quist[2]
G. E. Boyd[2]

The Raman and infrared spectra of ClO_3^- ion in molten salts and saturated aqueous solutions of $NaClO_3$

and $KClO_3$ were measured to determine the utility of the chlorate ion as a probe for investigating interionic interactions in liquid media. Specifically, the intention was to determine if spectral perturbations analogous to those observed with other oxy-anions such as NO_3^- and CO_3^{2-} in nitrate and carbonate melts and in aqueous solutions, respectively, could be observed with chlorate ion. In addition, two intense Raman bands were reported in the low-frequency region of molten $NaClO_3$ by other workers[3] which are inconsistent with results obtained from spectra of molten salts measured in this laboratory.

Raman spectra of molten and aqueous $NaClO_3$ are shown in Fig. 7.26. These spectra are also representative of those obtained with molten and aqueous $KClO_3$. The infrared spectrum of a 50 wt % solution of $KClO_3$ in molten KNO_3 is presented in Fig. 7.27. This spectrum was obtained by emission techniques, using the infrared Fourier transform spectrophotometer, FTS-20, system.

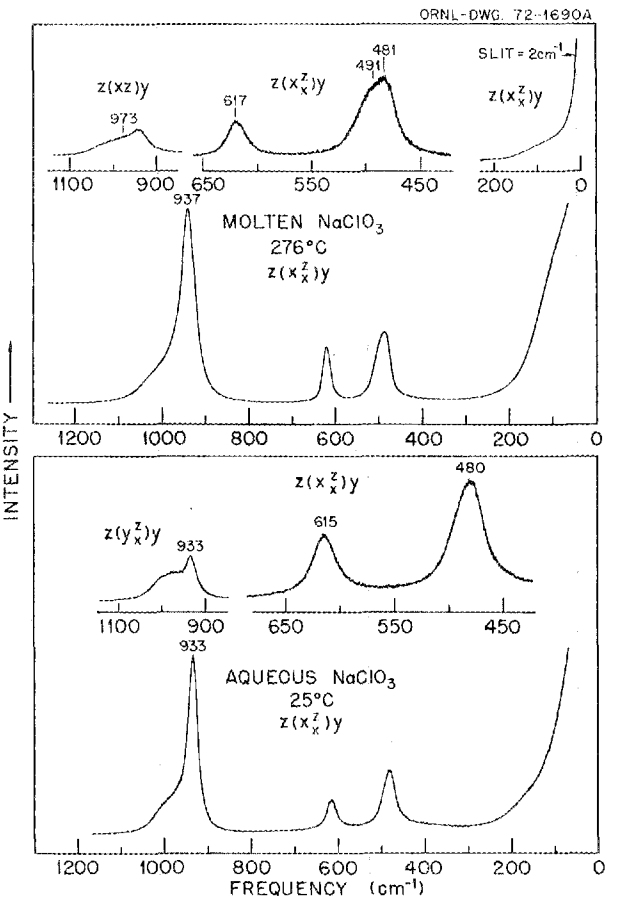

Fig. 7.26. Raman spectra of molten and aqueous $NaClO_3$.

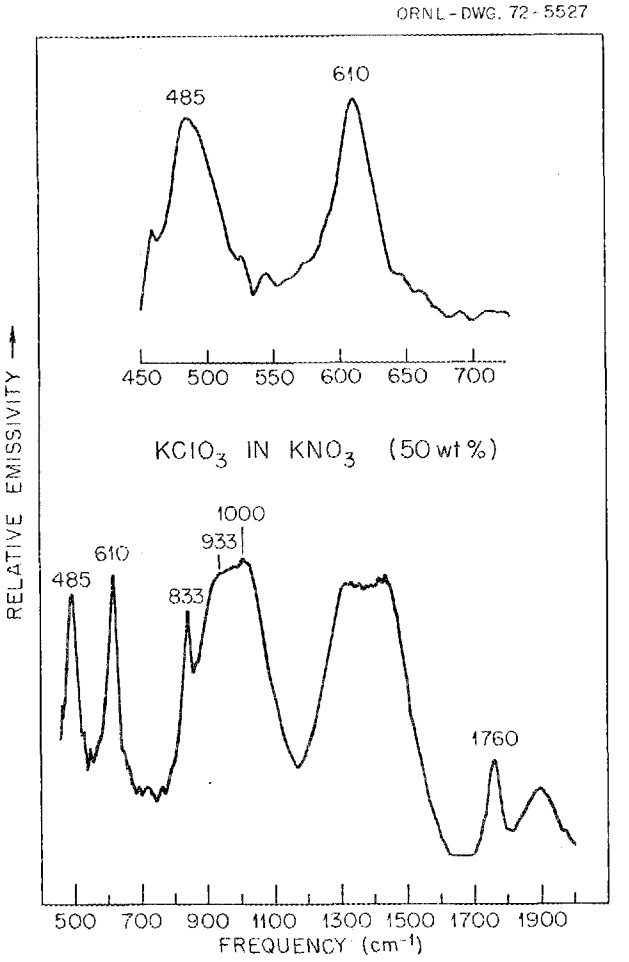

Fig. 7.27. Infrared emission spectrum of a 50 wt % mixture of $KClO_3$ and KNO_3.

Results from the molten salt and aqueous solution measurements are collected in Table 7.11.

The $\nu_4(e)$ ClO_3^- degenerate bending mode at about 480 cm^{-1} was split in Raman spectra of molten $NaClO_3$, and the ν_4 band in aqueous $NaClO_3$ exhibited an asymmetry indicating two components. The split of ν_4 in molten $KClO_3$ was less apparent. The $\nu_3(e)$ degenerate stretching mode exhibited a complex band centered at about 973 cm^{-1} in molten $NaClO_3$ (Fig. 7.26). There appear to be at least three components comprising this band envelope, but overlap of the strong $\nu_1(a_1)$ band at 937 cm^{-1} precluded the possibility of a meaningful line shape analysis. Split components of the doubly degenerate ν_3 vibration, as well as at least one component of $2\nu_4$, are expected in the 1000 cm^{-1} region.

Table 7.11. Bands observed from Raman and infrared spectra of molten and aqueous $NaClO_3$ and $KClO_3$. Frequencies in cm^{-1}

$NaClO_3$				$KClO_3$				Assignment
Aqueous (25°C)		Melt[a] (276°C)		Aqueous (25°C)		Melt (373°C)		
Raman	IR	Raman	IR	Raman	IR	Raman	IR	
976 dp[b]	1000 975	973 dp	1000	973 dp	970	963 dp	1000	$\nu_3(e)$and $2\nu_4$
933 p	935	937 p	935	930 p	n.o.	932 p	933	$\nu_1(a_1)$
615 p	621	617 p	614	611 p	n.o.	612 p	610	$\nu_2(a_1)$
480 dp	n.o.[b]	491 481 dp	495	478	n.o.	484 dp	485	$\nu_4(e)$
		120 (±10)				120 (±10)		

[a] Temperature of melts in emission experiments estimated at 350°C.
[b] p = polarized, dp = depolarized, n.o. = not observed.

The infrared band frequencies observed from the chlorate melts and aqueous solutions were not coincident in all cases with the Raman frequencies measured in the same system (Table 7.11). Noncoincidence of infrared and Raman frequencies and the splitting of degenerate fundamentals in melts and aqueous solutions appear to be characteristics of ClO_3^-, CO_3^{2-}, and NO_3^-. However, as a probe ion, ClO_3^- is not as suitable as NO_3^-, because the ν_3 mode, which exhibits the largest splitting, occurs in a region with $\nu_1(a_1)$ and $2\nu_4$.

A single broad band was observed in the low-frequency Raman spectrum of each molten chlorate (Fig. 7.26 and Table 7.11), as expected. The two strong bands previously reported[3] in Raman spectra of molten $NaClO_3$ apparently were caused by instrumental effects.

1. Expanded abstract of a paper submitted to *Chemical Physics Letters.*
2. Director's Division.
3. D. W. James and W. H. Leong, *Aust. J. Chem.* **23**, 1087 (1970).

RAMAN SPECTRA OF CRYSTALLINE CYCLOPROPANE, CYCLOPROPANE-d_6, AND C_3H_6-C_3D_6 SOLID SOLUTIONS[1]

J. B. Bates[2]

One of the purposes for measuring vibrational spectra of molecular crystals is to provide essential data for determining the magnitude of intermolecular interactions in condensed phases and in evaluating intermolecular potential functions. Detailed studies of the internal and external optical modes of organic crystals have been employed to calculate nonbonded atom-atom interaction constants.[3] The present study of crystalline cyclopropane purported to (1) evaluate the relative magnitudes of static and dynamic field effects and (2) determine the external optical mode frequencies. The separation of static and dynamic field effects requires measurements with dilute, isotopic mixed crystals, and the experiments described below represent one of the first reported attempts to measure the Raman spectra of such mixed crystals.

Raman spectra of neat polycrystalline C_3H_6 and C_3D_6 were measured from vapor-deposited samples at 77°K. The C_3H_6/C_3D_6 solid solutions containing about 5% of the solute species were prepared by mixing the gases in a volume ratio of 1/20 and sealing the mixture as a liquid at room temperature in 1-mm glass capillary tubes. Raman spectra of the neat crystals and solid solutions in the internal mode region are shown in Figs. 7.28 and 7.29. Spectra recorded in the external mode region of the neat crystals are presented in Fig. 7.30.

The spectra in Figs. 7.28 and 7.29 show the effects of dynamic coupling and the static field in neat crystals, compared with the effects of the static field only in the mixed crystals on the degenerate e' and e'' modes of C_3H_6 and C_3D_6. For example, in the 1400 cm^{-1} region of C_3H_6 (Fig. 7.28), the three components of $\nu_9(e')$ at 1434, 1432, and 1421 cm^{-1} in neat C_3H_6

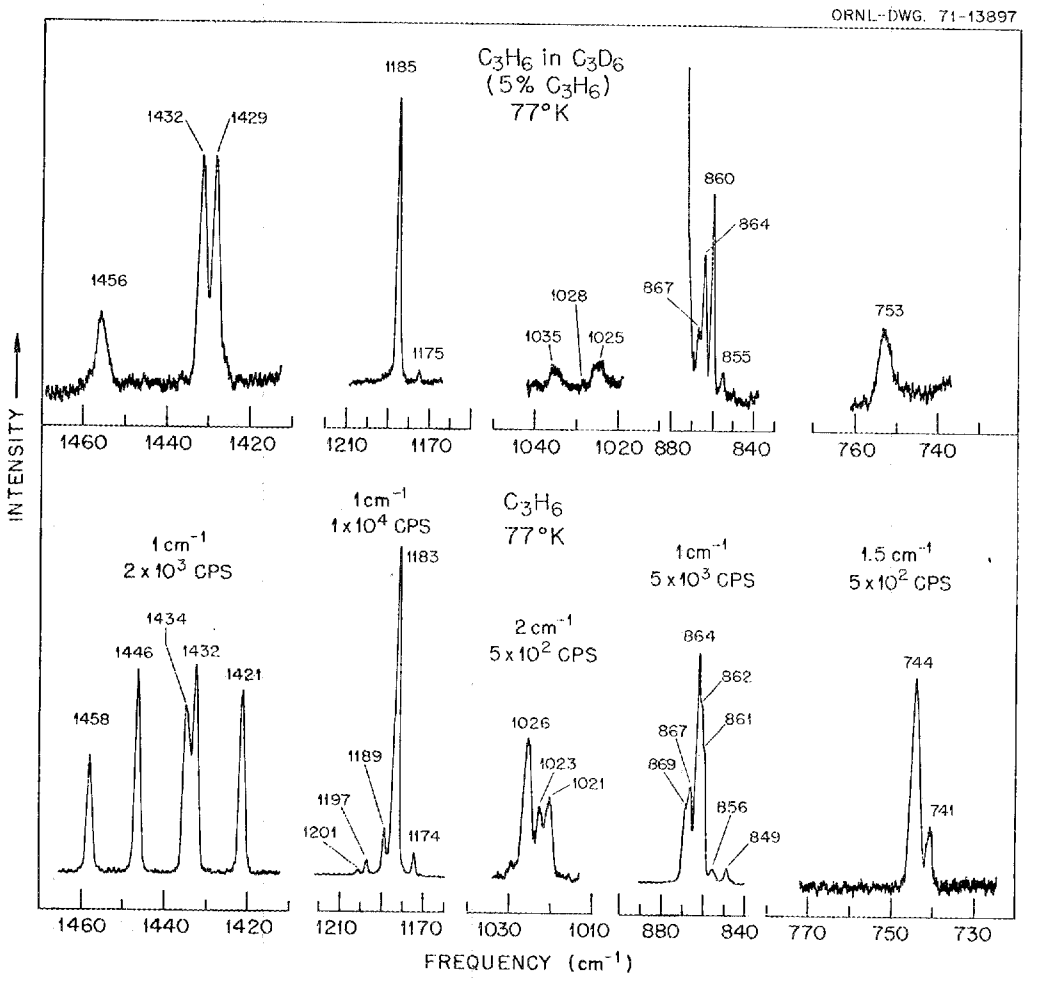

Fig. 7.28. Raman spectra of crystalline C_3H_6 and of a solid solution of 5% C_3H_6 in C_3D_6. Spectral slit width in cm^{-1} and sensitivity in counts per second.

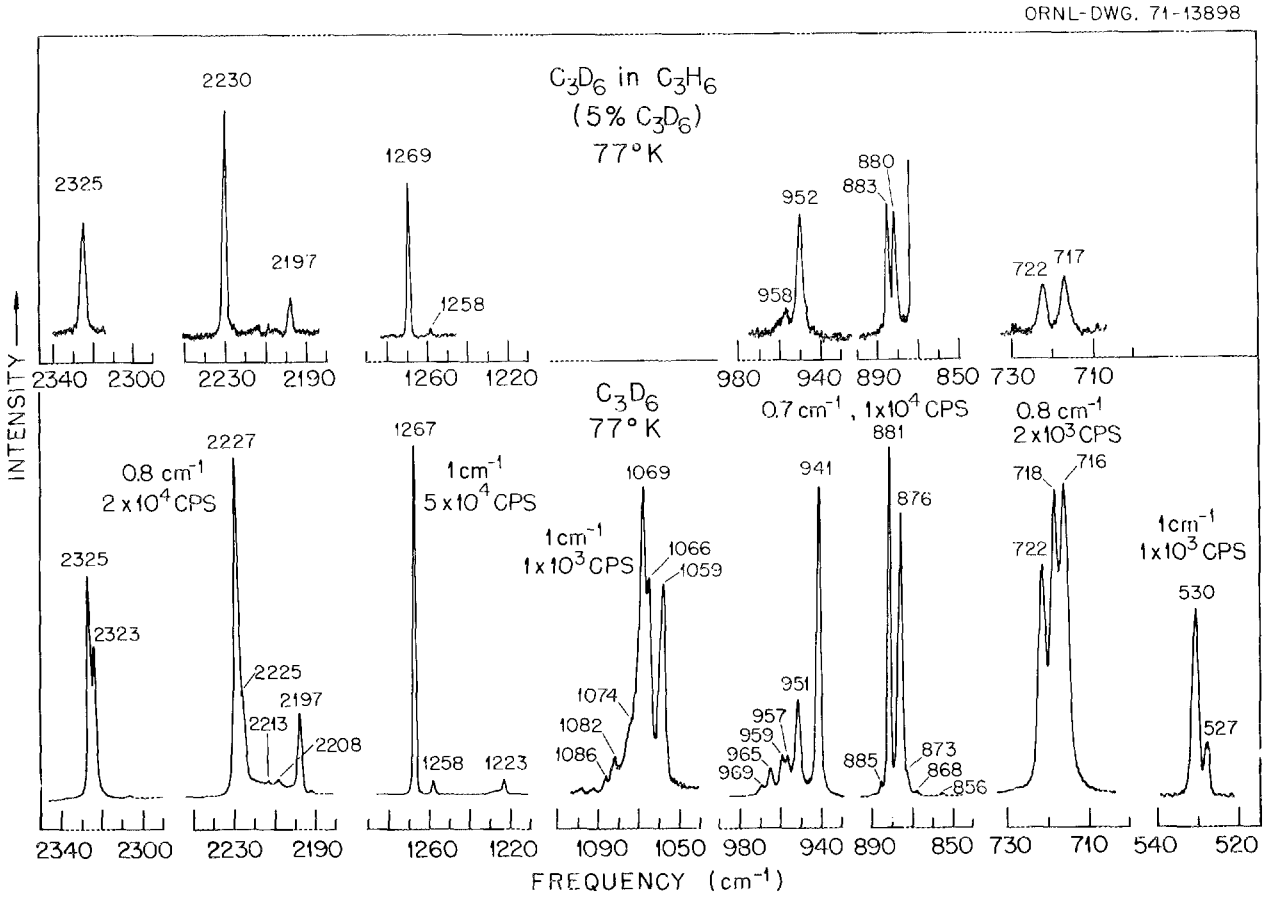

Fig. 7.29. Raman spectra of crystalline C_3D_6 and of a solid solution of 5% C_3D_6 in C_3H_6. Spectral slit width in cm^{-1} and sensitivity in counts per second.

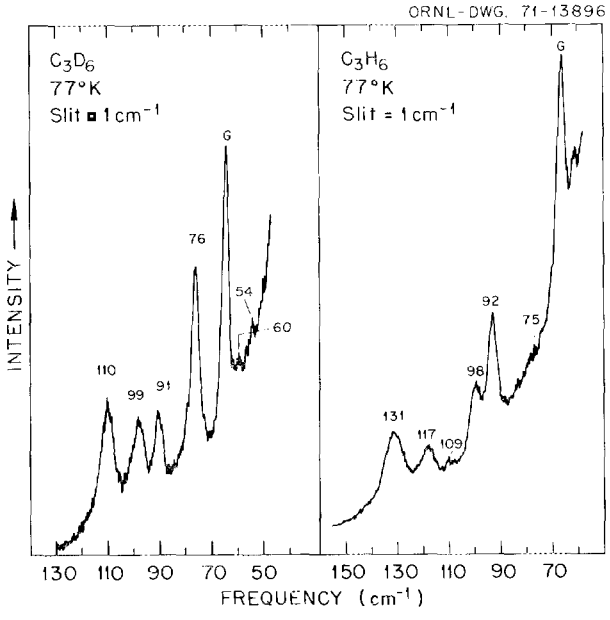

Fig. 7.30. Raman spectra of the external mode regions of crystalline C_3D_6 and C_3H_6.

collapse into two components at 1432 and 1429 cm^{-1} in the mixed crystal. Thus, the 13 cm^{-1} splitting of two ν_9 components is due primarily to dynamic interaction, since the splitting of ν_9 due to the static field is about 3 cm^{-1}.[4] In another case such as $\nu_{11}(e')$ of C_3D_6, Fig. 7.29 shows that the 6 cm^{-1} splitting of the components in the 700 cm^{-1} region is due primarily to a static field effect.

An assignment of the observed external mode frequencies of C_3H_6 and C_3D_6, assuming an orthorhombic C_{2v} lattice structure for cyclopropane,[5] is proposed in Table 7.12. The assignments were based on comparing measured isotopic frequency shifts with calculated values in which no coupling between internal and external modes was also assumed. Although the external modes can be mixtures of librational and translational motion (because of the acentric lattice structure), a consideration of the observed Raman intensities suggests that the 131 cm^{-1} band of C_3H_6 (110 cm^{-1} in C_3D_6) is due primarily to a librational motion. Likewise, the 117 cm^{-1} band (99 cm^{-1} in C_3D_6) was also assigned to an A_2 librational mode. The

Table 7.12. (*a*) Bands observed in the external mode regions in Raman spectra of crystalline C_3H_6 and C_3D_6 at 77°K. Frequencies in cm^{-1}. (*b*) Symmetry species for translations and rotations in the C_{2v} point group and calculated ratios for lattice modes in cyclopropane

C_3H_6	C_3D_6	ω_H/ω_D	Assignment
131	110	1.19	A_2
117	99	1.18	A_2
109	91	1.20	B_1
98	76	1.28	B_2
92		1.21	B_1
75	60	1.25	B_2
	54		

C_{2v}	ω_H/ω_D
A_1 T_z	1.07
A_2 R_z	1.19
B_1 T_x, R_y	1.19
B_2 T_y, R_x	1.27

109 cm^{-1} band in C_3H_6 was assigned to a B_1 mode of mainly translational-like motion, since it was the strongest infrared band[5] and a medium-to-weak Raman band.

1. Expanded abstract of a paper submitted to *Spectrochimica Acta.*
2. Director's Division.
3. Compare, for example, I. Harada and T. Shimanouchi, *J. Chem. Phys.* **44**, 2016 (1966).
4. The 1446 and 1458 cm^{-1} components in neat C_3H_6 and the 1456 cm^{-1} component in the mixed crystal are due to $\nu_2(a_1')$.
5. J. B. Bates, D. E. Sands, and W. H. Smith, *J. Chem. Phys.* **51**, 105 (1969).

MICROWAVE AND RADIO-FREQUENCY SPECTROSCOPY

PARAMAGNETIC RESONANCE STUDIES OF LIQUIDS DURING PHOTOLYSIS

Ralph Livingston Henry Zeldes

In an earlier report[1] a preliminary description was given of experiments using a rotating sector as a means of chopping the light used in photolytic studies so that direct physical measurement of radical lifetimes could be made. The technique consists in first recording the spectrum of a radical at steady-state concentration formed by continuous irradiation with ultraviolet light. The spectrometer is then adjusted to the peak of one of the lines of the spectrum, and the light is chopped with a rotating sector. The data are accumulated in a signal averager which records the changes in line intensity as the light turns on and subsequently as it turns off. A substantial improvement in the response time of the equipment has been made. The rise time of the electronic system is now slightly under 100 μsec, and the mechanical sector error (time for the light to change from full off to full on) is 240 μsec with good prospects for further improvement.

Extensive measurements have been made on the aqueous tartaric acid system.[1] Upon photolysis a carboxyl group is split off, leaving radical A, HOOCCH(OH)$\dot{C}$H(OH). This radical converts to an aldehyde form, HOOC$\dot{C}$HCHO, by an acid-catalyzed reaction. At high acidity (concentrated solutions of tartaric acid), where the conversion is rapid, the mean life of radical A is short, and its spectrum appears entirely in emission. At low acidity (dilute solutions of tartaric acid), where the mean life becomes long, the Zeeman states achieve thermal equilibrium, and the spectrum is, as normally expected, an absorption spectrum. This behavior has been studied[2] in steady-state experiments where the progressive conversion of an emission line to an absorption line was followed as the pH of the solution was increased. Rate curves have now been obtained for lines of radical A, as well as for lines of other radicals that appear in aqueous solutions of tartaric acid at various concentrations. Figure 7.31 shows rate curves for one of the eight hyperfine lines of radical A. The points are spaced at 50-μsec intervals. Figure 7.31*a* is for a concentrated solution which is highly acidic, and the lifetime of radical A is very short. When the light comes on, the spectrum appears promptly in steady-state emission within a time of about 350 μsec. This time is almost entirely controlled by the response time of the instrumentation. Upon turning the light off, the spectrum promptly goes to zero intensity. At a higher pH (less concentrated solution), Fig. 7.31*b*, the signal first rises to a strong emission peak, taking about 350 μsec, again instrumentally limited. A phenomenological theory describing the various rate curves has been developed, and it indicates that this rapid rise actually takes place in a time of several microseconds. If the response time of the equipment were faster, this transient peak would be more intense. Following the transient, the curve reverses to steady-state emission but at an intensity much less than that of Fig. 7.31*a*. When the light is turned

off, there is another transient response in the absorption direction, actually crossing to the absorption side of the base line. This is followed by decay (not instrumentally limited) to zero intensity. This final decay is a measure of the lifetime of radical A. Clearly, as the pH becomes higher (lower concentration), this chemical lifetime becomes longer and the steady-state concentration progressively changes from emission to absorption, as finally illustrated in Fig. 7.31*c*. Rate curves have been obtained for a greater range of concentration than that illustrated and also for the lowest-field hyperfine line of radical A.

It was initially felt[1] that this transient behavior meant that there is a moderately long-lived precursor of radical A. This is not true, nor is the lifetime of radical A as short as initially indicated. The phenomenological rate theory developed indicates a very *short* precursor lifetime. Moreover, the radicals are formed in a highly polarized state, rather than there being polarization processes taking place during the lifetime of the radical. The degree of this polarization must be exceptionally high. In Fig. 7.31*c*, for example, the initial transient requires about 600 μsec to return to a zero crossover. With a thermal relaxation time of the radical of the order of 1 μsec, it is estimated that the initial polarization is many percent.

If oxalic acid is added to a tartaric acid solution, a radical is formed from the oxalic acid by electron transfer[3] from all of the radicals (including radical A) present during photolysis. The polarization of radical A is transferred to the radical from oxalic acid, as indicated in Fig. 7.32. At higher values of pH the transient polarization of this radical becomes less pronounced. The lifetime of the radical is quite long.

Preliminary rotating sector experiments have been made on lines from $(CH_3)_2\dot{C}OH$. Some of the lines from this radical can be made to appear as emission

ORNL-DWG. 72-5514

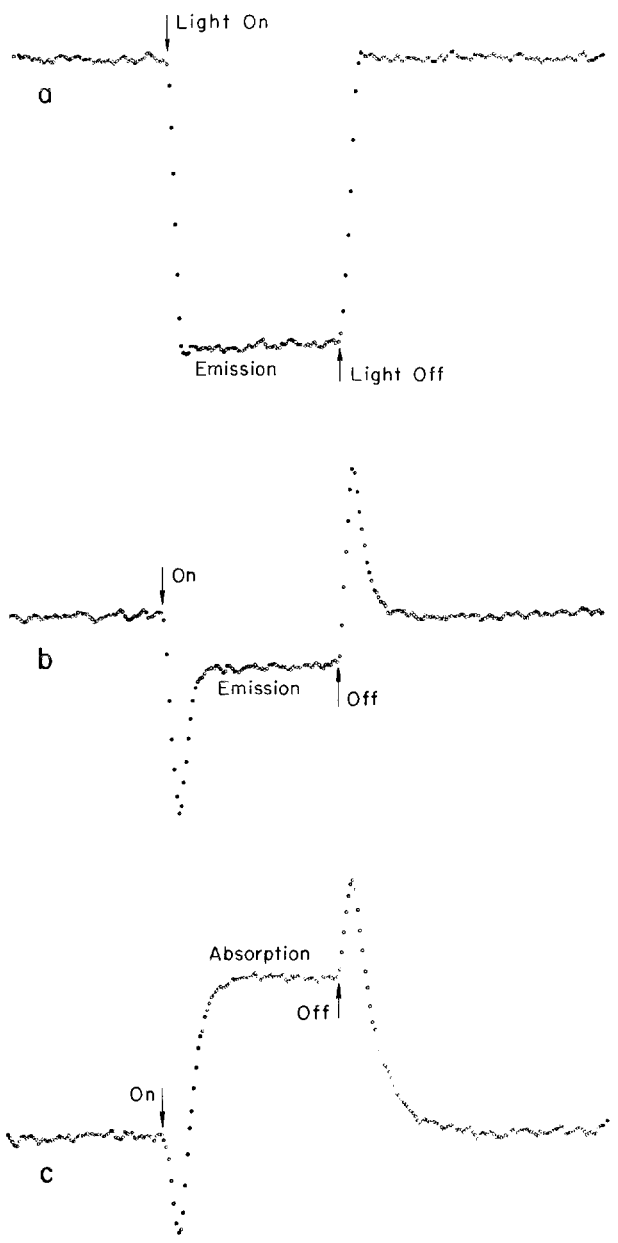

Fig. 7.31. Rate curves for the highest field hyperfine line of HOOCCH(OH)$\dot{C}$H(OH), radical A, formed by photolysis of aqueous solutions of tartaric acid. (*a*) 56.5%, (*b*) 30%, and (*c*) 8% tartaric acid. The points are spaced at 50-μsec intervals. Downward displacement from the base line corresponds to emission. About 1 hr of data accumulation was needed for each curve.

ORNL-DWG. 72-5513

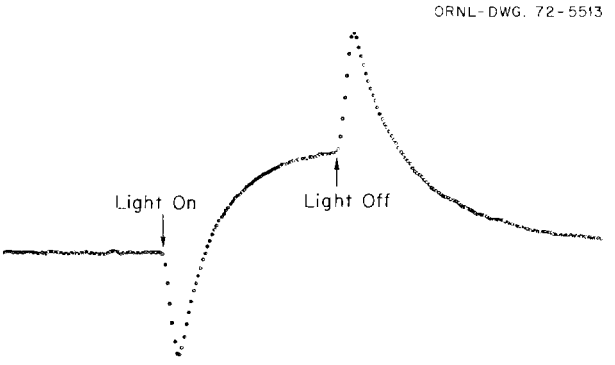

Fig. 7.32. Rate curve for the single line of the radical derived from oxalic acid formed by photolysis of 51.1% aqueous tartaric acid containing 2.3% oxalic acid. The points are spaced at 50-μsec intervals, and the downward direction corresponds to emission.

lines.[3] The rate curves are entirely different from those of the tartaric acid system, and it appears that the polarization takes place during the radical lifetime.

Electron paramagnetic resonance spectra of radicals derived from aromatic nitrogen heterocyclic compounds have been studied. Spectra were observed during steady-state photolysis near room temperature of solutions containing acetone and isopropyl alcohol as well as the parent compound. During photolysis, acetone is excited and reacts with isopropyl alcohol[4] to form the radical $(CH_3)_2\dot{C}OH$:

$$(CH_3)_2CO + (CH_3)_2CHOH \rightarrow 2(CH_3)_2\dot{C}OH\,. \qquad (1)$$

This radical, known to be a good electron donor,[5] then reacts with the parent compounds to form the nitrogen heterocyclic radicals. Experimental work is complete on radicals prepared in this way from pyridine (**a**), pyrazine (**b**), pyrimidine (**c**), and pyridazine (**d**). The

ORNL-DWG. 72-4966

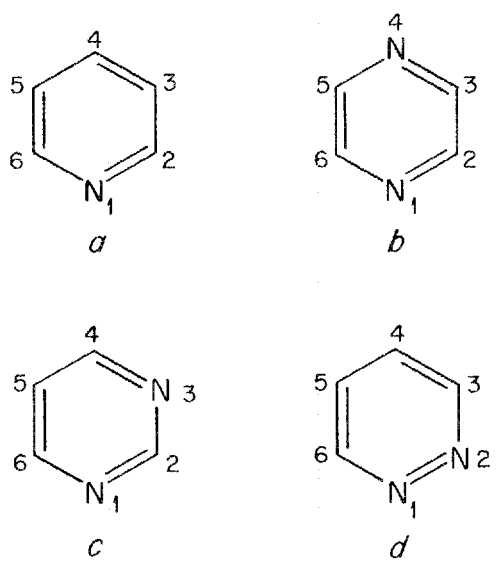

radical derived from pyridine was studied in isopropyl alcohol-rich, acetone-rich, and water-rich solutions. The others were studied in water-rich solutions. In each case the radical was identified as the one which would result from electron capture by the parent compound followed by protonation of every nitrogen atom. The radical derived from pyridine is neutral, and the others have one unit of positive charge. Each radical is a π-electron radical with a hydrogen substituent at every ring position. This makes it possible to estimate π-electron spin density ρ^{π}_i at every ring position i from the hydrogen couplings a^{H}_i rather than from molecular orbital calculations. This is done using the McConnell-type relationship[6]

$$a^{H}_i = Q^{H}_{XH}\,\rho^{\pi}_i\,, \qquad (2)$$

where X is C or N, depending upon whether carbon or nitrogen is at ring position i, and Q^{H}_{XH} is the spin polarization parameter. Molecular orbital calculations were made, but only to help in assigning hydrogen couplings to ring positions and in determining their signs. In order to assign hydrogen couplings to ring positions for the radical derived from pyridazine, it was necessary also to study the spectrum in D_2O-rich solutions. All couplings were assigned to ring positions for each radical, and all signs of couplings were determined except that for a weak coupling for a pair of equivalent hydrogens of the radical derived from pyridine. From the hydrogen couplings, Eq. (2), and the requirement that the total π-electron spin density for each radical is unity, consistent values of Q^{H}_{NH} and Q^{H}_{CH} for all the radicals were found. These Q values and Eq. (2) were then used to compute "experimental" spin densities at every ring position from the hydrogen couplings. The nitrogen couplings were expected to be given by a relation similar to the one developed by Karplus and Fraenkel[7] for ^{13}C couplings. This model, however, was not adequate. Numerical data and a full description of this work have been prepared for publication elsewhere.

Two computer programs were developed as aids in the analysis of complex spectra. These have been essential in the work on aromatic heterocyclics. Both calculate hyperfine couplings to second-order perturbation theory and can deal with a large number of groups of equivalent nuclei. Each group may contain a large number of nuclei of any spin. Line splittings which appear only in second-order theory may optionally be replaced by a single line at the center of gravity of the replaced lines. This feature is very useful when the splittings are within a line width. One program gives an ordered printout of magnetic fields of lines. For each line there is also given its strength, the field contribution arising from second-order theory, the coupled spin for each group of nuclei, and the nuclear magnetic quantum numbers. This same program may alternatively be used to find the best values for g and the hyperfine couplings to describe experimental data. This is done with a least-squares criterion. An error analysis is also given. The second program makes it possible to simulate spectra. Lines may be present from many radicals. Gaussian, Lorentzian, and first and second derivatives of Gaussian and Lorentzian line shape

functions may be used. Stick spectra and measured line positions may also be plotted. As many spectra as desired may be plotted at desired heights above the same field axis.

1. R. Livingston, H. Zeldes, and J. K. Dohrmann, *Chem. Div. Annu. Progr. Rep. May 20, 1971*, ORNL-4706, p. 236.
2. R. Livingston and H. Zeldes, *J. Chem. Phys.* **53**, 1406 (1970).
3. H. Zeldes and R. Livingston, *J. Phys. Chem.* **74**, 3336 (1970).
4. H. Zeldes and R. Livingston, *J. Chem. Phys.* **45**, 1946 (1966).
5. R. O. Norman and R. J. Pritchett, *J. Chem. Soc. (B)* 378 (1967).
6. H. M. McConnell, *J. Chem. Phys.* **24**, 632, 764 (1956).
7. M. Karplus and G. K. Fraenkel, *J. Chem. Phys.* **35**, 1312 (1961).

ELECTRON SPIN RESONANCE STUDY OF FREMY'S RADICAL IN SINGLE CRYSTALS OF POTASSIUM HYDROXYLAMINE TRISULFONATE

R. W. Holmberg B. J. Wilson[1]

Fremy's radical [the nitrosodisulfonate radical anion, $\dot{O}N(SO_3)_2^{2-}$] is a stable free radical which has been the subject of many ESR and chemical studies. Nevertheless, no definitive ESR study of it trapped in a diamagnetic single crystal has been reported. In a preliminary study[2] of the radical coprecipitated into a single crystal of its "chemical parent," potassium hydroxylamine disulfonate, anisotropic ^{14}N hyperfine spacings varying from 6 to 27 G were reported, but neither the hyperfine nor g tensor was evaluated.

Single crystals of potassium hydroxylamine trisulfonate, $K_3[SO_3ON(SO_3)_2]\cdot{}^3/_2H_2O$, were grown and were irradiated with ^{60}Co gamma rays at 77°K. ESR spectra from a number of nitrogen-containing free radicals which have not yet been identified were observed. On warming to room temperatures, these radicals decayed, and an ESR spectrum identified as being that of Fremy's radical appeared. The identification was made by comparing the ESR spectrum of this polycrystalline system with that seen when Fremy's radical was coprecipitated into polycrystalline potassium hydroxylamine disulfonate or into the diamagnetic phase[3] of potassium nitrosodisulfonate (Fremy's salt).

Measurements of the three anisotropic hyperfine lines arising from ^{14}N have been made, and the hyperfine and g tensors have been evaluated. Tentative principal values for g are 2.0025, 2.0059, and 2.0082, and those for the ^{14}N hyperfine tensor are 31.1, 6.8, and 6.1 G. The averages of these principal values, 2.0055 and 14.7 G, are similar to those of Fremy's radical in solution,[4] 2.0057 and 13.0 G, and indicate that the signs of the hyperfine tensor elements are all positive. An analysis of the hyperfine tensor indicates that the unpaired electron distribution in the vicinity of the nitrogen nucleus can be described by an almost pure N ($2p$) wave function with a spin density of about 48%.

1. Visiting scientist from Brigham Young University, Provo, Utah.

2. S. I. Weissman, T. R. Tuttle, Jr., and E. de Boer, *J. Phys. Chem.* **61**, 28 (1957).
3. W. Moser and R. A. Howie, *J. Chem. Soc. (A)* 3039 (1968).
4. J. E. Wertz, D. C. Reitz, and F. Dravnieks, *Free Radicals in Biological Systems*, ed. M. S. Blois, Jr., et al., p. 183, Academic Press, New York, 1961.

ESR STUDY OF RADICAL INTERCONVERSIONS IN SINGLE CRYSTALS OF STRONTIUM NITRATE AT 77°K

R. W. Holmberg

The radicals $\dot{N}O_3^{2-}$ and $NO_3^{\bullet}$ were found to be the predominant radical products when single crystals of $Sr(NO_3)_2$ were gamma irradiated at low temperatures. If the irradiations and ESR observations are carried out at sufficiently low temperatures (e.g., 64°K), both radicals are stably trapped; their concentrations do not change with time. While accurate assays of the radical concentrations have not been made, approximate integrations of the ESR lines indicate that their concentrations are roughly equal. When the crystals are warmed to 77°K, the line intensities from both radicals decrease with time, and a second form of $NO_3^{\bullet}$, not seen at the low temperature, grows. All changes occur irreversibly. Ultimately, the low-temperature form of $NO_3^{\bullet}$ (a) completely disappears, $\dot{N}O_3^{2-}$ partially decays to a steady-state concentration, and the second form of $NO_3^{\bullet}$ (b) increases to a steady concentration. The rates of these changes increase with radiation dose.

Hyperfine (^{14}N) and g tensors for the three radicals have been derived from measured spectra and are very similar to those of $\dot{N}O_3^{2-}$ and $NO_3^{\bullet}$ seen in other systems. All tensors are axially symmetric, with unique directions in the (111) direction of the cubic crystal. This suggests that the radicals are trapped in or very near nitrate positions.

The growth and decay of the ESR lines of the radicals have been followed at 77°K after irradiating for

different times at 64°K. While the proportionality between line intensity and various radical concentrations has not been established, the data have been semiquantitatively analyzed and are consistent with the following reaction scheme:

$$NO_3^{\bullet}\ (a) + \dot{N}O_3^{\ 2-} \rightarrow 2NO_3^{-}\ , \qquad (1)$$

$$NO_3^{\bullet}\ (a) + \text{“trap”} \rightarrow NO_3^{\bullet}\ (b)\ . \qquad (2)$$

In this scheme the $\dot{N}O_3^{\ 2-}$ and the "trap" are regarded as fixed in the lattice, while (at 77°K) the $NO_3^{\bullet}$ (*a*) is mobile. It migrates throughout the lattice as a hole (by electron transfer with adjacent nitrate ions). It eventually either finds and reacts with $\dot{N}O_3^{\ 2-}$ [reaction (1)] to form diamagnetic products (presumably nitrate ions) or finds an immobilizing trap [reaction (2)], yielding the second form of $NO_3^{\bullet}$ (*b*).

When the crystal is irradiated at 64°K, it is reasonable that trapping sites are available to stabilize both forms of $NO_3^{\bullet}$, yet no $NO_3^{\bullet}$ (*b*) was detected, even though it is the more stable form. Thus, one can conclude that there are many more *a* sites than *b*. This suggests that $NO_3^{\bullet}$ (*a*) is a "self-trapped" radical and that $NO_3^{\bullet}$ (*b*) is trapped near a stabilizing defect.

ELECTRON SPECTROSCOPY

Two programs employing the use of electron spectroscopy are supported by the Chemistry Division: one is located in the Physics Division and is carried out in joint collaboration with that Division; the other program is carried out at the Transuranium Research Laboratory.

The first program emphasizes the development of electron spectroscopy as a tool for the study of chemical problems. During the last year a substantial effort was employed in the use of angular distribution measurements on the photoelectron spectra of gaseous molecules. Some 40 systems have now been studied. The purpose of these studies is to develop a method for determining the nature of the molecular orbitals associated with each ionization band. A second major effort has been in the study of the chemical shifts in the core binding energies of a large variety of salts, particularly the alkali metal halides and members of groups III-A and V-B of the periodic table. The third major effort has been in the exploitation of electron spectroscopy for use in environmental research. Most of this work has been reported in the Physics Annual[1] as abstracts of papers. In addition, four brief summaries of recent work follow.

At the Transuranium Research Laboratory the binding energies of electrons in the 4*d* to 6*p* levels of americium have been determined.[2] Values of the atomic energy levels and x-ray energies of the actinides not yet measured are being determined in order to evaluate the consistency of the experimental results[3] obtained both here and elsewhere.

1. *Phys. Div. Annu. Progr. Rep. Dec. 31, 1971*, ORNL-4743, pp. 112–17.
2. M. O. Krause and F. Wuilleumier, "Electron Binding Energies in Americium," a contribution in chap. 2, this report.
3. M. O. Krause and F. Wuilleumier, "Evaluation of Atomic Energy Levels and X-Ray Energies for the Actinide Elements," a contribution in chap. 2, this report.

STUDY OF THE ANGULAR DISTRIBUTION FOR THE PHOTOELECTRON SPECTRA OF HALOGEN-SUBSTITUTED METHANE MOLECULES[1,2]

T. A. Carlson R. M. White[3]

The intensity of photoelectrons ejected from randomly oriented gaseous molecules as a function of the angle θ between the direction of the incoming photon and outgoing photoelectron is given from theory to be

$$1 + \frac{1}{2}\beta\left(\frac{3}{2}\sin^2\theta - 1\right)\ .$$

The angular parameter β is dependent on two factors: the photoelectron energy and the nature of the molecular orbital from which the photoelectron is ejected. Angular measurements should provide a powerful method for identifying an orbital associated with a given ionization band. The angular parameters β have been determined for most of the ionization bands found in photoelectron spectra of the following molecules: CH_3F, CH_2F_2, CHF_3, CF_4, CH_3Cl, CH_2Cl_2, CCl_4, CH_3Br, and CH_3I. To obtain these results, a dispersion electron spectrometer was employed, to which was attached a chamber containing a freely rotating gas discharge lamp that provided a directed beam of He I (589 Å) radiation. An attempt to correlate β with calculated population densities and atomic angular parameters was partially successful. The dependence of β on the vibrational structure has also been considered.

1. Work carried out jointly with the Physics Division.

2. Abstract of paper to be given at the General Discussion on Photoelectron Spectroscopy of Molecules, University of Sussex, sponsored by the Faraday Society, September 12–14, 1972.
3. On sabbatical leave from Baker University, Baldwin, Kan.

USE OF X-RAY PHOTOELECTRON SPECTROSCOPY TO STUDY BONDING IN Cr, Mn, Fe, AND Co COMPOUNDS[1,2]

J. C. Carver[3] G. K. Schweitzer[4]
T. A. Carlson

The photoelectron spectra of some 40 transition metal compounds have been measured using Al $K\alpha$ (1487 eV) and Mg $K\alpha$ (1254 eV) x rays. The compounds include both simple salts (halides and chalcogenides) and hexacoordinated complexes (cyano and fluoro) of Cr(III), Mn(II, III), Fe(II, III), and Co(III). From these data we have determined the chemical shifts of the core electrons and have related these results to a calculated charge based on Pauling electronegativities. In addition, multiplet splitting has been obtained for photoionization in the 3*s* shell and has been interpreted in terms of the exchange interaction between the partially filled 3*s* and 3*d* orbitals. To help in this explanation, calculations were made using both (1) Hartree-Fock solutions of the wave function for free ions and (2) a qualitative evaluation of the behavior of the exchange integral. The value of using x-ray photoelectron spectroscopy for studying chemical bonding in transition-metal compounds is amply illustrated.

1. Work carried out jointly with the Physics Division.
2. Abstract of paper to be published in the *Journal of Chemical Physics.*
3. Former graduate student from the University of Tennessee, Knoxville, supported by NSF grant.
4. Department of Chemistry, University of Tennessee, Knoxville.

STUDY OF THE X-RAY PHOTOELECTRON SPECTRUM OF TUNGSTEN–TUNGSTEN OXIDE AS A FUNCTION OF THICKNESS OF THE SURFACE OXIDE LAYER[1,2]

T. A. Carlson G. E. McGuire[3]

The photoelectron spectrum of tungsten metal using Al $K\alpha$ x rays has been studied as a function of a tungsten oxide layer on the surface. The photoelectron lines arising from the 4*f* shell of tungsten metal are clearly separate in energy from those coming from WO_3. The ratios of the intensities of these two sets of lines were measured for a series of metal samples which were anodized to a determined level of tungsten oxide. The data were shown to be consistent with a uniform deposition of oxide film. The escape depth, or thickness from which half the photoelectron intensity is derived, was found for a 1450-eV photoelectron to be 8.9 Å for W and 18.3 Å for WO_3.

1. Work carried out jointly with the Physics Division.
2. Abstract of paper to be submitted to the *Journal of Electron Spectroscopy.*
3. Graduate student, University of Tennessee, Knoxville, supported by National Science Foundation grant.

STUDY OF CORE BINDING ENERGIES OF SIMPLE AND COMPLEX SALTS USING X-RAY PHOTOELECTRON SPECTROSCOPY[1,2]

G. E. McGuire[3] T. A. Carlson
G. K. Schweitzer[4]

Chemical shifts in a wide variety of compounds were studied in order systematically to examine some of the factors causing these shifts. Systems that were studied included the alkali halides and compounds of indium, gallium, aluminum, niobium, tantalum, tungsten, and uranium.

An attempt was made to use photoelectron spectroscopy to distinguish halogen groups attached in bridging and terminal positions within some selected compounds. By itself, photoelectron spectroscopy cannot prove the existence of such groups, but in some cases it was found to give supportive evidence to available x-ray crystallographic data. The evidence used was the line broadening seen in the halogen spectra when compared with halogen reference lines in the simple salts NaF, NaCl, and KBr. The presence of line broadening may indicate the presence of bridging and terminal groups, but the absence of line broadening cannot be employed to rule out nonequivalent sites. The photoelectron spectra were sometimes found to be inadequately sensitive to the small separations expected in the binding energies of these groups. The expected maximum separations were predicted by a very simple calculation which took into consideration only the distances to nearest neighbors. These values were maxima, since a pure ionically bonded model was employed, which meant that actual values would be smaller because of covalent contributions. If a quantitative model could be developed that would take into consideration these covalent contributions and the influence of all the surrounding ions in the crystal, it might be possible to predict the expected values more accurately.

Chemical shifts observed in a number of solid compounds were related to a theoretical "free-ion" shift plus a crystal-potential shift. Using the simple alkali halides, we demonstrated that these two factors generally compete so that only small net chemical shifts are produced. The theoretical values of "free-ion" and crystal-potential shifts were based on an electrostatic model involving ionic charges (calculated by the Pauling method), empirical internuclear distances, and radii which were assigned to the crystal components. Since the Pauling charges agree at least approximately with more complex theoretical calculations, they were judged to be adequate. The internuclear distances, being experimentally derived, were also deemed appropriate. Thus major attention was turned toward the assignment of radii. Three types of radii were tried for the alkali halides: ionic radii, atomic radii, and radii based on electron density mapping. It was found that for the metal-ion shifts in the alkali halides, theoretical values based on ionic radii generally gave fair agreement with the experimental values. Because the differences in the Pauling charges were so small for the halogen ions in the alkali halides, it was found that the set of theoretical values which would give the best comparison with the experimental values could not be determined.

When this treatment was extended to metal-ion shifts in some alkaline-earth, aluminum, and gallium compounds, it was found that in general for highly ionic compounds, ionic radii gave the better results, while for more covalent compounds, atomic radii gave the better set of theoretical values.

Certain oxides of uranium can be prepared in pure form. It was desirable to show whether photoelectron spectroscopy can distinguish UO_2, UO_3, and U_3O_8. It was found that uranium core electrons have slightly different binding energies in each of these compounds.

The photoelectron spectra of analogous compounds of aluminum, gallium, and indium, as well as of niobium, tantalum, and tungsten, were compared to determine relative chemical shifts. This method was based on the assumption that crystal potentials of analogous compounds might be similar. Of the group III-A elements studied, aluminum was found to give shifts similar to those of gallium and larger than those of indium. The analogous compounds of all three of the transition elements — niobium, tantalum, and tungsten — were found to give similar chemical shifts.

1. Work carried out jointly with the Physics Division.

2. Summary taken from Ph.D. thesis of G. E. McGuire (University of Tennessee, Knoxville, 1972).

3. Graduate student, University of Tennessee, Knoxville, supported by National Science Foundation grant.

4. Department of Chemistry, University of Tennessee, Knoxville.

X-RAY ANALYSIS BY PHOTOELECTRON SPECTROMETRY[1]

M. O. Krause F. Wuilleumier[2]

As an important variant, photoelectron spectrometry has been shown[3] to be an excellent technique for the analysis of soft and ultrasoft x rays. Both in the customary ESCA method and in this new application of photoelectron spectrometry alike, the energies and flux of ejected photoelectrons are measured; but while in ESCA, binding energies of unknown molecular levels are derived using a fixed monochromatic x-ray line, in the new technique, energies of x rays from unknown x-ray emitters are derived using a fixed energy level of the converter. Thus, the Einstein relation $h\nu = E_{e,\mathrm{kin}} + E_B$ benefits us in a twofold way.

The electron spectrometer operated in the "x-ray mode" constitutes an instrument of high resolution, $\Delta E/E$, typically 0.1% in photoelectron energy. With Ne $2p$ as the converter level, the resolution in x-ray energy varies from 0.1 eV at 25 eV to about 0.4 eV at 400 eV, which equals the resolution obtainable with grating spectrometers but exceeds that of organic crystals and nondispersive devices. From about 400 eV to 600 eV, $\Delta E/E$ = 0.4 to 0.6 eV; the resolution is equal to or better than that of the potassium acid phthalate (KAP) crystal. From 600 eV to 3000 eV, $\Delta E/E$ = 0.6 to 2 eV; the conventional inorganic-crystal spectrometer exhibits better resolution provided the proper crystals are chosen for the various energy ranges.

Besides good resolution the new technique exhibits simple and well-defined intensity characteristics over the entire energy range. Thus, x-ray analysis by photoelectron spectrometry covers the energy range from 20 to 3000 eV *continuously* and provides a resolution of better than 2 eV with intensity characteristics that make accurate relative and absolute intensity measurements possible.

The new technique has been applied to studies in a number of areas. They are as follows:[3,4] (1) line widths and line energies of the ultrasoft $M\zeta$ x rays of Y, Zr, Nb, Mo, and Rh from 130 to 260 eV; (2) line intensities of the Zr L x rays between 1700 and 2500 eV; (3) band structure of Zr, Nb, and Mo scanned by the soft M x rays terminating in the conduction band; (4) structure of $4f$ level of Ho using the $3d$-$4f$ (1400 eV) and $4d$-$4f$ (150 eV) x rays; and (5) estimate of the oxygen content of Ho metal by comparing the intensities of oxygen K x

rays and holmium (*3d-4f*) x rays. Another promising area for application of the technique is qualitative and quantitative analysis, especially of light elements, in conjunction with the use of electron-optical viewing techniques.

1. Synopsis of a paper to be published in the *Proceedings of the International Conference on Inner Shell Ionization Phenomena,* April 1972, Atlanta, Ga.
2. Visiting scientist from Laboratoire de Chimie Physique de l'Université, Paris VI, France.
3. M. O. Krause, *Phys. Rev.* **177**, 151 (1969).
4. M. O. Krause, *Chem. Phys. Lett.* **10**, 65 (1971); M. O. Krause and F. Wuilleumier, *Phys. Lett. A* **35**, 341 (1971); M. O. Krause and F. Wuilleumier, *Proceedings of the International Conference on Inner Shell Ionization Phenomena,* Apr. 17, 1972, Atlanta, Ga. (to be published).

ATOMIC AND MOLECULAR COLLISIONS

VELOCITY DEPENDENCE OF ELECTRONIC TO VIBRONIC ENERGY CONVERSION FOR Hg (6^3P_2) IN MOLECULAR COLLISIONS

H. F. Krause S. Datz

We have completed a study of the collisional conversion of atomic electronic excitation to molecular vibronic excitation using velocity-selected crossed-molecular-beam techniques. The conversion of metastable Hg (6^3P_2) to Hg (6^3P_1) by collision with N_2, NO, CH_4, D_2, and H_2 was measured by observation of the light emanating from the decay of the Hg (6^3P_1) to the ground state (6^1S_0). The Hg (6^3P_2), formed by electron bombardment of a 400°K Hg atomic beam, intersected a velocity-selected beam of reactant molecules; the 2537-Å radiation was detected with a photomultiplier fitted with an interference filter.

For all reactant molecules studied, the quenching cross sections depend on the relative collision energy, E, according to $E^{-0.5}$ between 0.01 and 0.15 eV. The relative cross sections at 0.05 eV for N_2, NO, CH_4, D_2, and H_2 are in the ratio 1.00:0.92:0.78:0.18:0.58 respectively. These relative cross sections are in general agreement with relative total quenching cross sections obtained by Doemeny, Van Itallie, and Martin[1] in experiments that did not employ velocity selection. Two theoretical models have been proposed for Hg (6^3P) quenching. The model of Dickens, Linnett, and Sovers[2] assumes no crossing or near crossing of the initial- and final-state potential-energy curves. This theory is analogous in formalism to models for intermolecular vibration-vibration energy transfer. In contrast to the experimental results, it predicts a pronounced increase of the quenching cross section with increasing energy throughout the experimental energy range and cross-section magnitudes that resonantly depend on the closeness of match between the electronic energy given and the vibrational energy received during the collision.

The model of Bykhovskii and Nikitin (BN),[3] contrary to the assumptions of Dickens et al., suggests that the degeneracies of initial and final states of the triatomic quasi molecule must be considered during the collision. This assumption means that the quenching efficiency depends on the energy separation of the initial and final states for the quasi molecule and does not depend on the energy defect at infinite separation as in the Dickens et al. model. When the relative motions of the nonadiabatically interacting initial and final states are considered semiclassically, the transition probability far from threshold reduces to the form of the Landau-Zener model, which predicts an energy dependence of $E^{-0.5}$. The experimental quenching cross sections also behave in this manner in the energy region investigated, where Landau-Zener should be valid.

1. L. J. Doemeny, F. J. Van Itallie, and R. M. Martin, *Chem. Phys. Lett.* **4**, 302 (1969).
2. P. G. Dickens, J. W. Linnett, and O. Sovers, *Discuss. Faraday Soc.* **33**, 52 (1962).
3. V. K. Bykhovskii and E. E. Nikitin, *Opt. Spectrosc. (USSR)* **16**, 111 (1964).

IONIZING COLLISIONS OF FAST ALKALI ATOMS WITH Cl_2, Br_2, AND O_2

N. Kashihira[1] F. Schmidt-Bleek[2]
S. Datz

The study of energy loss accompanying chemi-ionizing collisions of fast alkali atoms (50–350 eV) has been completed.[3] The inelastic energy losses were found to be nearly energy independent for collisions of K or Cs with Cl_2, Br_2, and O_2 and ranged from about 8 to 10 eV, irrespective of the reactants. The collisions between alkali atoms and halogen molecules (Cl_2 and Br_2) yield as intermediates alkali ions (M^+) and excited molecular ions (X_2^-) in the $^2\Sigma_g$ state. This is followed by dissociation to the ground-state halogen ions or to excited halogen atoms. In the case of oxygen, excited molecular ions in the $^2\Pi_u$ state are formed, and these species either remain in the bound state of the $^2\Pi_u$ or decay to vibrationally excited molecular states ($^b\Sigma_g^+$, $^a\Delta_g$). The excitation functions (change of cross sections with incident energy variations) were interpreted in

terms of curve crossings near or inside the equilibrium distance of the $M\text{-}X_2$ potential surfaces.

1. Graduate student, Department of Chemistry, Purdue University, Lafayette, Ind.
2. Department of Chemistry, University of Tennessee, Knoxville.
3. Details have appeared in the Ph.D. thesis of N. Kashihira and will be submitted to the *Journal of Chemical Physics.*

SPECTATOR STRIPPING IN FAST ALKALI ATOM AND ION COLLISIONS WITH DIATOMIC MOLECULES

S. Datz F. Hwang[1]
F. Schmidt-Bleek[2]

A portion of the results of our previous work[3] on dissociative collisions between alkali atoms and hydrogen molecules has been reinterpreted in terms of a possible spectator stripping model[4] for high-energy (>30 eV) collisions. In this model the backscattered atom or ion is considered to interact elastically with only one atom of the diatomic molecule, and the coupling of the hydrogen atoms is neglected. This is justifiable if the collision time is short compared with the intramolecular coupling time. This model gives results which compare favorably with experimental observations. To test whether this is a general effect at high energies, Cs^+ ions of 50 to 200 eV were backscattered from N_2 molecules, and a peak appeared at energies corresponding to single-atom interactions. This type of energy transfer could lead to molecular dissociation and may prove to be an important mode for "hot atom" reaction kinetics.

1. Graduate student, Department of Chemistry, University of Tennessee, Knoxville.
2. Department of Chemistry, University of Tennessee, Knoxville.
3. P. F. Dittner and S. Datz, *J. Chem. Phys.* **54**, 4228 (1971).
4. R. E. Minturn, S. Datz, and R. L. Becker, *J. Chem. Phys.* **44**, 1149 (1966).

"HOT-ATOM" BEAM SOURCES FROM ELECTRON SPUTTERING OF ALKALI HALIDES

G. Ostrom[1] F. Schmidt-Bleek[2]
S. Datz

A study of a new "hot-atom" beam source has been initiated, and preliminary results have been obtained. This source is based on electron sputtering of alkali halides. The sputtering process is thought to take place through the formation and relaxation of V_K centers (ions). Sputtering yields of 3 halogen atoms per incident electron at 1 keV have been reported, but the energy distribution of the emergent atoms remained unknown. To investigate this, we constructed an electron sputtering apparatus and installed it in an existing mass spectrometer which we previously used to study the velocity distribution of iodine atoms sputtered from AgI by Ar ion bombardment.[3] Using KI targets, we have observed sputtered I atoms with energies greater than 1 eV, but the detailed energy distribution, yields, etc., remain to be determined. The results obtained from this work on a series of alkali halides will have relevance not only to hot-atom beam sources but to the basic mechanism of electron radiation effects on ionic crystals and to possible problems of Cl_2 generation in salt-mine storage of highly radioactive waste.

1. Graduate student, Department of Chemistry, University of Tennessee, Knoxville.
2. Department of Chemistry, University of Tennessee, Knoxville.
3. S. Datz, G. Ostrom, and F. Schmidt-Bleek, *Chem. Div. Annu. Progr. Rep. May 20, 1969,* ORNL-4437, p. 140; also, F. Schmidt-Bleek, G. Ostrom, and S. Datz, *Rev. Sci Instrum.* **40**, 1351 (1969).

INNER-SHELL IONIZATION IN FAST HEAVY-ION COLLISIONS

S. Datz H. O. Lutz[2]
C. D. Moak[1] J. Stein[2]

As reported last year,[3] we observed remarkable specificity in the creation of L-shell vacancies in iodine in atomic collisions at energies of from 15 to 60 MeV. The ratio of $2p_{3/2}$ to $2p_{1/2}$ or $2s$ vacancies varied by a factor of 7 depending on the target atom (Z_2 = 6 to 82) and showed two maxima over the range of targets used. Since that time, a theory including fine structure has been developed[4] involving curve crossing of molecular orbitals. This theory predicts that only $2p_{3/2}$ electrons can be promoted by quasi-molecular interaction of inner-shell atomic orbitals and that the process should be strongly dependent on the collision partner. However, the behavior with Z_2 is not yet explained, and the high cross section observed for $2p_{1/2}$ and $2s_{1/2}$ vacancy production ($\sim 10^{-18}$ cm^2) is not anticipated.

Even though the mechanism for vacancy formation in fast heavy ions is not thoroughly understood, application of these observations was made in the study of the states of ions as they penetrate matter.[5] In experiments using 50-MeV I, we observed that the L-ionization cross section of the iodine ion was larger by a factor of 10 in a solid medium as compared with a gaseous medium

(e.g., Se compared with Kr or Br_2). This difference could be explained in terms of the steady-state population of M-shell vacancies, which depended upon the collision frequency in the medium, the M-shell vacancies being necessary for molecular promotion of iodine L-shell electrons. In this work it was also observed that M-shell ionization cross sections are in the order of 10^{-17} cm^2. Relaxation of these M-shell vacancies takes place principally by Auger processes and hence should give a high yield of high-energy Auger electrons along the track of the penetrating particle. The presence of this Auger-electron component, in which a large number of energetic electrons are released in a very short distance, can have significance in terms of the efficacy of heavy-ion radiation therapy and certain forms of radiation damage. Preliminary experiments on the energy distribution of electrons emerging from thin carbon targets under iodine ion bombardment have indicated the existence of the Auger component.

1. Physics Division.
2. Kernforschungsanlage, Jülich, West Germany.
3. S. Datz, C. D. Moak, B. R. Appleton, and T. A. Carlson, *Chem. Div. Annu. Progr. Rep. May 20, 1971*, ORNL-4706, p. 246; also, *Phys. Rev. Lett.* **27**, 363 (1971).
4. H. Barat and W. Lichten, *Phys. Rev. A* (in press).
5. H. O. Lutz, J. Stein, S. Datz, and C. D. Moak, *Phys. Rev. Lett.* **28**, 8 (1972).

INNER-SHELL IONIZATION BY PROTON AND ALPHA-PARTICLE BOMBARDMENT

S. Datz J. U. Andersen[1]
E. Laegesgaard[1] L. C. Feldman[1]
J. L. Duggan[2]

The mechanism for inner-shell ionization by protons and alpha particles is understood in terms of Coulomb excitation of the electrons by the passing ion. Detailed calculations using the plane-wave Born approximation and relativistic electron wave functions have recently been carried out to predict cross sections for L-subshell ionization.[3] To check the theory, we analyzed L x-ray spectra of Au made by bombardment with 0.2- to 3.0-MeV/nucleon proton and alpha-particle beams[4] and found good qualitative agreement with the calculations for protons. However, the theory is not nearly exact enough, especially at the low energies, to fit the data to within 30%. Moreover, the behavior of alpha particles is significantly different from that anticipated from a properly scaled proton excitation cross section. This kind of information, aside from its intrinsic interest, is necessary for the proper interpretation of light-ion-induced x-ray spectra which may be used in analytical applications.

1. Physics Institute, University of Aarhus, Aarhus, Denmark.
2. Oak Ridge Associated Universities.
3. B. H. Choi and E. Merzbacher, private communication.
4. Details will be published in the *Physical Review*.

THE Z^2 DEPENDENCE OF THE X-RAY PRODUCTION CROSS SECTION BY 5-MeV/amu HEAVY IONS[1]

A. van der Woude[2] C. A. Ludemann[2]
M. J. Saltmarsh[2] R. L. Hahn
E. Eichler

Theoretical predictions for the cross section σ_I of ionization of inner-shell electrons by fast ions indicate that σ_I is proportional to Z^2, where Z is the projectile charge, as long as the electrons are not polarized by the projectile during the interaction.[3,4] Recently a few tests using He and Li ions have been made which indicate that appreciable deviations from this simple scaling law can occur in the K x-ray production cross section.[5,6] In order to test this further, we measured the cross section for the production of K x rays, σ_X, of Ti, Fe, Co, Zr, Sn, and Nd and for L x rays of Sn, Nd, and Au by 5-MeV/amu He, C, O, and Ne ions. We also measured σ_X for 10-MeV/amu C ions on the same targets. The 5-MeV/amu projectiles were obtained by accelerating He^{1+}, C^{3+}, O^{4+}, and Ne^{5+} ions in ORIC. By this particular choice of ions, only minor adjustments in the cyclotron are necessary in order to switch from one ion to another, while the energy per amu will be the same for each ion.

An absolute value of the x-ray production cross section σ_X can be obtained by comparing the yield of the x rays with the yield of Coulomb-scattered particles; in our case, the Coulomb cross section is independent of the nature of the projectiles at small angles of observation. This method eliminates the need to measure target thickness and beam current and thus enables one to perform accurate absolute measurements. The x-ray yield was measured at an angle of 135° with respect to the incoming beam by using an Si(Li) detector with a resolution of about 250 eV at 5.9 keV. Target thicknesses ranged from 200 to 1000 μg/cm^2. For most cases the absolute uncertainty in σ_X is ±6%; the uncertainty in the ratio between σ_X for different projectiles is, in most cases, better than ±2%.

A well-known phenomenon of heavy-ion-induced x rays is the shifting of x-ray energies, which is presumably due to the creation of multiple inner-shell vacan-

cies.[7,8] We measured these shifts for the $K\alpha$ lines of Fe, Co, Zr, and Sn and for the $K\beta$ lines of Fe and Co by fitting the observed spectra with a function consisting of Gaussian peaks superposed on a quadratic background. It was found empirically that for the bombarding energies of 5 and 10 MeV/amu the observed energy shift for each target is a nearly linear function of the stopping power of the bombarding ion. This is shown in Fig. 7.33; the stopping powers were obtained from Northcliffe and Schilling.[9]

Figure 7.34 shows the quantity $U_K{}^2\ \sigma_I{}^K/Z^2$ as a function of $E/\lambda U_K$ for the 5-MeV/amu He ions and the 10-MeV/amu ^{12}C ions. The quantity E/λ is the energy per nucleon, and U_K is the binding energy of the K-shell electron. The $\sigma_I{}^K$ are calculated from the relation $\sigma_X{}^K = \omega_K\ \sigma_I{}^K$. The fluorescence yields (ω_K) that were used are summarized in Table 7.13. The curve is the prediction of the binary-encounter model of ref. 3. In general there is a reasonable agreement between

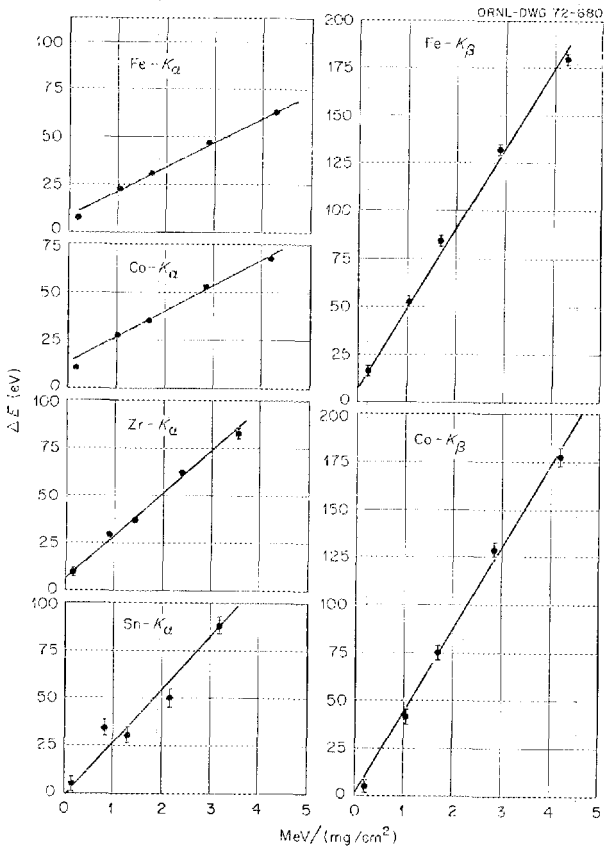

Fig. 7.33. Energy shift (ΔE) observed in the K x-ray spectra produced by 5-MeV/amu He, C, O, and Ne ions and 10-MeV/amu C ions vs the stopping power (S) of the ions. The curves illustrate the empirically observed nearly linear relation between ΔE and S.

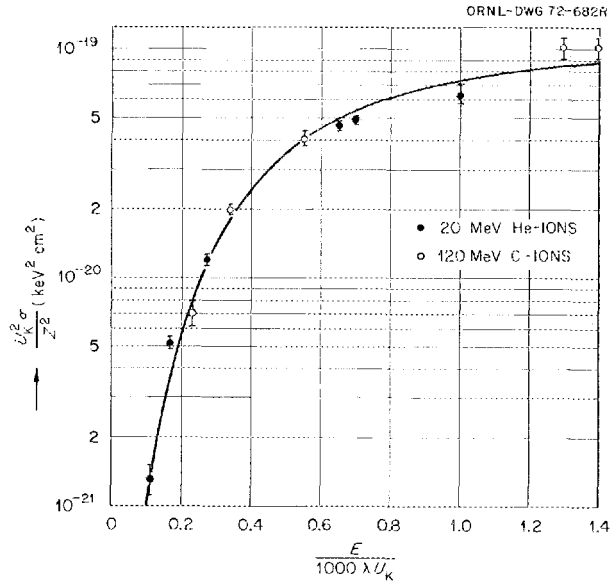

Fig. 7.34. Comparison of the experimentally observed ionization cross sections σ with the theoretical results of ref. 3. The values of σ are deduced from the experimentally measured x-ray production cross sections σ_X by using the fluorescence yields of Table 7.13.

Table 7.13. Fluorescence yields

Element	ω_K
Ti	0.221
Fe	0.344
Co	0.366
Zr	0.737
Sn	0.86
Nd	0.91

the predicted and experimental values for the He ions. The values for the 10-MeV/amu C ions for Fe and Co are about 10 to 15% above the predicted values.

In order to illustrate the Z^2 dependence of the x-ray production cross sections, we define the quantity

$$R_X(Z_1, Z_2) = [\sigma_X(Z_1)/\sigma_X(Z_2)](Z_2/Z_1)^2 .$$

Figure 7.35 shows $R_X(Z_1, Z_2)$ for $Z_2 = 2$ and $Z_1 = 6, 8$, and 10 as a function of $\xi = E/1000\lambda U$, where U is the binding energy of the K shell or a suitable average of the binding energies of the L shells. The experimental data suggest the following systematic trends: (1) For each projectile, R_X changes from values greater than 1 to values less than 1 at $\xi \sim 0.45$; (2) for each value of ξ, the value of $|R_X - 1|$ increases with increasing Z_1; (3) the behavior of R is approximately the same for K and L x rays.

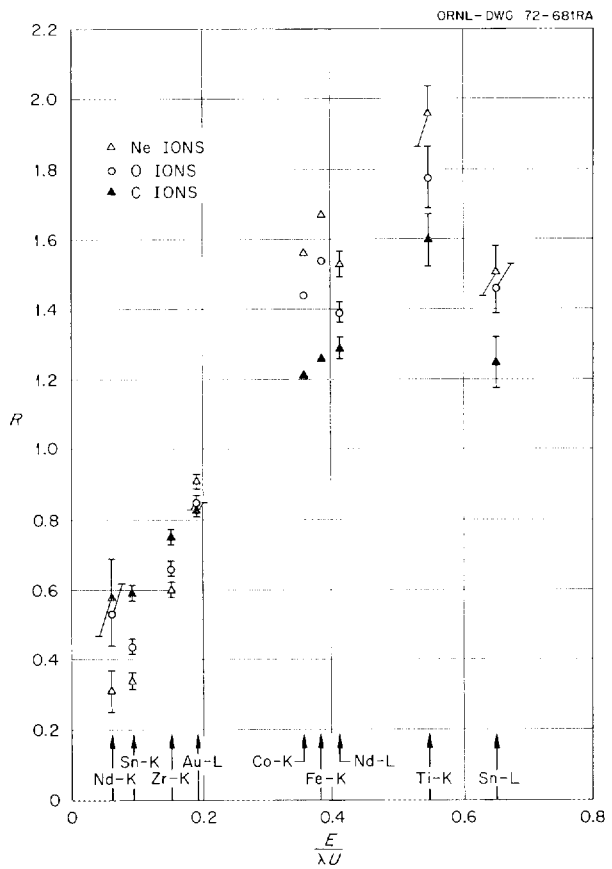

Fig. 7.35. Ratio $R(Z_1, Z_2) = [\sigma_x(Z)/\sigma_x(Z_2)](Z_2/Z_1)^2$ for K and L x rays with $Z_2 = 2$ and $Z_1 = 6$, 8, and 10 vs $E/1000\lambda U$, where E/λ is the energy per amu of the projectile and U is the appropriate electron binding energy.

Table 7.14. $|R(Z_1, Z_2) - 1|Z_t/(Z_1 - Z_2)$ with $Z_2 = 2$ for the K x-ray cross section

Target	Value for the projectile indicated		
	C	O	Ne
Ti	3.3 ± 0.1	2.9 ± 0.1	2.6 ± 0.1
Fe	1.7 ± 0.1	2.34 ± 0.1	2.2 ± 0.1
Co	1.4 ± 0.1	2.0 ± 0.1	1.4 ± 0.1
Zr	2.5 ± 0.2	2.3 ± 0.2	2.0 ± 0.1
Sn	5.1 ± 0.1	4.6 ± 0.2	4.1 ± 0.2
Nd	4.2 ± 1.0	4.7 ± 0.9	5.2 ± 0.5

The fact that $R_x \neq 1$ can be due to a Z_1 dependence of the fluorescence yield ω, or it can indicate that σ_I does not scale as Z_1^2. Most probably both effects have to be taken into account. However, in the case of Zr, Sn, and Nd, it is reasonable to assume that the fluorescence yield is not very Z-dependent, since the energy shifts indicate that the number of additional L vacancies created is only about unity[10] and the fluorescence yield of the undisturbed atoms is already large. Thus the observed discrepancy of a Z^2 dependence for the x-ray production cross section σ_x very likely reflects in these cases the behavior of the ionization cross section σ_I.

If we assume that the ionization cross section σ_I can be written as $\sigma_I = \sigma_I^0 [1 + \delta(Z_1/Z_t)^2]$, where σ_I^0 is the cross section calculated without taking polarization effects into account[3,4] and Z_t is the charge of the target atom, then the quantity $|R(Z_1, Z_2) - 1|Z_t/(Z_1 - Z_2)$ should be independent of Z_1. Table 7.14 shows that this is approximately true for the Zr, Sn, and Nd targets. This suggests that for small ξ values the effects of polarization of the electron orbits by the projectile can to a large extent be described by adding a Z_1^3 term in the ionization cross section. For the lighter elements, one first would have to establish either experimentally or theoretically the effect of multiple vacancies on the fluorescence yield before such an evaluation could be made. A similar remark can be made with respect to the L x rays of Sn, Nd, and Au, although it may be meaningful that all the data indicate the same trend of R vs $E/\lambda U$.

1. A similar report has appeared in *Phys. Div. Annu. Progr. Rep. Dec. 31, 1971*, ORNL-4743, p. 131.
2. Physics Division.
3. J. D. Garcia, *Phys. Rev. A* **1**, 280 (1970); *Phys. Rev. A* **4**, 955 (1971).
4. E. Merzbacher and H. W. Lewis, *Encyclopedia of Physics*, vol. 34, p. 166, Springer-Verlag, Berlin, 1958.
5. G. Basbas, W. Brandt, R. Laubert, A. Ratkowski, and A. Schwarzschild, *Phys. Rev. Lett.* **27**, 171 (1971).
6. C. W. Lewis, J. B. Natowitz, and R. L. Watson, *Phys. Rev. Lett.* **26**, 481 (1971).
7. D. Burch and P. Richard, *Phys. Rev. Lett.* **25**, 983 (1970).
8. D. Burch, P. Richard, and R. L. Blake, *Phys. Rev. Lett.* **26**, 1355 (1971).
9. L. C. Northcliffe and R. F. Schilling, *Nucl. Data Sect. A* **7**, 233 (1970).
10. T. A. Carlson, private communication.

Publications

NUCLEAR CHEMISTRY

E. Eichler and S. Raman,[1] "New Observations in the A = 49 Chain; Levels in ^{49}Sc and ^{49}Ti," *Phys. Rev. C* **3**, 2268 (1971).

B. R. Erdal,[2,3] A. C. Wahl,[2] and R. L. Ferguson, "Modes of Formation of Tin Fission Products," *J. Inorg. Nucl. Chem.* **33**, 2763 (1971).

C. E. Bemis, Jr., R. E. Druschel, J. Halperin, and J. R. Walton,[4] "Thermal-Neutron Capture Cross Section and Resonance Integral for 10.7-year Krypton-85," *Nucl. Sci. Eng.* **47**, 371 (1972).

N. K. Aras,[5] P. Fettweis,[6] G. Chilosi,[7] and G. D. O'Kelley, "Levels in ^{101}Ru Populated by the Decay of ^{101}Tc," *Nucl. Phys. A* **169**, 209 (1971).

N. C. Singhal,[8] N. R. Johnson, E. Eichler, and J. H. Hamilton,[9] "Energy Levels of ^{104}Pd Populated in the Decay of 43-sec ^{104}Rh and 4.41-min ^{104m}Rh," *Phys. Rev. C* **5**, 948 (1972).

N. D. Johnson,[9] J. H. Hamilton,[9] A. F. Kluk,[10] and N. R. Johnson, "Decay of ^{108}Ag," *Z. Phys.* **243**, 395 (1971).

B. H. Ketelle, A. R. Brosi, and J. R. Van Hise,[11] "Decay of ^{136}Pr and the Level Structure of ^{136}Ce," *Phys. Rev. C* **4**, 1431 (1971).

A. F. Kluk,[10] "Investigations of the Level Structure and of the Rotation-Vibration Interaction in ^{156}Gd and ^{158}Gd," Ph.D. thesis, Vanderbilt University, Nashville, Tenn., August 1971.

J. H. Hamilton,[9] P. E. Little,[9] A. V. Ramayya,[9] E. Collins,[9] N. R. Johnson, J. J. Pinajian,[12] and A. F. Kluk,[10] "$M1$ Admixtures of Transitions in ^{156}Gd," *Phys. Rev. C* **5**, 899 (1972).

E. Collins,[9] J. H. Hamilton,[9] P. E. Little,[9] A. V. Ramayya,[9] M. U. Kim,[9] A. F. Kluk,[10] and N. R. Johnson, "γ-γ Directional Correlations of the 961-89 and 2089-89 keV Cascades in ^{156}Gd," p. 245 in *Angular Correlations in Nuclear Disintegration,* edited by H. van Krugten and B. van Nooijen, Rotterdam University Press, 1971.

K. S. Toth,[13] R. L. Hahn, and M. A. Ijaz,[14] "Investigation of Thulium α Emitters; New Isotopes, ^{155}Tm and ^{156}Tm," *Phys. Rev. C* **4**, 2223 (1971).

---

1. Nuclear Data Project.
2. Washington University, St. Louis, Mo.
3. Present address: Iowa State University of Science and Technology, Ames.
4. Analytical Chemistry Division.
5. Middle East Technical University, Ankara, Turkey.
6. Centre d'Etude de l'Energie Nucléaire, Mol, Belgium.
7. Istituto di Fisica Superiore, Università di Napoli, Napoli, Italy.
8. Graduate research assistant from Vanderbilt University, Nashville, Tenn.
9. Vanderbilt University, Nashville, Tenn.
10. Oak Ridge Graduate Fellow from Vanderbilt University, Nashville, Tenn., under appointment with Oak Ridge Associated Universities. Present address: U.S. Atomic Energy Commission, Bethesda, Md.
11. Present address: Tri-State College, Angola, Ind.
12. Isotopes Division.
13. Physics Division.
14. Virginia Polytechnic Institute and State University, Blacksburg.

P. E. Little,[9] J. H. Hamilton,[9] A. V. Ramayya,[9] and N. R. Johnson, "Level Structure of ^{178}Hf," *Phys. Rev. C* **5**, 252 (1972).

R. L. Ferguson, F. Plasil,[13] G. D. Alam,[15] and H. W. Schmitt,[13] "Fission Fragment Mass Distributions and Kinetic Energies for Spontaneous Fission Isomers," *Nucl. Phys. A* **172**, 33 (1971).

M. F. Roche,[16,17] D. E. Troutner,[16] and R. L. Ferguson, "The Independent Yield of ^{112}Ag from Thermal Neutron Induced Fission of ^{233}U and ^{235}U," *Radiochim. Acta* **16**, 66 (1971).

S. C. Burnett,[18,19] R. L. Ferguson, F. Plasil,[13] and H. W. Schmitt,[13] "Neutron Emission and Fission Energetics in the Proton-Induced Fission of ^{233}U and ^{238}U," *Phys. Rev. C* **3**, 2034 (1971).

F. K. McGowan,[13] C. E. Bemis, Jr., J. L. C. Ford, Jr.,[13] W. T. Milner,[13] R. L. Robinson,[13] and P. H. Stelson,[13] "Equilibrium Quadrupole and Hexadecapole Deformation in ^{230}Th and ^{238}U," *Phys. Rev. Lett.* **27**, 1741 (1971).

G. D. O'Kelley, J. S. Eldridge,[4] E. Schonfeld,[20] and P. R. Bell,[21] "Abundances of the Primordial Radionuclides K, Th, and U in Apollo 12 Lunar Samples by Nondestructive Gamma-Ray Spectrometry: Implications for Origin of Lunar Soils," p. 1159 in *Proc. Second Lunar Science Conference, Geochim. Cosmochim. Acta, Suppl. 2,* vol. 2, MIT Press, 1971.

G. D. O'Kelley, J. S. Eldridge,[4] E. Schonfeld,[20] and P. R. Bell,[21] "Cosmogenic Radionuclide Concentrations and Exposure Ages of Lunar Samples from Apollo 12," p. 1747 in *Proc. Second Lunar Science Conference, Geochim. Cosmochim. Acta, Suppl. 2,* vol. 2, MIT Press, 1971.

G. D. O'Kelley, J. S. Eldridge,[4] E. Schonfeld,[20] and K. J. Northcutt,[4] "Primordial Radioelements and Cosmogenic Radionuclides in Lunar Samples from Apollo 15," *Science* **175**, 440 (1972).

CHEMISTRY AND PHYSICS OF TRANSURANIUM ELEMENTS

R. L. Hahn, "Inclusion of Fission and Charged-Particle Emission in Calculations of Nuclear Reactions," *Nucl. Phys. A* **185**, 241 (1972).

R. L. Hahn, K. S. Toth,[13] and M. F. Roche,[17] "On the Reactions of Protons with ^{231}Pa and ^{232}Th," *Nucl. Phys. A* **185**, 252 (1972).

J. L. C. Ford, Jr.,[13] P. H. Stelson,[13] C. E. Bemis, Jr., F. K. McGowan,[13] R. L. Robinson,[13] and W. T. Milner,[13] "Precise Coulomb Excitation $B(E2)$ Values for First 2^+ States of Actinide Nuclei," *Phys. Rev. Lett.* **27**, 1232 (1971).

M. Schmorak,[1] C. E. Bemis, Jr., M. J. Zender,[22] N. B. Gove,[23] and P. F. Dittner, "Ground State Rotational Bands in Even-Even Actinide Nuclei," *Nucl. Phys. A* **178**, 410 (1972).

Y. Y. Chu,[24] M. L. Perlman,[24] P. F. Dittner, and C. E. Bemis, Jr., "Electron Binding Energies, X-Ray Spectra and L-Shell Fluorescence Yields in Curium ($Z = 96$)," *Phys. Rev. A* **5**, 67 (1972).

J. E. McCracken,[25] J. R. Stokely,[4] R. D. Baybarz,[26] C. E. Bemis, Jr., and R. Eby,[4] "Determination of the Half Lives of ^{246}Cm and ^{248}Cm by an Absolute Specific Activity Technique," *J. Inorg. Nucl. Chem.* **33**, 3251 (1971).

---

15. Visiting scientist from the Pakistan Institute of Nuclear Science and Technology, Nilore, Pakistan, under the Sister Laboratory Arrangement between Oak Ridge National Laboratory and the Pakistan Atomic Energy Commission.
16. University of Missouri, Columbia.
17. Present address: Argonne National Laboratory, Argonne, Ill.
18. Graduate student, University of Tennessee, Knoxville.
19. Present address: Los Alamos Scientific Laboratory, Los Alamos, N.M.
20. NASA Manned Spacecraft Center, Houston, Tex.
21. Director's Division.
22. Oak Ridge Associated Universities Research Participant from Fresno State College, Fresno, Calif., summer 1969.
23. Mathematics Division.
24. Department of Chemistry, Brookhaven National Laboratory, Upton, Long Island, N.Y.
25. Present address: University of Georgia, Athens.
26. Chemical Technology Division.

R. J. Silva, "The Transcurium Elements," Chap. 3 in Vol. 8 (*Radiochemistry,* A. G. Maddock, ed.) of *MTP International Review of Science, Chemistry Division,* edited by H. J. Emeléus, Butterworths, London, 1972.

E. T. Chulick,[2,27] P. L. Reeder,[2,28] C. E. Bemis, and E. Eichler, "Analysis of Delayed-Neutron Yields from ^{252}Cf," *Radiochim. Acta* **16**, 8 (1971).

E. T. Chulick,[2,27] P. L. Reeder,[2,28] C. E. Bemis, Jr., and E. Eichler, "Energy Spectrum of Delayed Neutrons from the Spontaneous Fission of ^{252}Cf," *Nucl. Phys. A* **168**, 250 (1971).

P. F. Dittner and C. E. Bemis, Jr., "*K*-Series X-Ray Energies and Intensities for Curium, Berkelium, Californium, and Einsteinium," *Phys. Rev. A* **5**, 481 (1972).

R. L. Hahn, "Element 104," p. 175 in *World Book Encyclopedia,* vol. E, Field Enterprises Educational Corp., Chicago, 1972.

R. L. Hahn, "Element 105," p. 176 in *World Book Encyclopedia,* vol. E, Field Enterprises Educational Corp., Chicago, 1972.

R. V. Gentry,[29] "Radiohalos: Some Unique Lead Isotope Ratios and Unknown Alpha Radioactivity," *Science* **173**, 727 (1971).

R. V. Gentry,[29] "Radiohalos, Tektites, and Lunar Radioactive Chronology," p. 297 in *Lunar Science – III,* Lunar Science Institute Contribution No. 88 (1972).

L. J. Nugent, R. D. Baybarz,[26] J. L. Burnett,[30] and J. L. Ryan,[31] "Electron-Transfer and $f \rightarrow d$ Absorption Bands of Some Lanthanide and Actinide Complexes and the Standard (III-IV) Oxidation Potentials for Each Member of the Lanthanide and Actinide Series," *J. Inorg. Nucl. Chem.* **33**, 2503 (1971).

L. J. Nugent and K. L. Vander Sluis,[13] "Theoretical Treatment of the Energy Differences Between $f^q d^1 s^2$ and $f^{q+1} s^2$ Electron Configuration for Lanthanide and Actinide Atomic Vapors," *J. Opt. Soc. Amer.* **61**, 1112 (1971).

H. D. Harmon,[32,33] "The Thiocyanate and Chloride Complexes of Some Trivalent Actinides," Ph.D. thesis, University of Tennessee, Knoxville, August 1971; ORNL-TM-3486 (July 1971).

H. D. Harmon,[32,33] J. R. Peterson,[34] and W. J. McDowell,[26] "The Stability Constants of the Monochloro Complexes of Bk(III) and Es(III)," *Inorg. Nucl. Chem. Lett.* **8**, 57 (1972).

B. Weaver[26] and J. N. Stevenson,[35] "Relative Oxidation Potentials of the Bk(IV)-Bk(III) and Ce(IV)-Ce(III) Couples in Acid Solutions," *J. Inorg. Nucl. Chem.* **33**, 1877 (1971).

J. R. Stokely, Jr.,[4] R. D. Baybarz,[26] and J. R. Peterson,[34] "The Formal Potential of the Bk(IV)-Bk(III) Couple in Several Media," *J. Inorg. Nucl. Chem.* **34**, 392 (1972).

R. D. Baybarz,[26] J. R. Stokely, Jr.,[4] and J. R. Peterson,[34] "Absorption Spectra of Bk(III) and Bk(IV) in Several Media," *J. Inorg. Nucl. Chem.* **34**, 739 (1972).

J. A. Fahey,[35,36] "The Preparation and Some Properties of Berkelium Metal and Californium Dioxide," Ph.D. thesis, University of Tennessee, Knoxville, June 1971.

J. R. Peterson,[34] J. A. Fahey,[35,36] and R. D. Baybarz,[26] "The Crystal Structures and Lattice Parameters of Berkelium Metal," *J. Inorg. Nucl. Chem.* **33**, 3345 (1971).

---

27. Present address: Cyclotron Institute, Texas A & M University, College Station.
28. Present address: Battelle-Northwest, Richland, Wash.
29. Visiting scientist from the Institute of Planetary Science, Columbia Union College, Takoma Park, Md.
30. Present address: Division of Research, U.S. Atomic Energy Commission, Washington, D.C.
31. Pacific Northwest Laboratories, Richland, Wash.
32. Graduate student from the University of Tennessee, Knoxville, and supported by a National Defense Education Act Title IV fellowship.
33. Present address: Chemistry Department, Walters State Community College, Morristown, Tenn.
34. Consultant, Department of Chemistry, University of Tennessee, Knoxville.
35. Oak Ridge Graduate Fellow from the University of Tennessee, Knoxville, under appointment from the Oak Ridge Associated Universities.
36. Present address: Chemistry Department, Bronx Community College, Bronx, N.Y.

J. A. Fahey,[35,36] J. R. Peterson,[34] and R. D. Baybarz,[26] "Some Properties of Berkelium Metal and the Apparent Trend Toward Divalent Character in the Transcurium Actinide Metals," *Inorg. Nucl. Chem. Lett.* **8**, 101 (1972).

J. R. Peterson[34] and J. Fuger,[37] "The Dioxide of ^{248}Cm,"[38] *J. Inorg. Nucl. Chem.* **33**, 4111 (1971).

R. D. Baybarz,[26] J. B. Knauer,[26] and J. R. Peterson,[34] "New Encapsulation Techniques for the Fabrication of Californium-252 Neutron Sources," *Nucl. Technol.* **11**, 609 (1971).

R. D. Baybarz[26] and J. R. Peterson,[34] "Californium-252 Neutron Source and Method of Making Same," U.S. Pat. 3,640,888 (Feb. 8, 1972).

J. R. Peterson[34] and R. D. Baybarz,[26] "The Stabilization of Divalent Californium in the Solid State: Californium Dibromide," *Inorg. Nucl. Chem. Lett.* **8**, 423 (1972).

M. O. Krause and F. Wuilleumier,[39] "Electron Binding Energies in Americium," p. 759 in *Electron Spectroscopy: Proc. Int. Conf. on Electron Spectroscopy,* Asilomar, Calif., Sept. 7–10, 1971, edited by D. A. Shirley, North-Holland, Amsterdam, 1972.

J. H. Burns and P. G. Laubereau,[40] "The Crystal Structure of Triindenyluranium Chloride," *Inorg. Chem.* **10**, 2789 (1971).

P. G. Laubereau,[40] L. Ganguly,[41] J. H. Burns, B. M. Benjamin, J. L. Atwood,[42] and J. Selbin, "Preparation and Properties of Triindenylthorium Chloride and Triindenyluranium Chloride," *Inorg. Chem.* **10**, 2274 (1971).

R. L. Hahn, R. L. Stone,[43] J. R. Tarrant, L. D. Hunt, and M. L. Mallory, "Further Experience with a Fast-Closing Protective Valve," *Nucl. Instrum. Methods* **96**, 481 (1971).

ISOTOPE CHEMISTRY

G. M. Begun, C. R. Boston,[44] G. Torsi,[45] and G. Mamantov,[45] "The Raman Spectra of Molten Aluminum Trihalide–Alkali Halide Systems," *Inorg. Chem.* **10**, 886 (1971).

G. Torsi,[45] K. W. Fung,[45] G. M. Begun, and G. Mamantov,[45] "Mercury Species in Chloroaluminate Melts. Characterization of the New Ion Hg_3^{2+}," *Inorg. Chem.* **10**, 2285 (1971).

F. L. Whiting,[45] G. Mamantov,[45] G. M. Begun, and J. P. Young,[4] "Raman Spectra of Solute Species in Molten Fluorides; O_2^-, CrO_4^{2-}, and CO_3^{2-}," *Inorg. Chim. Acta* **5**, 260 (1971).

G. M. Begun, J. Brynestad,[44] K. W. Fung,[45] and G. Mamantov,[45] "Raman Spectra of the Molten $AlCl_3$-$ZnCl_2$ System and Molten Cs_2ZnCl_4," *Inorg. Nucl. Chem. Lett.* **8**, 79 (1972).

L. Schäfer,[46] G. M. Begun, and S. J. Cyvin,[47] "The Raman Spectrum of Benzene-Chromium-Tricarbonyl," *Spectrochim. Acta, Part A* **28**, 803 (1972).

RADIATION CHEMISTRY

C. J. Hochanadel, J. A. Ghormley, and P. J. Ogren,[48] "Absorption Spectrum and Reaction Kinetics of the HO_2 Radical in the Gas Phase," *J. Chem. Phys.* **56**, 4426 (1972).

---

37. Nuclear Chemistry Laboratory, University of Liège, Liège, Belgium.
38. Research jointly sponsored by the Universities of Tennessee (Knoxville) and Liège (Belgium) and by the U.S. Atomic Energy Commission under contract with the Union Carbide Corporation.
39. Visiting scientist from Laboratoire de Chimie Physique de l'Université, Paris VI, France.
40. Visiting scientist from Federal Republic of Germany, Bonn.
41. Visiting scientist from Louisiana State University, Baton Rouge.
42. Oak Ridge Associated Universities Research Participant from the University of Alabama, University, summer 1969.
43. Plant and Equipment Division.
44. Metals and Ceramics Division.
45. Department of Chemistry, University of Tennessee, Knoxville.
46. Department of Chemistry, University of Arkansas, Fayetteville.
47. Institute of Theoretical Chemistry, The Technical University of Norway, Trondheim.
48. Department of Chemistry, Maryville College, Maryville, Tenn.

R. W. Matthews,[49] H. A. Mahlman, and T. J. Sworski, "Elementary Processes in the Radiolysis of Aqueous Sulfuric Acid Solutions. Determinations of Both G_{OH} and $G_{SO_4^-}$," *J. Phys. Chem.* **76**, 1265 (1972).

A. R. Jones, "The Radiolysis of Aliphatic Carboxylic Acids: The Decarboxylation of Normal Acids at 38°," *Radiat. Res.* **47**, 35 (1971).

A. R. Jones, "The Radiolysis of Aliphatic Carboxylic Acids. On the Decarboxylation of Normal Acids in the Liquid State," *Radiat. Res.* **48**, 447 (1971).

P. S. Rudolph, "Preface to the Memoirs of Samuel Colville Lind," *J. Tenn. Acad. Sci.* **47**, 2 (1972).

ORGANIC CHEMISTRY

C. J. Collins and C. E. Harding,[50] "Molekulare Umlagerungen, XXVII. Relative Geschwindigkeiten der 6.2- und 3.2-Hydrid-Verschiebung im Norbornyl-Kation," *Justus Liebigs Ann. Chem.* **745**, 124 (1971).

C. J. Collins, "Reactions of Primary Aliphatic Amines with Nitrous Acid," *Accounts Chem. Res.* **4**, 315 (1971).

V. F. Raaen, B. M. Benjamin, and C. J. Collins, "A Deuterium Tracer Study of 6,1,2-Hydride Shift in Substituted Norbornyl Cations," *Tetrahedron Lett.* **28**, 2613 (1971).

PHYSICAL CHEMISTRY

R. M. Rush and J. S. Johnson, "Isopiestic Measurements of the Osmotic and Activity Coefficients for the Systems $HClO_4 + UO_2(ClO_4)_2 + H_2O$ and $NaClO_4 + UO_2(ClO_4)_2 + H_2O$ at 25°C," *J. Chem. Thermodyn.* **3**, 779 (1971).

M. H. Lietzke and R. J. Herdklotz,[35,51] "Electromotive Force Studies in Aqueous Solutions at Elevated Temperatures. XIII. The Thermodynamic Properties of HCl-$NaCl$-$MgCl_2$ Mixtures," *J. Inorg. Nucl. Chem.* **33**, 1649 (1971).

M. H. Lietzke and R. J. Herdklotz,[35,51] "Activity Coefficient Behavior in Aqueous Binary Salt Mixtures," *J. Tenn. Acad. Sci.* **46**, 133 (1971).

D. W. Gosbin,[18] "Predictions of Activity and Osmotic Coefficients for Aqueous Electrolyte Mixtures," M.S. thesis, University of Tennessee, Knoxville, August 1971.

Cynthia Daugherty,[18] "The Thermodynamic Properties of Aqueous HCl-KCl-$CaCl_2$ Mixtures as Calculated from Electromotive Force Measurements," M.S. thesis, University of Tennessee, Knoxville, March 1972.

F. Vaslow, "Thermodynamics of Solutions of Electrolytes," Chap. 12 in *Water and Aqueous Solutions*, edited by R. A. Horne, Wiley-Interscience, New York, 1972.

F. Vaslow, "Salt-Induced Critical-Type Transitions in Aqueous Solution. Heats of Dilution of the Lithium and Sodium Halides," *J. Phys. Chem.* **75**, 3317 (1971).

L. Dresner, "Phase-Plane Analysis of Nonlinear, Second-Order, Ordinary Differential Equations," *J. Math. Phys.* **12**, 1339 (1971).

L. Dresner, "Some Remarks on the Integration of the Extended Nernst-Planck Equations in the Hyperfiltration of Multicomponent Solutions,"[52] *Desalination* **10**, 27 (1972).

L. Dresner, "Geometric Effects in Piezodialysis through Charge-Mosaic Membranes,"[52] *Desalination* **10**, 47 (1972).

L. Dresner, "An Extension of the Radiometric Porous-Frit Method to the Measurement of Diffusion Coefficients of Non-Radioactive Counterions in Ion-Exchange Membranes,"[53] ORNL-4708 (July 1972).

---

49. Visiting scientist from the Australian Atomic Energy Commission Research Establishment, Lucas Heights, New South Wales.
50. Present address: University of Tennessee at Martin.
51. Present address: Chemistry Department, Bob Jones University, Greenville, S.C.
52. Research jointly sponsored by the National Science Foundation-IRRPOS and the Office of Saline Water under Union Carbide Corporation's contract with the U.S. Atomic Energy Commission.
53. Research sponsored by the National Science Foundation under Union Carbide Corporation's contract with the U.S. Atomic Energy Commission.

P. H. Wadia,[54] K. A. Kraus,[21] A. J. Shor,[55] and L. Dresner, "Preliminary Economic Analysis of Cross-Flow Filtration," ORNL-4729 (August 1971).

J. Csurny, J. S. Johnson, R. E. Minturn, G. E. Moore, C. G. Westmoreland, J. Acosta,[56] J. T. Day,[56] J. P. Jacks,[56] S. H. Ruben,[56] and P. H. Wadia,[56] "Hyperfiltration and Cross-Flow Filtration of Kraft Pulp Mill and Bleach Plant Wastes,"[57] ORNL-NSF-EP-14 (May 1972).

M. M. Irizarry[56] and D. B. Anthony,[56] "Adsorption and Filtration of Trace Contaminants in Aqueous Effluents," ORNL-MIT-129 (1971).

J. A. J. Sobota[56] and U. M. R. Lima,[56] "Adsorption and Filtration of Chromium from Aqueous Effluents," ORNL-MIT-133 (1971).

A. E. Marcinkowsky and H. O. Phillips, "Diffusion Studies. II. Tracer Diffusion Coefficients of Copper(II) in HCl and $HClO_4$ at 25°C,"[58] *J. Chem. Soc. A* **1971**, 101.

A. E. Marcinkowsky and H. O. Phillips, "Diffusion Studies. III. Tracer Diffusion Coefficients of Lanthanum(III) in Concentrated Solutions of HCl and $HClO_4$ at 25°C," *J. Chem. Soc. A* **1971**, 3556.

K. A. Kraus,[21] "Hydrous Oxide Cation Exchangers," U.S. Pat. 3,522,187 (July 28, 1970).

J. N. Baird, Jr., J. S. Johnson, Jr., K. A. Kraus,[21] and J. J. Perona, "Filtration Method of Separating Liquids from Extraneous Materials," U.S. Pat. 3,577,339 (May 4, 1971).

E. H. Taylor, "A Kinetic Argument Against the Existence of Anomalous Water," *J. Colloid Interface Sci.* **36**, 543 (1971).

A. S. Dworkin and M. A. Bredig, "Miscibility of Liquid Metals with Salts. X. Various Studies in Alkaline Earth Metal–Metal Fluoride and Rare Earth Metal–Metal Di- and Trifluoride Systems," *J. Phys. Chem.* **75**, 2340 (1971).

A. S. Dworkin, "Enthalpy of Uranium Tetrafluoride from 298–1400°K, Enthalpy and Entropy of Fusion," *J. Inorg. Nucl. Chem.* **34**, 135 (1972).

H. R. Bronstein and D. L. Manning,[4] "Lanthanum Trifluoride as a Membrane in a Reference Electrode for Use in Certain Molten Fluorides," *J. Electrochem. Soc.* **119**, 125 (1972).

R. H. Busey, R. B. Bevan, Jr., and R. A. Gilbert, "The Heat Capacity of Potassium Pertechnetate from 10 to 300°K. Entropy and Gibbs Energy. Entropy of the Aqueous Pertechnetate Ion," *J. Chem. Thermodyn.* **4**, 77 (1972).

R. E. Meyer, M. C. Banta,[59] P. M. Lantz, and F. A. Posey, "Rapid Batch and Continuous Electroanalysis for the Chloride Ion,"[58] *Desalination* **9**, 333 (1971).

G. H. Cartledge, "The Electrochemical Behavior of Technetium and Iron Containing Technetium," *J. Electrochem. Soc.* **118**, 1752 (1971).

CHEMICAL PHYSICS

G. M. Brown, "Symmetry Relations Among Structure Factors," *Acta Crystallogr., Sect. B* **27**, 1675 (1971).

---

54. Summer employee, 1971; present address: Department of Chemical Engineering, Massachusetts Institute of Technology, Cambridge.

55. Reactor Chemistry Division.

56. Massachusetts Institute of Technology School of Chemical Engineering Practice, Oak Ridge Station.

57. Research carried out under the ORNL-NSF Environmental Program, jointly sponsored by NSF-RANN and the U.S. Atomic Energy Commission under contract with the Union Carbide Corporation.

58. Research jointly sponsored by the Office of Saline Water, U.S. Department of the Interior, and the U.S. Atomic Energy Commission under contract with the Union Carbide Corporation.

59. Summer faculty employee, 1969; present address: Department of Chemistry, Sam Houston State University, Huntsville, Tex.

G. M. Brown, F. L. Hedberg,[60] and H. Rosenberg,[60] "Crystal Structure of Decachlororuthenocene. Noncoplanarity of Carbon and Chlorine Atoms Arising from Valence Forces," *Chem. Commun.* **1972**, 5.

W. E. Thiessen, H. A. Levy, W. G. Dauben,[61] G. H. Beasley,[61] and D. A. Cox,[61] "A Highly Twisted Double Bond," *J. Amer. Chem. Soc.* **93**, 4312 (1971).

R. D. Ellison, H. A. Levy, and K. W. Fung,[45] "Crystal and Molecular Structure of Trimercury Chloroaluminate, $Hg_3(AlCl_4)_2$," *Inorg. Chem.* **11**, 833 (1972).

R. Desiderato,[62] J. C. Terry,[62] G. R. Freeman,[62,63] and H. A. Levy, "The Molecular and Crystal Structure of 8-Hydroxyquinoline-N-oxide," *Acta Crystallogr., Sect. B* **27**, 2443 (1971).

W. R. Busing, "A Convenient Way of Applying Constraints in Structure-Factor Least-Squares Refinement," *Acta Crystallogr., Sect. A* **27**, 683 (1971).

A. H. Narten, "Diffraction Pattern and Structure of Non-Crystalline BeF_2 and SiO_2 at 25°C," *J. Chem. Phys.* **56**, 1905 (1972).

A. H. Narten and H. A. Levy, "Liquid Water: Molecular Correlation Functions from X-Ray Diffraction," *J. Chem. Phys.* **55**, 2263 (1971).

A. H. Narten, "Liquid Gallium: Comparison of X-Ray and Neutron Diffraction Data," *J. Chem. Phys.* **56**, 1185 (1972).

L. Blum[64,65] and A. J. Torruella,[65] "Invariant Expansion for Two-Body Correlations: Thermodynamic Functions, Scattering, and the Ornstein-Zernike Equation," *J. Chem. Phys.* **56**, 303 (1972).

J. K. Dohrmann,[66] R. Livingston, and H. Zeldes, "Paramagnetic Resonance Study of Liquids during Photolysis. XII. Alloxan, Parabanic Acid, and Related Compounds," *J. Amer. Chem. Soc.* **93**, 3343 (1971).

J. K. Dohrmann[66] and R. Livingston, "Paramagnetic Resonance Study of Liquids during Photolysis. XIII. Uracil and Derivatives," *J. Amer. Chem. Soc.* **93**, 5363 (1971).

E. G. Janzen[67] and R. Livingston, "The Second Symposium on Electron Spin Resonance Spectroscopy, Introductory Remarks," *J. Phys. Chem.* **75**, 3383 (1971).

R. W. Holmberg, "ESR Study of Gamma-Irradiated Single Crystals of Potassium Bicarbonate at 77°K," *J. Chem. Phys.* **55**, 1730 (1971).

T. A. Carlson, "Electron Spectroscopy for Chemical Analysis," *Phys. Today* **25**, 30 (1972).

T. A. Carlson and N. Fernelius,[68] "Applying Photoelectron Spectroscopy," *Ind. Res.* **14**, 46 (1972).

T. A. Carlson, "General Survey of Electron Spectroscopy," p. 53 in *Electron Spectroscopy: Proc. Int. Conf. on Electron Spectroscopy,* Asilomar, Calif., Sept. 7–10, 1971, edited by D. A. Shirley, North-Holland, Amsterdam, 1972.

T. A. Carlson, M. O. Krause, and W. E. Moddeman,[18,69] "Excitation Accompanying Photoionization in Atoms and Molecules and Its Relationship to Electron Correlation," *J. Phys. Paris Colloq.* **32**, C4-76 (1971).

M. O. Krause, T. A. Carlson, and W. E. Moddeman,[18,69] "Manifestation of Atomic Dynamics Through the Auger Effect," *J. Phys. Paris Colloq.* **32**, C4-139 (1971).

---

60. Non-metallic Materials Division, Air Force Materials Laboratory, Wright-Patterson Air Force Base, Ohio.
61. University of California, Berkeley.
62. North Texas State University, Denton.
63. Present address: University of Alabama Medical Center, Birmingham.
64. Oak Ridge Associated Universities research participant from the University of Puerto Rico, Rio Piedras, summer 1970.
65. Department of Physics, University of Puerto Rico, Rio Piedras.
66. Visiting scientist from Institut für Physikalische Chemie der Freien Universität Berlin, 1969–1970.
67. Department of Chemistry, University of Georgia, Athens.
68. Research Consultants, Inc., Oak Ridge, Tenn.
69. Present address: Vanderbilt University, Nashville, Tenn.

L. D. Hulett,[4] T. A. Carlson, B. R. Fish,[70] and J. L. Durham,[71] "Studies of Sulfur Compounds Adsorbed on Smoke Particles and Other Solids by Photoelectron Spectroscopy," pp. 187–95 in *Determination of Air Quality*, edited by G. Mamantov and W. D. Shultz, Plenum, New York, 1971.

W. E. Moddeman,[18,69] T. A. Carlson, M. O. Krause, B. P. Pullen,[35,72] W. E. Bull,[45] and G. K. Schweitzer,[45] "Determination of the *K-LL* Auger Spectra of N_2, O_2, CO, NO, and CO_2," *J. Chem. Phys.* **55**, 2317 (1971).

T. A. Carlson and A. E. Jonas,[18,73] "Angular Distribution of the Photoelectron Spectra for Ar, Kr, Xe, H_2, N_2, and CO," *J. Chem. Phys.* **55**, 4913 (1971).

T. A. Carlson and M. O. Krause, "Relative Abundances and Recoil Energies of Fragment Ions Formed from the X-Ray Photoionization of N_2, O_2, CO, NO, CO_2, and CF_4," *J. Chem. Phys.* **56**, 3706 (1972).

J. C. Carver,[18,25] "Photoelectron Multiplet Splitting and Chemical Shifts in Transition-Metal Compounds," Ph.D. thesis, University of Tennessee, Knoxville, March 1972.

J. C. Carver,[18,25] T. A. Carlson, L. C. Cain,[18] and G. K. Schweitzer,[45] "Use of X-Ray Photoelectron Spectroscopy to Study Bonding in Transition Metal Salts by Observation of Multiple Splittings," p. 803 in *Electron Spectroscopy: Proc. Int. Conf. on Electron Spectroscopy*, Asilomar, Calif., Sept. 7–10, 1971, edited by D. A. Shirley, North-Holland, Amsterdam, 1972.

A. E. Jonas,[18,73] "Photoelectron Spectroscopy of the Tetrafluoro and Tetramethyl Compounds of Group IV Elements," Ph.D. thesis, University of Tennessee, Knoxville, December 1971.

C. P. Anderson,[18] G. Mamantov,[45] W. E. Bull,[45] F. A. Grimm,[45] J. C. Carver,[18,25] and T. A. Carlson, "Photoelectron Spectrum of Chlorine Monofluoride," *Chem. Phys. Lett.* **12**, 137 (1971).

T. A. Carlson, G. E. McGuire,[18,74] A. E. Jonas,[18,73] K. L. Cheng,[75] C. P. Anderson,[18] C. C. Lu,[23,76] and B. P. Pullen,[35,72] "Comprehensive Examination of the Angular Distribution of Photoelectron Spectra from Atoms and Molecules," p. 207 in *Electron Spectroscopy: Proc. Int. Conf. on Electron Spectroscopy*, Asilomar, Calif., Sept. 7–10, 1971, edited by D. A. Shirley, North-Holland, Amsterdam, 1972.

T. A. Carlson and C. P. Anderson,[18] "Angular Distribution of the Photoelectron Spectrum for Benzene," *Chem. Phys. Lett.* **10**, 561 (1971).

C. C. Lu,[23,76] F. B. Malik,[77] and T. A. Carlson, "Calculation of the *K* X-Ray Intensities for Elements from $Z = 92$ to 126," *Nucl. Phys. A* **175**, 289 (1971).

C. C. Lu,[23,76] T. A. Carlson, F. B. Malik,[77] T. C. Tucker,[23] and C. W. Nestor, Jr.,[23] "Relativistic Hartree-Fock-Slater Eigenvalues, Radial Expectation Values, and Potentials for Atoms, $2 \leqslant Z \leqslant 126$," *At. Data* **3**, 1 (1971).

M. O. Krause, "Rearrangment of Inner Shell Ionized Atoms," *J. Phys. Paris Colloq.* **32**, C4-67 (1971).

M. O. Krause, "The $M\zeta$ X Rays of Y to Rh in Photoelectron Spectrometry," *Chem. Phys. Lett.* **10**, 65 (1971).

M. O. Krause and F. Wuilleumier,[39] "Energies of $M\zeta$ X Rays of Y to Rh," *Phys. Lett. A* **35**, 341 (1971).

F. Wuilleumier[39] and M. O. Krause, "Partition of the Photoionization Cross Section of Neon in Soft X-Ray Region," p. 259 in *Electron Spectroscopy: Proc. Int. Conf. on Electron Spectroscopy*, Asilomar, Calif., Sept. 7–10, 1971, edited by D. A. Shirley, North-Holland, Amsterdam, 1972.

P. F. Dittner and S. Datz, "Collision Induced Vibrational Excitation and Dissociation of Hydrogen with Alkali Atoms and Ions from 2 to 50 eV," *J. Chem. Phys.* **54**, 4228 (1971).

---

70. Health Physics Division.
71. Environmental Protection Agency, Research Triangle Park, North Carolina.
72. Present address: Southeastern Louisiana State College, Hammond.
73. Present address: University of Tennessee Research Center and Hospital, Knoxville.
74. Present address: Analytical Chemistry Division, ORNL.
75. University of Missouri, Kansas City.
76. Present address: University of Miami, Coral Gables, Fla.
77. Indiana University, Bloomington.

N. Kashihira,[78,79] "Ionizing Collisions of Fast Alkali Atoms with Cl_2, Br_2, and O_2," Ph.D. thesis, Purdue University, Lafayette, Ind., August 1971.

B. R. Appleton,[80] S. Datz, C. D. Moak,[13] and M. T. Robinson,[80] "Energy Loss Spectra of Channeled Iodine and Oxygen Ions in Gold," *Phys. Rev. B* **4**, 1452 (1971).

S. Datz, C. D. Moak,[13] H. O. Lutz,[81] L. C. Northcliffe,[82] and L. B. Bridwell,[83] "Charge States of 15–140 MeV Br Ions and 15 to 162 MeV I Ions in Solid and Gaseous Media," *At. Data* **2**, 273 (1971).

S. Datz, C. D. Moak,[13] B. R. Appleton,[80] M. D. Brown,[13] and T. A. Carlson, "Differentiation in $2p_{3/2}$ and $2p_{1/2}$ Vacancy Production in Iodine Ions in Atomic Collisions at 15 to 60 MeV," p. 409 in *Proc. VIIth Int. Conf. on the Physics of Electronic and Atomic Collisions*, North-Holland, Amsterdam, 1971.

S. Datz, C. D. Moak,[13] B. R. Appleton,[80] and T. A. Carlson, "Differentiation in *L*-Subshell Vacancy Production in Iodine Ions by Atomic Collisions at 15–60 MeV," *Phys. Rev. Lett.* **27**, 363 (1971).

H. O. Lutz,[81] J. Stein,[81] S. Datz, and C. D. Moak,[13] "Collisional X-Ray Excitation in Solid and Gaseous Targets by Heavy Ion Bombardment," *Phys. Rev. Lett.* **28**, 8 (1972).

---

78. Graduate student from Purdue University, Lafayette, Ind.
79. Present address: Institut für Radiochemie der Kernforschungsanlage, Jülich, W. Germany.
80. Solid State Division.
81. Kernforschungsanlage, Jülich, W. Germany.
82. Department of Physics, Texas A & M University, College Station.
83. Department of Physics, Murray State University, Murray, Ky.

Papers Presented at Scientific and Technical Meetings

NUCLEAR CHEMISTRY

K. S. Toth,*[1] R. L. Hahn, and M. A. Ijaz,[2] "Further Investigation of Thulium α-Emitters; New α-Emitting Isomer in ^{156}Tm," 1971 Fall Meeting, Division of Nuclear Physics, American Physical Society, Tucson, Ariz., Nov. 4–6; *Bull. Amer. Phys. Soc.* **16**, 1162 (1971).

R. O. Sayer,*[3] E. Eichler, N. R. Johnson, and D. C. Hensley,[1] "Coulomb Excitation of 10^+ States in ^{162,164}Dy," 1972 Annual Meeting, American Physical Society, San Francisco, Jan. 31–Feb. 3; *Bull. Amer. Phys. Soc.* **17**, 28 (1972).

K. S. Toth,*[1] R. L. Hahn, M. A. Ijaz,[2] and R. F. Walker, Jr.,[4] "Search for New Osmium Isotopes with $A < 172$," 1972 Spring Meeting, American Physical Society, Washington, D.C., Apr. 24–27; *Bull. Amer. Phys. Soc.* **17**, 559 (1972).

R. L. Ferguson,* F. Plasil,[1] G. D. Alam,[5] and H. W. Schmitt,[1] "Fragment Mass and Kinetic Energy Distributions for Spontaneously Fissioning Isomers," VII International Winter Meeting on Nuclear Physics, Villars, Switzerland, Jan. 25–30, 1971.

F. Plasil,*[1] R. L. Ferguson, F. Pleasonton,[1] and H. W. Schmitt,[1] "Neutron Emission in Proton-Induced Fission of ^{209}Bi at 36.1 MeV," 1972 Annual Meeting, American Physical Society, San Francisco, Jan. 31–Feb. 3; *Bull. Amer. Phys. Soc.* **17**, 138 (1972).

G. D. O'Kelley,* J. S. Eldridge,[6] K. J. Northcutt,[6] and E. Schonfeld,[7] "Some Consequences of Solar Proton Activation of Lunar Surface Materials," Conference on Modern and Ancient Particles from the Sun, Lunar Science Institute, Houston, Tex., Oct. 13–15, 1971 (invited).

J. S. Eldridge,*[6] K. J. Northcutt,[6] and G. D. O'Kelley, "Calibration and Use of a Large Low-Background Gamma-Ray Spectrometer for Lunar and Geochemical Samples," 10th National Meeting, Society for Applied Spectroscopy, St. Louis, Mo., Oct. 18–22, 1971.

J. S. Eldridge,[6] G. D. O'Kelley,* and K. J. Northcutt,[6] "Abundances of Primordial and Cosmogenic Radionuclides in Apollo 14 Rocks and Fines," Third Lunar Science Conference, Houston, Tex., Jan. 10–13, 1972.

G. D. O'Kelley,* J. S. Eldridge,[6] E. Schonfeld,[7] and K. J. Northcutt,[6] "Concentrations of Primordial Radioelements and Cosmogenic Radionuclides in Apollo 15 Samples by Nondestructive Gamma-Ray Spectrometry," Third Lunar Science Conference, Houston, Tex., Jan. 10–13, 1972.

---

*Speaker.

1. Physics Division.
2. Virginia Polytechnic Institute and State University, Blacksburg.
3. Furman University, Greenville, S.C.
4. Physics Department, Centenary College, Shreveport, La.
5. Visiting scientist from the Pakistan Institute of Nuclear Science and Technology, Nilore, Pakistan, under the Sister Laboratory Arrangement between Oak Ridge National Laboratory and the Pakistan Atomic Energy Commission.
6. Analytical Chemistry Division.
7. NASA Manned Spacecraft Center, Houston, Tex.

CHEMISTRY AND PHYSICS OF TRANSURANIUM ELEMENTS

G. T. Seaborg,*[8] J. L. Crandall,[9] P. R. Fields,[10] A. Ghiorso,[11] O. L. Keller, Jr., and R. A. Penneman,[12] "Recent Advances in the United States on the Transuranium Elements," Fourth United Nations International Conference on the Peaceful Uses of Atomic Energy, Geneva, Switzerland, Sept. 6–16, 1971 (invited).

R. L. Hahn,* K. S. Toth,[1] and M. F. Roche,[13] "Interactions of Protons (<85 MeV) with ^{231}Pa and ^{232}Th," 162nd National Meeting, American Chemical Society, Washington, D.C., Sept. 12–17, 1971; abstract NUCL-29.

R. L. Hahn and H. W. Bertini,[14] "Calculations of Spallation-Fission Competition in the Reactions of Protons with ^{238}U at Energies Below 3 GeV," 163rd National Meeting, American Chemical Society, Boston, Apr. 9–14, 1972; abstract NUCL-31.

R. L. Hahn,* P. F. Dittner, K. S. Toth,[1] and O. L. Keller, "Studies of (Heavy Ion, αxn) Reactions on Actinide Targets," 162nd National Meeting, American Chemical Society, Washington, D.C., Sept. 12–17, 1971; abstract NUCL-24.

N. R. Johnson,* E. Eichler, R. O. Sayer,[3] C. E. Bemis, Jr., D. Hensley,[1] and M. Schmorak,[15] "Heavy Ion Coulomb Excitation of Transuranium Nuclei," 162nd National Meeting, American Chemical Society, Washington, D.C., Sept. 12–17, 1971; abstract NUCL-13 (invited).

J. S. Boyno,*[16] Th. W. Elze,[17] J. R. Huizenga,[16] and C. E. Bemis, Jr., "Collective States Excited in the ^{236}U(d,d') Reaction," 1972 Spring Meeting, American Physical Society, Washington, D.C., Apr. 24–27; *Bull. Amer. Phys. Soc.* **17**, 463 (1972).

C. E. Bemis, Jr., "Electric Quadrupole and Hexadecapole Moments in ^{230}Th and ^{238}U," Fourth American Isotope Separator Symposium, National Bureau of Standards, Washington, D.C., Sept. 20, 1971 (invited).

F. K. McGowan,*[1] C. E. Bemis, Jr., J. L. C. Ford, Jr.,[1] W. T. Milner,[1] R. L. Robinson,[1] and P. H. Stelson,[1] "Electric Hexadecapole Moments in ^{230}Th and ^{238}U," 1971 Fall Meeting, Division of Nuclear Physics, American Physical Society, Tucson, Ariz., Nov. 4–6; *Bull. Amer. Phys. Soc.* **16**, 1157 (1971).

C. E. Bemis, Jr.,* F. K. McGowan,[1] J. L. C. Ford, Jr.,[1] W. T. Milner,[1] R. L. Robinson,[1] and P. H. Stelson,[1] "Equilibrium Quadrupole and Hexadecapole Deformations for Even-Even Transuranium Nuclei," 163rd National Meeting, American Chemical Society, Boston, Apr. 9–14, 1972; abstract NUCL-7 (invited).

C. E. Bemis, Jr.,* F. K. McGowan,[1] J. L. C. Ford, Jr.,[1] W. T. Milner,[1] R. L. Robinson,[1] and P. H. Stelson,[1] "Equilibrium Quadrupole and Hexadecapole Deformations for Even-Even Transuranium Nuclei," 1972 Spring Meeting, American Physical Society, Washington, D.C., Apr. 24–27; *Bull. Amer. Phys. Soc.* **17**, 538 (1972).

C. E. Bemis, Jr.,* P. F. Dittner, C. D. Goodman,[1] R. L. Hahn, D. C. Hensley,[1] and R. J. Silva, "Nuclear Spectroscopy and Single Particle States in the Region $Z \geqslant 100$," Third International Transplutonium Element Symposium, Argonne National Laboratory, Argonne, Ill., Oct. 20–22, 1972 (invited).

R. J. Silva,* N. Trautmann,[11] A. Ghiorso,[11] J. Harris,[11] and M. Nurmia,[11] "Automated System for Rapid Chemical Separation of Heavy Actinide and Transactinide Elements," Third International Transplutonium Element Symposium, Argonne National Laboratory, Argonne, Ill., Oct. 20–22, 1971.

C. E. Bemis, Jr., "The Identification of Transfermium Elements Using X-Ray Techniques," Gordon Research Conference on Nuclear Structure Physics, Andover, N.H., July 26–30, 1971 (invited).

---

8. U.S. Atomic Energy Commission, Washington, D.C.; Lawrence Berkeley Laboratory, Berkeley, Calif.
9. Savannah River Laboratory, Aiken, S.C.
10. Argonne National Laboratory, Argonne, Ill.
11. Lawrence Berkeley Laboratory, Berkeley, Calif.
12. Los Alamos Scientific Laboratory, Los Alamos, N.M.
13. Present address: Argonne National Laboratory, Argonne, Ill.
14. Neutron Physics Division.
15. Nuclear Data Project.
16. Nuclear Structure Research Laboratory, University of Rochester, Rochester, N.Y.
17. Institut für Kernphysik der Universität, Frankfurt, West Germany.

R. V. Gentry,[18] "Radiohalos, Tektites and Lunar Radioactive Chronology," Third Lunar Science Conference, Houston, Tex., Jan. 10–13, 1972.

K. L. Vander Sluis*[1] and L. J. Nugent, "Energy Differences Between the $f^q ps^2$ and the $f^{q+1}s^2$ Electron Configuration for the Lanthanide and Actinide Neutral Atoms," 1972 Annual Meeting, Optical Society of America, Ottawa, Canada, Oct. 5–8.

L. J. Nugent* and K. L. Vander Sluis,[1] "Theoretical Treatment of the Energy Differences Between $f^q d^1 s^2$ and $f^{q+1}s^2$ Electron Configurations for Lanthanide and Actinide Atomic Vapors," Ninth Rare-Earth Research Conference, Virginia Polytechnic Institute, Blacksburg, Oct. 10–14, 1971.

L. J. Nugent,* J. L. Burnett,[19] and L. R. Morss,[20] "Thermodynamic Systematics Among the Members of the Lanthanide and Actinide Series," Ninth Rare-Earth Research Conference, Virginia Polytechnic Institute, Blacksburg, Oct. 10–14, 1971.

L. J. Nugent, "Standard (II-III) Oxidation Potentials for Each Member of the Lanthanide and Actinide Series," Third International Transplutonium Element Symposium, Argonne National Laboratory, Argonne, Ill., Oct. 20–22, 1971 (invited).

M. O. Krause* and F. Wuilleumier,[21] "Electron Binding Energies in Americium," International Conference on Electron Spectroscopy, Asilomar, Calif., Sept. 7–10, 1971.

F. Wuilleumier*[21] and M. O. Krause, "Partition of the Photoionization Cross Section of Neon in Soft X-Ray Region," International Conference on Electron Spectroscopy, Asilomar, Calif., Sept. 7–10, 1971.

M. O. Krause, "Case Studies in Soft X-Ray Spectrometry Using an Electron Energy Analyzer of Well-Defined Characteristics," Nuclear Analytical Chemistry Conference, Oak Ridge, Tenn., Oct. 12–14, 1971 (invited).

J. H. Burns, "Preparation and Structure Determination of Compounds with Transuranium Elements Using Single-Crystal Methods," Third International Transplutonium Element Symposium, Argonne National Laboratory, Argonne, Ill., Oct. 20–22, 1971 (invited).

J. H. Burns,* W. H. Baldwin, and J. R. Stokely,[6] "Identification and Crystal Structure Analysis of a Compound of Heptavalent Neptunium, $LiCo(NH_3)_6Np_2O_8(OH)_2 \cdot 2H_2O$," Winter Meeting, American Crystallographic Association, Albuquerque, N.M., Apr. 4–7, 1972.

J. R. Peterson*[22] and J. Fuger,[23] "The Dioxide of Long-Lived Curium-248," 162nd National Meeting, American Chemical Society, Washington, D.C., Sept. 12–17, 1971; abstract NUCL-51.

J. R. Peterson,[22] "Microchemical Methods for the Synthesis and Study of Heavy Actinide Metals and Compounds," Third International Transplutonium Element Symposium, Argonne National Laboratory, Argonne, Ill., Oct. 20–22, 1971 (invited).

ISOTOPE CHEMISTRY

L. L. Brown, "Chemical Exchange Methods for Separating Carbon-13," National Symposium on Carbon-13, Los Alamos, N.M., June 9–11, 1971.

RADIATION CHEMISTRY

C. J. Hochanadel,* J. A. Ghormley, and P. J. Ogren,[24] "Absorption Spectrum and Reaction Kinetics of the HO_2 Radical in the Gas Phase," Pulse Radiolysis Symposium jointly sponsored by the Chemical Institute of Canada and Atomic Energy of Canada Limited, Whiteshell Nuclear Research Establishment, Pinawa, Manitoba, Canada, Oct. 25–27, 1971.

---

18. Visiting scientist from the Institute of Planetary Science, Columbia Union College, Takoma Park, Md.
19. Present address: Division of Research, U.S. Atomic Energy Commission, Germantown, Md.
20. Department of Chemistry, Rutgers University, New Brunswick, N.J.
21. Visiting scientist from Laboratoire de Chimie Physique de l'Université, Paris VI, France.
22. Consultant, Department of Chemistry, University of Tennessee, Knoxville.
23. Nuclear Chemistry Laboratory, University of Liège, Liège, Belgium.
24. Department of Chemistry, Maryville College, Maryville, Tenn.

C. J. Hochanadel,* J. A. Ghormley, J. W. Boyle, and P. J. Ogren,[24] "Studies of O_3 Formation, and the Absorption Spectrum and Reaction Kinetics of the HO_2 Radical Using Pulse Radiolysis and Flash Photolysis Techniques," Conference on Air Pollution sponsored jointly by the University of California and the AEC National Laboratories, California Statewide Air Pollution Research Center, University of California, Riverside, Feb. 23–24, 1972.

R. W. Matthews,[25] H. A. Mahlman, and T. J. Sworski, "Elementary Processes in the Radiolysis of Aqueous Sulfuric Acid Solutions: Determinations of Both G_{OH} and $G_{SO_4^-}$," Conference on Elementary Processes in Radiation Chemistry, University of Notre Dame, Notre Dame, Ind., Apr. 4–7, 1972.

ORGANIC CHEMISTRY

C. J. Collins, "The Mechanism of Aliphatic Deamination," Plenary Lecture, 22nd Conference on Reaction Mechanisms, Nagoya, Japan, Oct. 19, 1971 (invited).

PHYSICAL CHEMISTRY

M. H. Lietzke* and D. W. Gosbin,[26] "Simple Expressions for Representing Osmotic and Activity Coefficient Behavior in Mixed Electrolyte Systems," 23rd Southeastern Regional Meeting, American Chemical Society, Nashville, Tenn., Nov. 4–5, 1971.

J. S. Johnson, Jr., "Polyelectrolytes in Aqueous Solutions – Filtration, Hyperfiltration, and Dynamic Membranes," 162nd National Meeting, American Chemical Society, Washington, D.C., Sept. 12–17, 1971; abstract POLY-070 (invited).

J. S. Johnson, Jr., "Hyperfiltration. A Method for Treatment of Waste Streams," Conference on Textile Waste Water Treatment and Air Pollution Control, sponsored by Clemson University, Hilton-Head Island, S.C., Jan. 20–21, 1972 (invited).

R. E. Minturn* and J. S. Johnson, "Dynamically Formed Dual-Layer Membranes for Brackish Water Desalination," Third OSW Conference on Reverse Osmosis, Las Vegas, Nev., May 7–11, 1972 (invited).

C. A. Brandon,*[27] J. S. Johnson, Jr., R. E. Minturn, and J. J. Porter,[27] "Complete Reuse of Textile Dyeing Wastes Processed with Dynamic Membrane Hyperfiltration," Joint American Society of Mechanical Engineers/Environmental Protection Agency Symposium on Reuse and Treatment of Waste Water General Industry and Food Processing Symposium, New Orleans, La., Mar. 28–30, 1972.

M. A. Bredig, "Excess Free Energy in Some Binary Molten Salt Mixtures with a Common Cation," Gordon Research Conference on Molten Salts, Meriden, N.H., Sept. 1, 1971.

M. A. Bredig, "The Order-Disorder (Lambda) Transition in Uranium Dioxide and Other Solids of the Fluorite Type of Structure," International Colloquium on the Study of Crystal Transformations at High Temperature, above 2000°K, Odeillo, France, Sept. 29, 1971.

H. R. Bronstein, "Lanthanum Trifluoride as a Membrane in a Reference Electrode for Use in Certain Molten Fluorides," Gordon Research Conference on Molten Salts, Meriden, N.H., Sept. 1, 1971.

R. H. Busey, "Low-Temperature Heat Capacities of ^7LiH and ^7LiD," Second International Conference on Calorimetry and Thermodynamics (26th Annual Calorimetry Conference), Orono, Me., July 12–14, 1971.

---

25. Visiting scientist from the Australian Atomic Energy Commission Research Establishment, Lucas Heights, New South Wales.
26. Graduate student, University of Tennessee, Knoxville.
27. Clemson University, Clemson, S.C.

CHEMICAL PHYSICS

G. M. Brown,* D. C. Rohrer,[28] B. Berking,[28] C. A. Beevers,[29] R. O. Gould,[29] and R. Simpson,[29] "α,α-Trehalose Dihydrate, $C_{12}H_{22}O_{11}\cdot 2H_2O$. Three Independent Determinations," Winter Meeting, American Crystallographic Association, Albuquerque, N.M., Apr. 4–7, 1972.

P. A. Agron,* W. R. Busing, and H. A. Levy, "Lithium Hydroxide Monohydrate," Winter Meeting, American Crystallographic Association, Albuquerque, N.M., Apr. 4–7, 1972.

J. M. Williams,*[10] S. W. Peterson,[10] and H. A. Levy, "The Aquated Hydrogen Ion, $H_7O_3^+$: A High Precision Neutron Diffraction Study of Sulfosalicylic Acid Trihydrate (SSATH), $C_6H_3(COOH)(OH)SO_3H\cdot 3H_2O$," Winter Meeting, American Crystallographic Association, Albuquerque, N.M., Apr. 4–7, 1972.

W. E. Thiessen,* H. A. Levy, and B. D. Flaig,[30] "Non-Planarity of Two Hydroxamic Acids: 3-Hydroxyxanthine and Hydroxyurea," Winter Meeting, American Crystallographic Association, Albuquerque, N.M., Apr. 4–7, 1972.

W. R. Busing* and W. E. Thiessen, "The Effect of Intermolecular Forces on the Conformation of a Molecule in a Crystal," Summer Meeting, American Crystallographic Association, Ames, Iowa, Aug. 15–20, 1971.

C. K. Johnson, "A Set of Five Invariants for Reporting the Precision of Atomic Parameters," Summer Meeting, American Crystallographic Association, Ames, Iowa, Aug. 15–20, 1971.

C. K. Johnson* and G. D. Brunton,[31] "Hydrogen Isotope Fractionation, Phase Transformation and Dynamic Disorder in $Y(H_5O_2)(C_2O_4)_2H_2O$; A Neutron Diffraction Study," Winter Meeting, American Crystallographic Association, Albuquerque, N.M., Apr. 4–7, 1972.

C. K. Johnson, "New Computational Techniques, Particularly Refinement," Symposium on Computational Needs and Resources in Crystallography, Albuquerque, N.M., Apr. 8, 1972 (invited).

R. Livingston, "ESR Studies of Short-Lived Radicals Prepared by Photolysis of Liquids," Gordon Research Conference on Magnetic Resonance, New Hampton, N.H., June 16, 1971 (invited).

T. A. Carlson, "Evaluation of the Use of Electron Spectroscopy for the Study of Surfaces," 45th National Colloid Symposium, Atlanta, Ga., June 21–23, 1971 (invited).

T. A. Carlson, "Study of the Electronic Structure of Molecules by Photoelectron Spectroscopy," US-Japan Seminar on Current Problems in Spectroscopic Studies, Tokyo, Japan, Aug. 24–27, 1971 (invited).

T. A. Carlson, "General Survey of Electron Spectroscopy," International Conference on Electron Spectroscopy, Asilomar, Calif., Sept. 7–10, 1971 (invited).

T. A. Carlson, "Comprehensive Examination of the Angular Distribution of Photoelectron Spectra from Atoms and Molecules," International Conference on Electron Spectroscopy, Asilomar, Calif., Sept. 7–10, 1971.

J. C. Carver,*[26,32] T. A. Carlson, L. C. Cain,[26] and G. K. Schweitzer,[33] "Use of X-Ray Photoelectron Spectroscopy to Study Bonding in Transition Metal Salts by Observation of Multiplet Splitting," International Conference on Electron Spectroscopy, Asilomar, Calif., Sept. 7–10, 1971.

T. A. Carlson* and N. Fernelius,[34] "Chemical Shifts Observed in Photoelectron Spectroscopy as a Function of the Periodic Table," XVth Conference on Analytical Chemistry in Nuclear Technology, Oak Ridge, Tenn., Oct. 12–14, 1971 (invited).

---

28. Department of Crystallography, University of Pittsburgh, Pa.
29. Department of Chemistry, University of Edinburgh, Scotland.
30. Oak Ridge Associated Universities Summer Student Trainee from Moorhead State College, Moorhead, Minn., summer 1971.
31. Reactor Chemistry Division.
32. Present address: University of Georgia, Athens.
33. Department of Chemistry, University of Tennessee, Knoxville.
34. Research Consultants, Inc., Oak Ridge, Tenn.

J. C. Carver,*[26,32] T. A. Carlson, G. K. Schweitzer,[33] and F. A. Grimm,[33] "Photoelectron Spectroscopy of Transition Metal Compounds," XVth Conference on Analytical Chemistry in Nuclear Technology, Oak Ridge, Tenn., Oct. 12–14, 1971 (invited).

T. A. Carlson, "Recent Developments in the Use of Electron Spectroscopy for the Study of Chemical Problems," Maryland Section, American Chemical Society, Baltimore, Md., Jan. 26–27, 1972 (invited).

T. A. Carlson, "Recent Developments in the Use of Electron Spectroscopy for the Study of Chemical Problems," St. Joseph Valley Section, American Chemical Society, South Bend, Ind., Jan. 14–15, 1972 (invited).

T. A. Carlson, "Present and Future Applications of Auger Spectroscopy," International Conference on Inner Shell Ionization Phenomena, Georgia Institute of Technology, Atlanta, Apr. 17–22, 1972 (invited).

F. Wuilleumier*[21] and M. O. Krause, "Determination of Oscillator Strength for the First Discrete Transition in N_2 from the Auger Decay," International Conference on Inner Shell Ionization Phenomena, Georgia Institute of Technology, Atlanta, Apr. 17–21, 1972.

M. O. Krause* and F. Wuilleumier,[21] "X-Ray Analysis by Photoelectron Spectrometry," International Conference on Inner Shell Ionization Phenomena, Georgia Institute of Technology, Atlanta, Apr. 17–21, 1972.

M. O. Krause, "Creation of Multiple Vacancies," International Conference on Inner Shell Ionization Phenomena, Georgia Institute of Technology, Atlanta, Apr. 17–21, 1972 (invited).

M. J. Saltmarsh,*[1] A. van der Woude,[1] C. A. Ludemann,[1] R. L. Hahn, and E. Eichler, "Energy Shifts and Relative Intensities of *K* X-Rays Produced by Swift Heavy Ions," International Conference on Inner Shell Ionization Phenomena, Georgia Institute of Technology, Atlanta, Apr. 17–21, 1972.

A. van der Woude,*[1] M. J. Saltmarsh,[1] R. L. Hahn, and E. Eichler, "X-Ray Production Cross Sections by Swift Heavy Ions," International Conference on Inner Shell Ionization Phenomena, Georgia Institute of Technology, Atlanta, Apr. 17–21, 1972.

S. Datz,* E. Laegsgaard,[35] L. C. Feldman,[35] J. U. Andersen,[35] and J. L. Duggan,[36] "*L* Subshell Ionization Cross Sections in Gold for Proton and He Ion Bombardment (0.2–3 MeV/Nucleon)," International Conference on Inner Shell Ionization Phenomena, Georgia Institute of Technology, Atlanta, Apr. 17–21, 1972.

S. Datz, "Molecular Beam Studies of Collision-Induced Molecular Excitation," International Conference on Intermolecular Energy Transfer, Cambridge, England, July 19–23, 1971 (invited).

S. Datz, "Applications of Ion-Atom Collision Physics," International Seminar on Ion-Atom Collisions, Amsterdam, Netherlands, July 21–23, 1971 (invited).

S. Datz, "Atomic States of Energetic Ions in Solids," IInd International Conference on Atomic Collisions in Solids, Gausdal, Norway, Sept. 20–24, 1971 (invited).

---

35. Physics Institute, University of Aarhus, Aarhus, Denmark.
36. Oak Ridge Associated Universities, Oak Ridge, Tenn.

Lectures

NUCLEAR CHEMISTRY

R. L. Hahn, "Proposed APACHE Scientific Program (Nuclear Chemistry)," First Meeting of the Advisory Committee on the Experimental Facilities of Apache, Oak Ridge, Tenn., Oct. 11–12, 1971.

R. L. Ferguson, "Studies of the Double-Humped Fission Barrier at Oak Ridge," Institut für Kernphysik, Universität Tübingen, Germany, Dec. 17, 1970.

R. L. Ferguson, "Fission Isomer Studies at Oak Ridge," Physik Department, Technische Universität München, Garching, Germany, Feb. 9, 1971.

G. D. O'Kelley, "A New Look at the Moon: Analysis of Samples from the Apollo and Luna Missions," American Chemical Society Local Section Speaker Tour: Mobile, Birmingham, and Florence, Ala., October 1971.

CHEMISTRY AND PHYSICS OF TRANSURANIUM ELEMENTS

R. L. Hahn, "Super-Heavy and Sub-Super-Heavy Elements," Carnegie-Mellon University, Pittsburgh, Pa., Oct. 28, 1971.

R. L. Hahn, "Recent Research with Heavy Ions at Oak Ridge," Los Alamos Scientific Laboratory, Los Alamos, N.M., Feb. 22, 1972.

E. Eichler, "Coulomb Excitation of Actinide Nuclei with Heavy Ions from ORIC," Chemistry Department Seminar, Texas A and M University, College Station, May 5, 1972 (ORAU Traveling Lecture).

O. L. Keller, Jr., "Prediction of Chemical and Physical Properties of the Actinide and Superheavy Elements," Herbert S. Hamed Symposia on Chemistry of Heavy and Superheavy Elements, Yale University, New Haven, Conn., Mar. 9–10, 1972.

C. E. Bemis, Jr., "The Unequivocal Identification of Transfermium Elements by X-Ray Techniques," Chemistry Department Seminar, Washington University, St. Louis, Mo., Mar. 24, 1972.

R. J. Silva, "Predictions and Methods for the Chemical Separation of Superheavy Elements," Nuclear Chemistry Division Seminar, Lawrence Berkeley Laboratory, Berkeley, Calif., Apr. 14, 1972.

RADIATION CHEMISTRY

P. S. Rudolph, "The Study of the Radiolysis of Methane in a Mass Spectrometer," Chemistry Department Seminar, East Carolina University, Greenville, N.C., Oct. 29, 1971.

ORGANIC CHEMISTRY

C. J. Collins, "Der Gebrauch von Isotopen bei organischen Untersuchungen," Universität München, Germany, May 21, 1971; Universität des Saarlandes, Germany, July 5, 1971; Universität Frankfort, Germany, July 7, 1971.

C. J. Collins, "The Use of Isotopes to Study an Organic Reaction," Shionogi Inc., Osaka, Japan, Oct. 12, 1971; University of Hiroshima, Japan, Oct. 12, 1971; Sagami Research Center, Tokyo, Japan, Oct. 20, 1971; Sankyo Inc., Tokyo, Japan, Oct. 21, 1971; Sendai University, Japan, Oct. 22, 1971; University of Tennessee at Martin, Apr. 12, 1972.

C. J. Collins, "The Mechanism of 6,2-Hydride Shift in Norbornyl Cations," Osaka Section, Chemical Society of Japan, Oct. 13, 1971.

C. J. Collins, "Recent Experiments in the Deamination of Primary Aliphatic Amines," Chemistry Department Seminar, University of Tennessee, Knoxville, Jan. 13, 1972.

PHYSICAL CHEMISTRY

M. H. Lietzke, "Thermodynamic Properties of Electrolyte Solutions from Solubility and EMF Measurements," Chemistry Department Seminar, University of Tennessee, Knoxville, Nov. 11, 1971.

K. A. Kraus,[1] "Hyperfiltration and Related Techniques," Chemistry Division Seminar, Brookhaven National Laboratory, Upton, L.I., N.Y., June 9, 1971; Sterling Forest Research Center, Tuxedo, N.Y., June 10, 1971.

K. A. Kraus,[1] "Physical-Chemical Treatment Methods," Tennessee Water and Wastewater Association Meeting, Oak Ridge, July 29, 1971.

E. H. Taylor, "The Story of Polywater," American Chemical Society Local Section Lecture, University of Alabama, Tuscaloosa, Nov. 11, 1971.

H. R. Bronstein, "Emf Studies in Rare Earth Metal-Metal Halide Melts," University of New Brunswick, Fredericton, N.B., Canada, May 26, 1971.

H. R. Bronstein, "The Development of a Novel Reference Electrode System for Use in Certain Fluoride Melts," University of New Brunswick, Fredericton, N.B., Canada, May 27, 1971.

G. H. Cartledge, "The Ionic Potential," East Tennessee Section, American Chemical Society, Lind Lecture, University of Tennessee, Knoxville, Nov. 2, 1971.

G. H. Cartledge, "Effects in the Corrosion Interface," East Tennessee Section, American Chemical Society, Lind Lecture, Oak Ridge, Tenn., Nov. 3, 1971.

CHEMICAL PHYSICS

W. E. Thiessen, "Precise Molecular Geometry by X-Ray and Neutron Diffraction Techniques," Furman University, Greenville, S.C., Mar. 15, 1972.

T. A. Carlson, "Electron Spectra and Chemical Problems," Summer Institute on Low-Energy Accelerators for Teaching and Research, Oak Ridge, Tenn., July 5–Aug. 13, 1971.

M. O. Krause, "The Various Aspects of Electron Spectrometry," Aerospace Research Laboratory, Wright-Patterson Air Force Base, Dayton, Ohio (through University of Cincinnati), Jan. 21, 1972.

M. O. Krause, "Electron Spectrometry in Chemistry and Physics," Physics Department Colloquium, University of Virginia, Charlottesville, Mar. 24, 1972.

T. A. Carlson, "Recent Developments in the Application of Electron Spectroscopy to Chemical Problems," Rutgers University, New Brunswick, N.J., Apr. 5, 1972.

S. Datz, "Atomic States of Energetic Ions in Solids," Lecture Series, University of Aarhus, Aarhus, Denmark, June–September 1971.

---

1. Director's Division.

Supplementary Activities

STAFF

PROFESSIONAL AND EDUCATIONAL ACTIVITIES

W. R. Busing	President, American Crystallographic Association, 1971.
T. A. Carlson	Member, Organizing Committee, International Conference on Electron Spectroscopy, Asilomar, Calif., Sept. 7–10, 1971. Joint Editor-in-Chief, *Journal of Electron Spectroscopy*, December 1971–present. Member, Program Advisory Board, International Symposium on Future Applications of Inner Shell Ionization Phenomena, Atlanta, Ga., Apr. 22, 1972.
C. J. Collins	Professor of Chemistry, part time, University of Tennessee, Knoxville, January 1964–present. NATO Award, Universities of Munich and Saarbrücken, May 14–July 9, 1971.
S. Datz	Chairman, Gordon Research Conference on Dynamics of Molecular Collisions, 1972. Chairman, III International Conference on Atomic Collisions in Solids, 1972–73. Program Committee, Division of Electron and Atomic Physics, American Physical Society, 1969–71. Editorial Board, *Atomic Data*, 1969–present. Editorial Board, *Case Studies in Atomic Physics*, 1970–present. Guest Professor, Institute of Physics, Aarhus University, Aarhus, Denmark, June 1–Oct. 22, 1971.
L. Dresner	Lecturer in Chemical Engineering, University of Tennessee, Knoxville, 1963–present.
E. Eichler	Chairman, Symposium on Coulomb Excitation and In-Beam Gamma-Ray Spectroscopy, 162nd National Meeting, American Chemical Society, Washington, D.C., Sept. 12–17, 1971. Membership Committee, Division of Nuclear Chemistry and Technology, American Chemical Society, 1972.
R. L. Ferguson	Fellowship from Deutsches Bundesministerium für Wissenschaftliche Forschung, Garching, Germany, July 1970–July 1971.
J. A. Ghormley	Editorial Board, *Radiation Research*, 1972–1975.
R. L. Hahn	Secretary, Committee on Major Nuclear Facilities, Division of Nuclear Chemistry and Technology, American Chemical Society, 1970–1974.
C. K. Johnson	Member, USA National Committee for Crystallography, National Academy of Sciences–National Research Council, Jan. 1, 1972–Dec. 31, 1974. Member, National Research Council Committee on Chemical Crystallography. Consultant, Crystallographic Computing Committee, International Union for Crystallography.
O. L. Keller, Jr.	USAEC Transplutonium Program Committee, 1969–1974. Member, Nuclear Physics Survey Panel, National Academy of Sciences, 1969–1972.
K. A. Kraus	Editorial Board, *Journal of Chromatography*, 1958–present. Editorial Advisory Board, *Journal of Inorganic and Nuclear Chemistry*, 1958–present. Editorial Board, *Desalination*, 1966–present.
M. H. Lietzke	Professor of Chemistry, part time, University of Tennessee, Knoxville, January 1964–present.
Ralph Livingston	Professor of Chemistry, part time, University of Tennessee, Knoxville, January 1964–present. ORNL liaison officer for ORNL–University of Tennessee part-time teaching programs, 1968–present. Member, Graduate Council, University of Tennessee, Knoxville, January 1970–present. Chairman, East Tennessee Section, American Chemical Society, January 1972–present. Chairman, Third Southeastern Magnetic Resonance Conference, Oak Ridge, Oct. 20–22, 1971. Editorial Board, *The Journal of Magnetic Resonance*, January 1971–present. Editorial Board, *Magnetic Resonance Review*, September 1971–present. Judge, 23rd International Science and Engineering Fair, New Orleans, La., May 3, 1972.

G. E. Moore	Instructor in Chemistry, National Science Foundation In-Service Institute for Secondary School Science Teachers, Knoxville College, Knoxville, Tenn., 1967–present.
G. D. O'Kelley	Professor of Chemistry, part time, University of Tennessee, Knoxville, January 1964–present. Subcommittee on Radiochemistry, National Academy of Sciences–National Research Council, 1962–present. Chairman, Division of Nuclear Chemistry and Technology, American Chemical Society, 1971. Chairman, Nominating Committee, Division of Nuclear Chemistry and Technology, American Chemical Society, 1972.
R. W. Stoughton	Editorial Advisory Board, *Journal of Inorganic and Nuclear Chemistry,* 1958–present. Consulting Editor, *Inorganic and Nuclear Chemistry Letters,* 1965–present.
T. J. Sworski	Discussion leader, Chemistry Seminar for high school teachers and students, Cumberland College, Williamsburg, Ky., Mar. 31–Apr. 1, 1972.
E. H. Taylor	Board of Directors, Institute of Catalysis. Advisory Board, American Chemical Society and U.S. Atomic Energy Commission Monographs on Chemistry and Chemical Engineering in Nuclear Technology.

FOREIGN MEETINGS AND ACTIVITIES

Meeting and/or Activity	Location	Staff Member(s)
VIII International Meeting on Nuclear Physics, Jan. 25–30, 1971	Villars, Switzerland	R. L. Ferguson
International Conference on Intermolecular Energy Transfer, July 19–22, 1971	Cambridge, England	S. Datz
International Seminar on Ion-Atom Collisions, July 21–24, 1971	Amsterdam, Netherlands	
VII International Conference on the Physics of Electronic and Atomic Collisions, July 26–30, 1971	Amsterdam, Netherlands	
II International Conference on Atomic Collisions in Solids, Sept. 20–24, 1971	Gausdal, Norway	
Lecture Series, "Atomic States of Energetic Ions in Solids," June–September 1971	University of Aarhus, Aarhus, Denmark	
US-Japan Seminar on Current Problems in Spectroscopic Studies, Aug. 24–27, 1971	Tokyo, Japan	T. A. Carlson
OAS sponsored lectures and discussions on electron spectroscopy, May 6–21, 1972	University of Mexico, Mexico City, Mexico	
NATO Advanced Study Institute on Direct and Patterson Methods of Solving Crystal Structures, Sept. 6–18, 1971	University of York, York, England	G. M. Brown
International Colloquium on the Study of Crystal Transformations at High Temperature, Above 2000°K, September 1971	Odeillo, France	M. A. Bredig
Pulse Radiolysis Conference, Oct. 25–27, 1971	Whiteshell Nuclear Research Establishment, Pinawa, Manitoba, Canada	C. J. Hochanadel
22nd Conference on Reaction Mechanisms, October 1971	Nagoya, Japan	C. J. Collins

COLLABORATIVE RESEARCH

Institution	Collaborator(s)	Subject	Staff Member(s)
Argonne National Laboratory	A. Rahman S. W. Peterson J. M. Williams	Molecular dynamic studies of molten salts Neutron diffraction	A. H. Narten H. A. Levy
University of Arkansas	L. Schäfer	Raman spectra of metal-organo compounds	G. M. Begun
Brookhaven National Laboratory	J. Hudis	Search for superheavy elements in accelerator targets	J. Halperin R. W. Stoughton
Centenary College	R. F. Walker, Jr.	Properties of rare-earth and osmium alpha emitters	R. L. Hahn K. S. Toth[1]

1. Physics Division.

Institution	Collaborator(s)	Subject	Staff Member(s)
Clemson University	C. A. Brandon J. J. Porter	Hyperfiltration of textile dyeing wastes	J. S. Johnson, Jr. R. E. Minturn
University of Delft, Netherlands	B. van Nooijen A. C. Rester	Decay properties of ^{84}Y	N. R. Johnson
University of Delhi, India	S. C. Pancholi	Level structure of ^{59}Co	N. R. Johnson
Embassy of the Socialist Federal Republic of Yugoslavia	M. Mladjenovic	States in ^{249}Bk populated in alpha decay of ^{253}Es	C. E. Bemis, Jr.
EURATOM, Geel, Belgium	H. Weigmann	Search for conversion electrons from ^{236}U fission isomer	R. L. Ferguson
Florida State University	R. K. Sheline	Levels in ^{161}Tb excited by ($^{3}He,d$) reaction and by decay of 3.7-min ^{161}Gd	N. R. Johnson G. D. O'Kelley
Universität Frankfurt, Germany	P. Ostermann	Search for conversion electrons from ^{236}U fission isomer	R. L. Ferguson
Fresno State College	M. J. Zender	Energy levels in ^{236}U	P. F. Dittner C. E. Bemis, Jr.
Furman University	R. O. Sayer	Coulomb excitation of rare-earth and actinide nuclei	E. Eichler N. R. Johnson
Universität Giessen, Germany	G. Siegert H. Gunther	Nuclear charge distribution of heavy fission fragments in reaction $^{239}Pu(n_{th},f)$	R. L. Ferguson
Institut für Kernphysik der Universität Frankfurt, W. Germany	Th. W. Elze	Collective states excited in ^{236}U (d,d') reaction	C. E. Bemis, Jr.
Institute of Nuclear Research, Amsterdam, Netherlands	J. Konijn	Decay properties of ^{84}Y	N. R. Johnson
International Paper Company	K. J. Brown	Hyperfiltration of kraft pulp mill wastes	J. S. Johnson, Jr.
Lawrence Berkeley Laboratory	A. Ghiorso M. Nitchke	Automated system for rapid chemical separation of element 105	R. J. Silva
	G. T. Seaborg A. Ghiorso	Chemical separation and identification of superheavy elements	R. J. Silva
	E. Cheifetz R. C. Jared E. R. Giusti S. G. Thompson	Search for superheavy elements in nature	J. S. Drury J. Halperin R. J. Silva R. W. Stoughton
Lawrence Radiation Laboratory, Livermore	R. G. Lanier R. A. Meyer	Levels in ^{161}Tb excited by ($^{3}He,d$) reaction and by decay of 3.7-min ^{161}Gd	N. R. Johnson G. D. O'Kelley
University of Liège, Belgium	M. Noé	Self-irradiation effects on physical and chemical properties of curium	J. R. Peterson[2]
	J. Fuger	Experimental determination of heat of solution of berkelium metal	J. R. Peterson[2]
Los Alamos Scientific Laboratory	M. S. Moore A. N. Ellis	Neutron induced fission cross sections for ^{249}Cf at ORELA	C. E. Bemis, Jr.
Maryville College	P. J. Ogren	Pulse radiolysis and flash photolysis	C. J. Hochanadel J. A. Ghormley J. W. Boyle
Massachusetts Institute of Technology School of Chemical Engineering Practice, Oak Ridge Station	J. T. Day P. H. Wadia and various teams	Hyperfiltration with dynamically formed membranes	J. S. Johnson, Jr. K. A. Kraus
Middle East Technical University, Ankara, Turkey	N. K. Aras	Excited states in ^{184}W populated in the decay of ^{184}Ta	N. R. Johnson

2. Consultant, Department of Chemistry, University of Tennessee, Knoxville.

Institution	Collaborator(s)	Subject	Staff Member(s)
Universität München, Germany	H. J. Specht J. Weber	Search for conversion electrons from ^{236}U fission isomer	R. L. Ferguson
NASA Manned Spacecraft Center	E. Schonfeld	Determination of primordial and cosmogenic radionuclide content of lunar material by gamma-ray spectrometry	G. D. O'Kelley
University of Oklahoma	H. Fischbeck	Use of electron spectroscopy in biological systems[3]	T. A. Carlson
Laboratoire de Chimie Physique de l'Université, Paris VI, France	F. Wuilleumier	Electron spectrometry of actinides and their compounds	M. O. Krause
University of Puerto Rico	L. Blum	Theory of liquids	A. H. Narten
Purdue University	P. J. Daly S. W. Yates	Excited states in ^{184}W populated in decay of ^{184}Ta	N. R. Johnson
University of Rochester	J. R. Huizenga C. Kline	Odd proton in ^{249}Bk excited in $^{248}Cm(^{3}He,d)$ and $^{248}Cm(^{4}He,t)$ reactions	C. E. Bemis, Jr.
	J. R. Huizenga J. S. Boyno	Collective states excited in $^{236}U(d,d')$ reaction	C. E. Bemis, Jr.
Rutherford High Energy Laboratory	G. G. J. Boswell W. Newton	Search for superheavy elements in accelerator targets	J. Halperin H. W. Schmitt[1] R. W. Stoughton
Stanford Linear Accelerator Center	D. Busick D. Walz	Search for superheavy elements in accelerator targets	J. Halperin R. W. Stoughton
Technische Universität München, Germany	E. Konecny	Search for conversion electrons from ^{236}U fission isomer	R. L. Ferguson
University of Tennessee	L. L. Riedinger	Coulomb excitation of rare-earth and actinide nuclei	E. Eichler N. R. Johnson
	C. Bingham	Properties of rare-earth alpha emitters	R. L. Hahn K. S. Toth[1]
	G. Mamantov	Raman studies of molten-salt systems	G. M. Begun
	F. Schmidt-Bleek	Hot atom collision chemistry	S. Datz
	W. E. Bull G. K. Schweitzer	Use of electron spectroscopy for chemical analysis[3]	T. A. Carlson
	F. A. Grimm	Calculations of angular distribution of photoelectron spectra[3]	T. A. Carlson
	T. F. Williams	Pulse radiolysis study of succinonitrile in the rotator phase	J. A. Ghormley
Union Carbide Corp., Linde Laboratories	R. M. Milton	Search for superheavy elements in nature	J. Halperin R. W. Stoughton
U.S. Geological Survey	J. H. McCarthy	Search for superheavy elements in nature	J. Halperin R. W. Stoughton
UNISOR Project	A. C. Rester R. Mlekadj	Development of data-acquisition system	E. Eichler N. R. Johnson
Vanderbilt University	J. H. Hamilton A. V. Ramayya P. E. Little A. F. Kluk	Studies of deformed nuclei and of rotation-vibration interaction	N. R. Johnson
	J. H. Hamilton A. V. Ramayya A. C. Rester N. C. Singhal	Study of properties of some vibrational spherical nuclei	N. R. Johnson E. Eichler

3. In collaboration with the Physics Division.

Institution	Collaborator(s)	Subject	Staff Member(s)
Vanderbilt University	J. H. Hamilton P. E. Little A. V. Ramayya E. Collins A. F. Kluk	Determinations of $E2$-$M1$ mixing ratios in transitions from vibrational states of deformed nuclei	N. R. Johnson
	J. H. Hamilton L. Varnell	Heavy-ion Coulomb excitation of ^{178}Hf and ^{180}Hf	N. R. Johnson E. Eichler
Virginia Polytechnic Institute and State University	M. A. Ijaz	Properties of rare-earth and osmium alpha emitters	R. L. Hahn K. S. Toth[1]

ANNUAL INFORMATION MEETING AND ADVISORY COMMITTEE

The Annual Information Meeting of the Chemistry Division was held October 6 and 7, 1971, in the Central Auditorium, Building 4500N. Reports presented at the Meeting were:

Wednesday, October 6, 1971

E. H. Taylor	Introduction
E. J. Kelly	Electrochemical Behavior of Titanium
H. R. Bronstein	A Reference Electrode System for Use in Fluoride Melts
H. Zeldes	Paramagnetic Resonance Studies of Photolyzed Liquids
L. Dresner	Transport Through Ion-Exchange Membranes
R. H. Busey	Low-Temperature Heat Capacity of Lithium-7 Hydride and Lithium-7 Deuteride
C. J. Hochanadel	Absorption Spectrum and Reaction Kinetics of the HO_2 Radical in the Gas Phase

Thursday, October 7, 1971

C. E. Bemis	The Determination of the Electric Quadrupole and Hexadecapole Moments for Even-Even Actinide Nuclei
J. Halperin	A Neutron Multiplicity Counter
M. O. Krause	Electron Binding Energies in Americium
T. A. Carlson	Two New Aspects of Photoelectron Spectroscopy[3]
W. R. Busing	Effect of Interatomic Forces on Molecular Conformation in Crystals
A. H. Narten	Liquid Gallium: Interatomic Potential Function from X-ray and Neutron Diffraction Data

Members of the Advisory Committee were:

Prof. George S. Hammond
Department of Chemistry
California Institute of Technology
Pasadena, California 91109

Dr. Joseph J. Katz
Argonne National Laboratory
9700 South Cass Avenue
Argonne, Illinois 60493

Prof. Henry Taube
Department of Chemistry
Stanford University
Stanford, California 94305

On Nov. 17–18, 1971, the research program of the Chemistry Division was discussed with members of the Division of Research, U.S. Atomic Energy Commission. Reports presented at these meetings were:

Wednesday, November 17, 1971

E. Eichler	Heavy-Ion Coulomb Excitation of Deformed Nuclei (Lanthanides and Actinides) at ORIC
J. Halperin	Some Recent Neutron Cross Section Measurements
R. L. Ferguson	Fragment Mass-Energy Systematics and the Mechanism of Medium-Excitation Fission
C. E. Bemis	Determination of Intrinsic Electric Quadrupole and Hexadecapole Moments for Even-Even Actinide Nuclei
G. M. Begun	Molecular Spectroscopy
H. R. Bronstein	A Reference Electrode System for Use in Certain Fluoride Melts
E. Ricci[4]	Nuclear Methods in Chemical Analysis
D. J. Fisher[4]	Instrumentation Research in Analytical Chemistry
M. T. Kelley[4]	Small Computer Applications and In-Line Analyses
J. C. White[4]	Future Research Program Planning
T. A. Carlson	Recent Developments in the Use of Photoelectron Spectroscopy for Chemical Problems[3]
R. H. Busey	Low-Temperature Heat Capacity of Lithium-7 Hydride and Lithium-7 Deuteride
S. Datz	Inner- and Outer-Shell Chemistry from Collision Experiments

Thursday, November 18, 1971

L. J. Nugent	Systematics Correlating Some Thermodynamic Properties of the Lanthanide and Actinide Metals
C. J. Collins	The Memory of an Organic Reaction
W. E. Thiessen	The Molecular Geometry of Hydroxamic Acids: 3-Hydroxyxanthine and Hydroxyurea
E. J. Kelly	Electrode Kinetics and Corrosion: Electrochemical Behavior of Titanium; A Potentiostat Method for Conductance and Capacitance Measurements
C. J. Hochanadel	Absorption Spectrum and Reaction Kinetics of the HO_2 Radical in the Gas Phase
H. Zeldes	Paramagnetic Resonance Studies of Free Radicals in Solutions

The Annual Information Meeting of the Water Research Program of the Chemistry Division was held May 28, 1971, in the Central Auditorium, Building 4500N. Reports presented at the Meeting were:

J. S. Johnson, Jr.	Introductory Remarks
H. A. Mahlman	Cross-Flow Filtration in Treatment of Municipal Sewage
L. Dresner	Theoretical Studies Related to Ionic Transport through Membranes
R. E. Minturn	Recent Developments in Dynamic Membranes and Their Practical Applications
D. G. Thomas[5]	Hydrodynamic Effects on Fouling

VISITING SCIENTISTS

Name	Affiliation	ORNL Research Program	Sponsor
N. C. Fernelius	Research Consultants, Inc.	Electron Spectroscopy	Research Consultants, Inc.
F. H. Fink	Birmingham Southern College	Transuranium Research Laboratory	Birmingham Southern College
W. H. Fletcher	University of Tennessee	Isotope Chemistry	Consultant
R. V. Gentry	Columbia Union College	Transuranium Research Laboratory	Columbia Union College

4. Analytical Chemistry Division.
5. Reactor Division.

Name	Affiliation	ORNL Research Program	Sponsor
M. Mladjenovic	Embassy of the Socialist Federal Republic of Yugoslavia, Washington, D.C	Transuranium Research Laboratory	Government of Yugoslavia
J. R. Peterson	University of Tennessee	Transuranium Research Laboratory	Consultant
S. W. Peterson	Argonne National Laboratory	Neutron and X-Ray Diffraction	ANL
R. O. Sayer	Furman University	Nuclear Chemistry	ORAU Faculty Research Participation Program
F. K. Schmidt-Bleek	University of Tennessee	Molecular Beam	Consultant
R. Triolo	University of Palermo	Diffraction Studies of Liquids	NATO
J. A. Wargon	University of Tennessee	Organic Chemistry	University of Tennessee
R. M. White	Baker University	Electron Spectroscopy	Baker University
J. M. Williams	Argonne National Laboratory	Neutron and X-Ray Diffraction	ANL
B. J. Wilson	Brigham Young University	Microwave and Radio-Frequency Spectroscopy	Sabbatical leave and ORAU Faculty Research Participation Program
F. Wuilleumier	Laboratoire de Chimie Physique de la Faculté des Sciences de Paris, Paris, France	Transuranium Research Laboratory	Centre National de la Recherche Scientifique, NATO, and ORNL

STUDENTS

GRADUATE

Name	Major Professor and/or Institution	Staff Advisor	Field of Research	Sponsor
W. J. Carter	G. K. Schweitzer, University of Tennessee	T. A. Carlson	Electron spectroscopy applied to environmental problems[3]	Oak Ridge Graduate Fellowship Program
J. C. Carver	G. K. Schweitzer, University of Tennessee	T. A. Carlson	Photoelectron Multiplet Splitting and Chemical Shifts in Transition-Metal Compounds[3] (Ph.D. thesis, March 1972)	NSF Fellowship
L. L. Collins, Jr.	G. D. O'Kelley, University of Tennessee	G. D. O'Kelley E. Eichler N. R. Johnson	Decay properties of ^{206}Tl and ^{98}Tc	University of Tennessee
Cynthia Daugherty	M. H. Lietzke, University of Tennessee	M. H. Lietzke	The Thermodynamic Properties of Aqueous HCl-KCl-$CaCl_2$ Mixtures as Calculated from Electromotive Force Measurements (M.S. thesis, March 1972)	
J. A. Fahey	J. R. Peterson,[2] University of Tennessee	L. J. Nugent	The Preparation and Some Properties of Berkelium Metal and Californium Dioxide (Ph.D. thesis, June 1971)	Oak Ridge Graduate Fellowship Program
D. W. Gosbin	M. H. Lietzke, University of Tennessee	M. H. Lietzke	Predictions of Activity and Osmotic Coefficients for Aqueous Electrolyte Mixtures (M.S. thesis, August 1971)	
H. D. Harmon	J. R. Peterson,[2] University of Tennessee	C. F. Coleman[6]	The Thiocyanate and Chloride Complexes of Some Trivalent Actinides (Ph.D. thesis, August 1971)	National Defense Education Act Title IV Fellowship

6. Chemical Technology Division.

Name	Major Professor and/or Institution	Staff Advisor	Field of Research	Sponsor
A. Y. Herrell	Karl H. Gayer, Wayne State University	R. H. Busey	Enthalpies of formation of Tc_2O_7, TcO_3, and TcO_4^-(aq.)	National Science Foundation Science Faculty Fellowship
F. D. Hwang	F. K. Schmidt-Bleek, University of Tennessee	S. Datz	Fast collisions using molecular beams	University of Tennessee
S. G. Johnson	F. K. Schmidt-Bleek, University of Tennessee	S. Datz	Excited atom-molecule reactions	University of Tennessee
A. E. Jonas	W. E. Bull and G. K. Schweitzer, University of Tennessee	T. A. Carlson	Photoelectron Spectroscopy of the Tetrafluoro and Tetramethyl Compounds of Group IV Elements[3] (Ph.D. thesis, December 1971)	University of Tennessee Research Grant
N. Kashihira[7]	F. K. Schmidt-Bleek, University of Tennessee	S. Datz	Ionizing Collisions of Fast Alkali Atoms with Cl_2, Br_2, and O_2 (Ph.D. thesis, August 1971)	
A. F. Kluk	J. H. Hamilton, Vanderbilt University	N. R. Johnson	Investigations of the Level Structure and of the Rotation-Vibration Interaction in ^{156}Gd and ^{158}Gd (Ph.D. thesis, August 1971)	Oak Ridge Graduate Fellowship Program
G. E. McGuire	G. K. Schweitzer, University of Tennessee	T. A. Carlson	Study of complex metal salts by photoelectron spectroscopy[3]	NSF Fellowship
Joyce Ann Monard	P. G. Huray, University of Tennessee	O. L. Keller, Jr. R. L. Becker[1] F. E. Obenshain[1]	Transuranium Research Laboratory	NSF Fellowship
D. U. O'Kain	C. R. Bingham, University of Tennessee	R. L. Hahn K. S. Toth[1]	α/Ec Ratios in ^{150}Dy, ^{151}Dy, and ^{149}Tb	
G. L. Ostrom	F. K. Schmidt-Bleek, University of Tennessee	S. Datz	Sputtering studies	
P. R. Reed[7]	F. K. Schmidt-Bleek, University of Tennessee	C. J. Hochanadel T. J. Sworski	Radiation Chemistry of Gaseous Methane (Ph.D. thesis, August 1971)	AUA-ANL Predoctoral Fellowship
N. C. Singhal	J. H. Hamilton, Vanderbilt University	N. R. Johnson E. Eichler	Vibrational properties of even-even spherical nuclei	Vanderbilt University
D. P. Spears	H. Fischbeck, University of Oklahoma	T. A. Carlson	Use of electron spectroscopy for the study of heavy metals in biological systems[3]	Oak Ridge Graduate Fellowship Program
J. N. Stevenson	J. R. Peterson,[2] University of Tennessee	O. L. Keller, Jr. L. J. Nugent	Solid-state studies of some actinide elements and compounds	Oak Ridge Graduate Fellowship Program

UNDERGRADUATE

Name	Institution	ORNL Research Program	Sponsor
D. C. Ahlgren	DePauw University	Isotope Chemistry	Great Lakes Colleges Association
H. Lynn Button	University of Tennessee	Organic Chemistry	ORAU Summer Student Trainee Program
S. J. Conner[8]	Georgia Institute of Technology	Transuranium Research Laboratory	Columbia Union College
B. D. Flaig	Moorhead State College	Neutron and X-Ray Diffraction	ORAU Summer Student Trainee Program
W. D. Hopewell	University of Puget Sound	Spectroscopy of Transition Metal Complexes	ORAU Summer Student Trainee Program
F. A. Shirley	DePauw University	Organic Chemistry	Great Lakes Colleges Association

7. Purdue University, Lafayette, Ind.
8. Co-op student.

INTERNAL DISTRIBUTION

1. Biology Library
2–4. Central Research Library
5. Laboratory Shift Supervisor
6. MIT Practice School
7. ORNL – Y-12 Technical Library Document Reference Section
8–43. Laboratory Records Department
44. Laboratory Records, ORNL R.C.
45. H. I. Adler
46. P. A. Agron
47. S. I. Auerbach
48. J. A. Auxier
49. W. H. Baldwin
50. C. E. Bemis
51. D. S. Billington
52. F. F. Blankenship
53. E. G. Bohlmann
54. C. J. Borkowski
55–56. G. E. Boyd
57. M. A. Bredig
58. R. B. Briggs
59. H. R. Bronstein
60. A. R. Brosi
61. G. M. Brown
62. J. H. Burns
63. R. H. Busey
64. W. R. Busing
65. T. A. Carlson
66. G. H. Cartledge
67. C. J. Collins
68. D. R. Cuneo
69. F. L. Culler
70. M. D. Danford
71. S. Datz
72. L. Dresner
73. J. S. Drury
74. A. S. Dworkin
75. E. Eichler
76. R. L. Ferguson
77. J. L. C. Ford
78. W. Fulkerson
79. R. V. Gentry
80. J. A. Ghormley
81. J. H. Gibbons
82. R. A. Gilbert
83. J. H. Gillette
84. C. D. Goodman
85. W. R. Grimes
86. R. L. Hahn
87. J. Halperin
88. R. F. Hibbs
89. C. J. Hochanadel
90. H. P. Carter
91. C. K. Johnson
92–96. J. S. Johnson
97. N. R. Johnson
98. W. H. Jordan
99. O. L. Keller
100. E. J. Kelly
101. H. W. Kohn
102. M. T. Kelley
103. B. H. Ketelle
104. K. A. Kraus
105. M. O. Krause
106. W. C. Kuykendall
107. J. A. Lane
108. E. Lamb
109. H. A. Levy
110. M. H. Lietzke
111. T. A. Lincoln
112. J. L. Liverman
113. R. Livingston
114. R. S. Livingston
115. R. N. Lyon
116. H. G. MacPherson
117. Peter Mazur
118. J. R. McNally, Jr.
119. R. E. Meyer
120. R. E. Minturn
121–131. G. E. Moore
132. A. H. Narten
133. L. J. Nugent
134. G. D. O'Kelley
135. G. W. Parker
136–137. R. B. Parker
138. F. Plasil
139. J. J. Pinajian
140. F. A. Posey
141. A. S. Quist
142. R. J. Raridon
143. S. A. Reynolds
144. P. S. Rudolph
145. R. M. Rush
146. H. W. Schmitt

147. H. E. Seagren
148. E. D. Shipley
149. W. D. Shults
150. M. J. Skinner
151. H. G. Smith
152. A. H. Snell
153. P. H. Stelson
154. J. N. Stevenson
155. R. W. Stoughton
156. D. A. Sundberg
157. T. J. Sworski
158–211. E. H. Taylor
212. W. E. Thiessen
213. R. E. Thoma
214. K. S. Toth
215. D. B. Trauger
216. F. Vaslow
217. A. M. Weinberg
218. J. C. White
219. M. K. Wilkinson
220. J. J. Katz (Advisory Committee)
221. Henry Taube (Advisory Committee)
222. George S. Hammond (Advisory Committee)

EXTERNAL DISTRIBUTION

223. H. Miller, Office of Isotope Development, AEC, Washington 20545
224. R. H. Schuler, Radiation Research Laboratories, Mellon Institute, 4400 Fifth Ave., Pittsburgh, Pa. 15213
225. Division of Research and Development, AEC, Washington 20545
226. Union Carbide Corporation, Chemicals Division, P.O. Box 8361, South Charleston, W. Va. 25303
227. Masaharu Kondo, Professor of Chemistry, Radiation Chemistry Laboratory, Tokyo Metropolitan University, 1-950, Fukasawa-cho, Setagaya-ku, Tokyo, Japan
228. J. P. W. Houtman, Reactor Institute Delft, Technische Hogeschool, Delft, The Netherlands
229. Technion, Israel Institute of Technology, Department of Nuclear Science, Haifa, Israel
230. Ingmar Bergstrom, Nobel Institute of Physics, Stockholm 50, Sweden
231. Riki Kobayashi, William Marsh Rice University, Houston, Texas 77001
232. J. A. Swartout, Union Carbide Corporation, 270 Park Avenue, New York, N.Y. 10017
233. W. W. Grigorieff, Assistant to the Executive Director, Oak Ridge Associated Universities
234. Enrico Cerrai, CISE, Milan, Italy
235. H. E. Podall, Office of Saline Water, U.S. Department of the Interior, Washington, D.C. 20240
236. D. E. Troutner, Chemistry Department, University of Missouri, Columbia, Missouri 65201
237. J. H. Hamilton, Physics Department, Vanderbilt University, Nashville, Tennessee 37203
238. W. H. McCoy, Office of Saline Water, U.S. Department of the Interior, Washington, D.C. 20240
239. Sidney Langer, Gulf General Atomic, Box 1111, San Diego, California 92112
240. J. R. Peterson, Department of Chemistry, University of Tennessee, Knoxville, Tennessee 37916
241. Library, Wah Chang Albany Corporation, P.O. Box 460, Albany, Oregon 97321
242. S. B. Sachs, Weizmann Institute of Science, Rehovoth, Israel
243. F. Schmidt-Bleek, Department of Chemistry, University of Tennessee, Knoxville, Tennessee 37916
244. F. E. Walker, Chemistry Department, Lawrence Radiation Laboratory, P.O. Box 808, Livermore, California 94550
245. Robert Vandenbosch, Chemistry Department, University of Washington, Seattle, Washington 98105
246. S. R. Mohanty, Department of Chemistry, Utkal University, Bhubaneswar 4, India
247. G. Czapski, Department of Physical Chemistry, The Hebrew University, Jerusalem, Israel
248. G. Scatchard, Professor of Physical Chemistry, Emeritus, Massachusetts Institute of Technology, Cambridge, Mass. 02139
249. Craig A. Brandon, Department of Mechanical Engineering, Clemson University, Clemson, S.C. 29631
250. Kenton J. Brown, Group Director, Pulping & Processing Research, Corporate Research Center, International Paper Co., P.O. Box 797, Tuxedo Park, N.Y. 10987
251. H. F. Gibbard, Jr., Department of Chemistry, Southern Illinois University, Carbondale, Illinois 62901
252. M. A. Ijaz, Physics Department, Virginia Polytechnic Institute, Blacksburg, Virginia 24060
253. R. F. Walker, Jr., Physics Department, Centenary College, Shreveport, Louisiana 71104
254. Justin L. Bloom, U.S. Atomic Energy Commission, Washington, D.C. 20545
255. D. A. Bromley, Department of Physics, Yale University, New Haven, Conn. 06520

256. M. L. Perlman, Department of Chemistry, Brookhaven National Laboratory, Upton, Long Island, N.Y. 11973
257. R. A. Robinson, Department of Chemistry, University of Florida, Gainesville, Fla. 32601
258. Jerzy Jastrzedski, Institute for Nuclear Research, Swierk K. Otwocka, Poland
259. R. Bock, Physikalisches Institut, Max Planck Institut für Kernphysik, Heidelberg, West Germany
260. Director of the Institute for Nuclear Physics Research (I.K.O.), Ooster Ringdijk 18 a, Amsterdam, The Netherlands
261. Mme. G. Bastin, Centre de Spectrométrie Nucléaire, Et de Spectrométrie de Masse (C.N.R.S.), 15 Rue G.-Clémenceau, 91-Orsay, France
262. R. W. Benjamin, Savannah River Laboratories Aiken, South Carolina 29802
263. Henry R. Bungay, Division of Advanced Technology Applications, National Science Foundation, RANN, 1800 G Street, N. W., Washington, D. C. 20550
264. R. Chidambaram, Bhabha Atomic Research Centre, Nuclear Physics Division, Trombay Bombay 85, India
265. Mrs. K. M. Glover, Chemistry Division, Bldg. 220, A. E. R. E., Harwell Berks, England
266. A. C. Rester, Institut fur Strahlen-und Kernphysik, Der Universitat Bonn, Nussallee 14-16, Bonn, West Germany
267. R. C. Grimm, Technical Center, Union Carbide Corporation, South Charleston, West Virginia
268. Research and Technical Support Division, AEC, ORO
269. Patent Office, AEC, ORO

270–460. Given distribution as shown in TID-4500 under Chemistry category (25 copies – NTIS)